

UNCLASSIFIED

| |
|--|
| |
| |
| |
| AD NUMBER |
| AD910069 |
| NEW LIMITATION CHANGE |
| TO Approved for public release, distribution unlimited |
| FROM Distribution authorized to U.S. Gov't. agencies only; Test and Evaluation; MAR 1973. Other requests shall be referred to Air Force Materials Laboratory, Attn: LC, Wright-Patterson AFB, OH 45433. |
| AUTHORITY |
| AFWAL notice, 3 Nov 1983 |

THIS PAGE IS UNCLASSIFIED

UNCLASSIFIED

AD 910069

AUTHORITY:

AFWAL Notice

3 Nov 83



UNCLASSIFIED

THIS REPORT HAS BEEN DELIM.TED
AND CLEARED FOR PUBLIC RELEASE
UNDER DOD DIRECTIVE 5200.20 AND
NO RESTRICTIONS ARE IMPOSED UPON
ITS USE AND DISCLOSURE.

DISTRIBUTION STATEMENT A

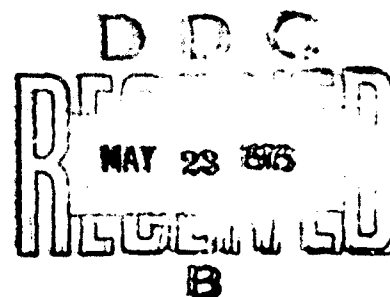
APPROVED FOR PUBLIC RELEASE;
DISTRIBUTION UNLIMITED.

COMPOSITE WING CONCEPTUAL DESIGN

W. D. Nelson, et al.
McDonnell Douglas Corporation
Douglas Aircraft Company

TECHNICAL REPORT AFML-TR-73-57

March 1973



Distribution limited to U.S. Government agencies; test and evaluation; statement applied March 1973. Request for this document must be referred to AFML (LC), Wright-Patterson Air Force Base, Ohio 45433.

Air Force Materials Laboratory
Air Force Systems Command
Wright-Patterson Air Force Base, Ohio 45433

AD910069

NOTICE

When Government drawings, specifications, or other data are used for any purpose other than in connection with a definitely related Government procurement operation, the United States Government thereby incurs no responsibility nor any obligation whatsoever; and the fact that the Government may have formulated, furnished, or in any way supplied the said drawings, specifications, or other data, is not to be regarded by implication or otherwise as in any manner licensing the holder or any other person or corporation, or conveying any rights or permission to manufacture, use, or sell any patented invention that may in any way be related thereto.

Copies of this report should not be returned unless return is required by security considerations, contractual obligations, or notice on a specific document.

COMPOSITE WING CONCEPTUAL DESIGN

W. D. Nelson et al

Distribution limited to U.S. Government agencies, test
and evaluation, statement applied March 1973.
Requests for this document must be referred to
AFML (IC), Wright-Patterson Air Force Base,
Ohio 45433.

FOREWORD

This report was prepared by Douglas Aircraft Company of McDonnell Douglas Corporation, Long Beach, California, under Contract No. F33615-71-C-1340, for the Advanced Development Division, Air Force Materials Laboratory, Air Force Systems Command, Wright-Patterson Air Force Base, Ohio. Mr. H. A. Wood and Mr. D. A. Roselius (AFML/LC) were the Air Force Project Engineers and Mr. W. D. Nelson was the Douglas Aircraft Company Program Technical Manager.

Work performance spanned the period 1 February 1971 to 17 January 1973.

Principal contributors to the Douglas activities described in this report were:

| | |
|--|--|
| Structural Design | C. A. van Pappelendam A. V. Hawley M. Ashizawa |
| Structural Mechanics | Dr. D. M. Purdy Dr. L. J. Hart-Smith C. G. Dietz |
| Materials and Process Engineering | H. M. Toellner R. J. Palmer |
| Manufacturing Engineering Research and Development | R. L. Zwart W. L. Romey |
| Instrumentation and Testing | D. E. McCay E. G. Willoughby |

Mr. van Pappelendam, now retired from the Douglas Aircraft Company, is given special recognition for his initial contribution of the truss web wing and fillet bond design concepts and for his creative design guidance within this effort.

This report was submitted by the authors on 16 February 1973.

This technical report has been reviewed and is approved.

Robert C. Tomashot
ROBERT C. TOMASHOT
Technical Area Manager
Advanced Development Division
Air Force Materials Laboratory

ABSTRACT

Design, analysis, fabrication and test work is described which was performed to identify and develop the potentials of the advanced composite truss web wing box concept. The aircraft on which the effort was based is the Advanced Medium STOL Transport (AMST). The truss web concept is unique in that it utilizes no ribs or bulkheads to redistribute chordwise loads or to support the covers. A weight saving of 36.6 percent with respect to the metal wing box was achieved for the baseline truss web utilizing a boron-epoxy tapered sandwich upper cover, a graphite-epoxy tapered sandwich lower cover and cutout-lightened substructure. Optimization studies showed an available range of weight savings from 28 to 56 percent, depending on the specific materials used, number of cells in the configuration, method of handling stress relief at bolted joints, bonded joint details, and tailoring of panel stiffening and substructure lightening detail. A multi-rib/multi-web design optimization study is reported. Finite anisotropic element analyses for the wing and final test component are described. Laminate tests utilizing mixed graphite materials are described. Element and subcomponent tests were conducted to verify features of the design, including the fillet bond concept for joining webs to covers. The testing effort culminated in a sweepbreak wing-fuselage intersection component which included a stress-relieved bolted upper cover and a fillet-bonded lower cover. It achieved 94 percent of ultimate combined bending and torsion load. The major design features under test were validated since failure occurred in a conventional locally overstressed area.

CONTENTS

| Section | | Page |
|---------|--|------|
| I | INTRODUCTION, SUMMARY, AND CONCLUSIONS | 1 |
| II | VEHICLE SELECTION | 5 |
| III | DESIGN CRITERIA AND LOADS | 9 |
| | 3.1 Basic Criteria | 9 |
| | 3.2 Baseline Description and Weights | 9 |
| | 3.3 Design Load Conditions | 12 |
| | 3.4 Allowable Stresses | 13 |
| IV | DESIGN CONCEPTS AND SENSITIVITY STUDIES | 21 |
| | 4.1 Initial Conceptual Wing Design | 21 |
| | 4.1.1 Application of Truss Web Concept to AMST Wing | 24 |
| | 4.1.2 Preliminary Materials and Ply Patterns | 30 |
| | 4.1.3 Configuration Optimization | 33 |
| | 4.1.4 Joints Investigation | 35 |
| | 4.1.5 Materials Optimization Analysis | 48 |
| | 4.1.6 Cover Optimization | 51 |
| | 4.1.7 Substructure Lightening | 63 |
| | 4.1.8 Initial Payoff Study | 77 |
| | 4.1.9 Selected Baseline Truss Web | 81 |
| | 4.2 Alternate Designs | 83 |
| | 4.2.1 Arch Web Concept | 83 |
| | 4.2.2 Torsional Stiffness Study | 86 |
| | 4.2.3 Multi-Web/Multi-Rib Optimization | 88 |
| | 4.2.4 Preliminary Configuration Weight Trade | 97 |
| V | STRUCTURAL ANALYSIS | 101 |
| | 5.1 Finite Element Analysis | 101 |
| | 5.1.1 AMST Conceptual Wing | 101 |
| | 5.1.2 Final Demonstration Component | 112 |
| | 5.2 Panel Stiffening Study | 121 |
| | 5.2.1 Introduction | 121 |
| | 5.2.2 Design Requirements | 121 |
| | 5.2.3 Stiffened Panel Design | 126 |
| | 5.2.4 Baseline Panel Design | 131 |
| | 5.2.5 Conclusions | 132 |
| VI | MATERIAL SELECTION | 133 |
| | 6.1 Data Summary | 133 |
| | 6.2 Laminate Allowables Tests | 134 |
| | 6.2.1 Boron Film/Graphite Fiber Testing | 138 |
| | 6.3 Adhesive Properties Tests | 142 |
| | 6.3.1 EA9306 Properties Tests | 142 |
| | 6.3.2 Mixed Graphite/Adhesive Laminate Tests | 147 |

CONTENTS (Continued)

| Section | | Page |
|---------|--|------|
| VII | DESIGN DEVELOPMENT AND VERIFICATION | 149 |
| | 7.1 Fabrication Feasibility | 149 |
| | 7.1.1 Truss Web to Skin Joint | 149 |
| | 7.1.2 Mixed Graphite Laminating | 154 |
| | 7.1.3 Co-curing Wing Skins to Honeycomb | 154 |
| | 7.2 Fabrication of Design Verification Specimens | 158 |
| | 7.2.1 Joint Tension Design Verification Specimens - Drawing Z3578686 | 159 |
| | 7.2.2 Truss Action Design Verification Specimens - Drawing Z5578684 | 161 |
| | 7.2.3 Bending, Torsion, and Joint Tension Box Beam Verification Specimens - Drawing Z5578687 | 164 |
| | 7.2.4 Final Demonstration Component - Drawing Z5569987 | 169 |
| | 7.3 Nondestructive Testing - Final Demonstration Component | 173 |
| | 7.4 Tooling and Drilling - Final Demonstration Component | 173 |
| | 7.5 Joint Design Allowables Tests | 182 |
| | 7.5.1 Bolt-Bearing Test Program | 182 |
| | 7.5.2 Boron Epoxy Bolt-Bearing Test Results | 183 |
| | 7.5.3 Open Hole Stress Concentration Factors | 192 |
| | 7.5.4 Compression K_T in Boron Laminates | 193 |
| | 7.5.5 Stress Concentration Relief Tests | 193 |
| | 7.5.6 Bonded Tension Joint | 196 |
| | 7.5.7 Bonded Fillet Joint | 196 |
| | 7.5.8 Small Bolted Tension Joint | 204 |
| | 7.6 Design Verification Tests | 204 |
| | 7.6.1 Wing/Fuselage Joint Tension Tests | 205 |
| | 7.6.2 Truss Action Tests | 205 |
| | 7.6.3 Substructure Tests | 211 |
| | 7.6.4 Box Beam Bending and Torsion Test | 211 |
| | 7.6.5 Fillet Bonded Box Beam Pressure Test | 223 |
| | 7.6.6 Final Demonstration Component | 224 |
| VIII | PAYOFF AND RECOMMENDATIONS | 237 |
| | 8.1 Weight Payoff | 237 |
| | 8.2 Recommendations | 242 |
| | APPENDIX A | 245 |
| | APPENDIX B | 277 |
| IX | REFERENCES | 281 |

ILLUSTRATIONS

| Figure | | Page |
|--------|---|------|
| 1 | AMST Conventional All-Metal Aircraft Model D915P | 6 |
| 2 | Fixed Wing Attack Aircraft - Model 252-2BF-3 | 7 |
| 3 | MST Metal Wing (Counterpart for Composite Wing) | 10 |
| 4 | Metal Wing Weight Distribution - One Side Only | 12 |
| 5 | Assumed Spanwise Airload Distribution Maximum Positive Bending Condition | 13 |
| 6 | Assumed Chordwise Airload Distribution Maximum Bending Condition | 14 |
| 7 | Maximum Torque Condition Airload Resultants | 15 |
| 8 | MST Chordwise Pressure Distribution, Maximum Torque Condition | 15 |
| 9 | 2G Taxi Condition Inertia Resultants | 16 |
| 10 | Lamina Failure Criteria | 18 |
| 11 | Truss Web Concept | 22 |
| 12 | Arch Web Concept - Chordwise Section | 22 |
| 13 | Web Fabrication Initial Concept | 23 |
| 14 | Web Crest Locations (MST Composite Truss-Web Wing) | 25 |
| 15 | MST Composite Wing Baseline Study Configuration | 27 |
| 16 | Sections at Movable Leading Edge and Flap Support Station - Baseline Study Configuration | 29 |
| 17 | Section Through Slat and Aileron - Baseline Configuration. | 29 |
| 18 | Assumed Internal Loads Due to Maximum Bending Condition | 31 |
| 19 | Assumed Internal Loads Due to Maximum Torque Condition. | 32 |
| 20 | Truss Web Configurations | 34 |
| 21 | Variation of Wing Weight with Configuration - Root Section | 36 |
| 22 | Variation of Wing Weight with Configuration - Station 276 | 37 |
| 23 | Joint Pressure Load and Web Requirements | 38 |
| 24 | Bolted Joint - Maximum Bolt Spacing Approach. | 39 |
| 25 | Bolted Cover to Web Joint - Minimum Bolt Spacing Approach | 40 |
| 26 | Bolted Joint Design Improvement | 41 |
| 27 | Bolt Spacing and Bolted Joint Weight | 42 |
| 28 | Bolted Joint Included - Web-Angle Geometry | 43 |
| 29 | Bonded-Joint Configurations | 45 |
| 30 | Design Verification Specimen A | 47 |
| 31 | Laminate Shear Stiffness | 52 |
| 32 | Upper Skin Weights (Bonded Construction) | 53 |
| 33 | Lower Skin Weights (Bonded Construction) | 53 |
| 34 | Metal Versus Composite Wing Stiffness Requirements | 54 |
| 35 | Pattern Provisions for Stress Concentration Relief | 56 |
| 36 | Collected Zero Degree Fiber Caps | 57 |
| 37 | Parallel Web Crest Configuration | 57 |
| 38 | Cover Panel Pattern and Material Concept at Web Crest Lines. | 58 |
| 39 | Panel Designs for Pressure Condition | 60 |
| 40 | A Thin Rectangular Sandwich Beam of Variable Thickness Under Action of Uniform Pressure | 61 |

ILLUSTRATIONS (Cont)

| Figure | | Page |
|--------|--|------|
| 41 | Web Hole Geometries - Constant A/B Ratio | 65 |
| 42 | Corrugated Shear Web Concept | 67 |
| 43 | Cutout Web Concept | 68 |
| 44 | Integrated Web Layup with Machined Corners | 69 |
| 45 | Improved Sandwich Strut Concept | 70 |
| 46 | Struts Attached by Skin Bolts | 71 |
| 47 | Truss - Posts Attached by Bonding | 72 |
| 48 | Corrugated Sheet Substructure Concept | 73 |
| 49 | Corrugated Hat Section Strut - STA 0 to 82 | 74 |
| 50 | Composite Wing Configurations | 77 |
| 51 | Multi-Web Baseline Composite Configuration | 78 |
| 52 | Configuration Relative Costs | 81 |
| 53 | Cost/Weight Comparison | 82 |
| 54 | Baseline Truss Web | 82 |
| 55 | 2-Dimensional Analysis - Configurations | 85 |
| 56 | 2-Dimensional Analysis - Deflections | 85 |
| 57 | 2-Dimensional Analysis - Stress Levels in Inner Cell | 85 |
| 58 | Basic Cross-Section | 86 |
| 59 | Torsional Stiffness Comparison of Several Candidate Designs | 87 |
| 60 | Typical Equivalent Sections for the Same J | 86 |
| 61 | Box Geometry | 89 |
| 62 | Fillet Joint Concepts for Wing Box Design | 90 |
| 63 | Multiweb Configuration Weights, Sta 107 | 92 |
| 64 | Multirib Configuration Weights, Sta 107 | 93 |
| 65 | Surface of Configuration Weights at Station 107 | 94 |
| 66 | Integral Stiffener Concept | 96 |
| 67 | Truss Rib Concept | 97 |
| 68 | Composite Wing Covers | 102 |
| 69 | Composite Wing Web | 102 |
| 70 | Composite Wing Finite Element Model | 103 |
| 71 | Triangular Membrane Elements | 103 |
| 72 | Ultimate Shear Loads Aft Edge of Lower Cover | 108 |
| 73 | Ultimate Spanwise Loads Aft Edge of Lower Cover | 109 |
| 74 | Ultimate Shear Loads Aft Web | 109 |
| 75 | Distributed Internal Chordwise Loads Web, Inboard of Sweep - Break Maximum Torque Condition (Limit) | 110 |
| 76 | Distributed Internal Loads Along Material Axis Aft Edge of Upper Cover Maximum Torque Condition (Limit) | 111 |
| 77 | Distributed Internal Loads Along Material Axis Aft Edge of Lower Cover 3G Balanced Maneuver Condition (Limit) | 111 |
| 78 | Distributed Internal Shear Loads Aft Shear Web Maximum Torque Condition (Limit) | 112 |
| 79 | Ultimate Upper Panel Loads at Aft Edge | 113 |
| 80 | Ultimate Upper Panel Shear at Aft Edge | 113 |
| 81 | Schematic - Z5569987-1 Design Verification Specimen | 114 |
| 82 | Bent Box Finite Element Idealization | 117 |
| 83 | Spanwise Stresses (KSI) | 122 |

ILLUSTRATIONS (Cont)

| Figure | | Page |
|--------|--|------|
| 84 | Chordwise Stresses (KSI) | 123 |
| 85 | Shear Stresses (KSI) | 124 |
| 86 | Chordwise Stresses (KSI) | 125 |
| 87 | Shear Stresses (KSI) | 125 |
| 88 | Stiffened Panel Configurations | 128 |
| 89 | Graphite-Epoxy Laminate Honeycomb Core Sandwich Panel Buckling Strength | 130 |
| 90 | Typical Mixed Graphite Compression Beam Failures | 139 |
| 91 | Mixed Boron Film and Graphite Beam After Failure | 140 |
| 92 | Thick Adherend Z4578680-509 Specimens | 144 |
| 93 | Cast Adhesive Tensile Specimen | 146 |
| 94 | EA9306 Tensile Stress/Strain - Room Temperature | 146 |
| 95 | EA9306 Tensile Castings - 200°F Stress/Strain | 147 |
| 96 | Sketch - Fabrication Feasibility Truss Web Joint | 150 |
| 97 | Layup Tool for Feasibility Study of Truss Web Design | 151 |
| 98 | First Truss Web Fabrication Feasibility Specimen | 151 |
| 99 | Conceptual Wing Joint Fabrication Test No. 2 | 152 |
| 100 | Bonded Truss Specimen, Load Application Joint, Graphite Cover | 152 |
| 101 | Bonded Truss Specimen, Upper Graphite Cover, Intermediate Joint | 153 |
| 102 | Exploded View of Cocure Panel Layup. | 156 |
| 103 | Interface Delamination - Sandwich - Precurred Ply Without Adhesive | 156 |
| 104 | Z3578686-1 Bonded Tension Specimen - Closeup of Bond Before Test. | 160 |
| 105 | Z3568686-501 Bolted Joint Tension Specimen | 160 |
| 106 | Z3578686-507 Bonded Fillet Joint Tension Specimen | 162 |
| 107 | Bolted Truss Action Specimen Overall View | 163 |
| 108 | Bolted Truss Action Specimen End Joint Closeup. | 163 |
| 109 | Bolted Truss Action Specimen Internal Joint Closeup. | 164 |
| 110 | Bonded Truss Action Specimen in Test Fixture | 165 |
| 111 | Bonded Truss Specimen, Upper Joint at Steel Doubler | 166 |
| 112 | Bonded Truss Specimen, Graphite to Boron End Joint | 166 |
| 113 | Bonded Truss Specimen, Graphite to Boron Lower Intermediate Joint | 167 |
| 114 | Z5578687-1 Box Beam Specimen, Before Attachment of Cover Panel | 167 |
| 115 | Z5578687-503 Design Verification Specimen | 168 |
| 116 | Z5578687-503 Specimen Before Test. | 168 |
| 117 | X-Ray Inspection of 5578687-505 Fillet Bond | 170 |
| 118 | Fit Check of Steel Bar Reinforcement - Z5578687-505 | 171 |
| 119 | Bolted Joint Reinforcement Specimen Z5578687-505 | 172 |
| 120 | Nondestructive Testing Method for Final Demonstration Component | 174 |
| 121 | Ultrasonic C-Scan Recording of Upper and Lower Panels. | 175 |
| 122 | Positive Radiographic Reproduction of View-8 Showing Discontinuities | 176 |

ILLUSTRATIONS (Cont)

| Figure | | Page |
|--------|---|------|
| 123 | Layup Mold for Z5569987-103 Lower Skin Assy | 177 |
| 124 | Truss Web Master Plaster Form - Sweep Break Specimen . . | 178 |
| 125 | Detail of Large Bolt Restraining Strap Layup Area - Master Plaster | 179 |
| 126 | Finished Laminating Tool - Sweep Break Specimen Truss Web | 180 |
| 127 | Shearout Stress as Function of Edge Distance. | 186 |
| 128 | Bearing Stress Contours for Various Laminate Patterns, AVCO 5505 Boron Epoxy | 187 |
| 129 | Shearout Stress Contours for Various Laminate Patterns, AVCO 5505 Boron Epoxy | 187 |
| 130 | Bearing Stress Contours for Various Laminate Patterns, Mixed Graphite Epoxy | 189 |
| 131 | Shearout Stress Contours for Various Laminate Patterns, Mixed Graphite Epoxy | 189 |
| 132 | Z3578686-1 Bonded Tension Specimen - Internal Failure Before Repair | 197 |
| 133 | Z3578686-509 Loop Tension Test, Room Temperature | 198 |
| 134 | Z3578686-511 Loop Tension Specimens | 199 |
| 135 | Z4569981-501, -503 Fillet Joint Rail Shear Specimens | 201 |
| 136 | Z4569981-505 Fillet Joint Rail Shear Specimens | 202 |
| 137 | Double-Lap Shear Tests on Z3569983 Specimen, EA9306 Adhesive | 202 |
| 138 | Peel Stress Failure of Thick Composite Bonded Joints | 203 |
| 139 | Z3569983-501 Double Lap Shear Fatigue Specimens | 204 |
| 140 | Z3578686-505 Laminate Combined Bearing and Tension Test | 206 |
| 141 | Large Joint Tension Test Results | 207 |
| 142 | Z5578687-503 Specimen in Test Machine | 207 |
| 143 | Z5578687-503 Specimen, Showing Failures in End | 208 |
| 144 | Truss Action Specimen Test Results | 208 |
| 145 | Load-Tensile Strain Relationship for Z5578684-1 Truss Specimen | 209 |
| 146 | Load-Compression Strain Relationships for Z5578684-1 . . . | 210 |
| 147 | Comparison of Truss Action Specimen Deflections | 210 |
| 148 | Photostress Pattern in 5578687-503 Near Failure | 211 |
| 149 | Cutout Truss Web Element Tension Test Setup | 212 |
| 150 | Cutout Truss Web Element Compression Test Setup | 213 |
| 151 | Box Beam Test Setup | 216 |
| 152 | Box Beam Load Introduction Details | 217 |
| 153 | Load Control and Data Acquisition System | 218 |
| 154 | Primary Failure, Skin Assembly - Reaction End | 219 |
| 155 | Secondary Failure, Skin Assembly - Loaded End | 220 |
| 156 | Secondary Failure, Web Assembly - Loaded End | 221 |
| 157 | Comparison Between Theory and Test for Test to Failure of Z5578687-1 Triangular Box Beam | 223 |
| 158 | Fillet Bonded Box Pressure Test | 225 |
| 159 | Closeup of Interlaminar Tension Failure - Z5578687 Web . . . | 225 |

ILLUSTRATIONS (Cont)

| Figure | | Page |
|--------|--|------|
| 160 | Conceptual Wing Bent Box Specimen | 226 |
| 161 | Load Geometry Sketch | 226 |
| 162 | Test Setup, Final Component | 228 |
| 163 | Actuator Setup | 229 |
| 164 | Strain Gage Installation | 229 |
| 165 | Specimen Failure | 232 |
| 166 | Specimen Failure - Sweep Break | 232 |
| 167 | Specimen Failure - Inboard | 233 |
| 168 | Ideal Strut with Initial Curvature | 234 |
| 169 | Truss Web Weight Distribution | 238 |
| 170 | Example Truss Web Wing Weight Distribution | 239 |

TABLES

| Table | | Page |
|-------|--|------|
| 1 | Aircraft Design Weights | 10 |
| 2 | Baseline Wing Weights | 11 |
| 3 | Wing Geometry | 12 |
| 4 | Monolayer Design Allowables | 16 |
| 5 | Preliminary Material Selection Study Results | 33 |
| 6 | Upper Cover Fiber Patterns (Strength and Stiffness) | 49 |
| 7 | Upper Cover Fiber Patterns (Strength Only) | 49 |
| 8 | Lower Cover Fiber Patterns (Strength and Stiffness) | 50 |
| 9 | Lower Cover Fiber Patterns (Strength Only) | 50 |
| 10 | Web Structure Patterns | 51 |
| 11 | Variable Depth Beam Analysis, Initial Cases, Lower and Aft Panels | 62 |
| 12 | Variable Depth Beam Analysis, Final Cases, Lower Panel Number 4 | 62 |
| 13 | Constant Versus Variable Thickness Panel Weights | 63 |
| 14 | Substructure Weight Comparison Pounds/Wing Box - Constant Weight Closure Webs and Edge Joints Excluded. . | 76 |
| 15 | Substructure Concepts Tooling and Fabrication Relative Cost | 77 |
| 16 | Interim Weight Study, Wing 40-Inch Section Weight Matrix (Lb/Section) | 79 |
| 17 | Weight Values for Design Features | 80 |
| 18 | Data Summary of Equivalent Sections | 87 |
| 19 | Matrix of Wing Cover Problems | 89 |
| 20 | Bonded Joint Configuration Weights Station 107, Alternate Box Designs | 91 |
| 21 | Multi-Rib/Web Configuration Weights Station 107 Lb/Inch Span | 94 |
| 22 | Multiweb Optimum Weight Configuration ($N_2 = 1$) | 95 |
| 23 | Multirib Optimum Weight Configuration ($N_1 = 1$) | 95 |
| 24 | Alternate Box Study Panel Facings | 95 |
| 25 | Revised 40-inch Selection Weight Comparison | 98 |
| 26 | Truss Web Vs Multiweb Theoretical Graphite Cover Weight Penalty (Designed by 20 PSI Pressure) | 98 |
| 27 | Element Lamination Pattern | 119 |
| 28 | Minimum Margins of Safety | 126 |
| 29 | List of Strength Analysis Cases | 129 |
| 30 | Comparison of Unstiffened and Stiffened Panels | 132 |
| 31 | HighTensile Strength Graphite Selection | 134 |
| 32 | Boron/Aluminum Material Selection | 135 |
| 33 | Summary of Rail Shear Tests on $(+45/-45)_S$ Thornel 75S/2544 | 136 |
| 34 | Summary of Picture Frame Tests on Ultra-Thin $(+45/-45)_T$ Narmco 5206 Face Sheets | 136 |
| 35 | Flatwise Strength of Graphite Laminate | 136 |
| 36 | Comparison of Mixed Laminate Properties Thornel 75S/2544 and Narmco 5206 | 137 |

TABLES (Cont)

| Table | | Page |
|-------|---|------|
| 37 | Summary of Test Results from Mixed Material Specimens (0 ₂ /+45/0 ₂ /90) _S Ply Pattern | 137 |
| 38 | Summary of Longitudinal Compression Test Results (0 _A /+45 _B /0 _A /-45 _B /90 _A) _S | 138 |
| 39 | Mixed Materials Compressive Tests | 141 |
| 40 | Stress-Strain Behavior of Thick Adherend Bonded Joints Z4578680 (Bond Area = 0.5 Sq In., Adherends 0.5 In. Thick Aluminum) | 143 |
| 41 | EA9306 Adhesive Tension Tests | 145 |
| 42 | EA9306 Tensile Casting Test Data, 200°F | 147 |
| 43 | Mixed Graphite/Adhesive Laminate Tests | 148 |
| 44 | Adhesive Flatwise Tensile Screening Tests | 153 |
| 45 | Average Results of Honeycomb Beam Tests | 155 |
| 46 | Strength and Stiffness of Cocured Sandwich Face with Precured Interlayer | 157 |
| 47 | Cocured Narmco 5206 Comparisons | 157 |
| 48 | Cocured AVCO 5505 Sandwich Facing Comparisons | 158 |
| 49 | Design Verification Specimens | 159 |
| 50 | Bolted Joint Test Laminates | 182 |
| 51 | Double-Lap Bolted Joint Strength Summary (0.25-Inch Bolt Diameter AVCO 5505 Boron-Epoxy) | 184 |
| 52 | Double-Lap Bolted Joint Strength Summary (0.25-Inch Bolt Diameter Mixed Graphite Epoxy) | 190 |
| 53 | Open Hole Stress Concentration Factors Narmco 5206 Graphite-Epoxy (0/+45/0) Laminate Pattern | 192 |
| 54 | Compression Tests on Unloaded Filled Holes in Boron-Epoxy | 194 |
| 55 | Double-Lap Bolted-Joint Strength Summary (0.25-Inch Bolt, 0 Deg Glass Softening Strip in 1004 Resin, Narmco 5206 Graphite-Epoxy or AVCO 5505 Boron-Epoxy) | 195 |
| 56 | Summary Z3578686 Joint Tension Tests | 199 |
| 57 | Bonded Fillet Joint Rail Shear Tests | 200 |
| 58 | Double-Lap Graphite-Epoxy EA9306 Fatigue Tests (R = 0.05) Specimen Z3569983 | 203 |
| 59 | Summary of Cutout Truss Web Element Tests - Z3569984 | 214 |
| 60 | Box Beam Test Summary | 214 |
| 61 | Ultimate Tes. | 230 |
| 62 | Test Correlation | 233 |
| 63 | Test Correlation | 234 |
| 64 | Initial Truss Web Wing Weight Savings | 240 |
| 65 | Final Wing Weight Breakdown Comparison | 241 |
| B-1 | Prepreg Quality Control Receiving Inspection Report | 278 |
| B-2 | Boron Control Receiving Inspection Report | 279 |
| B-3 | Receiving Quality Control - FM96 Adhesive | 279 |

SECTION I

INTRODUCTION, SUMMARY, AND CONCLUSIONS

INTRODUCTION

The objective of the Composite Wing Conceptual Design was to develop an advanced wing structural design concept which makes maximum and most effective use of advanced composite materials. This involved the consideration of the necessary manufacturing procedures as an integral part of the design process. Other general aspects of the program philosophy included the maximum use of structural bonding to achieve the lightest weight structure and the use of composite materials which are sufficiently characterized so as not to require significant program effort obtaining design allowables.

Benefits issuing from the program include composite design technology advancement and improved weight savings over more conventional wing box designs. It should be noted at the beginning that maximum weight savings along with effective and efficient manufacturing were design goals. The initial design selected was the truss web concept which offered great weight saving potential along with a promising manufacturing concept. Improved cost-effectiveness of composite primary structure was an additionally desired benefit which may have been achieved; however, absolute costs were not derived, actual program costing being limited to a few relative cost comparisons among composite designs.

The basic program was organized in five tasks:

- TASK I — Design Criteria and Analysis. This task included design evaluation and payoff determinations as well as establishment of the design criteria, design philosophy, and analytic techniques used within the program.
- TASK II — Materials Selection. This task included materials data summary, minimal laminate allowables testing, and adhesives and joints allowables tests.
- TASK III — Design Concepts. Subtasks under this task-head consisted of: Initial Conceptual Wing Design, Additional and Continuing Design Studies, Design and Analysis of the Wing-to-Fuselage Attachment, and Final Conceptual Wing Design (the latter was deleted from the program in August 1972).
- TASK IV — Fabrication, Quality Control, and Nondestructive Testing. The intent of subtasks under this head was to produce fabrication feasibility specimens of new design concepts, produce new materials and NDT specifications as required as well as a manufacturing outline. After initial fabrication feasibility work, this task was deleted in June 1972.

- TASK V — Structural Demonstration. This task was divided into two major subtasks, Design Verification Tests and the Final Static Test Component. The final static test was deleted in June 1972 when it was determined that completion and test of the final design verification component would adequately establish "proof of concept" for the conceptual wing design.

A TASK VI, AMST Structural Integration Study, was added to the program in May 1972 and has been reported under separate cover (Reference 1). The latter effort consisted of conceptual design studies of a composite Advanced Medium STOL Transport (AMST) fuselage, conceptual wing and fuselage integration, and determination of the impact of composite structure weight savings for total aircraft design and performance.

SUMMARY

Considering only practical materials and strength and stiffness requirements, the baseline truss web wing lower cover optimized using high-strength graphite epoxy for a 31.2 percent weight savings with respect to the metal lower cover. The upper cover optimized using boron-epoxy for a 29.2 percent savings with respect to the metal upper cover. These savings are based on wing bending material only. The truss web substructure optimized as a five-cell construction of high-strength graphite and incorporated unique cutouts in the form of struts. There was a 36.8 percent weight savings in substructure and 52.6 percent in penalties (cover cutouts, concentrated load introduction, etc.). This savings is related to the efficiency of the substructure concept and the method of joining. The total baseline wing box weight savings was 36.6 percent.

Other box weight savings ranging from 28-56 percent were determined to be a function of detail optimizations within the overall design concept, the best savings coming from stress concentration relief, methods of joining covers (bolting or bonding), more exotic materials such as mixed materials and boron/aluminum, and method of adding cutouts to the truss web.

The indicated trends were that considerable weight could be saved at very little cost increase for bolted, stress-relieved wing covers versus plain bolted covers. Use of the fillet bonding concept saved even more weight than bolting with stress relief and cost less than the plain bolted covers. Other weight saving features, such as lightened substructure, are achieved only with an indicated cost increase with respect to the plain composite structure.

CONCLUSIONS

- Equivalent sections for the same J, when investigated for torsional rigidity, showed the Arch Web design to have the highest torsion constant (J/A) and the J/A for the Truss Web design was greater than the Multi-Rib.
- The truss web is lighter than the multi-rib composite concept when concentrated load penalties are included. The projected pressure penalty for truss web does not appear because of the ease of providing complete stress relief in the covers with respect to the comparative multi-rib design.

- The thin anisotropic honeycomb wing cover panel with aspect ratio 1.3 and stiffened by hat stiffeners has equivalent weight to the unstiffened anisotropic faced sandwich panel with aspect ratio 3; however, both panels are less efficient than the variable thickness sandwich panel.
- The fillet bonded joint concept, when developed to its fullest potential, can provide the lightest and most economical method of joining composite components and assemblies.
- Weight savings are not a function of a peculiar design configuration, as witness the 28- to 56-percent range of savings available in the truss web wing. Weight saved depended on many things other than basic design concept, such as specific materials used, method of handling stress concentration, joint details, and expensive tailoring and optimization of design details. This can be true of any design.
- The final demonstration component which contained the sweepbreak and wing/fuselage reaction points, but which contained no bulkhead, was successfully tested to 94 percent of ultimate load. The failure initiated in a conventional detail over-stressed area. It is likely that 100-percent load would have been matched or exceeded in the four advanced technology areas under test - the lower cover fillet bond, the stress relief features at bolts, the major bolted tension/compression wing/fuselage intersection joint design, and the integral truss-rib sweepbreak reinforcement.

SECTION II

VEHICLE SELECTION

The first milestone in the program was the selection of a vehicle for which the conceptual wing would be designed. The aircraft selected by mutual agreement between the Air Force Materials Laboratory and the contractor was the proposed Douglas/Air Force Advanced Medium STOL Transport (AMST). See Figure 1. Prior to the selection, there had been three prime candidate vehicles: the McDonnell Douglas Model 252 fixed-wing attack aircraft, the AMST, and the C9-A, a military version of the commercial DC-9. The initially proposed vehicles were advanced design aircraft. The C9-A also was considered because of its well established weights, loads and design information.

Available data on the three aircraft were surveyed and rated against the following selection criteria, keeping in mind the design applicability of the proposed conceptual designs:

- High performance vehicle
- Design information availability
- Payoff information availability
- Convincing composites demonstration
- Payoff benefits
- Operating temperature for wing
- Potential composites application

Choice of the C9-A would have necessitated assumption of extensive redesign of existing fuselage structure at the wing intersection to avoid compromising the proposed truss web conceptual design. Although extensive wing design information existed, the cost/weight payoff potential of a vehicle already in service and not particularly performance critical for its military missions did not appear as good as composite payoffs for an advanced design vehicle. Although composite weight savings potential was rated good, the potential was not present for vehicle resizing or for taking advantage of performance gains.

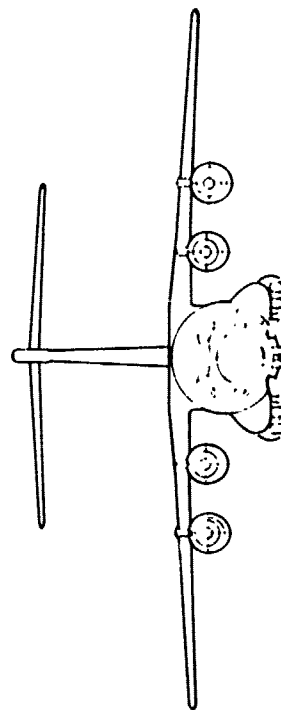
Although it was a very high performance vehicle, the Model 252-2BF-3, a typical SX configuration fixed-wing attack aircraft, proved to suffer in the ratings due to lack of firm design and payoff information, Figure 2. Also, the then relatively undefined high-speed performance indicated a wing temperature condition that would require a thermal/structural analysis and materials other than the well characterized epoxy matrix composites.

(4) 18,000-POUND THRUST GE-13 DERIVATIVE ENGINES

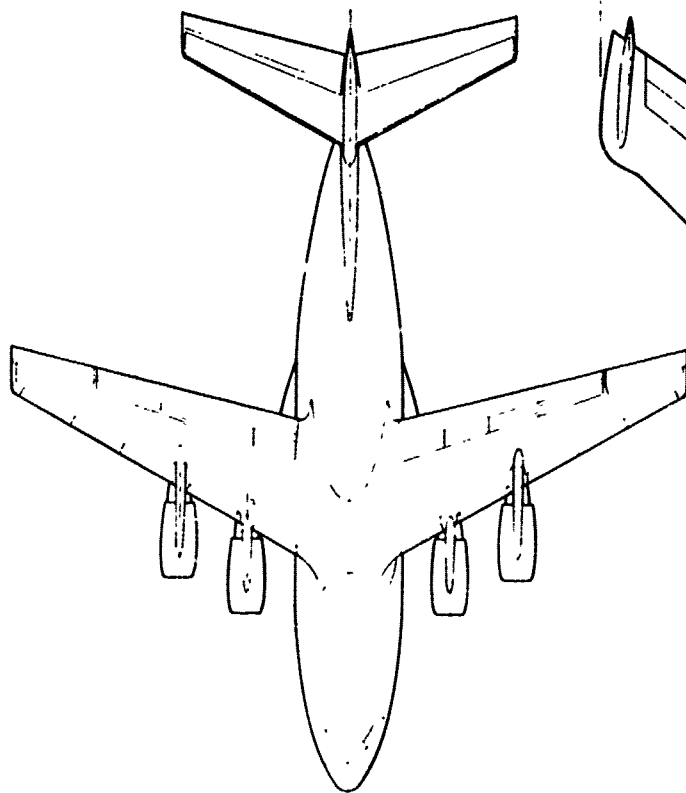
| | | |
|-------------------|---|--------------|
| WING AREA | = | 1,800 SQ. FT |
| WING ASPECT RATIO | = | 7 |
| PAYLOAD | = | 28,000 LB |
| STOL GW | = | 151,450 LB |

112 FT 3 IN. SPAN
(1347)

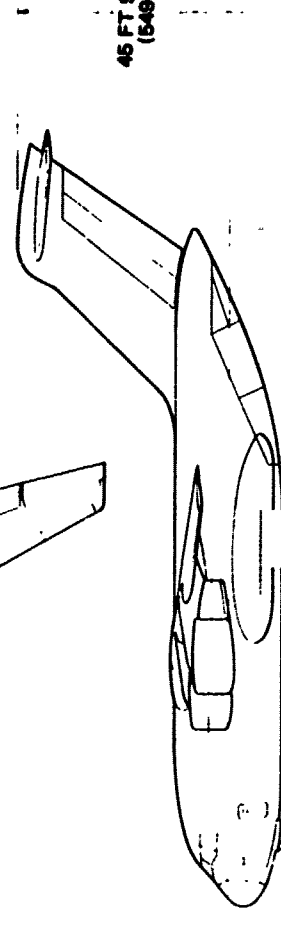
55 FT 6 IN. SPAN
(666)



124 FT 9 IN. OVERALL
(1497)



45 FT 9 IN.
(549)



108 FT 11 IN. FUSELAGE
(1307)

FIGURE 1. AMST CONVENTIONAL ALL-METAL AIRCRAFT - MODEL D915P

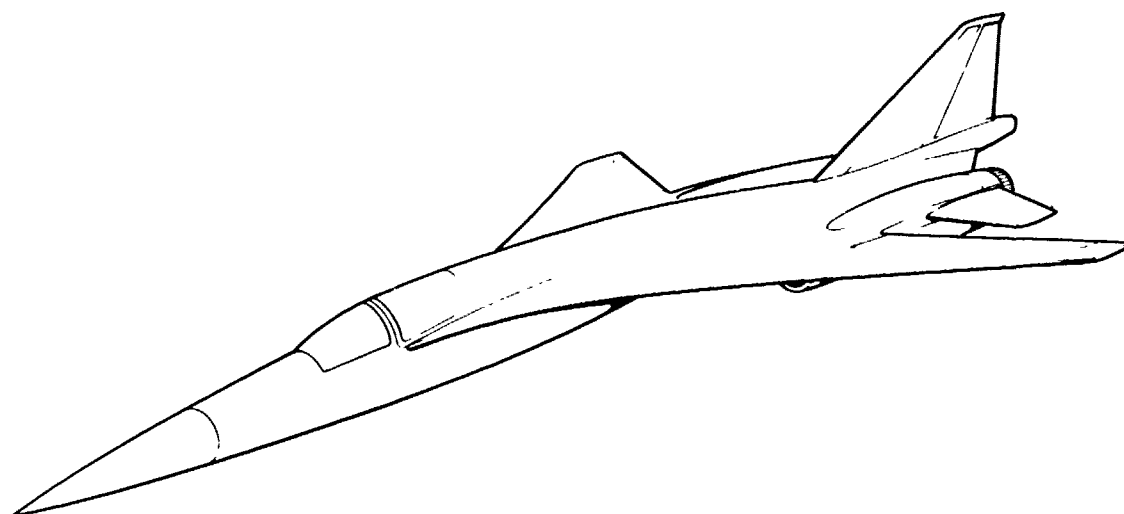


FIGURE 2. FIXED WING ATTACK AIRCRAFT - MODEL 252-2BF-3

The AMST had the best balance of potential payoffs and trade study information. Design information was adequate for initiating a program of this nature, modest operating temperatures existed, and it can be considered high performance in terms of thrust/weight ratio or takeoff performance. Therefore, the value of weight saved, and the potential for realizing that saving in a future system, made the AMST a logical choice. It also provides the Air Force with an opportunity to observe the use of composites in a transport-type aircraft.

Advanced Medium STOL Transport

The vehicle portrayed in the 3-view illustration (Figure 1) is the later Model D915P prototype and operational configuration proposed to the AMST System Program Office in March 1972. Its wing area is 1800 square feet and gross weight (STOL) is 151,450 pounds. At the beginning of the Conceptual Wing program, the Model D915B was the most well-defined configuration, with a wing area of 1660 square feet and a STOL TOGW of 132,800 pounds. The D915B was the configuration used for the basic wing program (Tasks I through V), and all design, analytic, and weights work was accomplished to the D915B size. The D915P was selected for the later Task VI study. This indicates the flexibility of configuration on advanced design aircraft and the necessity of fixing a study configuration at the beginning of a subsidiary program even though the work must be updated for later or follow-on application.

SECTION III

DESIGN CRITERIA AND LOADS

3.1 BASIC CRITERIA

The wing is designed for the maximum combination of loads to which it is subjected from the balance, pitch, roll, yaw, and gust flight conditions and for the landing and ground conditions. In a full-scale wing these conditions will be analyzed for variations in payload, engine thrust, cg location, fuel load, and fuselage pressurization. Survivability will be ensured by providing alternate load paths such that sufficient margins of strength exist for the damaged vehicle loads from the failure of any one principal structure element. For areas where fast fracture would result from damage, crack stoppers are to be provided such that damage will be contained.

In addition to the established criteria, composite structures will have additional requirements which are subject to change as the state of the art advances, but at the present time include the following:

- The stress analysis procedures consider the non-isotropic characteristics of the materials.
- Ultimate load effective stress concentrations of joints and cutouts based on the failing load tests are considered in the stress analysis.
- No panel instability is allowed up to ultimate load.
- Skin-to-substructure connections in primary structure, if not fully bonded, must have mechanical attachments capable of carrying at least limit load if used in a bonded-bolted assembly or at least ultimate load if used in a bolted assembly.
- Unrestrained laminates are constructed such that all in-plane failure modes are filament controlled.
- All purely bonded joints will have a strength capability at least 50 percent greater than surrounding laminates.
- All multiple fastener joints will have a class 5 or better fit (generally 0.000 to 0.003).

3.2 BASELINE DESCRIPTION AND WEIGHTS

The STOL airplane used in this study is a four-engine high-wing airplane employing a T-tail, tricycle landing gear and the externally blown flap lifting concept in the general arrangement shown (Figure 1). The basic aircraft weights used in this study are given in Table 1.

TABLE 1
AIRCRAFT DESIGN WEIGHTS

| CONDITION | WEIGHT (LB) |
|-----------|-------------|
| TAXI | 133,800 |
| TAKEOFF | 132,800 |
| LANDING | 131,800 |
| ZERO FUEL | 118,600 |
| PAYLOAD | 28,000 |

High wing lift for STOL operation is achieved by using the externally blown flap concept. Performance optimization is achieved by positioning the two segment flaps well below the wing and drooping the spoilers ahead of the flaps to promote good forward slot effectiveness. A maximum lift coefficient of 4.9 is achieved for normal takeoff thrust and flap settings. Values as high as 8.0 are achieved with full power at landing flap settings. Pertinent features of the wing weight are summarized in Table 2 and the geometry in Table 3 and Figure 3. The assumed metal wing weight distribution is given in Figure 4.

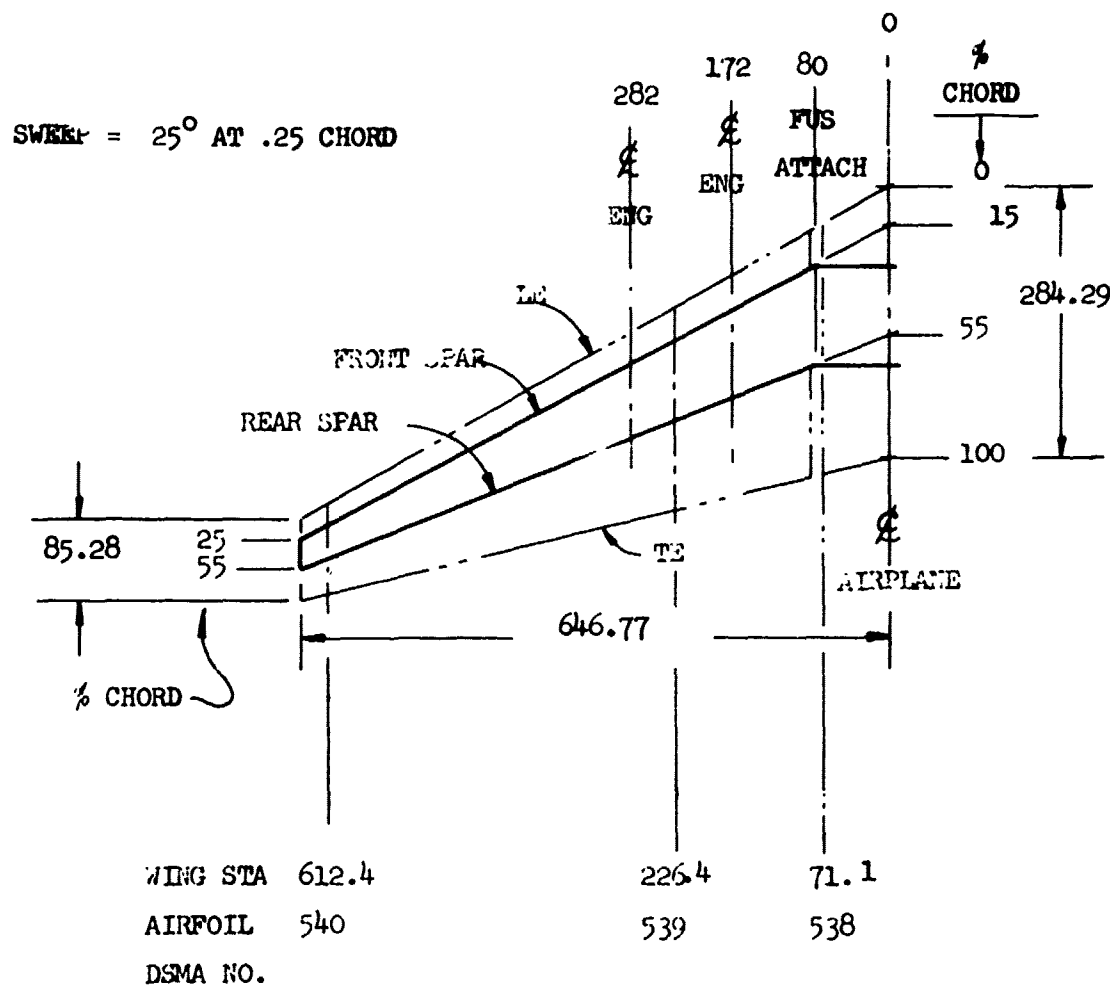


FIGURE 3. MST METAL WING (COUNTERPART FOR COMPOSITE WING)

TABLE 2
BASELINE WING WEIGHTS

| | | LB/AIRCRAFT |
|---------------------------------------|-----|--------------------|
| THEORETICAL BENDING MATERIAL | | 4,574 |
| SPLICES AND JOINTS | | 376 |
| DOORS, DOUBLERS AND ASSOCIATED ATTACH | | 496 |
| SPAR WEBS | | 916 |
| RIBS AND BULKHEADS (30 IN. SPACING) | | 1,639 |
| THEORETICAL RIBS | 560 | |
| C.W. PRESSURE BULKHEAD PENALTY | 135 | |
| WING TO FUSELAGE BULKHEAD PENALTY | 256 | |
| FLAP BULKHEAD PENALTY | 305 | |
| AILERON BULKHEAD PENALTY | 38 | |
| FUEL BULKHEAD PENALTY | 105 | |
| POWER PLANT ATTACH BULKHEAD PENALTY | 200 | |
| AERODYNAMIC BREAK BULKHEAD PENALTY | 40 | |
| WING TO FUSELAGE ATTACH | | 234 |
| SUBTOTAL - WING BOX WEIGHT | | 8,235 |
| LEADING EDGE | | 806 |
| TRAILING EDGE | | 746 |
| FAIRING AND FILLETS | | 469 |
| TIPS | | 45 |
| FLAPS | | 4,342 |
| AILERONS | | 551 |
| SPOILERS | | 318 |
| L.E. DROOP PENALTY | | 253 |
| SLATS | | 863 |
| TOTAL WING STRUCTURAL WEIGHT | | 16,628 |
| SYSTEMS | | 3,822 |
| | | 20,450 |

TABLE 3
WING GEOMETRY

| | |
|---------------------------------------|--------|
| AREA (SQ FT) | 1660 |
| ASPECT RATIO | 7.0 |
| TAPER RATIO | 0.3 |
| SWEEP (C/4) | 25° |
| SWEEP (ELASTIC AXIS) | 23.9° |
| t/c ROOT | 0.158 |
| t/c TIP | 0.1175 |
| PERCENT CHORD – FRONT SPAR (ROOT/TIP) | 15/25 |
| PERCENT CHORD – REAR SPAR | 55 |

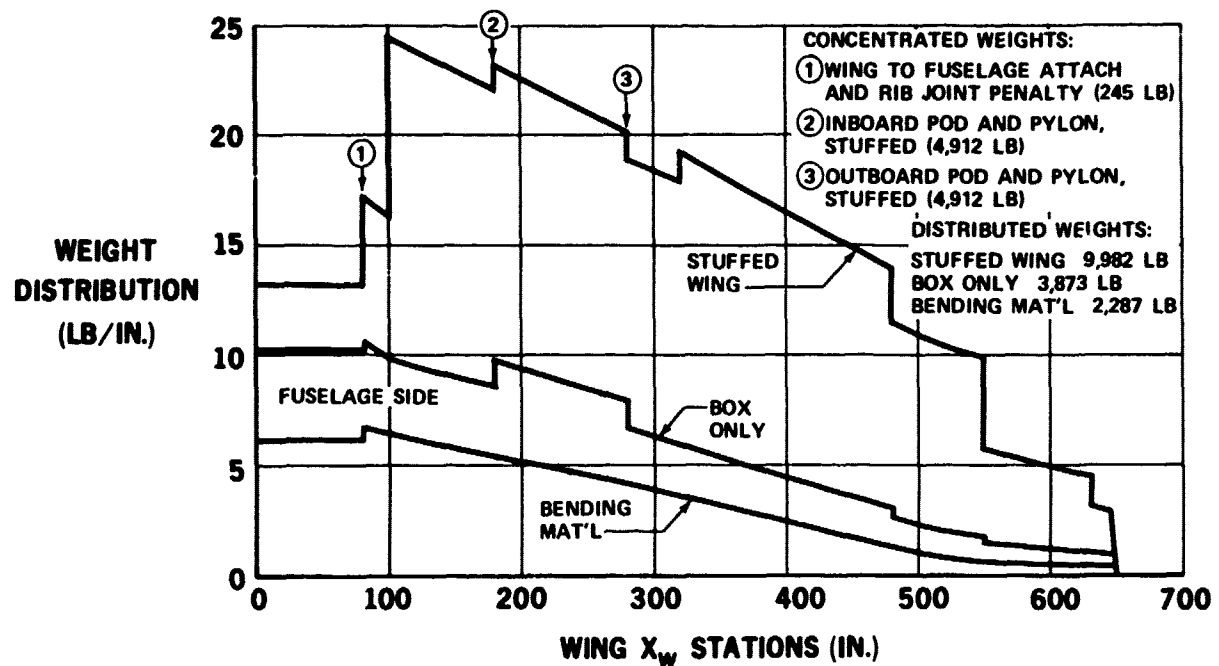


FIGURE 4. METAL WING WEIGHT DISTRIBUTION – ONE SIDE ONLY

3.3 DESIGN LOAD CONDITIONS

Three load conditions were selected from the flight spectrum for use in this study. The three conditions are identified as maximum positive bending, maximum torque, and maximum negative bending conditions. These conditions were selected as representing the extreme values of the load envelope. Loads in terms of pressure distributions over the wing surface were used for the two flight conditions. The maximum bending condition resulted from a 3-g symmetric maneuver. The assumed spanwise and chordwise airload distributions are presented in Figures 5 and 6, respectively. The maximum torque condition is a 2-g, fully extended flap condition. The assumed spanwise airload resultant distribution and chordwise airload distributions are

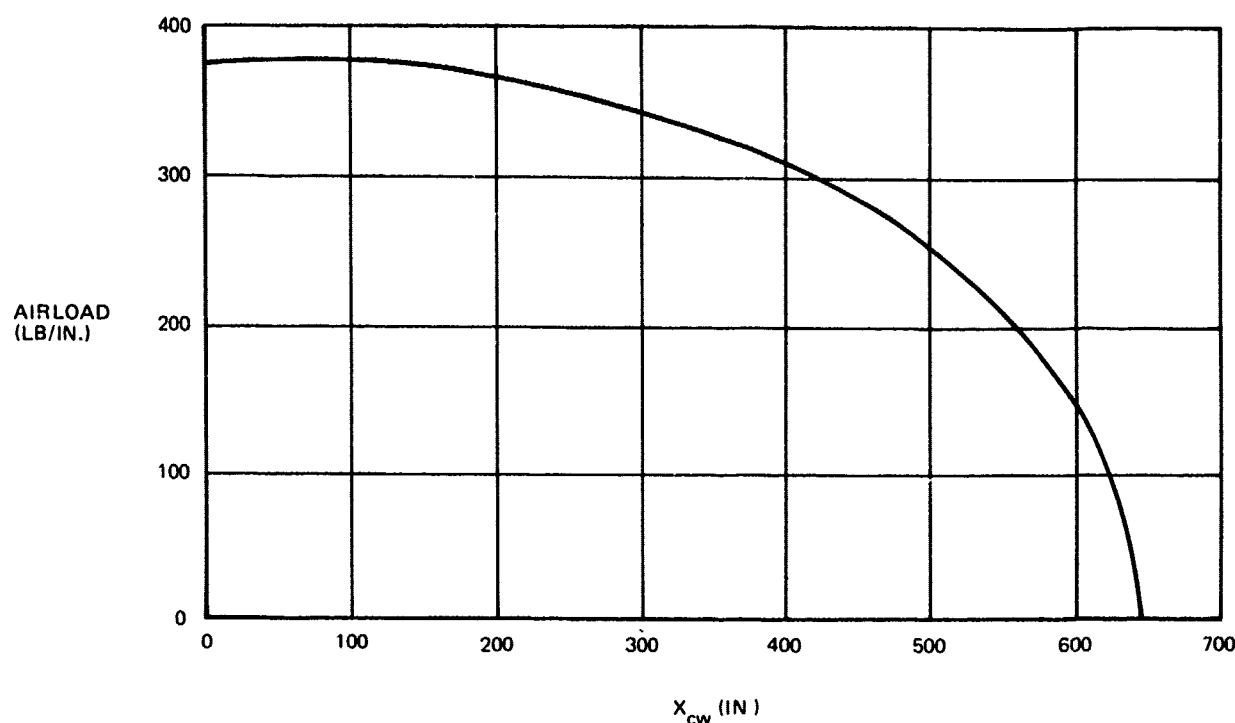


FIGURE 5. ASSUMED SPANWISE AIRLOAD DISTRIBUTION MAXIMUM POSITIVE BENDING CONDITION

presented in Figures 7 and 8, respectively. No airload was considered for the maximum negative bending condition which was associated with a 2-g taxi condition. The inertia resultants for this condition are presented in Figure 9. For the flight conditions the onboard fuel was taken as 8,300 pounds and for the ground condition 43,100 pounds of fuel was assumed.

3.4 ALLOWABLE STRESSES

Five composite materials were considered as candidates for application on the wing. These materials were Avco 5505 boron/epoxy, Narmco 5206, AS/286, and Thornel 75S graphite/epoxy and boron/aluminum. Basic mono-layer properties were developed without benefit of test in this program and are based upon the experience of the contractor and a review of available literature. The allowables (Table 4) selected should be considered as "B" basis allowables.

For patterned laminates the three allowable single-stress components are determined using a Hill type quadratic interaction formula for each of the individual lamina. This criterion, however, has been modified in several ways. The first modification is a limitation to ensure that neither of the basic normal-stress allowables are exceeded. Another modification has been incorporated to counter premature failure predictions of the laminate due to low transverse tensile allowables, characteristic of most composite lamina.

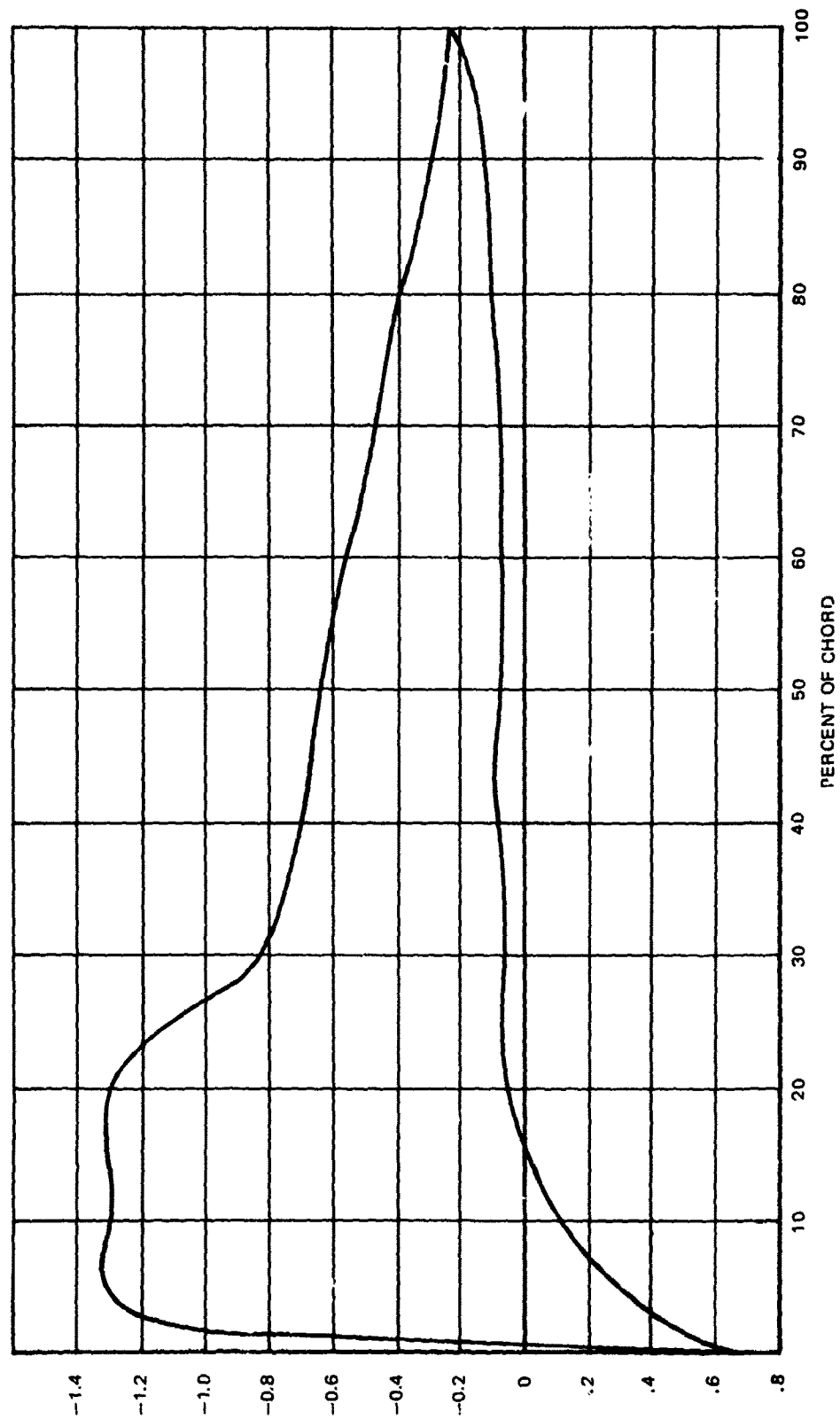


FIGURE 6. ASSUMED CHORDWISE AIRLOAD DISTRIBUTION MAXIMUM BENDING CONDITION

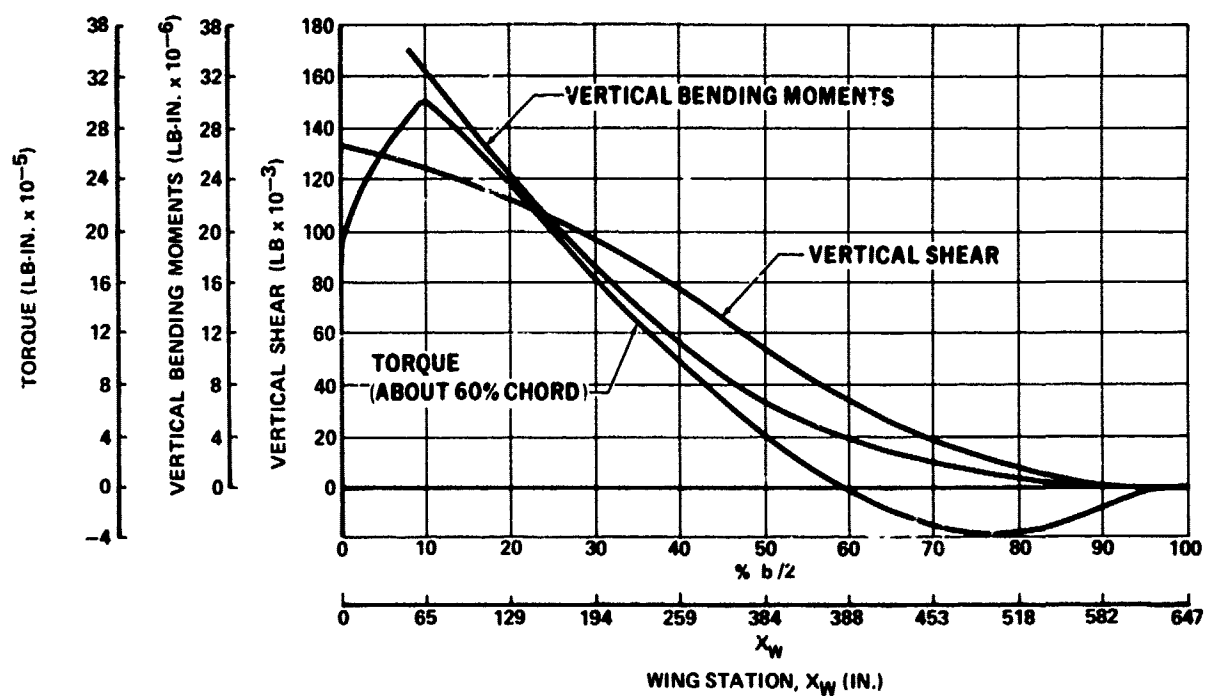


FIGURE 7. MAXIMUM TORQUE CONDITION AIRLOAD RESULTANTS

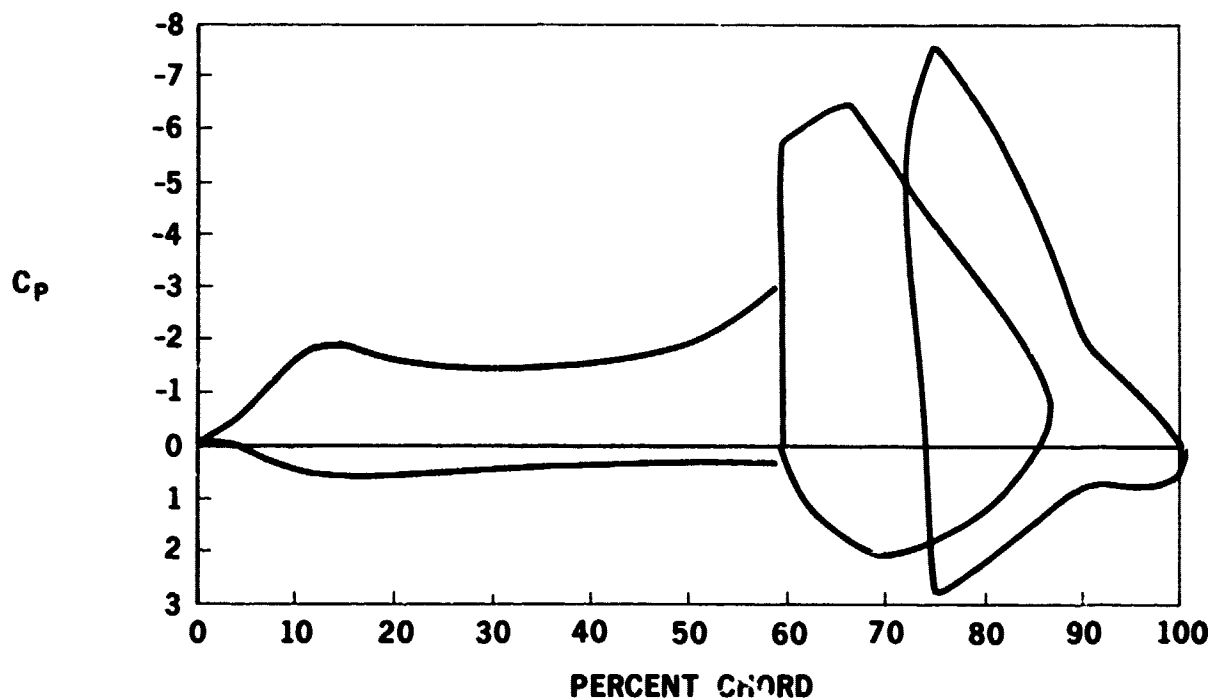


FIGURE 8. MST CHORDWISE PRESSURE DISTRIBUTION, MAXIMUM TORQUE CONDITION

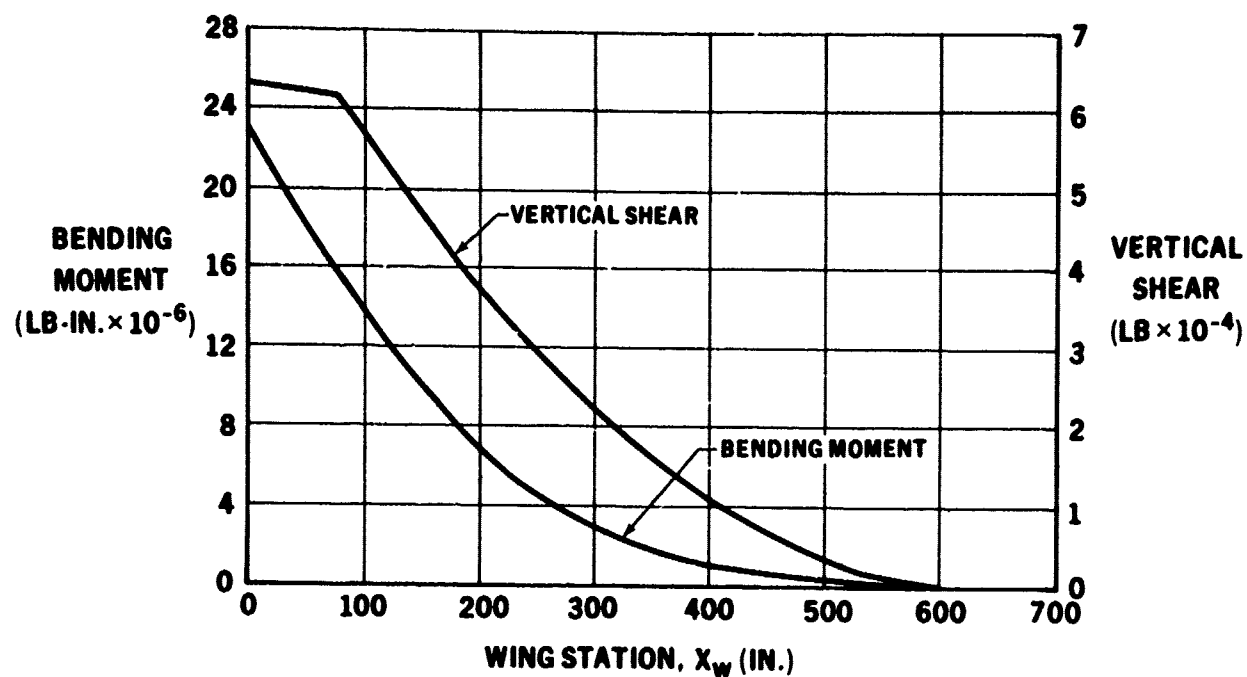


FIGURE 9. 2G TAXI CONDITION INERTIA RESULTANTS

TABLE 4
MONOLAYER DESIGN ALLOWABLES

| | UNITS | AVCO 5505 | AS/286 | NARMCO 5206 II | THORNEL 75S/1004 | BORON/ ALUMINUM |
|--------------------------|-------|--------------|--------|-------------------|---------------------|--------------------|
| STRENGTH | | | | | | |
| LONGITUDINAL TENSION | KSI | 192.0 | 174.0 | 165.0 | 174.0 | 130.0 |
| LONGITUDINAL COMPRESSION | KSI | 350.0 | 195.0 | 168.0 | 71.5 | 150.0 |
| TRANSVERSE TENSION | KSI | 10.4 | 8.5 | 8.0 | 3.5 | 10.0 |
| TRANSVERSE COMPRESSION | KSI | 40.0 | 30.0 | 29.5 | 20.0 | 24.0 |
| INPLANE SHEAR | KSI | 10.0 | 12.0 | 13.6 | 6.0 | 7.6 |
| STIFFNESS | | | | | | |
| LONGITUDINAL TENSION | MSI | 31.9 | 17.9 | 21.0 | 42.7 | 28.0 |
| LONGITUDINAL COMPRESSION | MSI | 31.9 | 17.9 | 21.0 | 42.7 | 28.0 |
| TRANSVERSE TENSION | MSI | 3.1 | 2.10 | 1.3 | 0.88 | 18.5 |
| TRANSVERSE COMPRESSION | MSI | 3.1 | 2.10 | 1.3 | 0.88 | 18.5 |
| INPLANE SHEAR | MSI | 1.0 | 0.55 | 0.7 | 0.7 | 10.0 |
| MAJOR POISSON'S RATIO | | 0.22 | 0.31 | 0.31 | 0.38 | 0.36 |

The ultimate strength of a laminate is not necessarily recorded at the first sign of a lamina transverse tensile fracture. This mode of failure is precluded until a specified fraction of the ultimate load is reached. These failure modes are permissible in a limiting sense for the ultimate laminate strength predictions. This specified fraction of ultimate load is generally taken as 2/3, corresponding to limit load for aircraft structures. Of course, the other lamina stresses can be expected to increase as transverse tensile fractures occur. A final modification of Hill's interaction formula accounts for these increases. The finally adopted failure criterion for the individual lamina may be defined mathematically by the use of two functions, F_1 and F_2 .

$$F_1(\sigma_L, \sigma_T, \sigma_{LT}) = \max \left\{ \left| \frac{\sigma_L}{F_L} \right|, \left| \frac{\sigma_T}{F_T} \right|, \text{SQRT} \left[\left(\frac{\sigma_L}{F_L} \right)^2 + \left(\frac{\sigma_T}{F_T} \right)^2 - \left(\frac{\sigma_L}{F_L} \right) \left(\frac{\sigma_T}{F_T} \right) + \left(\frac{\sigma_{LT}}{F_{LT}} \right)^2 \right] \right\}$$

$$F_2(\sigma_L, \sigma_T, \sigma_{LT}, \bar{\sigma}_L, \bar{\sigma}_T, \bar{\sigma}_{LT}) = \min \{ F_1(\sigma_L, \sigma_T, \sigma_{LT}), \max [F_1(\bar{\sigma}_L, \bar{\sigma}_T, \bar{\sigma}_{LT}), \phi \sigma_T, \sigma_{LT}] \}$$

$$F_1(\bar{\sigma}_L, \bar{\sigma}_T, \bar{\sigma}_{LT}) \dots \text{when } \sigma_T > 0$$

$$= F_1(\bar{\sigma}_L, \bar{\sigma}_T, \bar{\sigma}_{LT}) \dots \text{when } \sigma_T \leq 0$$

where

F_L, F_T, F_{LT} are the basic lamina stress allowables

$\sigma_L, \sigma_T, \sigma_{LT}$ are the lamina stresses

$\bar{\sigma}_L, \bar{\sigma}_T, \bar{\sigma}_{LT}$ are the lamina stresses corresponding to $E_T = 0$

ϕ is the specified fraction of ultimate load below which transverse tensile fracture must be precluded.

Hill's failure criterion with the first modification is defined by the inequality $F_1 \geq 1$. The adopted failure criterion is governed by the inequality $F_2 \geq 1$.

It may be observed that the equation for F_2 , corresponding to positive transverse tensile stress, is simply a comparison of three terms. The first term accounts for Hill's criterion with the first modification of single-stress cut-offs, as illustrated by the solid lines of Figure 10. The second term is an allowance for transverse tensile strain beyond fracture and is illustrated by the dotted lines (Figure 10). The third term checks for increased stresses accompanying possible transverse fractures and is indicated by the dashed

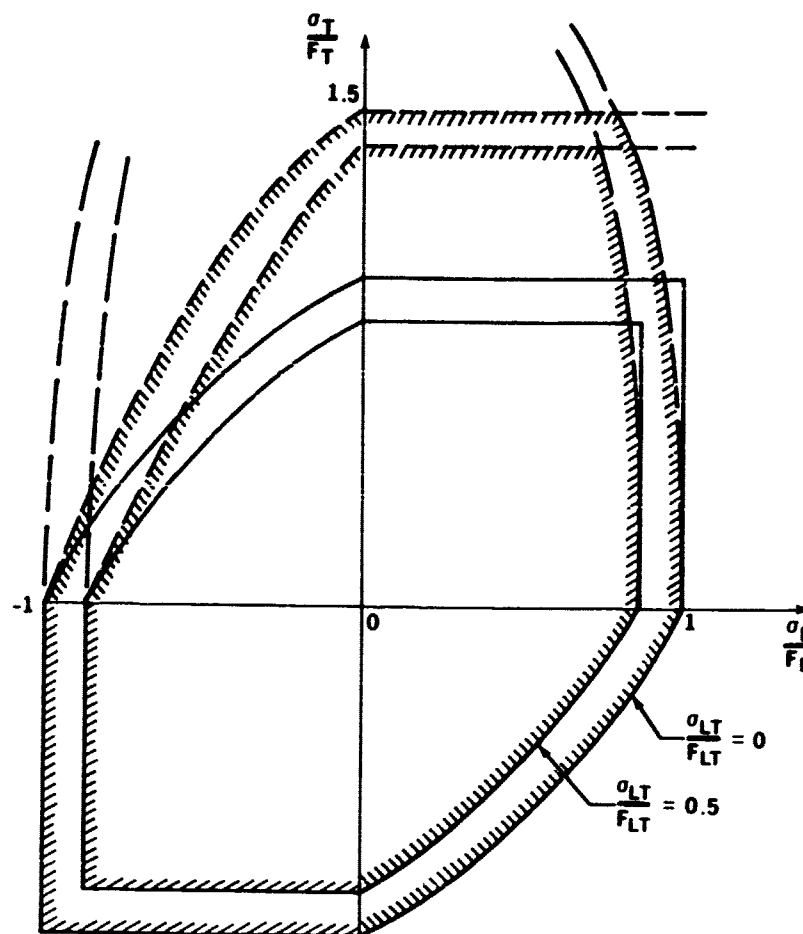


FIGURE 10. LAMINA FAILURE CRITERIA

cutoff lines (Figure 10). It should be realized that the dashed line cutoffs are dependent on the particular laminate design as well as the laminate loading. But, of course, the loadings are being restricted to the three single-stress allowables.

The stress state of each lamina is a function of the single-stress allowables (F_x , F_y , F_{xy}) being sought for the laminate as a whole. These single-stress allowables are determined once any corresponding lamina stress state exceeds the failure criteria of that lamina. Once the single-stress allowables are determined for a laminate, a laminate interaction formula can be used to assess the factor of safety associated with that laminate for any loading case. Loading cases may consist of any combination of panel loads, N_x , N_y , and N_{xy} .

Combined Loading: In order to determine the safety factor associated with any given laminate subject to a particular case of combined loads (N_x , N_y , N_{xy} pounds/inch), an interaction criterion established in Reference 1 was used. This criterion is based on a parameter $\gamma = 3F_{xy}^2 / F_x F_y$ which reflects the degree to which the laminate simulates an ideal noninteracting material.

When $\gamma \leq 1$, the factor of safety, FS, is the smaller of the quantities μ_1 and μ_2 defined below.

$$\frac{1}{\mu_1^2} = \left(\frac{N_x}{F_x t} \right)^2 + \gamma \left\{ \left(\frac{N_y}{F_y t} \right)^2 - \frac{F_y}{F_x} \left(\frac{N_x}{F_x t} \right) \left(\frac{N_y}{F_y t} \right) \right\} + \left(\frac{N_{xy}}{F_{xy} t} \right)^2$$

$$\frac{1}{\mu_2^2} = \left(\frac{N_y}{F_y t} \right)^2 + \gamma \left\{ \left(\frac{N_x}{F_x t} \right)^2 - \frac{F_x}{F_y} \left(\frac{N_x}{F_x t} \right) \left(\frac{N_y}{F_y t} \right) \right\} + \left(\frac{N_{xy}}{F_{xy} t} \right)^2$$

When $\gamma > 1$, the factor of safety is the smaller of the quantities μ_1 and μ_2 defined below.

$$\begin{aligned} \frac{1}{\mu_i^2} = & \left(\frac{N_x}{F_x t} \right)^2 + \left(\frac{N_y}{F_y t} \right)^2 + \left(\frac{N_{xy}}{F_{xy} t} \right)^2 - 2 h \\ & + (-1)^i 2 g(\gamma) \left(\frac{N_{xy}}{F_{xy} t} \right) \left(\frac{N_x}{F_x t} + \frac{N_y}{F_y t} \right) \end{aligned}$$

$$\text{where } h(\gamma) = 1 - \frac{1}{2} f(\gamma)$$

$$g(\gamma) = \sqrt{\gamma/12} \left[\frac{3 f(\gamma)}{f(\gamma) - 4} + 1 \right] f(\gamma)$$

$$f(\gamma) = \frac{1}{10} \left[-\left(\frac{3}{\gamma} + 4 \right) + \sqrt{\left(\frac{3}{\gamma} + 4 \right)^2 + \frac{240}{\gamma}} \right]$$

SECTION IV

DESIGN CONCEPTS AND SENSITIVITY STUDIES

Two promising wing-box design concepts were selected for investigation at the beginning of the program. These were the truss web and arch web designs shown as schematic cross sections in Figures 11 and 12. Multi-rib and multi-web concepts were later considered and configuration work accomplished on them, as will be detailed; however, primary work effort was directed in the program to the truss web concept. The arch web, after preliminary work, was de-emphasized early in the program due to its fuel volume limitation in a wing application.

4.1 INITIAL CONCEPTUAL WING DESIGN

The truss web concept selected as the primary initial concept consists basically of three parts (Figure 11): the internal web structure, the upper cover and the lower cover. When these three parts are joined, every fore and aft cross section is a truss structure. Since the centroidal axes of the truss members intersect at a point, a pure truss is formed.

A fabrication concept is also implied along with the structural concept. The covers are conceived as large, monolithic co-cured and bonded assemblies. The entire internal web structure is laid up on a mold and cured into one composite assembly. This does away with many adhesive and bolted joints that would occur in an assembly made of many cured parts. The wing box is noted to be one of the high cost and weight components of a conventional airframe. The high cost items of the conventional metal wing box are fabrication of the cover panels and the assembly of the structural box. The essential truss web fabrication feature is that detail effort is expended in making large subassemblies, thus minimizing final assembly.

This construction has the capability of transporting shear loads in any direction and ribs are not required. Eliminating ribs allows spanwise load-carrying material to run from wing tip to wing tip without any discontinuities in the load path. Discontinuities add stress concentrations which are undesirable in the non-ductile composite materials. Elimination of ribs also eliminates problems associated with the crossing of two loaded members where one of the two members must be cut and joined together, resulting in many clips, cutouts, and joints which complicate manufacture and assembly and add many undesirable stress risers.

The multi-triangular cell box created by the truss configuration provides a wing with good torsional stiffness. The triangular cells provide supports for the skin which have both vertical and lateral stiffness for maximum skin buckling allowables under compression and shear loading.

Concentrated torsional and shear loads, such as those coming from the flaps or engine pylon into the wing box, are distributed across the truss section by local thickening of the truss member skins. Fuselage attachment loads are distributed in a similar manner. Bending cap material is distributed in the covers across the chord which provides the most efficient placement of the composite material. Where bolted joints are used, a small portion of the cap material is placed on the webs.

TRUSS WEB DESIGN

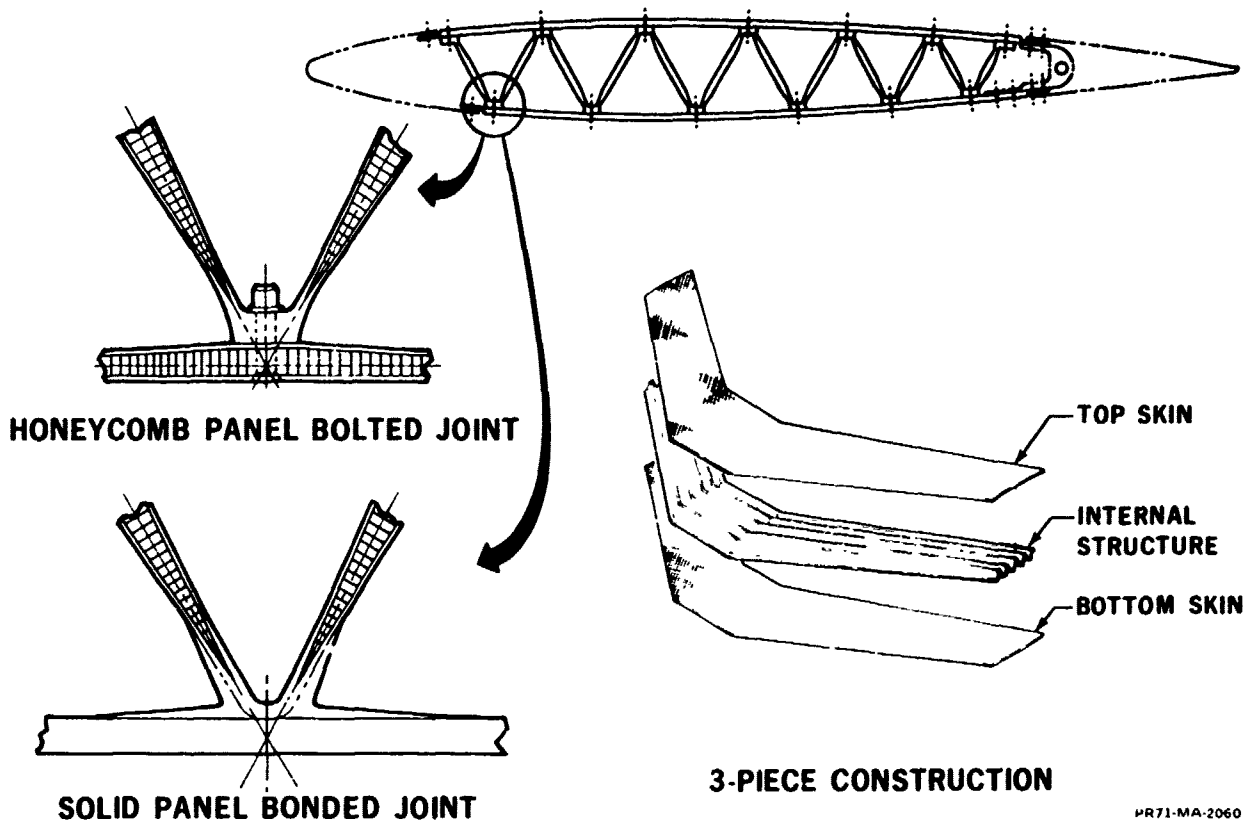


FIGURE 11. TRUSS WEB CONCEPT

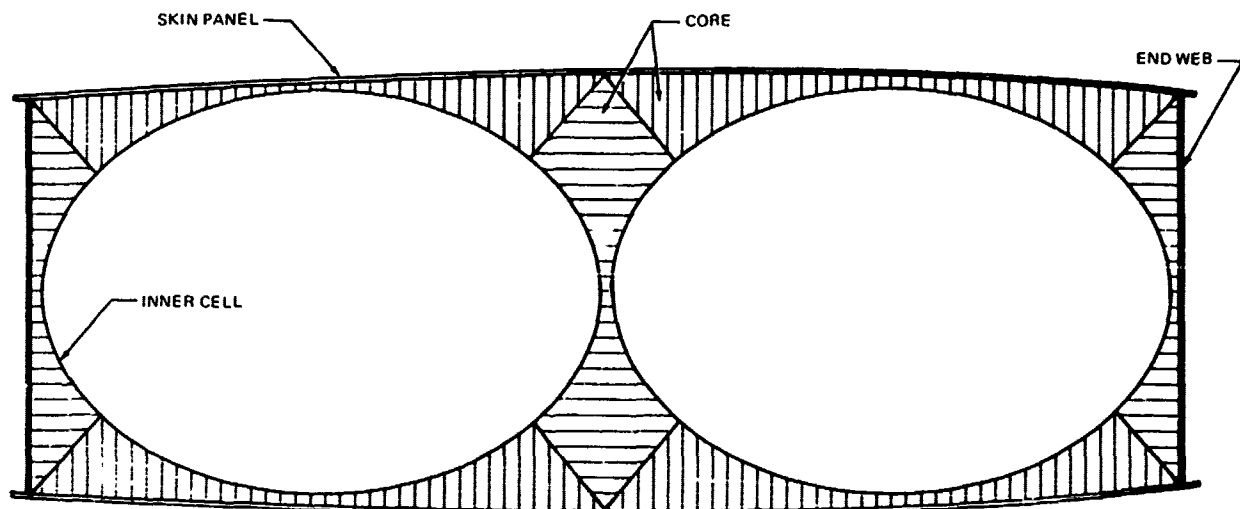


FIGURE 12. ARCH WEB CONCEPT - CHORDWISE SECTION

The primary structure of airplane wings characteristically has many "hard points" or places where concentrated loads are introduced. Some of these are the points at which aileron, flap, slat, spoiler, external stores, engine pylons, and landing gear loads are introduced. Concentrated loads can be dissipated or "fanned out" in the truss web with a small amount of added material in truss web construction, since loads can theoretically travel in all directions from the point of application.

The thin composite material in covers and webs is stabilized against buckling by honeycomb core. For a wing of the size and running loads of the selected AMST wing, all wing panels and webs require stabilizing. On a highly loaded thin wing, unstabilized solid panel construction would be used where loading is sufficiently high to require a skin thick enough to be buckle resistant. Honeycomb core stabilization was selected for initial truss web panels rather than solid panels stabilized by stiffeners or corrugations since judgment and preliminary calculations indicated honeycomb panels to be minimum weight and the simplest construction.

The crests of the internal web structure follow straight lines in the plan-view of the wing. These lines are located for maximum structural advantage and may or may not follow the straight element lines of the wing surface. Thus, the lines along the crests may be slightly curved in a vertical direction. The fabrication procedure is designed to accommodate this curvature. As shown in Figure 13, the web sheet is not continuous but is made of a series of sheets which overlap at the crest. Thus, only a narrow strip at the edge of the uncured composite sheet is folded over the slightly curved crest. This curvature can be accommodated within the forming capability of the uncured composite. The overlap provides the desired thickening or reinforcing for the bend in the web material at the crests.

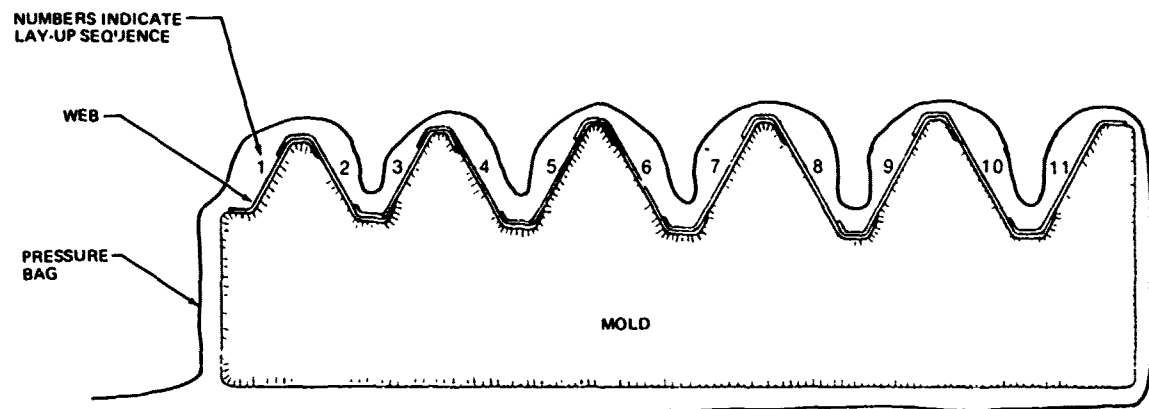


FIGURE 13. WEB FABRICATION INITIAL CONCEPT

The angle of the triangular web cells is not constant, but is allowed to vary along the wing span to adapt to airfoil changes. The fabrication procedure and the geometry of the structure are able to accommodate this angle change. Good truss geometry can be maintained through an included angle range of 60 to 90 degrees.

Allowing the web angle to vary and the crest line to deviate from the element lines gives the designer freedom to place the structural elements of this concept in a structurally efficient location for a minimum weight design. Additional general design features of the truss web concept were discussed in Reference 2.

4.1.1 Application of Truss Web Concept to AMST Wing

The AMST wing is a typical swept wing configuration (Figure 3). The cross section is relatively thick for the loading. Each side supports two engines, a large multiple flap, spoilers, an aileron, movable leading edges and leading edge slats. Each of these items, by means of numerous attachment points, introduces concentrated loads which must be picked up and distributed over the wing box structure.

Location of Front and Rear Spars - After examining the mechanism needed for actuation of the slats and movable leading edges it was concluded that the front spar would remain vertical and in the same location as on the metal wing. This location is a straight line joining the points at 15 percent of the root chord and 25 percent of the tip chord, Figure 14.

Investigation of the rear spar area showed it would be advantageous to move the upper edge aft and to move, by a lesser amount, the lower edge forward. Moving the upper edge aft did not interfere with the flap leading edge and allowed the spoiler hinge to be moved farther aft to an even more effective aerodynamic position. The rear spar in the metal wing was on the 55-percent line. In the truss web wing the upper edge of the rear spar was established as the 60-percent line. Changing the rear spar location resulted in a slight increase in box overall volume. This is desirable to offset the fuel volume that would be lost by the contemplated use of sandwich in both covers and webs.

Location of Web Crest Lines - The intersections of the diagonal webs (crests) were placed in flat planes perpendicular to the wing reference plane and thus appear as straight lines from root to tip in a planview of the wing. At the root and tip sections the crests are located aft of the rear spar the same fraction of the chordwise distance between the front and rear spar (Figure 14). This would place the crest lines on the wing percent lines if the front spar were on a percent line. But since the front spar crosses the percent lines (15 percent at root to 25 percent at tip) the crest lines also cross percent lines. However, the percent lines on this wing are not straight lines but are slightly curved, when viewed in a fore and aft direction, since the basic airfoils are not constant throughout the wing.

The number of crests was mainly determined by the minimum angle between the webs required for making a bolted connection and the minimum angle required for an efficient truss; both of these requirements turn out to be approximately a 60-degree angle. This approach produced the arrangement shown which was considered to provide for an efficient connection at crests numbers 2, 3, 4, 5, and 6, but to compromise the connections at crests 0 and 1 at the front spar. Here the penalty comes from having to leave the front spar vertical.

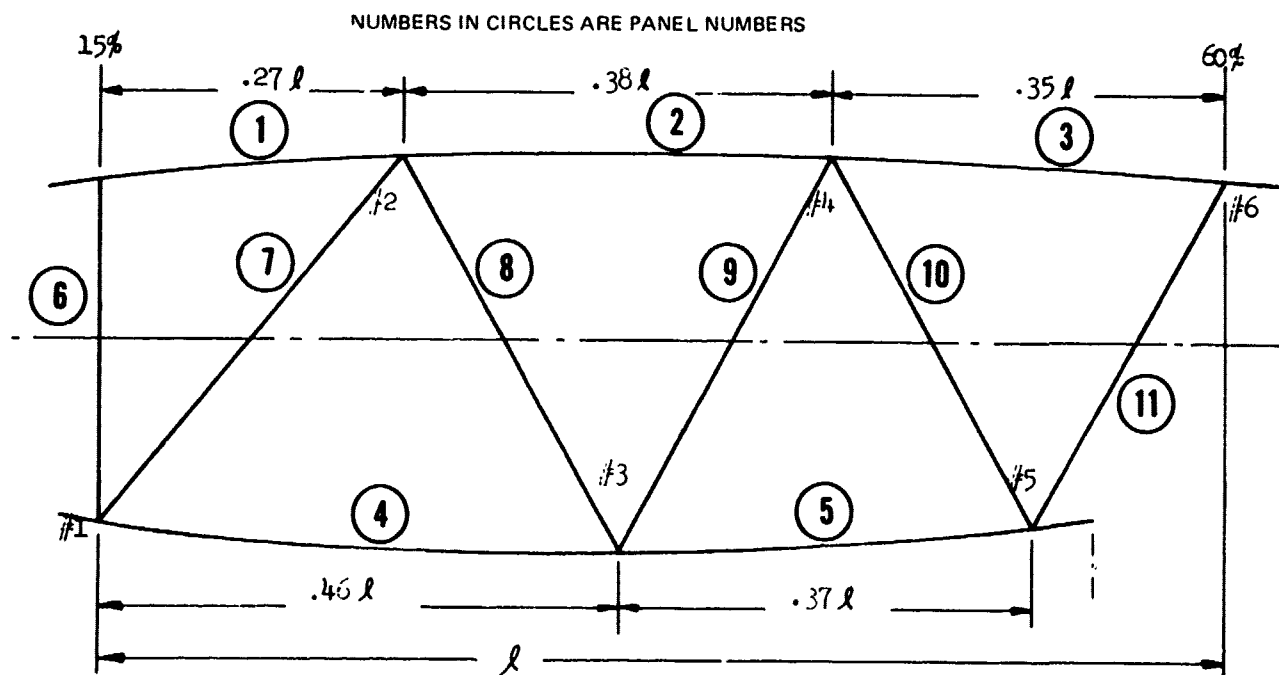
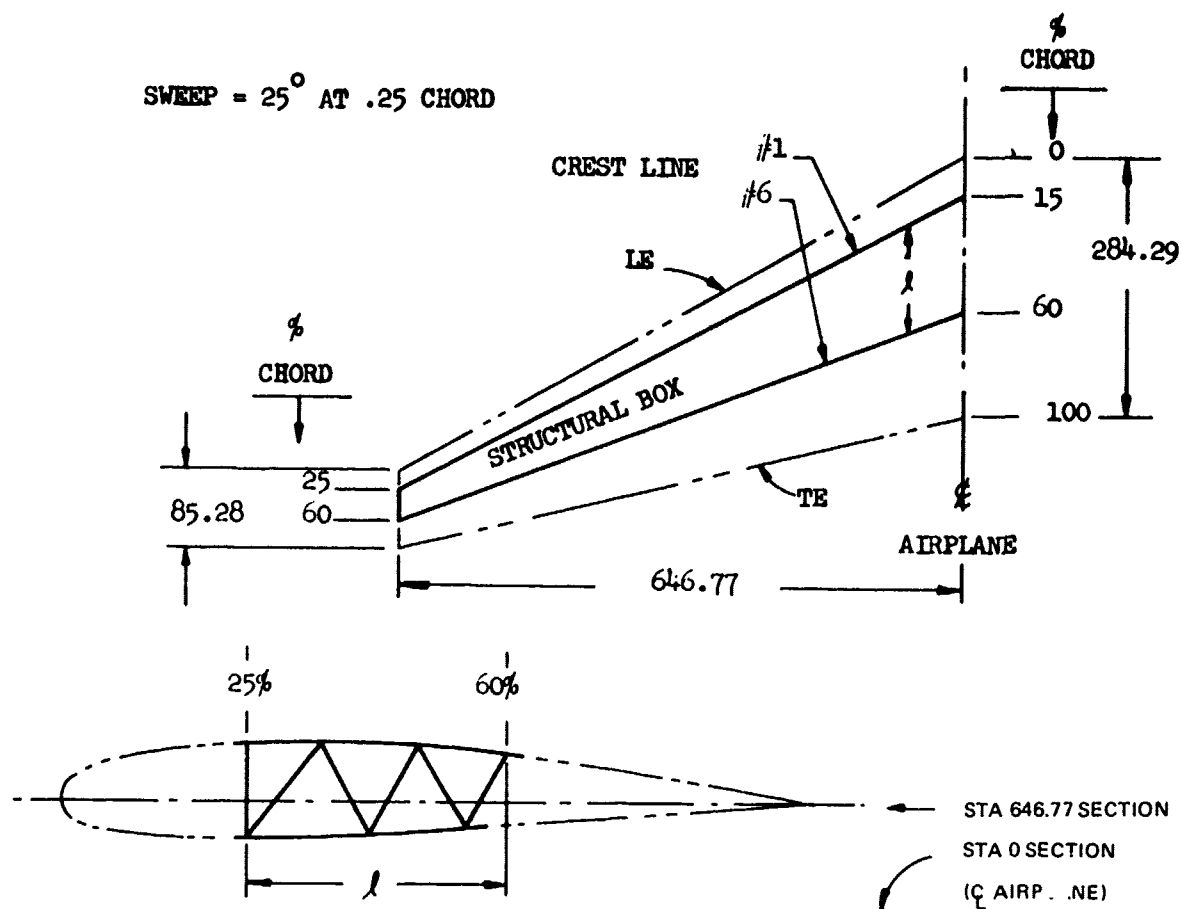


FIGURE 14. WEB CREST LOCATIONS (MST COMPOSITE TRUSS-WEB WING)

Later optimization work (Paragraph 4.1.3) showed the initially chosen five-cell configuration to be optimum weight with bolted cover to web joints.

Baseline Truss Web Configuration - A baseline truss web wing general configuration was established as a basis for a finite element analysis model, for various design studies, and for design of the verification test specimens. See Figures 15, 16 and 17.

The fuselage structure for the AMST airplane was initially arranged to accommodate the truss web wing design. Initially, the fuselage was 200 inches in diameter and the wing was required to be higher with respect to the top of the fuselage, due to fixed cargo box size, thus it was convenient to put a gentle depression in the upper fuselage and run the fuselage bending loads under the wing. Large fuselage frames are placed under each of the three truss points on the lower skin (Figure 15). The connection to each frame consists generally of two widely spaced bolts (approximately 25 inches on center, in an in-and-outboard direction). This provides for continuity of frame and wing structure which is particularly desirable for resisting lateral wing loads by the fuselage. At the rear outer location two outer bolts are used to divide the 340,000-pound ultimate tension load and provide a failsafe feature. Fore and aft wing loads are transferred from the wing mounting bolts to an angle running fore and aft which distributes the load into the fuselage skin. An all-aluminum fuselage was assumed.

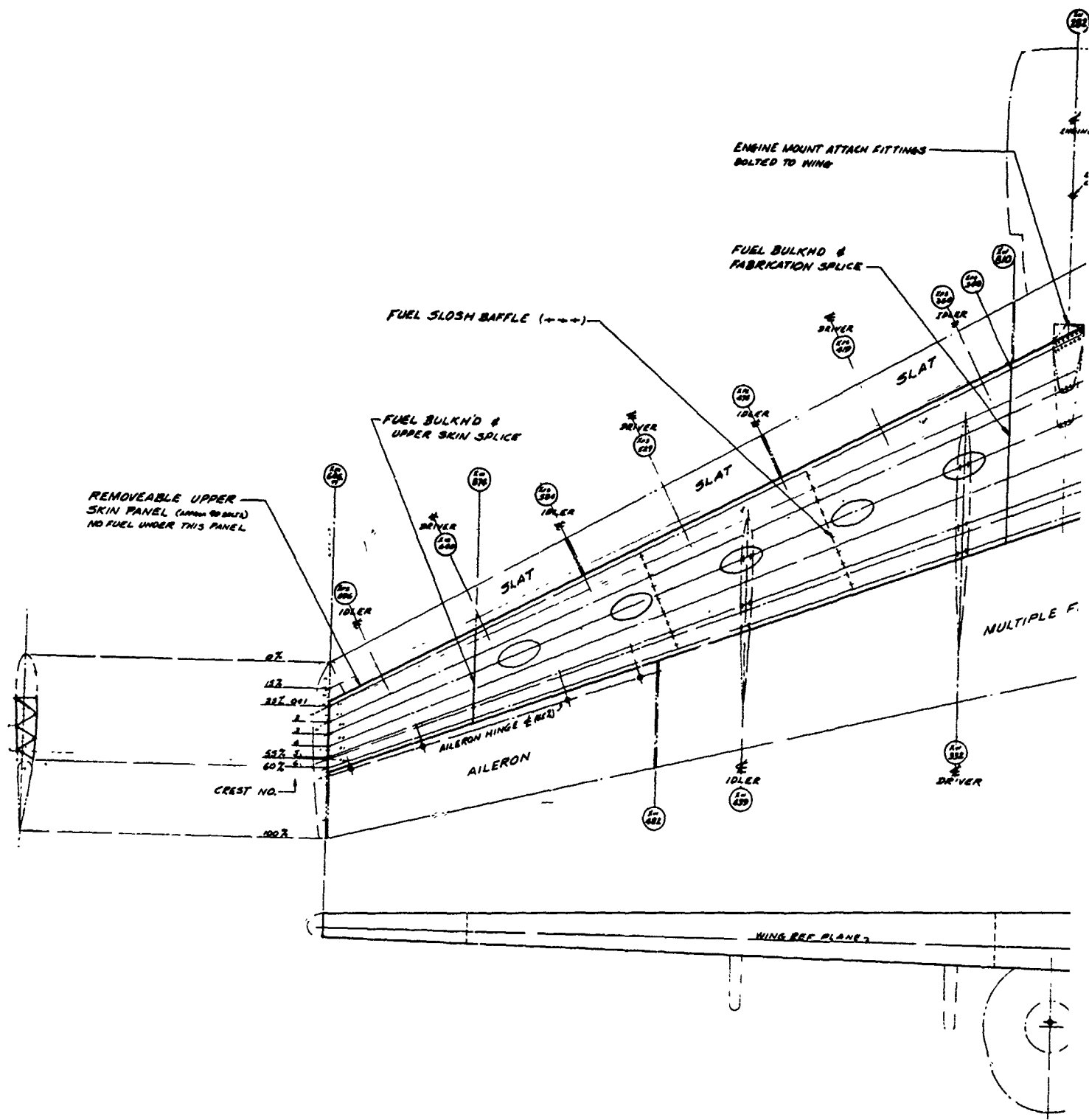
The outer 5 feet of wing tip are dry since it is a primary lightning attachment area and to provide space for fuel dump valve, antennas and lights. Access to this tip area is provided by removing the 30-x 60-inch upper wing panel. The truss web caps are capable of satisfying the bending material requirement in this area.

Other than in the tip area, access holes of adequate size for head and shoulders are spaced along the upper surface. Wing tank barriers and baffle locations are also indicated (Figure 15).

A chordwise manufacturing joint is indicated outboard of the outboard engine (Figure 15). The center wing assembly of covers and web are judged to be of sufficient size to fulfill the "3-piece wing" concept and still not require inordinately large curing and bonding facilities. (The later Task VI study added an additional splice at fuselage centerline, thus making four rather than three major wing subassemblies, further reducing autoclave cost and providing opportunity for greater numbers of workmen to fabricate simultaneously.)

At the engine pylons which essentially project straightforward from the wing box, it is possible to put fittings on the upper and lower exterior surfaces, the upper one being under a fairing which is an extension of the pylon leading edge. It was envisioned these fittings would be bolted to the wing through the truss crests only (Figure 15), similar to the flap linkage support brackets (Figure 16). The lower pylon attachment fitting carries vertical, fore and aft, and in-and-outboard loads. The upper fitting carries the same loads except none in the vertical direction. The composite wing structure is locally reinforced at the bolt connections and the truss is reinforced to spread the bolt loads into the structural box.

1



ENGINE

FUEL BULKHEAD

DROOPABLE L.E.

SLAT

FLAP

MULTIPLE FLAP

FLAP LINKAGE ATTACH BOLTS PAIRING

AERODYNAMIC BREAK

FUEL BAGS OVER FUSELAGE

CABIN PRESSURE BOUNDARY

FAIRING

FUSELAGE SKIN

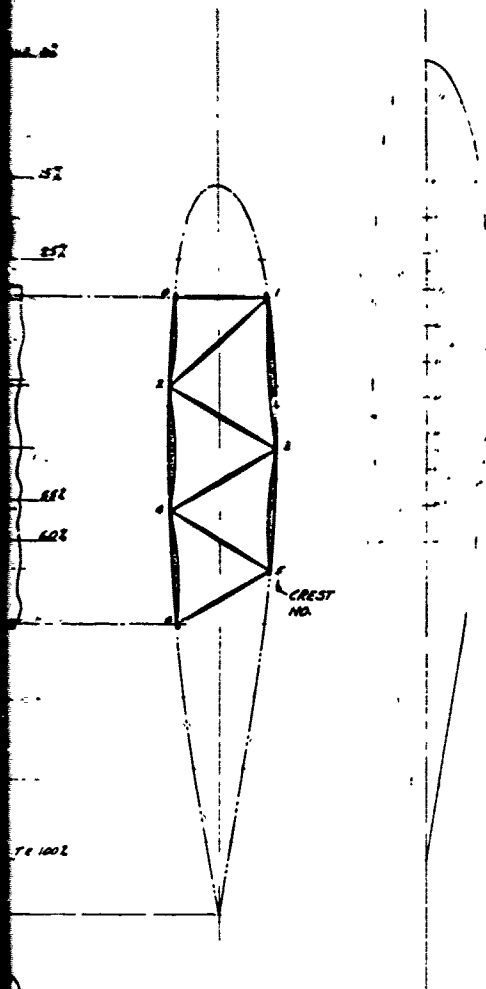
FUS. STRINGERS

FUS. WING ATTACH

ACCESS DOORS

FUSELAGE ATTACH BOLTS

CREST NO.



PLANE

*UPPER STRINGERS ARE CONTINUOUS UNDER WING. SIDE STRINGERS ARE SPACED AT WING ATTACH FRAMES

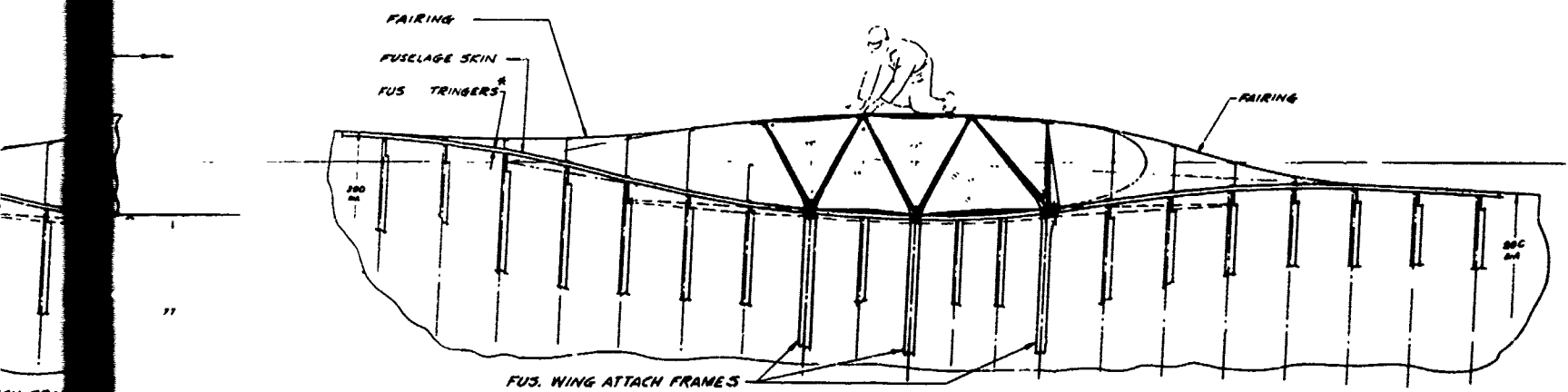


FIGURE 15. MST COMPOSITE WING BASELINE STUDY CONFIGURATION

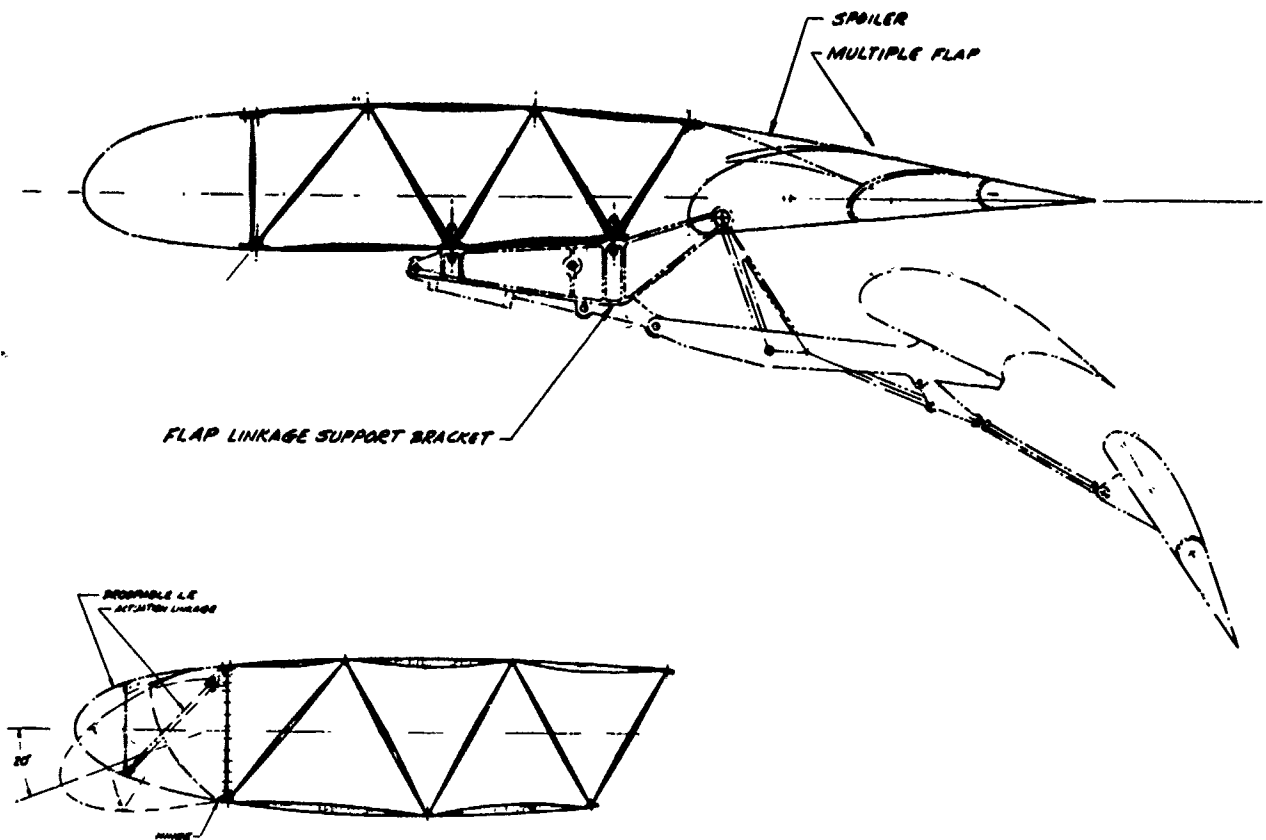


FIGURE 16. SECTIONS AT MOVABLE LEADING EDGE AND FLAP SUPPORT STATION - BASELINE STUDY CONFIGURATION

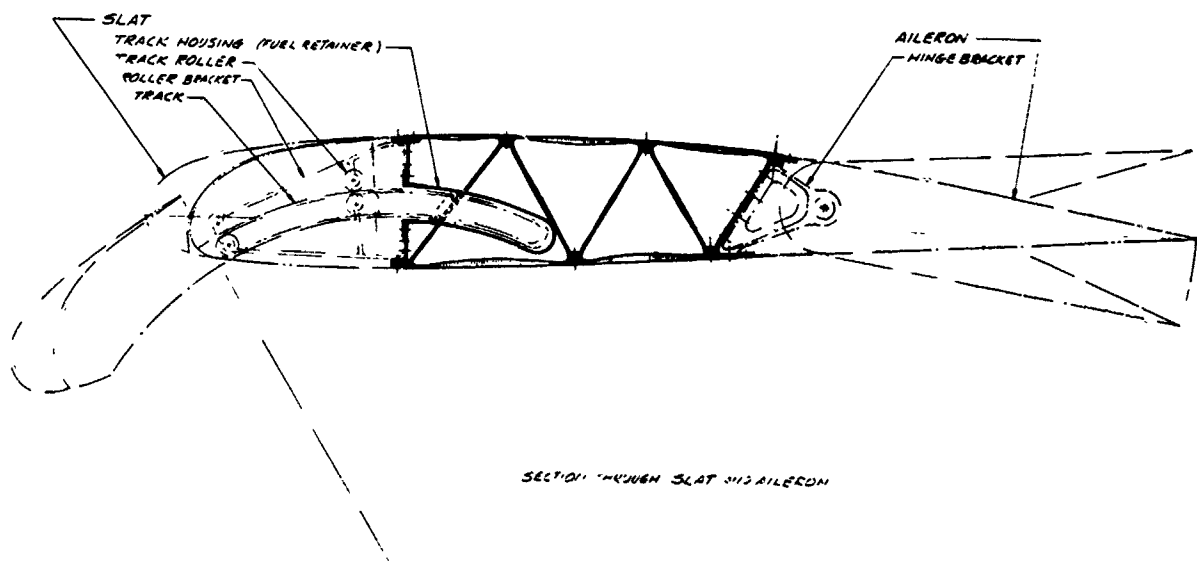


FIGURE 17. SECTION THROUGH SLAT AND AILERON - BASELINE CONFIGURATION

Center Wing Geometry-Baseline Configuration - Brief consideration was given to continuing the composite wing sweep angle inboard to the fuselage centerline (Figure 14), rather than having a sweepbreak and constant center section. This question was not resolved since it became apparent that to judge relative internal load intensities and effect of lack of support at fuselage centerline in the case of the "vee" configuration required a trade study based on finite element analysis models. In light of ply pattern changes at the present sweepbreak, load distributions in the ribless truss web at that location, and the required dihedral changes (meaning significant vertical kick loads) at the sweepbreak, the vee configuration might prove to have design and weight advantages.

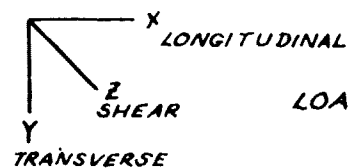
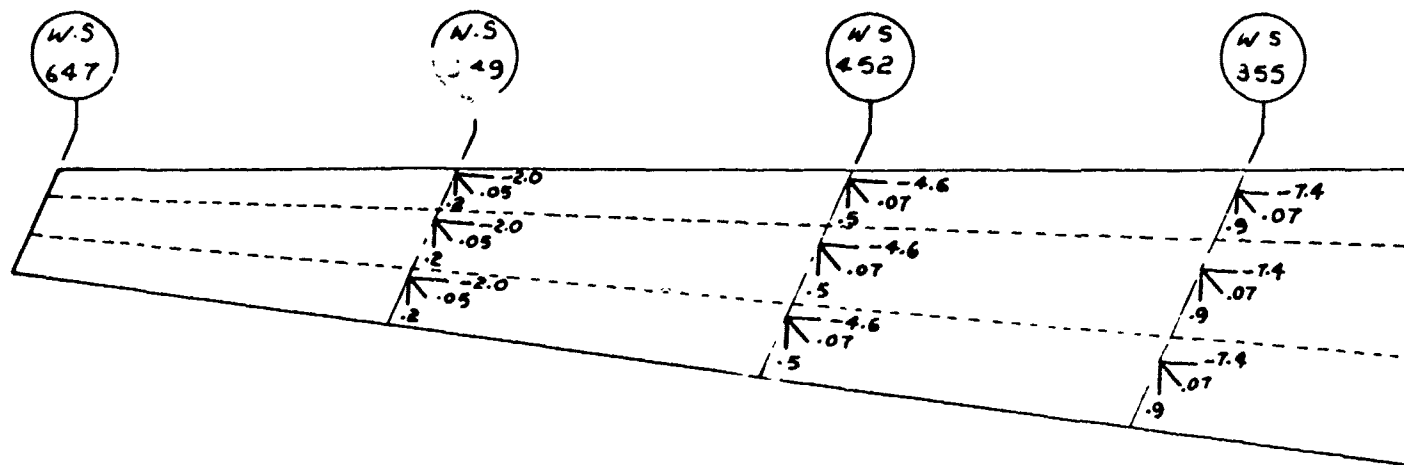
Access Philosophy, AMST Composite Conceptual Wing - Access holes through covers of the wing box in fuel-carrying areas (Figure 15) will be limited to the wing upper surface and front and rear webs of the wing center section. This is based primarily on use of the Line Replaceable Unit maintenance concept, minimization of ground support equipment, and safety on a high wing aircraft. For all areas in the wing it is assumed that large enough holes can be provided in the internal truss webs to allow intercell accessibility. Cover holes are modelled after DC-10 wing access hole size and shape.

4.1.2 Preliminary Materials and Ply Patterns

Preliminary monolayer design allowables were developed for Avco 5505 boron epoxy, Narmco 5206II high-strength graphite epoxy, Thornel 75S high-modulus graphite epoxy and boron/aluminum. Using the external bending and torsion loads, an estimate of the cover internal load distributions was made, Figures 18 and 19. Using these allowables and internal loads, the M6LA laminate optimization (strength only) program selected orientations and numbers of plies for one wing station (Root Sta 97). All combinations of the four materials were tried for the covers, whereas high-strength graphite was held constant for the truss web.

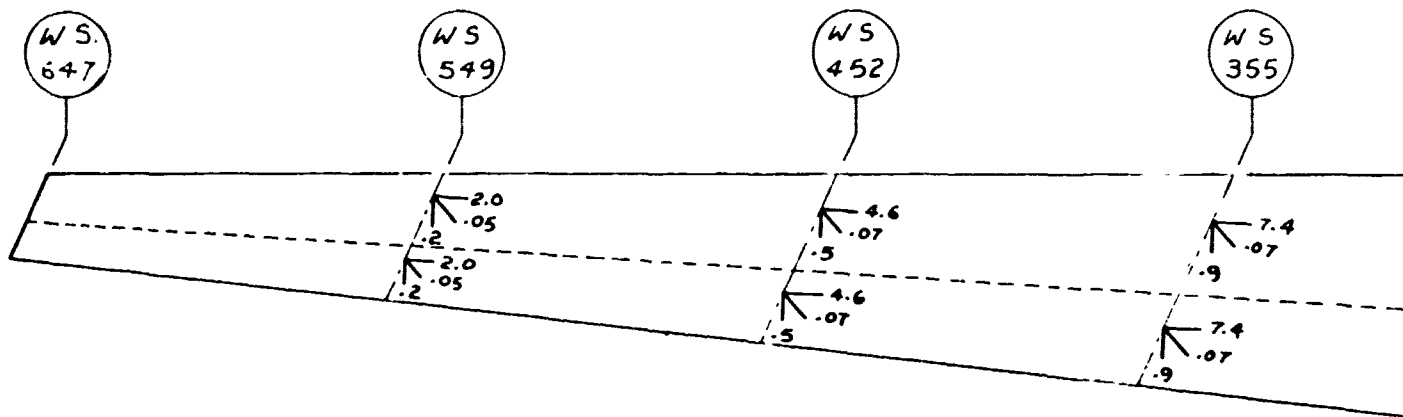
Since the initial stiffness criterion was to match the metal wing stiffness, the selected strength laminates in boron/epoxy and Narmco 5206II were found not to satisfy the torsional stiffness requirement. Additional plies at +45 degrees had to be added and the skin weights increased about 30 percent. Because of the torsional stiffness weight penalty, the Narmco 5206 skins were resized with Thornel 75S in +45-degree plies. The results of this preliminary study (Table 5) indicated that a significant weight reduction could be obtained using mixed epoxy laminates. Thornel 75S was also considered for use with Avco 5505 since the mixture was of lower density at potentially equivalent laminate strength and stiffness.

The wing was also sized at Station 97 for boron/aluminum skins. The pattern used was undirectional and no additional plies were added to meet the torsional stiffness requirement. Because no additional plies had to be added, boron/aluminum skins resulted in the lightest weight structure at Station 97. Although this finding must be viewed with some skepticism since local conditions might require angle or transverse plies, it does indicate that in structural areas where shear stiffness is important, boron/aluminum is a strong candidate.



LOADS IN 1000 LBS/INCH

UPPER SURFACE



LOWER SURFACE

2

W.S.
355

W.S.
258

W.S.
97

ENG

ENG

7.4
-9
.07

10.2
-10.2
1.0
.07

7.4
1.0
.05

7.4
-9
.07

10.2
-10.2
1.0
.07

14.8
1.0
.05

7.4
-9
.07

10.2
-10.2
1.0
.07

22.0
1.0
.05

SURFACE

W.S.
355

W.S.
258

W.S.
97

ENG

ENG

7.4
-9
.07

10.2
1.0
.07

7.4
1.0
.05

7.4
-9
.07

10.2
1.0
.07

22.0
1.0
.05

SURFACE

FIGURE 18. ASSUMED INTERNAL LOADS DUE TO MAXIMUM BENDING CONDITION

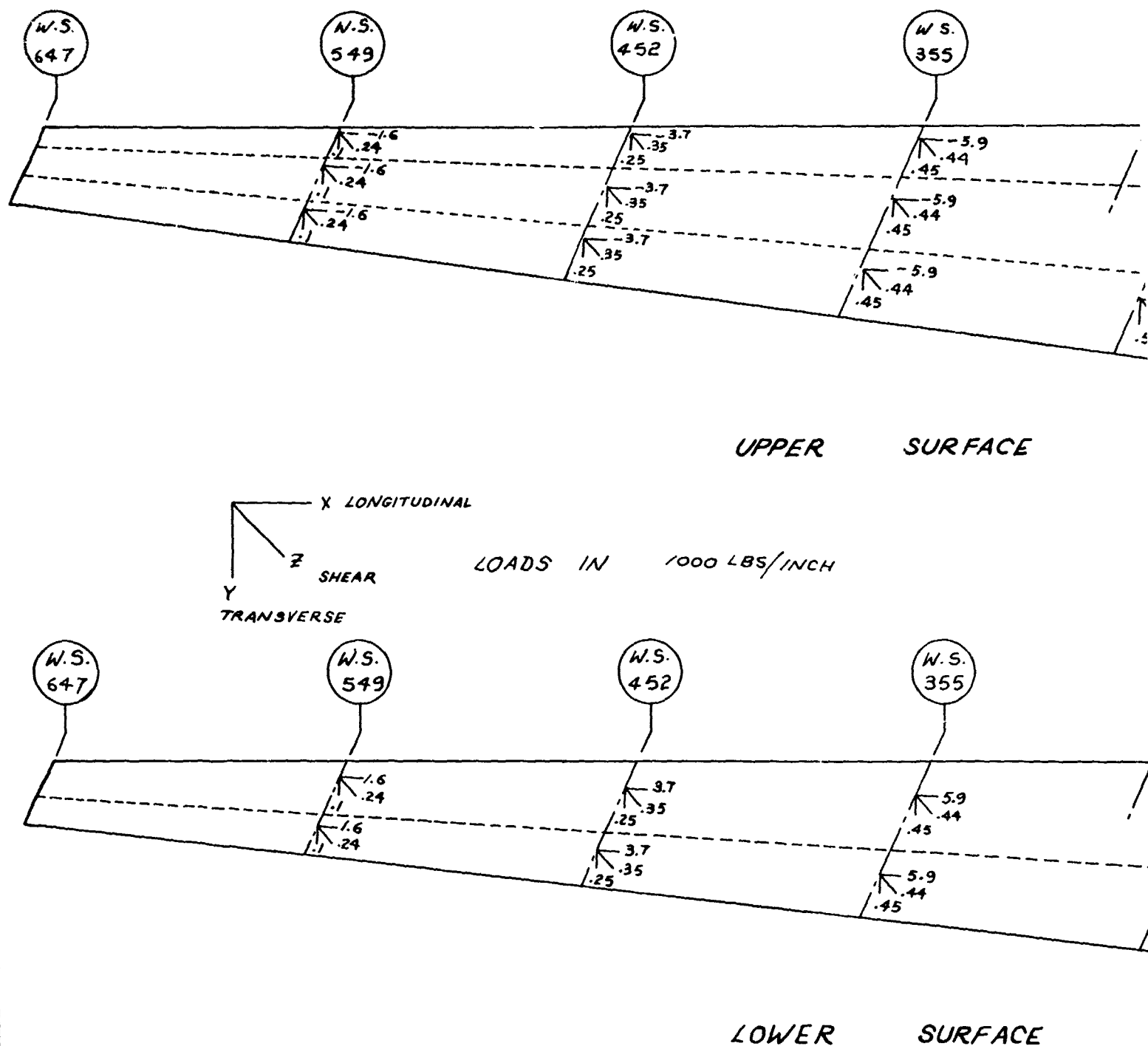


FIGURE 19. ASSUMED INTERNAL LOADS DUE TO MAXIMUM TORQUE CONDITION

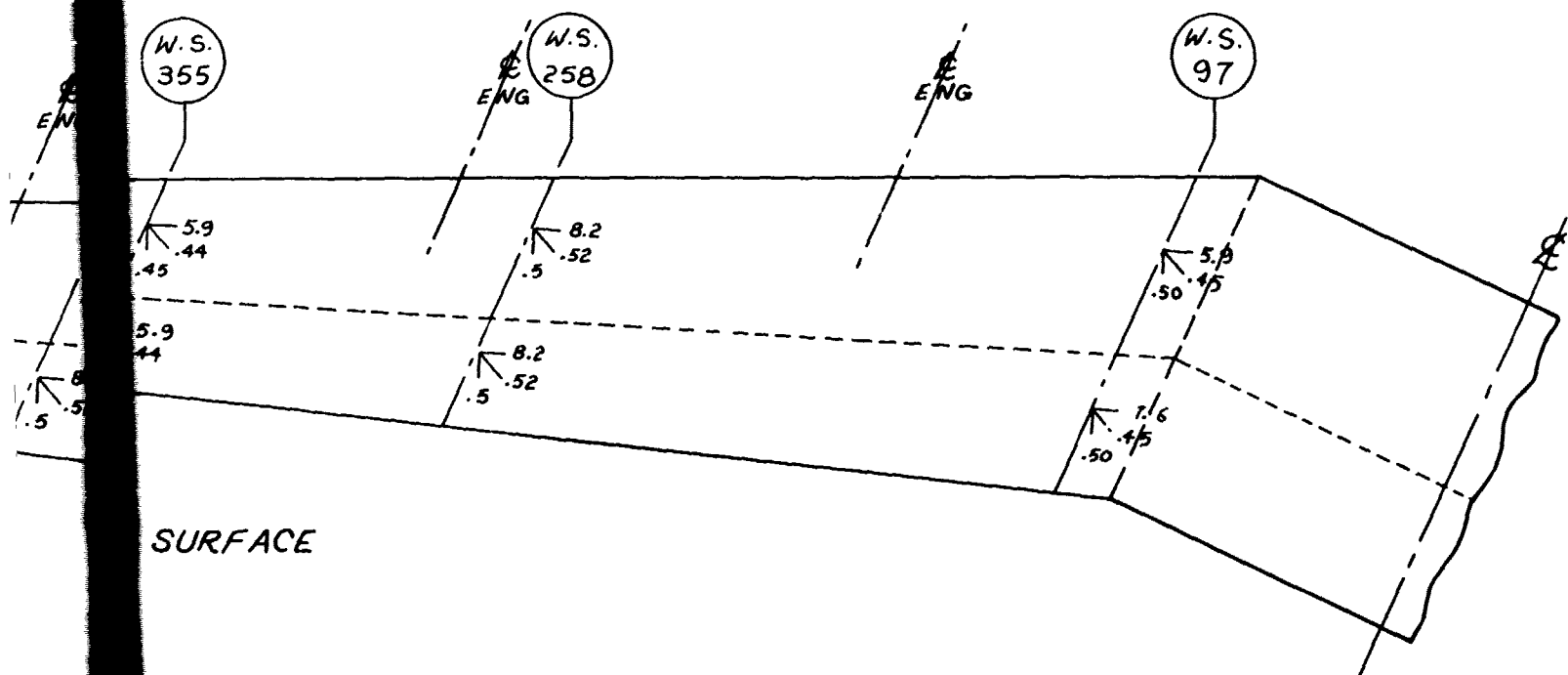
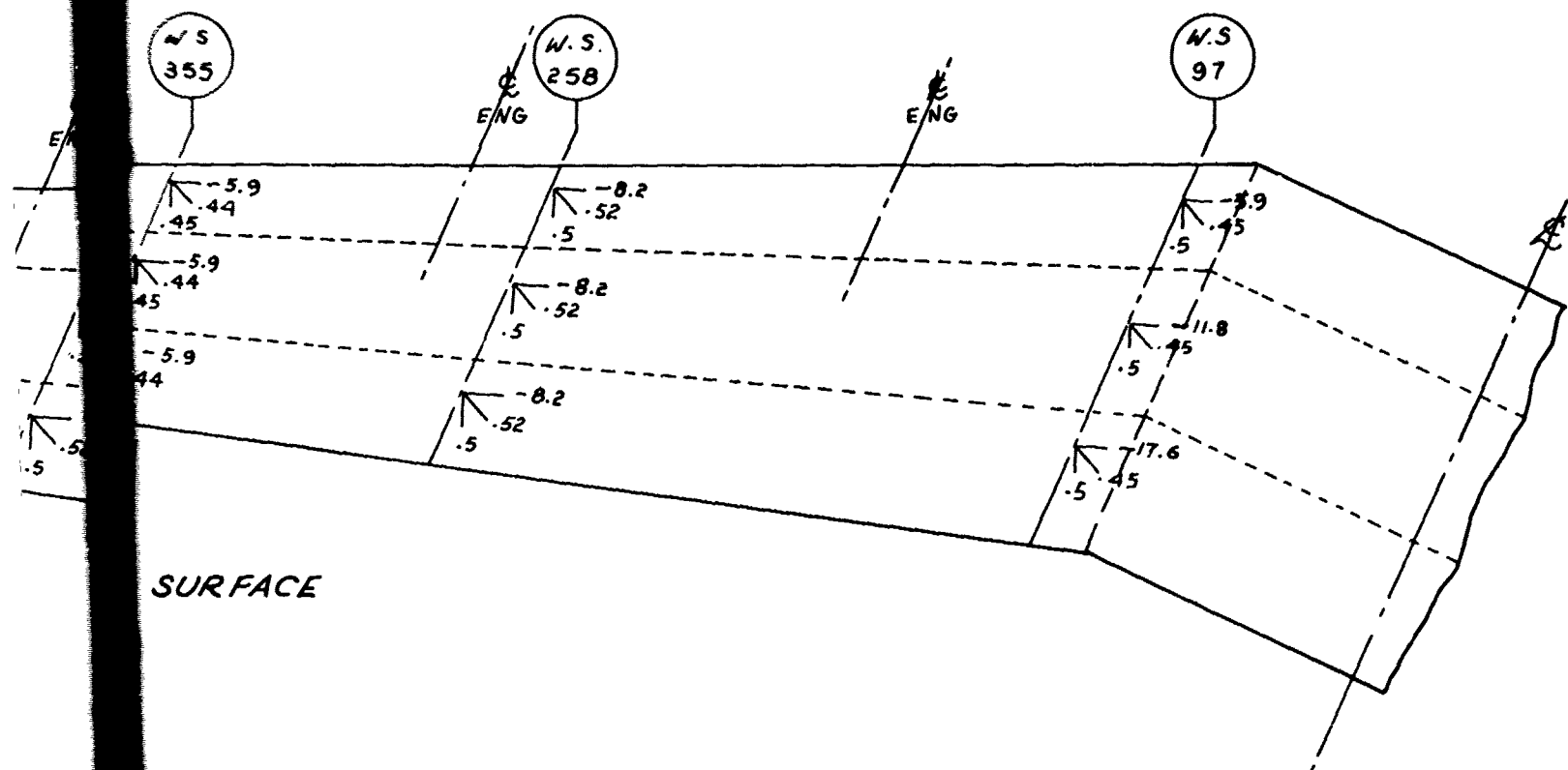


TABLE 5
PRELIMINARY MATERIAL SELECTION STUDY RESULTS

| UPPER SKIN | LOWER SKIN | SUBSTRUCTURE | WEIGHT (LB/IN. SPAN) ⁽¹⁾ |
|--|--|--------------|--|
| NARMCO 5206 | NARMCO 5206 | NARMCO 5206 | 4.80 |
| NARMCO 5206 WITH THORNEL 75S AT $\pm 45^\circ$ | NARMCO 5206 WITH THORNEL 75S AT $\pm 45^\circ$ | NARMCO 5206 | 4.26 |
| BORON/EPOXY | BORON/EPOXY | NARMCO 5206 | 4.20 |
| BORON/EPOXY | NARMCO 5206 WITH THORNEL 75S AT $\pm 45^\circ$ | NARMCO 5206 | 4.12 |
| BORON/ALUMINUM | BORON/ALUMINUM | NARMCO 5206 | 3.93 |

(1) WEIGHTS DO NOT INCLUDE SKIN PANEL CORE, ADHESIVE, OR JOINING PENALTIES.

A laminate test program was initiated to determine initial allowables for laminate strength, stiffness and bolt bearing strength for Thornel 75S/Narmco 5206II (Section 6), and this mixed material was adopted for the baseline study wing lower cover. The baseline upper cover remained all-boron epoxy in the baseline since no experimental work to support mixed boron/graphite or boron/aluminum allowables was authorized for the program. Boron/graphite and boron/aluminum remained under theoretical consideration but were not adopted for the study baseline for design verification specimen fabrication due to lack of sufficient design properties information.

4.1.2 Configuration Optimization

Detailed weights per inch of span were computed for the five configurations shown on Figure 20. Two sections, one at the root and one at Station 276, were investigated, and the following basic assumptions were made:

1. The weights computed were those necessary to carry the basic wing bending and shear and a fuel overpressure condition of 30 psi ultimate. It was assumed all webs equally resisted shear flow.
2. The skin thicknesses used were those derived in Paragraph 4.1.2. The upper skin was all boron, but the lower cover was the Thornel 75S/5206II mixture. The variations in cover skin strength requirements resulting from the various configurations were accommodated by varying the core thickness.
3. Weight required for the introduction of concentrated loads was not included, neither were the penalties for access holes and other stress concentrations.

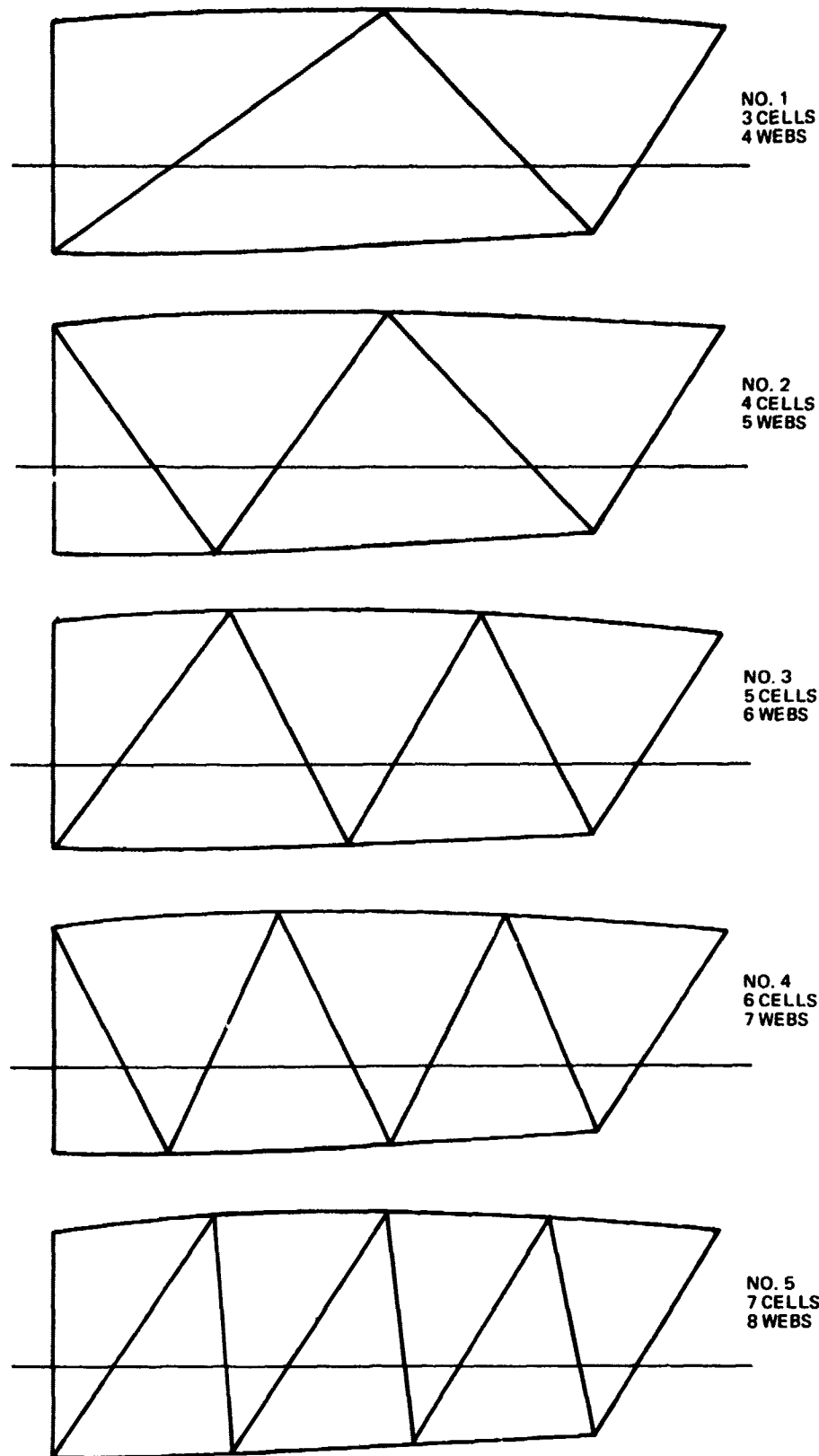


FIGURE 20. TRUSS WEB CONFIGURATIONS

4. The unit weights used were:

- | | |
|--|--|
| a. Mixed graphite Composite lower cover and web | 0.056 lb/cu in. |
| b. Boron Composite upper cover | 0.075 lb/cu in. |
| c. Core | 5 lb/cu ft |
| d. Adhesive | 0.10 lb/sq ft/joint on covers 0.06 lb/sq ft/joint on webs |
| e. Web caps (fittings) | 0.52 lb/ft |
| f. Bolt strip on skin | 0.52 lb/ft |

5. The bolt strip is assumed to deduct 1 inch from each edge of a panel (2 inches total) for weight calculation purposes. Similarly the panel length was reduced by 0.875 in calculating core weights on the assumption that one-quarter of the core will be linearly tapered.

The results of this study are shown in the graphs of Figures 21 and 22. Configuration No. 4 is the most efficient, however, Configurations No. 5 and 3 are within 3 and 6 percent, respectively, of the minimum weight. The weights of the cover panels are influenced greatly by the fuel pressure condition which dictates that relatively narrow panels be used. High cover weights in Configurations No. 1 and 2 are the result of having wide panels. On the other hand, a separate theoretical investigation (Reference 3, Appendix C) shows that the webs are minimum weight when their angle relative to the vertical is 45 degrees, an angle characteristic of Configurations No. 1 and 2. These conflicting influences give an optimum configuration (No. 4) having a web half-angle of approximately 26 degrees.

The five-cell baseline wing configuration corresponds to No. 3. Evaluation of whether or not to adopt the six-cell configuration No. 4 for the final wing design effort involves consideration of joint type, whether bonded or bolted, and if bolted, additional weight penalty associated with more acute web angles. Manufacturing cost for additional number of cells and joints would also be considered. See Paragraphs 4.1.8 and 4.1.9.

4.1.4 Joints Investigation

Bolted and bonded joints were to be considered in this program. The bonded/bolted approach was not considered since emphasis was placed on full bonding with minimum stress concentration in the joint. Bolted joints were to be considered to determine the penalty versus bonding and to have a design for a removable wing cover panel. Joint type was not specified for the baseline study configuration since a selection would be made after trade study.

4.1.4.1 Web to Cover Attachment - The purpose of this connection is to transfer shear loads from the webs to covers and to resist outward tension loads produced by fuel pressure. The initial web to cover joint tension

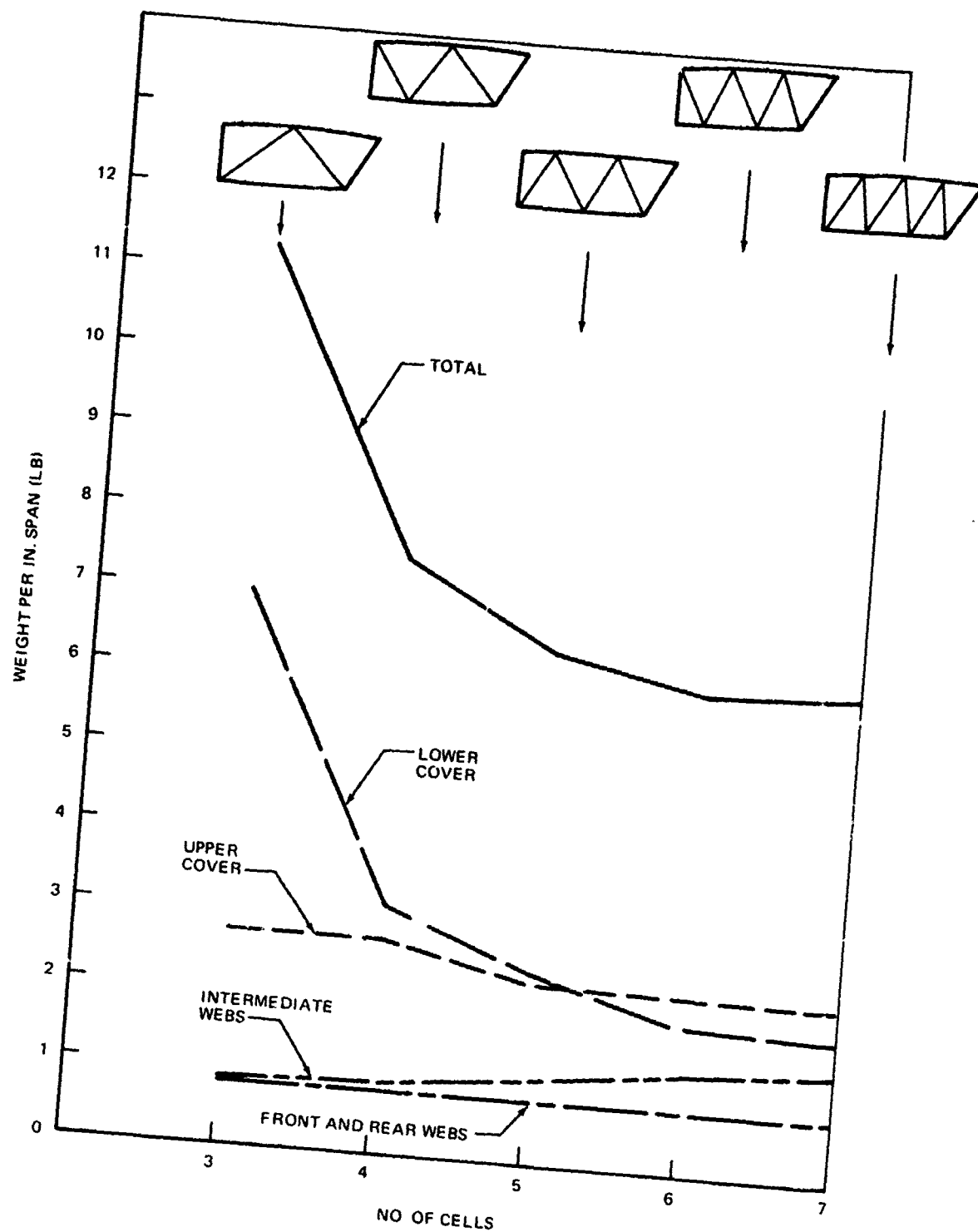


FIGURE 21. VARIATION OF WING WEIGHT WITH CONFIGURATION - ROOT SECTION

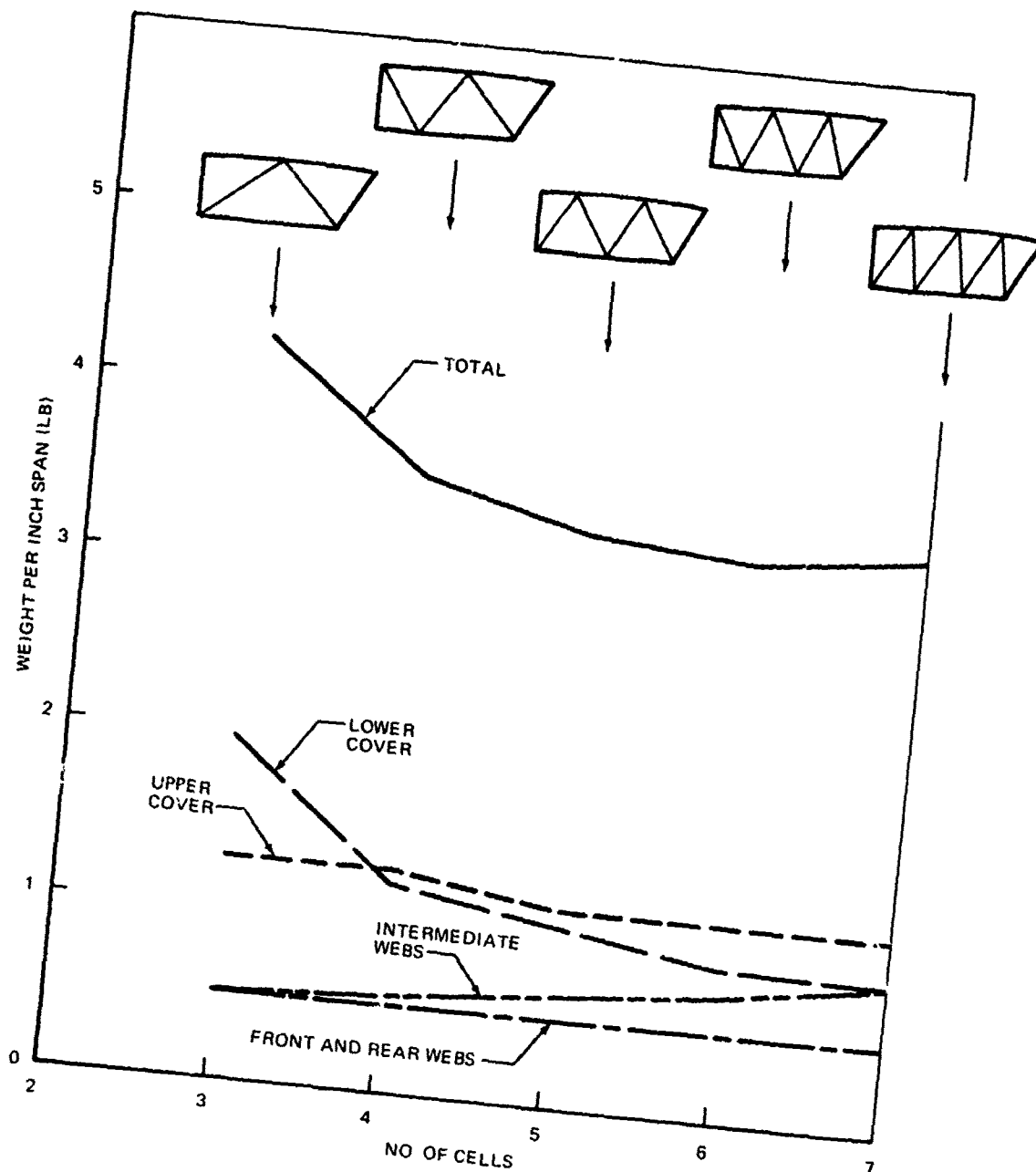


FIGURE 22. VARIATION OF WING WEIGHT WITH CONFIGURATION - STATION 276

design load was 1731 pounds per inch tension based on 30 psi internal pressure on the largest panel of the baseline five-cell configuration (Figure 23). The requirement was later reduced to 20 psi after assessment that there is much less penalty for the fuel vent system to be sized for a reduced overfill pressure relief than to carry the weight in the structure. Thirty psi remained the design goal for the joint testing program.

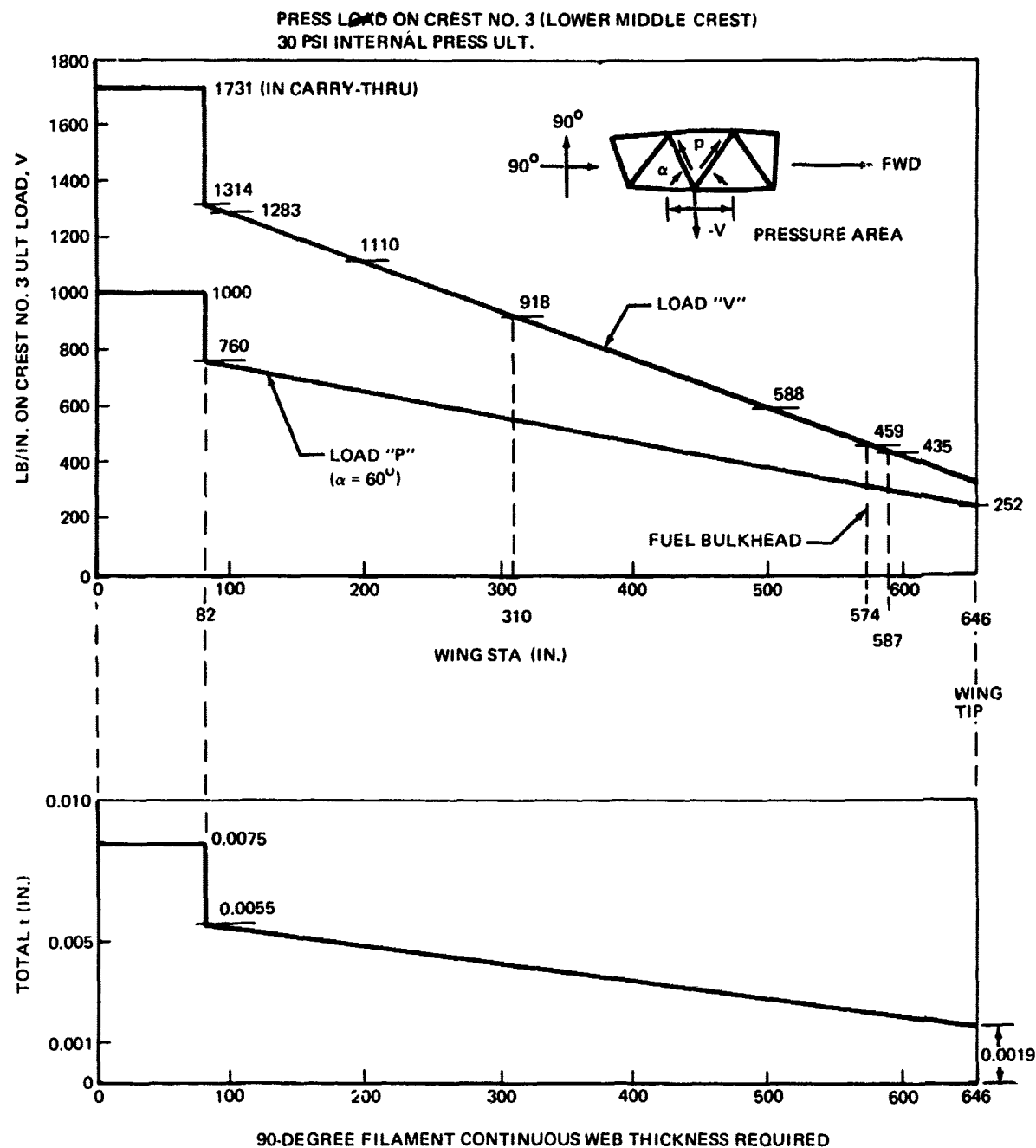


FIGURE 23. JOINT PRESSURE LOAD AND WEB REQUIREMENTS

The joint design shear load was taken from the finite element analysis. Maximum shear occurred in the rear web outboard of the sweepbreak for the truss-post concept (in which internal webs are not required to carry shear) and its value was 5280 pounds/inch ultimate at the joint. Joint design factors were applied (Section III).

The bolted joint design investigation began by considering a typical internal web crest joint designed by both tension and shear. Allowance was made for both kinds of stress concentrations (load introduced at the bolt and load in the panel going past the hole).

Maximum Bolt Spacing Approach - The web to skin connection shown in Figure 24 uses a 1/4-inch-diameter bolt as standard throughout the wing except at special locations. It accommodates the varying angle between the webs of 55 to 60 degrees, caused by wing contour changes, so as to provide a seat for a nutplate, barrel nut, or standard nut. Bolt spacing is based on shear strength of the bolt. At full shear strength, the nominal bearing stresses used are about 1/3 of the allowable in both cover and web cap to allow for bearing stress concentration factor. A special bolt could be fabricated with 3/8-inch-diameter shank and 1/4-inch-diameter threads for additional bearing stress reduction.

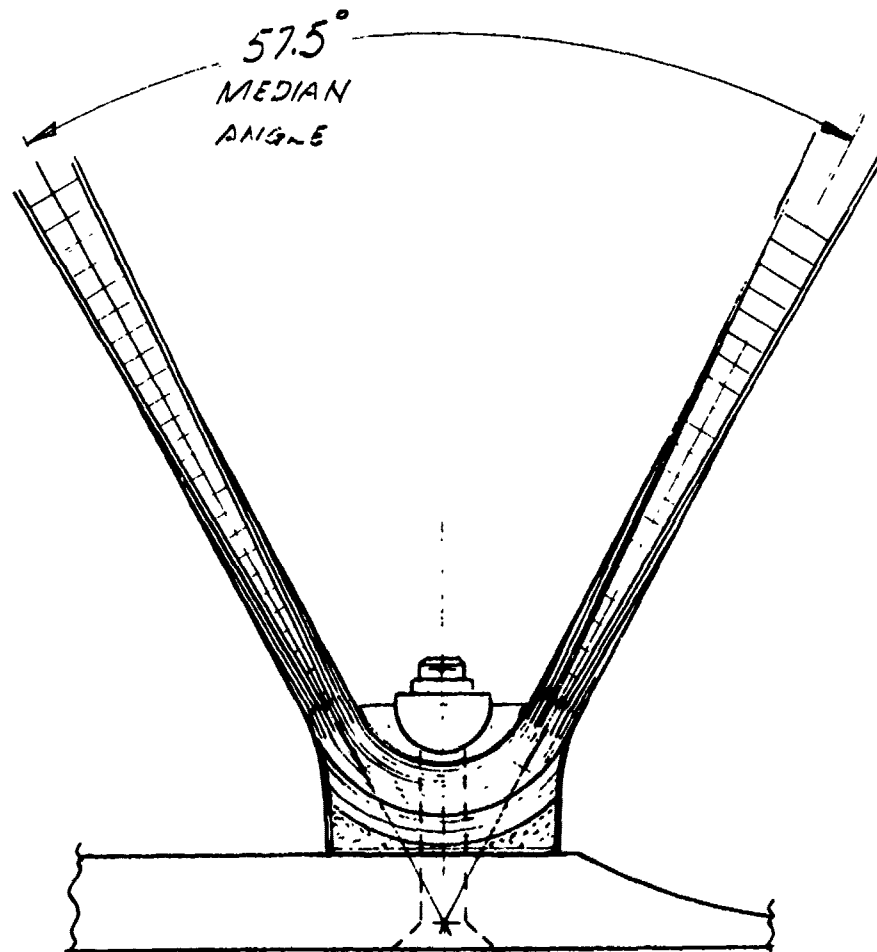


FIGURE 24. BOLTED JOINT - MAXIMUM BOLT SPACING APPROACH

While concentricity and joint fixity for carrying truss type loading is excellent, the weight added to webs using standard nuts is 1.145 lb/ft of web crest with most of the weight in composite material. This weight is not objectionable near the wing root since it can be counted as wing bending material thereby reducing the cover skin requirement. Going outboard, the skins become so thin that web caps can no longer be subtracted from the cover material required and the web cap becomes excess wing weight. The excess material comes from the necessity of having web cap and cover self stable between bolts.

Also fabrication of the web cap provides a difficult layup task because of variations in layup thickness at each wing station.

Minimum Bolt Spacing Approach - Figure 25 shows a web-to-skin connection which was developed to overcome some of the objections to the preceding joint. The bolts are not utilized to their full shear strength which reduces the bearing load per bolt and the required composite thickness. While the number of bolts is increased, the total weight of the joint is decreased even in the areas of maximum wing shear loads. For the same shear loads and with comparable fasteners as in the preceding connection, this joint adds 0.550 lb/ft of crest to the web weight for 1-1/2-inch bolt spacing at the root.

0.550 LB/FT

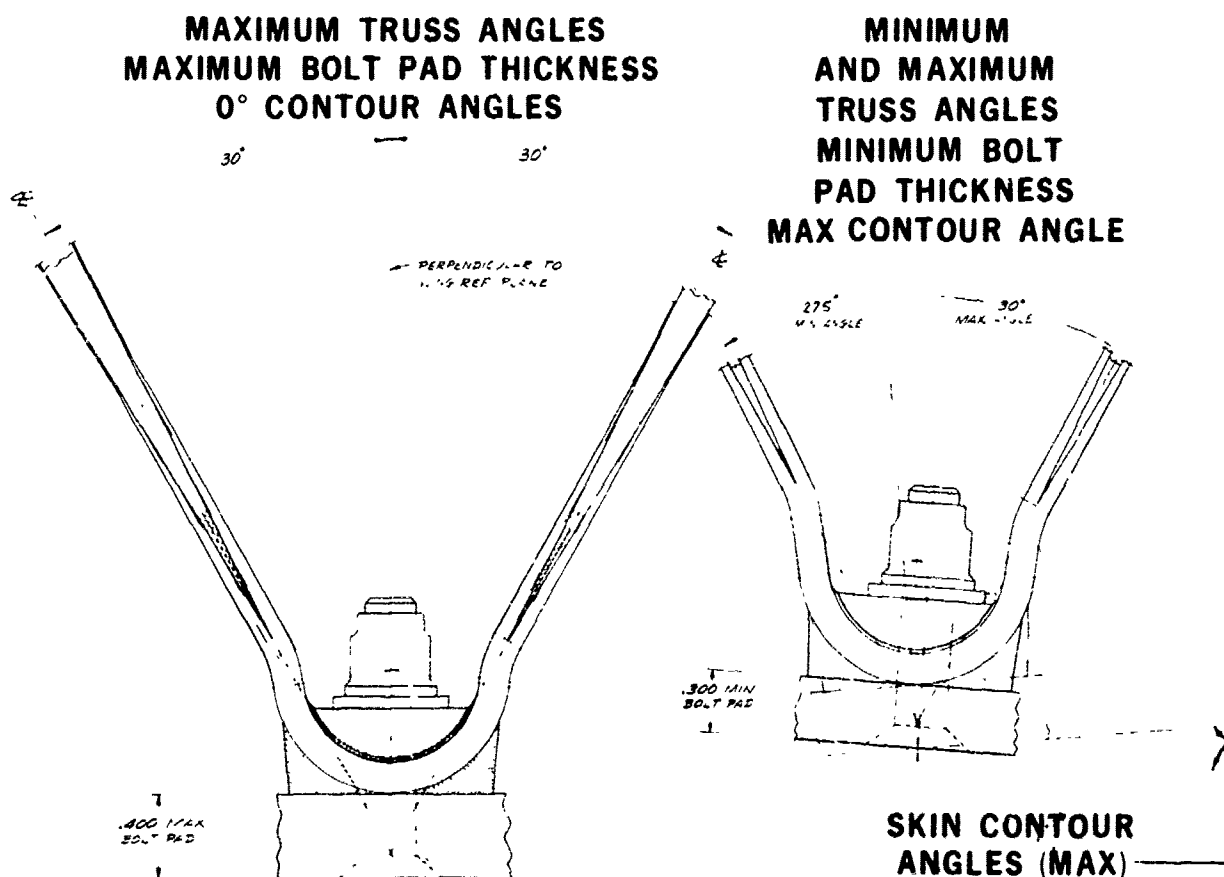


FIGURE 25. BOLTED COVER TO WEB JOINT - MINIMUM BOLT SPACING APPROACH

This joint configuration makes use of the thinner composite sections to provide constant composite cross sections which can accommodate varying web and skin angles to facilitate composite layup operations. The rounded end (or "kink") introduces some eccentricity and bending at the end of the webs. The reinforcing required for low bolt bearing stresses is adequate to resist the maximum axial load in the normal or unreinforced web. In areas where the web is reinforced to sustain highly concentrated truss loads the joint also will be reinforced.

Further improvements to the bolted joint were made as a corollary to the substructure lightning task (Paragraph 4.1.7) and the pressure panel study (Paragraph 4.1.6). It was found for this wing that shear loads in the webs were so low that full panel internal webs were not required. A "cutout web" concept was introduced to eliminate excess core, adhesive and minimum gage web skins. This made the substructure between front and rear pressure/shear webs into members resisting tension or compression and chordwise shear only. Also, the pressure panel study revealed the need for greater thickness in the cover panels at the web crests to limit chordwise bending stresses due to internal pressure. These two factors allowed a joint redesign which removed the reverse curve web kink and allowed a general lightening of the joint. Figure 26 shows a comparison of the orig-

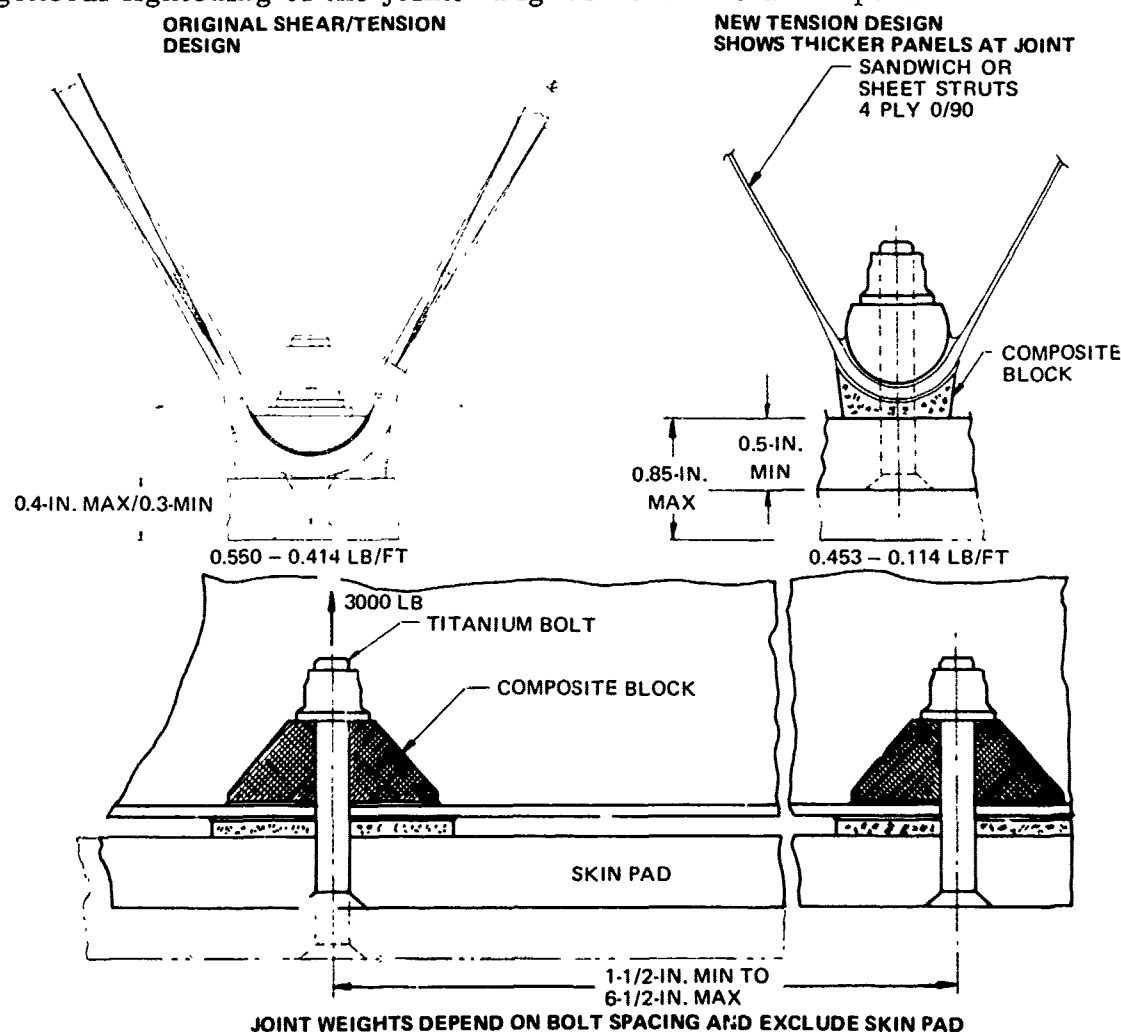


FIGURE 26. BOLTED JOINT DESIGN IMPROVEMENT

inal and improved joints. The bolt spacing (minimum bolt spacing approach) could now be increased in the outboard wing areas from a previous 4-inch to 6-1/2-inch maximum due to the thicker cover panel being more stable under compression between bolt supports. Figure 27 shows the improved design bolt spacing and section weights as a function of span. Bolt spacing was determined chiefly by pressure loads on cover panels. Actual design spacing (also shown in Figure 27) was worked out to practical considerations of the corrugated hat section lightened web concept (Paragraph 4.1.7).

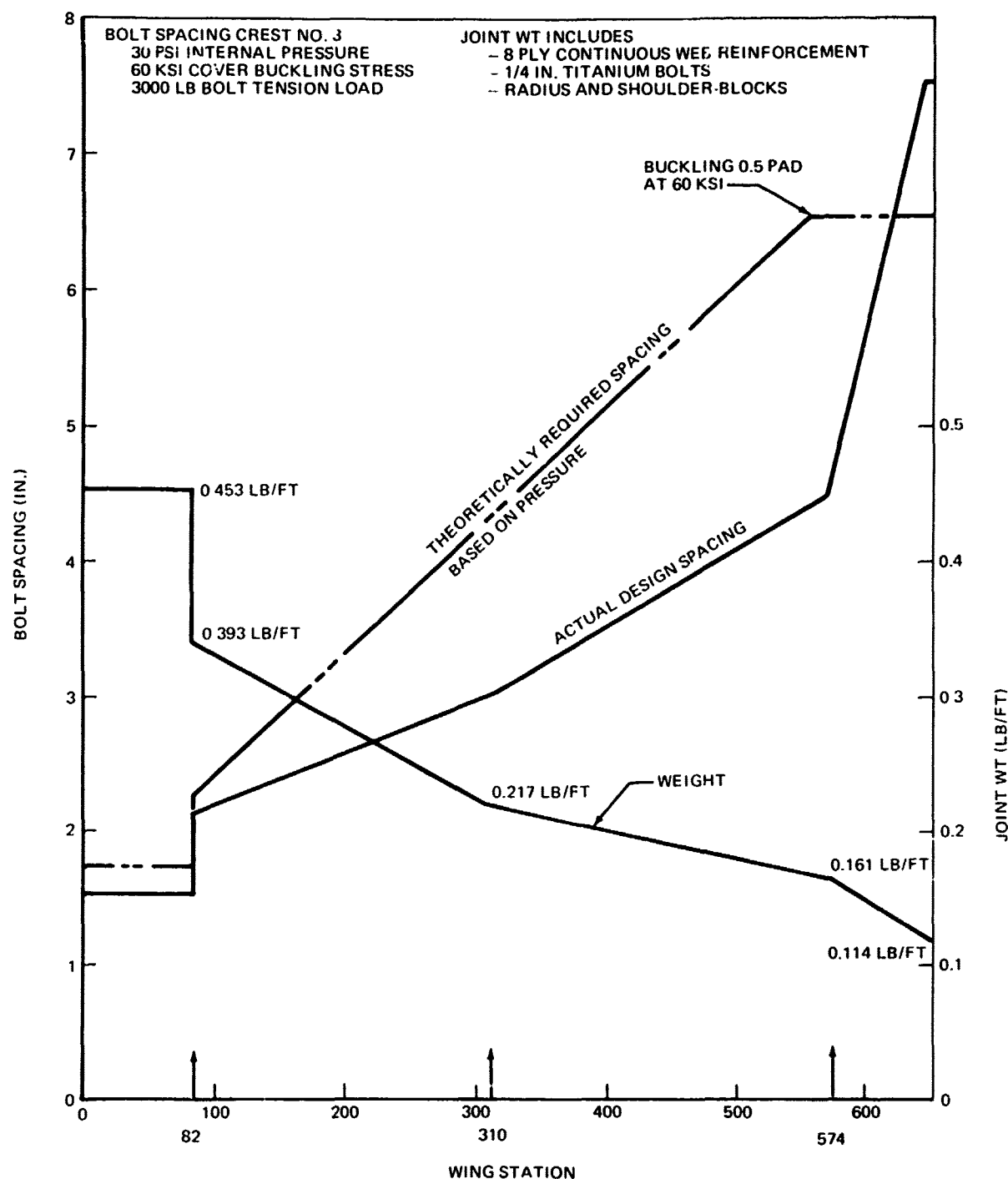


FIGURE 27. BOLT SPACING AND BOLTED JOINT WEIGHT

Bolted and Bonded Joints versus Optimum Configuration - As described for the shear-carrying web-to-cover joint, a kink was introduced into the web at the joint due to its universal application for varying truss and cover intersection angles. The kink was required due to the width of the nut bearing pad coupled with the constraint of intersecting truss load lines within the solid laminate portion of the cover. The kink is not required for a tension-only joint due to the longer bolt used at wider spacing. For the five-cell baseline wing, the kink joint was the lightest bolted shear connection as indicated in Figure 28.

The optimum configuration study (Paragraph 4.1.3) indicated the six-cell configuration to be minimum weight based on the same joint weights as the five-cell. Figure 28 shows the six-cell bolted joint wing configuration actually to have a greater joint weight. When optimum weight curves are drawn with the bolted joint weights varying with included web angle, the baseline five-cell configuration is seen to be true minimum weight. If the joints could be lightened by bonding, then the six-cell becomes the true minimum weight truss configuration, showing a sensitivity of configuration to joint type. The improved tension joint (Figure 26) may be usable with a six-cell configuration at a joint weight competitive with bonding but this was not investigated.

MINIMUM BOLT SPACING APPROACH

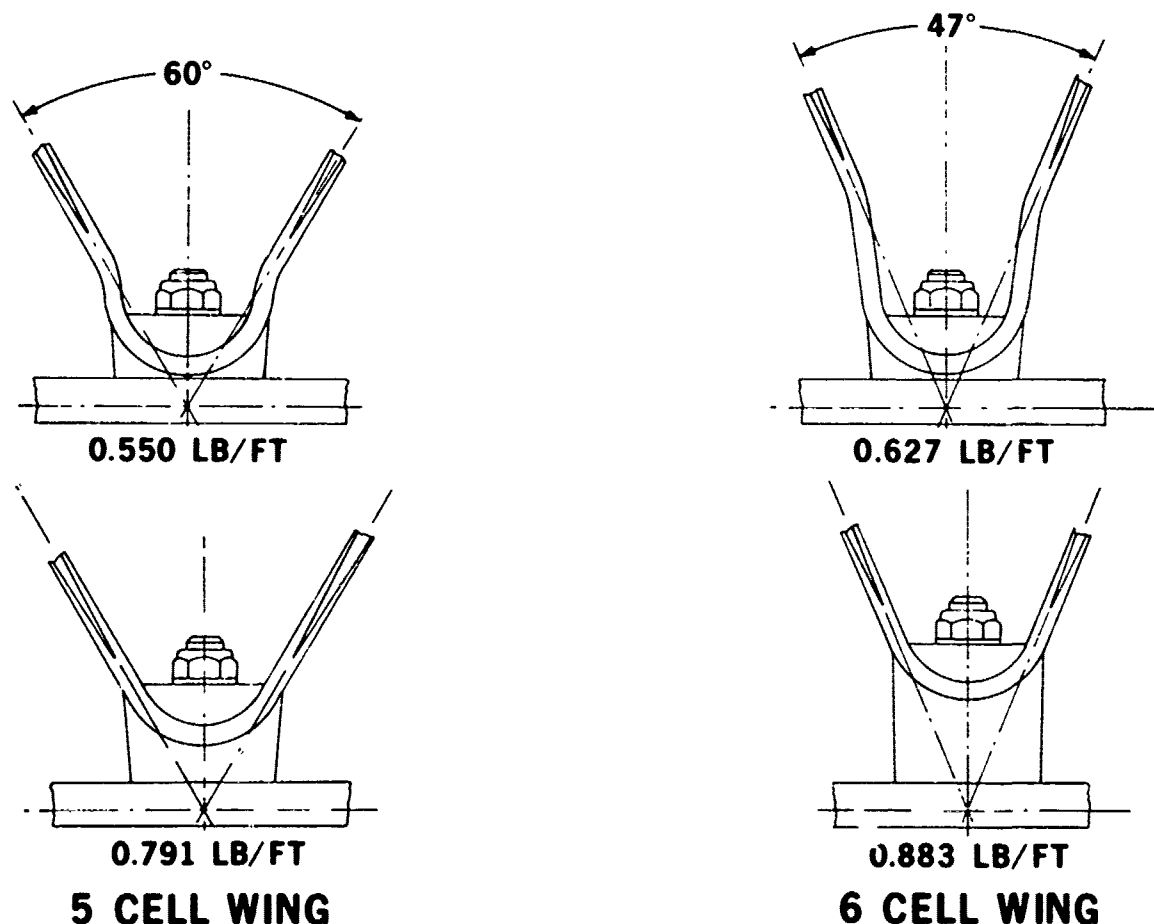


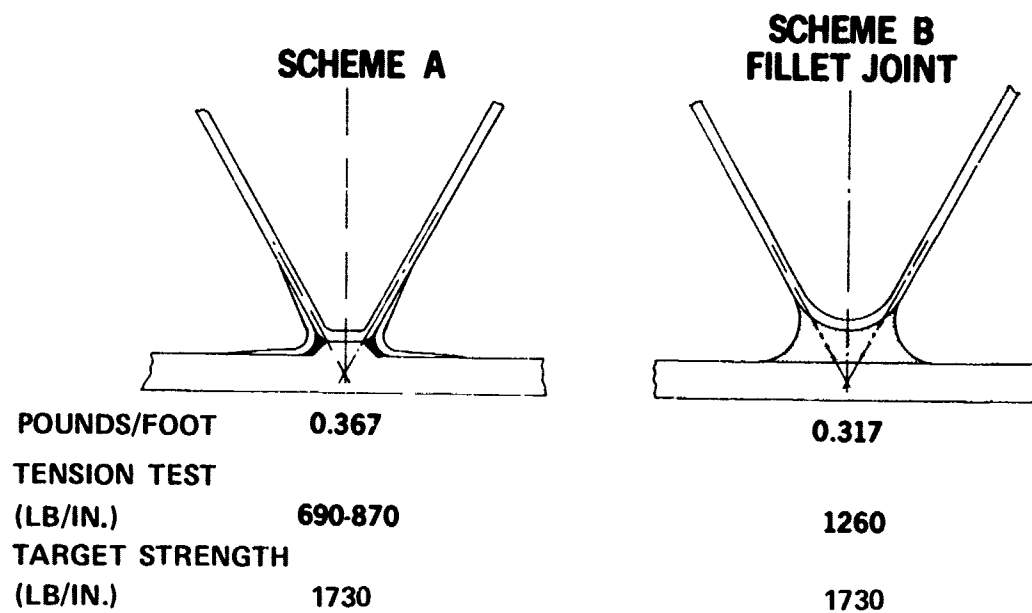
FIGURE 28. BOLTED JOINT INCLUDED - WEB-ANGLE GEOMETRY

The conclusion was reached that the optimum weight truss web with bolted shear joints was the five-cell configuration. The six-cell was optimum if lightweight bonded (or bolted tension-only) joints could be developed to accommodate the smaller included web angles. An extension of the truss web optimization study (Paragraph 4.1.3) showed no weight advantage for a seven-cell configuration over the six-cell using lightweight bonded joints. Also the inclusion of a lightened "cutout" truss web did not alter these basic optimization findings except to lower total weights. The above discussion also assumes that cover weights do not vary with joint type in order to isolate the effect of joint type. Actually, the stress concentration factors at the bolt holes would cause heavier covers as discussed elsewhere.

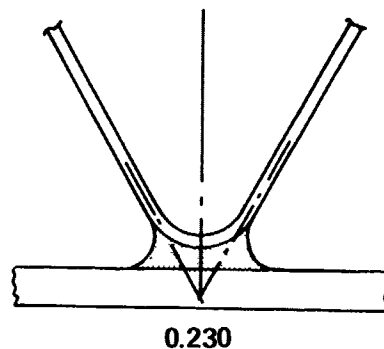
Bonded Web to Cover Connections - Various types of bonded joints were examined to reduce truss web to cover joint weight. Besides joint weight, wing cover weight due to the presence of bolt holes is the other factor making all-bonded joints attractive. Transferring shear loads does not present as much of a problem as transferring the tension loads produced by internal pressure, such as that caused by malfunction of the fuel filling system or aircraft roll maneuvers. The very low interlaminar tension strength of the composite must be satisfied by the bonded vee or tee joint. This value for Narmco 5206II is 2000-2500 psi which is lower than the tensile strength of the adhesive. Two primary types of bonded joints were prepared for testing (Section VII). Bonded joints Scheme A and Scheme B are shown in Figure 29 where it can be seen that the weights are less than for bolted joints.

Initial development tension test results were established using the Z3578686-1 and Z3578686-507 specimens (Figure 29). The Scheme B (or fillet) thick bondline joint appeared more attractive not only because of higher initial load capability but also it is less costly than the matched-bonded surfaces (Scheme A) concept with cocured reinforcing angles. A fillet bond material with the appropriate handling characteristics was selected from adhesive screening tests (Hysol EA9306) for the fillet bond. Although risks are associated with reliability of such a joint, its promise merited additional developmental work. During the testing of the fillet joint (Section VII) its configuration was modified to increase its strength and further lower its weight, i.e., the original 1/4-inch minimum bond thickness was reduced to 1/8 inch and weight from 0.317 to 0.230 lb/inch. See drawing Z3578686-511 in Appendix A.

It might be questioned why a very thick bondline design is expected to be as strong as a thin bondline. Theoretical analyses predict improved joint-strengths with thicker bondlines, subject to the assumption that bond properties do not change. Very thin (starved) glue lines are weaker than joints with 0.005-inch bondline, probably because of a magnification of local stress concentration effects and a lack of sufficient bond material. Experience has shown that relatively thick (0.030-inch) bondlines are weaker; however, the reason is poor quality of bond (voids, etc), due to processing problems. There is also the problem of increased eccentricity on unsupported single-lap joints. Unsupported single-lap joints are not recommended in design because they severely degrade the laminate load capacity ("Z" direction stresses) as well as that of the bond. Douglas is working to vacuum degas adhesive prior to application to obtain high quality material in the thick bondline.



IMPROVED FILLET JOINT
Z3578686-511



| | |
|-----------------------|-----------------------|
| POUNDS/FOOT | |
| TENSION TEST (LB/IN.) | 2412 (REPRESENTATIVE) |
| TARGET STRENGTH | 1730 |

FIGURE 29. BONDED-JOINT CONFIGURATIONS

Box Corner Joints - The front and rear webs (conventionally the spar webs) are subject to pressure and shear loads. The joints joining these webs to the covers experience lower direct tension loads than interior truss web joints but joint chordwise moment and peeling are increased. The rear web joint near the sweepbreak develops as much as 5280 lb/inch ultimate shear. Designing a bolted shear joint for this area appeared to be straightforward and was not worked out in any detail in this program. Attention turned to the bonded corner joint.

The bonded EA9306 adhesive fillet joint with metal adherends developed 5600 lb/inch at failure in the Z4569981-501 rail shear test series and testing at 160°F indicated a 27-percent shear strength reduction. Also, bonded joint design criteria required a strength capability of at least 25 percent better than surrounding laminates and 50 percent better in the adhesive. Further testing in shear with graphite adherends, rather than steel adherends, showed the laminate interlaminar shear and interlaminar tension strength to govern joint failure at a lower stress than could be achieved in the adhesive. Thus, it was apparent the basic bonded fillet joint design could not merely be scaled up geometrically to attain the required strength in high load areas.

The room temperature shear stress-strain curve of this fillet adhesive (EA9306) does not indicate a yield point. Even with adhesive yielding, it is doubted that bolts through this thick bondline joint (bonded/bolted) would increase joint shear strength. A double-step, fillet-bonded joint is proposed but was not worked out and tested in this program. An alternate design offering more than sufficient strength is a bonded/bolted double step joint utilizing a yielding (EA951) film adhesive and bolts. The latter requires closely fitted adherends and would require abandonment of the fillet-bond assembly concept, therefore it is de-emphasized in favor of further fillet bond development.

Joint peel is another development area for the fillet joint concept. The loop tension joint test series (Z3578686) used base plates with actual wing cover thickness which were thick enough to minimize plate bending at the toe of the fillet. The premature failure of the pressurized box beam specimen (Z5578687-501) was attributed to excessive plate bending at the toe of the fillet bond. In all such tension tests utilizing graphite adherends the failure consistently occurred by interlaminar tension with the laminate. A tension bolt through the center of the joint would help only if the EA9306 fillet adhesive had a stress-strain characteristic similar to EA951, since the stress concentration is at the edge of the joint. The bolt, of course, is undesirable since it doubles joint weight and adds cover stress concentrations as well. Interleaving adhesive plies between graphite plies to improve interlaminar tension strength and to add some ductility to the laminate is a promising concept. EA951 doubled interlaminar tension strength of Narmco 5206II and tripled that of Thornel 75S-1004 in screening tests. Testing at service temperature revealed excessive plate bending with interleaved EA951 so the proper material combination for the interleaved concept was not defined within the program. Sufficient strengths were obtained from joint shear, tension, and fatigue tests to warrant using Narmco 5206 plain laminates and EA9306 for fillet bonded program design verification specimens.

4.1.4.2 Wing to Fuselage Joint - The wing to fuselage reactions at truss Crests No. 1, 3 and 5 were defined from the output of the finite element analysis. A preliminary estimate for design indicated the highest load is at the rear web (Crest No. 5) of approximately 340,000 pounds tension during the wing maximum torque condition. A 1-1/4 fitting factor is included. Since this is a large load it was deemed best to divide the load between two 1-1/8-inch-diameter bolts for failsafe design. One of these bolts formed the basis for the subsequent design verification specimen design except the specimen was scaled down to 3/4-inch-diameter bolt to reduce specimen size. See Figure 30 and drawing Z5578687-503. The concept is a wraparound composite fitting with a tension bolt and a bearing block. This type of design fits nicely into the "V" formed by the diagonal webs and can be used in a number of places on the wing.

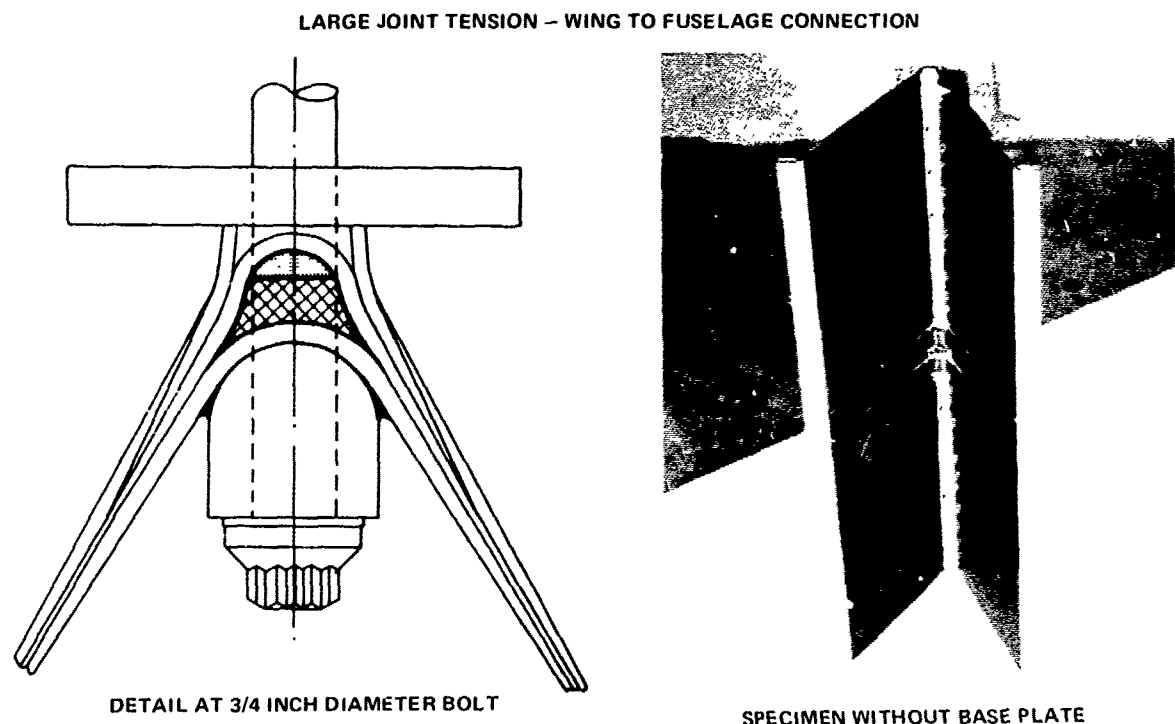


FIGURE 30. DESIGN VERIFICATION SPECIMEN A

Composite properties needed for design of this joint were flatwise crushing strength and the interaction curves for flatwise compression with in-plane tension. Because of this data lack, simple loop tension/bearing block specimens using 1/4-inch bolts were tested to develop allowables for the larger specimen tension straps (Z3578686-505). Test of the larger Z5578687-503 specimen verified the capability of this type design to be scaled up to the required loads and the same design was used for the rear bolt reaction area of the Z5569987-1 sweepbreak specimen.

Other load conditions, as well as bolt torquing apply compression loads to web crest bolt joints at the wing/fuselage intersection. In the case of the fillet bonded lower cover, it was doubted the EA9306 adhesive would have sufficient crushing strength without design development testing, therefore, the joint was designed with a graphite laminate bolt pad contacting, and film-bonded to the graphite lower cover. (See Z5569987 specimen drawing) This

removed one desirable feature of fillet bonding, the adjustable bondline thickness for assembly tolerance takeup. Compression testing of fillet-bonded major joints is recommended.

4.1.5 Materials Optimization Analysis

A weight study for several materials was conducted for the wing covers and webs. The materials which were evaluated are listed below.

Upper and Lower Covers:

Narmco 5206 Type II Graphite

Avco 5505 Boron

AS/286 Graphite

5206II/5206I Mixed Graphite (Type I in 45-degree plies)

Webs:

Narmco 5206 Type II Graphite

Thornel 75S Graphite

In this study, no attempt was made to optimize the core depth and face sheet design simultaneously. It has been assumed that buckling and fuel pressure bending requirements imposed on the panels governed the core depth, once the faces have optimally designed for the membrane loads derived from overall wing bending loads.

Each of the panels was subjected to membrane loads N_x , N_y , and N_{xy} derived from the finite element analyses. A computer program was written to determine the optimum orientation of plies for the multiple loading conditions and stiffness constraints dictated by previous flutter analyses. This program is described in detail in Reference 7. A summary of panel design and total weights of the covers and webs is presented in Tables 6 through 10, for each of the selected materials.

Some conclusions from the summary are:

- Mixed graphite covers do not offer sufficient weight reduction to be considered further. This comment is particularly pertinent, considering that the weight predictions were based on the maintenance of panel stiffness constraints only, and not strength. If mixed graphite is ever to be seriously considered, an elaborate strength check would be necessary. Exclusion of mixed 5206/Thornel 75 is discussed in 4.1.6.
- AS/286 graphite is heavier because of its lower stiffness properties.
- Avco 5505 boron upper cover weighs the least.
- Narmco 5206 Type II graphite lower cover and webs weigh the least.

TABLE 6
UPPER COVER FIBER PATTERNS (STRENGTH AND STIFFNESS)

| <u>STA</u> | <u>PANEL</u> | <u>5206 II</u> | <u>5505</u> | <u>AS/286</u> | <u>MIXED</u> |
|---------------|--------------|----------------|-------------|---------------|--------------|
| 20 | FWD | 28, 2, 12* | 20, 2, 8 | 38, 2, 12 | 28, 2, 12 |
| | MID | 30, 2, 8 | 22, 2, 8 | 42, 2, 8 | 30, 2, 8 |
| | AFT | 30, 2, 12 | 20, 2, 12 | 42, 2, 12 | 30, 2, 8 |
| 60 | FWD | 28, 2, 12 | 20, 2, 8 | 38, 2, 12 | 28, 2, 8 |
| | MID | 30, 2, 8 | 22, 2, 8 | 42, 2, 8 | 30, 2, 8 |
| | AFT | 30, 4, 12 | 20, 2, 12 | 42, 2, 12 | 30, 4, 8 |
| 107 | FWD | 28, 2, 12 | 20, 2, 8 | 38, 2, 12 | 28, 2, 8 |
| | MID | 30, 2, 8 | 22, 2, 4 | 42, 2, 8 | 30, 2, 8 |
| | AFT | 30, 2, 12 | 22, 2, 8 | 42, 2, 12 | 30, 2, 8 |
| 152 | FWD | 30, 2, 12 | 22, 2, 8 | 42, 2, 12 | 30, 2, 8 |
| | MID | 32, 2, 6 | 22, 2, 8 | 42, 2, 12 | 32, 2, 8 |
| | AFT | 30, 2, 8 | 20, 2, 8 | 40, 2, 12 | 30, 2, 8 |
| 202 | FWD | 20, 2, 16 | 14, 2, 12 | 26, 2, 20 | 20, 2, 12 |
| | MID | 20, 2, 12 | 14, 2, 8 | 28, 2, 16 | 20, 2, 8 |
| | AFT | 24, 2, 8 | 18, 4, 8 | 28, 2, 12 | 24, 2, 8 |
| 257 | FWD | 18, 2, 12 | 14, 4, 12 | 20, 2, 16 | 18, 2, 8 |
| | MID | 20, 2, 16 | 12, 6, 12 | 26, 2, 24 | 20, 2, 12 |
| | AFT | 22, 8, 12 | 20, 8, 8 | 30, 2, 20 | 22, 8, 8 |
| TOTAL WEIGHT: | | 356.11 LB | 344.18 LB | 407.38 LB | 352.21 LB |

TABLE 7
UPPER COVER FIBER PATTERNS (STRENGTH ONLY)

| <u>STA</u> | <u>PANEL</u> | <u>5206 II</u> | <u>5505</u> | <u>AS/286</u> | <u>MIXED</u> |
|---------------|--------------|----------------|-------------|---------------|--------------|
| 20 | FWD | 12, 4, 8* | 10, 2, 8 | 8, 2, 12 | 12, 4, 8 |
| | MID | 12, 4, 8 | 8, 2, 12 | 10, 2, 12 | 12, 4, 8 |
| | AFT | 14, 2, 12 | 12, 2, 12 | 10, 2, 16 | 14, 2, 8 |
| 60 | FWD | 12, 2, 8 | 10, 2, 8 | 8, 2, 12 | 12, 2, 8 |
| | MID | 10, 2, 12 | 10, 2, 8 | 10, 2, 12 | 10, 2, 8 |
| | AFT | 20, 2, 16 | 16, 2, 16 | 16, 2, 20 | 20, 2, 12 |
| 107 | FWD | 14, 2, 4 | 12, 2, 4 | 10, 2, 8 | 14, 2, 4 |
| | MID | 16, 2, 4 | 12, 2, 4 | 16, 2, 4 | 16, 2, 4 |
| | AFT | 22, 2, 8 | 16, 4, 8 | 18, 2, 12 | 22, 2, 8 |
| 152 | FWD | 16, 4, 4 | 12, 4, 4 | 18, 4, 4 | 16, 4, 4 |
| | MID | 16, 2, 4 | 12, 4, 4 | 16, 4, 4 | 16, 2, 4 |
| | AFT | 18, 2, 8 | 12, 4, 8 | 14, 2, 12 | 18, 2, 8 |
| 202 | FWD | 16, 2, 4 | 12, 2, 4 | 14, 4, 4 | 16, 2, 4 |
| | MID | 14, 4, 8 | 12, 4, 8 | 14, 2, 12 | 14, 4, 8 |
| | AFT | 24, 2, 8 | 18, 4, 8 | 18, 2, 12 | 24, 2, 8 |
| 257 | FWD | 18, 2, 12 | 14, 4, 12 | 18, 2, 12 | 18, 2, 8 |
| | MID | 14, 8, 8 | 10, 8, 8 | 16, 10, 8 | 14, 8, 8 |
| | AFT | 22, 8, 12 | 20, 8, 8 | 20, 12, 12 | 22, 8, 8 |
| TOTAL WEIGHT: | | 243.69 LB | 270.91 LB | 221.27 LB | 249.69 LB |

*CODE: L, M, N
 L = NO. OF 0° PLIES
 M = NO. OF 90° PLIES
 N = NO. OF ±45° PLIES

TABLE 8
LOWER COVER FIBER PATTERNS (STRENGTH AND STIFFNESS)

| <u>STA</u> | <u>PANEL</u> | <u>5206 II</u> | <u>5505</u> | <u>AS/286</u> | <u>MIXED I/II</u> |
|---------------|--------------|------------------------|------------------------|------------------------|-----------------------|
| 20 | FWD AFT | 20, 2, 8* 34, 2, 12 | 16, 2, 8 24, 4, 12 | 26, 4, 8 46, 2, 16 | 20, 2, 8 34, 2, 8 |
| 60 | FWD AFT | 20, 4, 4 34, 2, 16 | 14, 2, 8 24, 2, 20 | 26, 2, 8 46, 2, 20 | 20, 4, 4 34, 2, 12 |
| 107 | FWD AFT | 22, 4, 4 34, 2, 12 | 14, 2, 8 26, 2, 8 | 26, 2, 8 46, 2, 16 | 22, 4, 4 34, 2, 8 |
| 152 | FWD AFT | 24, 2, 4 28, 2, 8 | 16, 2, 8 20, 2, 8 | 32, 2, 4 38, 2, 8 | 24, 2, 4 28, 2, 8 |
| 202 | FWD AFT | 16, 2, 12 22, 4, 12 | 14, 2, 12 20, 2, 12 | 22, 2, 12 32, 2, 12 | 16, 2, 8 22, 4, 8 |
| 257 | FWD AFT | 26, 2, 8 24, 2, 20 | 18, 4, 8 22, 2, 12 | 34, 4, 8 32, 2, 24 | 26, 2, 8 24, 2, 16 |
| TOTAL WEIGHT: | | 262.21 LB | 278.69 LB | 298.01 LB | 261.95 LB |

TABLE 9
LOWER COVER FIBER PATTERNS (STRENGTH ONLY)

| <u>STA</u> | <u>PANEL</u> | <u>5206 II</u> | <u>5505</u> | <u>AS/286</u> | <u>MIXED I/II</u> |
|---------------|--------------|-------------------------|------------------------|------------------------|-----------------------|
| 20 | FWD AFT | 12, 2, 12* 18, 2, 16 | 12, 2, 12 16, 2, 16 | 18, 2, 12 22, 2, 20 | 12, 2, 8 18, 2, 12 |
| 60 | FWD AFT | 12, 4, 8 26, 2, 20 | 12, 2, 8 24, 2, 20 | 16, 2, 12 32, 2, 24 | 12, 4, 8 26, 2, 16 |
| 107 | FWD AFT | 16, 2, 8 24, 6, 8 | 14, 2, 8 26, 2, 8 | 18, 2, 12 38, 2, 8 | 16, 2, 8 24, 6, 8 |
| 152 | FWD AFT | 16, 4, 8 20, 4, 8 | 16, 2, 8 16, 2, 12 | 24, 2, 8 26, 2, 12 | 16, 4, 8 20, 4, 8 |
| 202 | FWD AFT | 14, 2, 12 22, 4, 12 | 14, 2, 12 20, 2, 12 | 20, 2, 12 32, 2, 12 | 14, 2, 8 22, 4, 8 |
| 257 | FWD AFT | 14, 6, 8 20, 6, 12 | 14, 4, 8 22, 2, 12 | 22, 2, 12 32, 4, 12 | 14, 6, 8 20, 6, 8 |
| TOTAL WEIGHT: | | 226.10 LB | 270.02 LB | 249.91 LB | 227.62 LB |

*CODE: L, M, N
 L = NO. OF 0° PLIES
 M = NO. OF 90° PLIES
 N = NO. OF ±45° PLIES

TABLE 10
WEB STRUCTURE PATTERNS

| STA | PANEL | (STRENGTH AND STIFFNESS) | | (STRENGTH ONLY) | |
|---------------|-------|--------------------------|-----------|-----------------|-----------|
| | | 5206 II | 75 S | 5206 II | 75 S |
| 20 | FWD | 2, 2, 8* | 2, 2, 4 | 2, 2, 4 | 2, 2, 4 |
| | AFT | 2, 2, 8 | 2, 2, 4 | 2, 2, 4 | 2, 2, 4 |
| 60 | FWD | 2, 2, 8 | 2, 2, 8 | 2, 2, 4 | 2, 2, 8 |
| | AFT | 2, 2, 8 | 2, 2, 8 | 2, 2, 4 | 2, 2, 8 |
| 107 | FWD | 2, 2, 8 | 2, 2, 8 | 2, 4, 4 | 2, 2, 8 |
| | AFT | 2, 2, 16 | 4, 4, 20 | 2, 2, 16 | 4, 4, 20 |
| 152 | FWD | 2, 2, 8 | 2, 2, 8 | 2, 2, 4 | 2, 2, 8 |
| | AFT | 2, 2, 12 | 2, 4, 16 | 2, 2, 12 | 2, 4, 16 |
| 202 | FWD | 2, 2, 12 | 2, 2, 4 | 2, 2, 4 | 2, 2, 4 |
| | AFT | 2, 2, 12 | 2, 4, 16 | 2, 2, 12 | 2, 4, 16 |
| 257 | FWD | 2, 2, 12 | 2, 6, 16 | 2, 2, 12 | 2, 6, 16 |
| | AFT | 2, 6, 16 | 4, 6, 20 | 2, 6, 16 | 4, 6, 20 |
| TOTAL WEIGHT: | | 85.76 LB | 133.59 LB | 71.75 LB | 133.59 LB |

*CODE: L, M, N L = NO. OF 0° PLIES
 M = NO. OF 90° PLIES
 N = NO. OF ±45° PLIES

4.1.6 Cover Optimization

4.1.6.1 Laminate Selection - Final materials optimization for cover strength and stiffness was covered in the preceding paragraph. The materials used in that study were considered practical for cover fabrication and the stiffness requirements were those due to composite wing flutter optimization.

The preliminary materials optimization study had indicated mixed Avco 5505/Thornel 75, mixed Thornel 75/Narmco 5206II and Boron/Aluminum to be promising candidates for optimum weight materials (Paragraph 4.1.2). Experimental work was undertaken to determine preliminary allowables for the high-modulus/high-strength graphite mixture, since both boron/aluminum and boron/graphite were excluded except for theoretical consideration by agreement with the Air Force Materials Laboratory. The experimental work showed that Thornel 75-1004 did not have sufficient interlaminar shear strength to be a practical material for wing design (Section VI). In the meantime, however, an interim study of optimum cover materials, including the mixtures, had been accomplished and it will be reported here.

A laminate optimization program, STOP3 (developed by Northrop Corporation under Air Force funding), was utilized to determine the optimum laminate pattern. This program increments ply orientations by a specified amount to pick the optimum number and orientation. The increment specified in this study was 45 degrees. Internal loads (N_x , N_y , N_{xy}) from the finite element analysis, plus a shear stiffness originating from the wing torsional stiffness requirement were input to STOP3. The internal chordwise loads

N_y , are relatively small as determined from the finite element analysis, so that these loads are likely to exhibit a large percentage error. To be conservative, both values $\pm N_y$ were input to STOP3. The torsional stiffness requirement was the same as that reported in Reference 2, specifically, a demand for equal torsional rigidity to that reflected by the metal STOL wing.

The optimum number of plies in 0, ± 45 , and 90 degree orientations for both upper and lower cover panels were determined using four different material combinations. The material combinations considered are:

- 5206 graphite, type II
- 5505 boron
- 5206 graphite (0- , 90-degree plies)/Thornel 75S (45-degree plies)
- 5505 boron (0- , 90-degree plies)/Thornel 75S (45-degree plies).

Figure 31 was used to determine the number of ± 45 ply replacement by Thornel 75S since STOP3 could not be used for mixed materials. The skin weights for the upper and lower covers, each with the above four material combinations are shown in Figures 32 and 33. In both covers, it is again noted the lower weight designs are theoretically possible with Thornel 75 shear plies. However, compression and bolted-joint tests (described in Section VI) with this mixed-graphite laminate revealed inadequate interlaminar strength to benefit from this concept at present.

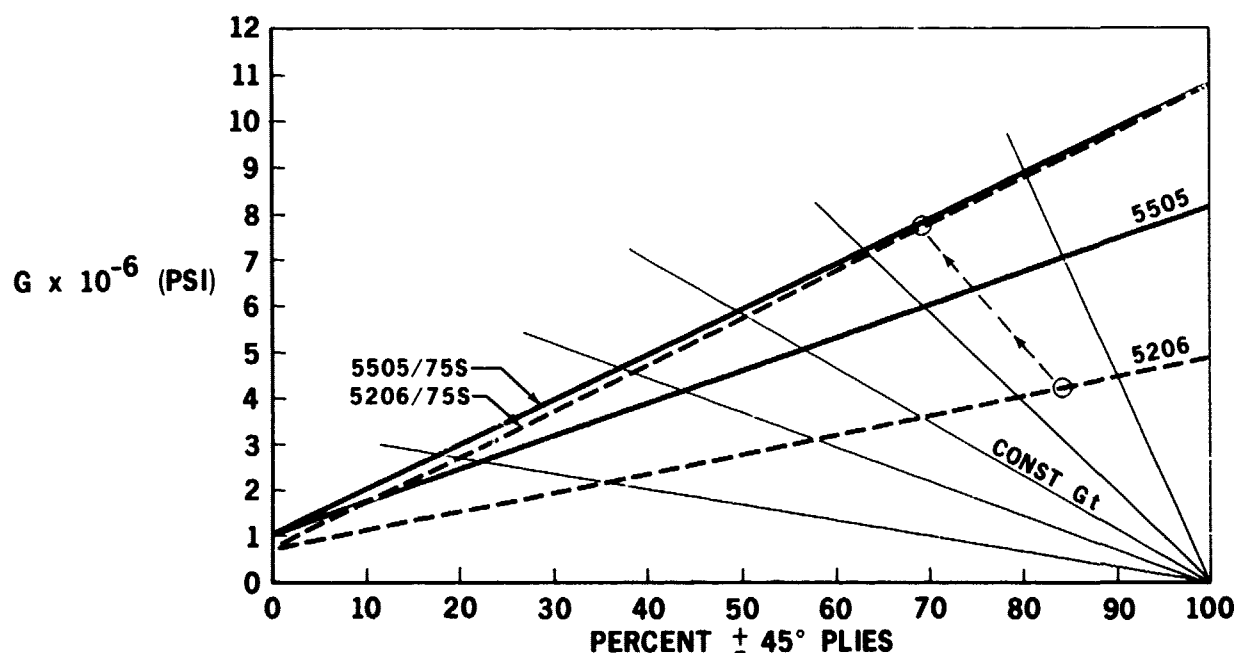


FIGURE 31. LAMINATE SHEAR STIFFNESS

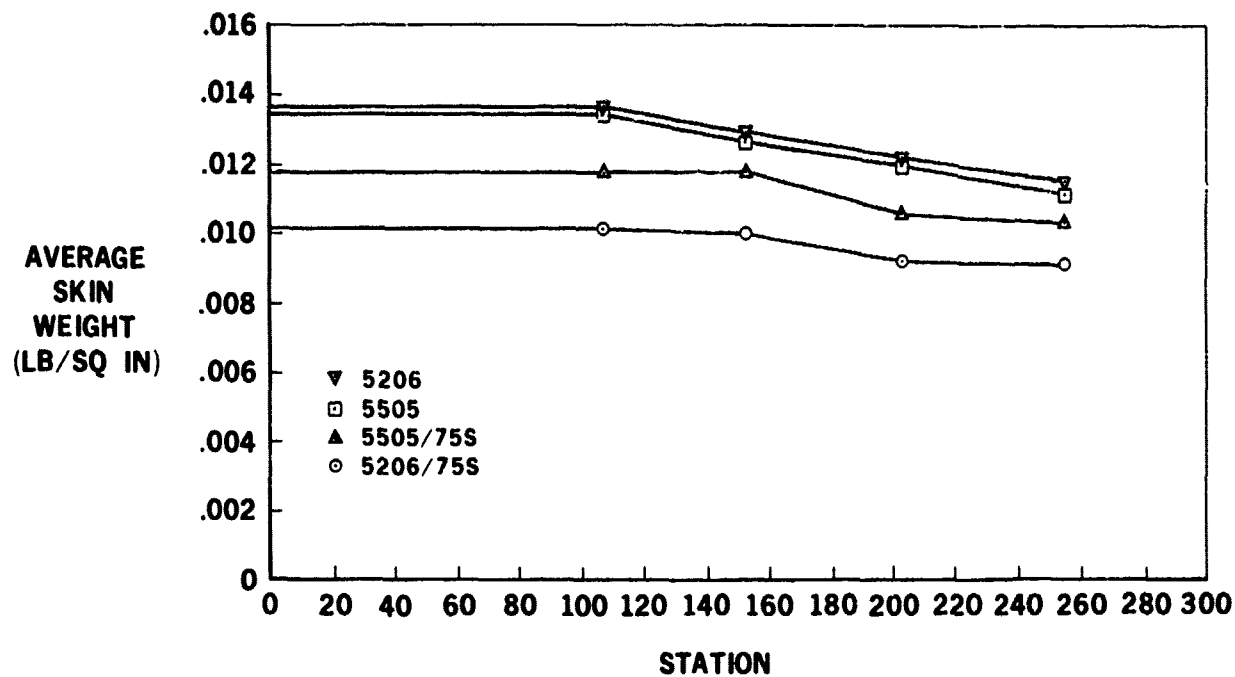


FIGURE 32. UPPER SKIN WEIGHTS (BONDED CONSTRUCTION)

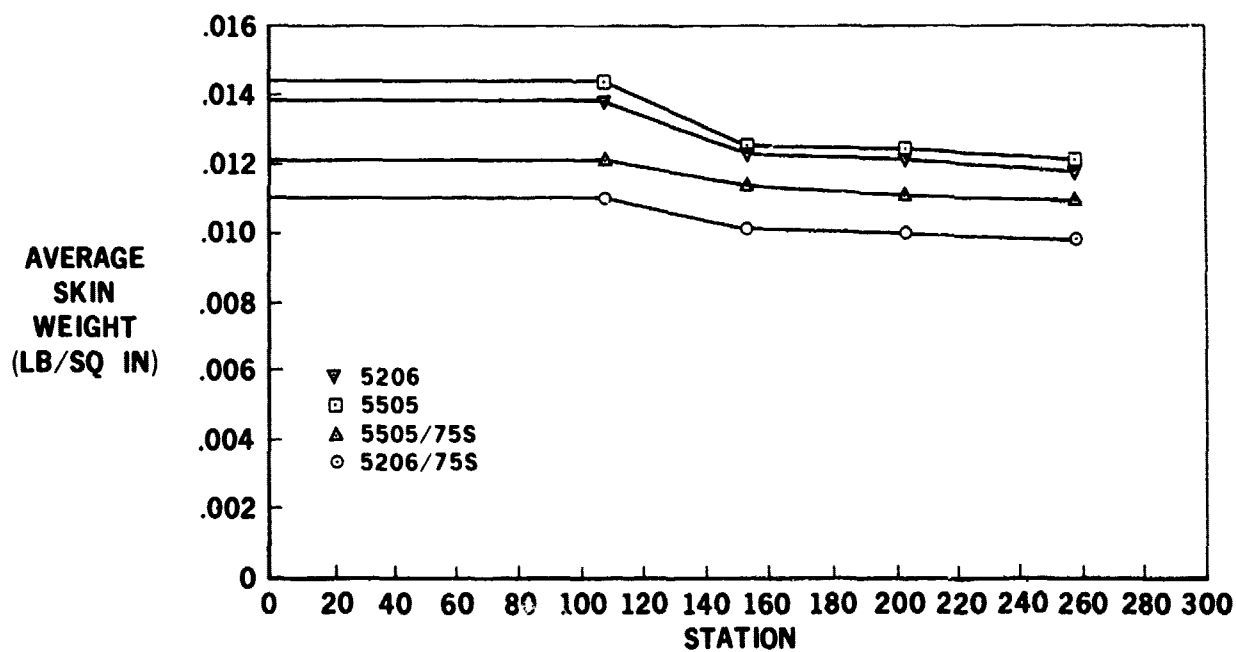


FIGURE 33. LOWER SKIN WEIGHTS (BONDED CONSTRUCTION)

Since Thornel 75 was unable to develop its potential, attention turned to other mixed materials in the attempt to achieve the theoretical optimum material. These were GY70/5206II, 5206I/5206II, and 5206II/boron film combinations. The film was supplied by National Research Corporation. Test results are presented in Section VI. The 5206I/5206II was the selected mixed material based on highest interlaminar and compressive strengths and it was used for the aforementioned final materials optimization analysis (Paragraph 4.1.5). The boron film/graphite fiber mixture achieved even better results in the screening tests; however, it was judged in too-embryonic a developmental stage to consider for full wing application at present.

Several factors conspired to eliminate the mixed graphite concept from the final baseline wing design.

The torsional stiffness requirement, which motivated the use of VHM mixed graphite, was modified by a Company-funded composite wing flutter stiffness study. The result is shown in Figure 34 and shows the GJ requirement based on the AMST metal wing is a needless constraint on the composite wing. Reference 5 includes additional material on the optimization of wing cover laminates for flutter. The new GJ/EI requirement was adopted for the program and used for the final cover laminate optimization.

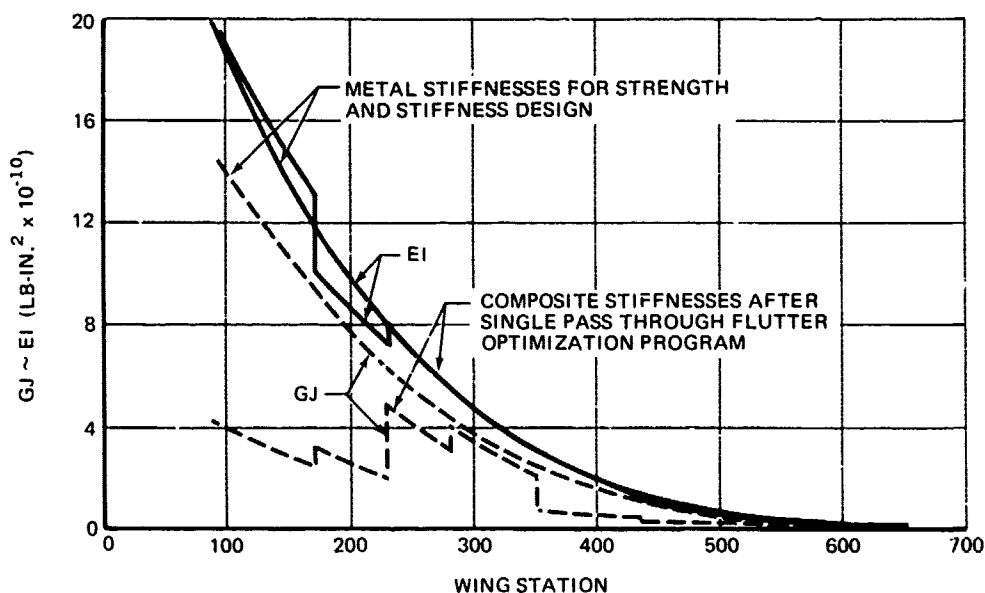


FIGURE 34. METAL VERSUS COMPOSITE WING STIFFNESS REQUIREMENTS

An upgrading of strength and stiffness allowables for 5206II based on receiving inspection testing batch records and the reduced stiffness requirements combined to eliminate even the mixed 5206I/II. Mixed 5206I/II was only 1/2 percent lighter in the lower cover than all-5206II; so to reduce cost, an all-Type II lower cover was selected for the recommended baseline wing. Also, mixed Type I/Type II graphite was 1 percent lighter than all-Type II for the upper cover, but the Avco 5505 was 2.2 percent lighter than the mixture. An all-boron upper (compression) cover was thus selected.

The introduction of stress concentrations due to bolting either cover was neglected in these optimization studies but it is judged, based on present estimates of K_T for the various materials and ply patterns, that bolting will not change the relative weights.

4.1.6.2 Stress Concentration Relief Provisions - It was recognized that the converging web crest geometry posed a problem to the selected stress concentration relief technique which utilized glass strips at spanwise bolt lines to locally replace graphite or boron 0-degree fibers. Convergence between adjacent crestlines can amount to 0.5 degree. A preferred design provision for stress relief strips is illustrated in Figure 35. In this concept, each web crest establishes its own 0-degree direction which requires the spanwise 0-degree layers to butt splice at the center of each upper cover panel and at crest number three in the lower cover. Stress relief strips change direction at the sweepback since web crests also change direction at that location. The 0-degree layer splices associated with each (0/+45/90) 4-ply group continue across the wing center section to fuselage centerline without direction change where an isotropic group pattern splice is effected. Forty-five- and 90-degree layer directions are not changed to conform to the variable 0-degree direction for a half wing. The extra zeros in the general pattern (those in excess of isotropic) change direction at the sweepbreak by means of overlapping those plies changing direction as indicated in the triangular area of Figure 35.

Alternate solutions for spanwise stress relief are to collect the 0-degree fibers into caps adjacent to each web crest, Figure 36, or to require parallel crestlines, Figure 37. The first idea leaves only 45- and 90-degree plies in the covers, which is good for both spanwise stress relief and pressure panel design. More importantly, however, it is better design philosophy to keep the 0-degree layers distributed across the wing chord rather than collect them into "caps" which would lead to splicing, load introduction, and load direction-change design problems. The truss web configuration change (Figure 37) illustrates the problems in the outboard wing for such a concept. It can hardly be of optimum weight from the standpoint that outboard panels are as wide as at the wing root and are subject to the same pressure load requirements as inboard panels, yet inplane load requirements are much reduced.

The addition of bolts in the fillet bonded edges of the baseline graphite lower cover for leading and trailing edge attachment will require stress relief to avoid cover weight penalties. Isolated bolts will occur through the bonded fillet joint, but these are generally for chordwise loads and stress concentration can be handled by localized doublers. The degree of stress relief offered by the rigid adhesive attached to the laminate around a bolt hole is unknown and is assumed to be negligible at this time.

An additional complication is introduced in order to achieve the minimum weight stiffened cover panel which is essentially designed by normal pressure rather than inplane stability alone. See the Pressure Panel Study (Paragraph 4.1.6.3) and Panel Stiffening Study (Paragraph 5.2). This complication is a pattern change in the covers along web crestlines in order to enrich the proportion of 90-degree plies and thereby reduce the solid laminate thickness requirements at panel edges. Figure 38 indicates a technique for integrating this pattern change with the stress concentration relief provisions. Glass 90-degree plies are used in the band of solid laminate along web crests with

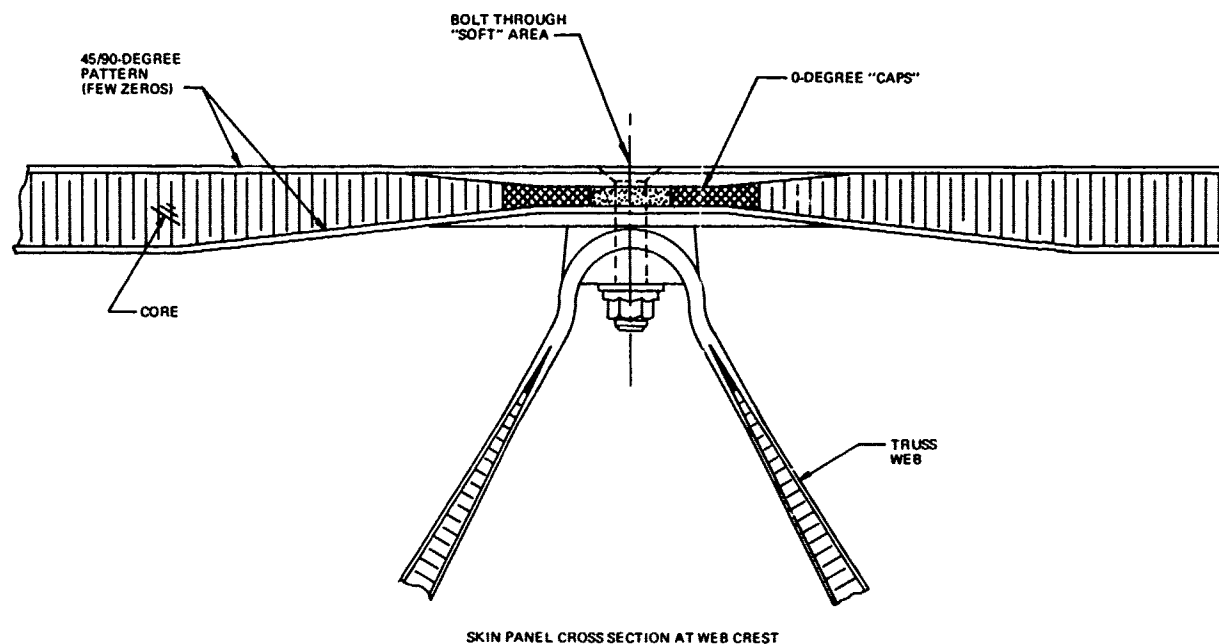


FIGURE 36. COLLECTED ZERO DEGREE FIBER CAPS

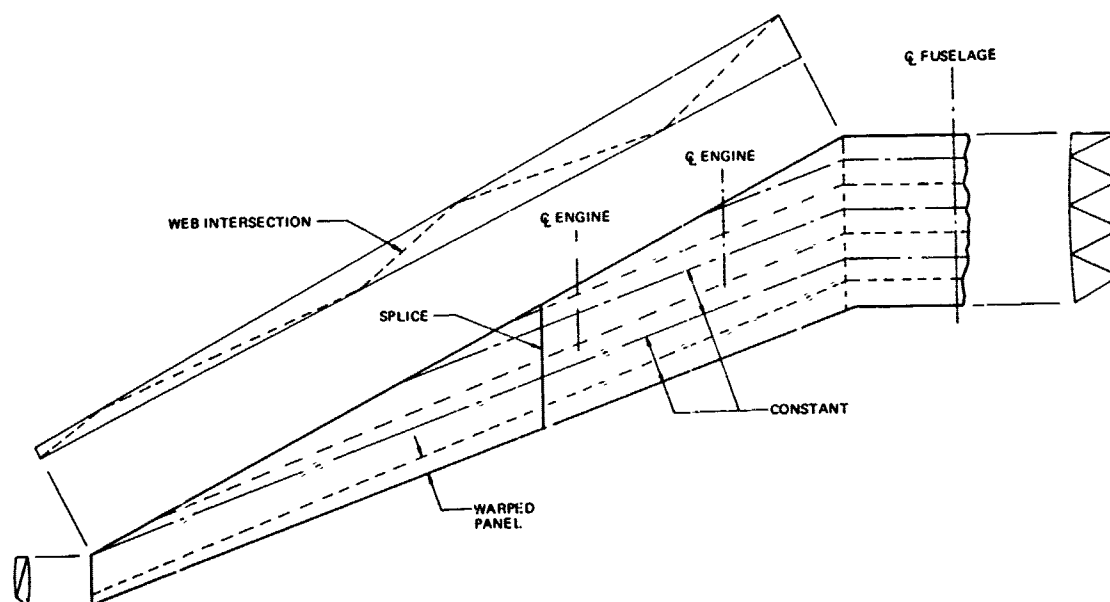


FIGURE 37. PARALLEL WEB CREST CONFIGURATION

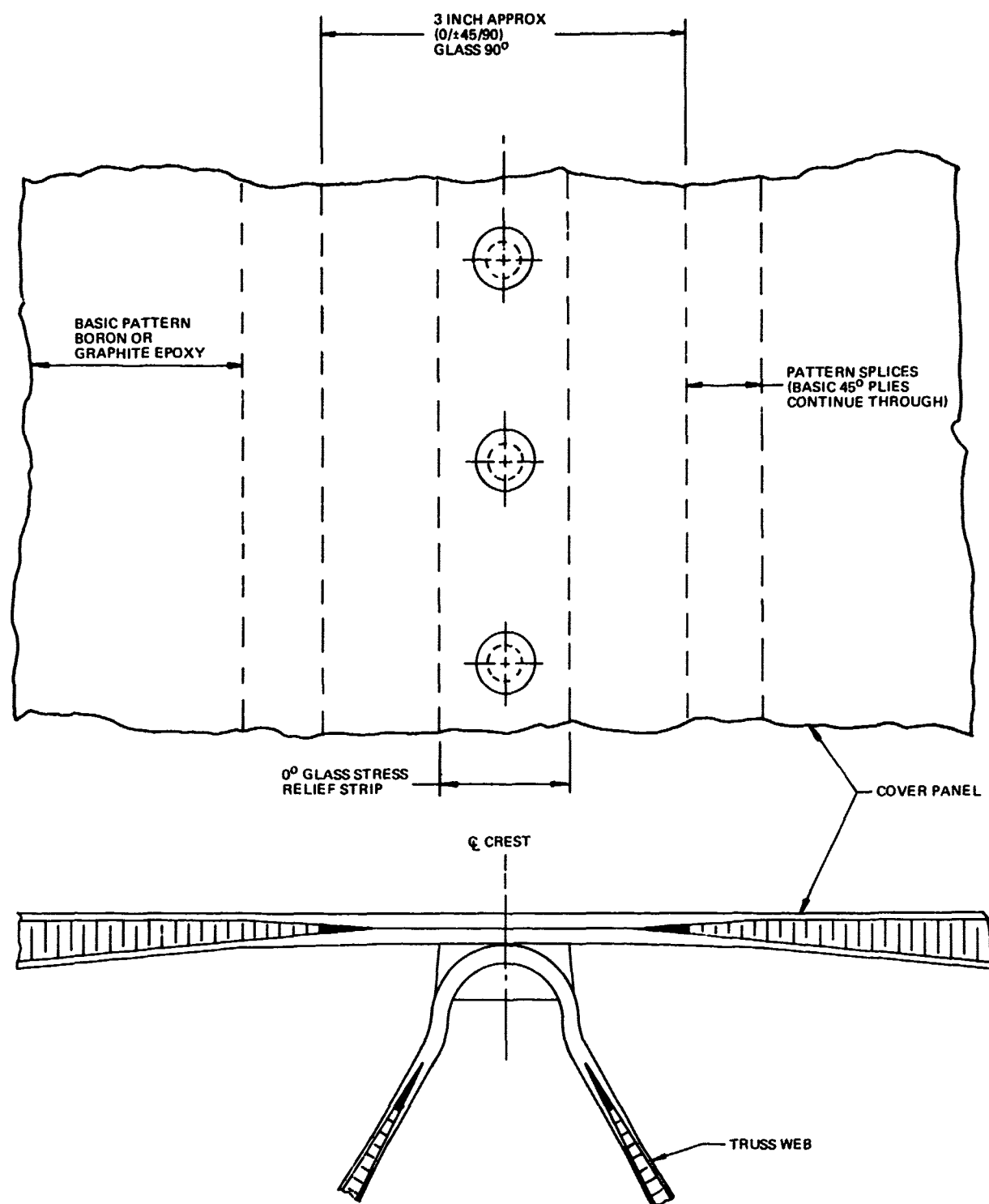


FIGURE 38. COVER PANEL PATTERN AND MATERIAL CONCEPT AT WEB CREST LINES

local 0-degree SCR glass plies. The 90-degree glass plies reduce the laminate local chordwise modulus without sacrificing bending strength. This moves the chordwise bending inflection point (due to pressure) closer to the web crest and minimizes laminate thickness.

In anticipation of this mixed glass/boron or glass/graphite concept at web crests, bearing and shearout tests were conducted on such laminates. See specimen drawing Z3569985 and test results in Paragraph 7.5. The data indicate that this mixed materials concept is at least as good as the all-graphite or all-boron laminates for bolted joint load transfer and it also offers reduced chordwise stress concentration factor.

The complexities introduced by these measures are deemed less costly than an equivalent bond assembly of separate parts to achieve the same least-weight design objective.

4.1.6.3 Pressure Panel Optimization Study - The covers are generally constructed of advanced composite face sheets and fiberglass honeycomb and are of infinite aspect ratio. The face sheets are sized by the finite element analyses for membrane loading. The honeycomb core depth is sized by buckling and the fuel pressure condition. For the panels investigated, it appeared that the fuel pressure condition governs the core sizing.

The following three configurations of the cover panels were investigated for the fuel over-pressure condition:

- uniform section
- parabolic shaped section
- fully stressed shape section.

Except for the last of these configurations, the core sizing at the nodes was conservatively assumed to be governed by the fixed-end moment existing in a beam model, simply supported at one edge, and fixed at the other. For the fully stressed design, a fixed-fixed beam model was used. The core sizing at the middle of the span was conservatively assumed to be governed by a beam model simply supported at each end. In each case, the beam was loaded by a uniform load of 30 pounds per inch. The most critical panel for this fuel pressure loading is the forward, lower cover panel spanning 50 inches at Station 107. Of the configurations investigated, the parabolic shaped section with local strengthening at the nodes is the more appealing from a practical viewpoint of designing the truss web joints. The designs of each of the above three configurations with their respective weights are shown in Figure 39.

From this preliminary optimization, it was apparent further optimization of the parabolic panel edges would remove additional weight. To obtain panel thickness dimensions for use throughout the wing design a generalized computer analysis was programmed.

Concurrently, the 30-psi ultimate pressure criterion was changed to 20 psi. Fuel bulkheads with flapper valves spaced at appropriate locations can limit fuel inertia load in the outboard wing due to roll maneuvers and it is much less a penalty for the fuel system than the composite structure to limit fuel

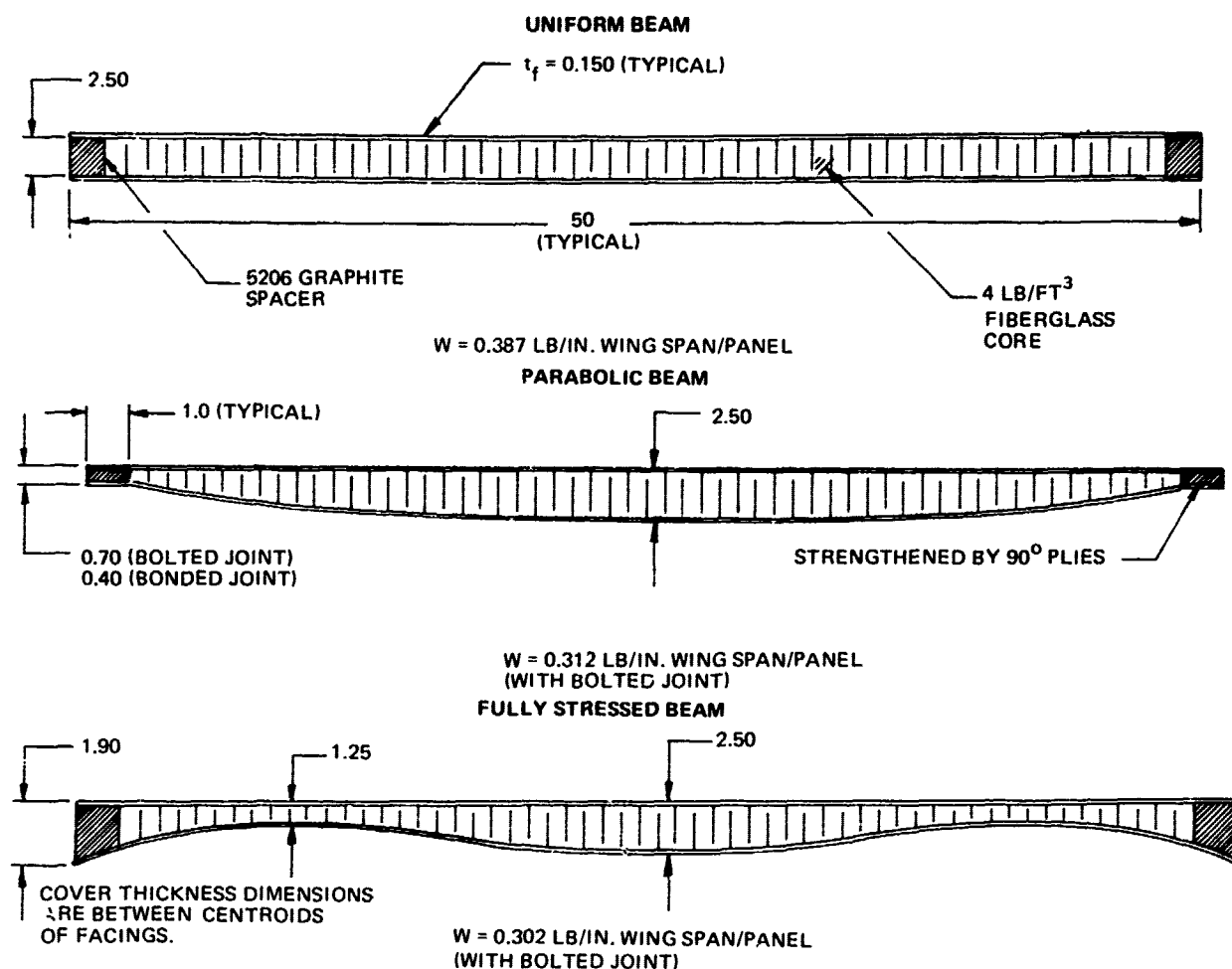


FIGURE 39. PANEL DESIGNS FOR PRESSURE CONDITION

overflow pressure to 11.6 psi limit. The fuel vapor explosion suppression criterion had not been established for the AMST operational vehicle, therefore, no arbitrary criterion was established for this program.

A thin rectangular sandwich beam of variable thickness under the action of uniform pressure was analyzed. The beam was rigidly built-in at the two ends. Over a small portion of the length from the two ends, the beam thickness was constant and then increased symmetrically, with respect to the midspan, until a maximum thickness was reached at the midspan. The purpose of this analysis was to determine the beam thicknesses, both at the built-in ends and at the midspan, such that the maximum bending stresses at these locations just reached the allowable stress of the material.

Reference 6 describes the derivation and method. Figure 40 shows idealizations from that reference. A computer program was developed and calculations for 80 different beam configurations were obtained. This represented 40 cases with generous l_1 (end beam lengths) and 40 cases with minimum l_1 . Four representative panels (front, rear, upper, lower) were taken at six stations along the wing span. Within a set of 40 cases, some upper and lower panels were represented with pseudoisotropic, rather than "design" laminate, patterns in the end beams to determine the effect on panel dimensions and weights.

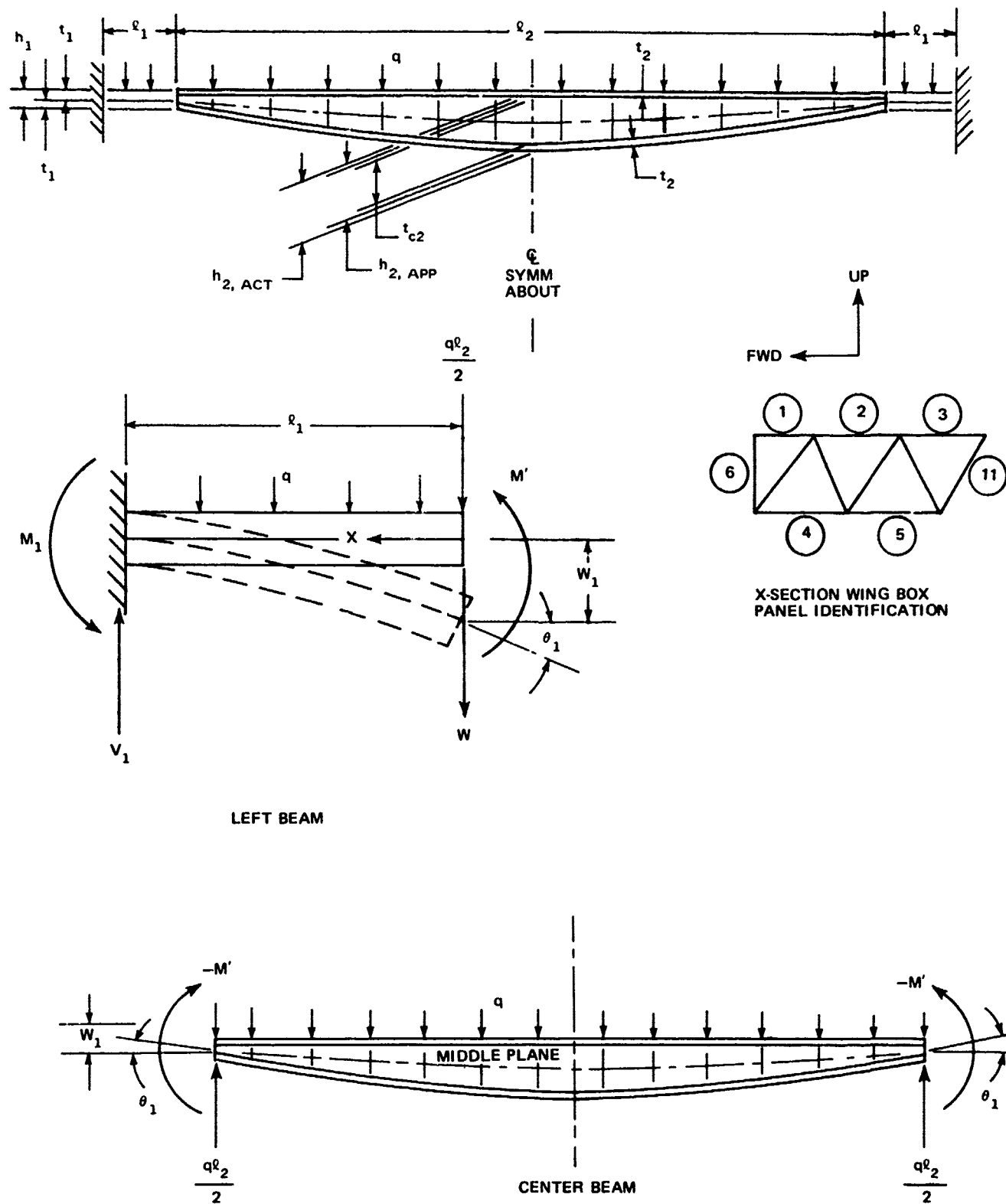


FIGURE 40. A THIN RECTANGULAR SANDWICH BEAM OF VARIABLE THICKNESS UNDER ACTION OF UNIFORM PRESSURE

Table 11 illustrates input and output data for an initial run for panels 4 (lower) and 11 (aft). The end beam length (l_1) was not minimum for the cover. The third case at stations 350 and 550 was run in the event panel weights were desired for a parallel truss crest configuration. Table 12 illustrates modified data for panel 4 with minimum end beam length and pseudoisotropic end laminates. Similar tables were constructed for upper and forward panels. Comparison, on a basis of end beam weights, showed use of isotropic buffer strips at truss crests saved an average of 31 percent weight, with respect to design laminate end beams which were weak and relatively soft in the chord-wise direction. On a wing basis, this is a 2-percent saving. Such tailoring of plies would be evaluated on a cost effective basis, but are incorporated in covers of the conceptual design for weight saving, and because of the probability they would act as rip stop areas.

TABLE 11
VARIABLE DEPTH BEAM ANALYSIS, INITIAL CASES, LOWER AND AFT PANELS

| PANEL NO | PRESSURE (PSI) | WING STATION | INPUT DATA | | | | | | | | | | OUTPUT DATA | | | | | | | |
|-------------------|----------------|--------------|--------------------------|--------------------------|------------------------------|----------------------------|------------------------------|--------------------------|------------------------------|----------------------------|-------------------------------------|----------------------------------|----------------------------------|---------------------------|---------------------------|------------------------------|------------------------------|---------------------------|---------------------------|--|
| | | | END BEAMS | | | | CENTER BEAM | | | | | | END BEAMS | | | | CENTER BEAM | | | |
| | | | ℓ_1 (IN.) | E_1 (10^6 PSI) | ν_1 | σ_1 (ALLOW. KSI) | ℓ_2 (IN.) | E_2 (10^6 PSI) | ν_2 | σ_2 (ALLOW. KSI) | t_2 (IN.) | t_1 (IN.) | h_1 (IN.) | D_1 (10^3 IN.-LB) | σ_1 (MAX) (KSI) | t_{C2} (IN.) | h_2 (ACT.) (IN.) | D_2 (10^3 IN.-LB) | σ_2 (MAX) (KSI) | |
| 4 4 11 | 20 | 60 | 2 0 2 0 1 2 | 8 0 5 0 6 3 | 0 33 0 08 0 77 | 65 40 48 | 49 5 49 5 36 6 | 5 0 5 0 6 3 | 0 08 0 08 0 77 | 40 40 48 | 0 077 0 077 0 0275 | 0 313 0 422 0 180 | 0 626 0 843 0 359 | 183 251 60 | 65 40 48 | 3 11 3 11 1 65 | 3 26 3 26 1 70 | 1962 1962 597 | 40 40 48 | |
| 4 4 11 | | 107 | 2 0 2 0 1 2 | 8 0 5 0 4 5 | 0 33 0 08 0 78 | 65 40 33 | 40 5 40 5 36 0 | 5 0 5 0 4 5 | 0 08 0 08 0 78 | 40 40 33 | 0 0825 0 0825 0 0495 | 0 261 0 351 0 209 | 0 521 0 701 0 418 | 06 145 70 | 65 40 33 | 1 89 1 89 1 21 | 2 05 2 05 1 31 | 807 807 450 | 40 40 33 | |
| 4 4 11 | | 257 | 2 0 2 0 1 2 | 8 0 3 0 7 7 | 0 33 0 09 0 76 | 65 27 58 | 33 0 33 0 27 6 | 3 0 3 0 7 7 | 0 09 0 09 0 76 | 27 27 58 | 0 099 0 099 0 0605 | 0 217 0 355 0 128 | 0 433 0 709 0 256 | 61 90 25 | 65 27 58 | 1 50 1 50 0 30 | 1 69 1 69 0 43 | 381 381 74 | 27 27 58 | |
| 4 4 4 11 | | 350 | 1 5 1 5 1 5 1 2 | 8 0 4 2 4 2 2 6 | 0 33 0 40 0 40 0 79 | 65 35 35 20 | 28 0 28 0 32 0 23 0 | 4 2 4 2 4 2 2 6 | 0 40 0 40 0 40 0 79 | 35 35 35 20 | 0 088 0 088 0 088 0 0495 | 0 181 0 240 0 271 0 174 | 0 363 0 480 0 542 0 348 | 36 46 66 24 | 65 35 35 20 | 0 76 0 76 1 03 0 75 | 0 94 0 94 1 20 0 85 | 159 159 274 109 | 35 35 35 20 | |
| 4 4 11 | | 450 | 1 0 1 0 1 2 | 8 0 5 5 2 6 | 0 33 0 14 0 79 | 65 45 20 | 22 5 22 5 18 0 | 5 5 5 5 2 6 | 0 14 0 14 0 79 | 45 45 20 | 0 0385 0 0385 0 011 | 0 143 0 181 0 140 | 0 287 0 362 0 280 | 17 22 13 | 65 45 20 | 1 11 1 11 2 16 | 1 19 1 19 2 19 | 143 143 180 | 45 45 20 | |
| 4 4 4 11 | | 550 | 1 0 1 0 1 0 1 2 | 8 0 7 0 7 0 2 6 | 0 33 0 20 0 20 0 79 | 65 55 55 20 | 17 2 17 2 33 0 13 1 | 7 0 7 0 7 0 2 6 | 0 20 0 20 0 20 0 79 | 55 55 55 20 | 0 0275 0 0275 0 0275 0 011 | 0 112 0 127 0 231 0 106 | 0 225 0 254 0 462 0 212 | 8 10 60 5 | 65 55 55 20 | 0 72 0 72 2 78 1 11 | 0 77 0 77 2 84 1 13 | 55 55 790 48 | 55 55 55 20 | |

TABLE 12
VARIABLE DEPTH BEAM ANALYSIS, FINAL CASES, LOWER PANEL NUMBER 4

| PRESSURE (PSI) | WING STATION | INPUT DATA | | | | | | | | | | OUTPUT DATA | | | | | | | |
|-------------------|-----------------|----------------|------------------------|---------|------------------------------|----------------|------------------------|---------|------------------------------|----------------|----------------|----------------|---------------------------|---------------------------|-------------------|--------------------------|---------------------------|---------------------------|--|
| | | END BEAMS | | | | | CENTER BEAM | | | | | END BEAMS | | | | CENTER BEAM | | | |
| | | l_1 (IN.) | E_1 (10^6 PSI) | ν_1 | σ_1 (ALLOW KSI) | l_2 (IN.) | E_2 (10^6 PSI) | ν_2 | σ_2 (ALLOW KSI) | t_2 (IN.) | t_1 (IN.) | h_1 (IN.) | D_1 (10^3 IN.-LB) | σ_1 (MAX) (KSI) | t_{C2} (IN.) | h_2 (ACT.) (IN.) | D_2 (10^3 IN. LB) | σ_2 (MAX) (KSI) | |
| 20 | 60 | 0.75 | 8.0 | 0.33 | 65 | 49.5 | 5.0 | 0.08 | 40 | 0.077 | 0.299 | 0.597 | 159 | 65 | 3.175 | 3.329 | 2050 | 40 | |
| | 107 | 0.75 | 8.0 | 0.33 | 65 | 40.5 | 5.0 | 0.08 | 40 | 0.0825 | 0.246 | 0.492 | 89 | 65 | 1.943 | 2.108 | 852 | 40 | |
| | 257 | 0.75 | 8.0 | 0.33 | 65 | 33.0 | 3.0 | 0.09 | 27 | 0.099 | 0.202 | 0.404 | 49 | 65 | 1.551 | 1.749 | 408 | 27 | |
| | 350 | 0.75 | 8.0 | 0.33 | 65 | 28.0 | 4.2 | 0.40 | 35 | 0.088 | 0.173 | 0.345 | 31 | 65 | 0.78 | 0.956 | 156 | 35 | |
| | 450 | 0.75 | 8.0 | 0.33 | 65 | 22.5 | 5.5 | 0.14 | 45 | 0.0385 | 0.141 | 0.281 | 17 | 65 | 1.122 | 1.99 | 145 | 45 | |
| | 550 | 0.75 | 8.0 | 0.33 | 65 | 17.2 | 7.0 | 0.20 | 55 | 0.0275 | 0.109 | 0.219 | 8 | 65 | 0.726 | 0.781 | 57 | 55 | |

The additional feature of using glass 90-degree fibers in these buffer strips was not evaluated by the present effort, since the analysis did not have a variable point of inflection between end and center beams to determine the effect of lowered modulus on bending stress. Further analytic refinement was felt to be beyond the scope of the program, but would be of value in a detail wing design optimization effort.

Minimization of end beam lengths caused 1 to 3.5 percent increases in center beam core thicknesses (h_2).

In addition to deriving panel weights as a function of the pressure condition for wing weight analysis, a comparison was made to define the weight efficiency of the variable thickness panels, with respect to constant thickness panels. As shown in Table 13, the variable thickness panels are somewhat lighter.

TABLE 13
CONSTANT VERSUS VARIABLE THICKNESS PANEL WEIGHTS

| | WING STA | FACING THICKNESS (IN.) | PANEL WIDTH (IN.) | CORE THICKNESS | | W _{TOT} (PSF) | | ΔW (PERCENT) |
|-------------|----------|------------------------|-------------------|----------------|---------------|------------------------|-------|--------------|
| | | | | CONSTANT (IN.) | MAX VAR (IN.) | CONSTANT | VAR | |
| UPPER COVER | 107 | 0.088 | 38.5 | 0.847 | 2.01 | 3.047 | 2.923 | 4 |
| | 257 | 0.0825 | 31.0 | 0.349 | 0.837 | 2.267 | 2.265 | 0 |
| | 350 | 0.088 | 26.5 | 0.292 | 0.60 | 2.304 | 2.253 | 2 |
| | 450 | 0.039 | 21.0 | 0.380 | 0.829 | 1.406 | 1.376 | 2 |
| LOWER COVER | 107 | 0.0825 | 42.0 | 0.808 | 1.95 | 2.502 | 2.388 | 5 |
| | 257 | 0.099 | 34.5 | 0.643 | 1.55 | 2.547 | 2.448 | 4 |
| | 350 | 0.088 | 29.5 | 0.383 | 0.78 | 2.020 | 1.919 | 5 |
| | 450 | 0.039 | 24.0 | 0.547 | 1.12 | 1.451 | 1.306 | 11 |

NOTES: (1) ATTACHMENT EDGE WEIGHT INCLUDED IN CONSTANT PANELS, AND ISOTROPIC "END BEAM" INCLUDED FOR VARIABLE THICKNESS PANELS.

(2) FIXED EDGE PANELS, DESIGNED BY 20 PSI PRESSURE.

(3) UPPER COVER BORON FACINGS, LOWER COVER GRAPHITE FACINGS, ALL CORE 8 PCF, ADHESIVE 0.00031 LB/IN.²

4.1.7 Substructure Lightening

Preliminary wing weight computations revealed an excess of web strength in the internal webs of the wing. Front and rear webs did not present this minimum gage problem because of being well above minimum thickness to provide required wing torsional stiffness and resistance to internal pressure. They are thus capable of carrying a considerable proportion (or all) of the shear.

Several approaches were considered for reducing this excess weight.

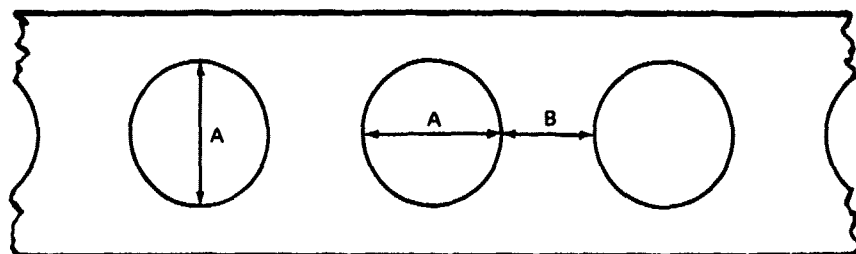
1. Use two plies (+45) in place of four for each facing and balance warpage across the core.

2. Use three mils per ply graphite in place of six.
3. Replace solid sandwich webs with open or truss-type members which can be tailored to match load requirements.

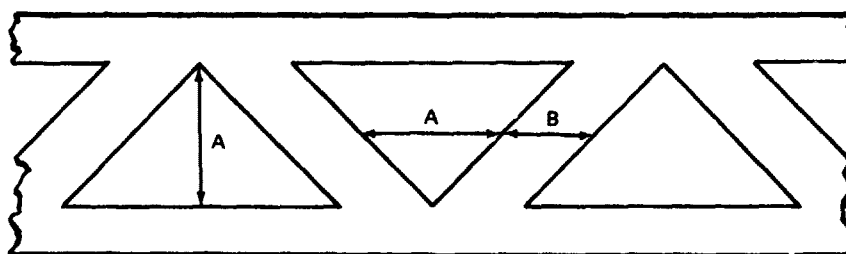
Four plies per facing were used in the initial wing analysis finite element model and for the design verification specimens. Fabrication feasibility panels have been fabricated with two-ply cocured facings without warpage. The shear strength and stiffness of 3-mil/ply graphite has been tested (see Paragraph 6.2) and wing weight estimates were made on the basis of two-ply minimum web facing for continuous panel webs.

Core and adhesive weight is also a significant and relatively invariant weight (typically 33 percent of web weight) and can be removed by cutting holes. Access through the webs is also a requirement, therefore an investigation has been conducted into possible ways of incorporating lightening holes in the webs. The holes under consideration are not reinforced and only require sealing around the edges of the honeycomb panel. Four basic hole geometries are shown in Figure 41 and these are discussed below.

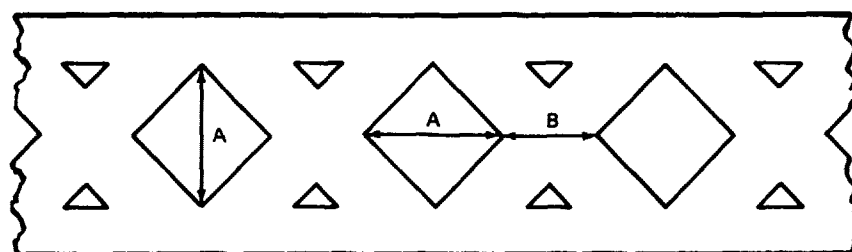
1. Circular Holes. Circular holes are typical of traditional holes commonly used in metal webs. A high capability of carrying shear and vertical tension and compression is retained with a minimum of stress concentration effects, but this is the heaviest of the configurations.
2. Single Truss. When webs are loaded primarily in shear, triangular holes can be used to produce a shear truss effect. Since the individual truss members are loaded in pure tension or compression, it is possible to have filament directions along the length of the members only. However, adjacent members meet at the apex of each triangle and there is a region where the filaments cross under biaxial (shear) stress. Although the thickness is doubled where the filaments cross, the allowable shear stress is less than half of the direct tensile and compressive strengths of the uniaxial truss members. Hence a stress concentration factor exists in this region, but this effect can be reduced by allowing the ± 45 -degree filament to extend across the whole region above and below the holes. These portions of the webs act as stiffeners between the truss nodes and are required to support the compressive skin panel against buckling. Their ability to do this will be enhanced by the addition of 0-degree filaments. Although the hole area is greater than for circular holes, and also the actual truss members can be lighter due to their uniaxial direction, the additional layers along the stiffener regions will offset these advantages to some extent.
3. Double Truss. In this concept, two trusses are superimposed to leave main diamond-shaped holes, and smaller triangular holes. Hole area is very much reduced compared with the single truss, but since there are twice the number of truss members, the load carrying capacity is nominally doubled. Again, where the truss members cross, there is a biaxial stress condition and a corresponding stress concentration factor. The number of supports for the skin panel is increased, making the compressive buckling condition less critical. The small triangular holes can be omitted to improve the skin panel buckling stress still further. This concept is appropriate in the inner wing regions where skin panel loads are high and wing thickness is greater.



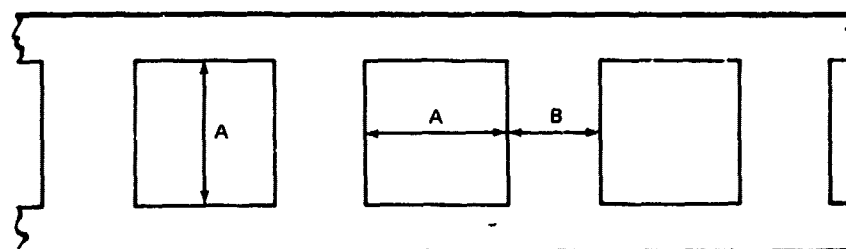
A) CIRCULAR HOLES (HOLE AREA = $0.785 A^2$)



B) SINGLE TRUSS (HOLE AREA = A^2)



C) DOUBLE TRUSS (HOLE AREA = $0.556 A^2$
FOR A/B RATIO SHOWN)



D) SQUARE HOLES (HOLE AREA = A^2)

FIGURE 41. WEB HOLE GEOMETRIES – CONSTANT A/B RATIO

4. Square Holes. This shape of hole is more appropriate to webs in which the shear stresses are not high. Compared with a web with circular holes, shear capability is reduced but hole area is increased. If shear loading is not critical, the dominant stress direction will be transverse to the web longitudinal axis and hence, it would be preferable to replace the usual $+45$ -degree pattern with layers at 90 degrees. In fact, the use of such a pattern will discourage the internal webs from carrying shear loads, by transferring the shear to the end webs of the box. This is a more efficient structural arrangement and is to be generally recommended.

Once the use of 90-degree filaments was accepted, consideration was given to further reducing the number of layers rather than resorting to lightening holes. For sandwich panels with $+45$ -degree facings, the minimum number of plies per facing is four, if thermal and shear balance of each facing is required. This can be reduced to two if the facings are cocured, in which case thermal and shear balance of the whole panel rather than the individual facings is achieved. No such balance problem exists with 90-degree filaments, and facings as thin as a single ply are theoretically possible. Hence, the need for lightening holes is minimized, although holes for access and fuel flow are still required.

Finally, a solid laminate corrugated shear web concept was under consideration, see Figure 42. This eliminates core, adhesive, and edge sealing requirements. Cutting access holes through such a web is not considered feasible unless such holes are produced by isolating panel sections, in which case edge reinforcement is required.

In all web concepts, the difficulty was recognized of cutting holes without adding weight due to edge reinforcement for stress concentrations and edge sealing. It became possible to circumvent the problem when the finite element analysis (Section V) showed the front and rear webs, designed to meet requirements of internal pressure and torsional stiffness, are adequate to carry wing shear. This reduced the intermediate truss web function to that of cover support, and only in cases of concentrated load introduction do they need to carry local shear.

The cutout web concept of Figure 43 was proposed to fulfill the functions of:

- Cover stability due to wing bending
- Compression from bending and airloads; and
- Tension from internal pressure and airloads
- Concentrated load distribution by truss action.

The chordwise sections become closely spaced truss ribs and the former truss crests and joints are preserved as stringers. Post spacing is determined by stringer bending stiffness and stringer column lengths for cover stabilization. This web concept is integrally laid up and cocured with cutouts in place. Although this concept weighed only 36 percent of solid sandwich, excluding crest joint reinforcement and edge sealing, the concurrent determination of wing configuration relative costs showed this weight saving was achieved only with a considerable cost penalty. See initial payoff study, Paragraph

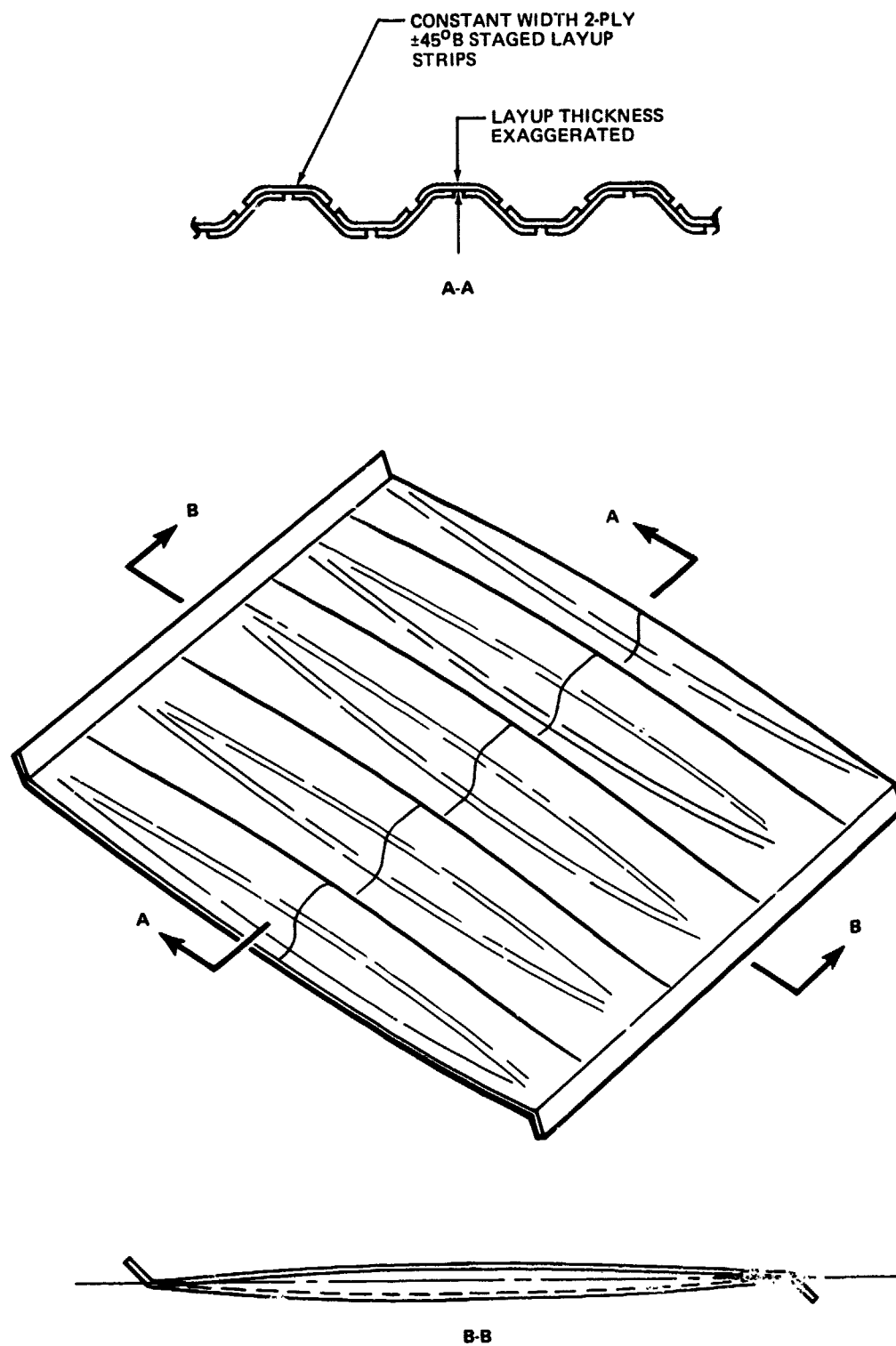


FIGURE 42. CORRUGATED SHEAR WEB CONCEPT

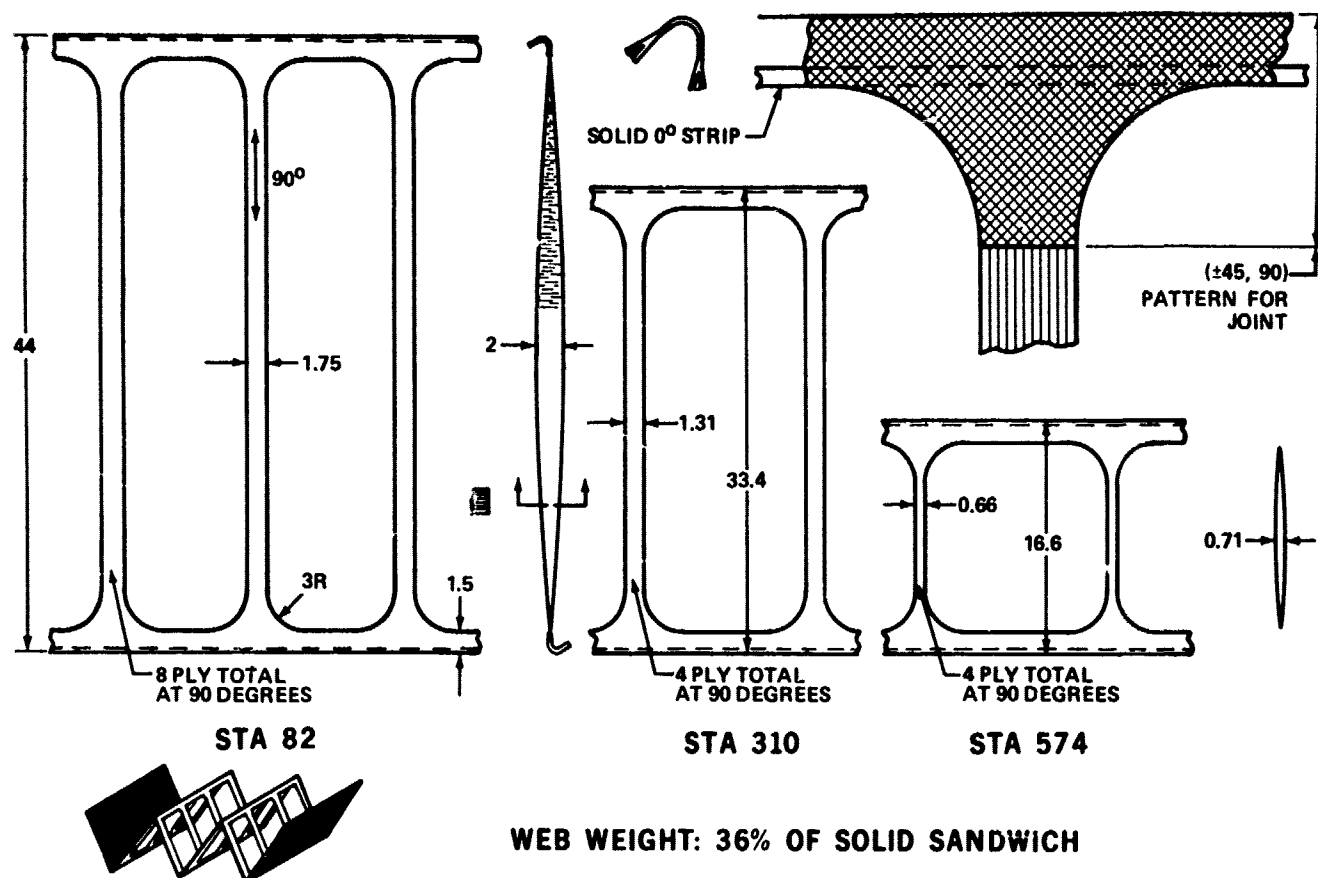


FIGURE 43. CUTOUT WEB CONCEPT

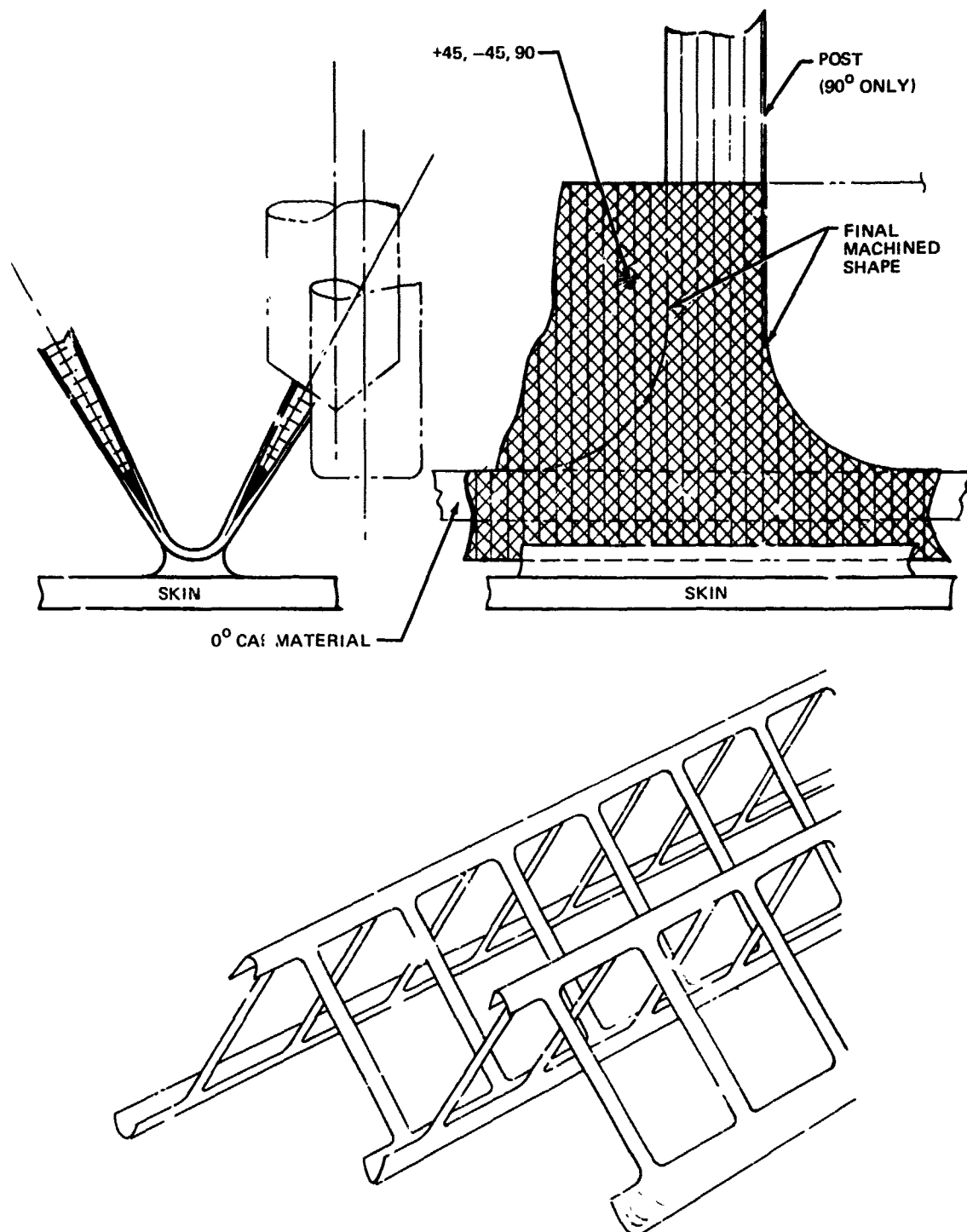
4.1.8. The cutout web was preferred over other web concepts since a large amount of web weight was saved and the required access holes were integral with the concept.

If only a small amount of weight is to be saved, circular holes in sandwich could be cut but strength disappears rapidly with hole size. Shear truss and double truss concepts saved more weight but introduced fabrication cost increases and shear panels were not really needed in this application. Corrugated panels were the lightest of the shear web concepts (Figure 42) but were not pursued when the shear panel requirement disappeared. The general conclusion if intermediate shear webs were to be retained, and given the access requirement, was that only a small amount of weight could be saved by cutting any kind of holes in sandwich panels.

Other post-truss concepts were developed to improve fabricability and to lower cutout-web fabrication cost without sacrificing maximum weight saving. These are illustrated in Figures 44 through 49.

Alternate Substructure Concept 1 (Figure 41) - A first design variation simplified the integral layup technique by laying up extra wide stringers but the posts are laid up to the net width in the large mold, thus producing square corners. After cure, the corner radii and stringer net flange width is produced by machining with a movable cutter rotating about a vertical axis. Only small weight penalties accrue with respect to the original concept where the corners

were laid up net. This concept is called Alternate Substructure Concept 1. Fabrication and tooling considerations for this and the succeeding concepts will be found in Reference 4, Appendix C. General design description is given here.

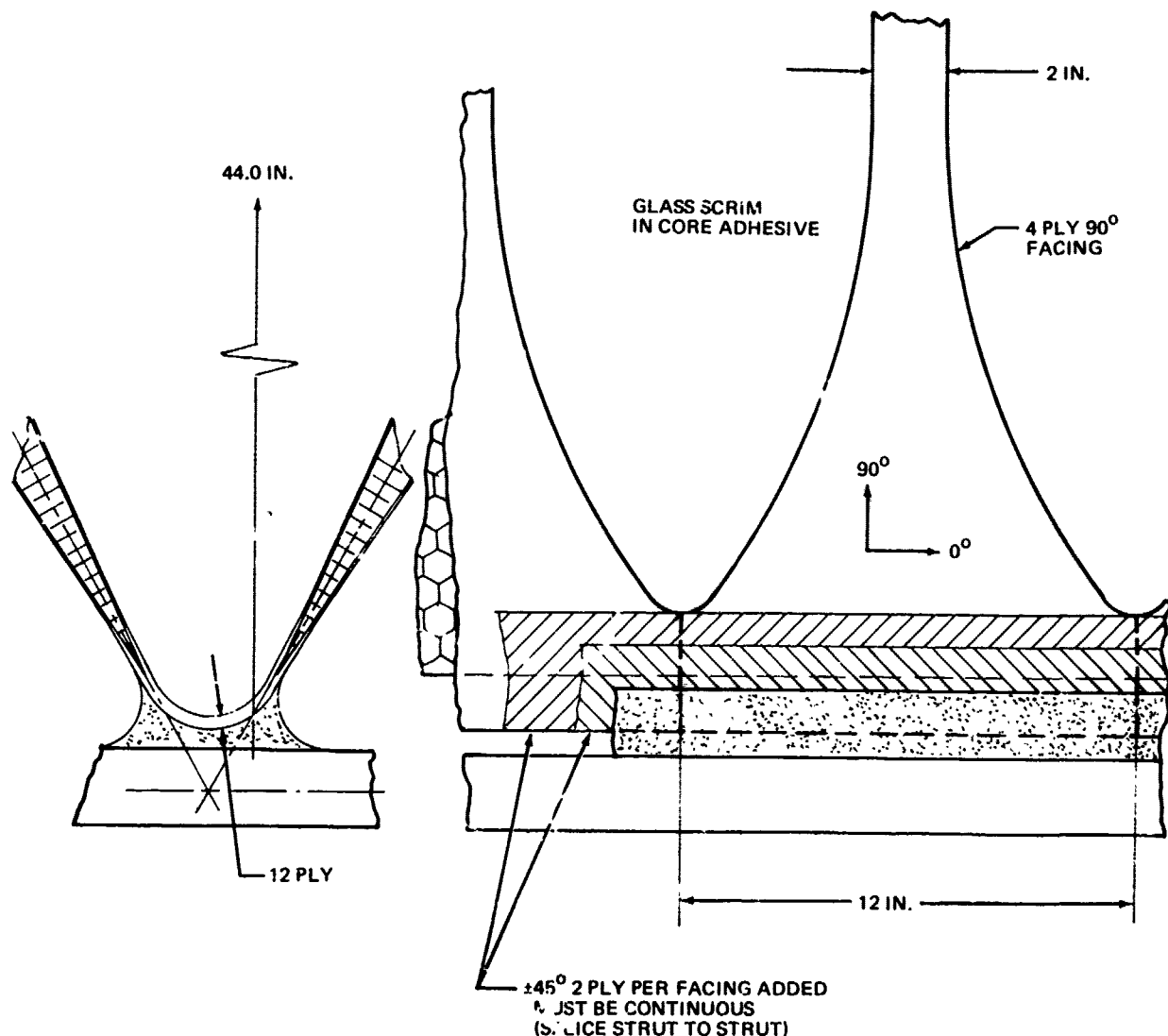


ALTERNATE SUBSTRUCTURE CONCEPT NO. 1

FIGURE 44. INTEGRATED WEB LAYUP WITH MACHINED CORNERS

To avoid the necessity of strut-stringer corner radii, a variation of this concept that bolted (pinned) the struts to the stringer was considered and rejected. The bolted joint requires bolt-bearing pads in strut and stringer and a heavier stringer to stabilize the cover resulting in a net weight and labor increase over the other concepts.

Alternate Substructure Concept 1A - Improved Sandwich Strut Concept (Figure 45) - Because Concept 1 would be very difficult to lay up by hand in situ (i.e., working from above on a mold as much as 40 inches deep, 7 feet wide and 50 feet long), additional alternate concepts consider the web/strut assembly to be made of separately laid up subassemblies. Alternate Concept 1A was selected for fabrication and test (see drawing Z3569984, Appendix A), because of its simplicity and tractability from an engineering design sense. The strut facings are made entirely from unidirectional material. Pending test, only the glass scrim cloth in the core adhesive is being considered for cross-plying for minor shear stresses. Since the covers are continuously supported by these struts, stringer cap material is unnecessary.



STATION 0-82 SUBSTRUCTURE CONCEPT 1A

FIGURE 45. IMPROVED SANDWICH STRUT CONCEPT

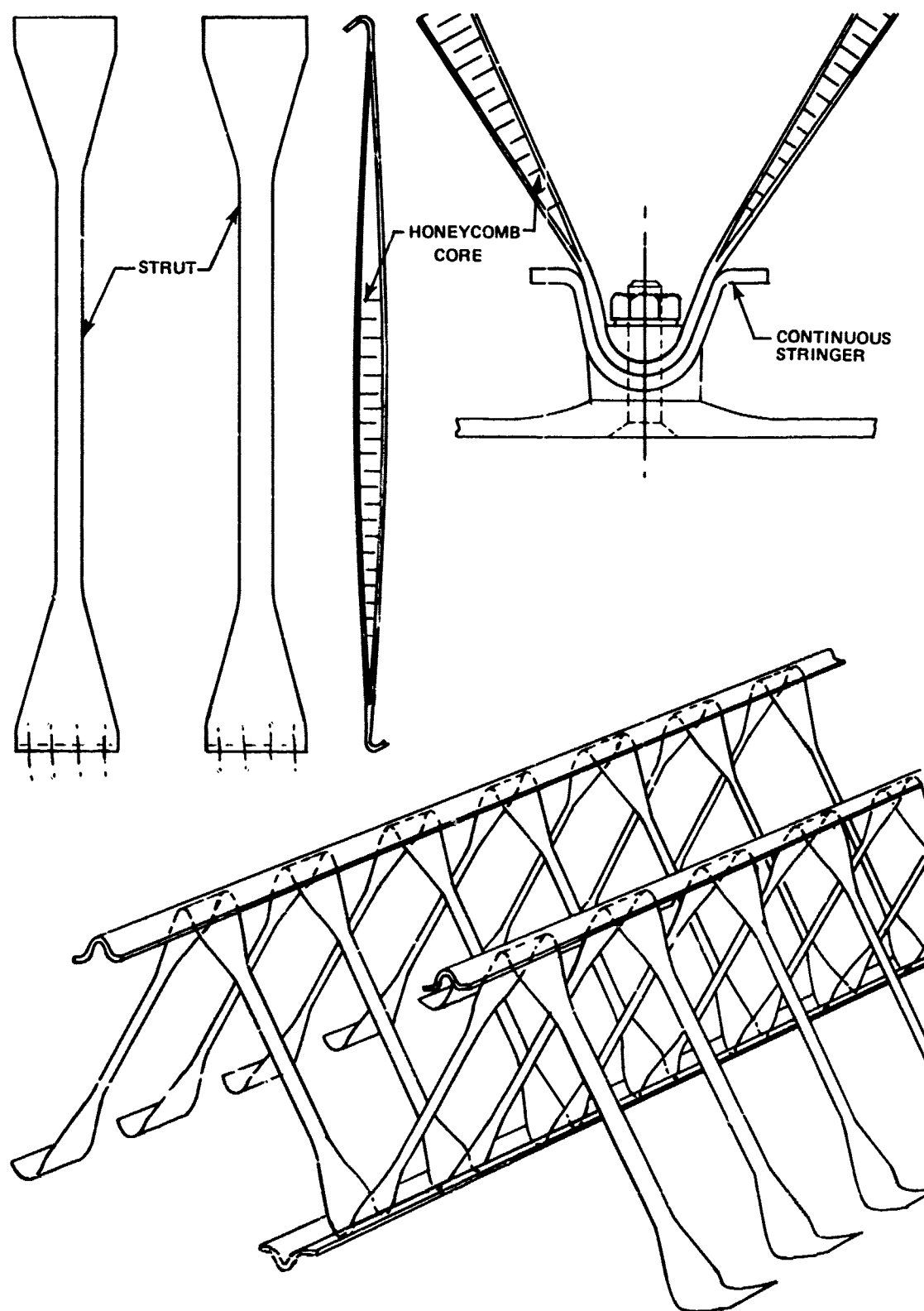
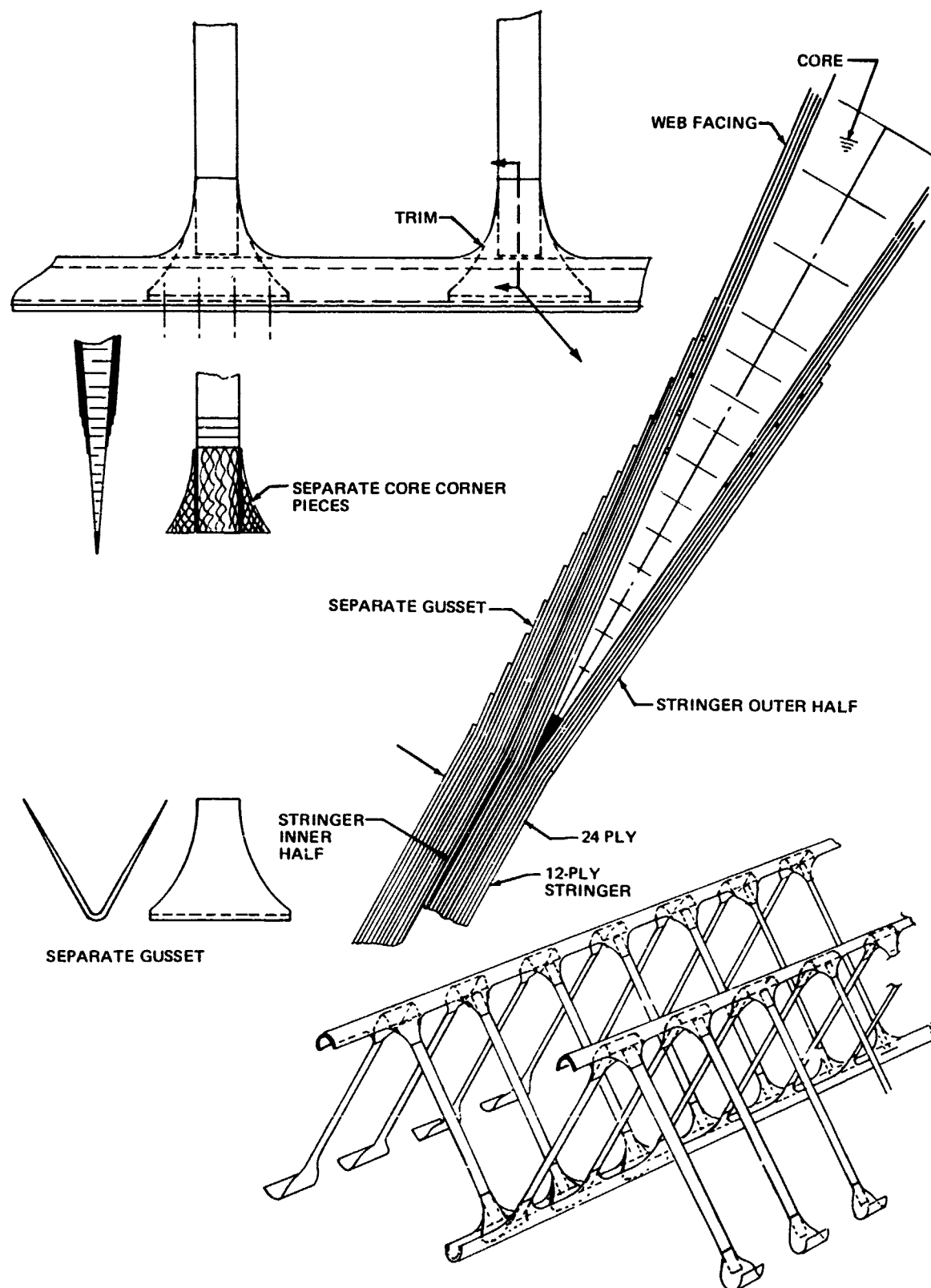


FIGURE 46. STRUTS ATTACHED BY SKIN BOLTS



SUBSTRUCTURE CONCEPT NO. 3

FIGURE 47. TRUSS - POSTS ATTACHED BY BONDING

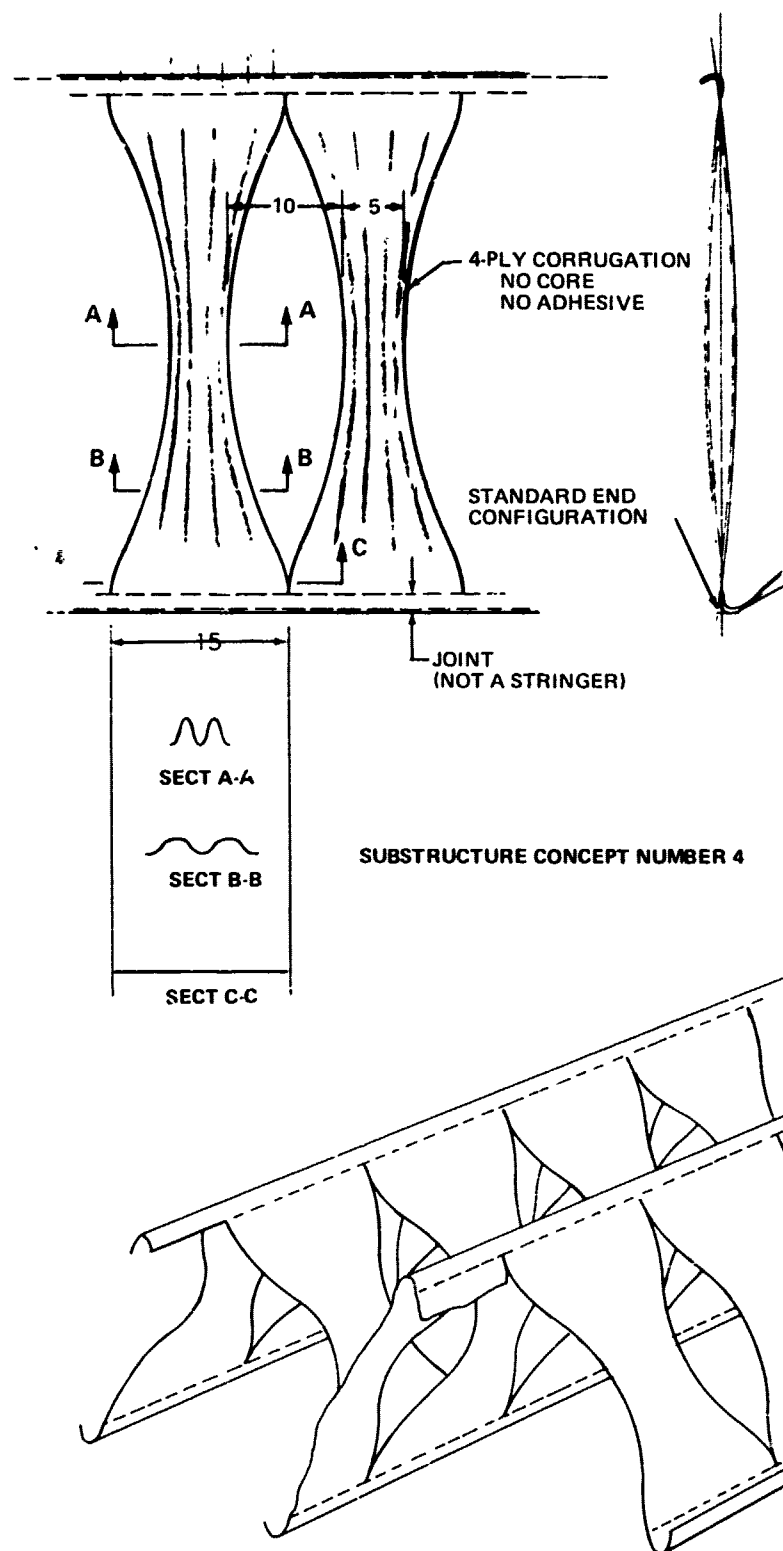


FIGURE 48. CORRUGATED SHEET SUBSTRUCTURE CONCEPT.

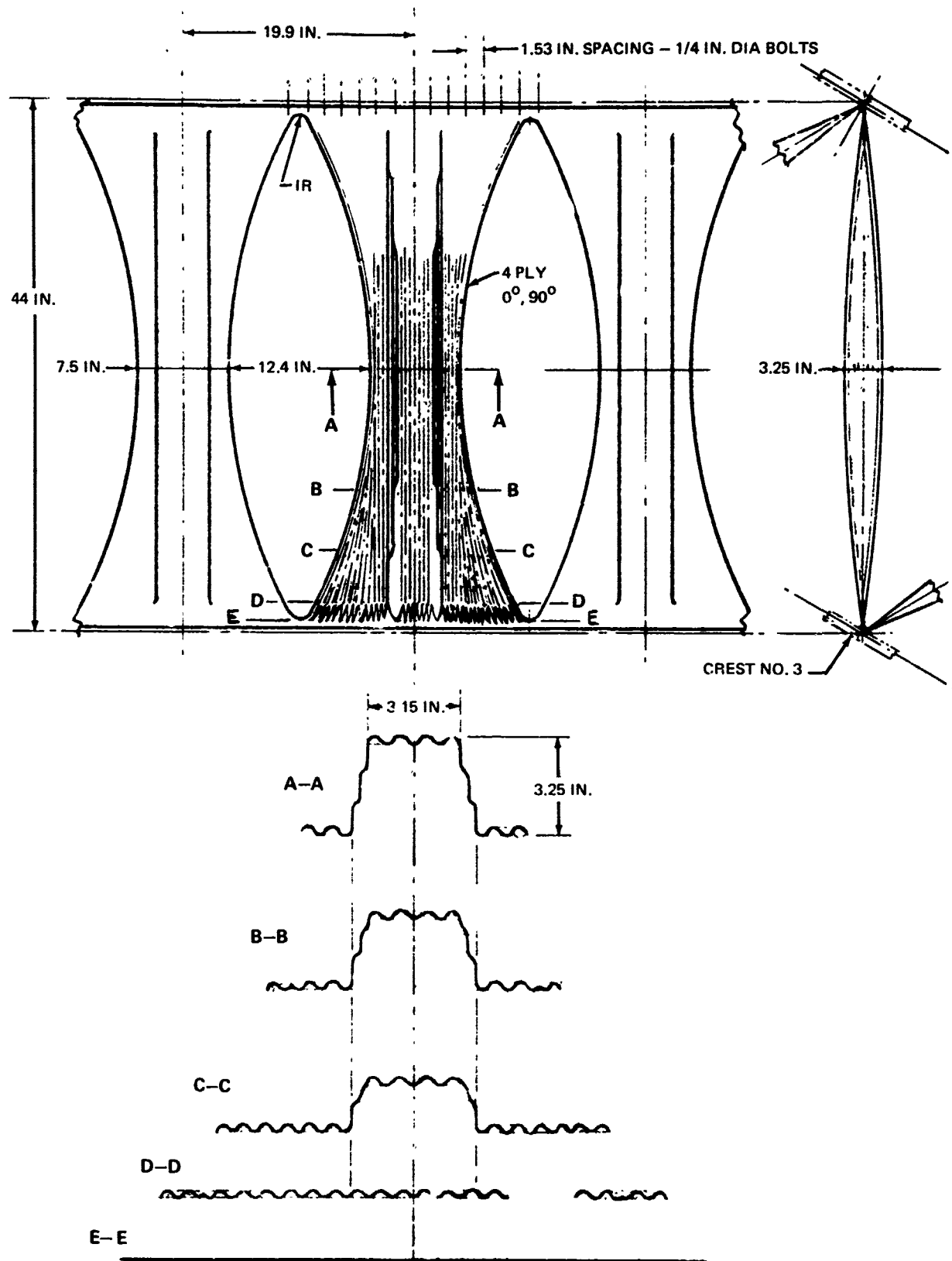


FIGURE 49. CORRUGATED HAT SECTION STRUT - STA 0 TO 82

Alternate Substructure Concept 2 - Strut Attached by Skin Bolts (Figure 46) - Truss posts attached by bolting through the stringer to the skin were attractive since the struts could be precured as a chordwise truss. A 1-3/4-inch-wide strut at the wing root must flare at the end to 6 inches to accommodate the four 1/4-inch bolts required for pressure load at a post spacing of 11.3 inches. The material volume of this concept is roughly twice that of the original integral post but still less than that of the uncut truss web. Since every post is a different length in the wing, the problem exists how to fabricate struts in great quantities and still maintain good fits. Gang molding of many trusses on a foreshortened taper mold is possible but the exaggerated taper fits and tolerance problems require a "liquid shim" assembly technique which in turn adds weight. A thick glue line bonded version of this design could be considered when the truss web itself is bonded to the covers.

Alternate Substructure Concept 3 - Truss Posts Attached by Bonding (Figure 47) - Consideration of truss posts attached by bonding leads to a gusset-splice concept. The stringers are laid up in separate tooling including the outer and inner splice gusset which is integral with the stringer. Precured and machined stringer cap strips are included in the layup and the inner and outer integral gussets are kept from adhering together by separator film. The stringer layups are then densified. After densification, the gusset corner radii may readily be trimmed to shape in the "B" stage since there are only a few plies of graphite. Struts are gang molded and cut apart as in Concept 3; however, they are of constant width and the end tapers are not critical since strut ends may be trimmed to fit on the assembly. The struts are inserted into the layup as all parts are transferred to a final-bond tool. Separate vee-shaped B-staged gussets also are inserted at this time to complete the joints and the assembly is cured and bonded in a single cycle. No final machining is necessary.

Alternate Substructure Concept 4 - Corrugated Sheet Concept (Figure 48) - A particularly interesting concept evolved from an attempt to eliminate the stringers, core, and associated adhesive. A rectangular layup (4-ply $[0/90]_S$ or 3 ply $[90/0]_S$) sheet is draped over a corrugated mold made so that the middle of the resulting layup has deep corrugations while the ends that attach to the covers remain flat. The transition between ends and middle occurs in gentle curves. Micro-wrinkles are formed into the thin walls of the general corrugations to provide local stability. The hourglass planform of the three-dimensional self-stiffened shape is such that 10-inch gaps exist between adjacent struts at their centers while maintaining butt-edges at their ends. This gap can be used for access through the web. At the root, each web segment carries the cover-pressure load from seven bolts. The continuous-joint member is not a stringer in that it does not have an EI depth requirement. The web segments which bond it to continuously support the skin. This concept has geometric proportioning difficulties in the outboard wing areas and requires fabrication and tooling development for realization of its generally superior weight saving characteristics. Design investigation of this concept revealed that section shaping is critical for local and general stability so that Concept 4 may be considered a partial solution leading to Concept 5.

Alternate Substructure Concept 5 - Corrugated Hat Section Strut - Figure 49 illustrates the design evolved from the corrugated sheet concept. The geometry variations required at several stations along the wing are shown in Reference 4. For proper detail design of such a concept, the following work is indicated:

- Testing of short wrinkled sheet columns
- Fabrication feasibility work to determine layup possibilities and techniques
- Testing of long, tapered, wrinkled sheet columns to determine overall stability.

Web Concept Evaluation - Although the self-stabilized sheet strut concept was not the design selected for the strut test and subsequent specimens, its weight aspects were investigated. Table 14 shows the weight comparison between the original solid sandwich web and Concept 5, corrugated hat section struts. Joint weights are included since solid sandwich webs required shear-carrying joints whereas the strut webs do not. It will be noted that the new bolted tension joint was much lighter than the previous tension/shear joint.

TABLE 14
SUBSTRUCTURE WEIGHT COMPARISON
POUNDS/WING BOX - CONSTANT WEIGHT
CLOSURE WEBS AND EDGE JOINTS EXCLUDED

| | SOLID SANDWICH | ORIGINAL CUTOUT WEB | CORRUGATED HAT | IMPROVED SANDWICH STRUT |
|--------------------------|----------------|---------------------|----------------|-------------------------|
| INTERNAL WEBS OR FACINGS | 380.0 | 143.6 | 288.0 | 158.0 |
| CORE | 124.6 | 26.8 | 0.0 | 28.7 |
| ADHESIVE | 116.0 | 24.4 | 0.0 | 26.7 |
| BOLTED JOINT* | 197.2 | 197.2 | 86.8 | 86.8 |
| | 817.8 | 392.0 | 374.8 | 300.2 |

*BASED ON AVERAGE WEIGHT/SPAN OF JOINTS OR STRINGERS AT CRESTS NO. 2, 3, 4.

The improved sandwich strut concept (Figure 45), when weighed on a wing basis, was found to be 1.4 percent lighter than the corrugated hat concept. The original cutout web was still heavier because of the stringer required between struts.

As the designs were developed for web concepts, concurrent manufacturing feasibility and relative cost were established. The problem of machining complex tooling shapes such as for the corrugated sheet (Concept 4) are reduced to a minimum through computer programs linked to the large numerically controlled mill or jig bore. Tool costs are generally the minor item in a production run. One method or type of tool versus another may not have a determining effect on the overall amortized production cost. This can be illustrated by referral to Table 15, where first article labor cost is seen relative to tooling labor cost. The table is based on fabrication of 60-inch-long by 2-panel-wide web sections. The differences in tooling cost tend to disappear as soon as 10 or 20 parts are made and recurring costs become dominant.

Although the machined, integrally laid-up substructure (Concept 1) shows least fabrication cost (machining cost is included), this would be very difficult to

TABLE 15
SUBSTRUCTURE CONCEPTS TOOLING AND FABRICATION RELATIVE COST

| CONCEPT | NAME | FIRST UNIT FABRICATION COST | NON-RECURRING TOOLING |
|---------|---|-----------------------------------|--------------------------|
| 1 | INTEGRATED WEB LAYUP WITH MACHINED CORNERS | 0.156 | 1.34 |
| 1A | IMPROVED SANDWICH STRUT | 0.200 | 1.00 |
| 2 | "W" STRUTS — BOLTED TO COVER | 0.228 | 1.50 |
| 3 | TRUSS/POST BOND ASSEMBLY | 0.205 | 1.55 |
| 4(1) | CORRUGATED SHEET | 0.220 | 1.39 |
| 5(2) | CORRUGATED HAT SECTION STRUT | (2) | — |

(1) DESIGN FEASIBILITY NOT FULLY ESTABLISHED

(2) FABRICATION FEASIBILITY NOT FULLY ESTABLISHED

scale-up to wing size and do hand layup in the 40-inch-deep wing center section. If the layup mold were oriented with the wing chord plane vertical, gravity would be working against much of the layup procedure. For this reason, Concept 1A is deemed the least cost practical design. It is also the least weight concept.

4.1.8 Initial Payoff Study

The preliminary weight payoff study for the truss web wing included an investigation of the weight effect of several design features. A configuration rate was established as shown in Figure 50 which displays the configurations

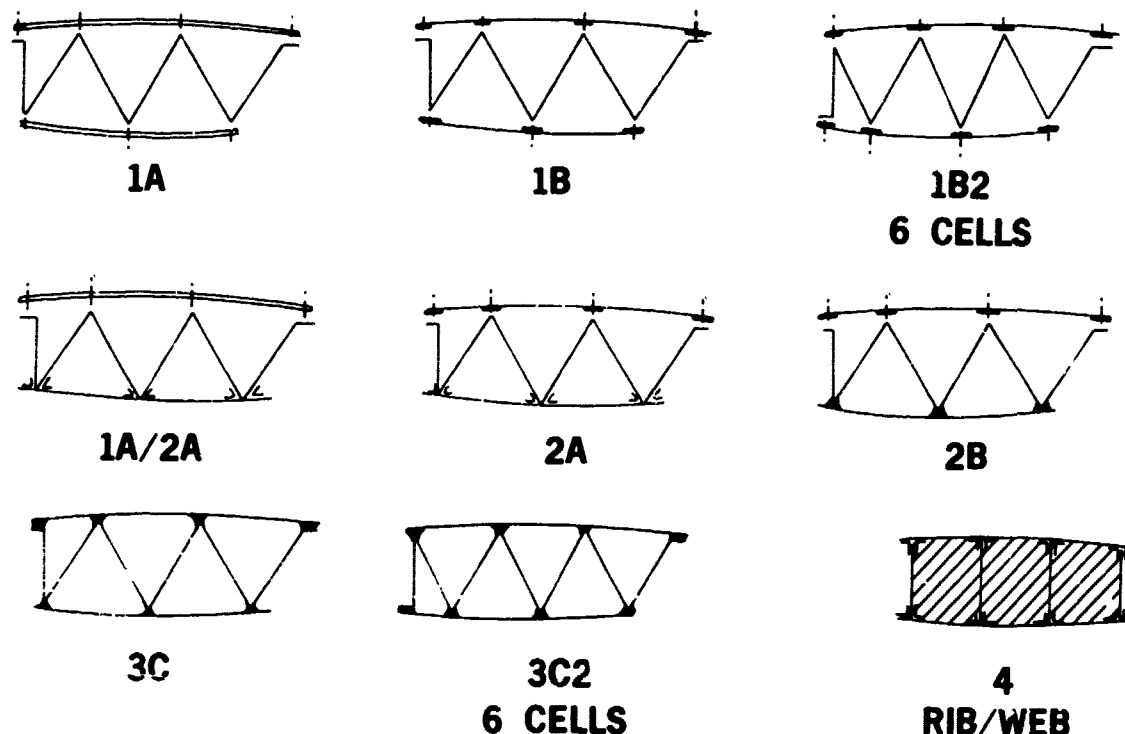


FIGURE 50. COMPOSITE WING CONFIGURATIONS

as generalized wing box sections. It was assumed that the same number of cells were maintained from root to tip. Configurations 1A and 1B both indicate bolted-cover-to-substructure connections but differ by the addition of stress concentration relief (SCR) at the spanwise bolt rows of 1B. Two major bonded joint schemes are indicated in Configurations 2 and 3. Bond Schemes A and B (fillet bond) were used for the lower cover only of Configurations 2A and 2B, respectively, with an SCR bolted upper cover. All configurations designated 3 utilized bond scheme B for both upper and lower cover. Configurations 3C and 3C2 were intended to show cost and weight differences for changing overall configuration from five to six cells, as was done for Configurations 1B and 1B2 for an all-bolted case.

Configuration 4 is a composite rib/web configuration against which the truss web was compared. Figure 51 presents more detail of this concept.

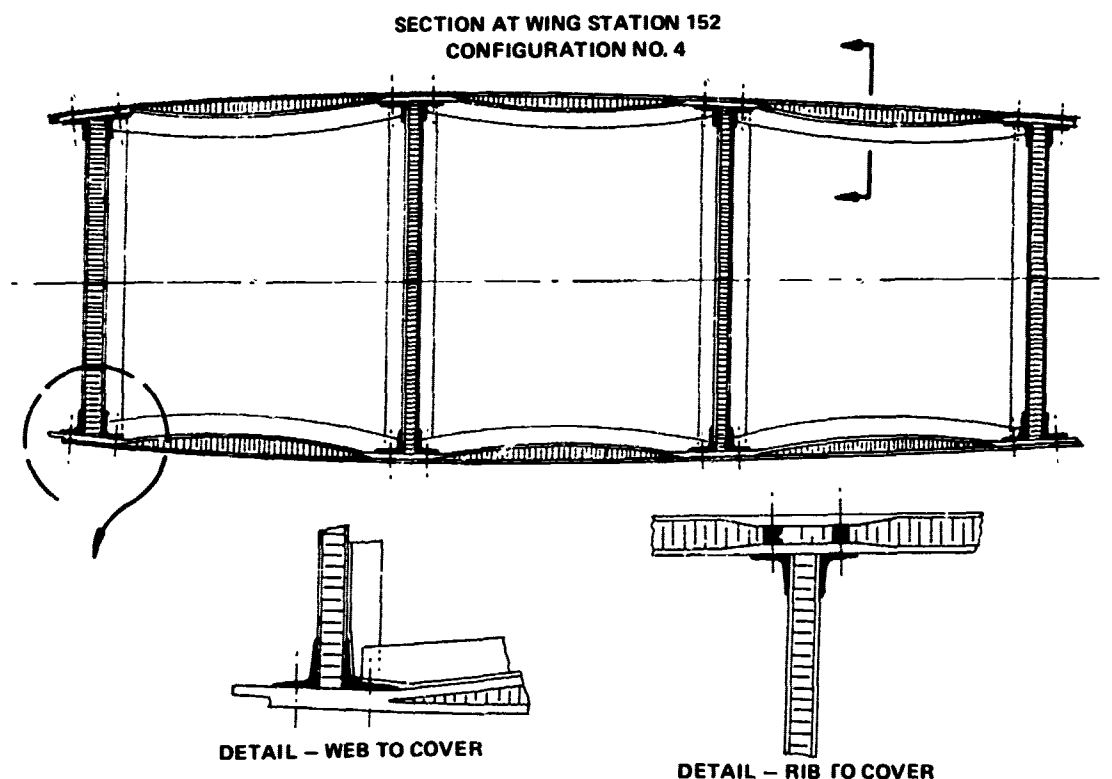


FIGURE 51. MULTI-WEB BASELINE COMPOSITE CONFIGURATION

A 40-inch section (Stations 132-172) of the wing box was used for initial detail weight comparisons of the several design features, different material combinations, and methods of fabrication. Table 16 shows the matrix with results in pounds of weight for the 40-inch sections and also relative weights in parentheses compared to Configuration 3C, the baseline five-cell configuration with joints fillet bonded per scheme B.

TABLE 16
INTERIM WEIGHT STUDY, WING 40-INCH SECTION WEIGHT MATRIX
(LB/SECTION)

| | | BASE 5 CELL | | | | | 6 CELL | | COMPARATIVE COMPOSITE BASELINE | |
|---------------------------|-------------------------------|--------------------|--------------------|-------------------|--------------------|--------------------|--------------------|-------------------|--------------------------------------|------------------|
| | | ALL BOLTED | | 1/2 BONDED | | ALL BONDED | ALL BOLTED | ALL BONDED | | |
| GEOMETRIC CONFIGURATION | | 1A | 1B | 1A/2A | 2A | 2B | 3C | 1B2 | | 3C2 |
| MATERIALS AND FABRICATION | ALL 5206 | 257.39 (1.401) | - | - | - | - | - | - | - | - |
| | BORON COVERS/5206 WEB | 228.49 (1.250) | 193.92 (1.061) | - | - | - | - | - | - | - |
| | BASELINE MATERIALS | 233.69* (1.271) | 192.22* (1.050) | 200.21 (1.095) | 189.15* (1.035) | 188.54* (1.030) | 183.01* (1.000) | 185.56 (1.013) | 174.32* (0.952) | 239.0* (1.3%) |
| | OPTIMUM WT MATERIALS | 213.31 (1.165) | 187.07 (1.022) | - | 183.35 (1.002) | 182.74 (0.997) | 187.06 (0.912) | - | 157.94 (0.863) | - |
| | BASELINE MATERIALS COCURED | 240.24* (1.325) | 198.77* (1.087) | 206.76 (1.133) | 195.70* (1.070) | 195.09* (1.067) | 189.53* (1.036) | 192.28 (1.050) | 181.04* (0.992) | - |

*COST CONFIGURATIONS

The fifth row (Table 16) shows weights resulting from the cocure fabrication technique. All other rows show precured laminate weights. Baseline materials were all-boron/epoxy (5505) upper cover, Narmco 5206 substructure, and mixed Narmco 5206/Thornel 75S-1004 lower cover. Optimum weight materials differed with configuration, and their selection was seen to be sensitive to stress concentration factors, bolt bearing strength, laminate pattern, and failure criteria used for laminate design. This complex situation indicated optimum materials could only be generally assigned for the 40-inch section and would not necessarily be the same for the whole wing. In general, the (0/+45) boron/aluminum laminate family was the lightest upper (compression) cover when no weight penalty factor for the presence of bolt holes was assigned. This is revealed in the 0.912 and 0.863 relative weights for Configurations 3C and 3C2 (Table 16). The other weight reductions in the optimum materials row over the baseline materials row is a result of using mixed boron/Thornel 75 or mixed 5206/Thornel 75 for the upper cover since the mixed graphite lower cover was already optimum.

It can be seen that the heaviest 40-inch sections were those utilizing bolting without stress concentration relief as a means of cover attachment. It was interesting that Configuration 1A with boron covers was lighter than 1A with baseline materials due to assignment of somewhat lower stress concentration factors for the boron. The comparative composite baseline Configuration 4 was barely competitive with truss web Configuration 1A, to which it should be compared since both had bolting without SCR.

The 40-inch sections provided data for cost comparisons and showed weight trends and relative effect of design features only.

Table 17 displays a summary of the weight values for the truss web wing of the various design features. It is seen that web lightening cutouts, stress concentration relief or bonding, and the use of optimum materials provide the maximum weight payoffs aside from the basic concept itself. These weight saving sources imply varying degrees of technological risk and fabrication cost. It is judged that the highest risks are associated with the reliability of the fillet bonded joint concept but only in the sense that additional developmental work is needed. Use of mixed materials or boron/aluminum is judged the next order of risk, and stress concentration relief is seen to be only a matter of further work by this and other contractors to define the best methods. The cutout web concept is seen as not so much a risk as it is a cost item to be aggressively improved. (See Substructure Lightening Study, Paragraph 4.1.7, for improved designs.)

TABLE 17
WEIGHT VALUES FOR DESIGN FEATURES

| TOTAL WING BOX BASIS - APPROXIMATE PERCENT SAVED | |
|---|---------|
| o WEB LIGHTENING CUTOUTS | 4.8 |
| o COCURING | -2.5 |
| o BOLTED STRESS CONCENTRATION RELIEF | 9.0 |
| o BONDING OVER BOLTING WITH SCR | 3.0-5.0 |
| o ADD A CELL - ALL BONDED SCHEME B | 2.8 |
| o ADD A CELL - BOLTED WITH SCR | 0.1 |
| o USE OPTIMUM MATERIALS IN COVERS INSTEAD OF 5505 | 0-9%* |
| o USE OPTIMUM MATERIALS IN COVERS INSTEAD OF 5206 | 12-19%* |

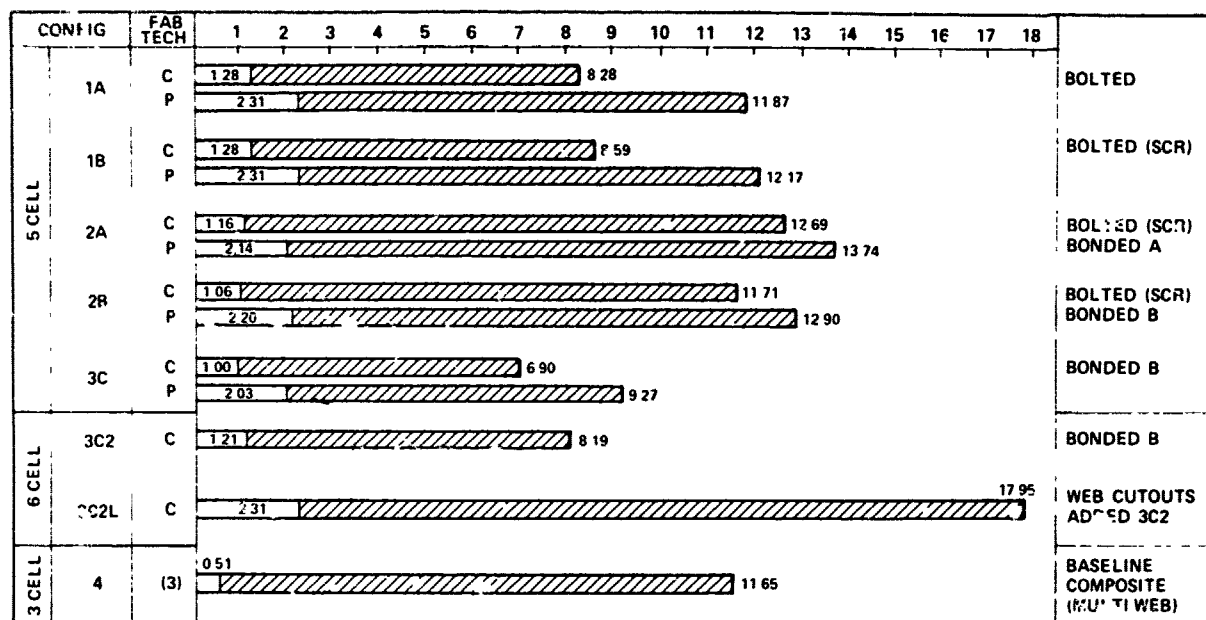
*EXCLUDING BORON/ALUMINUM.

Configuration Relative Cost/Weight - Balancing the technical risks of the weight-saving design features is the cost to produce. Figure 52 indicates configuration relative costs from which the cost effect of design features may be observed. Costs were generated for 40-inch wing sections on the basis of initial tooling and 50-unit fabrication labor. The effect of materials optimization was not included since materials cost was a small percentage of the totals.

Comparing Configuration 3C2L with 3C2 (Figure 52), it can be seen that the cutout web concept is presently a significant cost item compared to the continuous sandwich web. Fabrication and design aspects will bear considerable work to make the additional box weight saving worthwhile.

By contrast, stress concentration relief (Configuration 1B versus 1A in Figure 52) is seen to add very little cost for the large weight saving produced. Of the two bonded joint concepts (Configuration 2A versus 2B), the fillet joint (Configuration 2B) is less costly than the matched-bonded surfaces A concept with cocured reinforcing angles. In fact, fillet bonding both covers provides the least costly as well as the lightest weight attachment configuration.

A cost/weight comparison of the truss web configurations with the composite baseline (multi-web) design concept can also be made (Figure 52). The tooling cost for Configuration 4 is the lowest due to the flat panel substructure,



P PRECURED LAMINATES
C CO CURED⁽²⁾

▨ PART FAB □ TOOLING (NON-RECURRING)

(1) ESTIMATE BASIS: MANHOURS TO MAKE 50-40 INCH SECTIONS. 85 PERCENT LEARNING CURVE.

(2) FULLY CO CURED WEB WITH PRECURED INSERTS, PARTIALLY CO CURED COVERS

(3) PRECURE AND BOND RIBS AND WEBS, CO CURE/ BOND SUBSTRUCTURE, PARTIALLY CO-CURED COVERS, CO CURE/BOND ASSEMBLY.

FIGURE 52. CONFIGURATION RELATIVE COSTS

however, fabrication labor makes it noncompetitive with several truss web configurations. The comparison is better seen in Figure 53 where the numbers of Figure 52 and the weights of Table 16 have been normalized to Configuration 4. Again, Configuration 3C2 is the most attractive when considering both cost and weight.

4.1.9 Selected Baseline Truss Web

An isometric visualization of the selected baseline truss web wing concept is shown in Figure 54. The boron/epoxy sandwich upper cover and Type II graphite/epoxy lower cover are shown removed from the improved cutout web graphite sandwich substructure assembly. Front and rear shear webs are, of course, without cutouts (except for access, control surface, and subsystems requirements) while the internal web structure consists of tension and compression posts with unidirectional facings, except in areas such as flap and pylon attachment where beefup is required. As indicated (Figure 54), the upper cover is bolted and removable, whereas the lower cover is fillet-bonded and not removable. This figure should be considered as a schematic since many details, such as discontinuous bolt shoulder pads at web crests, are omitted for clarity.

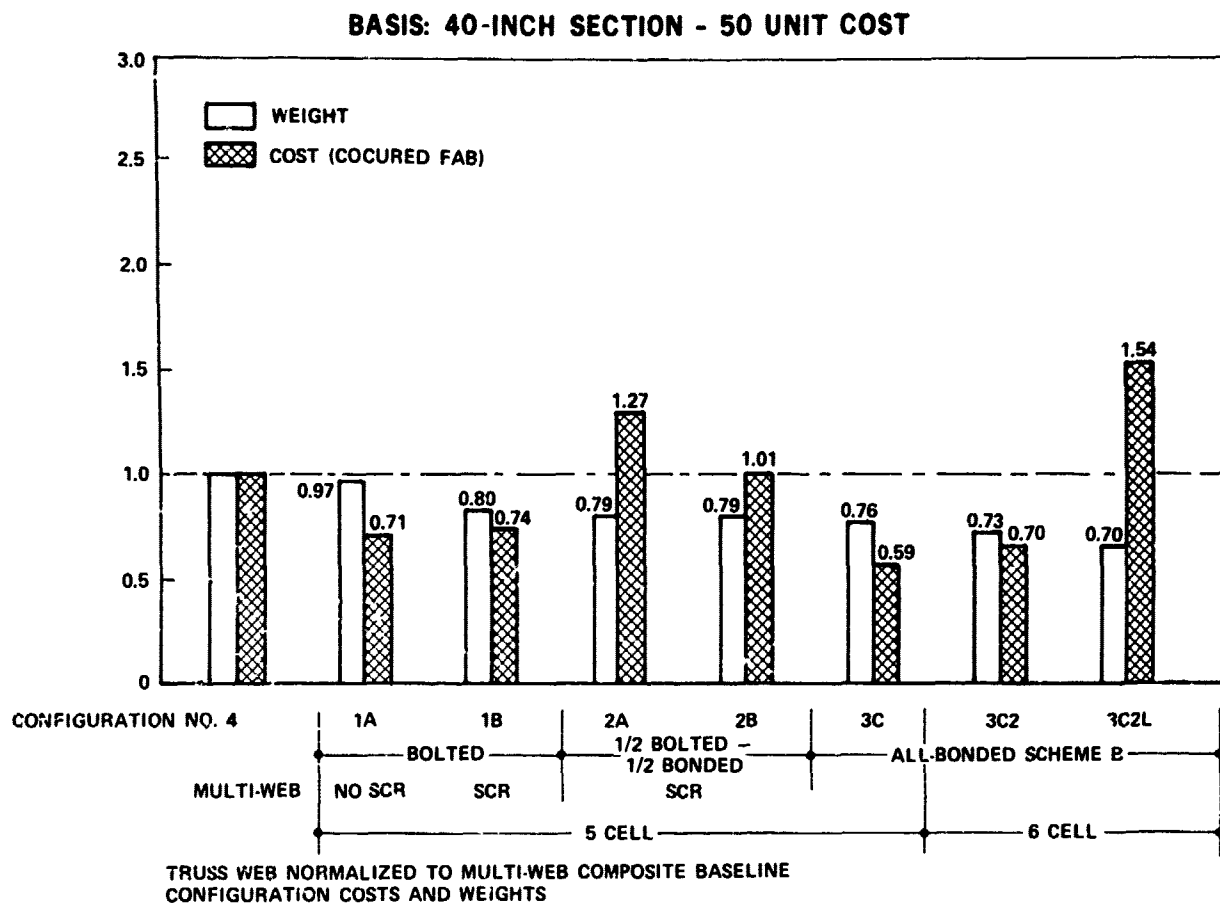


FIGURE 53. COST/WEIGHT COMPARISON

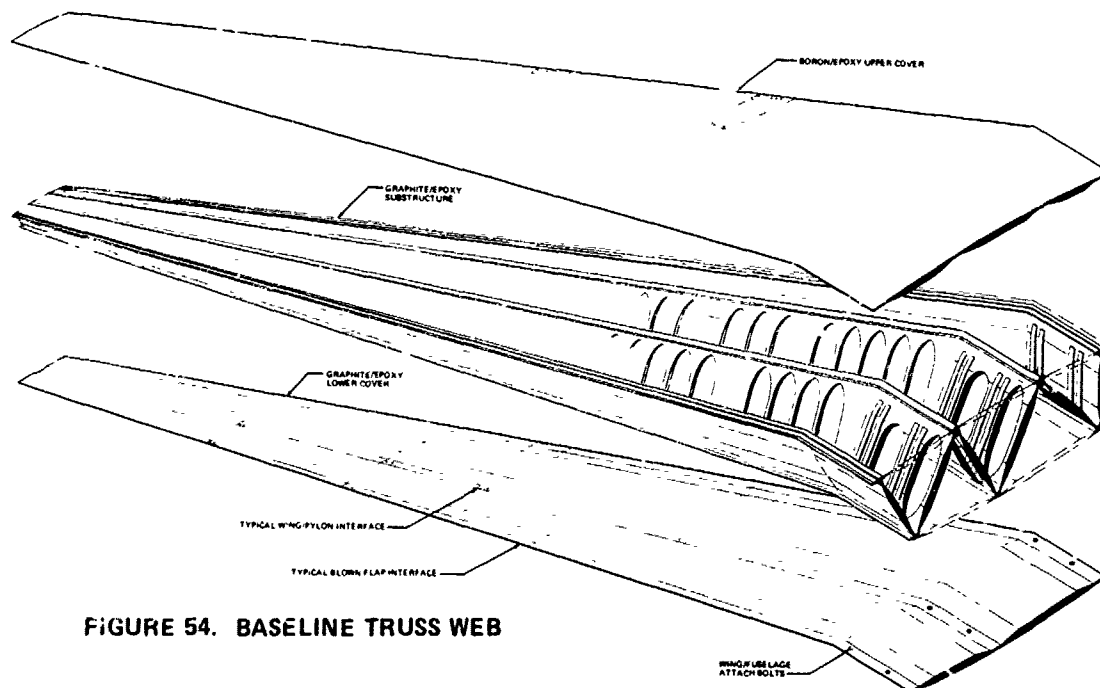


FIGURE 54. BASELINE TRUSS WEB

The preceding Initial Payoff Study (Paragraph 4.1.8) indicated configuration 3C2 (all bonded, six cells, no web cutouts) should be selected rather than Configuration 2B. The baseline truss web selection was intended to represent the design verification specimens actually built. It was desired to test both bonded and bolted joints for this concept so a configuration was selected that included both. Baseline materials were selected later in time than the initial payoff study when it had been determined the mixed graphite concept utilizing Thornel 75 was unworkable and the mixed graphite concepts utilizing other Type I materials offered insufficient payoff.

The more expensive configuration with web cutouts was selected because of the practical requirement for intercell accessibility, not offered by solid panel webs, and the desire to achieve best possible weight saving within other constraints.

4.2 ALTERNATE DESIGNS

4.2.1 Arch Web Concept

This concept was pictured in Figure 12. An analytical study was made to verify that the arch-web concept is a satisfactory structural configuration. The investigation was a two-dimensional chordwise analysis. Loads and geometry are an idealized representation of the conditions that exist at the root of the MST wing, ignoring the local effect that the sweep break has on the stress distribution. The box cross-sectional geometry was defined as:

- Box Chord = 100 inches
- Box Depth = 30 inches
- Skin Panels = 0.30 inch, 0/+45/90 Narmco 5206
- End Webs = 0.10 inch, 0/+45/90 Narmco 5206
- Inner Cells = 0.024 inch, 90-deg Narmco 5206
- Core = 2.0 pcf, fiberglass honeycomb.

In this investigation, a chordwise slice was analyzed to determine the capability of the arch web structure in distributing the locally applied loads to the main structural box members. A secondary purpose was to establish whether the internal structure was effective in maintaining the shape of the box cross section. The maximum bending condition has been considered, with air and structural inertia loadings being represented by asymmetric loads applied to the outside of the box. These included loads from the leading- and trailing-edge structural boxes. Fuel inertia loads were applied to the inside of the internal cell, zero and

maximum fuel conditions being investigated. Additionally, the effect of an internally applied ultimate pressure of 30 psi was considered, to represent the refueling malfunction condition.

Two geometries of internal cell shape were analyzed, Figure 55. Configuration A had an elliptical cell shape, and a deep internal arch structure. However, the fuel volume was only 65.7 percent of the main box volume and this could be a severe limitation in a wing-box application. The alternative Configuration B, having a fuel volume of 81.8 percent, was included to determine the practicality of increasing fuel capacity by reducing the stiffness of the arch.

A two-cell configuration, symmetrical about the centerline, was chosen for analysis. Reactions to applied bending and torsion loads were calculated on the assumption that only the end webs and the skin panels were effective in carrying shear. These reactions were then applied to the structure to form an internally balanced loading system. Deflected shapes of Configurations A and B are shown in Figure 56. In the maximum bending condition with zero fuel, Configuration B has a maximum deflection of 1.60 inches, which is considered to be excessive. The corresponding value for Configuration A is 0.18 inch which is acceptable. In practice, the presence of discrete ribs might reduce these deflections considerably.

Configuration A was selected as the more practical of the two designs. The analysis showed that the skin panels and end webs were lightly loaded, which was to be expected since the size of these members was determined by spanwise loading consideration.

Stress levels in the inner cell for Configuration A are shown in Figure 57, maximum of 50,000 psi being reached in the fueling malfunction condition.

This stress is well within the strength capability of the 90-degree laminate, but local stiffening might be required to avoid face wrinkling on the honeycomb core. Generally, Configuration A appears to be a satisfactory structure. Some increase in fuel volume might be possible, but it is doubtful whether the extreme geometry used in Configuration B could be achieved unless the stiffness of the internal cell and the core were increased.

Although the internal structure must inevitably strain with the skin to some extent, it is not required to have any spanwise strength or stiffness. The inner unidirectional membrane which acts to stabilize the outer primary structural membrane, via an elastic medium connecting the two membranes, is the basic idea behind this structure. The continuous stabilization of the covers is thought to offer a unique structural efficiency. Unfortunately, the difficulties inherent in a three-dimensional stability analysis of such a structure proved to be beyond the scope of the program.

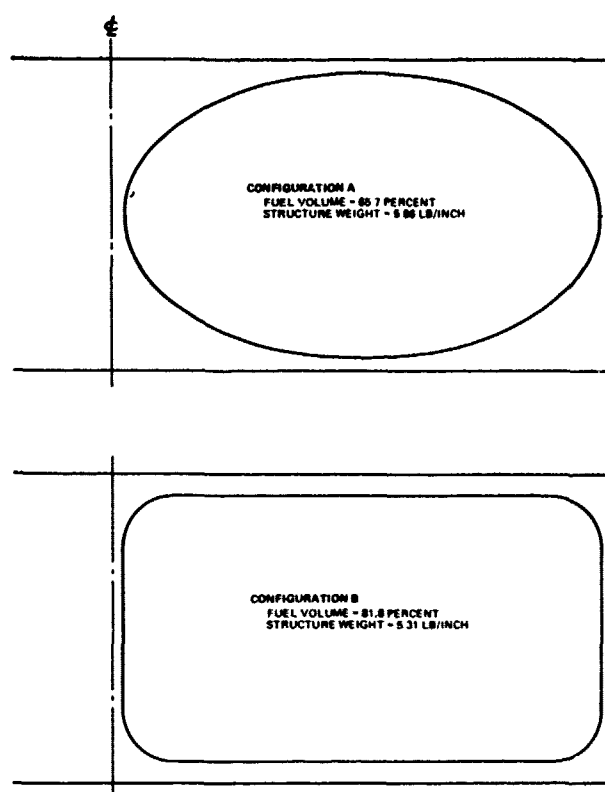


FIGURE 55. 2-DIMENSIONAL ANALYSIS - CONFIGURATIONS

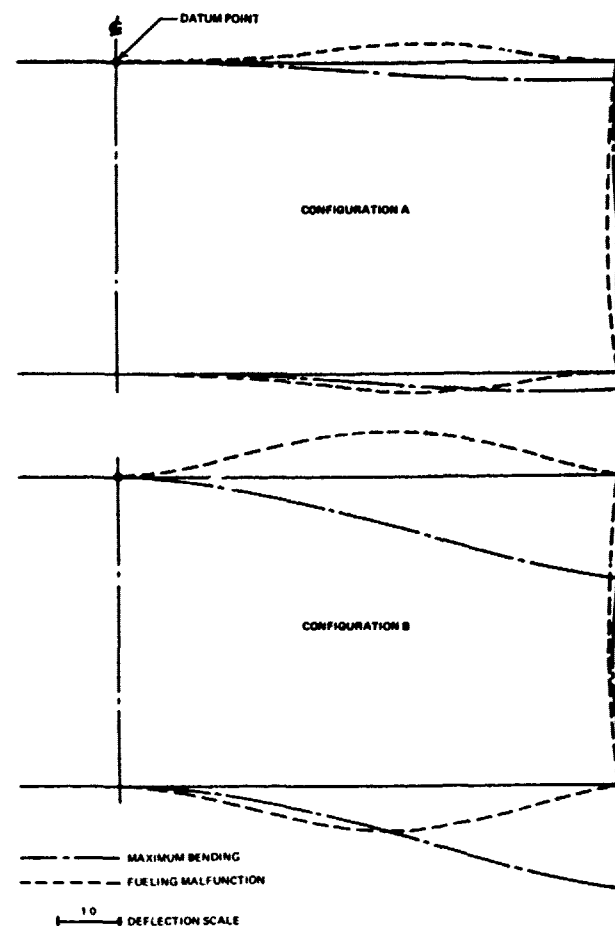


FIGURE 56. 2-DIMENSIONAL ANALYSIS - DEFLECTIONS

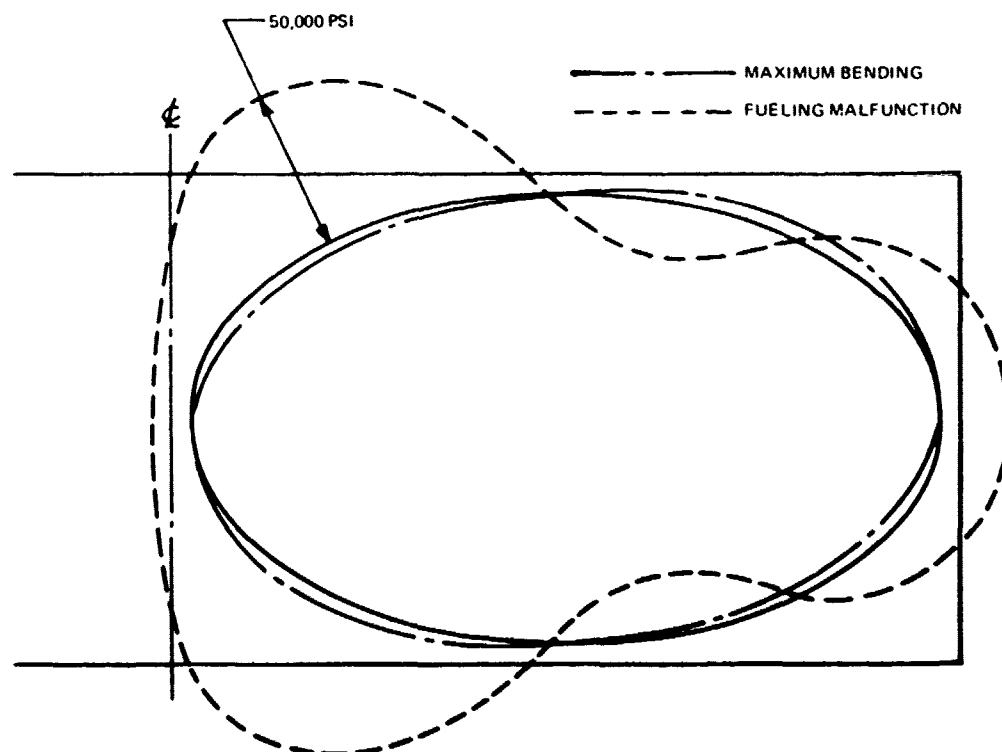


FIGURE 57. 2-DIMENSIONAL ANALYSIS - STRESS LEVELS IN INNER CELL

4.2.2 Torsional Stiffness Study

A brief study was made to compare relative torsional stiffness capabilities of several wing designs under consideration. Designs considered were the base case multi-web, the truss-web, and an approximation to the arch-web. St. Venant torsion was assumed and the elementary Bredt formulation for thin-walled sections was used to develop appropriate simultaneous equations. The approach is considered to be adequate for preliminary design purposes where relative ranking and initial sizes are sought.

The typical constant section wing box illustrated in Figure 58 was chosen in order to fix numerical values. Although somewhat arbitrary for this study, the same cross section has been used in the two-dimensional arch web box design study and the preliminary configuration weight trade. A change in the section should not significantly change the relative results given here..

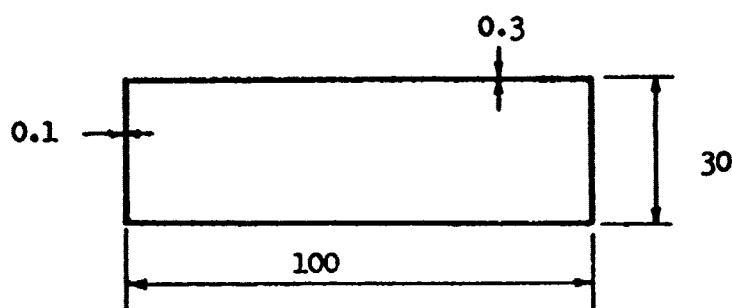


FIGURE 58. BASIC CROSS-SECTION

Figure 59 presents a summary of the results comparing the truss-web and multi-web designs on the basis of the required weight to obtain the same value of the constant, J . Tabulated results are presented in Table 18. Truss-web weight was calculated as that to give the same torsion constant as its comparable multi-web design, the total weight of interior webs in both cases being held constant. Comparable truss-web and multi-web designs were taken to be those that divide the covers into the same number of chordwise panels. Thus, for example, a truss-web design would require six cells to divide the covers into the same number of panels as a three-cell multi-web design. Additional cells were formed in the basic multi-cell box by adding interior webs that were 0.1 inch thick. Equivalent truss-web and multi-web designs are illustrated in Figure 60 for a basic three-cell case.

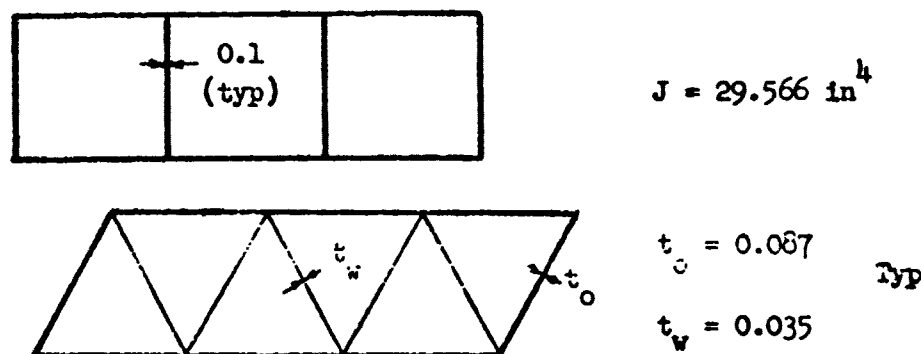


FIGURE 60. TYPICAL EQUIVALENT SECTIONS FOR THE SAME J

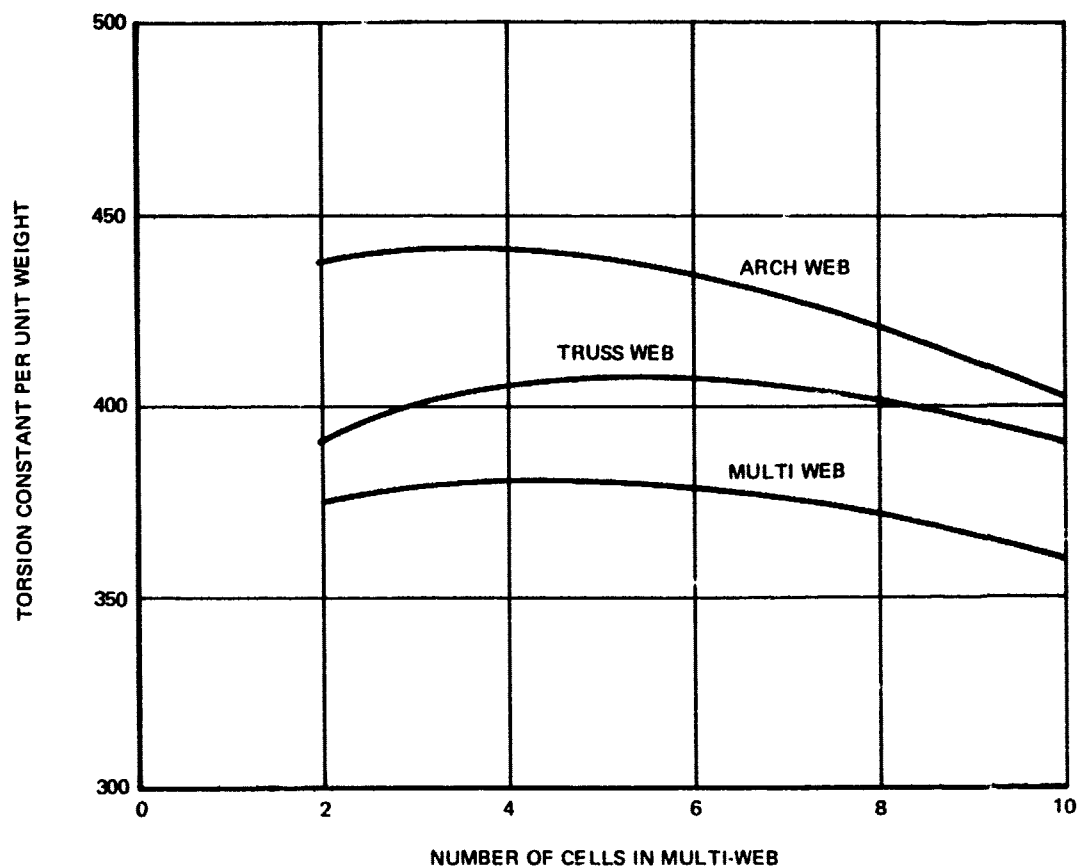


FIGURE 59. TORSIONAL STIFFNESS COMPARISON OF SEVERAL CONDIDATE DESIGNS

TABLE 18
DATA SUMMARY OF EQUIVALENT SECTIONS

| NO. OF CELLS ⁽¹⁾ | MULTI-WEB | | TRUSS-WEB ⁽⁶⁾ | ARCH WEB | | J/A | | |
|-----------------------------|-----------|---------------------|--------------------------|------------------|---------------------|-----------|-----------|---------|
| | J | AREA ⁽²⁾ | AREA ⁽⁴⁾ | J ⁽³⁾ | AREA ⁽⁵⁾ | MULTI WEB | TRUSS WEB | ARCHWEB |
| 2 | 28421 | 75.6 | 72.7 | 30335 | 69.0 | 375.9 | 390.6 | 439.6 |
| 3 | 29566 | 78.6 | 73.3 | 31874 | 72.0 | 376.1 | 402.9 | 442.6 |
| 4 | 30809 | 81.6 | 75.4 | 33147 | 75.0 | 377.5 | 408.3 | 442.3 |
| 5 | 31964 | 84.6 | 73.0 | 34208 | 78.0 | 377.8 | 409.7 | 438.5 |
| 6 | 33000 | 87.6 | 60.7 | 35113 | 81.0 | 376.7 | 408.6 | 433.5 |
| 8 | 34743 | 93.4 | 60.4 | 36599 | 87.0 | 371.1 | 401.8 | 420.6 |
| 10 | 36136 | 99.6 | 92.2 | 37718 | 93.0 | 362.8 | 391.6 | 405.5 |

- (1) Number of Cells in multiweb design.
- (2) Includes 10% of base area for ribs (6.6 in²)
- (3) 50 cells
- (4) Material added to outside webs
- (5) Also base area for given case
- (6) Same J as multiweb

In general, the torsion constant for the truss-web design will be somewhat smaller than the multi-web design if the total web weight is held constant.

To obtain the same torsion constant, additional material was added to the exterior webs because for these proportions less weight is required when it is added to the webs rather than the covers. However, the additional weight of added material was in the order of one percent for the cases studied and so was not significant.

The torsional constant for the arch-web case was approximated by distributing the material weight of the interior webs for a given multi-web case into an equivalent web weight case with 50 cells. Thus, the approximation to the arch-web is a section with a full-depth core, and the different cases can be taken to represent different core densities. Cases with 100 cells showed only a fraction of a percent increase over the 50-cell case and so the latter was used for the comparison because the increase in computational time is not justified. These results would be expected to be somewhat low since for a constant weight the hollow sections of the arch-web would allow more material to be moved toward the exterior webs, thus increasing the torsion constant slightly.

Implicit in all of the calculations is the assumption that all of the material involved has the same effective in-plane shear modulus. To account for the ribs in the base multi-web design, the weight was increased by 10 percent of the basic box weight. This increase reflects the additional weight of the ribs in the multi-web design compared to the material required to transfer concentrated loads, etc., in the truss-web design.

It is emphasized that the weights shown are approximate only, but are adequate to establish the desired trends. The trend appears to be that the arch web design is a strong candidate for torsion-critical structures. The continuous truss web also has a greater torsion constant (J/A) than the multi-web by virtue of not requiring ribs. A comparison of torsion stiffness of the truss web with shear carrying inner webs versus unidirectional post internal structure was obtained by the finite element analysis (Paragraph 5.1) and showed a 6-percent decrease in GJ for the lighter-weight post/web box. If worked out on the above comparison basis of equivalent torsion constants, the truss-web box with cutout post/webs would still have a higher J/A than the multi-web/rib design.

4.2.3 Multi-Web/Multi-Rib Optimization

The objective of the multi-rib and multi-web optimization study was to determine the optimum composite baseline wing box configuration for this family of designs. Constant thickness honeycomb panels for all covers, webs and ribs are assumed for ease of parametric design. At four stations of the wing, in-plane loads and stiffness requirements (E_t and G_t) are input to the sandwich panel design program (SPADE). Panel dimensions and aspect ratio are varied at each station to obtain designs and weights for the family of substructure configurations at each station.

Table 19 shows the matrix of wing upper and lower cover problems solved: N_1 represents number of chordwise subdivisions in the wing box, see Figure 61,

TABLE 19
MATRIX OF WING COVER PROBLEMS

| | | N_1 | | | | | |
|-------|----|-------|---|---|---|----|----|
| | | 1 | 2 | 4 | 8 | 12 | 16 |
| N_2 | 1 | X | X | X | X | X | X |
| | 2 | X | | | | | |
| | 4 | X | | X | | X | |
| | 8 | X | | | | | |
| | 12 | X | | X | | X | |

N_1 = NUMBER OF CHORDWISE SUBDIVISIONS IN BASIC PANEL

N_2 = NUMBER OF SPANWISE SUBDIVISIONS IN BASIC PANEL

X = SPADE PROBLEMS SOLVED (OTHER CASES INTERPOLATED OR EXTRAPOLATED)

BASIC PANEL: $N_1 = 1$ AND $N_2 = 1$

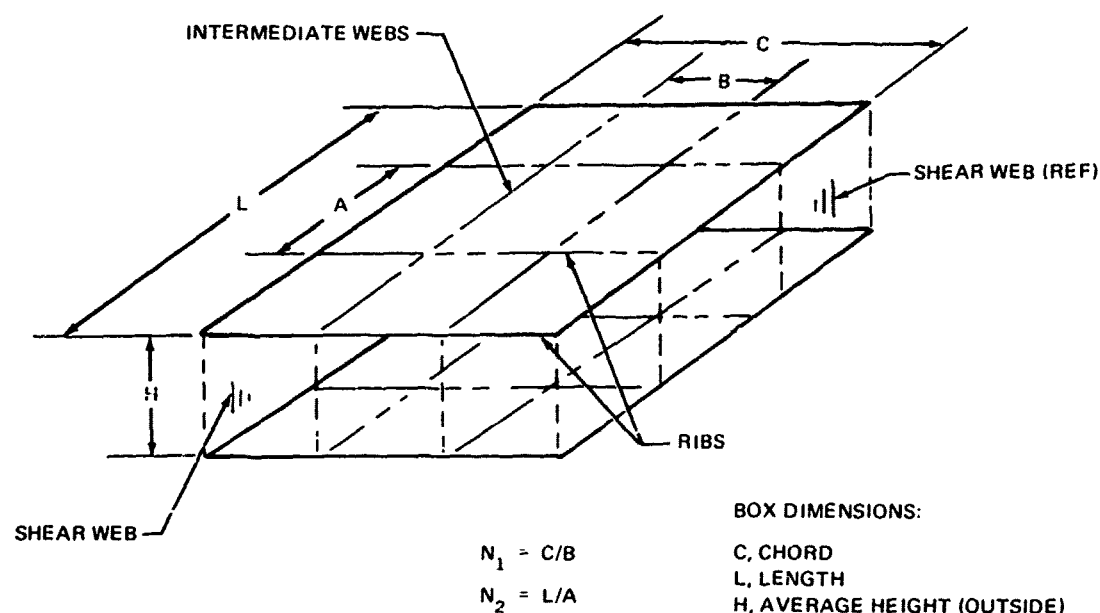


FIGURE 61. BOX GEOMETRY

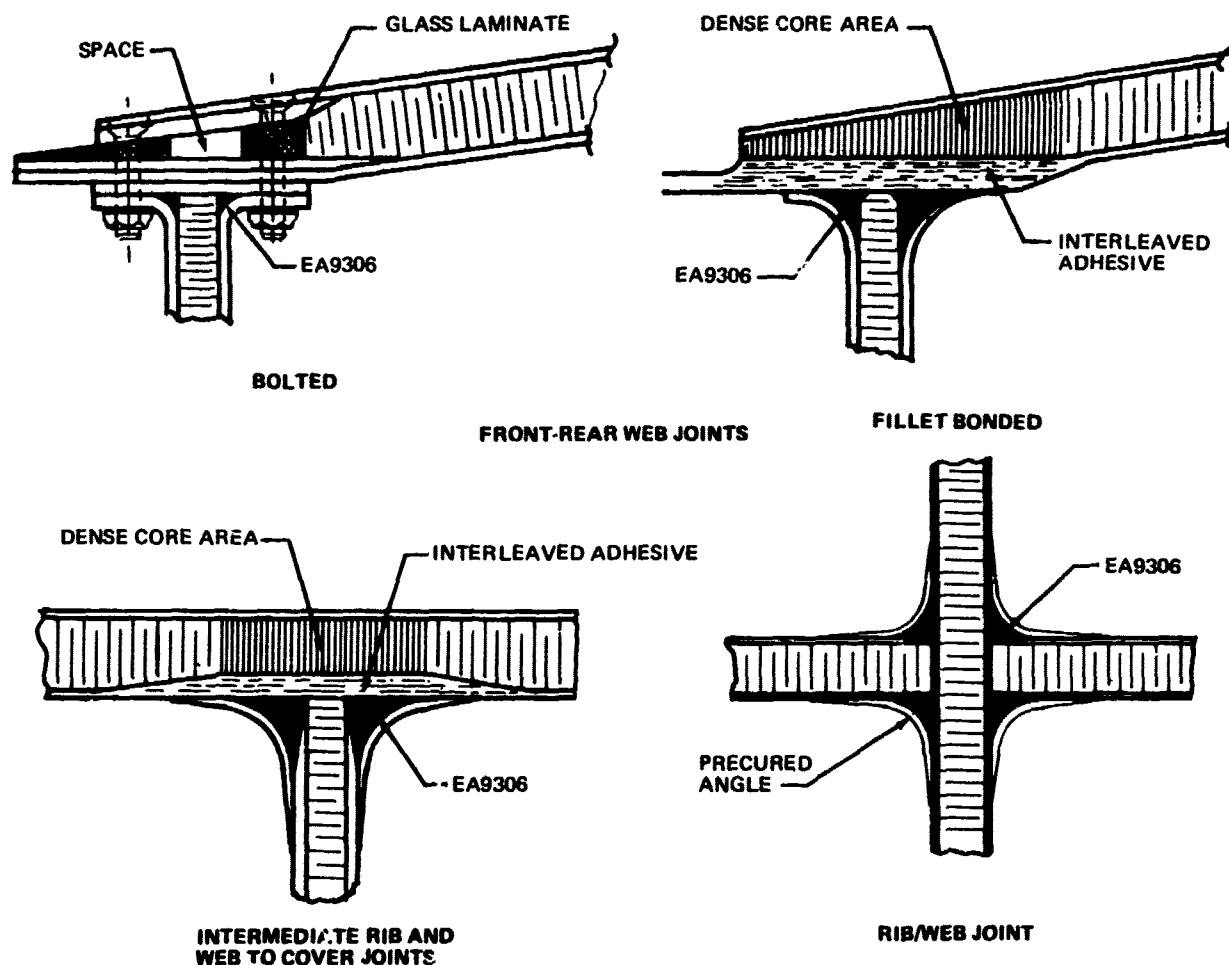
and N_2 represents the number of spanwise subdivisions between major ribs 55 inches apart (i.e., concentrated load input stations). The $N_2 = 1$ row (Table 19) represents the family of multi-web configurations. The $N_1 = 1$ column represents multi-rib configurations. Rows and columns greater than one represent multi-web/rib configurations. Front and rear shear web problems corresponding to the $N_1 = 1$ column are also solved at the four stations.

Ribs are assumed to transfer cover air loads to front and rear shear webs and to resist compression due to wing bending. Intermediate ribs (closer than 55 inches apart) redistribute no wing shear. With these rules it was discovered that, even at the wing root, two-ply ± 45 -degree sandwich facings were more

than adequate for the load levels. SPADE was run to determine core thickness requirements for a few rib cases to aid determination of representative rib panel weights.

Webs intermediate to front and rear webs ($N_1 > 1$) were assumed to support covers only. They were sized with two-ply facings and core thickness of 0.25 inch minimum. Also, large cutouts were introduced that removed 50 percent of the web panel weight.

Weights of joints to connect all panels were generated on the basis of the fillet joint design concept. Constant thickness honeycomb panels were connected to covers ("tee" joints) with filleting adhesive and co-cured angles with large bend radii. See Figure 62. The figure also shows a comparison of box corner joint designs using a conventional bolted concept and the contrasting fillet joint concept. Weights of box corner joints were considered constant for all configurations and were omitted from section weight comparisons. Other joints (cover to web and cover to rib) were assumed designed for maximum internal pressure and to vary in weight as a function of panel area, down to a minimum practical joint weight. Table 20, showing joint weights at Station 107, is typical.



NOTE: SKETCHES - NOT TO SCALE.

FIGURE 62. FILLET JOINT CONCEPTS FOR WING BOX DESIGN

TABLE 20
BONDED JOINT CONFIGURATION WEIGHTS STATION 107, ALTERNATE BOX DESIGNS

| (1) N ₁ | (1) N ₂ | K | (2) JOINT WEIGHT (LB/55-INCH SPAN) | BOX CONFIGURATION |
|------------------------------|-----------------------|--|---|-------------------|
| 1 2 4 8 12 16 | 1 | 2.0 1.0 0.55 0.30 0.23 0.15 | 8.2 6.24 6.39 7.99 10.12 11.04 | MULTI-WEB |
| 1 1 1 1 | 2 4 8 12 | 1.0 0.55 0.30 0.23 | 8.25 8.96 9.78 11.20 | MULTI-RIB |
| 4 12 4 12 | 4 4 12 12 | 0.15 0.15 0.15 0.15 | 8.52 24.70 24.05 68.20 | MULTI-RIB/WEB |

(1) SEE TABLE 2 FOR N_2 (2) JOINT WEIGHTS INCLUDE END RIB JOINTS

Figures 63 through 65 are plots of box configuration weights per inch of span at Station 107. End rib weights and box corner joint weights are excluded, being considered constant. These plots include the effect of pressure on covers and front and rear webs. Although the cover panels at Station 107 were highly anisotropic (90-percent 0-degree fibers), due to the reduced GJ and the significant EI requirement for the box in this area (refer to Figure 34), the addition of 30-psi pressure to the cover panels did not require additional cross plies. Apparently these high aspect ratio panels ($a/b = 10$) will carry the pressure load to their narrow ends and unload preferentially on the ribs rather than carry the load across the narrow width to the webs. The front and rear shear panels (+45-degree pattern) designed by stability did require addition of core and/or facing thickness due to application of pressure for cases $N_2 = 1$ and 2.

It may be observed that in the inboard wing areas, where GJ requirement is lower, directional panel stiffening concepts may show a weight advantage. Observations from Figures 63 through 65 include the following:

- The multi-web configuration total weights (Figure 63) indicate an optimum at $N_1 = 6$. Detail variation in method of joint weight derivation should not significantly alter this finding.
- The multi-rib configuration total weights (Figure 64) indicate an optimum at $N_2 = 4$, with an indicated minimum weight less than multi-web.
- The multi-rib/web minimum weight configurations (dotted curve on the surface plotted in Figure 65) were not characterized by a sufficient number of numerical calculations; however, inspection (Figure 65) indicates they probably do not offer any significant weight advantage over (in fact their weights probably are intermediate between) the rib and web configurations. This is supported by the four multi-rib web cases run. See Table 21.

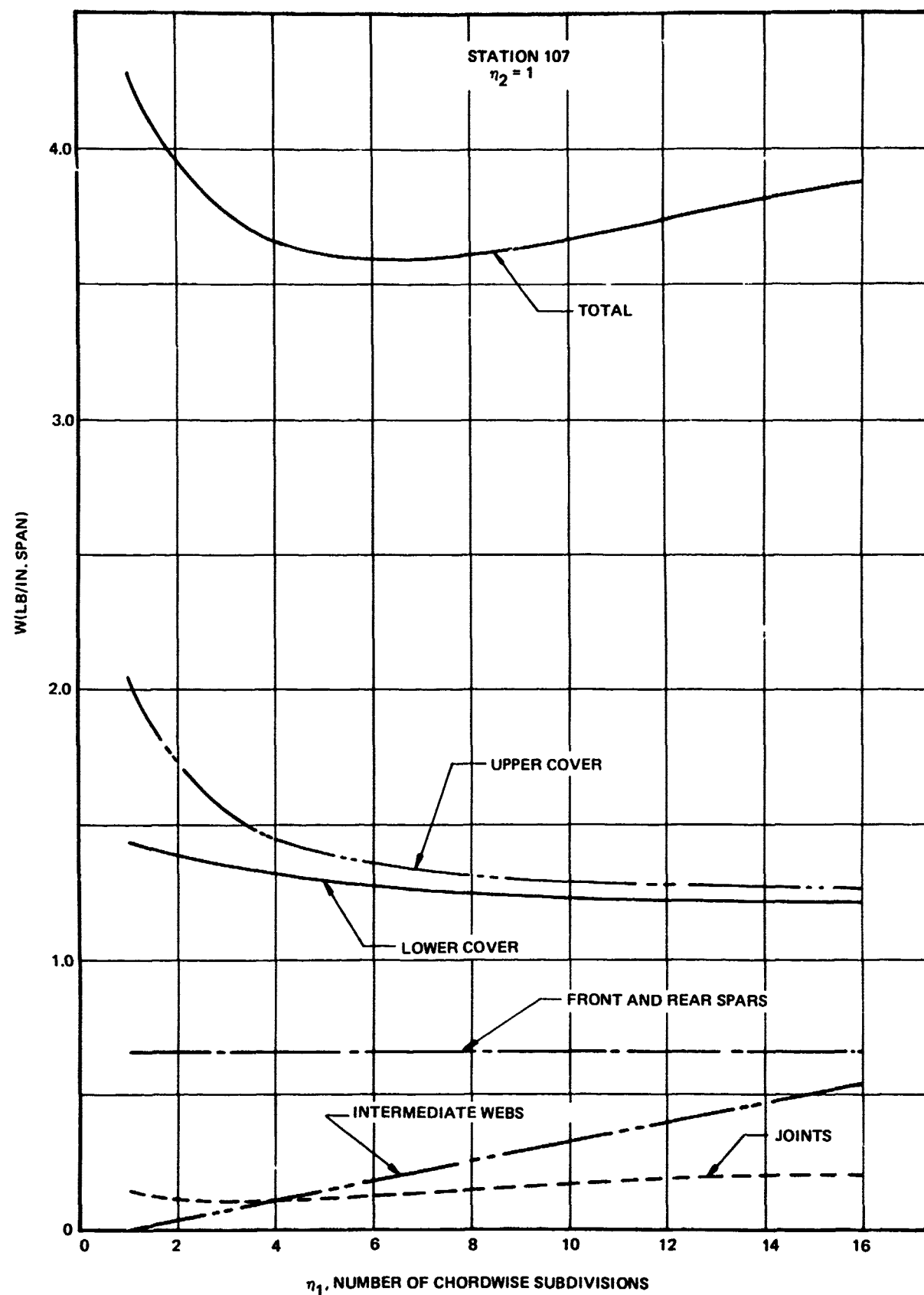


FIGURE 63. MULTIWEB CONFIGURATION WEIGHTS, STA 107

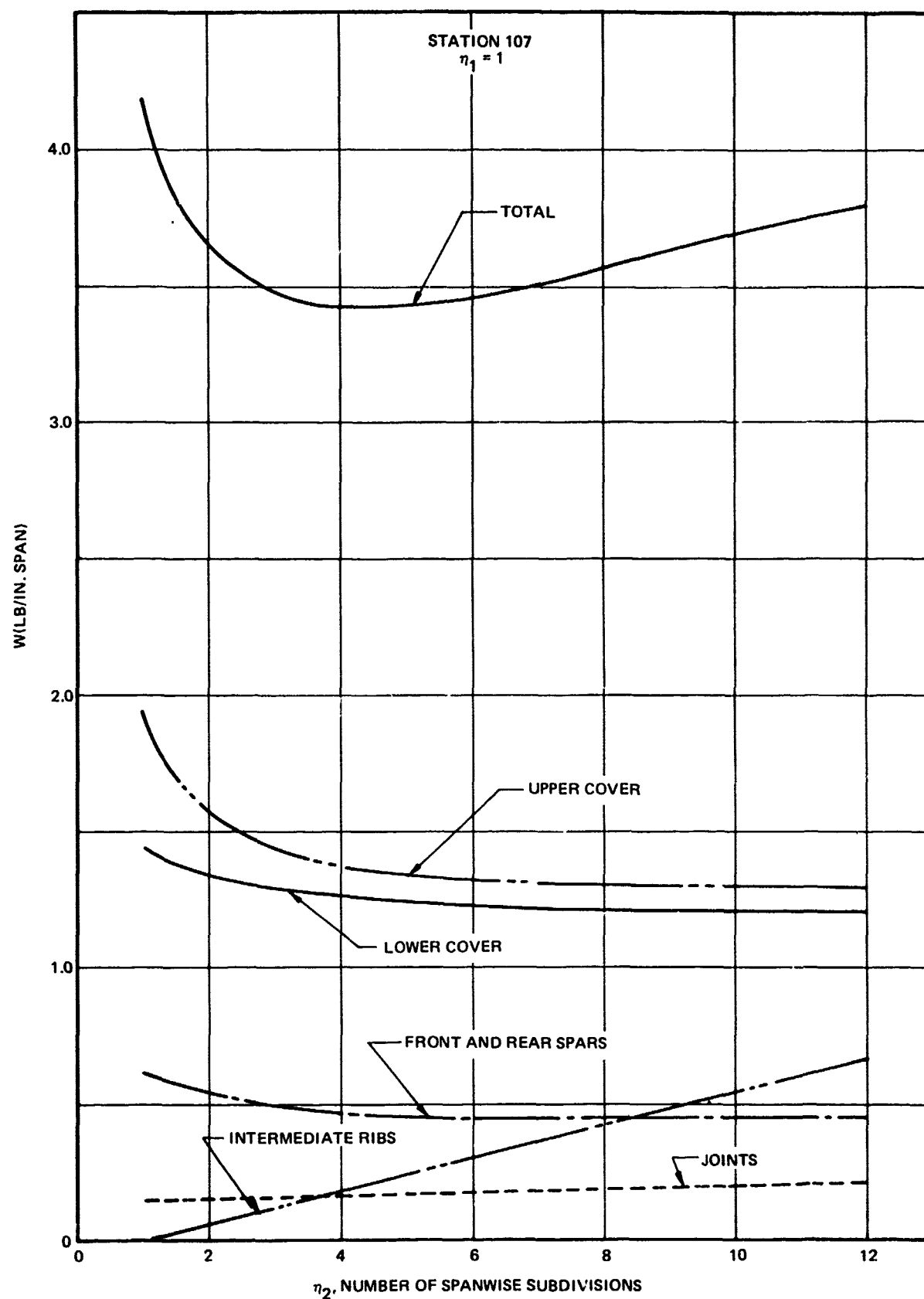


FIGURE 64. MULTIRIB CONFIGURATION WEIGHTS, STA 107

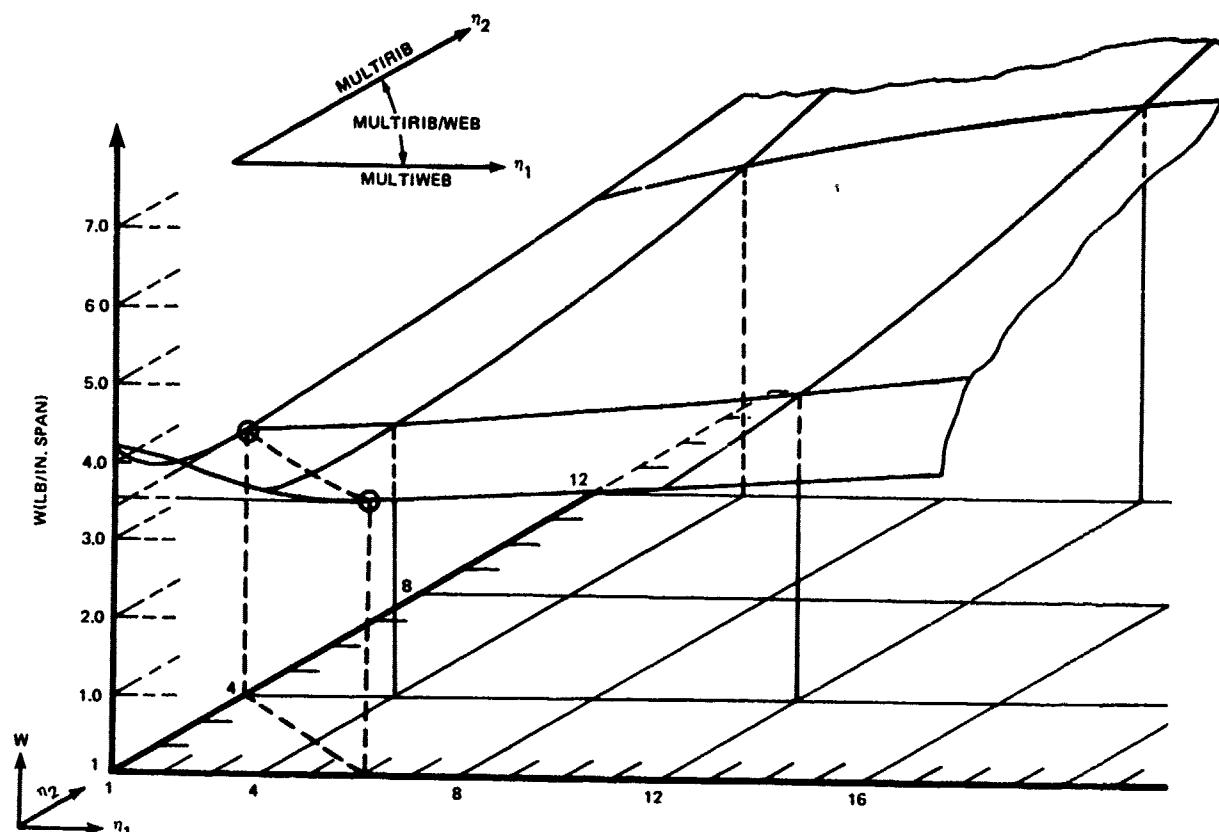


FIGURE 65. SURFACE OF CONFIGURATION WEIGHTS AT STATION 107

TABLE 21
MULTI-RIB/WEB CONFIGURATION WEIGHTS
STATION 107
LB/INCH SPAN

| N_1 | N_2 | UPPER COVER | LOWER COVER | INTERMEDIATE RIBS AND WEBS | JOINTS | FRONT/ REAR WEBS | TOTAL WITHOUT JOINTS | TOTAL |
|-------|-------|-------------|-------------|----------------------------|--------|------------------|----------------------|--------|
| 4 | 4 | 1.3520 | 1.2590 | 0.2866 | 0.1545 | 0.4642 | 3.3618 | 3.5163 |
| 12 | 4 | 1.2770 | 1.2200 | 0.5762 | 0.4490 | 0.4457 | 3.5189 | 3.9679 |
| 4 | 12 | 1.3370 | 1.2080 | 0.7606 | 0.4385 | 0.4642 | 3.7698 | 4.2083 |
| 12 | 12 | 1.2760 | 1.0490 | 1.0502 | 1.2400 | 0.4457 | 3.8206 | 5.0609 |

Corresponding investigation at the other wing stations confirmed a slight weight advantage for the optimum multi-rib over the optimum multi-web, even when internal pressure is neglected. When pressure (20 psi ultimate) is included, stations outboard of Station 350 are affected, with the most weight being added for the multi-web. It should be remembered the multi-web also includes ribs at 55-inch spacing, which prevents the panels from being of infinite aspect ratio. It was also noted that weight penalty for pressure is added only for box closure (shear) webs for the multi-rib design. See Tables 22 and 23. Reference 7 includes charts of configuration weights.

TABLE 22
MULTIWEB OPTIMUM WEIGHT
CONFIGURATIONS ($N_2 = 1$)

| STA | OPT N_1 | b (IN.) | SECTION MINIMUM WEIGHT (LB/INCH SPAN) | |
|-----|--------------|------------|--|--------------------|
| | | | NO PRESSURE | 20 PSI PRESSURE |
| 107 | 6 | 15 | 3.60 | 3.60 |
| 257 | 4-5 | 18-14.4 | 2.65 | 2.65 |
| 350 | 3 | 20.3 | 1.55 | 1.586 |
| 450 | 2-3 | 25-16.7 | 0.81 | 1.255 |

TABLE 23
MULTIRIB OPTIMUM WEIGHT
CONFIGURATIONS ($N_1 = 1$)

| STA | OPT N_2 | a (IN.) | SECTION MINIMUM WEIGHT (LB/INCH SPAN) | |
|-----|--------------|------------|--|--------------------|
| | | | NO PRESSURE | 20 PSI PRESSURE |
| 107 | 4 | 13.75 | 3.40 | 3.40 |
| 257 | 3-4 | 18.3-13.75 | 2.65 | 2.65 |
| 350 | 3 | 18.3 | 1.60 | 1.609* |
| 450 | 3 | 18.3 | 0.80 | 0.942* |

*MULTIRIB WEIGHT PENALTY DUE TO
END WEB INCREASES ONLY.

versus number of bays at the various stations to support these tables. Table 24 presents the HTS graphite laminates designed by the SPADE computer program and which were used in this study.

The advantage of the multi-rib is due chiefly to the high percentage of span-wise 0-degree plies in the covers which find support on the ribs, allowing minimum thickness sandwich cover panels.

TABLE 24
ALTERNATE BOX STUDY PANEL FACINGS

| STA | COVER STIFFNESS INPUT | | UPPER AND LOWER COVERS | | | END SHEAR PANELS | | |
|-----|--------------------------|-----------------------|--|-------------------------|-----------------------------|---------------------------------------|-------------------------|-----------------------------|
| | ET x 10 ⁻⁴ | GT x 10 ⁻⁴ | NO. PLIES AT ANGLE | NO. PLIES PER FACING | LAMINATE WEIGHT (PSF) | NO. PLIES AT ANGLE | NO. PLIES PER FACING | LAMINATE WEIGHT (PSF) |
| 107 | 395.0 | 55.0 | (0 ₁₈ /+45/-45) | 20 | 1.678 | (+45 ₅ /-45 ₅) | 10 | 0.8392 |
| 257 | 252.0 | 52.0 | (0 ₁₁ /+45 ₄ /-45 ₄) | 19 | 1.595 | (+45 ₅ /-45 ₅) | 10 | 0.8392 |
| 350 | 161.0 | 47.9 | (0 ₇ /+45 ₄ /-45 ₄) | 15 | 1.259 | (+45 ₄ /-45 ₅) | 9 | 0.7553 |
| 450 | 82.0 | 9.4 | (0 ₄ /45/-45) | 6 | 0.504 | (+45/-45) | 2 | 0.1678 |

A multi-rib box panel stiffening concept was briefly investigated, Figure 66. This offers increased fuel volume compared with constant depth honeycomb. This concept, unlike discrete stiffeners, supports the panel continuously so that panel stress level is uniform. Fabrication, cost, or weight comparison were not accomplished for this concept. It is presented for idea only.

Further multi-rib design work must contend with the close rib spacing (13.75 inches) of the optimum weight configurations. Ribs with a single large elliptical cutout in each rib are envisioned. Ribs could be spaced further apart through use of an integral stringer stiffening concept such as pictured in Figure 66.

Figure 67 displays an alternative multi-rib box design. It is a two-cell wing box with three shear webs to the outboard flap attachment station and a single

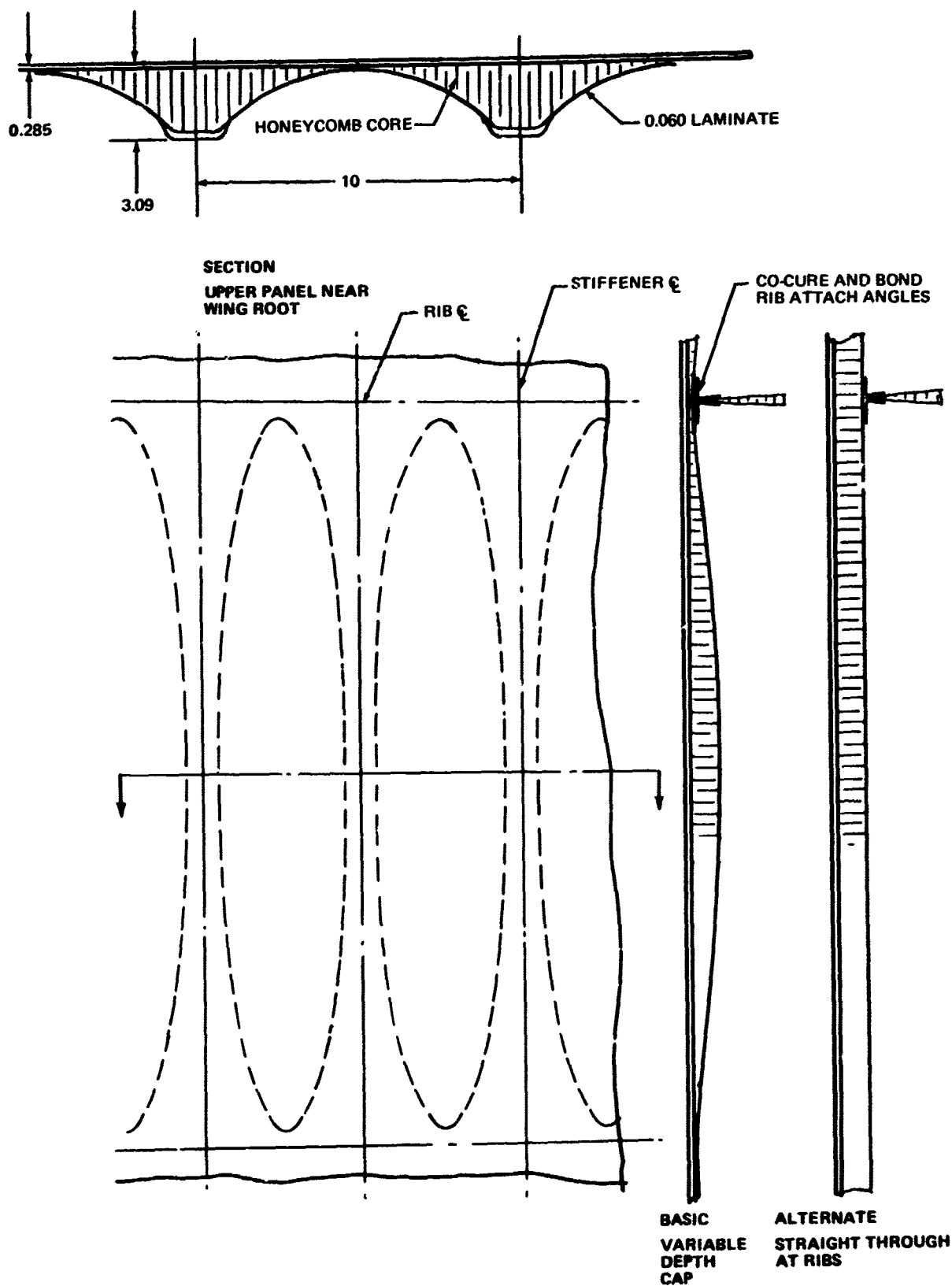


FIGURE 66. INTEGRAL STIFFENER CONCEPT

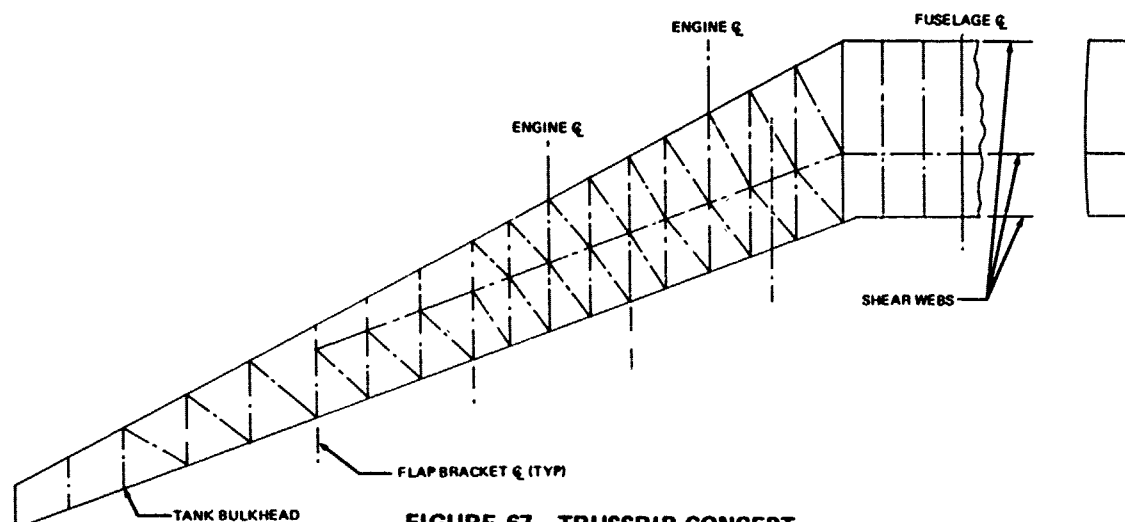


FIGURE 67. TRUSSRIB CONCEPT

cell from there outboard. The diagonal truss-rib design serves to space the basic streamwise ribs farther apart by limiting the cover panel buckle size to the circle inscribed in the triangles. A further function of the diagonal trussing is to stiffen the box in torsion, allowing removal of excess 45-degree plies and replacing them with diagonal rib cap material. In this way the covers are stabilized for compression and stiffened in shear by the same structure. In the MST wing box, the greatest torsional stiffness is required inboard of each engine pylon. Like the baseline truss web design, the substructure (Figure 67) may be laid up on sawtooth-shaped molds, allowing a few large bonded subassemblies to go into a final assembly. For bolted covers, stress relief strips would appear only along the three spanwise web connections. The covers would contain doublers following the diagonal ribs which would reduce stress concentrations due to attachment of those members. The doublers also serve as rib caps.

4.2.4 Preliminary Configuration Weight Trade

The weight advantages or disadvantages of the truss-web concept compared to other more conventional composite concepts was desired. The composite concept selected as a comparative composite baseline for the initial payoff study (Paragraph 4.1.8, Configuration 4, three-cell multi-web/rib) was later found not to be optimized. Configuration 4 (Ref Table 16) was 4.3 percent heavier on an equivalent basis than the optimum multi-rib of Paragraph 4.2.3, and 8 percent heavier if pressure penalty is included.

If the optimum multi-rib configuration is designed with bolted covers with stress concentration relief and is put on the same weight basis as Table 16, thus replacing Configuration 4 as a composite comparative baseline, its relative weight value would be 1.028, or 2.2 percent lighter than the comparable 1B truss-web configuration. See Table 25. Using truss-web weight penalties from the payoff study (Paragraph 8.1.), the optimum multi-rib is seen to be approximately 2 percent lighter than the Configuration 1B truss web and equal to the 2B truss web. Actually, the percentage penalties for a multi-rib designed in metal (i.e., the baseline metal wing) are greater than for a truss web, so this comparison is not complete. If wing internal pressure is added into this comparison, the truss web is found to be at a theoretical weight disadvantage with respect to the multi-rib. Apparent cover weight increases for the truss-web infinite aspect ratio panels compared with panels supported on 55-inch centers are shown in Table 26.

TABLE 25
REVISED 40-INCH SECTION WEIGHT COMPARISONS

**BASIS: NO WEIGHT PENALTIES, NO INTERNAL
PRESSURE, BASELINE MATERIALS**

| CONFIGURATION | | LB/40-IN. SECTION | RELATIVE WEIGHT* | Δ PERCENT |
|---|---------------|----------------------|---------------------|-----------|
| NAME | NUMBER | | | |
| SCR SOLTED TRUSS WEB | 1B | 192.22 | 1.050 | 0.0 |
| BASELINE TRUSS WEB (WITHOUT CUTOUT WEBS) | 2B | 188.54 | 1.030 | -2.0 |
| 3-CELL COMPARATIVE COMPOSITE M-W/R | 4 | 196.54 | 1.072 | 2.2 |
| OPTIMUM SCR BOLTED MULTI-RIB | OPTIMUM MR | 188.15 | 1.028 | -2.2 |

*REF. TABLE 16.

TABLE 26
**TRUSS WEB VS MULTIWEB THEORETICAL GRAPHITE COVER
WEIGHT PENALTY (DESIGNED BY 20 PSI PRESSURE)**

| UPPER COVER | | | | |
|-------------|-------------------------|--------------------|--------------------|---------------------------|
| STA | PANEL WIDTH (IN.) | TRUSS WEB (PSF) | MULTIWEB* (PSF) | TRUSS WEB ΔW (PERCENT) |
| 107 | 43 | 3.165 | 2.720 | 11.6 |
| 257 | 34 | 2.330 | 2.208 | 6.0 |
| 350 | 28 | 1.767 | 1.480 | 12.0 |
| 450 | 22.7 | 1.334 | 1.182 | 15.8 |
| LOWER COVER | | | | |
| 107 | 50 | 3.555 | 2.300 | 54.2 |
| 257 | 43 | 2.575 | 1.927 | 49.6 |
| 350 | 36 | 1.992 | 1.520 | 31.0 |
| 450 | 28.7 | 1.680 | 1.328 | 26.5 |

SCF'S NEGLECTED

* $\eta_2 = 1$, RIBS AT 55-INCH SPACING

The pressure panel analysis assumed uniform thickness sandwich panels, using cover laminates and core density established by the Multi-Web/Multi-Rib Optimization Study. Core thicknesses were obtained by calculation of maximum longitudinal and transverse panel bending moments for 20-psi pressure. No attempt was made to optimize the patterns for the pressure case.

It should be noted (Table 26) that the suggested penalties do not accrue in real design when the stress concentrations due to mechanical attachment to substructure are considered. Unless the multi-rib has all-bonded attachment of ribs to covers, the frequent rows of chordwise holes would require a considerable attachment penalty not computed in this program. The truss web, on the other hand, does not require frequent chordwise stress relief except at local areas of chordwise concentrated load introduction and at the dihedral change in upper cover, and spanwise stress relief along web crests is relatively easy to achieve.

In short, the rib attachment penalty for a multi-rib is believed to be much greater than the penalty for the relatively few chordwise load introduction points on the truss web. If an all-bonded rib to cover connection, such as the tension-fillet bond, is perfected to withstand internal pressure loads, then a multi-rib design is possible that would be competitive.

SECTION V

STRUCTURAL ANALYSIS

5.1 FINITE ELEMENT ANALYSIS

5.1.1 AMST Conceptual Wing

Model Definition and Geometry - A finite element analysis of the truss web design concept was conducted. The finite element model which was adopted for this analysis incorporated the current wing geometry at the time the finite element analysis was initiated. This geometry was for the Model 915B, 1660-square-foot wing. Since most of the large concentrated loads from engine mounts, and flap hinges occur on the inboard half of the wing, and since internal forces can be expected to differ from those determined from engineering beam theory most in the sweep-break region, economy dictated that the wing should be modeled only outboard as far as wing Sta 282. However, for a final design of the truss web concept, extension of the idealization to the tip should be considered. The finite element model reflects a double curvature of the wing covers, corresponding as close as the fineness of the model would allow, to the true topology of the AMST wing surface. The idealization which is reflected in the model is compatible with a membrane solution, although bending bars were required to carry kick forces produced by the effect of double curvature on the membrane element forces. These kick forces are transmitted to locations where they are reintroduced into the membrane elements of the model.

The AMST truss web wing box (Figure 54) is made up of three components: an upper cover, a lower cover, and a web structure. The finite element model of these same three components is shown in Figures 68, 69, and 70. The idealization of the web structure is shown in Figure 69 in a developed form. Nodes numbered 1 through 7 are located on the aircraft plane of symmetry, and consistent with symmetric loading cases which were analyzed, the reactions on this plane are of a symmetric type, and hence no tangential type of reactions are assumed to act on the plane of symmetry. The model dimensions may be characterized by the following sizes:

47 nodes

143 bars

132 triangular membranes

28 reactions

1903 unknown forces

1227 equations

676 redundants.

Elements - The principal element used in the model is a triangular membrane equilibrium element, which is based on an assumed linear stress

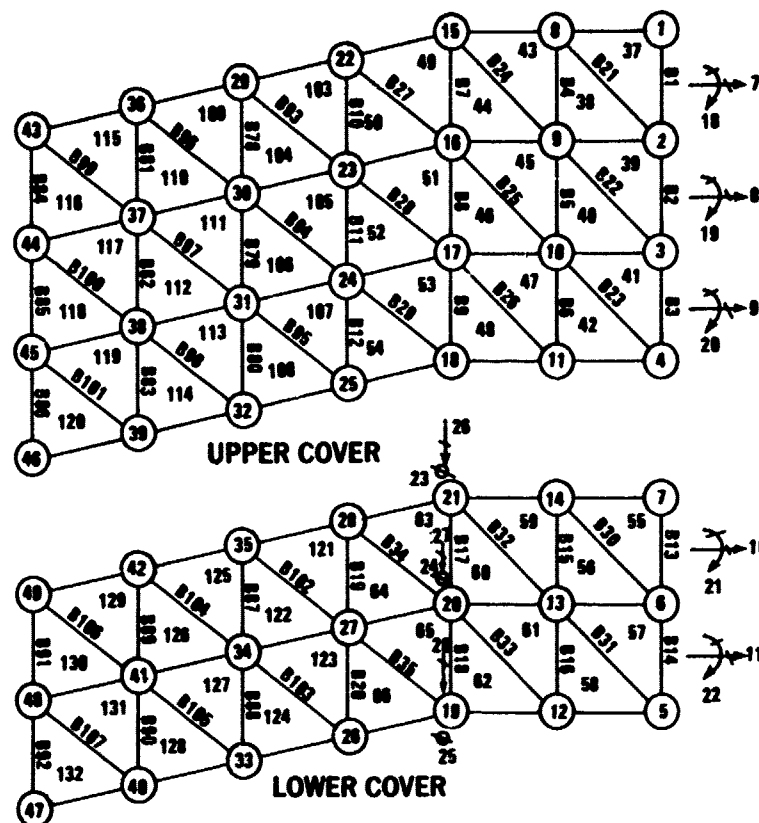


FIGURE 68. COMPOSITE WING COVERS

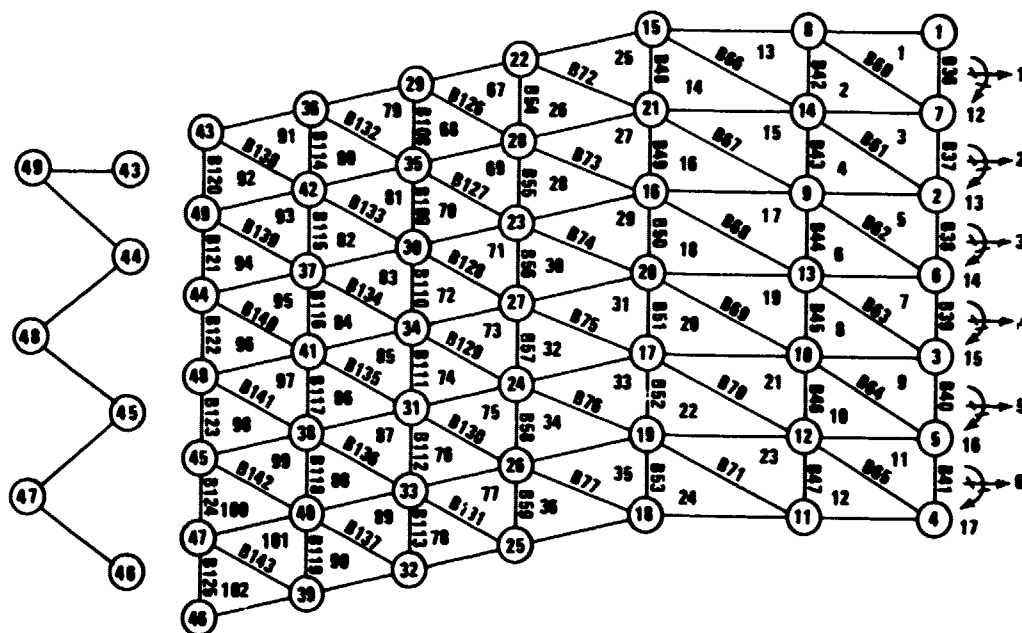


FIGURE 69. COMPOSITE WING WEB

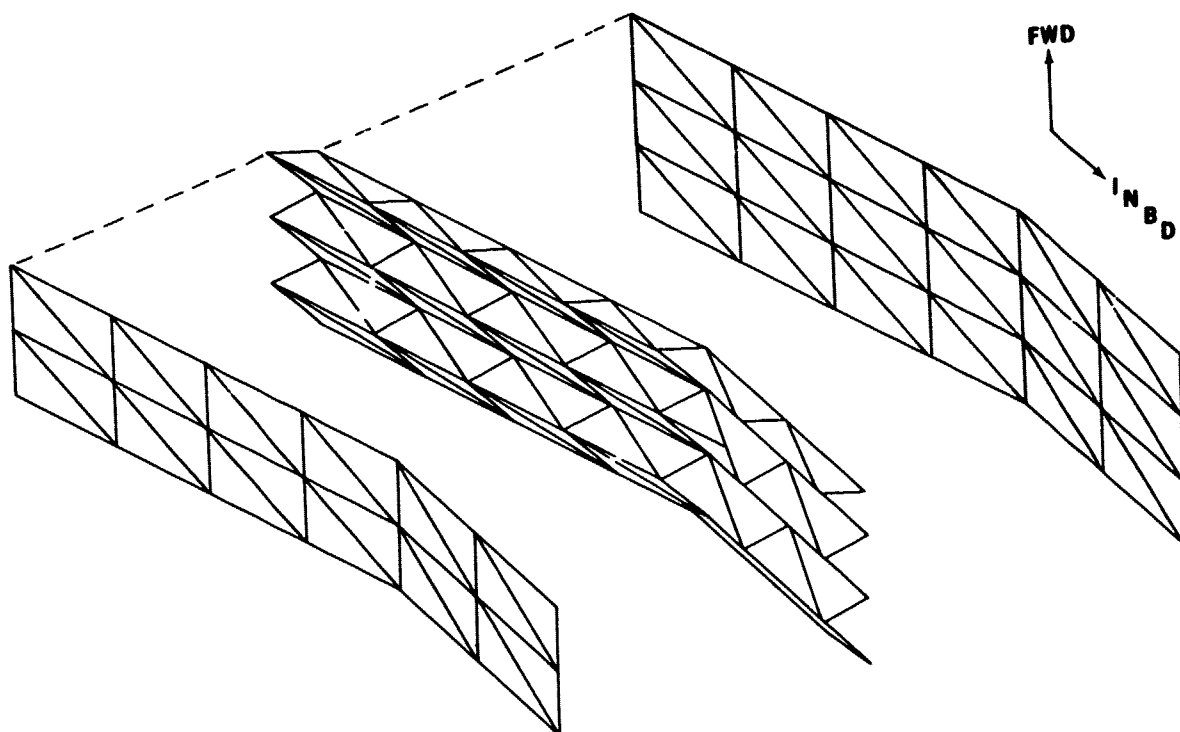
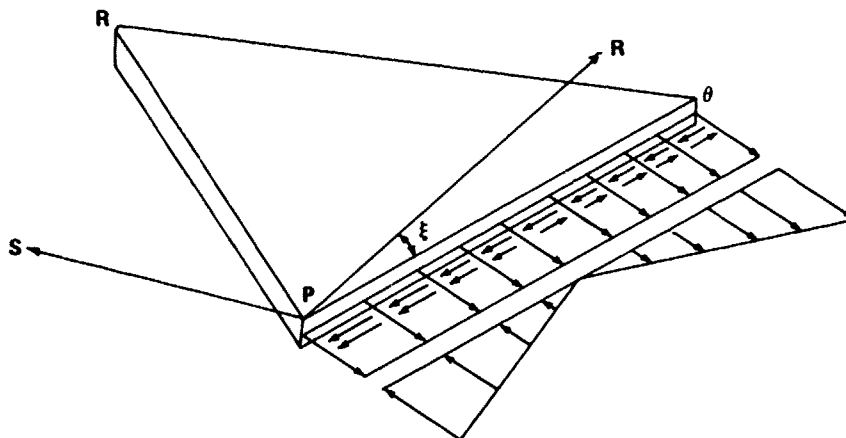


FIGURE 70. COMPOSITE WING FINITE ELEMENT MODEL

field within the element. This element is referred to as an equilibrium element because the element forces associated with this element are actually linearly distributed forces along the edges, which allow for edgewise equilibrium to be maintained when an assemblage of these type elements are connected. The linearly distributed forces on the element edges are treated by considering their lumped equivalent. Thus, the linearly distributed normal forces on an edge are defined by two element forces; the first captures the uniform part of the distribution, and the second captures the moment part of the distribution. Similarly, the linearly distributed tangential forces are defined in a lumped equivalent form by two element forces. Hence, each edge of the triangle has associated with it four element forces as shown in Figure 71. Retaining three of the edge forces



- LINEAR NORMAL AND TANGENTIAL FORCE DISTRIBUTIONS ASSUMED TO ACT ON EACH EDGE
- EACH LINEAR FORCE DISTRIBUTION IS DEFINED BY TWO COMPONENT DISTRIBUTIONS
- 12 FORCE COMPONENTS ARE DEFINED PER ELEMENT; 9 ARE CHOSEN AS ELEMENT FORCES; 3 OTHERS ARE USED AS ELEMENT REACTIONS
- ANISOTROPIC MATERIAL PROPERTIES MAY BE USED IN THE R-S MATERIAL AXES

FIGURE 71. TRIANGULAR MEMBRANE ELEMENTS

as reactions to eliminate the rigid body displacements of the element, a total of nine element forces are associated with each triangular membrane element. The element reactions are a statically determinate function of the nine independent element forces. The membrane stiffnesses of the elements may be of an anisotropic form, referenced to a material axis which is rotated from the p-q base edge by some angle ξ , (Figure 71). In the case of the AMST conceptual wing, the material properties of all the elements were orthotropic since laminates were chosen using only 0-, ± 45 -, and 90-degree ply orientations, relative to the quarter-chord line.

The finite element model constitutes an assemblage of these triangular membrane elements plus a minimum number of bending bars necessary for a membrane solution of a doubly-curved surface. Equations of equilibrium are written at the mid points of intersecting element edges, in terms of the element forces defined there. For this analysis, a total of 1227 such equations were solved. A biaxial stress state is output at each of the corners of the triangular membrane elements, while displacements are specified in directions of the equilibrium equations which are written at the midpoints of the element edges.

Applied Loads - For each finite element analysis solution that was performed, three different loading conditions were considered. These three conditions are listed below and are detailed in Paragraph 3.3 in which the weights and airload pressure distributions are specified. All three conditions are symmetrical about the airplane centerline.

- 3g symmetrical maneuver condition (maximum bending)
- 2g maximum torque condition
- 2g taxi condition

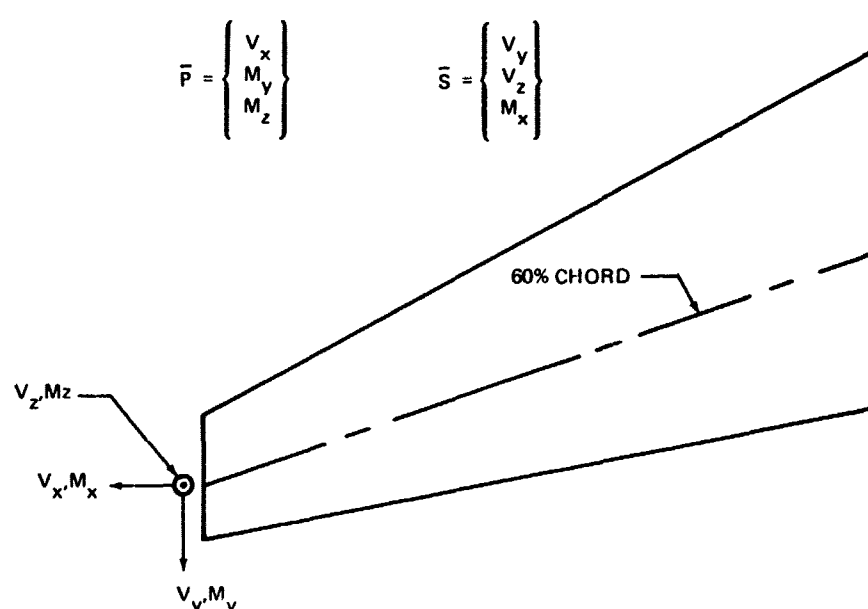
The second condition represents a flaps down landing approach at 132 knots. The third condition is included to provide a lower surface compression design.

In general, loads may be applied in each of the equilibrium directions for which equations are written. However, in the case of the AMST conceptual wing, for which only a membrane solution was sought, a much smaller set of applied loads was required.

For each of the three conditions which were analyzed, the distributed airload distribution and distributed weight distribution were replaced by a set of discrete forces and moments, corresponding to the equilibrium directions of the model. Discrete vertical forces were applied to the upper cover on the nodal lines defined by the intersection of the web structure and the upper cover. These vertical forces were therefore transmitted directly into the web structure, compatible with a membrane solution. Chordwise drag forces were introduced equally into the upper and lower covers. Bending moments were used to capture the effect of airloads acting on the leading and trailing edges and the flaps, producing an overhanging effect on the wing box structure. These bending moments were actually transmitted to the structure by equal and opposite chordwise forces applied to the upper and lower covers.

In addition to the discrete forces which were applied to the model, simulating airload and inertia loads acting inboard of Sta 282, a distribution of forces acting on the outboard section of the model was required to simulate the effect of the airloads and inertia loads acting outboard of Sta 282. Of course, by Saint-Venant's Principle, the internal stresses away from the outboard edge of the model will be relatively unaffected by whatever distribution is used, as long as that distribution is statically equivalent to the airloads and inertia loads outboard of Sta 282. However, with a realistic distribution of forces applied to the outboard boundary of the model, a greater confidence in resulting stresses near that boundary will be gained.

A realistic distribution of forces on the outboard boundary was determined as follows. Consider the resultants of the wing loading outboard of Sta 282, partitioned as two vectors.



Define the vector \bar{P} to consist of all the applied load vectors acting on the outboard boundary of the model which contribute toward \bar{P} sums.

Define the vector \bar{S} to consist of all the remaining force vectors acting on the outboard boundary of the model. With the use of three transformation matrices, a , b , and c , the resultant vectors \bar{P} and \bar{S} can be written in terms of the local applied load vectors P and S .

$$\bar{P} = aP$$

$$\bar{S} = bS + cP$$

To approximately incorporate the bending and shear stiffness distribution of the wing two diagonal matrices are utilized.

$$K_P = \begin{bmatrix} \cdot & \cdot & \cdot & \cdot & \cdot \\ & \cdot & \cdot & \cdot & \cdot \\ & & \cdot & \cdot & \cdot \\ & & & \cdot & \cdot \\ & & & & \cdot \end{bmatrix} \quad K_S = \begin{bmatrix} \cdot & \cdot & \cdot & \cdot & \cdot \\ & \cdot & \cdot & \cdot & \cdot \\ & & \cdot & \cdot & \cdot \\ & & & \cdot & \cdot \\ & & & & \cdot \end{bmatrix}$$

A diagonal element of K_p denotes the panel membrane stiffness associated with the corresponding P vector element, while a diagonal element of K_s denotes the panel shear stiffness associated with the corresponding S vector element. The vectors P and S are then determined from

$$P = K_p a^T (a K_p a^T)^{-1} \bar{P}$$

$$S = K_s b^T (b K_s b^T)^{-1} (\bar{s} - cP)$$

The first of these expressions is derived below in terms of vectors σ (stress), ϵ (strain), U (displacements associated with P), \bar{U} (generalized displacements associated with \bar{P}), and diagonal matrices A (areas) and E (moduli).

$$P = A\sigma$$

$$\bar{P} = aP = aA\sigma$$

$$U = a^T \bar{U}$$

by virtual work since

$$\delta P^T U = \delta \bar{P}^T \bar{U} = \delta P^T a^T \bar{U}$$

$$\epsilon = \frac{\partial U}{\partial x} = a^T \frac{\partial \bar{U}}{\partial x}$$

$$\sigma = E\epsilon = Ea^T \frac{\partial \bar{U}}{\partial x}$$

$$\bar{P} = aAE a^T \frac{\partial \bar{U}}{\partial x}$$

$$\frac{\partial \bar{U}}{\partial x} = (aK_p a^T)^{-1} \bar{P}$$

$$P = AE a^T (aK_p a^T)^{-1} \bar{P} = K_p a^T (aK_p a^T)^{-1} \bar{P}$$

The expression for S is similarly derived. In effect, only the stiffness of one bay has been accounted for. Furthermore, chordwise stresses have been assumed to be small compared with spanwise stresses. The fundamental assumption underlying this derivation is that the outboard boundary at Sta 282 remains plane as the wing is deformed, consistent with ordinary engineering beam theory.

Equations - The equations which were employed in the finite element analysis are presented below:

equilibrium: $P_F F + P = 0$

compatibility: $e = P_F^T U = 0$

constitutive: $e = DF + E$

In these equations,

- F is a vector of all the element forces, the size of the vector, n_F , being dependent on the number of elements in the model.
- U is a vector of all the displacements, the size of the vector equal to the number of equilibrium equations written at the connection points of the elements in the model.
- E is a vector of initial deformations and thermal strains, in the direction of the element forces.
- P is a vector of applied loads in the direction of the displacements, the size of the vector denoted by n_p .
- P_F is a matrix of size $n_p \times n_F$ which transforms the element forces into the equilibrium directions.
- D is the nonsingular flexibility matrix of size $n_F \times n_F$. This matrix is simply a stacking along the diagonal of each of the element flexibilities. The flexibility D_{ij} is the element deformation in the i^{th} element force direction due to a unit of the j^{th} element force. Thus, a vector of element deformations, e , can be expressed $e = DF$ when no initial deformations are present..

Substituting the constitutive relation into the compatibility equation, the above system of equations can be conveniently expressed in a partitioned matrix form as

$$\begin{bmatrix} D & P_F^T \\ P_F & \end{bmatrix} \begin{bmatrix} F \\ u \end{bmatrix} = \begin{bmatrix} E \\ P \end{bmatrix}$$

Rather than solve this equation for all the unknowns, F and u , at once, it is more efficient to solve the equations first for U , which is tantamount to a displacement method solution.

$$U = (P_F D^{-1} P_F^T)^{-1} (P - P_F D^{-1} E)$$

$$F = -D^{-1} (P_F^T U + E)$$

The displacement solution expressed in this form, in terms of P_F and D , is a more expedient solution when equilibrium type elements are employed.

Solutions - Several finite element solutions were obtained during the course of the AMST conceptual wing design and development. These solutions corresponded to the basic truss web concept, plus two modifications. The first modification incorporated a truss-shaped rib at the sweep-break, where the truss members were assumed to be of a one-square-inch area graphite

epoxy material. The second modification was a replacement of the continuous inner truss webs (excluding the front and rear web) by webs with regularly spaced elliptical cutouts and unidirectional properties. This modification was incorporated in the finite element model by reducing the shear and spanwise longitudinal stiffnesses to an insignificant amount relative to the chordwise stiffness. The pitch of the cutouts is assumed to be small enough to validate this idealization scheme.

The effect of the first modification on the stresses resulting from the 3g symmetrical maneuver condition is illustrated in Figures 72 through 74. These figures demonstrate the beneficial effect of a trussed rib at the sweep-break. The effect of the regularly spaced elliptical cutouts is illustrated in Figures 75 through 78. These figures reveal how little the stresses are increased due to the cutouts. The effect of the unidirectional faced webs with the regularly spaced elliptical cutouts on torsional stiffness was found to be minimal. This conclusion was reached by a comparison of torsional deflection, measured at the outboard boundary of the model for the maximum torque condition. The post design produced only 6 percent more torsional deflection than did the base design.

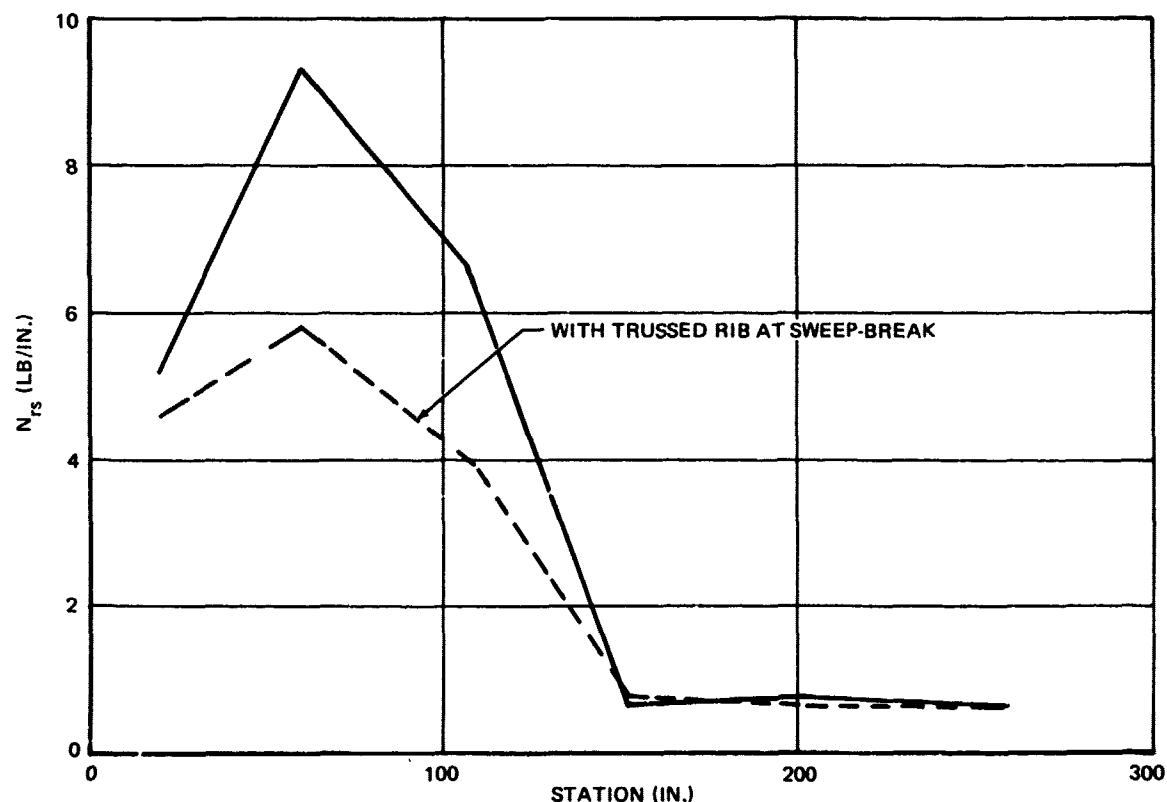


FIGURE 72. ULTIMATE SHEAR LOADS AFT EDGE OF LOWER COVER

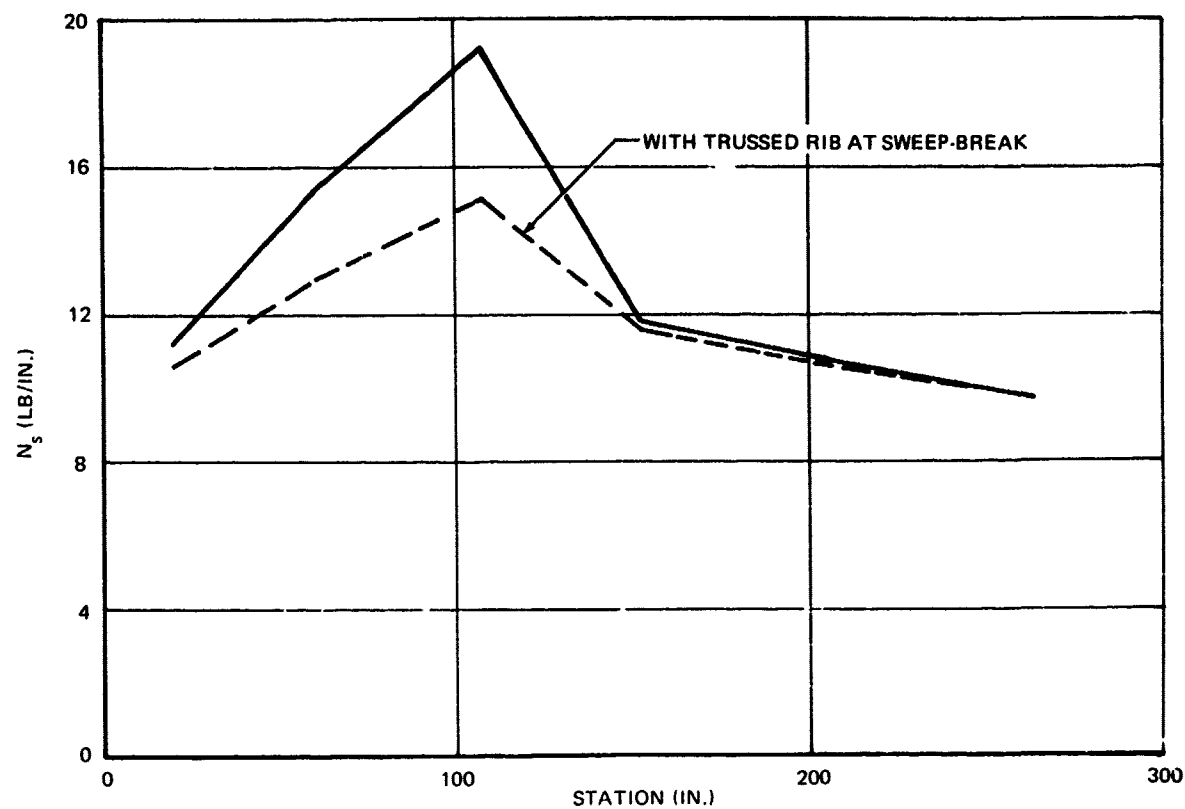


FIGURE 73. ULTIMATE SPANWISE LOADS AFT EDGE OF LOWER COVER

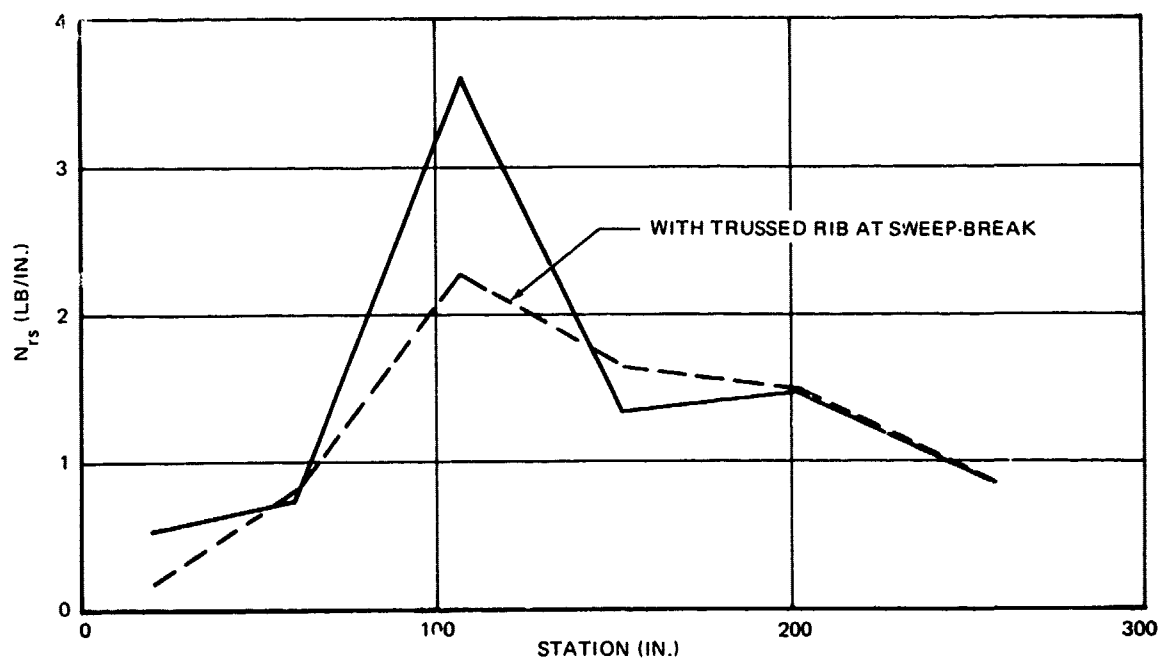


FIGURE 74. ULTIMATE SHEAR LOADS AFT WEB

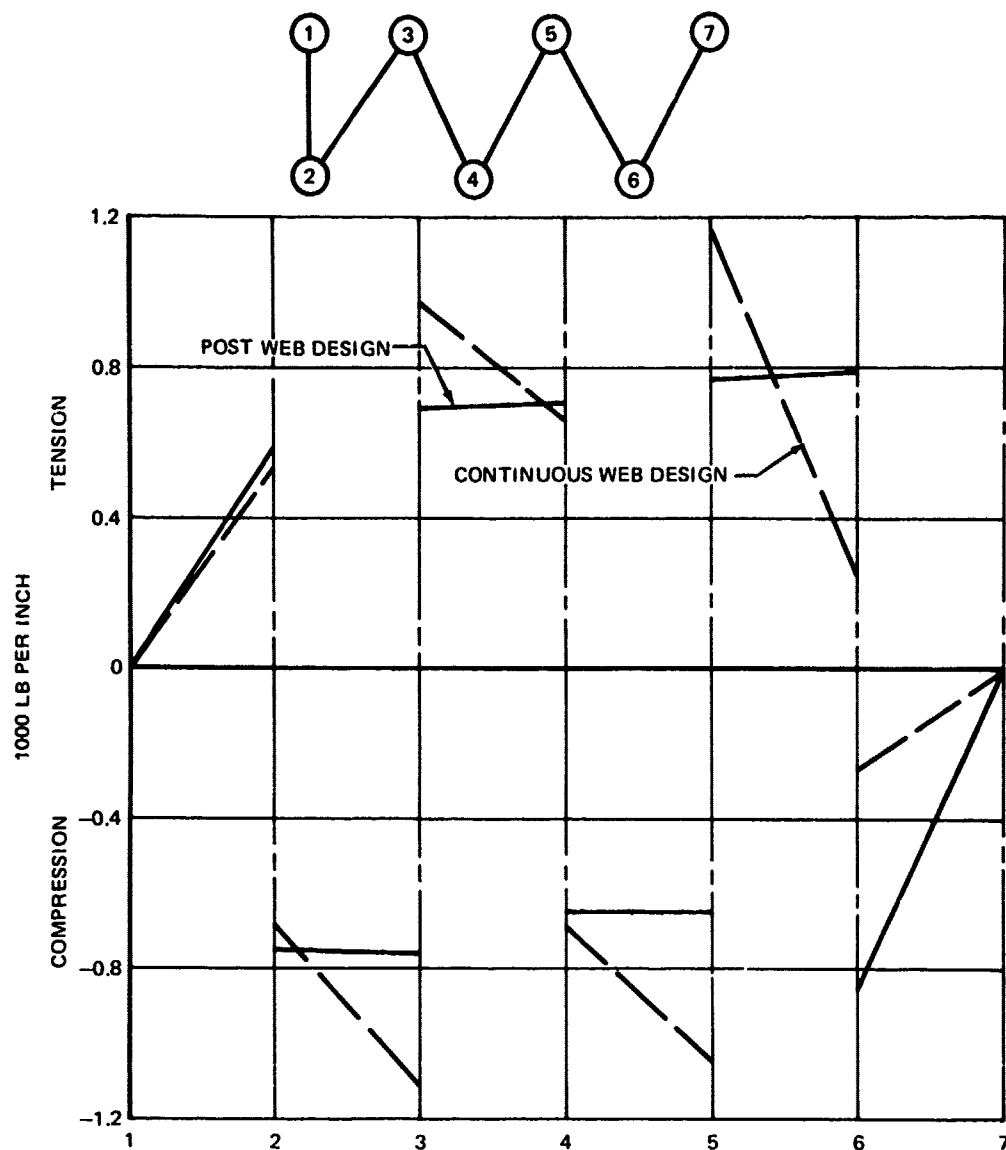


FIGURE 75. DISTRIBUTED INTERNAL CHORDWISE LOADS WEB, INBOARD OF SWEEP – BREAK MAXIMUM TORQUE CONDITION (LIMIT)

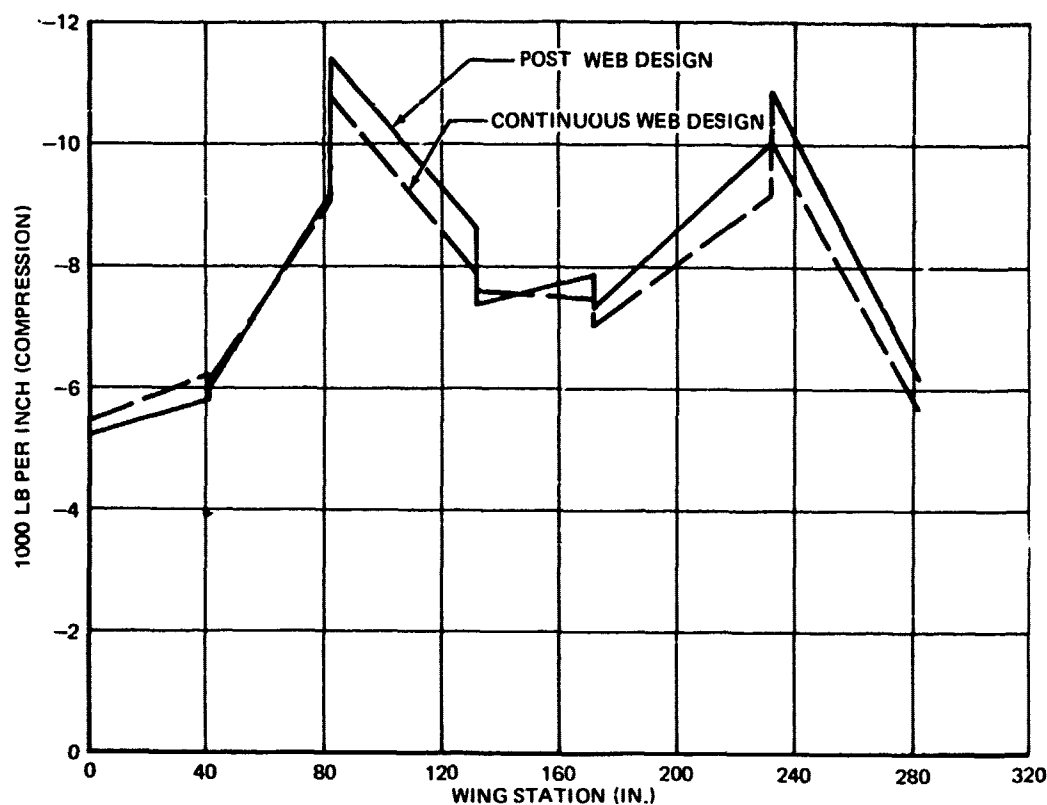


FIGURE 76. DISTRIBUTED INTERNAL LOADS ALONG MATERIAL AXIS AFT EDGE OF UPPER COVER
MAXIMUM TORQUE CONDITION (LIMIT)

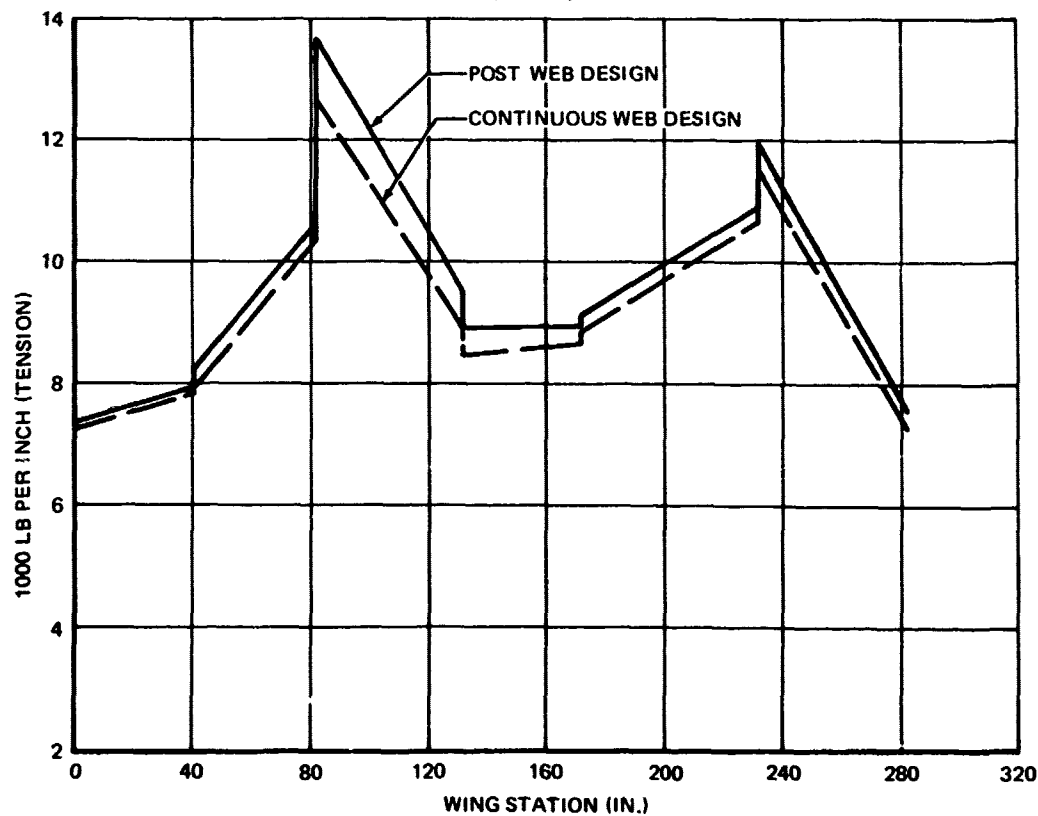


FIGURE 77. DISTRIBUTED INTERNAL LOADS ALONG MATERIAL AXIS AFT EDGE OF LOWER COVER
3G BALANCED MANEUVER CONDITION (LIMIT)

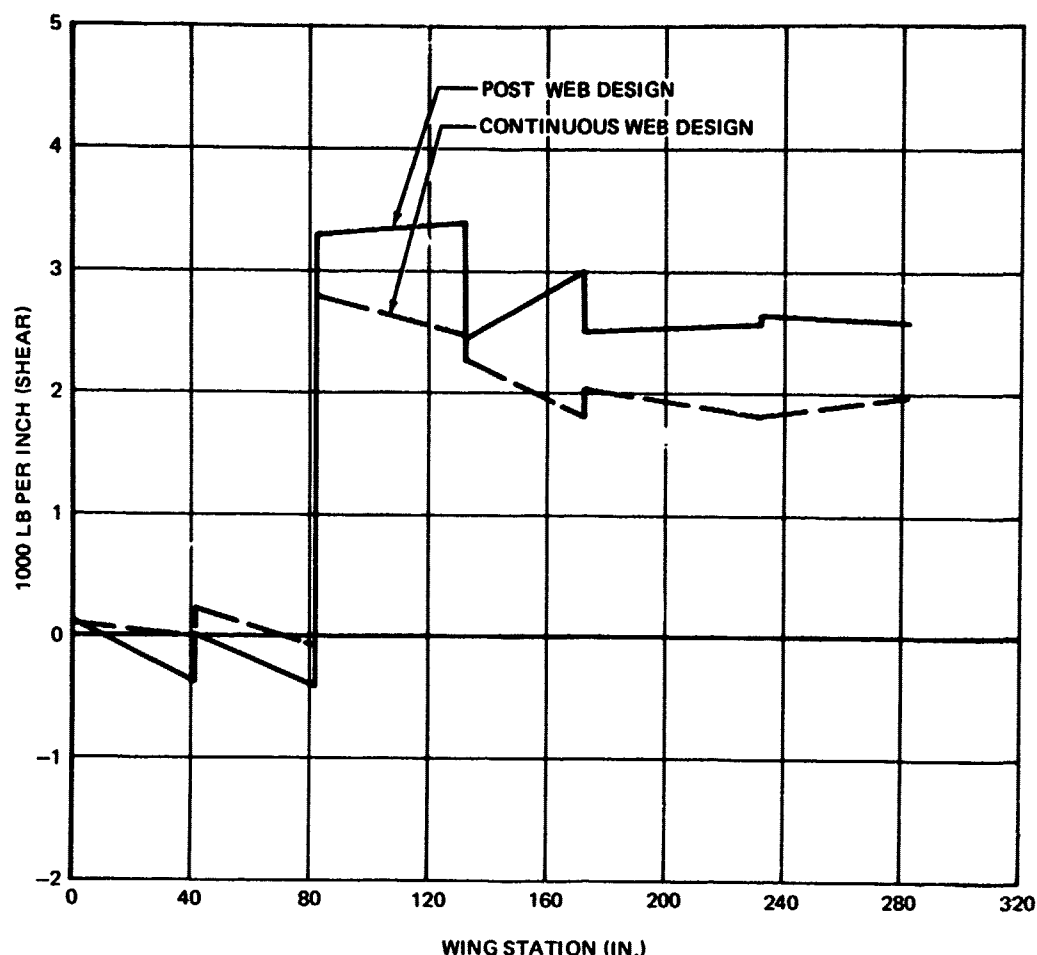


FIGURE 78. DISTRIBUTED INTERNAL SHEAR LOADS AFT SHEAR WEB MAXIMUM TORQUE CONDITION (LIMIT)

Based on the configuration incorporating both modifications, a final pass was made through the finite element analysis reflecting revised element stiffnesses. The stresses obtained from the initial pass finite element analysis were used to optimally select new laminate patterns. The membrane element stiffnesses in the finite element model were then updated accordingly, and a second iteration finite element solution obtained. Convergence of this iteration cycle was rapid as demonstrated by Figures 79 and 80.

5.1.2 Final Demonstration Component

Introduction - In order to verify the analytical methods used to design the wing as well as to prove the joining concepts employed in the wing design, a final demonstration component was selected for a test. This component was required to reflect as many of the wing design difficulties and complexities as possible. It was decided that a scaled specimen of the aft two cells of the five-cell wing box would adequately demonstrate such a set of requirements. It was dictated that the specimen was to reflect as many of the characteristics of the wing box as possible, including a sweep-break, wing attach bolts at the sweep-break, a boron upper cover, a graphite lower cover, and a graphite web structure including elliptic cutouts in the center

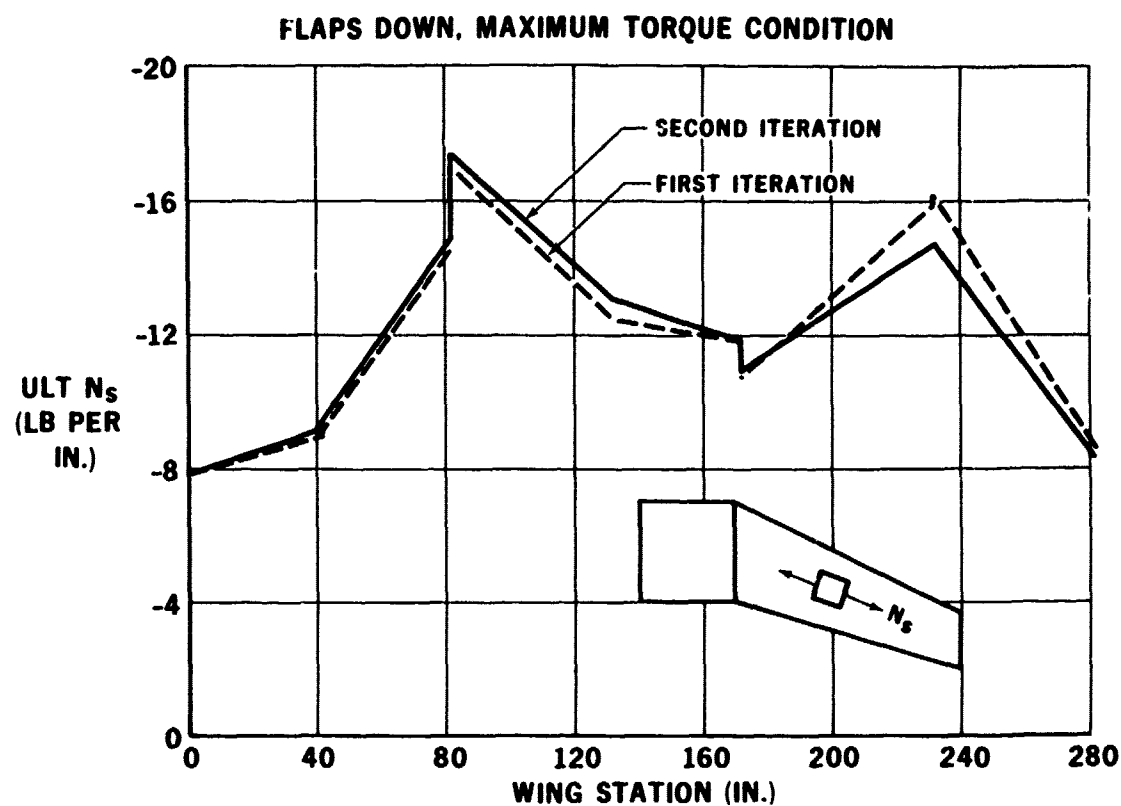


FIGURE 79. ULTIMATE UPPER PANEL LOADS AT AFT EDGE

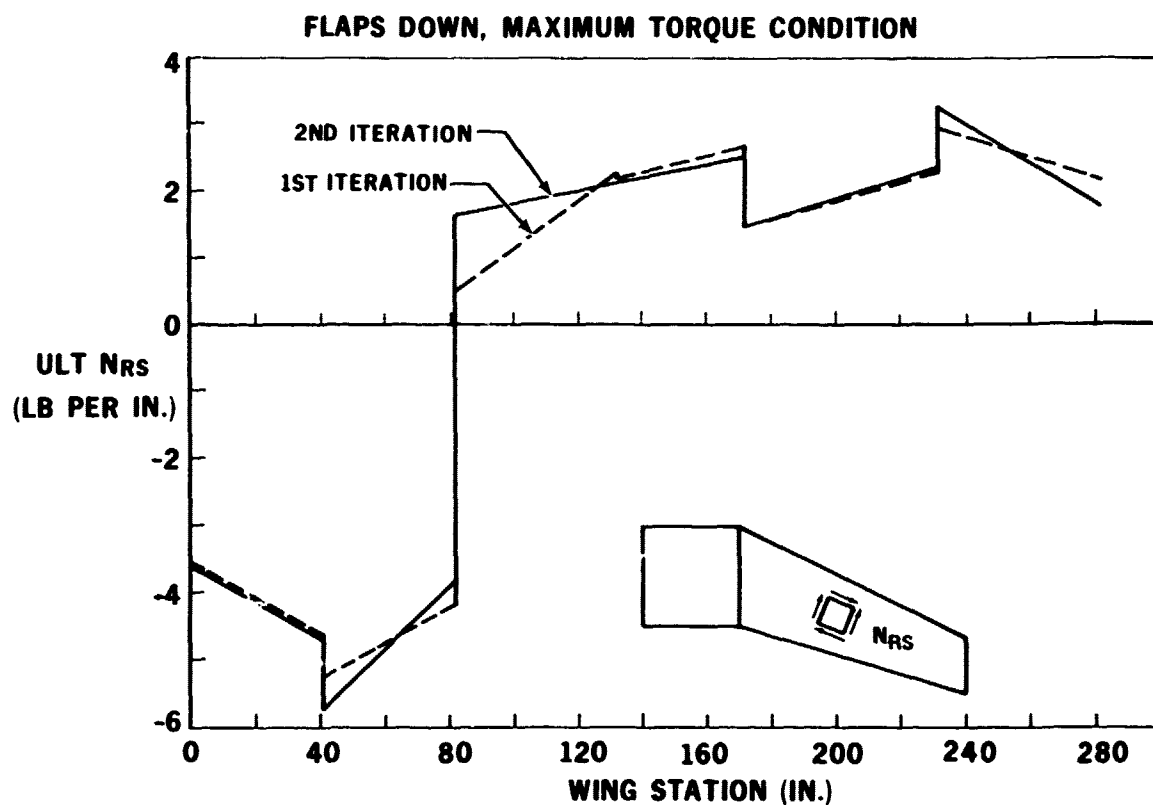


FIGURE 80. ULTIMATE UPPER PANEL SHEAR AT AFT EDGE

web. In addition, the upper cover was to be joined to the web structure by titanium bolts incorporating fiberglass protection against stress concentrations in the upper cover bolt holes, the same concept employed in the wing design. Likewise, the lower cover was to be jointed to the web structure using the fillet bond concept, as in the wing design. See engineering drawing Z5569987 in Appendix A.

The laminate patterns for the covers duplicate the wing root pattern and consist mainly of 0-degree plies, with a minimum number of ± 45 degree plies and 90-degree plies. The forward and aft web laminates consist principally of ± 45 -degree plies with a minimal number of 90-degree plies. The center web struts are constructed of laminates of 90-degree plies only. The strut construction of the center web is formed by elliptical cutouts. Extra plies are added to "beef-up" the structure at both ends of the structure where the test fixture is attached to relieve expected stress concentrations. Additional plies are also provided at the sweep-break to help redistribute the concentrated bolt loads. The material axes systems (0-degree ply direction) turn at the sweep-break and are defined parallel to the cover edges.

The box is loaded at the outboard end and restrained at the inboard end. The inboard restraint has been chosen to simulate symmetric wing loading conditions. Hence, the reactions at the inboard end lie in the plane of the covers. Moreover, chordwise components of these reactions have been omitted so that restraint is provided in the X-direction only, Figure 81. Bolts on the lower cover, just inboard of the sweep-break, provide vertical and chordwise displacement restraint and simulate wing attachment to the fuselage.

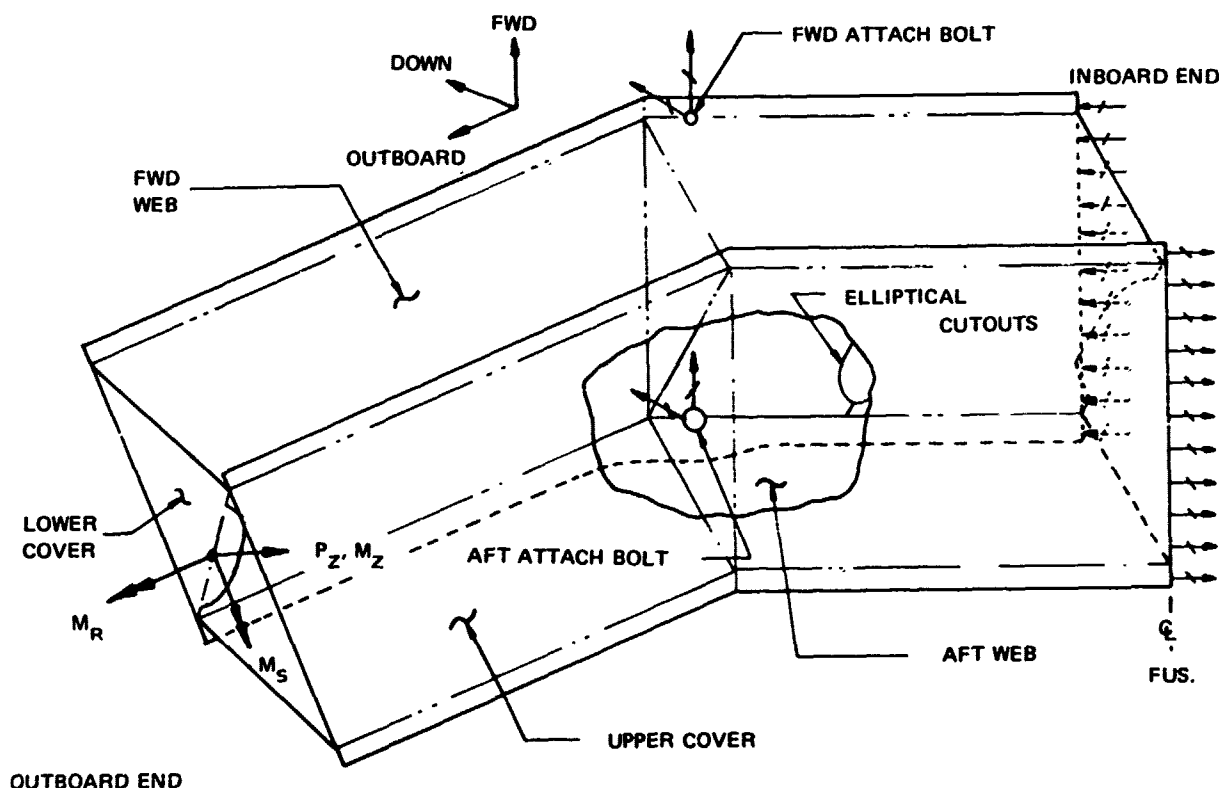


FIGURE 81. SCHEMATIC - Z5569987-1 DESIGN VERIFICATION SPECIMEN

Unidirectional glass for stress concentration relief is substituted for 0-degree boron plies at upper cover edges where bolting to substructure truss web occurs. The lower cover is fillet-bonded to the truss web and glass is again used locally at the two reaction bolts, in place of 0-degree graphite layers. Stress relief was not necessary in lower covers at the bolted ends to the test fixture because of the bonded steel doublers.

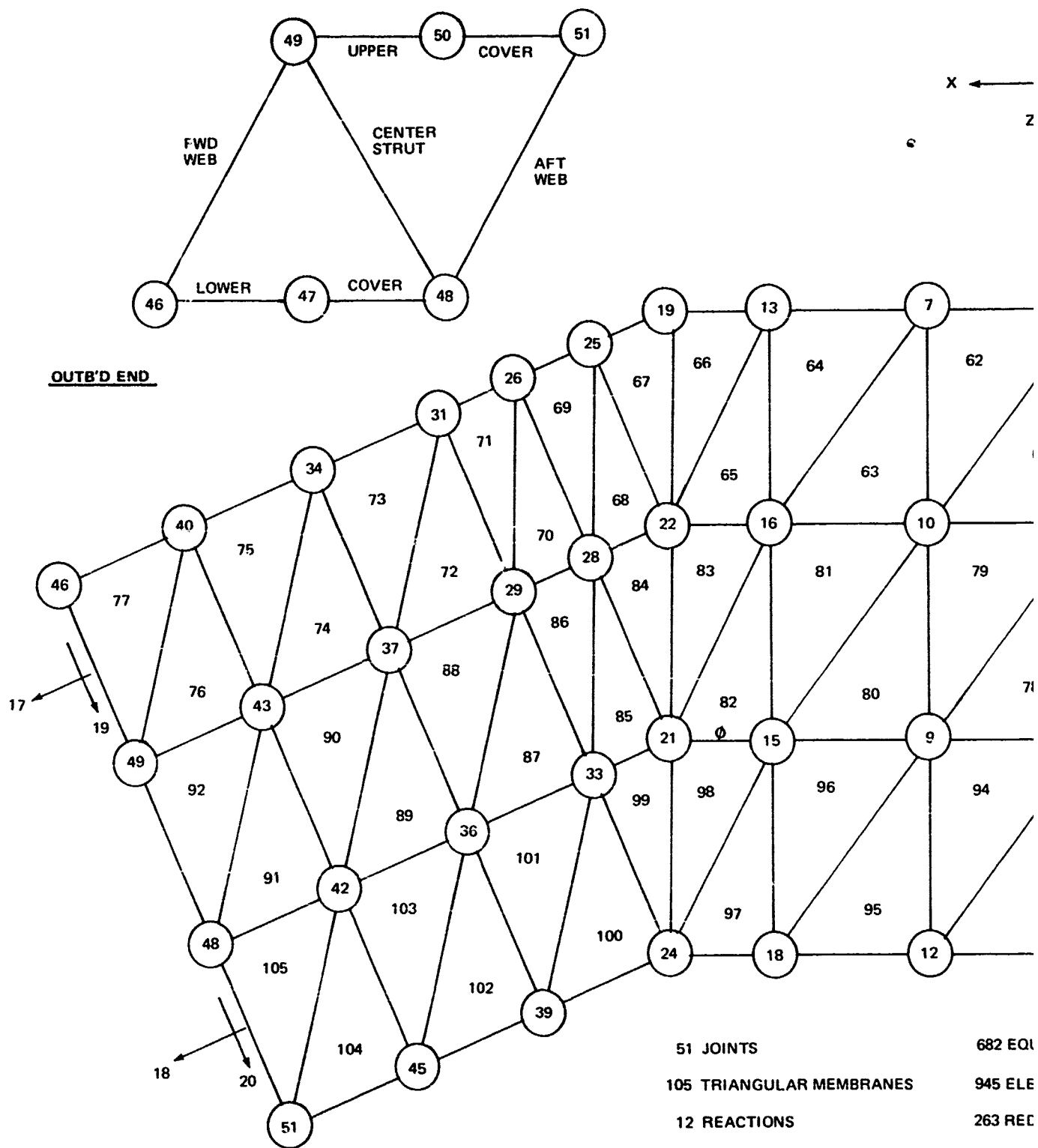
The covers are perfectly flat and the depth between surfaces is constant. The box structure is bent 22-1/2 degrees to match the sweep-break of the wing. No planform taper was introduced in order to simplify tooling and fabrication.

Analysis - In order to substantiate the analytical methods employed in the structural aspects of the wing design, the same type of analysis was performed on the final demonstration component. First of all, a finite element analysis was performed by modeling the test specimen with the same type elements as were used in the wing model, and a gridwork of similar fineness. Secondly, a stress analysis was conducted similar to that employed for the design of a wing. For example, a similar stability analysis was conducted for the upper cover, the bolted and bonded joints were similarly investigated, and the same failure criteria for the composite laminates were utilized.

Finite Element Analysis - A finite element analysis was conducted for the final demonstration component to determine the internal stress states for each of six unit load cases. Membrane action only was treated, while neglecting bending degrees of freedom. Triangular, equilibrium-type elements, based on an assumed linearly varying stress state were used in this model. These elements are described in detail in the preceding section on the wing finite element analysis. In contrast to the wing model, this model required no bars since the covers are perfectly flat. The model for the final demonstration component is shown in Figure 82. Reactions 1 through 8 simulate the inboard center-line restraint associated with the wing symmetric loading cases, while reactions 9 through 12 simulate the restraint offered by the fuselage attach bolts.

The number and orientation of laminate plies assumed for the elements is listed in Table 27. It should be noted in this table that the local support straps for the aft attach bolt and the beefed-up column structure on the forward web have not been accounted for at the sweep-break. The model based on the laminates defined in Table 6 reflects a lower bound on the chordwise stiffness associated with the sweep-break. After the publication of the Sixth Quarterly Technical Report (Report MDC-J4187), the model was modified to reflect an upper bound on the chordwise stiffness at the sweep-break, in order to determine the effect of the -43 and -45 straps and the added layers bonded to the front web at the sweep-break. It was determined from this second run that although the stresses of the elements changed were significantly decreased, the panel loads measured in pounds per inch were not significantly altered. The expected stress states at the specified strain gage locations corresponding to these two bounding analyses are tabulated in tables of Paragraph 7.6.6. The results of both analyses were obtained for the same set of loads defined below.

PRECEDING PAGE I LAME NOT FILMED



2

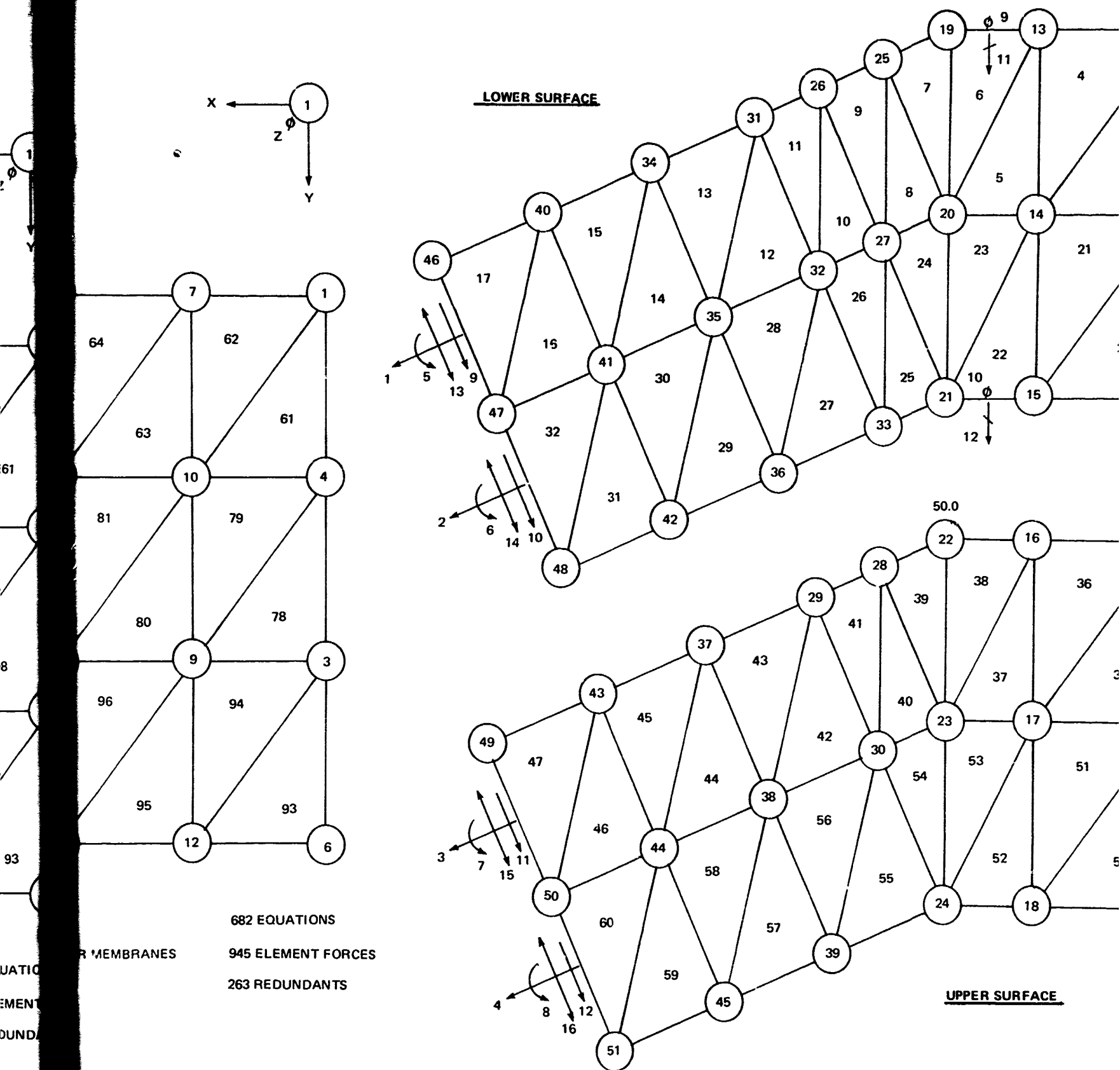
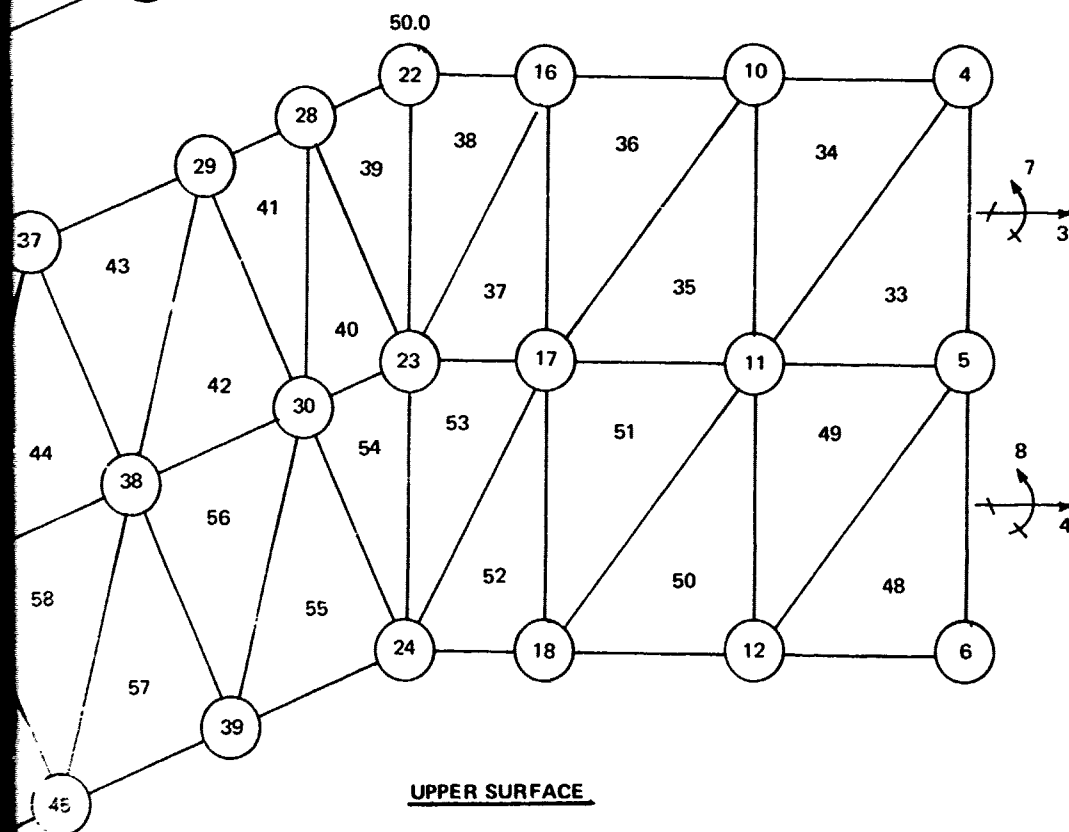
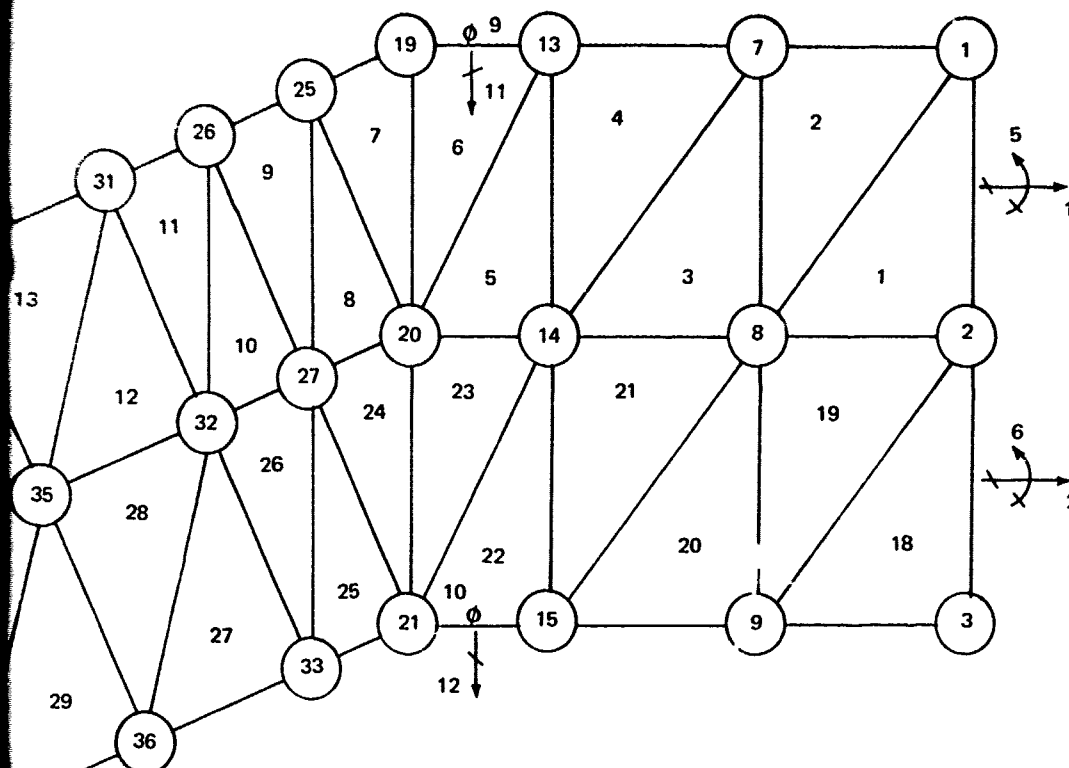


FIGURE 82. BE
IC

3



UPPER SURFACE

FIGURE 82. BENT BOX FINITE ELEMENT IDEALIZATION

TABLE 27
ELEMENT LAMINATION PATTERN

| ELEMENTS | θ (PLY ORIENTATION) N (PLY NUMBER) | | | | | |
|------------------------------------|--|--------------|--------------|---------------|---------------|-----------|
| | | | | | | |
| 1-4 18-21 33-36 48-51 | 0° 10 | 22-1/2° 2 | 67-1/2° 2 | -22-1/2° 2 | -67-1/2° 2 | |
| 5, 6, 22, 23 37, 38, 52, 53 | 0° 10 | 22-1/2° 2 | 67-1/2° 2 | -22-1/2° 2 | -67-1/2° 2 | -90° 6 |
| 7, 8, 24, 25 39, 40, 54, 55 | 0° 12 | 45° 2 | -45° 2 | 90° 2 | 67-1/2° 6 | |
| 9-17 26-32 41-47 56-60 | 0° 12 | 45° 2 | -45° 2 | 90° 2 | | |
| 61-64 69-77 93-96 101-105 | 45° 4 | -45° 4 | 90° 2 | | | |
| 65, 66 97, 98 | 45° 4 | -45° 4 | 90° 6 | | | |
| 67, 68 99, 100 | 45° 4 | -45° 4 | 90° 2 | 67-1/2° 4 | | |
| 78-81 86-92 | 90° 4 | | | | | |
| 82, 83 | 90° 12 | | | | | |
| 84, 85 | 90° 4 | 67-1/2° 8 | | | | |

NOTE: THESE PLY PATTERNS ARE DEFINED FOR THE MODEL ELEMENTS, AND ARE NOT NECESSARILY ACTUALLY EXISTING IN THE SPECIMEN. THERE ARE VERY LOCAL AREAS WHERE THE SPECIMEN IS ACTUALLY STIFFER THAN THE MODEL.

Loads - Solutions for each of the six-unit load cases were obtained for the finite element model. These unit-load cases correspond to three resultant forces and three resultant moments applied to a rigidized outboard end.

This type of loading can be visualized as three-unit forces and three-unit moments being applied to the hub of an infinitely stiff "wagon wheel" attached to the outboard end of the model. This infinitely rigid wagon wheel is used to simulate the test fixture.

In order to stress the test specimen to a level approximating the stressing of the composite wing, a method of least squares was used to determine a proper set of loads to apply at the outboard end. Nine pertinent wing stresses were selected for a matchup with the test specimen:

1. Maximum bending stress at sweep-break, upper cover.
2. Maximum bending stress at Sta 132, upper cover.
3. Maximum bending stress at sweep-break, lower cover.
4. Maximum bending stress at Sta 132, lower cover.
5. Maximum shear stress, aft web.
6. Maximum bending fwd stress at fuselage centerline, lower cover.
7. Maximum bending aft stress at fuselage centerline, lower cover.
8. Maximum bending fwd stress at fuselage centerline, upper cover.
9. Maximum bending aft stress at fuselage centerline, upper cover.

Four resultant loads were used to obtain a least square matchup of the stresses. These resultant loads were a vertical force and three moments. The values of these resultant loads were determined to be:

$$P_Z = 20,120 \text{ lb}$$

$$M_R = 59,800 \text{ in-lb}$$

$$M_S = -410,260 \text{ in-lb}$$

$$M_Z = 376,750 \text{ in-lb}$$

See Figure 81 for load definition.

These loads yielded the following stress matchups:

| Stress Number | Wing Stresses (psi) | Model Stresses (psi) |
|------------------|------------------------|-------------------------|
| 1 | -77,200 | -57,700 |
| 2 | 0 | -4,100 |
| 3 | 58,600 | 68,800 |
| 4 | 0 | -3,100 |
| 5 | 33,000 | 36,900 |
| 6 | 58,600 | 64,700 |
| 7 | 58,600 | 66,800 |
| 8 | -77,200 | -76,200 |
| 9 | -77,200 | -68,100 |

The wing stresses were, in general, selected from the composite wing finite element analysis. However, to keep the application point of the vertical load from being too far removed from the specimen (i.e., to keep M_S relatively small), the bending stresses at Sta 132 were specified as zero.

Superimposing the four applicable unit solutions, a solution associated with the loads listed (P_Z , M_R , M_Z) was obtained. This solution yielded 44,900 pounds tension in the aft attach bolt just inboard of the sweep-break. A previously-conducted component test, for the purpose of demonstrating the ultimate strength of a similarly designed bolted joint, indicated an ultimate bolt tensile load of 44.0 kips. Accounting for a 20-percent scatter in this value, it was decided to scale the applied loads by a factor of $(44.0/44.9)$ $(0.80) = 0.784$. Hence, the final applied loads were:

$$P_Z = 20,120 (0.784) = 15,800 \text{ lb}$$

$$M_R = 59,800 (0.784) = 46,900 \text{ in-lb}$$

$$M_S = -410,260 (0.784) = -322,000 \text{ in-lb}$$

$$M_Z = 376,750 (0.784) = 296,000 \text{ in-lb}$$

Stresses - The stresses in the specimen associated with the final loads noted are shown in Figures 83 through 87. Minimum margins of safety for these stresses are listed in Table 28. The sandwich core depth of the panels was determined so that the panels would be free of buckling instability when exposed to these stresses.

5.2 PANEL STIFFENING STUDY

5.2.1 Introduction

The objective was to investigate the weight efficiency of stiffened panels as compared to an unstiffened constant thickness honeycomb panel. The design strength, buckling and stiffness requirements were those of the AMST wing. The panel stiffening concepts are considered to be applicable to the primary (truss web) and alternate composite wing box designs.

5.2.2 Design Requirements

The panel design requirements are based on the AMST wing strength and stiffness design. The following load conditions were selected as representative of the AMST wing design requirements:

ULTIMATE LOAD ~ LB/IN

| Conditions | N_s | N_c | N_{sc} |
|------------|---------|--------|----------|
| 1 | -10,050 | -1,005 | 1,650 |

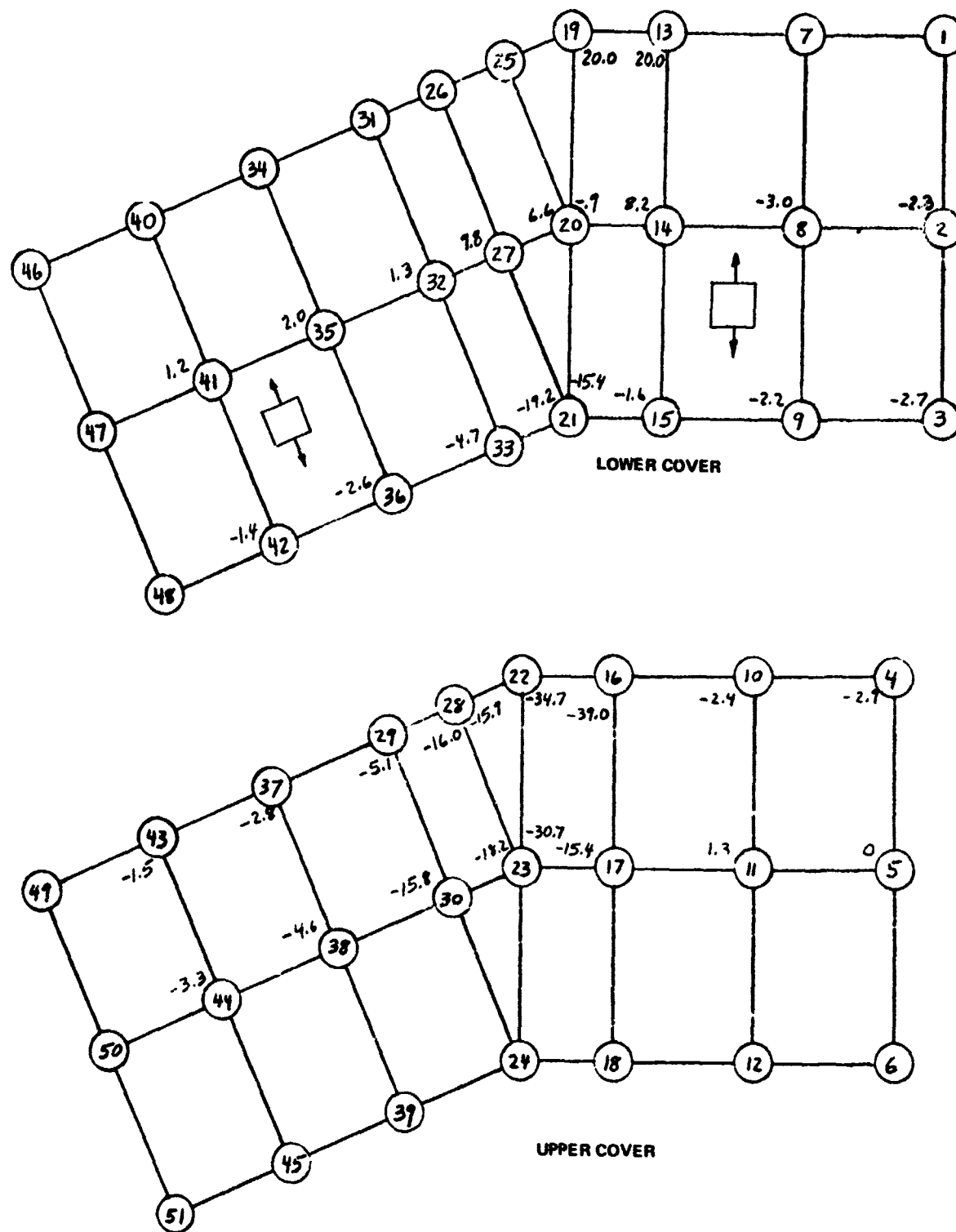


FIGURE 84. CHORDWISE STRESSES (KSI)

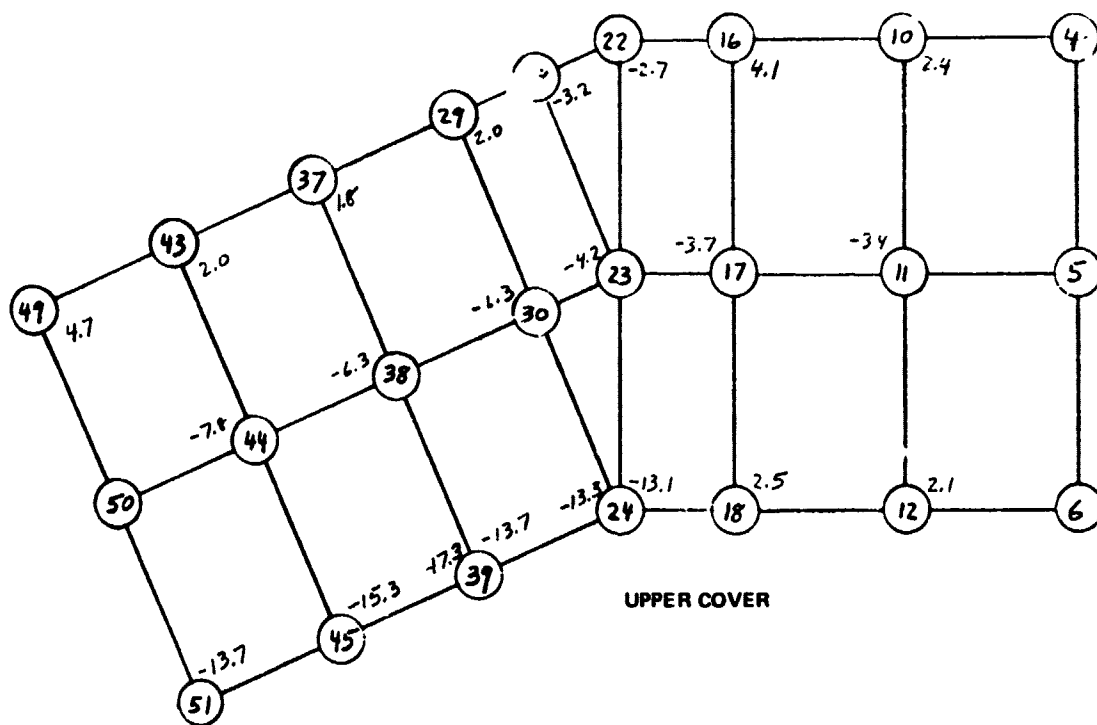
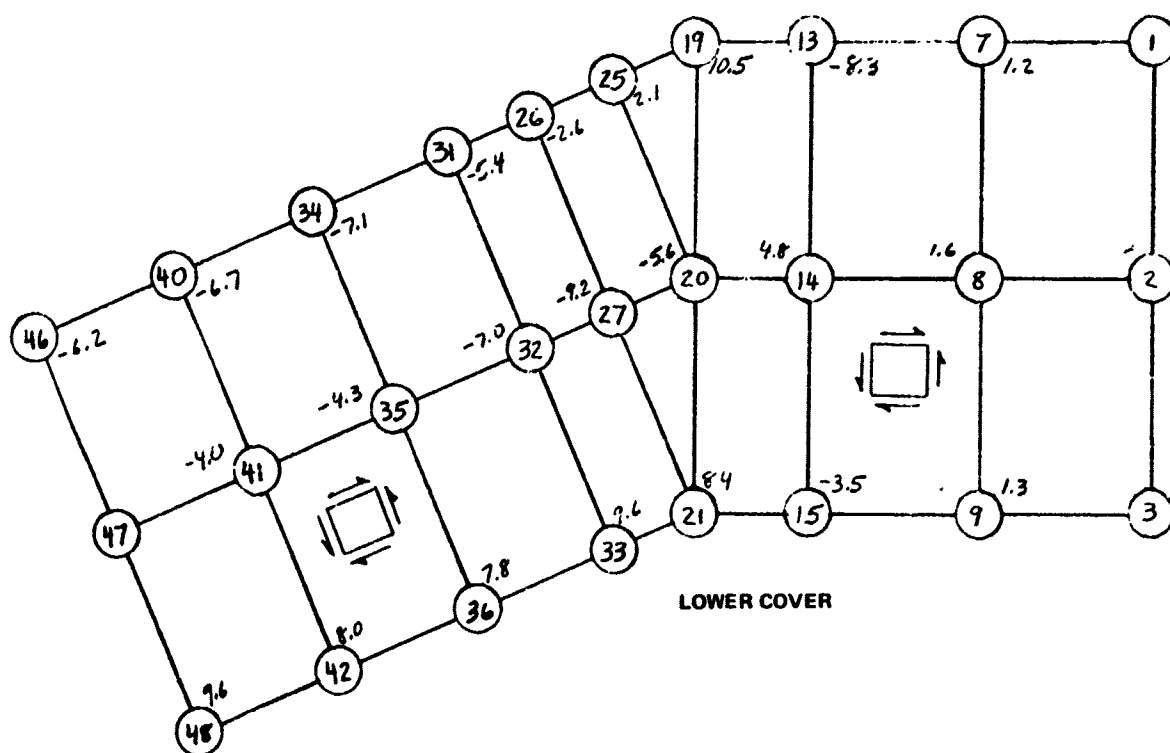
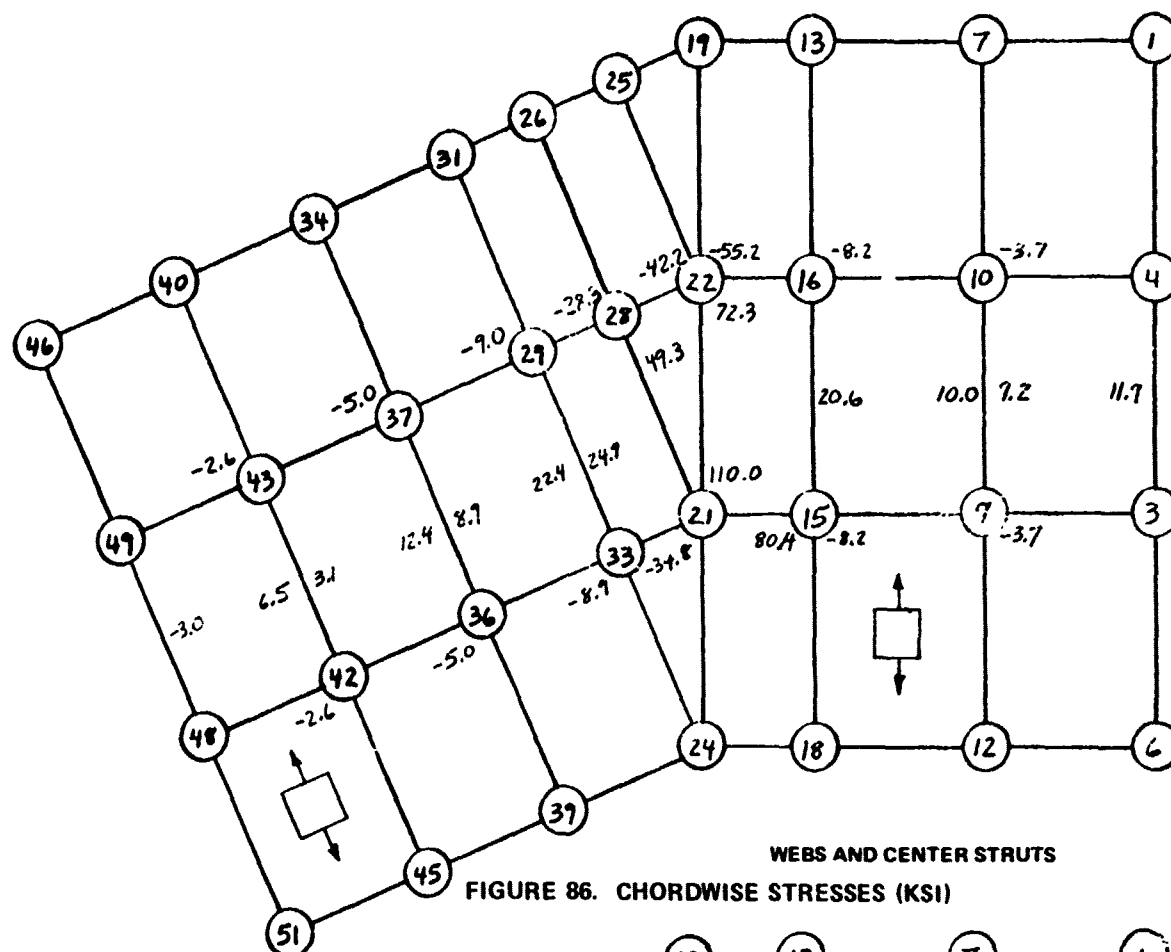
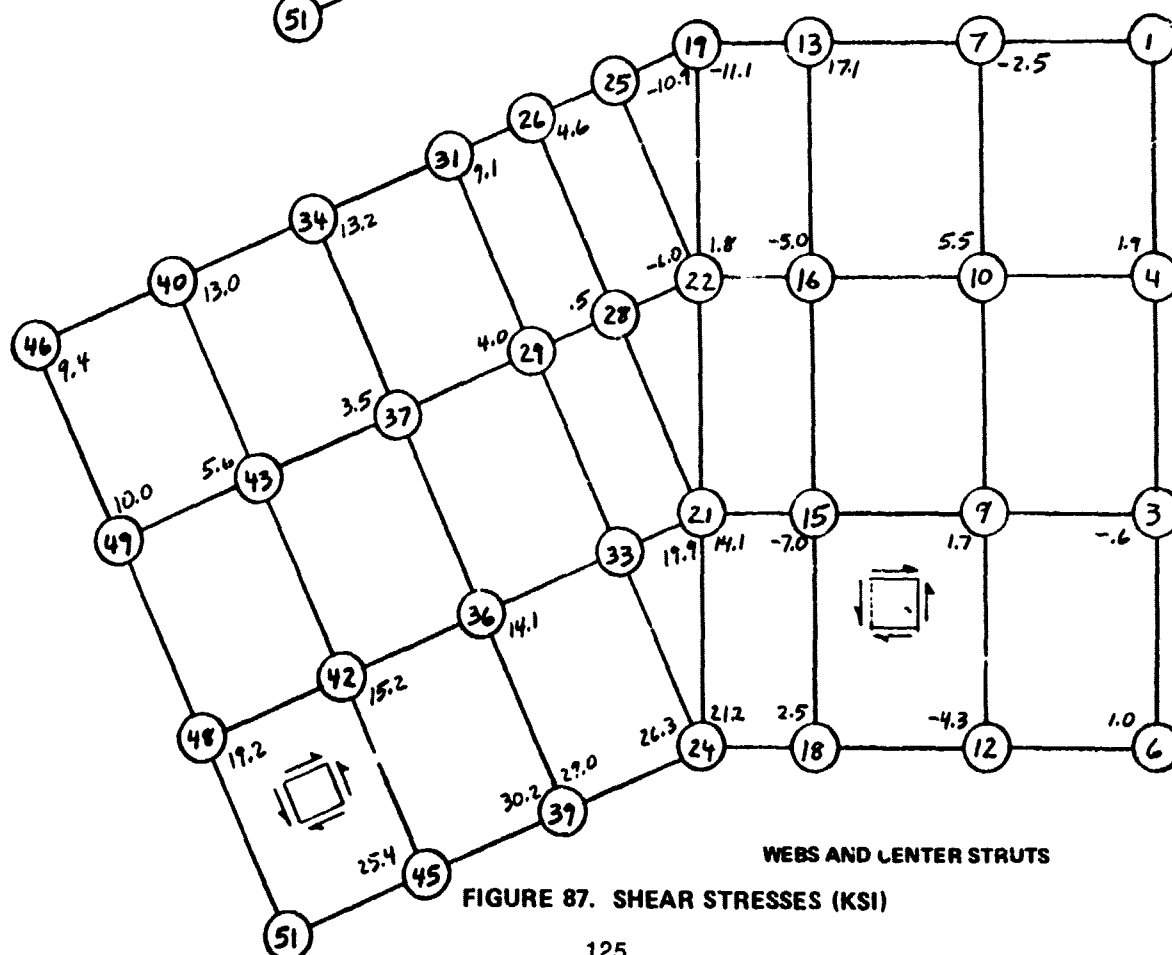


FIGURE 85. SHEAR STRESSES (KSI)



WEBS AND CENTER STRUTS
FIGURE 86. CHORDWISE STRESSES (KSI)



WEBS AND CENTER STRUTS
FIGURE 87. SHEAR STRESSES (KSI)

TABLE 28
MIN MARGINS OF SAFETY

| STRUCTURAL ITEM | LOCATION | MODE OF FAILURE | MARGIN OF SAFETY |
|--------------------------------|-------------------------|-------------------|------------------|
| UPPER COVER | SWEEP-BREAK | COMBINED MEMBRANE | +0.28 |
| LOWER COVER | INBOARD OF SWEEP-BREAK | COMBINED MEMBRANE | +0.27 |
| AFT WEB | OUTBOARD OF SWEEP-BREAK | COMBINED MEMBRANE | +1.07 |
| CENTER STRUT | OUTBOARD OF SWEEP-BREAK | TENSION | +0.22 |
| ATTACH BOLTS (COVER TO WEB) | SWEEP-BREAK | BOLT SHEAR | +0.09 |

2 13,800 0 2,550

3 - 3,960 - 390 5,250

where, N_s = spanwise load

N_c = chordwise load

N_{sc} = inplane shear

Although no one particular point in the wing experiences all of these loadings exactly, the three conditions are typical average values of the AMST wing design loads.

In addition to these three conditions the panel must support a 20-psi (ultimate) pressure condition. The panel must satisfy the static and buckling strength and stiffness requirements. For the purpose of defining the panel geometry and wing stiffness requirements, wing lower surface rear panel between Sta 172 and 232 is chosen. The panel average width over this length is 37 inches for the truss web wing design. The average stiffnesses are:

$$ET = 2.42 \times 10^6$$

$$G^T = 0.16 \times 10^6$$

Panel lengths of approximately 50 inches were assumed since, to use a stiffened panel design, it is practical to modify the truss web to supply cover supports at that interval.

5.2.3 Stiffened Panel Design

Three stiffening concepts were considered for comparison to the baseline unstiffened panel design:

1. Honeycomb core sandwich with laminate face sheets and laminate hat stiffeners.
2. Laminate truss core with laminate covers.

3. Laminate skin with laminate hat stiffeners.

The three configurations are illustrated in Figure 88. General features of these configurations are:

- All laminates are graphite-epoxy, Narmco 5206, Type II.
- All laminates, except the uniaxial reinforcements, are composed entirely of a combination of 0-, 90-, and ± 45 -degree/plies. The 0-degree direction is in the wing spanwise direction.
- Bonding is considered to be the mode of attachment.

The stiffened panel design procedure was:

1. To select the optimum (weight efficiency) stiffened panel configuration on the basis of static strength requirements of the three design conditions and,
2. To optimize the selected configuration with respect to the other design requirements: buckling strength, pressure condition and stiffness.

Strength analysis was performed on the three configurations using computer program C2KD. This finite element analysis program was used to calculate the panel weight, panel internal stresses, and static strength margins of safety. Panel geometry and ply orientation were varied to define the optimum design. Table 29 presents a summary of the strength analysis cases. On the basis of weight efficiency (lb/ft^2) and static strength requirements, the optimum panel is Configuration 1, case 46, with a weight efficiency of $2.61 \text{ lb}/\text{ft}^2$. Configuration 3 was 14 percent heavier.

The buckling strength characteristics of the selected panel, case 46, were investigated through the use of a modified version of the PANBUC computer program. The results are shown in Figure 89. Local buckling between stiffeners ($A = W = 8 \text{ in.}$) is considered.

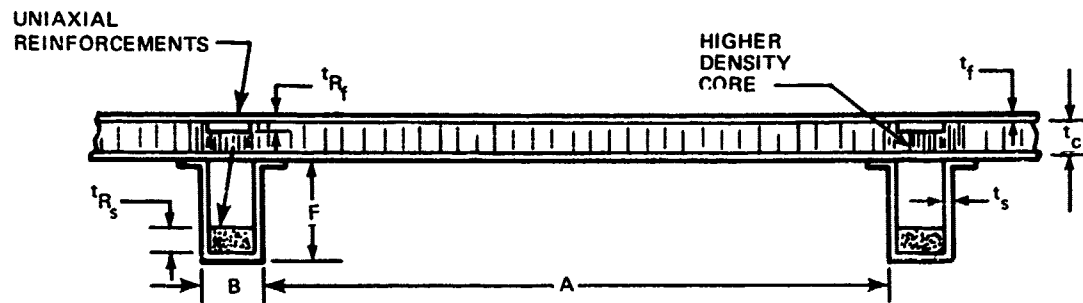
The analysis element critical loadings (ultimate, psi) for the compression loading conditions are:

| Elem | Cond | F_x | F_y | F_{xy} | F_y/F_x | F_{xy}/F_x | $F_{x_{cr}}$ | MS |
|------|------|---------|---------|----------|-----------|--------------|--------------|------|
| 103 | 3 | -12,180 | -12,930 | 31,950 | 1.06 | 2.62 | -14,500 | 0.19 |
| 105 | 1 | -31,640 | -11,450 | 9,420 | 0.36 | 0.30 | -51,000 | 0.61 |

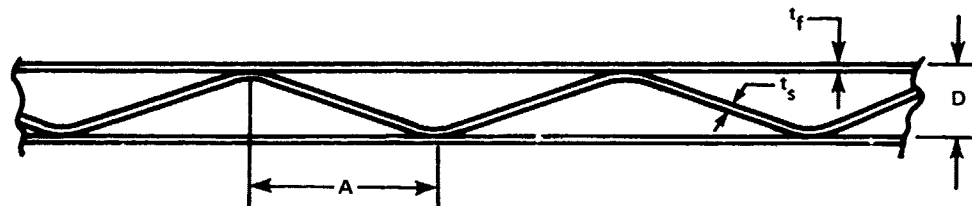
F_x , F_y and F_{xy} were obtained from the finite element analysis and $F_{x_{cr}}$ from Figure 89. It is seen that the panel has satisfactory buckling strength characteristics. Also, the panel satisfies the stiffness requirements.

| | Required | Stiffened Panel |
|----|--------------------|--------------------|
| Et | 2.42×10^6 | 2.58×10^6 |
| Gt | 0.16×10^6 | 0.67×10^6 |

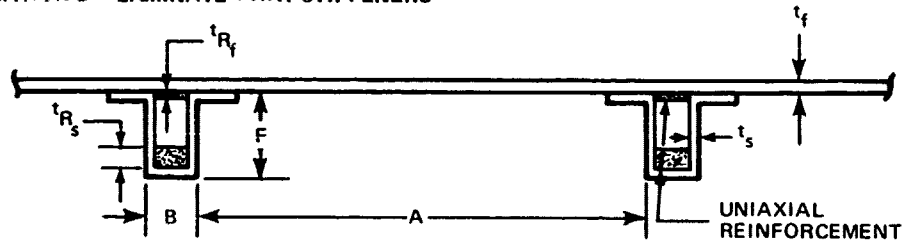
CONFIGURATION 1 – HONEYCOMB SANDWICH + HAT STIFFENERS



CONFIGURATION 2 – TRUSS CORE WITH LAMINATE COVERS



CONFIGURATION 3 – LAMINATE + HAT STIFFENERS



- A = SPACING BETWEEN STIFFENERS (OR BETWEEN TRUSS CORE NODES)
- B = STIFFENER WIDTH
- F = STIFFENER HEIGHT
- D = TRUSS CORE DEPTH (HEIGHT)
- t_c = SANDWICH CORE HEIGHT
- t_f = SKIN THICKNESS
- t_s = STIFFENER THICKNESS
- t_r = REINFORCEMENT THICKNESS

FIGURE 88. STIFFENED PANEL CONFIGURATIONS

TABLE 29
LIST OF STRENGTH ANALYSIS CASES

CONFIGURATION 1

| A | t_c | SKIN PLY PROPERTIES | CASE NUMBER | | | | | | | |
|----|-------|---------------------|-------------|-------|----------|-------|----------|----------|----------|----------|
| | | | 20/20/60 | | 20/10/70 | | | 30/10/60 | | |
| | | | t_f | t_s | t_f | t_s | t_{Rf} | t_{Rs} | t_{Rf} | t_{Rs} |
| 16 | 0.5 | | 3 | 7 | | 11 | 15 | | 19 | 23 |
| | 0.75 | | 4 | 8 | | 12 | 16 | | 20 | 24 |
| 14 | 0.5 | | 1 | 5 | | 9 | 13 | 25 | 17 | 21 |
| | 0.75 | | 2 | 6 | | 10 | 14 | 26 | 18 | 22 |
| 12 | 0.25 | | 29 | | 34 | 39 | 44 | | | 50 |
| | 0.5 | | 30 | | 35 | 40 | 45 | | | 51 |
| 10 | 0.25 | | 27 | | 32 | 37 | 42 | | | 48 |
| | 0.5 | | 28 | | 33 | 38 | 43 | | | 49 |
| 8 | 0.25 | | 31 | | 36 | 41 | 46 | | | |

STIFFENER PLY PROPERTIES = 10/10/80; CORE: HPP - 3/16 - 8.0
B = 1.0, F = 1.66 REINFORCEMENT THICKNESS: t_{Rf}/t_{Rs}

| A | t_f/t_s | 0.036/0.06 | 0.06/0.084 | 0.084/0.108 |
|-------|-----------|-------------|-------------|-------------|
| 14-16 | | 0.166/0.309 | 0.166/0.374 | 0.166/0.49 |
| 8-12 | | 0.125/0.232 | 0.125/0.30 | 0.125/0.368 |

CONFIGURATION 2

| CASE NO. | A | t_f | t_s | D | PLY PROPORTIONS | |
|----------|---|-------|-------|-----|-----------------|----------|
| | | | | | SKIN | TRUSS |
| 1 | 3 | 0.1 | 0.08 | 1 | 20/10/70 | 20/20/60 |
| 2 | 4 | 0.1 | 0.08 | 1 | 20/10/70 | 20/20/60 |
| 3 | 4 | 0.1 | 0.08 | 1.5 | 20/10/70 | 20/20/60 |
| 4 | 3 | 0.06 | 0.04 | 1 | 20/10/70 | 20/20/60 |
| 5 | 4 | 0.06 | 0.04 | 1 | 20/10/70 | 20/20/60 |
| 6 | 4 | 0.06 | 0.04 | 1.5 | 20/10/70 | 20/20/60 |
| 7 | 3 | 0.1 | 0.08 | 1 | 30/10/60 | 20/20/60 |
| 8 | 4 | 0.1 | 0.08 | 1 | 30/10/60 | 20/20/60 |
| 9 | 4 | 0.1 | 0.08 | 1.5 | 30/10/60 | 20/20/60 |
| 10 | 3 | 0.08 | 0.06 | 1 | 20/10/70 | 20/20/60 |

CONFIGURATION 3

| CASE NO. | A | t_f | t_s | t_{Rf} | t_{Rs} |
|----------|---|-------|-------|----------|----------|
| 1 | 4 | 0.168 | 0.152 | 0.09 | 0.353 |
| 2 | 6 | 0.168 | 0.131 | 0.07 | 0.274 |
| 3 | 8 | 0.168 | 0.138 | 0.077 | 0.306 |
| 4 | 4 | 0.12 | 0.109 | 0.09 | 0.278 |
| 5 | 8 | 0.12 | 0.099 | 0.077 | 0.241 |

B = 0.8, F = 1.33
PLY PROPORTIONS:
SKIN = 20/10/70
STIFFENERS: 10/10/80

NARMCO 5206, TYPE II GRAPHITE

0 - 90° - ±45° $t_c = 0.25$ IN. $L = 42$ IN.
 20 - 10 - 70% $t_f = 0.084$ IN. $W = 8$ IN.
 40 PLY

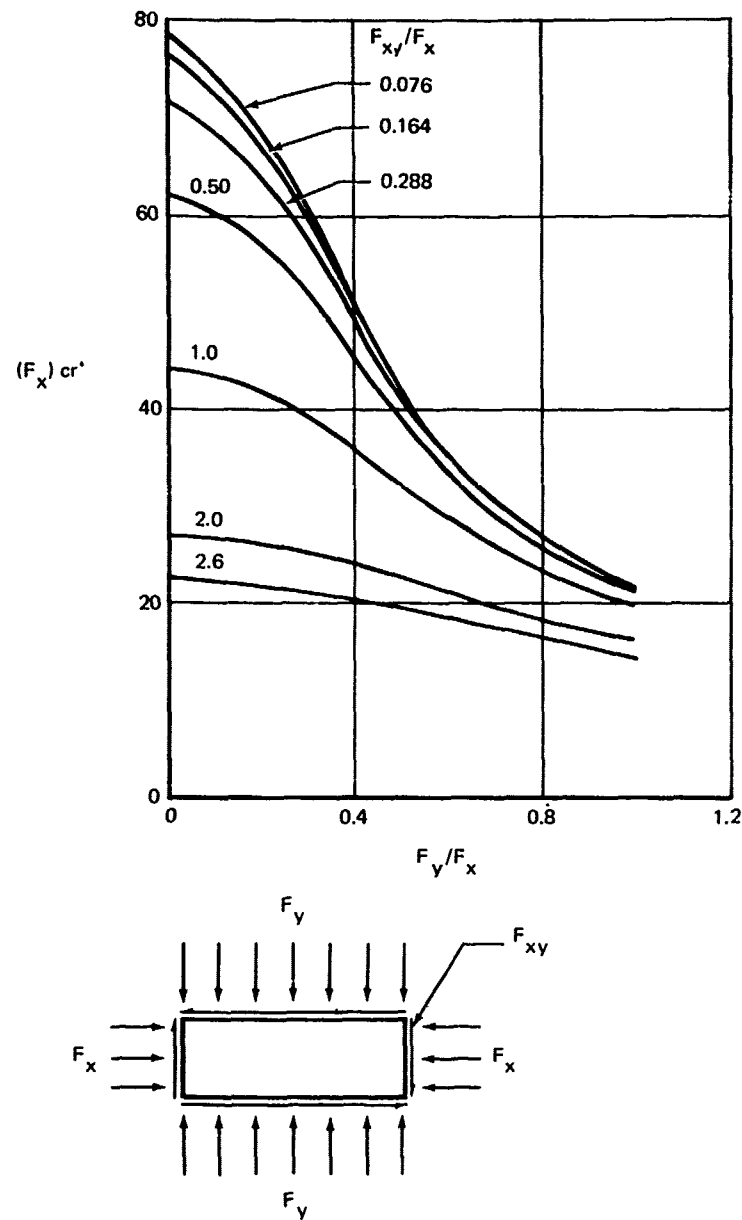


FIGURE 89. GRAPHITE-EPOXY LAMINATE HONEYCOMB CORE SANDWICH PANEL BUCKLING STRENGTH

where E_t is the equivalent stiffness of the honeycomb sandwich face sheets, stiffeners and reinforcements while the torsional stiffness, G_t , of the honeycomb sandwich alone is more than satisfactory.

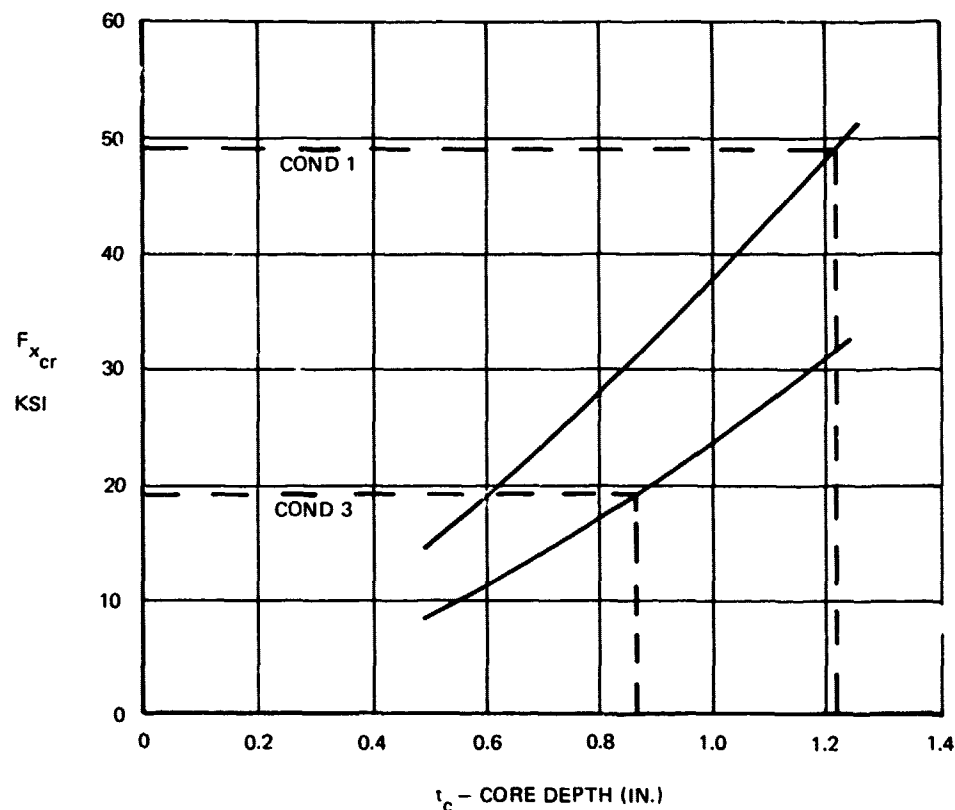
The honeycomb core depth $t_c = 0.25$ in. does not provide sufficient bending stiffness to support the 20-psi pressure condition. Based on the bending analysis of a simply supported infinite aspect ratio anisotropic panel 37 in. wide, the required core depth is $t_c = 0.76$ in.

5.2.4 Baseline Panel Design

The unstiffened baseline panel design is based on the same strength, stiffness, pressure and buckling strength requirements as the stiffened panel. The panel is a constant thickness honeycomb sandwich with graphite-epoxy (Narmco 5206, Type II) laminate face sheets. The laminates are a combination of 0-, 90- and ± 45 -degree plies.

The face sheet laminate ply proportions and thickness were optimized for strength (three load conditions) and stiffness requirement using the Douglas laminate strength and stiffness optimization program. The required thickness of each face sheet is $t_f = 0.105$ in. with the following proportions of plies: 0- (52.5 percent), 90- (5.3 percent) and ± 45 -degree (42.2 percent).

The core depth was first determined on the basis of buckling strength by considering a panel 37 inches wide with an aspect ratio of 3. Analysis was performed using the PANBUC program. The required core depth for buckling is $t_c = 1.21$ inch. Critical buckling strength versus core depth is shown below for the two companion design conditions:



The core depth required to support the 20-psi pressure condition, on the basis of a bending analysis of a simply supported infinite aspect ratio anisotropic panel, 37 inches wide, is $t_c = 1.83$ inch.

5.2.5 Conclusions

Comparison of the baseline unstiffened panel and the hat reinforced stiffened panel is presented in Table 30. The panel is representative of the truss web wing design, lower surface, aft panel, Sta 172-232. Weight efficiency (lb/ft^2 of the panel area) for the two panels is about the same with the stiffened panel showing a very marginal superiority in this respect over the unstiffened panel. This is true even if the 20-psi pressure condition is not considered.

If stiffener support is neglected, it appears that the stiffened panel is just as efficient as the unstiffened with respect to weight in wing cover applications. A more substantial weight saving for the stiffened panel may be possible through additional study using a more refined analysis and design. Unfortunately, the weight of stiffener supporting ribs within the truss web, and spaced 40 to 50 inches apart, would be assessed as a penalty against the stiffened panel concept. A variable thickness panel, on the other hand, was found to be more efficient than constant sandwich panels in the pressure panel study. See Paragraph 4.1.6.

TABLE 30
COMPARISON OF UNSTIFFENED AND STIFFENED PANELS

| GRAPHITE-EPOXY LAMINATES NARMCO 5206, TYPE II 0°/90°/±45° PLIES | UNSTIFFENED HONEYCOMB SANDWICH | | STIFFENED HONEYCOMB SAND- WICH WITH HAT STIFFENERS AND REINFORCEMENTS | |
|---|--------------------------------------|------|---|------|
| DESIGN REQUIREMENTS | (1) | (2) | (1) | (2) |
| PLY PROPORTIONS, % FACE SHEET HAT STIFFENERS | 52.5/5.3/42.2 — | | 20/10/70 10/10/80 | |
| t_f | 0.105 | | 0.084 | |
| t_c | 1.21 | 1.83 | 0.25 | 0.76 |
| t_s | — | | 0.108 | |
| A | — | | 8 | |
| t_{Rf} | — | | 0.125 | |
| t_{Rs} | — | | 0.30 | |
| B | — | | 1.0 | |
| F | — | | 1.66 | |
| WEIGHT LB/SQ FT OF PANEL AREA: | | | | |
| FACE SHEETS | 1.66 | | 1.36 | |
| CORE | 0.81 | 1.23 | 0.18 | 0.55 |
| STIFFENERS | — | | 0.48 | |
| REINFORCEMENTS | — | | 0.44 | |
| ADHESIVE | 0.14 | | 0.14 | |
| TOTAL | 2.61 | 3.03 | 2.60 | 2.97 |

(1) STRENGTH, STIFFNESS AND BUCKLING.

(2) STRENGTH, STIFFNESS, BUCKLING AND PRESSURE.

SEE FIGURE 88 FOR PANEL AND SYMBOL DESCRIPTION, CONFIGURATION 1.

SECTION VI

MATERIAL SELECTION

6.1 DATA SUMMARY

The selection of prepreg materials for this program was governed by the following constraints:

1. Design requirements, including service temperatures not exceeding 200°F
2. Availability of characterization data developed on Government-sponsored programs
3. Relatively long range price, 1 and 2 above having been satisfied.

Suppliers of raw materials and fabricators of advanced composites were contacted for latest data on the following classes of materials:

1. High tensile strength graphite/epoxy
2. High modulus (50×10^6 psi) graphite/epoxy
3. Very high modulus (70×10^6 psi) graphite/epoxy
4. Boron/epoxy
5. Boron/aluminum.

The resultant information was screened, tabulated, and presented in Appendix A of Reference 2. It was apparent that reliable design allowables would be almost impossible using the data available. However, there was sufficient information to permit a selection when coupled with other factors such as corporate backing, Douglas familiarity with the product, proximity of supplier, price, etc. Where more than one prepreg was available in a class, specifically the high tensile strength graphite/epoxy and boron/aluminum, a simple weighting of factors was used. Tables 31 and 32 display this.

A review of program design needs eliminated the high modulus graphite (50×10^6 psi) and boron/aluminum as materials for fabrication consideration. The former contributed no weight or cost saving and the latter would present fabrication problems beyond the scope of the program although the properties of boron/aluminum were included in design analysis trades. As a consequence of the foregoing, the following materials were selected:

1. High tensile strength graphite - Narmco 5206 (Morganite II/1004 resin)
2. Very high modulus graphite - Union Carbide Thornel 75S/2544 resin, the resin later being changed to Whittaker 1004.
3. Boron/epoxy - Avco or Narmco 5505.

TABLE 31
HIGH TENSILE STRENGTH GRAPHITE SELECTION

| | <u>Narmco 5206</u> | <u>Hercules 3002</u> | <u>Fiberite X904</u> | <u>CIBA BSL907</u> |
|--------------------|------------------------|--------------------------|--------------------------|------------------------|
| <u>Tensile</u> | | | | |
| 0° Tensile | 2 | 2 | 1 | 2 |
| 0° Tensile Mod. | 1 | 2 | 1 | 2 |
| 90° Tensile | 1 | 2 | 3 | 1 |
| 90° Tensile Mod. | 1 | 1 | 2 | 2 |
| <u>Compressive</u> | | | | |
| 0° Comp. | 2 | 1 | ND. | ND. |
| 0° Comp. Mod. | 1 | 2 | ND. | ND. |
| 90° Comp. | 1 | ND. | 2 | ND. |
| } Not Considered | | | | |
| <u>Shear</u> | | | | |
| 0° In-plane | 1 | 1 | 2 | 2 |
| Amount of Data | 1 | 2 | 2 | 4 |
| Corporate Backing | 1 | 1 | 1 | 1 |
| Immediate Cost | 2 | 1 | 1 | 2 |
| Proximity | 1 | 2 | 3 | 4 |
| DAC Familiarity | 1 | 4 | 2 | 3 |
| Rating Total* | 12 | 18 | 18 | 23 |

*Lowest is best.

ND = NO DATA

Unsatisfactory experience with Thornel 75S in the ensuing test program led to consideration of Celanese GY70/1004, and several Type I (high-modulus) graphites, specifically Narmco 5206 I for substitute use in the mixed graphite materials concept. As explained elsewhere none of these mixed material concepts was selected for wing application.

6.2 LAMINATE ALLOWABLES TESTS

A series of laminate tests was scheduled to confirm the procedures for establishing design allowables for some of the materials concepts, specifically the feasibility of using mixed graphite laminates in the wing lower cover and ultra-thin Narmco 5206 on truss webs.

TABLE 32
BORON/ALUMINUM MATERIAL SELECTION

| | General Technology | Amercon | Harvey Aluminum |
|-------------------|--------------------|---------|-----------------|
| 0° Tensile | 1 | 1 | 2 |
| 0° Modulus | 1 | 1 | 1 |
| 90° Tensile | 3 | 1 | 2 |
| 0° Comp. | 1 | 1 | 3 |
| 90° Comp. | ND. | 1 | ND. |
| 0° Shear in Plane | ND. | 1 | 1 |
| Amount of Data | 3 | 1 | 1 |
| Corporate Backing | 2 | 3 | 1 |
| Immediate Cost | 3 | 2 | 1 |
| Fab Shapes | 1 | 1 | 1 |
| Delivery | 1 | 1 | 1 |
| Proximity | 2 | 1 | 1 |
| Rating Total* | 18 | 13 | 14 |

*Lowest is best.

ND = NO DATA

Table 33 shows results of rail shear tests of Thornel 75S/2544. The shear strength of ($\pm 45/\pm 45$)S Thornel 75S/2544 is slightly better than the 20,000 psi anticipated and shear modulus is lower than the 10.7 million predicted. The response was essentially linear to failure. Individual Design Guide data sheets were published in Appendix A of Reference 3.

Table 34 shows that ultra-thin 5206 has apparent shear strength values about 50 percent of the values for standard thickness 5206. The modulus values are not changed from the standard thickness 5206. The stress strain curves were essentially linear to failure.

The design of the all-bonded truss-to-cover joints (Z3578686-1, -507, -509) and the design work relating to the wing-to-fuselage joint concept (Z5578687-503) required establishment of representative values for transverse tension and compression for the graphite laminates being considered. Table 35 indicates results. Flatwise tensile tests were on 2- x 2-inch laminates bonded between aluminum loading blocks. The flatwise compression specimens were approximately 0.5 x 0.5 inch. Note the low value for interlaminar tension with Thornel 75 present.

An initially encouraging evaluation of mixed graphite properties was obtained from receiving inspection tests, Table 36. The flexural strength and short beam shear results are essentially the same as for Thornel 75S alone while the flexural modulus roughly follows the rule of mixtures.

TABLE 33
SUMMARY OF RAIL SHEAR TESTS ON $[\pm 45/\mp 45]_S$ THORNEL 75S/2544

| SPECIMEN NUMBER | ULTIMATE STRENGTH (PSI) | SHEAR MODULUS (PSI X 10^{-6}) |
|-----------------|-------------------------|----------------------------------|
| 1 | 25,750 | (1) |
| 2 | 24,200 | 9.55 |
| 3 | 21,700 | 9.25 |

(1) STRAIN GAGE DATA INDICATED THE PRESENCE OF SPECIMEN BENDING

TABLE 34
SUMMARY OF PICTURE FRAME TESTS ON ULTRA-THIN $[\pm 45/\mp 45]_T$ NARMCO 5206 FACE SHEETS

| SPECIMEN NUMBER | ULTIMATE STRENGTH (PSI) | SHEAR MODULUS (PSI X 10^{-6}) |
|-----------------|-------------------------|----------------------------------|
| 1 | 19,675 | (1) |
| 2 | 21,975 | 5.10 |
| 3 | 15,040 | 5.35 |

(1) NO STRAIN GAGE DATA

TABLE 35
FLATWISE STRENGTH OF GRAPHITE LAMINATE

| MATERIAL | FLATWISE TENSILE STRESS (PSI) | COMMENTS |
|---|--|---|
| MODMOR 5206 [0/45/-45/90] _S | 2,500 | 4 SPECIMENS |
| MIXED GRAPHITE [0/45/-45/90] _S MODMORE IN 0, 90 DEG THORNEL 75S/1004 IN ± 45 DEG | 900 | 2 SPECIMENS. BOTH FAILED AT THORNEL 75S PLIES |
| | FLATWISE COMPRESSIVE STRESS (PSI) | |
| MODMOR 5206 [(0/90) ₁₂] _T AVG | 76,400 82,800 92,000 83,800 78,500 82,700 | LOAD/STRAIN UNIFORM TO FAILURE |
| MODMOR 5206 24 PLY - [0] _C AVG | 38,400 38,100 37,200 37,300 36,300 37,500 | DITTO |

TABLE 36
COMPARISON OF MIXED LAMINATE PROPERTIES
THORNEL 75S/2544 AND NARMCO 5206

| PROPERTY | MATERIAL | | |
|------------------------|--|-----------------------------|------------------------|
| | 0° MIXED THORNEL 75S/2544 (50%) AND NARMCO 5206 (50%) | TYPICAL THORNEL 75S/2544 | TYPICAL NARMCO 5206 |
| FLEXURAL STRENGTH, PSI | 120,000 | 130,000 | 195,000 |
| FLEXURAL MODULUS, PSI | 29,700,000 | 43,000,000 | 18,500,000 |
| SHORT BEAM SHEAR, PSI | 7,300 | 6,500 | 15,000 |

The mixed graphite material concept was originated as a means of providing increased torsional rigidity for the wing while incurring the least weight penalty. Table 37 shows that not only did the predicted (5×10^6 psi) inplane shear rigidity fail to materialize, but also there was a serious deterioration in longitudinal compressive strength. The low shear modulus is attributed to inadequate adhesion between the Thornel 75S fibers so there is not complete continuity between groups of Modmor II layers even at low stress levels. The scanning electron micrograph of the failure surface of interlaminar tension specimens shows evidence of poor adhesion between the Thornel 75S filaments and the matrix. Reference 10 contains the photograph, data sheets, and a more complete discussion of this subject.

The search for a mixed graphite/epoxy material with high longitudinal strengths and high shear stiffness continued. Two materials were selected for further evaluation: Narmco 5206/I and GY70/1004. The receiving inspection tests indicated that the Narmco 5206/I has an interlaminar shear strength

TABLE 37
SUMMARY OF TEST RESULTS FROM MIXED MATERIAL SPECIMENS
[0₂/±45/0₂/90]_s PLY PATTERN

| PROPERTY | TYPE OF TEST | ULTIMATE STRENGTH (PSI) | | EXPERIMENTAL ELASTIC MODULUS (MSI) |
|--------------------------|-----------------------------|----------------------------|------------|---|
| | | EXPERIMENTAL | ANALYTICAL | |
| LONGITUDINAL TENSION | 4-POINT SANDWICH BEAM | 108,800 | 102,000 | 13.07 |
| LONGITUDINAL COMPRESSION | 4-POINT SANDWICH BEAM | 64,500 | 129,000 | 12.75 |
| TRANSVERSE TENSION | MODIFIED ITTRI | 16,300 | 24,000 | 5.26 |
| TRANSVERSE COMPRESSION | CELANESE | 16,800 | 30,600 | — |
| INPLANE SHEAR | RAIL SHEAR | 11,100 | 14,200 | 3.14 |

of 9,100 psi, and the GY70/1004 has an interlaminar shear strength of 7,900 psi. Sandwich beam compression tests (Table 38) were run on specimens with Narmco 5206 II at 0 and 90 degrees and the high stiffness graphite at +45 degrees. The results indicate that the materials exhibit premature failures and high scatter of strength results. The failures had significant brooming and separation of plies (see Figure 90). Although the strength results were better than the previous results using Thornel 75S, it was concluded that neither material had characteristics which enable it to be considered for application.

TABLE 38
SUMMARY OF LONGITUDINAL COMPRESSION TEST RESULTS
(0_A/+45_B/0_A/-45_B/90_A)_S

| MATERIAL | | TYPE OF TEST | ULTIMATE COMPRESSION STRENGTH (KSI) | MODULUS (MSI) |
|----------|-----------|-----------------------|-------------------------------------|---------------|
| A | B | | | |
| 5206/II | 5206/I | 4-POINT SANDWICH BEAM | 103.2 | 11.39 |
| | | | 102.4 | 11.70 |
| | | | 68.1 | 10.70 |
| 5206/II | GY70/1004 | 4-POINT SANDWICH BEAM | 95.6 | 11.40 |
| | | | 76.8 | 10.67 |
| | | | 75.7 | 11.21 |

See Z4578682 in Appendix A for sandwich beam specimen drawing.

6.2.1 Boron Film/Graphite Fiber Testing

Compression beam screening tests were conducted on a mixed fiber/film laminate to compare it on the same basis as the other mixed graphite laminates tested in the program. These laminates were sensitive in the compression failure mode because of interlaminar and fiber/resin interface problems.

Seven-ply boron film stacks were constructed at the National Research Corporation (NRC), Cambridge, Massachusetts, using 1004 resin supplied by Douglas. These were colaminated with unidirectional 5206 II graphite per drawing Z4578682 (configuration -507) and three beams fabricated at Douglas. The test laminate consisted of three seven-ply stacks of film between which two plies of 0-degree 5206 were laminated.

Beam No. 1 broke under one of the two loading heads at a boron/graphite splice area (see drawing) at a compression stress of approximately 107 ksi. It was not anticipated that the failing stress would be above 50 ksi, based on incomplete understanding of NRC work not then reported. To conserve film, the splice within the test laminate was introduced. Beam No. 2 was tested under three-point (central) loading and broke at 140 ksi, again in the film-to-graphite joint area. Accordingly, an aluminum reinforcing plate was bonded over the joints of the third beam and the beam was three-point loaded to a failure stress of 150 ksi. Figure 91 shows this beam after failure. Strain data were obtained for one beam. The calculated 16.7×10^6 psi laminate modulus is approximately as expected from the rule of mixtures. The film stacks met the drawing requirement of less than 0.7 mil/ply since the five-ply mixed laminate thickness was 0.024 (0.027 on the drawing).

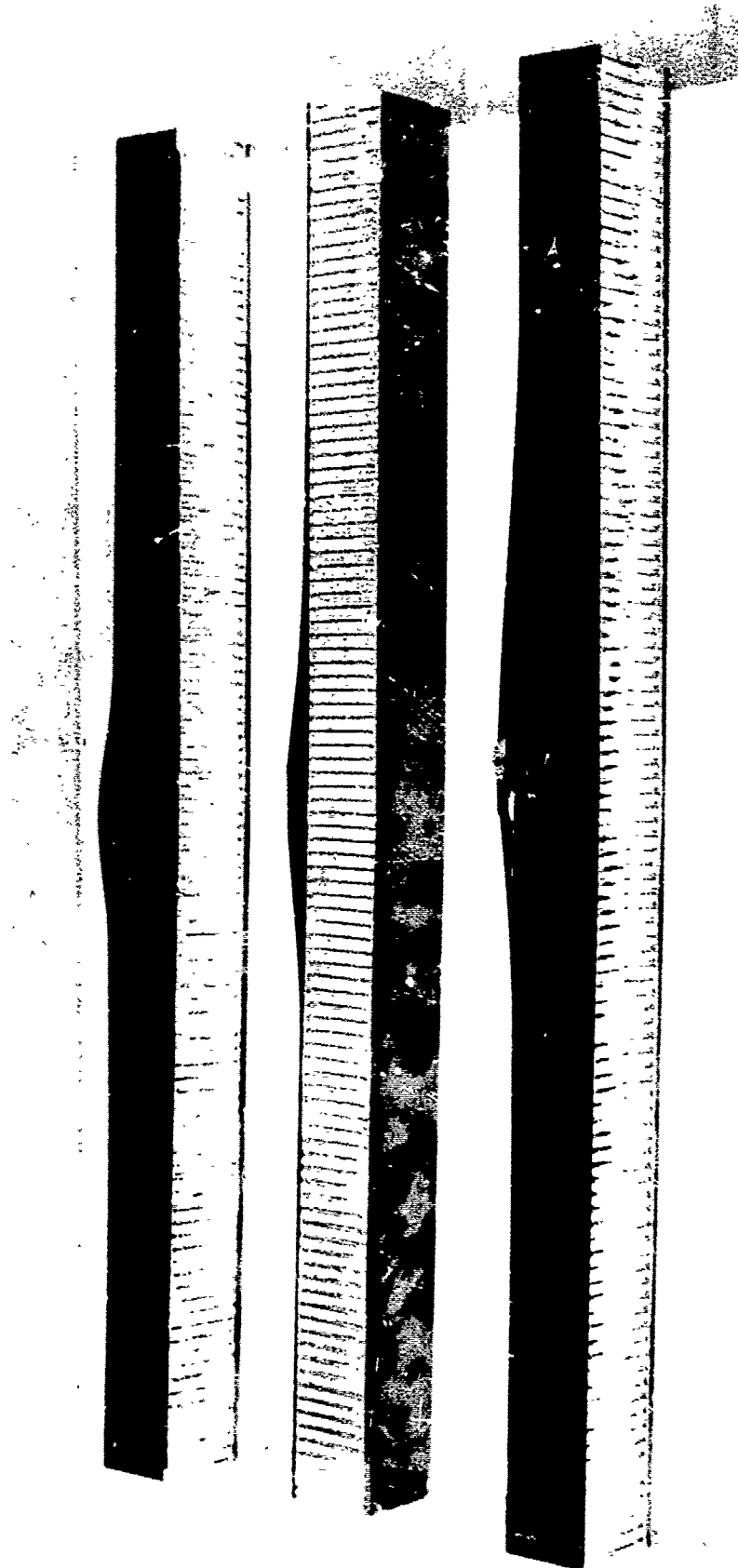


FIGURE 90. TYPICAL MIXED GRAPHITE COMPRESSION BEAM FAILURES

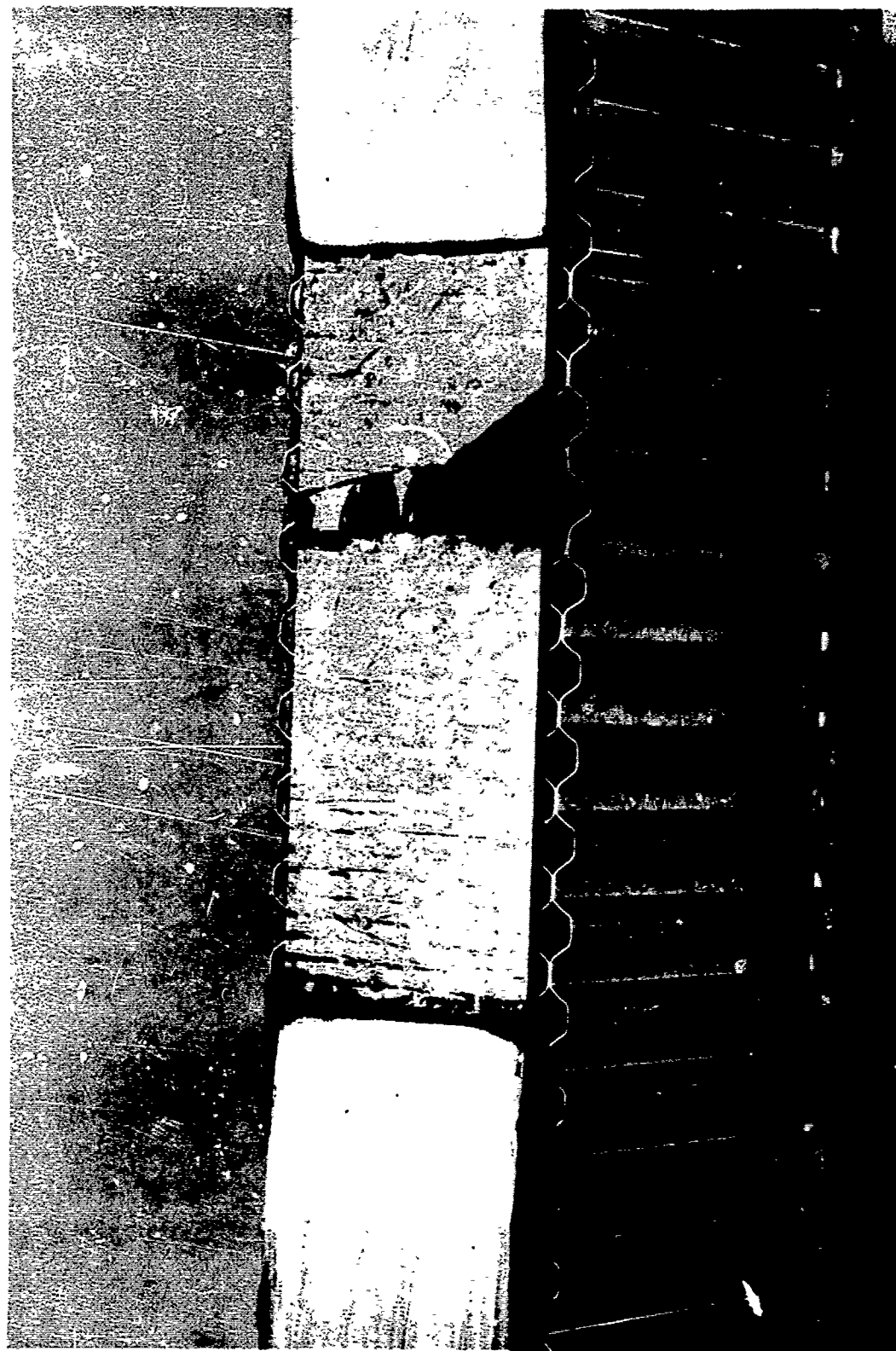


FIGURE 91. MIXED BORON FILM AND GRAPHITE BEAM AFTER FAILURE

The compressive strain at failure for the boron film laminate alone was reported to be 3,100 microinches and its compressive strength 71,500 psi (Reference 11), however, conversation with Dr. Padawer at NRC established that his earlier results were conditioned by the graphite-type used and the CIBA resin system. Our results, using 5206/II, indicate a greater strain to failure and compressive strength than previously reported for the film/graphite mixture.

It is now indicated that shear modulus and shear and tension strength of this combination be investigated, since it achieved better compression and interlaminar shear properties than the mixed fiber laminates screened on this program (see Table 39). Short beam interlaminar shear specimens of this material combination developed an average F_{ILS} of 11,000 psi, failing generally at the interface between film and polyimide film carrier.

Various design use potentials of the film/fiber concept:

- Prevent fiber separation under load for unidirectional facings such as truss web struts.
- Panel edge reinforcement at bolted chordwise wing cover splices.
- Stress relief doublers at chordwise hole rows.
- Wing compression covers and shear webs, particularly for high shear stiffness without use of high modulus angle plies.

TABLE 39

MIXED MATERIALS COMPRESSIVE TESTS

| REFERENCE | MATERIAL | PERCENT BY VOLUME | | | | | COMPRESSION ULTIMATE (PSI) | COMPRESSION MODULUS (PSI) |
|-----------------------|--|-------------------|------|-----|---------------|-------|---|---------------------------------|
| | | GRAPHITE FIBERS | | | BORON FILM | RESIN | | |
| | | 0° | ±45° | 90° | | | | |
| NEW | 5206 TYPE 2/BORON FILM (B ₇ /0 _{GR} /B ₇ /0 _{GR} /B ₇ /T | 28 | — | — | 21 | 51 | 107,100 (1) 140,000 (2) 150,000 (3) | 16.7 × 10 ⁶ |
| PAGE 31 MDC J-4110 | 5206 TYPE 2/1004 THORNEL 75 (0 ₂ /±45/0 ₂ /90) _S | 36.5 | 18.5 | 5 | — | 40 | 64,500 | 12.75 × 10 ⁶ |
| PAGE 27 MDC J-4181 | 5206 TYPE 2/5206 TYPE 1 (0/45/0/—45/90) _S | 27 | 27 | 6 | — | 40 | 91,000 | 11.3 × 10 ⁶ |
| | 5206 TYPE 2/GY70 CF ¹ LANESE (0/45/0/—45/90) _S | 27 | 27 | 6 | — | 40 | 83,000 | 11.1 × 10 ⁶ |
| PAGE 24 MDC J-0945 | 5206 TYPE 2/5206 TYPE 2 [(0/±45) ₃] _S | 20 | 40 | — | — | 40 | 75,000 | 7.2 × 10 ⁶ |
| | 5206 TYPE 2/5206 TYPE 2 [(0/±45/90) ₂] _S | 15 | 30 | 15 | — | 40 | 69,000 | 6.6 × 10 ⁶ |

6.3 ADHESIVE PROPERTIES TESTS

The design of bonded joints in a structure is based primarily on the complete stress-strain curves for the adhesive bonds under shear loading (Reference 12). Such data are needed at at least three temperatures throughout the design operating environment because of changes in adhesive behavior with temperature. Specimens and test instrumentation were prepared to generate these data for several selected adhesives in accordance with drawing Z4578680, however, the data were not obtained at all temperatures.

Hysol EA951 adhesive film was selected for cured composite-to-composite or composite-to-metal bonds because of its high strength and high strain to failure. The ultimate shear strain serves as a failure criterion for the joint. Douglas had derived information for EA951 at room temperature in an earlier program.

3-M FM96 adhesive film was selected for sandwich face sheet bonding to core and for an interface between cocured and precured laminates. EA951 could also have been and was used for the latter purpose also.

A thixotropic paste adhesive, Hysol EA9306, was also selected as a result of specific design requirements associated with the fillet bond concept. The material screening tests were conducted under the Fabrication Feasibility Task (Paragraph 7.1.1) and design properties were required for the selected EA 9306.

Table 40 summarizes thick-adherend testing of the selected adhesives. Figure 92 shows some of the Z4578680-509 specimens. A specially modified Tinius Olsen breakaway extensometer was used. Previously unpublished IRAD tests on Metlbond 329 are included for comparison. Briefly, the EA 951 proved extremely tough and ductile, while the others were extremely brittle.

The -505 and -507 specimens (Table 40) were to gather data for the influence of the graphite-epoxy shear deformation on the bond strength. Unfortunately, many specimens were broken by splitting (peeling) along the laminate after the specimen slots were cut. It is now realized that interlaminar tension behavior in a joint is the crucial influence, rather than shear as originally believed, so shear testing was discontinued.

6.3.1 EA9306 Properties Tests

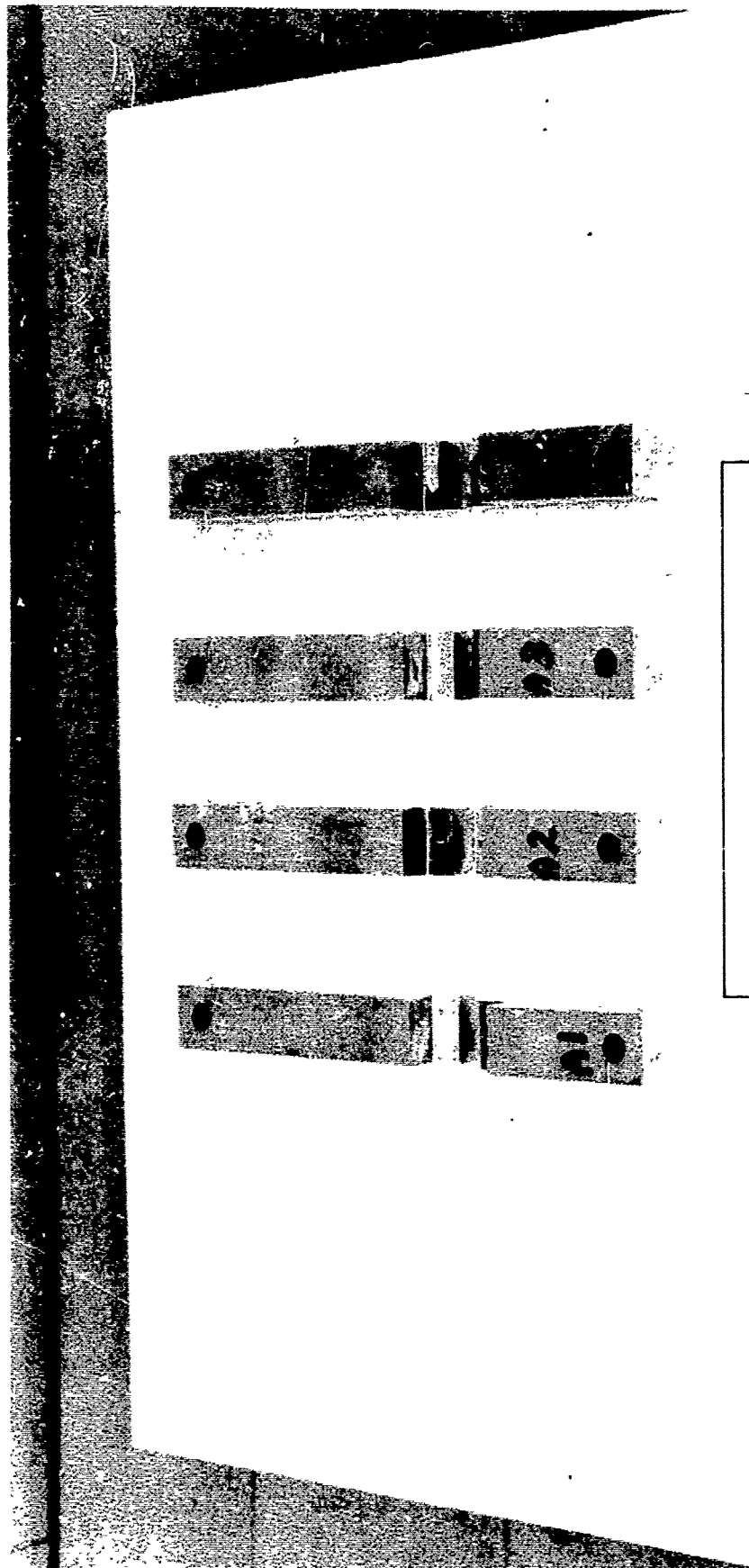
The initial set of flatwise tension test results, Table 41, was obtained to determine the effect of bond thickness and temperature on the strength of EA9306. The first set of specimens was full of voids and pointed up the need for degassing the adhesive prior to application. The second set of flatwise block tests showed the material to be stronger after degassing. The 2600-3500 psi values represent the effect of severe stress risers in the material.

The bottom portion of Table 41 indicates a much higher room temperature strength (9000 psi) using a cast dogbone specimen from which modulus can be

TABLE 40
STRESS-STRAIN BEHAVIOR OF THICK ADHEREND BONDED JOINTS Z4578680
(BOND AREA = 0.5 SQ IN., ADHERENDS 0.5 IN. THICK ALUMINUM)

| CONFIGURATION SPECIMEN I.D. | ADHESIVE | TEST TEMP (°F) | FAILURE LOAD (LB) | MAXIMUM BOND STRESS (PSI) | MAXIMUM BONDLINE DISPLACEMENT (IN.) | BONDLINE DISPLACEMENT AT YIELD (IN.) | NOMINAL BONDLINE THICKNESS* (IN.) | MAXIMUM BOND SHEAR STRAIN | COMMENTS |
|--------------------------------|-------------------------------------|----------------------|-------------------------|---------------------------------|--|---|--|---------------------------------|---|
| 1 NO. 4 | FM96 | RT | 2490 | 4980 | 0.00005 | 0.00005 | 0.005 | 0.01 | EXTREMELY BRITTLE FAILURE |
| 1 NO. 5 | FM96 | RT | 2950 | 5900 | 0.0024 | 0.0023 | 0.005 | 0.48 | APPARENTLY COMPLETE CHARACTERISTIC |
| 1 NO. 6 | FM96 | RT | 2400 | 4800 | 0.0012 | 0.0011 | 0.005 | 0.24 | BRITTLE PREMATURE FAILURE |
| (-1) NO. 1 | N329 | RT | 3000 | 6000 | 0.0011 | 0.0001 | 0.005 | 0.22 | SLIGHT YIELD AT 5400 PSI |
| (-1) NO. 2 | N329 | RT | 2440 | 4880 | ≈0 | ≈0 | 0.005 | 0 | BRITTLE PREMATURE FAILURE |
| (-1) NO. 3 | N329 | RT | 2685 | 5370 | 0.0008 | 0.0002 | 0.005 | 0.16 | SLIGHT YIELD AT 4200 PSI |
| (-1) NO. 4 | N329 | RT | 2900 | 5800 | 0.0012 | 0.0002 | 0.005 | 0.24 | SLIGHT YIELD AT 4200 PSI |
| (-1) NO. 5 | N329 | RT | 2410 | 4820 | ≈0 | ≈0 | 0.005 | 0 | BRITTLE PREMATURE FAILURE |
| (-509) NO. 6 | N329 | RT | 3140 | 6280 | 0.0044 | ~0.002 | 0.005 | 0.88 | NO DISTINCT YIELD. MODULUS = 15,000 PSI |
| (-501) NO. 1 | EA951 | RT | 3750 | 7500 | 0.0200 | 0.0024 | 0.005 | 4.0 | VERY DUCTILE YIELD AT 5300 PSI |
| (-501) NO. 2 | EA951 | RT | 3890 | 7780 | 0.0130 | 0.0016 | 0.002 | 6.5 | VISIBLY STARVED GLUE LINE. VERY DUCTILE. |
| (-501) NO. 3 | EA951 | RT | 2960 | 5920 | 0.0152 | 0.0010 | 0.005 | 3.0 | VERY DUCTILE YIELD AT 4300 PSI INFINITE INITIAL MODULUS |
| (-501) NO. 4 | EA951 | RT | 3950 | 7900 | 0.0140 | 0.0020 | 0.005 | 2.8 | VERY DUCTILE. YIELD AT 4300 PSI |
| -503 NO. 1 | EA9306 | RT | 280 | -- | ≈0 | ≈0 | 0.032 | -- | EXCESSIVE VOIDS. DEFECTIVE SPECIMEN |
| -503 NO. 2 | EA9306 | RT | 1775 | 3550 | ≈0 | ≈0 | 0.032 | -- | BRITTLE PREMATURE FAILURE |
| -503 NO. 3 | EA9306 | RT | 2300 | 4600 | 0.0023 | ≈0 | 0.032 | -- | INFINITE INITIAL MODULUS |
| -509 NO. B1 | EA9306 | RT | 3115 | 6230 | 0.0078 | 0.0064 | 0.032 | 0.24 | NO DISTINCT YIELD |
| -509 NO. B2 | EA9306 | RT | 2695 | 5390 | 0.0083 | 0.0070 | 0.032 | 0.26 | NO DISTINCT YIELD |
| -509 NO. B3 | EA9306 | RT | 2650 | 5300 | 0.0090 | 0.0060 | 0.032 | 0.28 | NO DISTINCT YIELD |
| -509 NO. B4 | EA9306 | RT | 2660 | 5320 | 0.0085 | 0.0068 | 0.032 | 0.27 | NO DISTINCT YIELD |
| -509 NO. A1 | EA9306 | 160 | 1875 | 3750 | 0.0064 | 0.0050 | 0.032 | 0.20 | SLIGHT YIELD AT 3700 PSI |
| -509 NO. A2 | EA9306 | 160 | 2150 | 4300 | 0.0037 | 0.0031 | 0.032 | 0.12 | SLIGHT YIELD AT 4300 PSI |
| -509 NO. A3 | EA9306 | 160 | 2115 | 4230 | 0.0074 | 0.0057 | 0.032 | 0.23 | SLIGHT YIELD AT 4200 PSI |
| -509 NO. A4 | EA9306 | 160 | 2395 | 4790 | 0.0053 | 0.0049 | 0.032 | 0.17 | SLIGHT YIELD AT 4700 PSI |
| -505 NO. A2 | 45° N5206 LAMINATE | RT | 2350 | 4700 | 0.0052 | | | | SLIGHT YIELD AT 4700 PSI |
| -505 NO. A4 | 8 LAYERS BETWEEN | RT | 2400 | 4800 | 0.0054 | | | | SLIGHT YIELD AT 3700 PSI |
| -505 NO. A5 | EA951 | RT | 1900 | 3800 | 0.0048 | | | | VERY BRITTLE FAILURE |
| -505 NO. A1 | ADHESIVE (ALUMINUM ADHERENDS) | -67 | 1040 | 2080 | 0.0005 | | | | SLIGHT YIELD AT 3000 PSI |
| -505 NO. A6 | | -67 | 1650 | 3300 | 0.0024 | | | | VERY PREMATURE FAILURE |
| -505 NO. A7 | | -67 | 445 | -- | ≈0 | | | | ABRUPT PREMATURE FAILURE |
| -507 NO. B4 | 0°/45°/90° N5206 LAMINATE LIKE -505 | RT | 1075 | 2150 | 0.0004 | | | | |

*CONTROLLED BY WIRE STOPS IN BOND OUTSIDE TEST SECTION
 () IRAD TESTS INCLUDED FOR COMPARISON



THICK ADHEREND SPECIMENS

FIGURE 92. THICK ADHEREND Z4578680-509 SPECIMENS

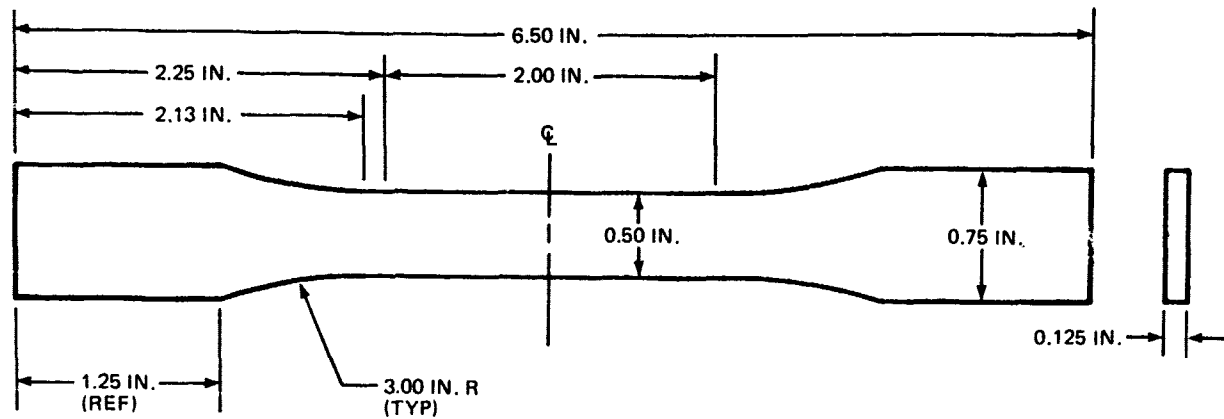
TABLE 41
EA9306 ADHESIVE TENSION TESTS

| TYPE SPECIMEN | t (IN.) | A (SQ IN.) | F _Z ^T (PSI, ULTIMATE) | | TEMP (°F) | COMMENT |
|---|-------------------|---------------|--|--------------------------------------|--------------|-----------------------------------|
| 2 x 2 AL BLOCKS 1 x 2 TEST AREA OF AS NOTED FLATWISE | 0.250 | 2.00 | 4278 | | RT | AL BLOCK FAILED 10,045 LB |
| | 0.250 | 2.00 | 3740 | | RT | |
| | 0.125 | 2.00 | 5022+ | | RT | |
| | 0.125 | 2.00 | 3035 | | RT | |
| | FIRST SET AVERAGE | | 4019 | | | ALL OF FIRST SET HAD VOIDS |
| | 0.250 | 2.00 | 1542 | | 200 | |
| | 0.250 | 2.00 | 1202 | | 200 | |
| | 0.125 | 2.00 | 1850 | | 200 | |
| | 0.125 | 2.00 | 1794 | | 200 | |
| | FIRST SET AVERAGE | | 1597 | | | |
| | 0.125 | 2.00 | 5920 | | RT | AL BLOCK FAILED 11,650 LB |
| | 0.125 | 2.00 | 5830+ | | RT | |
| | AVERAGE | | 5900 | | | |
| | 0.125 | 1.00 | 2600 | | RT | |
| | 0.250 | 1.00 | 3550 | | RT | SAWCUTS - STRESS RISERS |
| | 0.250 | 1.00 | 2670 | | RT | SAWCUTS - STRESS RISERS |
| | AVERAGE | | 2940 | | | |
| | - | 1.00 | 2668 | | 200 | SAWCUTS - STRESS RISERS |
| | - | 1.00 | 2940 | | 200 | SAWCUTS - STRESS RISERS |
| | - | 1.00 | 2120 | | 200 | SAWCUTS - STRESS RISERS |
| | - | 1.00 | 2310 | | 200 | SAWCUTS - STRESS RISERS |
| | AVERAGE | | 2509 | | | |
| CAST TENSILE PER ASTM D-638 6.5 IN. LONG | 0.1196 | 0.0583 | F _X ^T (PSI) | E _X ^T (PSI) | RT | MODULUS TO 32 PERCENT ULTIMATE |
| | 0.1195 | 0.0578 | 9091 | 8.0 x 10 ⁵ | RT | MODULUS TO 32 PERCENT ULTIMATE |
| | 0.1166 | 0.0558 | 9429 | 9.6 x 10 ⁵ | RT | MODULUS TO 32 PERCENT ULTIMATE |
| | AVERAGE | | 6810* | 9.6 x 10 ⁵ | RT | MODULUS TO 45 PERCENT ULTIMATE |
| | AVERAGE | | 8443 | 9.0 x 10 ⁵ | | |

*BROKE IN END AT A VOID

obtained. Figure 93 shows the specimen configuration. The modulus values placed the adhesive in the high strength brittle category. As seen in Figure 94 instrumentation difficulties prevented obtaining stress-strain data to failure. The 200°F tensile strengths are shown in Table 42, showing a serious (80 percent) strength reduction at that temperature. It is speculated that properties may be relatively stable to 180°F, a characteristic of the

EA9306 TENSILE SPECIMEN (REF: ASTM D-638)



USE Z5825808 PRECISION ALIGNMENT TEST FIXTURE, IF NOT AVAILABLE, USE TEMPLIN GRIPS

EXTENSOMETER: INSTRON G-15-13 OR EQUIVALENT

TEST TEMP: RT AND 200°F (3 REPLICATES)

TOTAL NUMBER OF SPECIMENS: 6

RECORD STRESS-STRAIN CURVE TO 80 PERCENT ULTIMATE STRENGTH.

FIGURE 93. CAST ADHESIVE TENSILE SPECIMEN

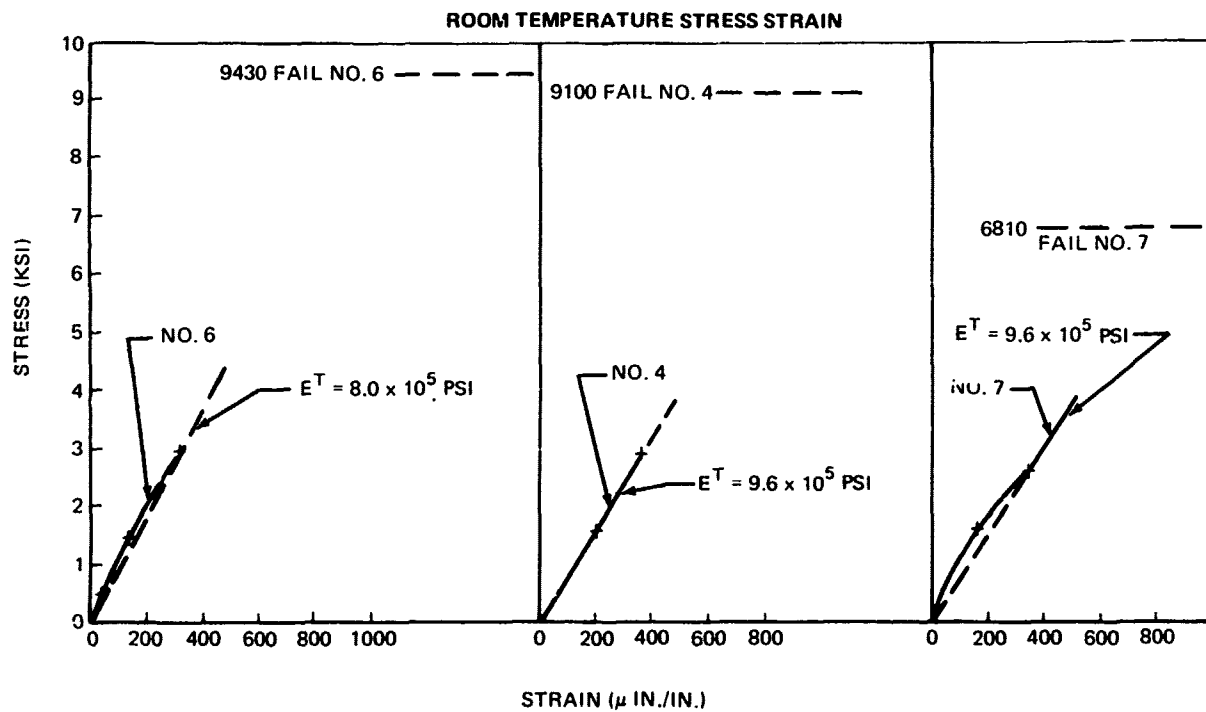


FIGURE 94. EA9306 TENSILE STRESS/STRAIN - ROOM TEMPERATURE

TABLE 42
EA9306 TENSILE CASTING TEST DATA, 200°F

| | t (IN.) | A (SQ IN.) | F _x ^T (PSI, ULT) | E _x ^T | TEMP (°F) |
|--------------------------------|------------|---------------|---|-----------------------------|--------------|
| CAST TENSILE PER ASTM D-638 | 0.1223 | 0.0593 | 1686 | • | 200 |
| | 0.1182 | 0.0570 | 1771 | • | 200 |
| | 0.1200 | 0.0574 | 1707 | • | 200 |
| | AVERAGE | | 1721 | | |

*SEE STRESS/STRAIN CURVES

250°F curing epoxies of which EA9306 is a type. Use of this material in any primary joint must be evaluated in terms of further tests at actual temperatures experienced at the bondline. Figure 95 shows a reduced modulus and a pronounced yield at 200°F.

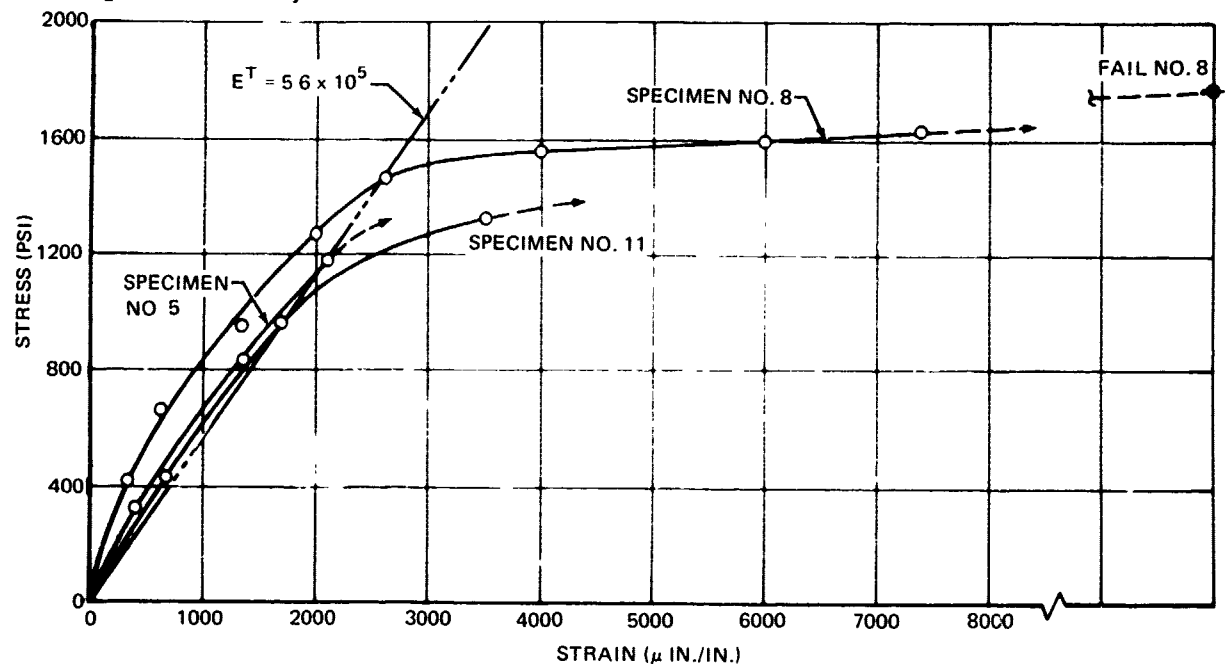


FIGURE 95. EA9306 TENSILE CASTINGS - 200°F STRESS/STRAIN

6.3.2 Mixed Graphite/Adhesive Laminate Tests

Interlaminar tensile and interlaminar shear tests on laminates consisting of alternating plies of Narmco 5206 and EA951 adhesive are summarized in Table 43. The resulting laminate is apparently stronger, transversely, by a factor of 2 for 5206 than for the graphite laminate alone. The 4000-psi test results were conditioned by failure of EA951 at the interface with the metal block. The 5000+ psi result was a limitation of the test block since no failure occurred. The 4925-psi result was the only failure within the laminate.

The 6775-psi short beam shear strength of the interleaved laminate was governed by the EA951, which in torsion ring tests has displayed a 6500-psi shear strength.

TABLE 43
MIXED GRAPHITE/ADHESIVE LAMINATE TESTS

| MATERIAL | TYPE TEST | SPAN (IN.) | t (IN.) | F _{ILS} (PSI) | COMMENT |
|--|------------------|------------|---------------------------|---|------------------------|
| NARMCO 5206/II (0/45/90/-45) _S WITH 7 PLIES EA951 INTERLEAVED | SHORT BEAM SHEAR | 0.2507 | 0.0990 | 6646 | ALI FAILED IN ADHESIVE |
| | | 0.2580 | 0.0998 | 6902 | |
| | | 0.2505 | 0.0945 | 6786 | |
| | | 0.2508 | 0.0955 | 6732 | |
| | | 0.2501 | 0.0934 | 6809 | |
| | AVERAGE | | | 6775 | |
| | FLATWISE TENSION | A (SQ IN.) | F _T Z (PSI) | NO FAILURE, TEST TERMINATED. BONDED WITH 9306 TO METAL BLOCKS BONDED WITH 951 WHICH FAILED AT METAL BONDED WITH 9306. FAILED IN LAMINATE | |
| | | | | | |
| | | | | | |
| | | | | | |
| | | | | | |
| 2 x 2 AL BLOCKS | 2.0 | 5000+ | | | |
| 1 x 2 TEST AREA | 2.0 | 4000 | | | |
| | 2.0 | 4925 | | | |
| AVERAGE | | 4641 | | | |
| ALL TESTS AT ROOM TEMPERATURE | | | | | |

SECTION VII

DESIGN DEVELOPMENT AND VERIFICATION

7.1 FABRICATION FEASIBILITY

Several new concepts, both from a design and fabrication standpoint, were attempted in this program. This necessitated some fabrication feasibility studies. The following areas were of primary concern:

1. Joining the truss web to the wing skins by primary bonding.
2. Mixing Modulite 5206/II graphite with Thornel 75S/epoxy graphite.
3. Cocuring the skins to the honeycomb.

7.1.1 Truss Web to Skin Joint

A sample truss web bolted joint, similar to those shown on Design Verification Drawing Z5578684, was layed up and cured in a simple sheet metal tool as shown in Figures 96 and 97. Figure 98 is a photograph of this specimen clearly indicating the need to precure the bolt pads and shoulders. A second part made utilizing precured pads and shoulders indicated a problem of pulldown of the prepreg during cure, causing wrinkles in the web facing and dislocation of the honeycomb (see Figure 99). Great care in the layup and intermediate densification was indicated. A similar situation was shown later to exist in the bonded joints as indicated in Figures 100 and 101.

The bonded joint concepts studied in the program required some feasibility study to determine adequate materials for the bond. Candidate materials were screened to the following criteria:

1. Flatwise tensile strength equal to or greater than that of the composite laminate and shear strength greater than 3000 psi.
2. Maintain shape during cure.
3. Easily applied with only simple preforming.
4. Modulus greater than 1×10^6 psi.
5. Good peel strength (high strain).

Only those materials with available data indicating shear strength in excess of 3000 psi were investigated. Flatwise tensile testing of adhesives and reinforced adhesives was used to screen candidates. The results are shown in Table 44. While none of these materials meets all of the criteria, the Hysol EA9306 had such excellent wetting characteristics, coupled with good bond strengths, that it was selected. However, the low temperature resistance (as determined in subsequent tests) and relative brittle nature at room temperature would dictate further material evaluation for an actual wing material evaluation for an actual wing material. It was felt that the EA9306 would adequately verify the concept.

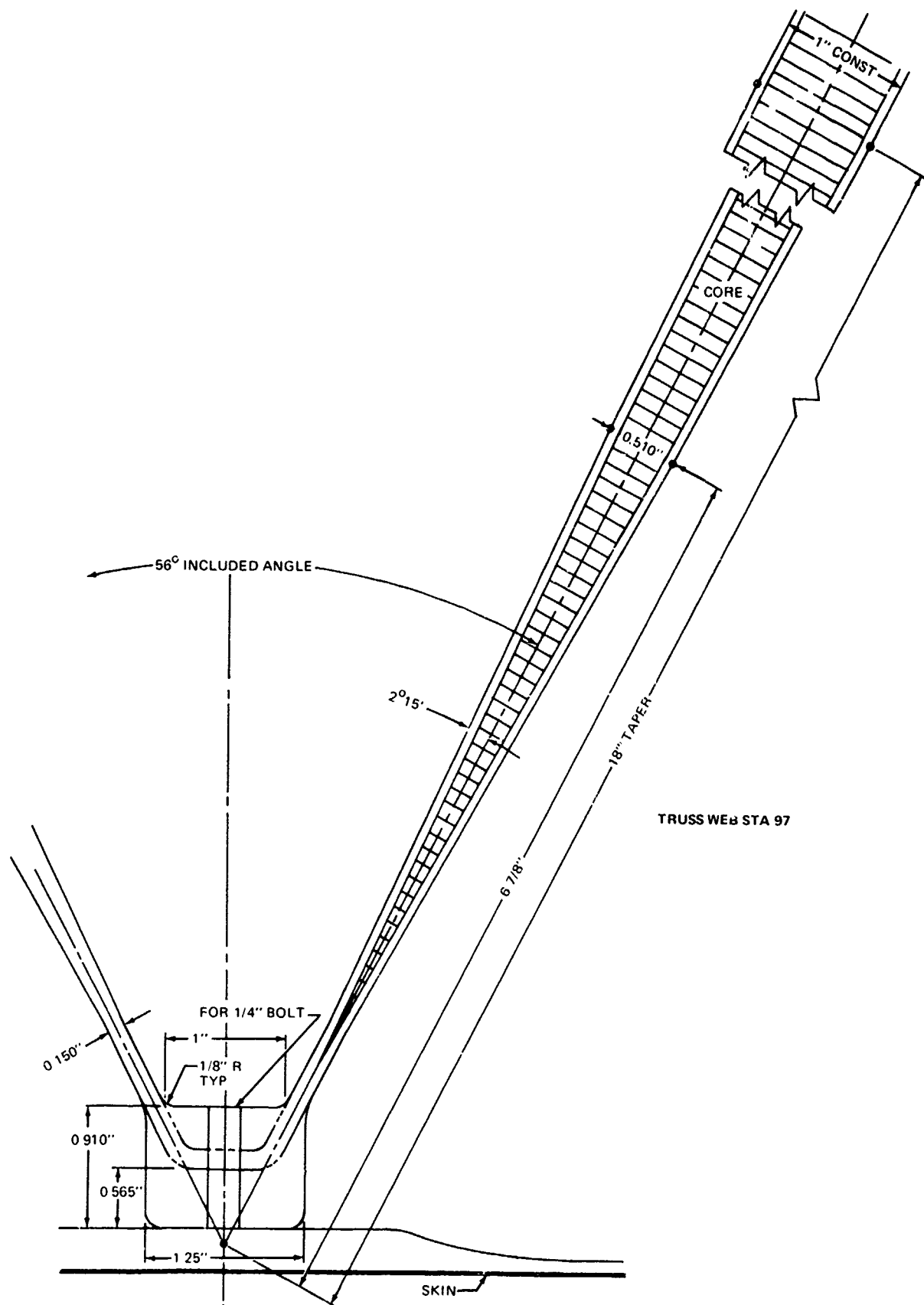


FIGURE 96. SKETCH - FABRICATION FEASIBILITY TRUSS WEB JOINT

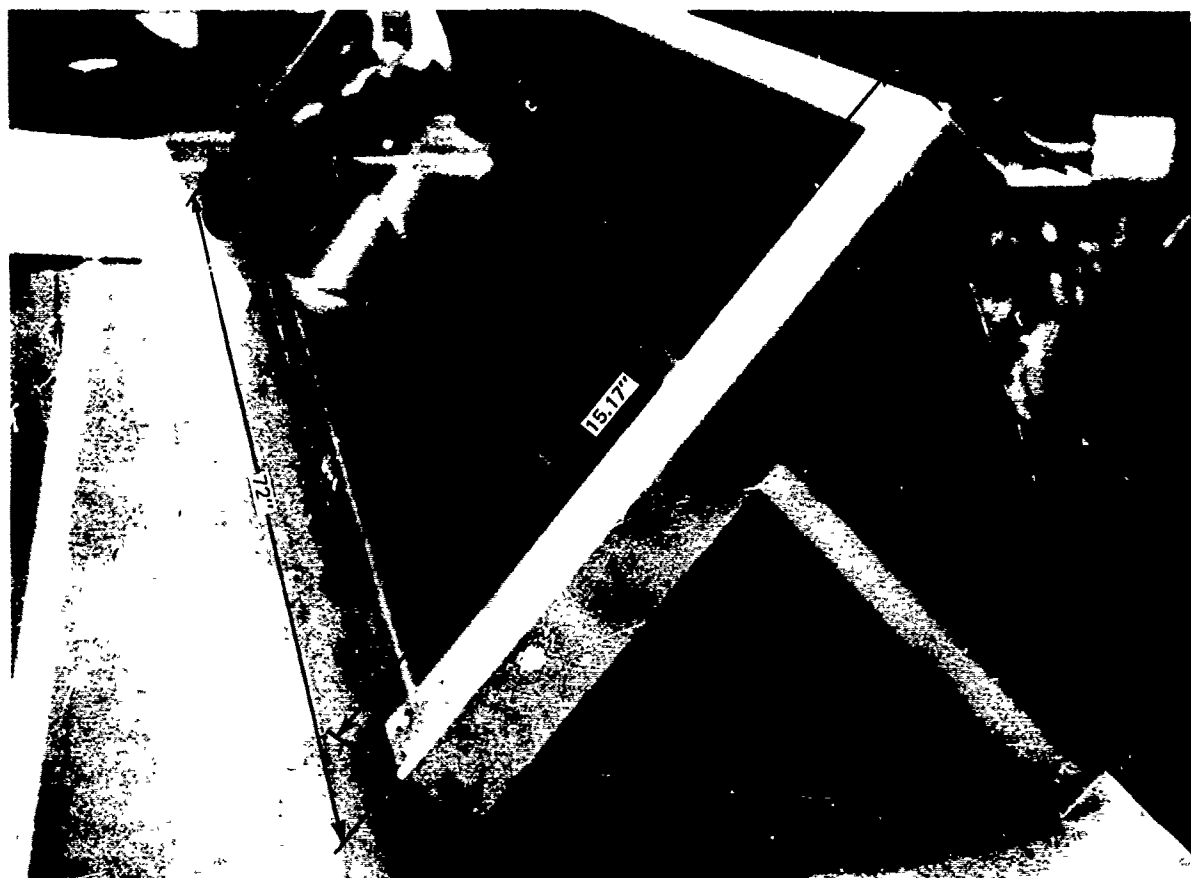


FIGURE 97. LAYUP TOOL FOR FEASIBILITY STUDY OF TRUSS WEB DESIGN



FIGURE 98. FIRST TRUSS WEB FABRICATION FEASIBILITY SPECIMEN



FIGURE 99. CONCEPTUAL WING JOINT FABRICATION TEST NO. 2



FIGURE 100. BONDED TRUSS SPECIMEN, LOAD APPLICATION JOINT, GRAPHITE COVER

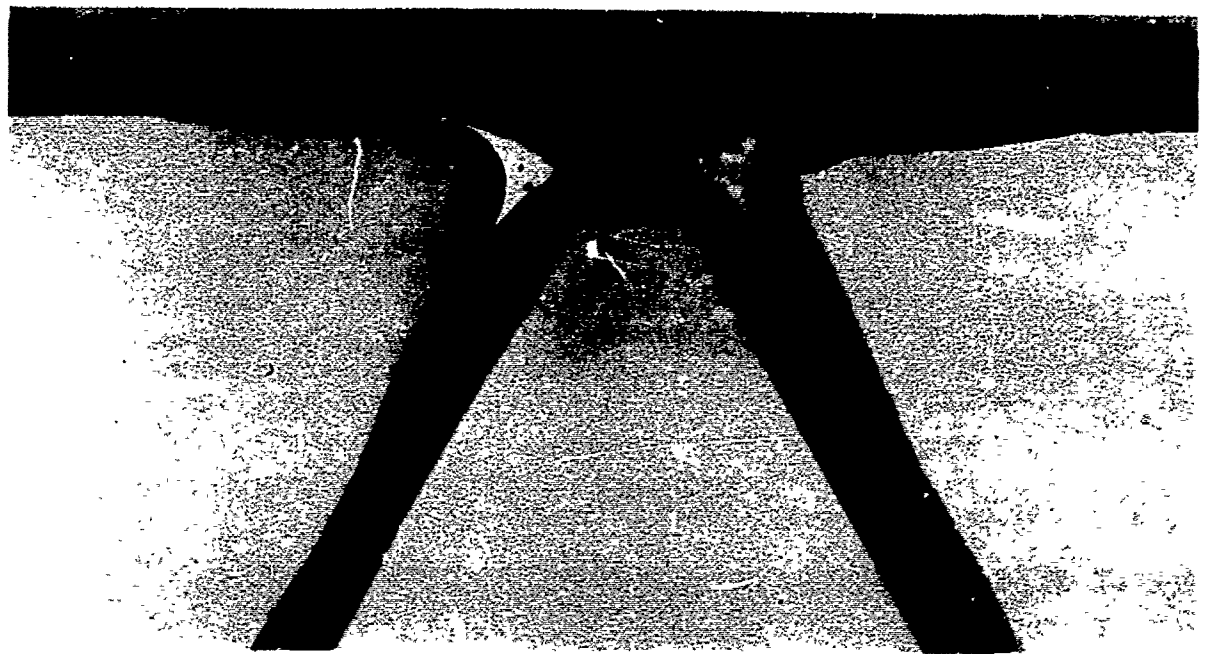


FIGURE 101. BONDED TRUSS SPECIMEN, UPPER GRAPHITE COVER, INTERMEDIATE JOINT

TABLE 44
ADHESIVE FLATWISE TENSILE SCREENING TESTS

| MATERIAL | TRANSVERSE TENSILE STRENGTH (PSI) | COMMENT | NUMBER SPECIMENS |
|---|---|---|------------------|
| HYSOL POTTING COMPOUND 10001 (DMS 1803B) WITHOUT FIBER | 2100 | DIFFICULT TO APPLY | 2 |
| WITH 3-5 PERCENT FIBER (CHOPPED MORGANITE II GRAPHITE) | 600 | — | 2 |
| EA951 ADHESIVE 18 LAYERS IN 1/4 IN. | 2100 | THICK, UNREINFORCED | 1 |
| DAPCOTAC 3003 POTTING COMPOUND WITHOUT FIBER | 1800 | — | 1 |
| WITH 3-5 PERCENT FIBER (CHOPPED MORGANITE II GRAPHITE) | 600 | — | 1 |
| WITH 5 PERCENT FIBER (CHOPPED E-GLAS _s /VOLAN FINISH) | 1400 | — | 2 |
| PREIMPREGNATED UNIDIRECTIONAL CHOPPED GRAPHITE MOLDING MAT (FOTHERGILL AND HARVEY SAMPLE) | 1900 | HIGH PRESSURE CURE | 1 |
| | 36 | LOW PRESSURE CURE | 1 |
| | 1500 MINIMUM (PREMATURE FAILURE-NONPARALLEL LOADING BLOCKS) | ALTERNATING PLIES: MAT AND EA951 ADHESIVE (LOW PRESSURE CURE) | 1 |
| HYSOL EA9306 (PASTE) | 4000 | 1/4 INCH THICKNESS | 1 |
| | 4200 | 1/8 INCH THICKNESS | 1 |
| THORNEL 75S/1004 (0, ±45, 90) _s | 2275 | ALTERNATING PLIES: 75S AND EA951 ADHESIVE | 1 |

7.1.2 Mixed Graphite Laminating

The design studies indicated a desire to blend very high modulus graphite material with the 5206 graphite and with the 5505 boron. While there is no fabrication concern regarding the mixing of the different reinforcements, mixing of two resins of radically different cure rate represented a potential problem. While initial trial laminates indicated no problem with mixtures of Thornel 75S/2544 and Modulite 5206/II, subsequent panels (Z3578685-22 through -41) showed excessive voids and poor resin bleed. Since it was possible that the mixture of resins was the cause, it was decided that any subsequent fiber mixtures would have the same resin system. While the concept of the blend of very high and moderate modulus reinforcements was later eliminated for other reasons, the use of one resin system provided good lamination.

7.1.3 Co-curing Wing Skins to Honeycomb

A small amount of investigative effort was conducted on the cocuring of graphite skins to HRP honeycomb. This work was conducted to establish whether significant dimpling would occur and whether the bond strengths were adequate. The following honeycomb sandwich panels were prepared:

1. Narmco 5206 (0.006 in. /ply), 8 plies, 0/+45/90-degree pattern, precured and bonded both sides with FM96U adhesive.
2. Narmco 5206 (0.006 in. /ply), 8 plies, 0/+45/90-degree pattern, one skin precured and bonded with FM96U and the other cocured and bonded with FM96U.
3. Narmco 5206 (0.006 in. /ply), 8 plies, 0/+45/90-degree pattern, cocured and bonded both sides with FM96U.
4. Narmco 5206 (0.006 in. /ply), 4 plies, +45-degree pattern, precured and bonded both sides with FM96U.
5. Narmco 5206 (0.006 in. /ply), 4 plies, +45-degree pattern, one skin precured and bonded with FM96U and the other cocured and bonded with FM96U.
6. Narmco 5206 (0.003 in. /ply), 4 plies, 0/90 degree pattern, precured and bonded both sides with FM96U.
7. Narmco 5206, (0.003 in. /ply), 4 plies, 0/90-degree pattern, one skin precured and bonded with FM96U and the other cocured and bonded with FM96U.

Each of the above panels was cut into replicate specimens to be tested to failure in a beam bending test with the precured skin in tension and some with the cocured skin in tension. All of the cocured skins showed significant dimpling with the severity proportional to the skin thickness. The bending test failures were in the cocured skin whenever it was in compression. When the cocured skin was in tension, the failures were mixed. Table 45 shows a summary of the average test results by layup and failure mode. It is apparent that the dimpling results in a significant loss of compression strength.

TABLE 45

AVERAGE RESULTS OF HONEYCOMB BEAM TESTS

| SKIN CONFIGURATION | COCURED SKIN | | | PRECURED SKIN | | |
|--|-------------------------------|-----------------|--------------------------------|-------------------------------|-----------------|--------------------------------|
| | STRESS 10 ³ PSI | NO. OF TESTS | MODULUS 10 ⁶ PSI | STRESS 10 ³ PSI | NO. OF TESTS | MODULUS 10 ⁶ PSI |
| 8 PLIES 0°/±45°/90° 0.044 INCH THICK | 27.5 | 5 | 4.39 | 39.5 | 3 | 4.63 |
| 4 PLIES ±45° 0.022 INCH THICK | 23.6 | 3 | 2.14* | 32.7 | 3 | 2.39 |
| 4 PLIES 0°/90° 0.012 INCH THICK | 40.6 | 1 | 8.15 | 47.4 | 5 | 8.28 |

*2 TESTS

As a consequence, a small amount of laboratory work was conducted to determine whether a single ply of precured skin placed next to the honeycomb would prevent the dimpling. Figure 102 is a schematic of the panel construction. The first panel made had no adhesive layer between the precured skin and the cocured outer plies. Even though the precured skin was grit-blasted, there was delamination at this interface when the specimens were subjected to bending (see Figure 103). A second panel was fabricated by placing a layer of 0.05 lb/ft² FM96U adhesive between the precured ply and the two outer plies. The outer surfaces of the fully cured panel were smooth (no dimpling). Four specimens were cut and tested for flexural strength and flexural modulus. The results of these tests on the second panel are shown in Table 46. A specimen was measured and weighed, and a cocured facing was removed. Thickness at the honeycomb cell wall was 0.017 inch. Since the inner surface was dimpled, it was concluded that the extra adhesive had collected in the skin between cell walls. An "effective thickness" of the cocured 2-1/2-ply laminate with extra adhesive was calculated from sandwich weight and dimensions as that thickness required to give the same density as a precured laminate. It is for that thickness listed in Table 46 that strength and initial modulus were calculated.

The truss web structure was the design application in mind for this method of cocuring; however, comparisons with precured laminate are difficult on the basis of such limited testing. In addition, the truss web basic pattern was (45/-45)_T. Comparison of the above cocured (0₁/2/45/-45)_T laminate with a (0/45/-45)_T precured laminate on a specific basis is presented in Table 47.

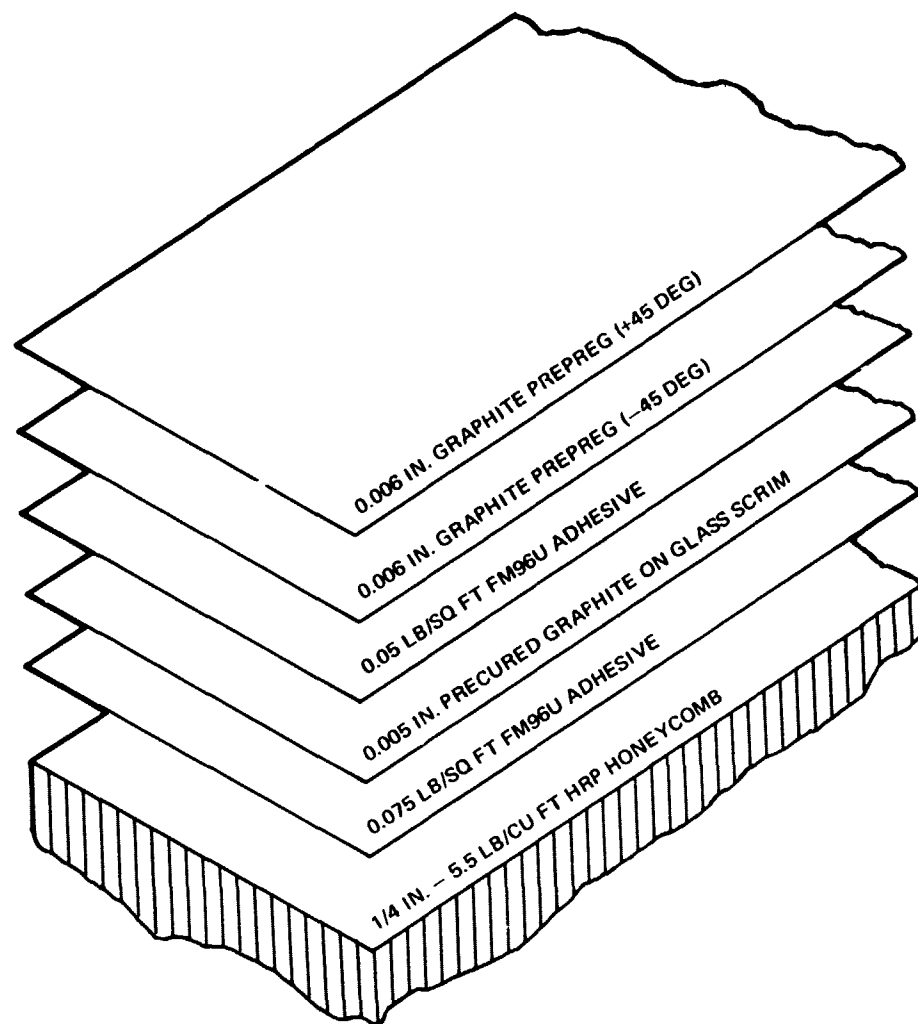


FIGURE 102. EXPLODED VIEW OF COCURE PANEL LAYUP



FIGURE 103. INTERFACE DELAMINATION - SANDWICH - PRECURED PLY WITHOUT ADHESIVE

TABLE 46
STRENGTH AND STIFFNESS OF COCURED SANDWICH FACE WITH PRECURED INTERLAYER

| SPECIMEN | t_{eff} (IN.) | F_{TU}^X (KSI) | INITIAL MODULUS ($\times 10^{-6}$ PSI) |
|----------|--------------------|---------------------|--|
| 1 | 0.0214 | 38.4 | 3.82 |
| 2 | 0.0214 | 36.0 | 3.80 |
| 3 | 0.0214 | 34.4 | 3.68 |
| 4 | 0.0214 | 32.0 | 3.65 |
| | AVERAGE | 35.2 | 3.73 |

NOTES: 1. SIMPLE BEAM LOADING, 12 INCH SPAN.
2. PATTERN [$1/2/45/-45$]_T
3. MATERIAL: NARMCO 5206
4. t_{eff} = SEE TEXT.

TABLE 47
COCURED NARMCO 5206 COMPARISONS

| | COCURED ^{1, 3} [$0_1/2/45/-45$] _T (PSI) | | PRECURED ² [$0/45/-45$] _T (PSI) | SPECIFIC COMPARISON |
|-------|---|---------|---|------------------------|
| F_x | 35,200 | F_x^T | 57,730 | 0.61 |
| | | F_x^C | 75,070 | — |
| E_x | 3.73×10^6 | E_x^T | 7.88×10^6 | — |
| | | E_x^C | 7.33×10^6 | 0.51 |

NOTES: 1. VALUES CALCULATED ON BASIS OF t_{eff} , SEE TEXT
2. VALUES FROM REFERENCE 3.
3. 0.003 INCH/0 DEG PLY NARMCO 5206 PRECURED ON NO. 104 GLASS SCRIM

Since significant dimpling and loss of strength occurred when graphite was cocured directly to honeycomb, it was deemed necessary to ascertain the extent of this problem with boron. Two panels were fabricated as follows, using a curing pressure of 50 psi:

1. Two plies at ± 45 degrees were cocured on each face of 1/4 in. -5 pound HRP honeycomb using a single FM96U adhesive ply at the core.
2. Two plies at ± 45 degrees and one precured ply at 0 degree were cocured on each face of 1/4 in. -5 pound HRP honeycomb using FM96U adhesive on each side of the precured plies.

The panel with precured layer was relatively smooth whereas the fully cocured panel showed minor dimpling. These panels were cut into specimens and tested for flexural strength and modulus. The loss in strength due to dimpling was less difficult to estimate since the precured interlayer

was a full ply thickness. The comparisons in Table 48 assume the cocured laminates have the same thickness as the corresponding precured laminates since they contain the same amount of reinforcement. For specific comparisons, one must add the weight of the extra adhesive (0.05 lb/ft²) to the three-ply laminate, and for the four-ply fully cocured laminate, one should include the prepreg resin that remains in the core if an external bleeder is not used.

These tests were exploratory in nature and were aimed at assessing the potential of cocuring as a fabrication technique. It is apparent that development of design allowables for the various cocuring techniques requires a more extensive test program. Findings to date indicate:

1. A precured interlayer is necessary to prevent dimpling.
2. A ply of adhesive is required at the interlayer to B-staged laminate interface.
3. For the +45-degree laminate, direct cocuring produces about the same stiffness loss for both boron and graphite, and a slightly greater strength loss for graphite than boron.
4. Strength and stiffness loss for cocured 0/45/-45 laminate with precured 0-degree ply is greater for graphite/epoxy than for boron/epoxy.

TABLE 48
COCURED AVCO 5505 SANDWICH FACING COMPARISONS

| PATTERN | COCURED | | PRECURED (PREDICTED) | | COCURED FACTOR AVCO 5505 | | COCURED REDUCTION FOR NARMCO 5206 (REF 1) | |
|---------------------------------------|--------------------------------------|--------------------|----------------------------------|----------------|-----------------------------|-----------------------|--|-----------------------|
| | E_{x_c} ($\times 10^{-6}$ PSI) | F_{x_c} (PSI) | E_x ($\times 10^{-6}$ PSI) | F_x (PSI) | $\frac{E_{x_c}}{E_x}$ | $\frac{F_{x_c}}{F_x}$ | $\frac{E_{x_c}}{E_x}$ | $\frac{F_{x_c}}{F_x}$ |
| (0 ¹ /45/-45) _T | 9.65 | 62,400 | 12.9 | 86,000 | 0.75 | 0.73 | — | — |
| (45/-45) _S | 2.89 | 30,900 | 3.6 | 35,000 | 0.80 | 0.88 | 0.72 | 0.90 |

NOTES: 1. 0-DEG LAYER PRECURED
2. VALUES FROM TEST OF SIMPLE SANDWICH BEAMS ON 12 IN. SPAN.

7.2 FABRICATION OF DESIGN VERIFICATION SPECIMENS

Eleven different design verification specimens were fabricated throughout the program. In every case detailed Fabrication and Control Travelers (FACT) were prepared prior to manufacture. Table 49 is a list of these specimens by drawing number and title. In addition, all raw materials were purchased and approved to appropriate Douglas Material Specifications.

TABLE 49
DESIGN VERIFICATION SPECIMENS

| DRAWING NO. | DASH NO. | NAME |
|-------------|----------|---|
| Z3578686 | -1 | JOINT TENSION - RONDED - COVERED ANGLES |
| | -501 | JOINT TENSION - BOLTED - GRAPHITE CAP |
| | -503 | JOINT TENSION - BOLTED - BORON CAP |
| | -505 | JOINT TENSION - STRAP |
| | -507 | JOINT TENSION - THICK ADHESIVE BOND |
| Z5578684 | -1 | BOLTED TRUSS |
| | -501 | BONDED TRUSS |
| Z5578687 | -1 | BOX BEAM - BOLTED COVER |
| | -503 | LARGE JOINT TENSION |
| | -505 | BOX BEAM - BONDED COVER |
| Z5569987 | -1 | BENT BOX |

All of the specimens were considered of adequate quality for the purpose. However, each had specific fabrication challenges and/or problems. The following discussion covers the highlights of these. Additional detail is presented for the Final Demonstration Component since its fabrication was not reported in program quarterlies.

7.2.1 Joint Tension Design Verification Specimens - Drawing Z3578686

1. Bolted Joint (-1), Figure 104

One problem that occurred during fabrication of the -3 web is worth discussion. The first attempt was made on a male tool and resulted in a poor external surface (bag side). Due to the simplicity of the part and its relatively short length, no intermediate densification was utilized. It was also decided that a female tool was necessary since the surface to be bonded to the cap had to be as flat as possible. The second attempt was made in the female mold and was densified every eight plies at 140°F under vacuum. The resultant part after final cure was deemed adequate. However, there was still evidence of unwanted graphite movement resulting in variable part thickness, particularly at the small radii. In addition, the typical phenomenon of "springback" was experienced when the webs were removed from the tool. The web angle decreased 1 to 2 degrees after removal from the tool for both the male and female molded articles. The explanation for this springback is not known but its occurrence is well documented in composite fabrication.

2. Bolted Joint - Graphite Cap (-501), Figure 105

The -9 graphite web was densified every eight plies then cocured and bonded with the previously cured -11 glass shoulder and -13 glass boltpad. The part was of excellent quality.



FIGURE 104. Z3578686-1 BONDED TENSION SPECIMEN ~ CLOSEUP OF BOND BEFORE TEST

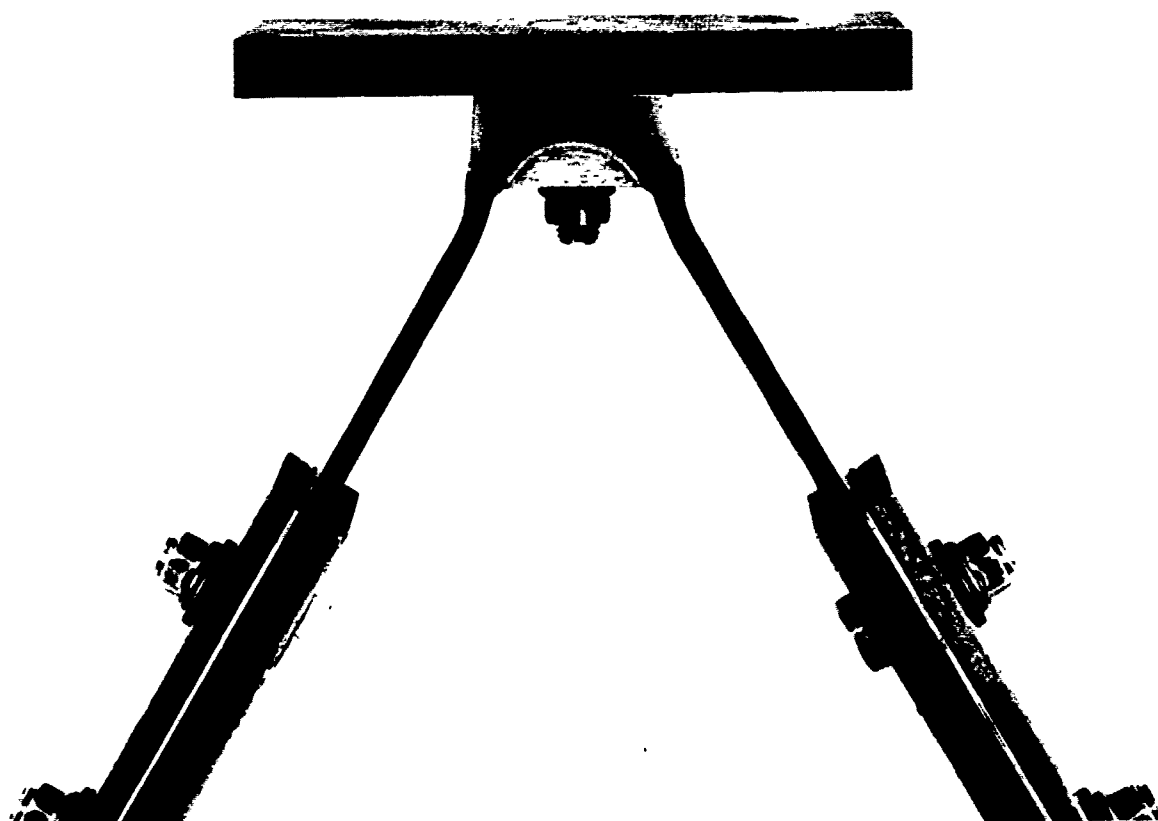


FIGURE 105. Z3568686-501 BOLTED JOINT TENSION SPECIMEN

3. Bolted Joint - Boron Cap (-503), Figure 105

The undamaged web and shoulder assembly from the tested -501 specimen was used with the -17 boron cap.

4. Strap (-505)

Some difficulty was experienced in producing a wrinkle-free composite loop (-17 web). This was resolved by applying a conforming thin plate over the layup around the smaller radius and extending up both sides to a point past the points of tangency of the larger radius. In this manner, any material accumulation or wrinkles occurred in an area of the web not critical to the test.

5. Thick Adhesive Bond (-507), Figure 106

No significant fabrication problems were experienced. It was necessary to degas the Hysol EA9306 adhesive to reduce the voids to an acceptable size and level. These comments also apply to the subsequent Z3578686-509 and -511 thick adhesive bond specimens.

7.2.2 Truss Action - Design Verification Specimens - Drawing Z5578684

1. Bolted (-1), Figure 107

The upper (graphite) and lower (boron) sandwich skins were made by precuring the skin pads, the outer facings, one ply of 0-degree graphite prepreg (on 104 glass scrim) and one ply of 0-degree boron prepreg. The skin pads, tapered honeycomb, and adhesive were located on the precured outer facings, followed by the single precured 0-degree ply. The inner facings were then layed up and the assemblies cured. The only problem was tapering the honeycomb. Attempts to fill the edge cells with Organoceram and then machining the taper were unsuccessful. It was found that the machining must be done first, followed by application of the Organoceram along the edges and curing under a tapered pressure plate.

The web section was made by cocuring both skins with the precured shoulders and honeycomb in place. The first 12 plies were densified at 150°F under 100-psi pressure before the honeycomb was positioned. No significant problems (other than honeycomb tapering mentioned above) were encountered. However, the cured web was only marginally satisfactory. There was some unwanted movement of graphite fibers that collected near the tips of the honeycomb and some indication of slight crushing of the honeycomb at the inner edges of the Organoceram filler. These defects can be seen in Figures 108 and 109.

The assembly of the skins to the web and the part of the test jig presented some alignment problems due to (1) springback of the web upon removal from the tool, (2) slight warpage of the sandwich skin panels, and (3) the roughness of the internal facing of the graphite upper skins. These were overcome by light sanding of appropriate surfaces (graphite internal skin and bolt shoulders) and by holding the components in place with slight pressure while bolting.

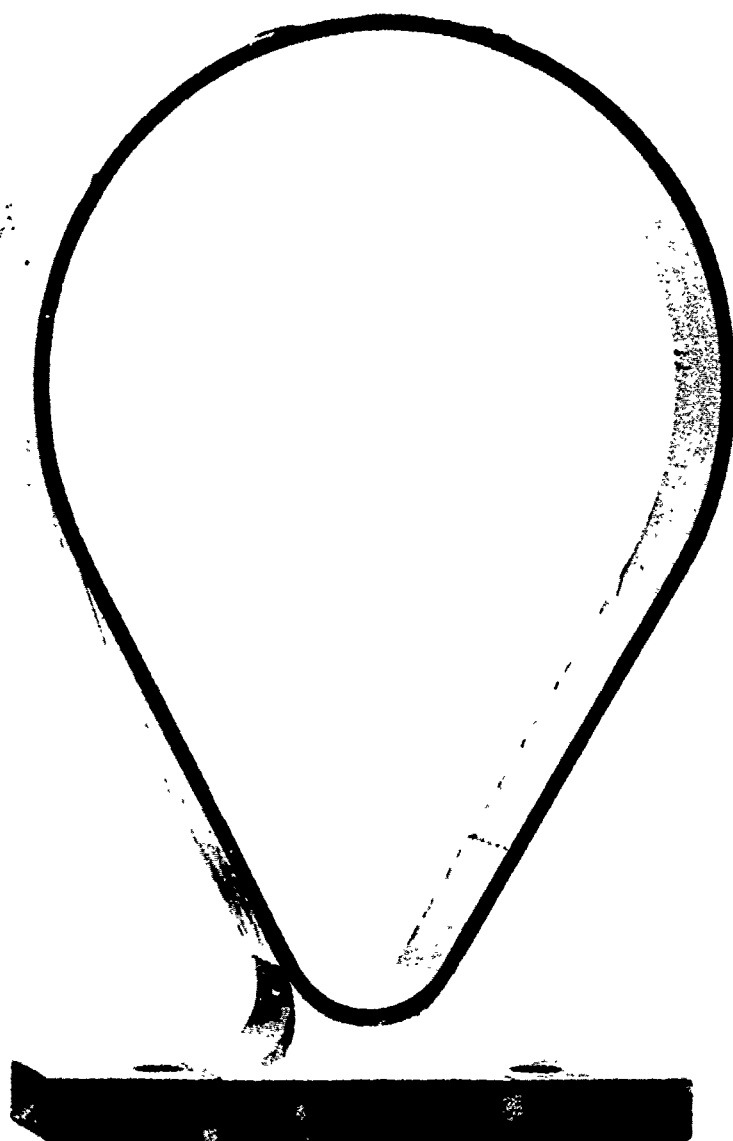


FIGURE 106. Z3578686-507 BONDED FILLET JOINT TENSION SPECIMEN

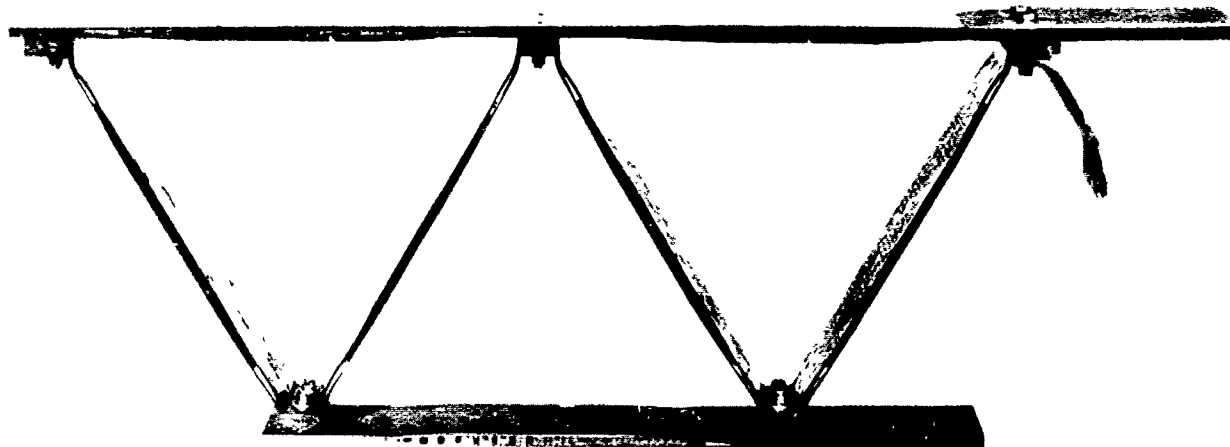


FIGURE 107. BOLTED TRUSS ACTION SPECIMEN OVERALL VIEW



FIGURE 108. BOLTED TRUSS ACTION SPECIMEN END JOINT CLOSEUP



FIGURE 109. BOLTED TRUSS ACTION SPECIMEN INTERNAL JOINT CLOSEUP

2. Bonded Joint (-501), Figure 110

The bonded truss action specimen web was fabricated in a similar manner to that for the -1 bolted specimen except that surface plates of 0.020 aluminum were formed and placed over the layup before bagging and curing. The web surfaces were greatly improved but some material bunched at the nodes due to failure of the plates to seat against the node surfaces. Consequently, there was very little pressure on some of the nodes during cure. Figures 111 through 113 are close-up views of selected nodes showing the effects of this lack of pressure. This condition was corrected in future laminations by simple redesign of the surface plates to allow them to conform to the part surface.

Some difficulty was also experienced in bonding the upper and lower skins to the web. Bridging of the bleeder fabric caused distortion of a portion of the attach angles and insufficient degassing of the filler fillets caused voids to form. Both of these problems should be easily remedied. Again, Figures 111 through 113 show these defects.

Even though the above problems were experienced, the part was considered acceptable.

7.2.3 Bending, Torsion, and Joint Tension Box Beam Verification Specimens - Drawing Z5578687

1. Box Beam - Bolted Cover (-1), Figure 114

The only fabrication problem encountered was a debonding of the -5 face skins from the -17 inserts when the -15 spacer was cocured to the skins.

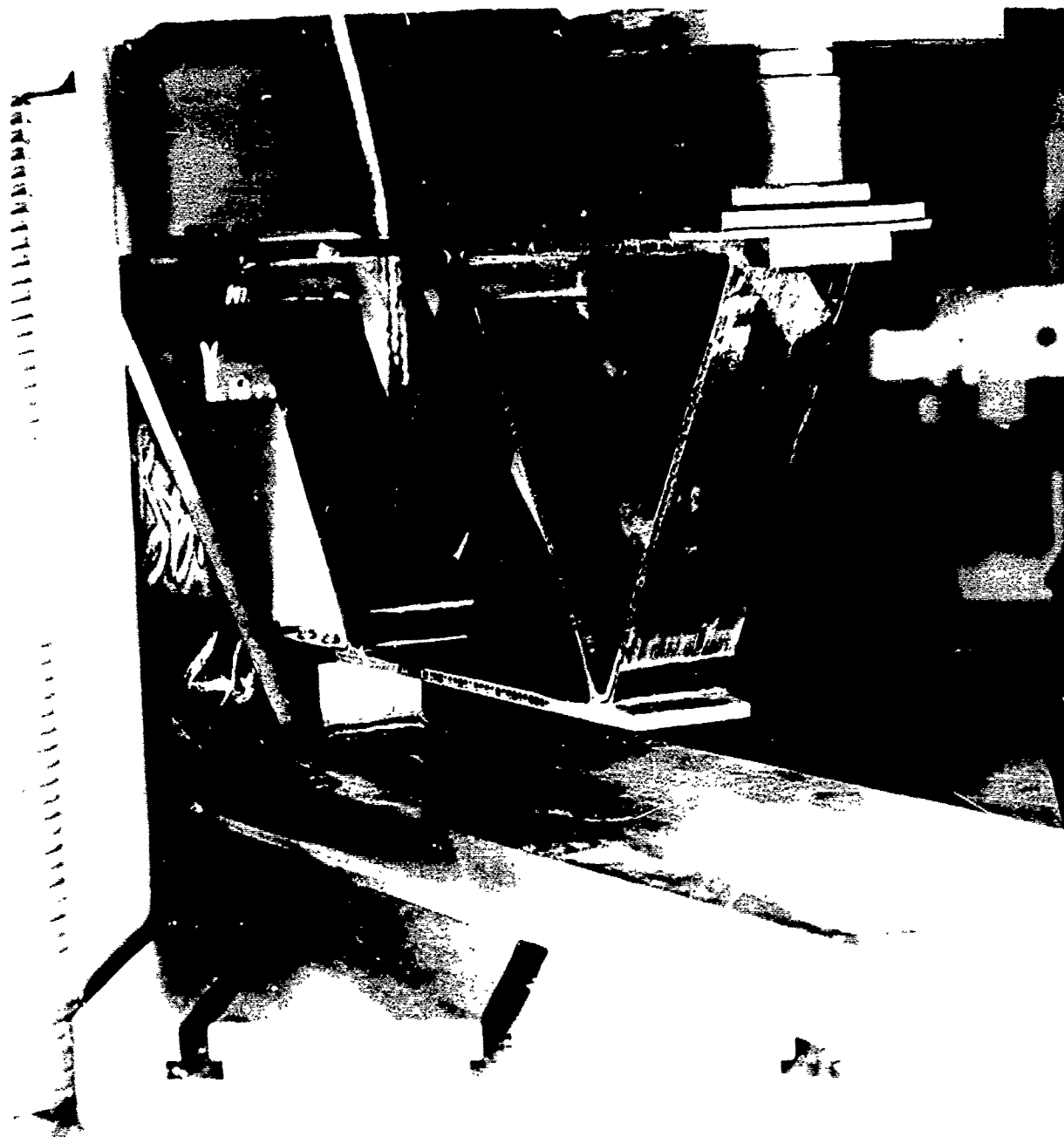


FIGURE 110. BONDED TRUSS ACTION SPECIMEN IN TEST FIXTURE



FIGURE 111. BONDED TRUSS SPECIMEN, UPPER JOINT AT STEEL DOUBLER

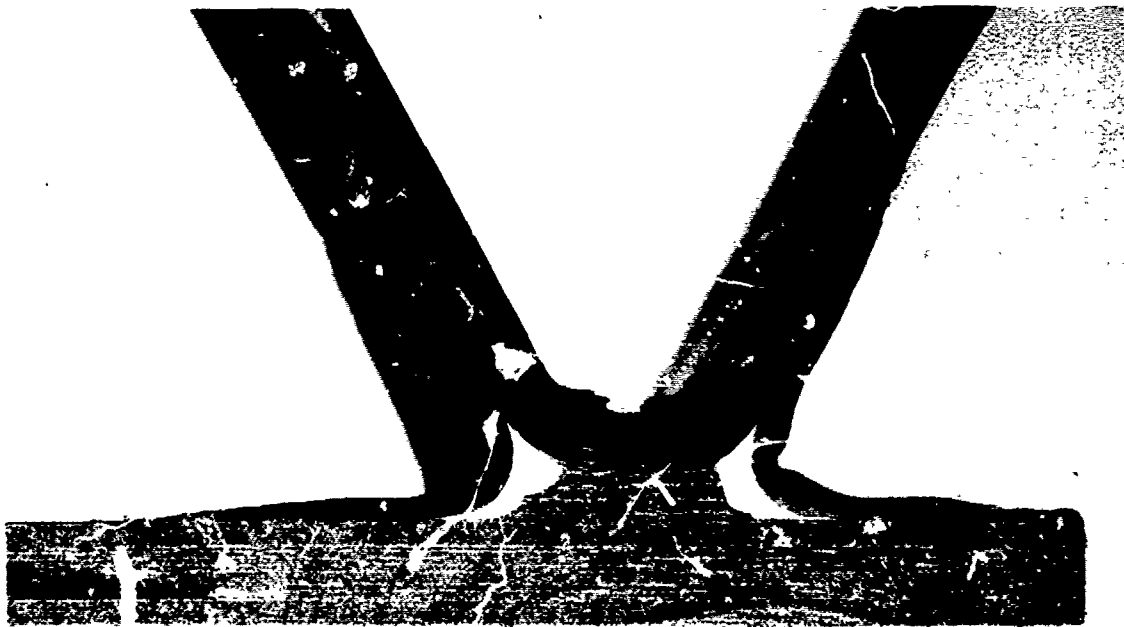


FIGURE 112. BONDED TRUSS SPECIMEN, GRAPHITE TO BORON END JOINT

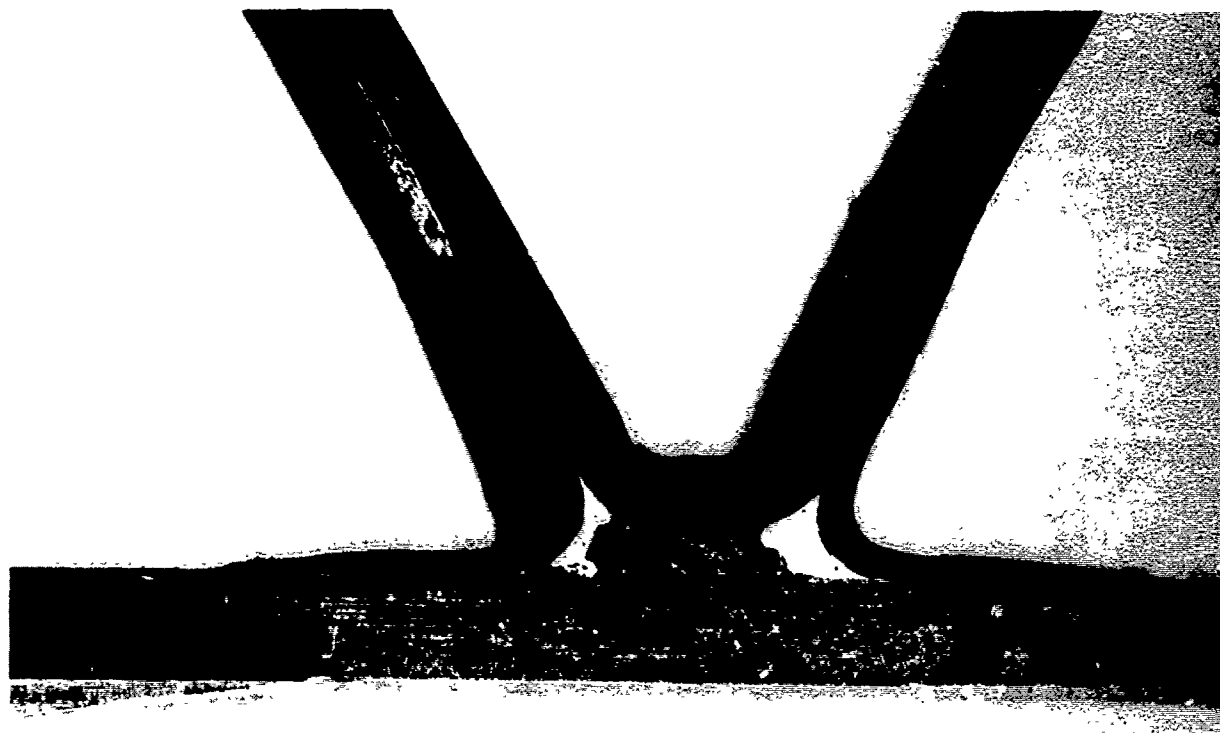


FIGURE 113. BONDED TRUSS SPECIMEN, GRAPHITE TO BORON LOWER INTERMEDIATE JOINT

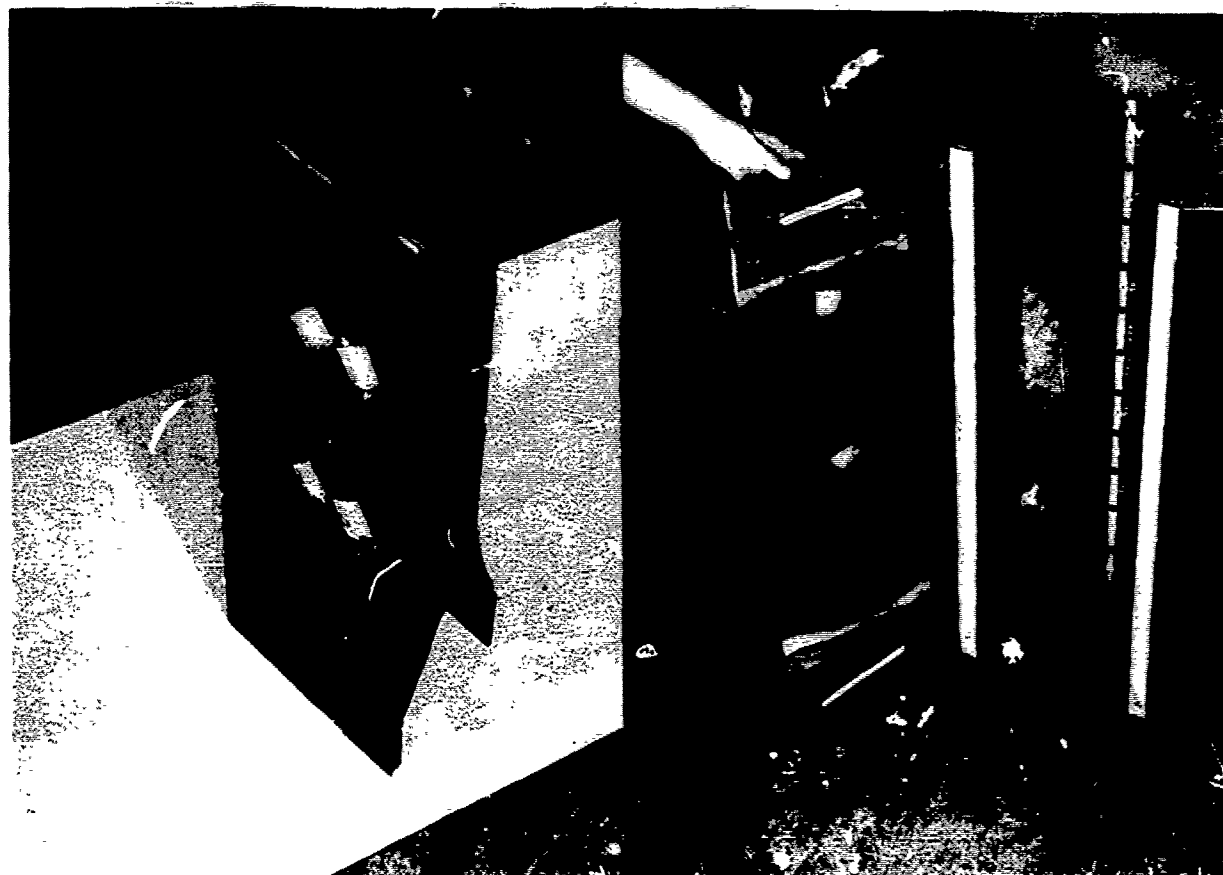


FIGURE 114. Z5578687-1 BOX BEAM SPECIMEN, BEFORE ATTACHMENT OF COVER PANEL

The apparent reason was release of volatiles from the -17 phenolic glass inserts which had been cured at 300°F but not postcured. It is recommended that, where glass inserts are used, epoxy resin be employed. Even a postcured phenolic laminate will absorb significant amounts of moisture during storage before use whereas an epoxy laminate will absorb much less (0.5 percent versus 0.1 percent).

2. Wing/Fuselage Interface Joint Tension Specimen (-503), Figures 115 and 116

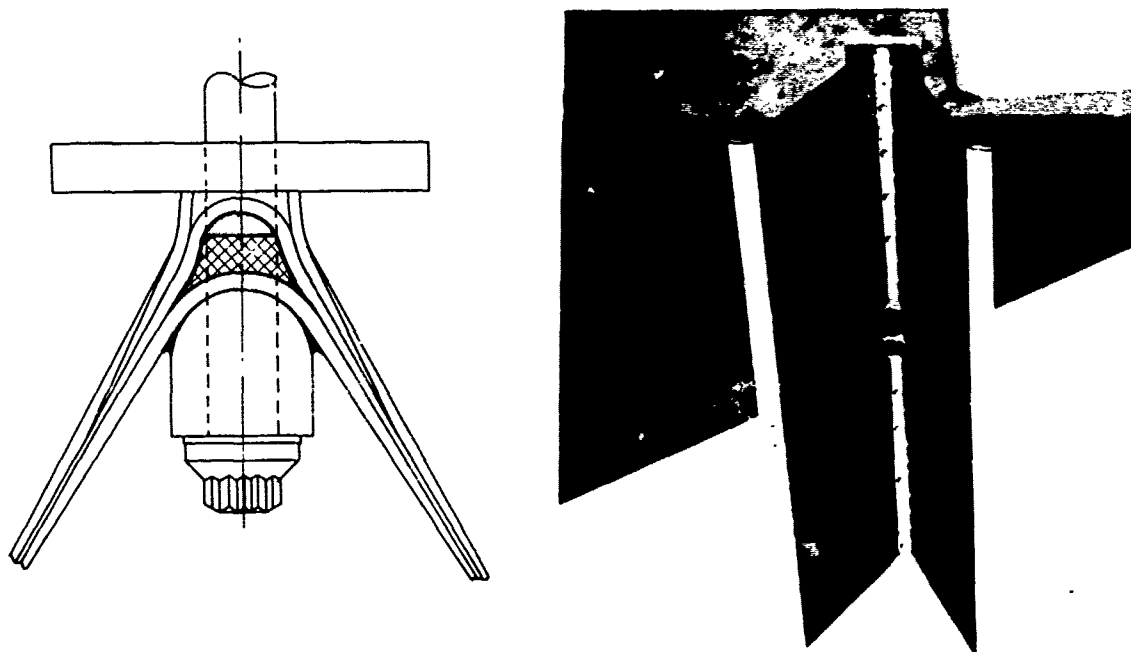


FIGURE 115. Z5578687-503 DESIGN VERIFICATION SPECIMEN

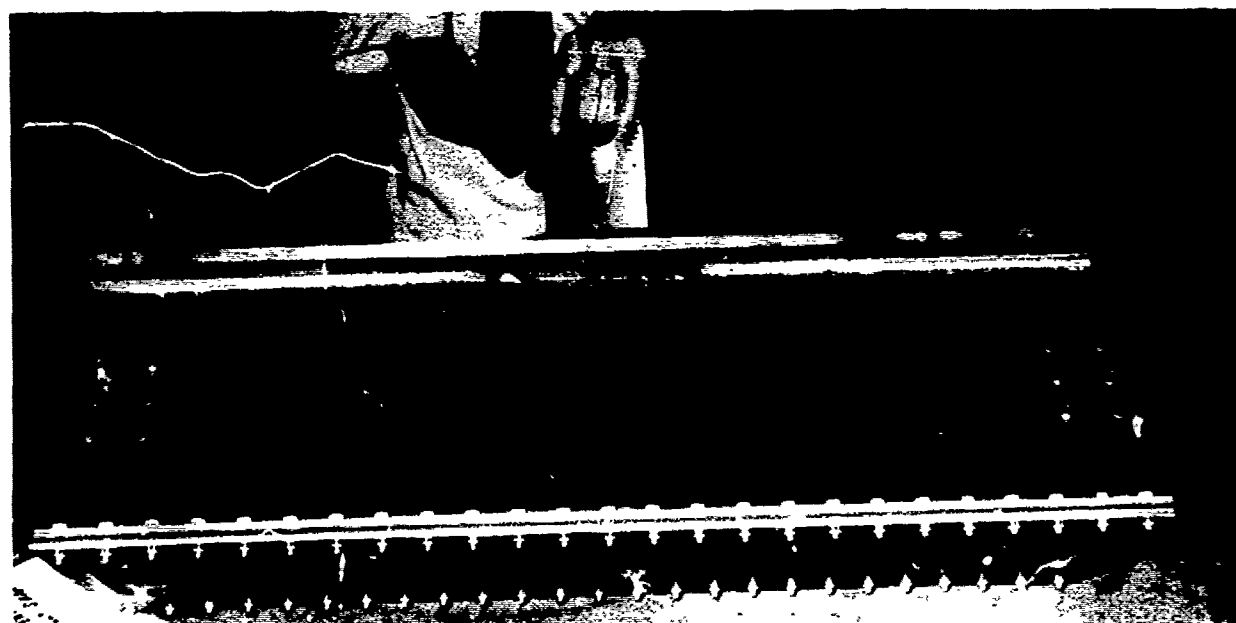


FIGURE 116. Z5578687-503 SPECIMEN BEFORE TEST

The web fabrication proceeded without incident even though the layup sequence was quite complex. The part was excellent in overall quality. However, the -67 saddle proved to be troublesome. Type II graphite fiber molding compounds are not available. Consequently, one had to be developed on short notice. The third attempt resulted in a molded part adequate for the purposes of the test but still far from a high quality molding. Should a molded piece of this nature be needed in the final item, further development will be necessary.

3. Box Beam - Bonded Cover (-505)

The fabrication of the Z5578687-505 box-beam specimen proceeded with only minor difficulties. However, it may prove instructive to list these difficulties as a matter of record.

- The honeycomb was oversize in the 90-degree direction and had to have a portion of the flat area removed. This then required longitudinal cutting and splicing to obtain correct length between tapered ends.
- The short plies in the area of the bolted joint were somewhat difficult to lay up accurately.
- The cured part was removed from the mold with difficulty, causing some delamination damage to the glass shoulder strip. The damage was repaired and considered not significant to the test.
- The cured web part had springback of approximately one degree from the female mold.
- The cured bonded joint had evidence of some small voids and a large one. The small ones were typical of thick section cures of Hysol 9306 made to date and were accepted. The large void was accessible and was repaired by drilling and filling with 9306 resin.

X-rays were taken of the bonded joints before and after repair and one is shown in Figure 117.

Figure 118 is a photograph of the Z5578687-505 specimen prior to preparation for bonding the cover and prior to part cleanup. This photograph shows the joint inner reinforcement and bar, added to the bolted joint (Figure 119). The main fabrication problem experienced in adding the reinforcement was unequal resin bleed in the radius along the length of the specimen. This caused a high spot in the center of the specimen which had to be sanded out, using care not to disturb fibers.

7.2.4 Final Demonstration Component - Drawing Z5569987

The fabrication of the bent box will be covered in somewhat greater detail than the previous specimens. The manufacturing sequence is conveniently divided into four categories: upper cover, lower cover, web, and final assembly.

1. Upper Cover - The upper cover was fabricated by cocuring both skins to the core. The layup did not prove difficult and the final part quality was excellent.

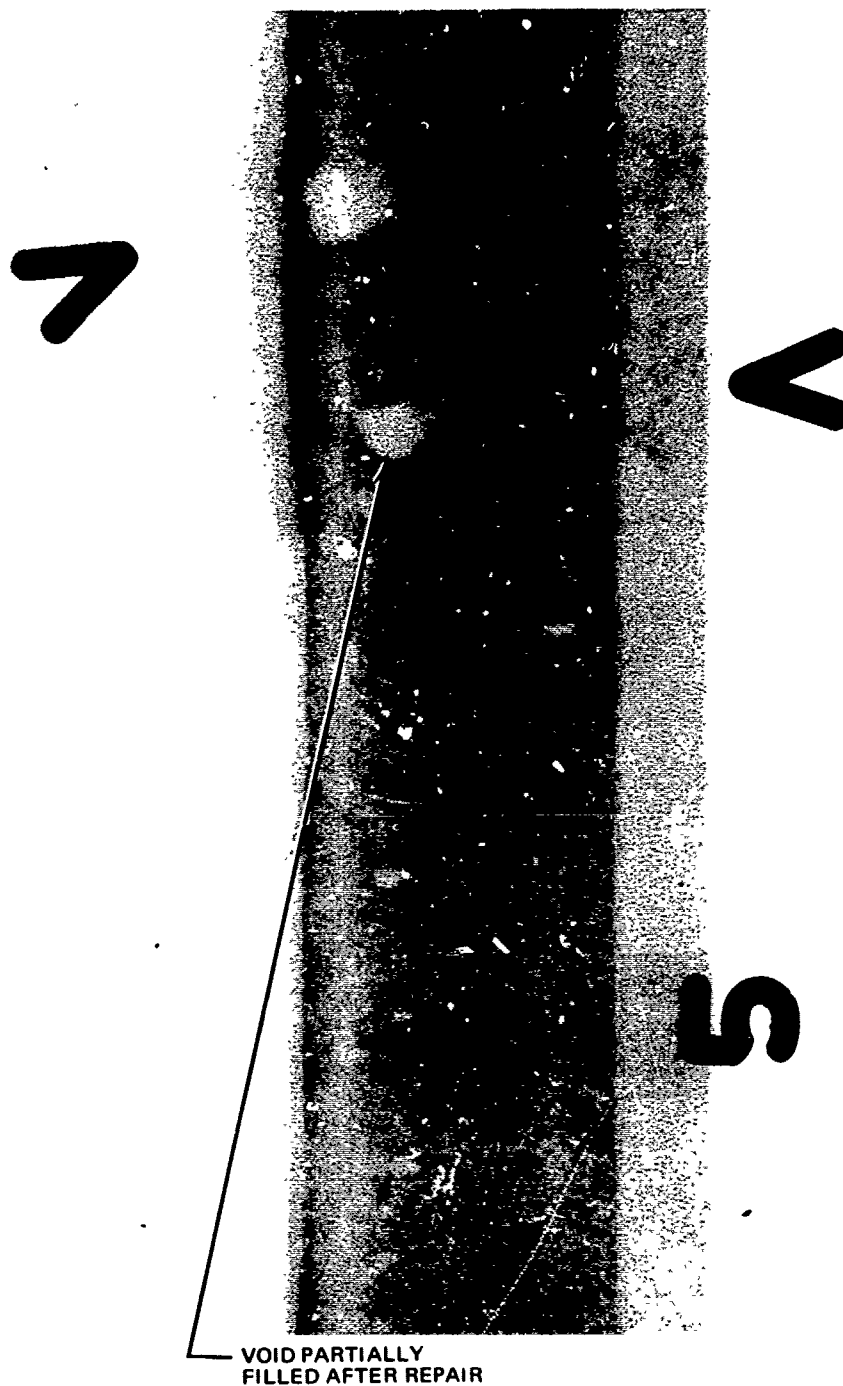


FIGURE 117. X-RAY INSPECTION OF 5578687-505 FILLET BOND



FIGURE 118. FIT CHECK OF STEEL BAR REINFORCEMENT - Z5578687-505

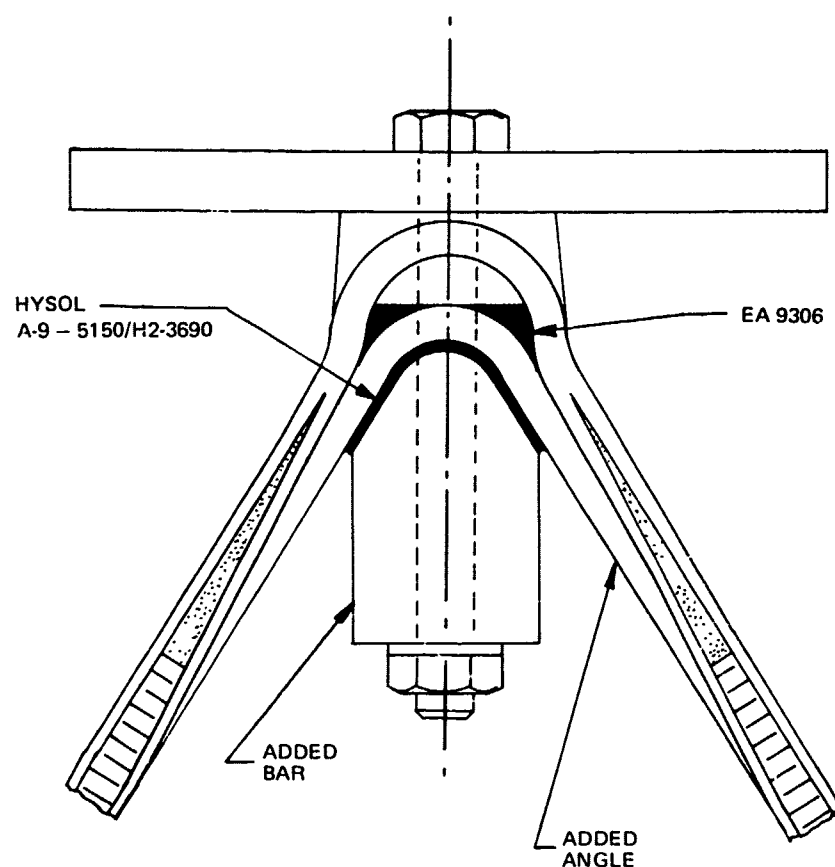


FIGURE 119. BOLTED JOINT REINFORCEMENT SPECIMEN Z5578687-505

2. Lower Cover - The lower cover also utilized cocuring. However, the graphite prepreg was predensified after layup for 1/2 hour at 150°F and 100 psi and then placed on the tapered honeycomb. The special stress relief layup around the holes proved somewhat time consuming but proceeded without other difficulties. The part after cure was excellent in composite quality and though slightly warped was well within an acceptable degree.
3. Web - As in previous truss webs the bolt pads, shoulders, saddle and inserts were precured. The saddle (-53) was machined from a 160-ply solid laminate rather than attempting to develop a molding compound. The resultant part was excellent. The layup of the web itself proved very time consuming around the lightening holes. The center web honeycomb was very fragile and, as a result, difficult to hold in place without damage. The layup around the lightening hole inserts was tedious, but more importantly, would be even more difficult on a full wing section because of accessibility. In addition, sealing the edges of the honeycomb (not done for the test part) would be troublesome. The layup was densified for 1/2 hour at 175°F and 100 psi before insertion of honeycomb and for 1/2 hour at 150°F and 50 psi when honeycomb was present. Thin gage surface plates were placed on the web surfaces, and the part was bagged and cured. The quality of the cured web was considered good. Springback was present and there was some material bunching near the nodes, particularly at the strap. However, the bunching was significantly less than in the previous truss specimens.

4. Final Assembly - The final assembly consisted of attaching the covers. The upper cover was bolted and comments appear later in this report. The lower cover was bonded with EA9306 adhesive. This bond was attempted with only simple tooling jigs and presented problems. Simultaneous maintenance of a specified glue line thickness and fillet radius proved to be beyond the capabilities of the tooling. The buildup section around the large hole (to have been bonded with FM123) did not bond since tool movement left a gap. The fillet bond radii had large amounts of excess resin behind the points of tangency with the parts. The gap was rebonded by vacuum impregnating with heat Hysol A9-51501/HZ-3690. The excess fillet resin was removed in critical areas by hand filling and sanding. The bond quality after repair was considered adequate for the purpose of the specimen after X-ray of the repaired fillet bond revealed a remaining void which was not repairable. (See 7.3, Nondestructive Inspection.)

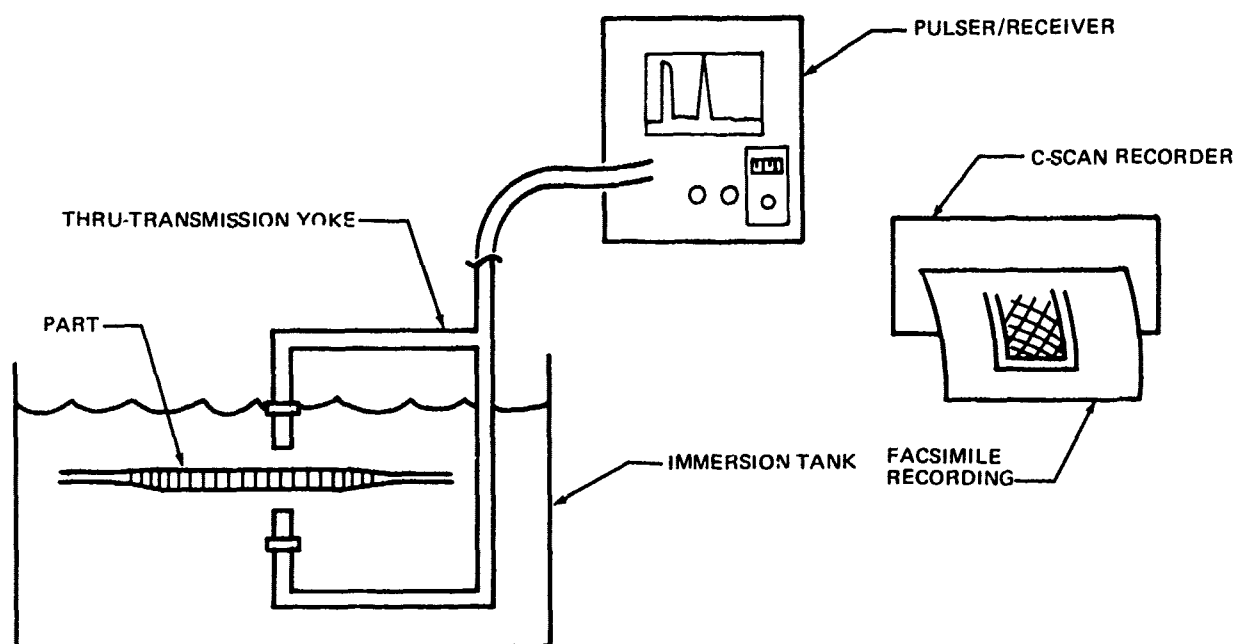
7.3 NONDESTRUCTIVE TESTING - FINAL DEMONSTRATION COMPONENT

The 5569987-101 upper panel (boron composite) was submitted for ultrasonic inspection on 9-5-72. The 5569987-103 lower panel (graphite composite) was submitted for inspection on 9-6-72. Both panels were inspected with the immersed through-transmission technique using 2.25 MHz focused search units as shown in Figure 120. The ultrasonic C-scan facsimile recordings for both panels are shown in Figure 121. The dark areas indicate good ultrasonic transmission through the specimens. It is obvious from the results that the graphite composite is more homogenous than the boron composite. The peripheral areas show good transmission through the laminates themselves indicating a lack of delaminations or voids. The poor transmission through the honeycomb areas is difficult to assess without destructive analysis. However, it is felt that the poor transmission is caused by micro-porosity in the cocured laminate between the core cell walls.

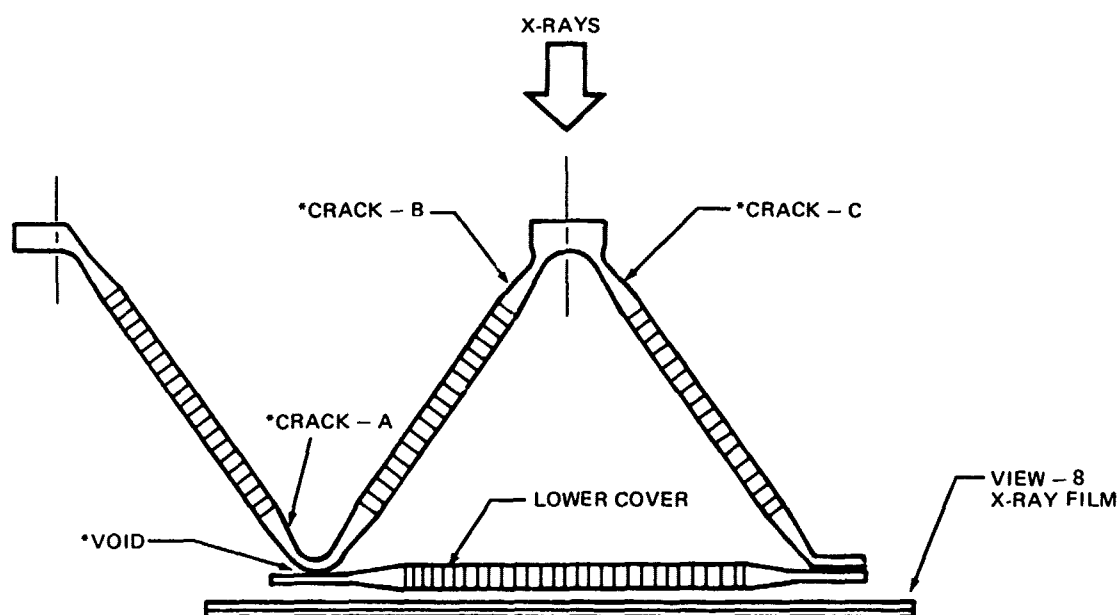
The -103 lower graphite panel was bonded to the -105 graphite Z-web and submitted for radiographic inspection on 11-6-72 along with the upper boron panel. Figure 120 shows the source and film location for View-8. The discontinuities revealed in View-8 are shown in Figure 122 with location within the part being indicated in Figure 120. The void in the bond line between the lower panel and Z-web was repaired prior to static test. Crack A was parallel to the unidirectional fibers and cracks B and C were apparently shrinkage cracks within the core potting material. They were not considered detrimental to the strength of the assembly.

7.4 TOOLING AND DRILLING - FINAL DEMONSTRATION COMPONENT

Figure 123 shows the aluminum layup mold for fabrication of the graphite-epoxy sandwich lower cover for specimen Z5569987. A similar tool was made for the boron-epoxy upper cover. The tool was made from 1-inch-thick wrought aluminum plate with layers and indentations milled in its surface to generate the cover contours. The problem associated with this type of tooling was to hold the flatness tolerances required. When a cut was made on one



ULTRASONIC TEST



*NOTE. SEE FIGURE 122

RADIOGRAPHY

FIGURE 120. NONDESTRUCTIVE TESTING METHOD FOR FINAL DEMONSTRATION COMPONENT

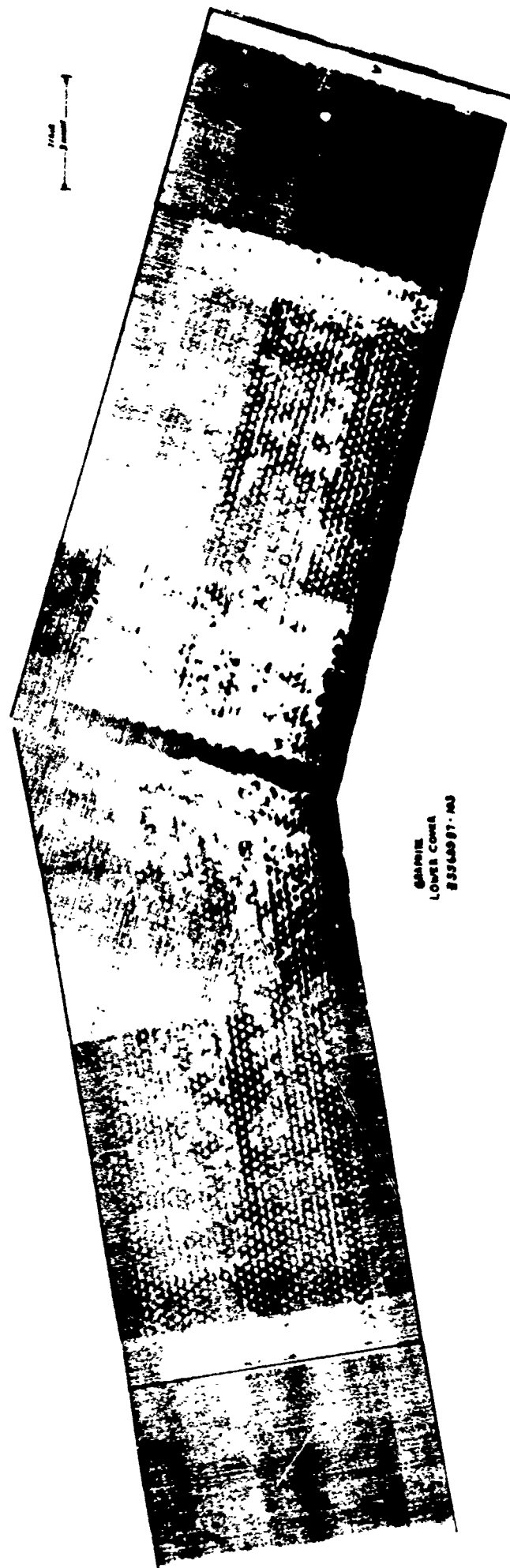
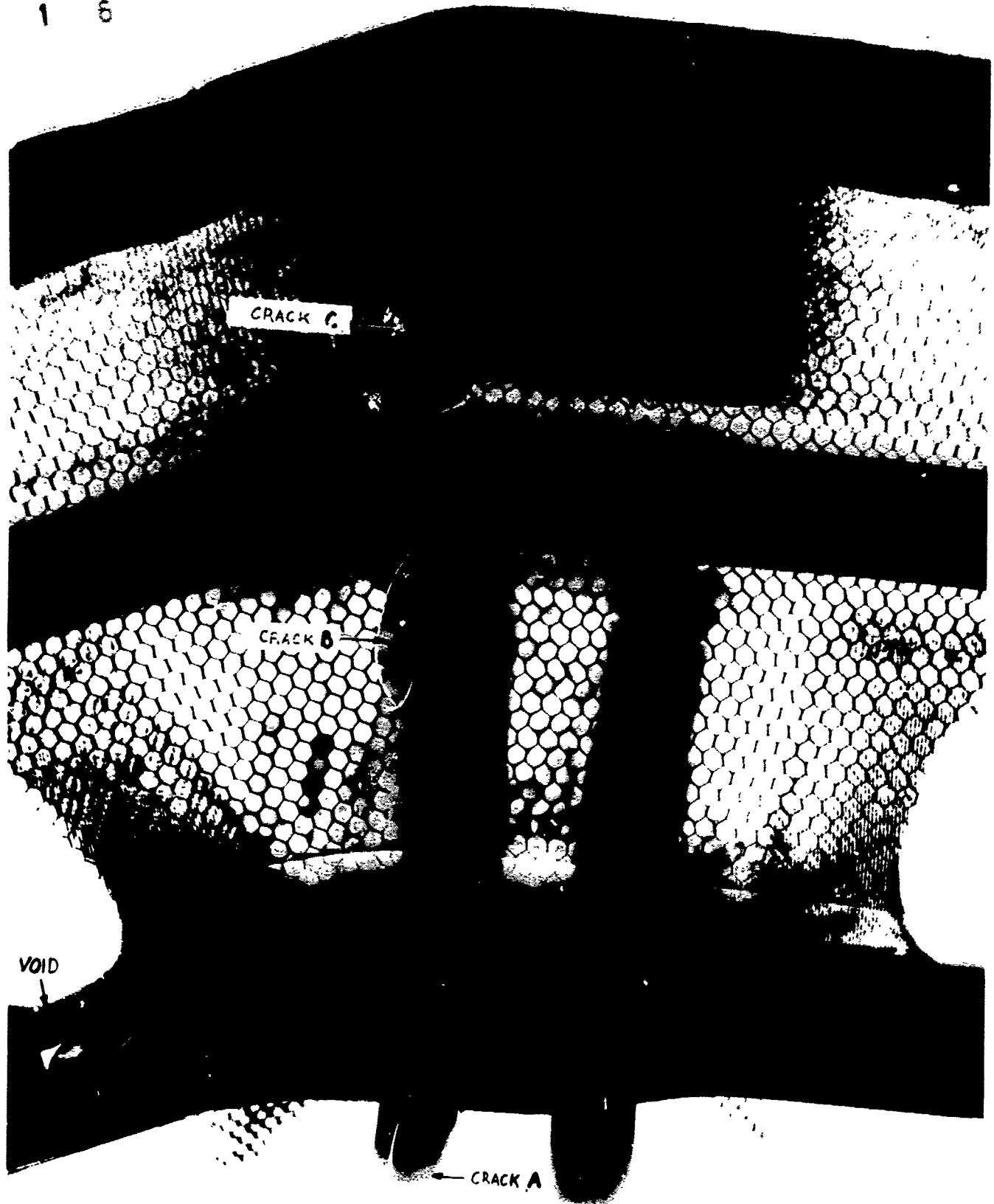


FIGURE 121. ULTRASONIC C-SCAN RECORDINGS OF UPPER AND LOWER PANELS

8

RAF

1 6



Z5569987

FIGURE 122. POSITIVE RADIOGRAPHIC REPRODUCTION OF VIEW-8 SHOWING DISCONTINUITIES

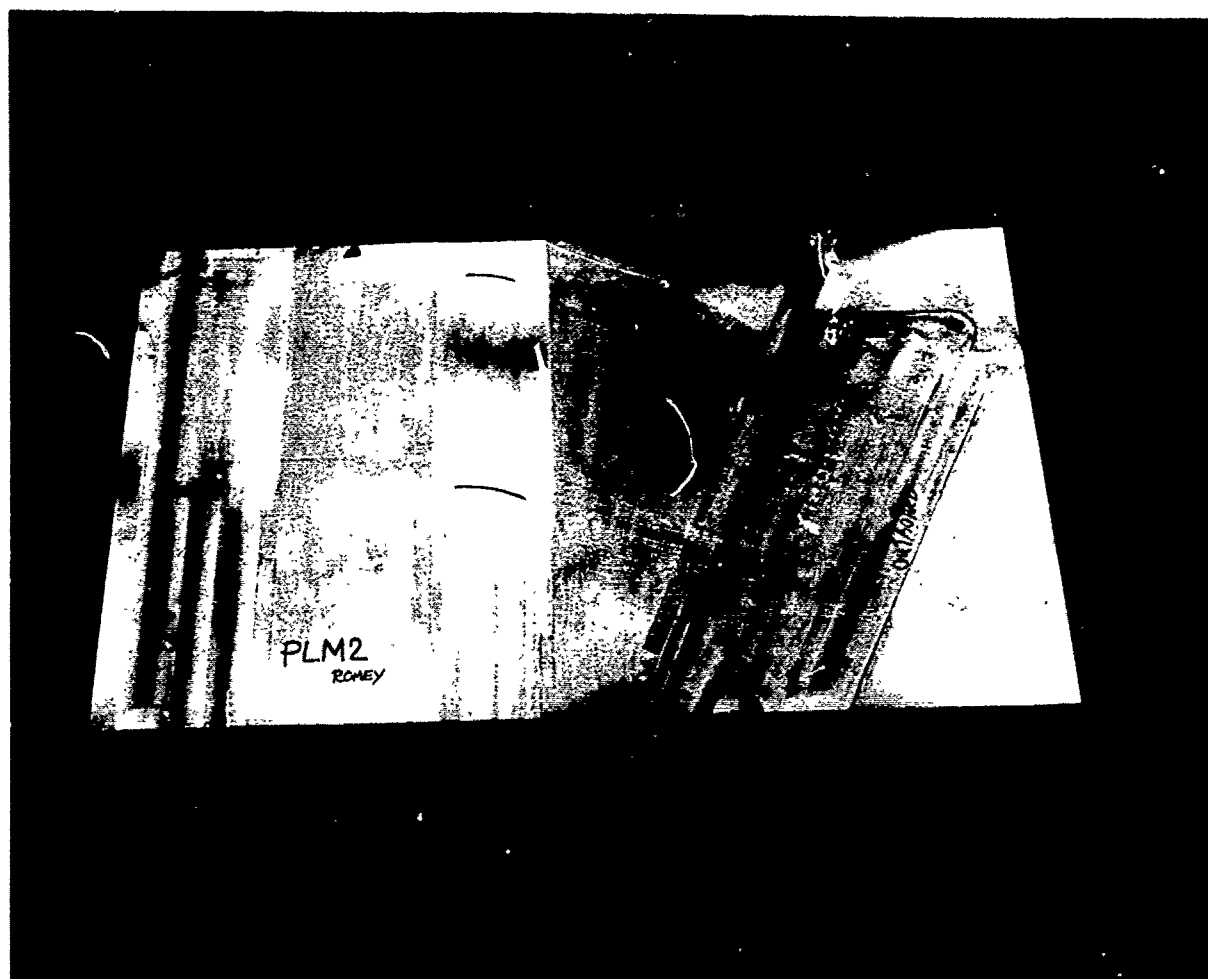


FIGURE 123. LAYUP MOLD FOR Z5569987 - 103 LOWER SKIN ASSY

side of the tool it would bow because of the internal stress in the tool. Stress relief heat treatment and a skin cut on both sides of the plate were required to hold the flatness tolerance.

The layup mold for the truss web was the most complex of any tooling required for the program. Precision drawing layouts were made by MLO (Master Lay Out) of various cross sections within the web structure. These drawings were transferred to template stock by a photographic process. Templates were then made to aid in the construction of the MPP (Master Plaster Pattern).

Figure 124 shows the truss web MPP which was particularly difficult to make because of the numerous tapers and double tapers which can be seen in the figure as shaded areas. Figure 125 shows the recesses necessary for the graphite-epoxy strap reinforcement layup for the lower surface bolted joint. Notice tapers on each side of the strap area.

A plastic faced plaster tool (Thixfiber) was layed up from the MPP. This tool was needed to layup and cure the final layup mold for the test specimen. The plastic-faced plaster provides heat resistance and vacuum integrity which cannot be achieved with plaster alone.

Techniques developed in a 1972 IRAD program, Improved Methods and Techniques of Plastics, were used to make a high quality fiberglass-epoxy layup mold, Figure 126. The construction of the tool consisted of a thin (0.030-inch



FIGURE 124. TRUSS WEB MASTER PLASTER FORM — SWEEP BREAK SPECIMEN



FIGURE 125. DETAIL OF LARGE BOLT RESTRAINING STRAP LAYUP AREA - MASTER PLASTER

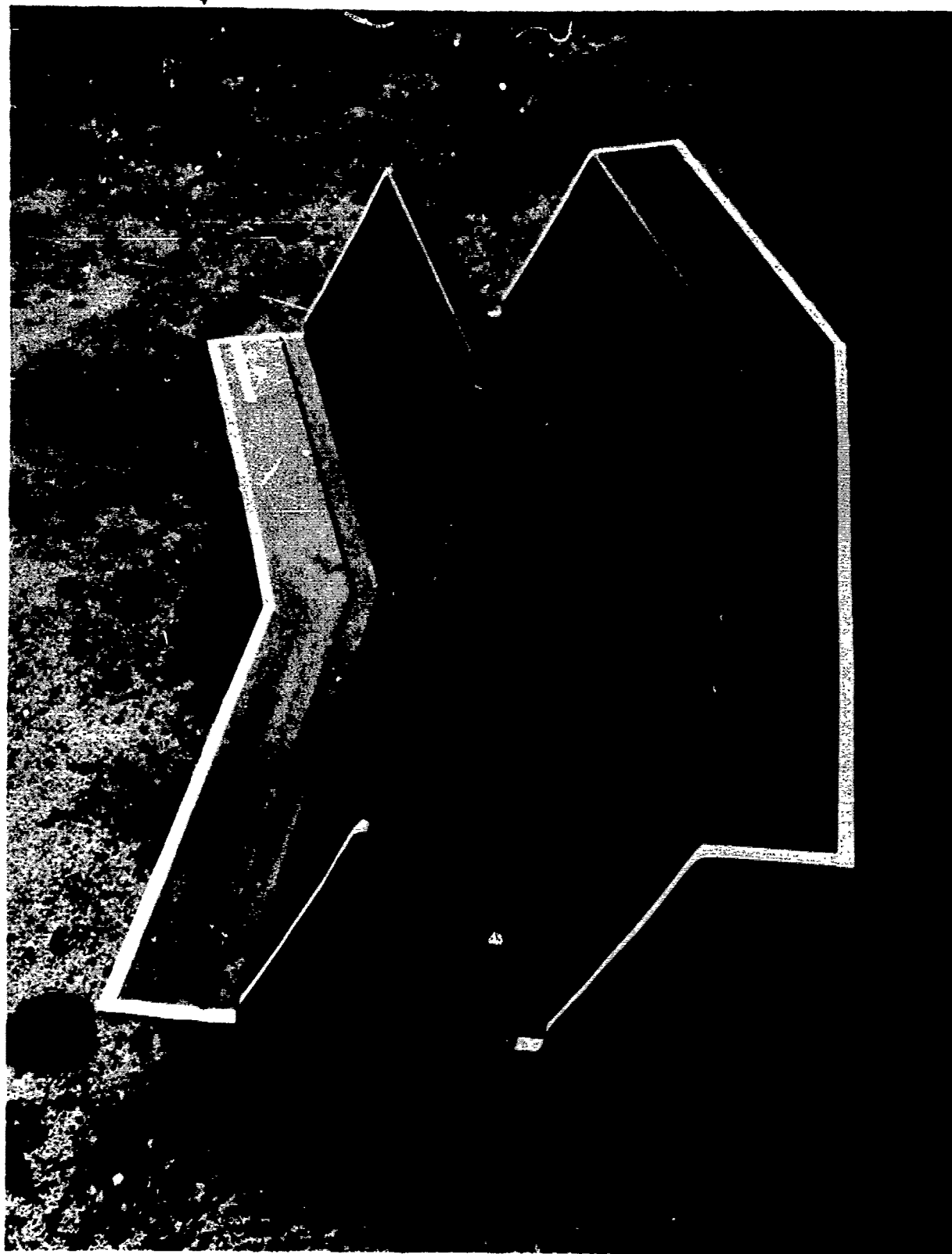


FIGURE 126. FINISHED LAMINATING TOOL – SWEEP BREAK SPECIMEN TRUSS WEB

max) gel coat over a 1/4-inch-thick shell. The structure was backed up with 1/4-inch-thick high-temperature epoxy stiffening board.

During the layup and cure of the graphite web, the epoxy-fiberglass layup tool performed according to expectation. Very little warpage and no vacuum leakage was attributed to the layup tool.

The materials used in this specimen included boron/epoxy, graphite/epoxy and S-glass laminates. Steel doublers were incorporated on each end of the cover sections for load application. The resulting composite sections consisted of steel, boron, and fiberglass. Engineering tolerances were specified at ± 0.002 -inch diameter for holes to be drilled through these material mixes.

The hard, abrasive characteristics of boron fibers required the use of diamond drills to provide a clean hole-surface finish.

The first holes to be drilled were located in the boron cover, approximately 0.312 inch thick. A 0.250-inch diamond core drill from Permattach Company, Milford, N. H., was used at 1800 rpm in a jig boring machine with externally flooded coolant in the form of water soluble oil. Manual feed was necessary to provide "pecking" of the drill and permit fluid to flush away debris. Considerable skill was required by the machinist to control the feed rate into the work. A dial indicator on the machine was used to judge feed rate - approximately 0.25 inch per minute. The fluid chuck was not used because of excessive runout. Attempts at correcting the problem were unsuccessful.

Each hole was backed up on the bottom breakout side by a 0.25-in-thick piece of micarta. This backup prevented delamination of the boron fibers on the lower surface. A "wiggler" was used to precisely locate the core drill holes on the panel.

A drilling progressed, it was observed that the hole diameters were decreasing, indicating that the core drill was beginning to wear slightly. After drilling 20 holes with one core drill, the minimum hole diameter was 0.248 inch. The wear of the drill was approximately 0.002 inch on the diameter.

The holes were slightly tapered, with the bottom diameter 0.002 inch less than the upper hole diameter in the 0.312-inch-thick boron section. By using a second core drill as a reamer coming through from the bottom side, the final hole profile was of uniform diameter.

The most difficult portion of the drilling occurred in penetrating through the steel doubler section which also contained boron and fiberglass. Diamond core drills were found to be ineffective in drilling into steel, even though these particular core drills were coated with diamond plus tungsten carbide particles. The tungsten carbide addition was intended for use in penetrating the steel. To effectively drill the holes, conventional HSS drills were used to pass through the steel and upper boron layers. The dull drill was changed and the next penetration progressed through fiberglass and the lower boron layer. A third drill was used to complete the hole through the bottom steel doubler. Although many drill changes were necessary, this procedure was most efficient both time-wise and in drill costs. Penetration rates through the 1.0-inch-thick section were approximately 5 minutes per hole, including drill changes. The two boron layers did not suffer any reduction in surface integrity because they were sandwiched on both sides, thus preventing delamination or breakout.

The specimen lower cover consisted of a graphite/epoxy, fiberglass/epoxy and steel doubler section. Conventional HSS drills with coolant were used to drill this area. The steel doublers on both sides of the composite section provided a material backup and prevented degradation of the holes.

During the transfer drilling of holes from the boron cover into the fiberglass flanges of the structure, an aluminum backup sheet was used to minimize breakout of fiberglass. This method was not very effective, possibly because of an uneven lower surface which prevented good intimate contact between the aluminum and the fiberglass so some breakout occurred on the fiberglass.

7.5 JOINT DESIGN ALLOWABLES TESTS

7.5.1 Bolt-Bearing Test Program

Bolted joints in composite laminates can fail in essentially three modes under in-plane loading: bearing, shearout, and tension-through-the-hole. Of these, the first achieves the greatest strengths and the other two can be eliminated by careful design of the joint geometry. This conceptual wing design is predicated on ensuring that only bearing failures occur at ultimate load in order to prevent large fractures from originating at any bolt hole. The test program reflects this philosophy. The ultimate bearing stresses are determined for a variety of laminate patterns encompassing those to be used on the skins, and shearout tests have been conducted to establish allowable bolt pitches and minimum edge distances.

An economical multipurpose test specimen has been designed to provide the necessary data. It is the two-ended specimen depicted in Drawing Z3578685. The laminate fiber orientations tested are recorded in Table 50 and reflect the greater magnitude of spanwise loads in comparison with the chordwise loads. Sufficient suitable data for the chordwise load stress concentrations were available from an earlier program by interpolation with respect to the percentage of 0-degree filaments. Tests on both all-boron and mixed-graphite (0-degree, 90-degree Narmco 5206, ± 45 -degree Thronel 75S/1004) are included.

TABLE 50
BOLTED JOINT TEST LAMINATES

| | | | | | | | | | | |
|-------------------------|----|----|----|------|------|------|----|----|----|-----|
| PERCENT (0 DEG) | 25 | 50 | 75 | 25 | 50 | 75 | 25 | 50 | 75 | 0 |
| PERCENT (± 45 DEG) | 75 | 50 | 25 | 62.5 | 37.5 | 12.5 | 50 | 25 | 0 | 100 |
| PERCENT (90 DEG) | 0 | 0 | 0 | 12.5 | 12.5 | 12.5 | 25 | 25 | 25 | 0 |

In addition to this basic laminate data, a small number of tests are included to provide a basis for assessing the merits of including "softened" (± 45 -degree) strips in the vicinity of the bolt seams. The ± 45 -degree pattern is tested as above, for Narmco 5206, Thronel 75S, and a 50-percent mixture of these graphites.

It was suggested that countersunk fastener data not be generated under this program because of the results of such testing conducted during an earlier program. It was established therein that for the practical proportions of head size, bolt diameter, and laminate thickness tested, shear load was transferred through the shank and the 100-degree countersunk head was essentially ineffective. The successful completion of this design rests on low bearing stresses to minimize the stress concentrations in the skins, so there will be no situations in which the countersunk head approaches the total thickness of the skin.

7.5.2 Boron Epoxy Bolt-Bearing Test Results

Table 51 presents bearing and shearout results for 32-ply boron epoxy panels. A special effort was made in the design of the specimen to ensure pure bearing failure modes not influenced by the tension-through-the-hole or shearout failures. This attempt was substantially successful but the (0/45/0/-45) and (0₃/45/0₃/-45) patterns proved so weak in shearout that a pure bearing failure may be inherently unobtainable, no matter how great the edge distance.

The shearout tests were conducted at an edge distance of two bolt diameters. One salient result is that, for a given percentage of 0-degree plies, 90-degree plies are far more effective in improving the resistance to shearout loads than are +45-degree plies. Likewise, the greater the proportion of 0-degree plies, the lower is the shearout stress. A further important finding is that, for the minimum practical edge distance of $e = 2d$, there is a preferential tension-through-the-hole failure mode for laminates with 90-degree (lateral) plies. The failure surface for the (45/-45) laminates in tension is along the +45-degree filament directions rather than the 0-degree or 90-degree orientations.

Some interesting observations have become apparent for the (0/45/0/-45) and (0/45/-45/0) patterns. The first of these is illustrated in Figure 127. The shearout stress

$$\sigma_s = P/2t(e - \frac{d}{2})$$

is obviously a monotonically decreasing function of the edge distance ratio e/d . The shearout stress is not constant as had been believed hitherto. In view of this potential complication in the comparison of test data, the opportunity has been taken to standardize on the presentation of the data in accord with the "Structural Design Guide for Advanced Composite Applications."

Figure 127 contains the results from the current tests as well as those from previous Douglas tests (Reference 13), and a single test result from General Dynamics (Convair) (Reference 14). Only the last result did not indicate failure along two parallel shear planes extending from the bolt right to the edge. The Convair result was a combination of a bearing failure with limited shearout. On one other panel in this (Douglas) program, a pronounced compression shake was developed. This leads on to the hypothesis of a constant effective shearout distance. Were this so, the shearout load, as distinct from stress, would be independent of total edge distance and the "average"

TABLE 51
DOUBLE-LAP BOLTED JOINT STRENGTH SUMMARY
(0.25-INCH BOLT DIAMETER AVCO 5505 BORON-EPOXY)

| CONFIGURATION Z3578885 | LAMINATE THICKNESS (IN.) | LAMINATE WIDTH (IN.) | SHEAROUT TESTS | | | | BEARING TESTS | | | | |
|--|--------------------------------|----------------------------|---------------------------|--------------------------|----------------------|---|---------------------------|--------------------------|-----------------|---|--------|
| | | | EDGE DISTANCE (IN.) | ULTIMATE LOAD (LB) | FAILURE MODE | STRESSES AT FAILURE (PSI) BEARING SHEAROUT TENSION | EDGE DISTANCE (IN.) | ULTIMATE LOAD (LB) | FAILURE MODE | STRESSES AT FAILURE (PSI) BEARING SHEAROUT TENSION | |
| 5 (25% 0 DEG, 75% +45 DEG) | 0.160 | 2.508 | 0.483 | 3,290 | CLEAVAGE | 82,300 | 28,719 | 9,110 | BEARING | 197,500 | 21,870 |
| | 0.160 | 2.508 | 0.490 | 3,040 | CLEAVAGE, TENSION | 76,000 | 26,027 | 8,410 | TENSION | 221,300 | 24,560 |
| | 0.161 | 2.499 | 0.500 | 3,260 | SHEAROUT, TENSION | 81,500 | 27,167 | 9,060 | TENSION | 213,800 | 23,770 |
| | 0.160 | 2.496 | 0.498 | 3,100 | TENSION, SHEAROUT | 77,500 | 25,972 | 8,626 | BEARING | 217,500 | 24,210 |
| -7 (50% 0 DEG, 50% +45 DEG) | 0.162 | 2.511 | 0.498 | 2,750 | SHEAROUT | 68,800 | 23,040 | | SHEAROUT | 179,400 | 12,457 |
| | 0.164 | 2.503 | 0.496 | 2,125 | SHEAROUT | 53,100 | 17,899 | | SHEAROUT | 175,500 | 12,140 |
| | 0.162 | 2.503 | 0.504 | 2,425 | SHEAROUT | 60,600 | 19,995 | | SHEAROUT | 157,500 | 10,254 |
| | 0.162 | 2.511 | 0.501 | 2,590 | SHEAROUT | 64,800 | 21,526 | | GRIP FAILURE | | |
| 9 (75% 0 DEG, 25% +45 DEG) | 0.161 | 1.996 | 0.517 | 2,075 | SHEAROUT | 50,600 | 14,000 | | SHEAROUT | 61,800 | 3,327 |
| | 0.162 | 1.993 | 0.590 | 2,190 | SHEAROUT | 54,800 | 14,718 | | SHEAROUT | 83,500 | 4,691 |
| | 0.162 | 1.999 | 0.578 | 2,175 | SHEAROUT | 54,400 | 15,004 | | SHEAROUT | 98,800 | 5,548 |
| | 0.162 | 1.994 | 0.589 | 2,185 | SHEAROUT | 54,600 | 14,716 | | SHEAROUT | 108,800 | 6,082 |
| -11 (25% 0 DEG, 12-1/2% 90 DEG, 62-1/2% +45 DEG) | 0.165 | 2.501 | 0.504 | 4,120 | TENSION, CLEAVAGE | 103,000 | 33,971 | 11,440 | TENSION* | 138,200 | 15,360 |
| | 0.164 | 2.503 | 0.500 | 3,940 | TENSION, CLEAVAGE | 98,500 | 32,833 | 10,330 | TENSION* | 143,500 | 15,470 |
| | 0.165 | 2.498 | 0.496 | 3,875 | TENSION, CLEAVAGE | 96,900 | 32,640 | 10,770 | BEARING | 212,300 | |
| | 0.164 | 2.492 | 0.497 | 4,175 | TENSION, CLEAVAGE | 104,400 | 35,072 | 11,640 | BEARING† | 212,500 | |
| -13 (50% 0 DEG, 12-1/2% 90 DEG, 37-1/2% +45 DEG) | 0.163 | 2.506 | 0.498 | 2,730 | SHEAROUT | 68,300 | 22,872 | | BEARING† | 188,800 | |
| | 0.162 | 2.509 | 0.497 | 2,980 | SHEAROUT | 74,500 | 25,034 | | SHEAROUT | 211,000 | |
| | 0.162 | 2.506 | 0.500 | 2,525 | SHEAROUT | 63,100 | 25,042 | | SHEAROUT | 218,800 | |
| | 0.164 | 2.509 | 0.500 | 2,870 | SHEAROUT | 71,800 | 23,917 | | BEARING | 180,000 | |

NOTES: STRESSES COMPUTED ON BASIS OF NOMINAL 0.005 IN PLATE,
SHEAROUT STRESSES DERIVED BY FORMULA $\sigma = P/2t$ (P = 0.50 d)
* FAILURE INFLUENCED BY OUT OF PLANE BENDING FROM MISALIGNMENT BOLT
† PHONOUNDED COMPRESSION SHAKE'S VISIBLE
‡ NO VISIBLE DAMAGE WHATSOEVER, MAXIMUM LOAD RECORDED ON LOAD DEFLECTION TRACE
** CLEARLY DEFINED PARALLEL SPLIT PLUG SHEARED OUT ALL THE WAY TO THE EDGE

TABLE 51 (CONTINUED)
DOUBLE-LAP BOLTED JOINT STRENGTH SUMMARY
(0.25-INCH BOLT DIAMETER AVCO 5505 BORON-EPOXY)

| CONFIGURATION | LAMINATE THICKNESS (IN.) | LAMINATE WIDTH (IN.) | SHEAROUT TESTS | | | | BEARING TESTS | | | |
|--|--------------------------|----------------------|---------------------|--------------------|--------------------|---------------------------|---------------------|--------------------|--------------|---------------------------|
| | | | EDGE DISTANCE (IN.) | ULTIMATE LOAD (LB) | FAILURE MODE | STRESSES AT FAILURE (PSI) | EDGE DISTANCE (IN.) | ULTIMATE LOAD (LB) | FAILURE MODE | STRESSES AT FAILURE (PSI) |
| -15 (75% 0 DEG, 12-1/2% 90 DEG, 12 1/2% +45 DEG) NO. 1 - 1A, 2A NO. 1 - 1B, 2B NO. 2 - 1A, 2A NO. 2 - 1B, 2B | 0.160 | 2.006 | 0.503 | 2,230 | SHEAROUT | 55,800 | | | | |
| | 0.157 | 2.003 | 0.506 | 1,880 | SHEAROUT | 47,000 | 18,436 | 5,675 | BEARING | 141,900 |
| | 0.159 | 2.003 | 0.487 | 1,935 | SHEAROUT | 48,400 | 15,420 | 5,750 | BEARING | 143,800 |
| | 0.162 | 2.004 | 0.505 | 1,780 | SHEAROUT | 44,500 | 14,638 | 3,300 | BEARING | 82,500 |
| | | | | | | | | 5,375 | BEARING | 134,400 |
| 17 (25% 0 DEG, 25% 90 DEG, 50% +45 DEG) NO. 1 - 1A, 2A NO. 1 - 1B, 2B NO. 2 - 1A, 2A NO. 2 - 1B, 2B | 0.167 | 2.507 | 0.495 | 3,600 | TENSION, CLEAVAGE | 90,000 | 30,405 | 4,300 | BEARING | 107,500 |
| | 0.168 | 2.499 | 0.486 | 3,510 | TENSION, CLEAVAGE | 87,800 | 29,565 | 4,475 | BEARING | 111,900 |
| | 0.167 | 2.501 | 0.487 | 3,840 | TENSION, CLEAVAGE | 96,000 | 33,149 | 5,190 | BEARING | 129,800 |
| | 0.166 | 2.505 | 0.501 | 3,775 | TENSION, CLEAVAGE | 94,400 | 31,375 | 5,400 | BEARING | 135,000 |
| | | | | | | | | | | |
| -19 (50% 0 DEG, 25% 90 DEG, 25% +45 DEG) NO. 1 - 1A, 2A NO. 1 - 1B, 2B NO. 2 - 1A, 2A NO. 2 - 1B, 2B | 0.169 | 2.505 | 0.505 | 3,100 | SHEAROUT, TENSION | 77,500 | 25,493 | 5,750 | BEARING | 143,800 |
| | 0.169 | 2.507 | 0.504 | 3,410 | SHEAROUT, TENSION | 85,300 | 28,117 | 6,150 | BEARING | 153,800 |
| | 0.172 | 2.503 | 0.507 | 3,065 | SHEAROUT, TENSION | 76,600 | 25,074 | 5,700 | BEARING | 142,500 |
| | 0.170 | 2.503 | 0.507 | 3,165 | SHEAROUT, TENSION | 79,100 | 25,892 | 6,240 | BEARING | 156,000 |
| | | | | | | | | | | |
| -21 (75% 0 DEG, 25% 90 DEG) NO. 1 - 1A, 2A NO. 1 - 1B, 2B NO. 2 - 1A, 1B NO. 2 - 2A, 2B | 0.167 | 2.010 | 0.510 | 2,065 | SHEAROUT | 51,600 | 16,761 | 5,400 | BEARING | 135,000 |
| | 0.167 | 2.014 | 0.502 | 2,050 | SHEAROUT | 51,300 | 16,993 | 5,400 | BEARING | 140,500 |
| | 0.171 | 2.003 | 0.503 | 2,130 | SHEAROUT | 53,500 | 17,609 | 5,890 | BEARING | 147,300 |
| | 0.167 | 2.009 | 0.504 | 1,970 | SHEAROUT | 49,300 | 16,243 | 5,790 | BEARING | 144,800 |
| | | | | | | | | | | |
| -23 (100% +45 DEG) NO. 1 - 1A, 2A NO. 1 - 1B, 2B NO. 2 - 1A, 2A NO. 2 - 1B, 2B | 0.159 | 3.003 | 0.507 | 3,040 | TENSION AT +45 DEG | 76,000 | 24,869 | 4,570 | BEARING | 114,300 |
| | 0.159 | 3.006 | 0.511 | 2,940 | TENSION AT +45 DEG | 73,500 | 23,802 | 4,590 | BEARING | 114,800 |
| | 0.159 | 3.003 | 0.513 | 3,075 | TENSION AT +45 DEG | 76,900 | 24,786 | 4,400 | BEARING | 110,000 |
| | 0.159 | 3.002 | 0.514 | 3,050 | TENSION AT +45 DEG | 76,300 | 24,502 | 4,740 | BEARING | 118,500 |
| | | | | | | | | | | |

NOTES: STRESSES COMPUTED ON BASIS OF NOMINAL 0.005 IN PLIES.
SHEAROUT STRESSES DERIVED BY FORMULA $\sigma = P/2t$ (P = 0.50 IN)

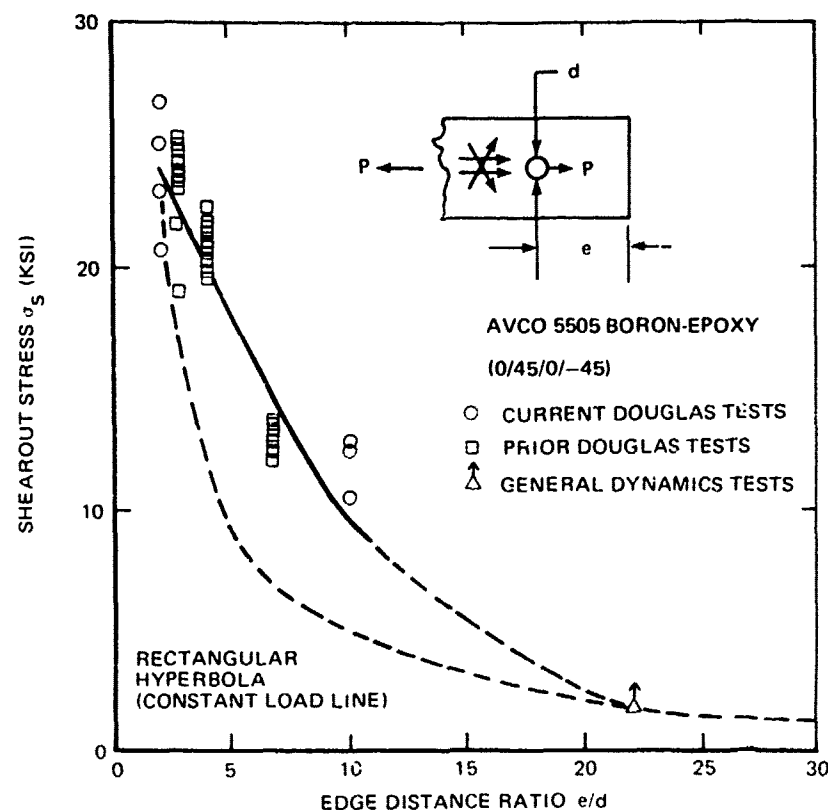


FIGURE 127. SHEAROUT STRESS AS FUNCTION OF EDGE DISTANCE

shearout stress would be inversely proportional to the edge distance. Figure 127 demonstrates that this is not so. The rectangular hyperbola drawn through the test results for $e/d = 2$ would have to follow the test results for all e/d were the hypothesis valid. On the contrary, the test data indicate that the load capacity increases with edge distance for the Douglas tests. It seems that the Convair test is conservative because of the influence of the bearing damage. In the Convair test the unloaded end of the specimen was heavily reinforced, effectively suppressing the possibility of establishing shearout cracks running to the free edge. Consequently, the shearout behavior for extremely large edge distance has not yet been established.

These shearout data above have an important impact on the design of softening strips around bolt seams in boron-epoxy laminates. The pattern proposed for the inboard skin planks is close to the (0/45/0/-45) pattern. In one of these tests on this pattern with $e/d = 10$, a shearout crack was observed to run down the 0-degree direction displaced from the hole edge by a tension crack about 1/8 inch long. This same behavior was observed also in some of the shearout tests with $e/d = 2$. This suggests the possibility of running a spanwise crack between the boundary of such a laminate and any (45/-45) softening strips, particularly since the proposed e/d is less than 10.

These tests suggest that continuous chordwise (90-degree) filaments at about 12-1/2 percent of the laminate would effectively suppress this undesirable failure mode. It would offer the further advantage of a direct load path for the chordwise skin loads.

Figures 128 and 129 depict results for the boron panels in terms of stress contours for bearing and shearout failures.

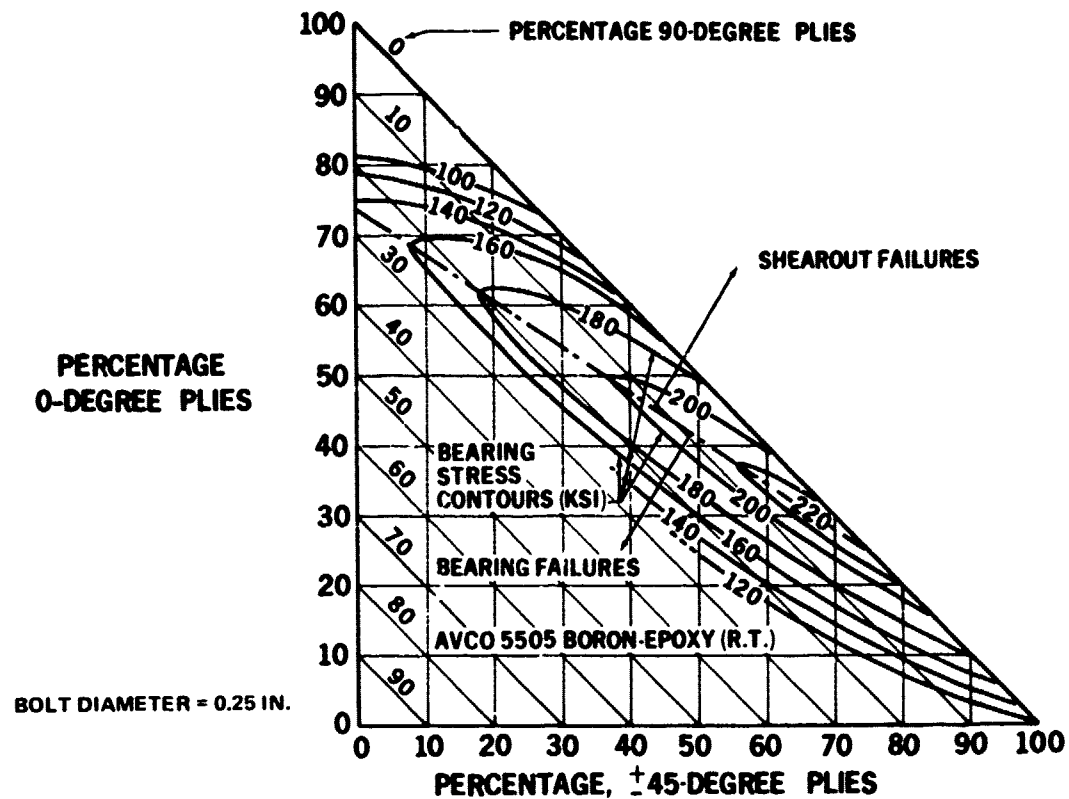


FIGURE 128. BEARING STRESS CONTOURS FOR VARIOUS LAMINATE PATTERNS, AVCO 5505 BORON EPOXY

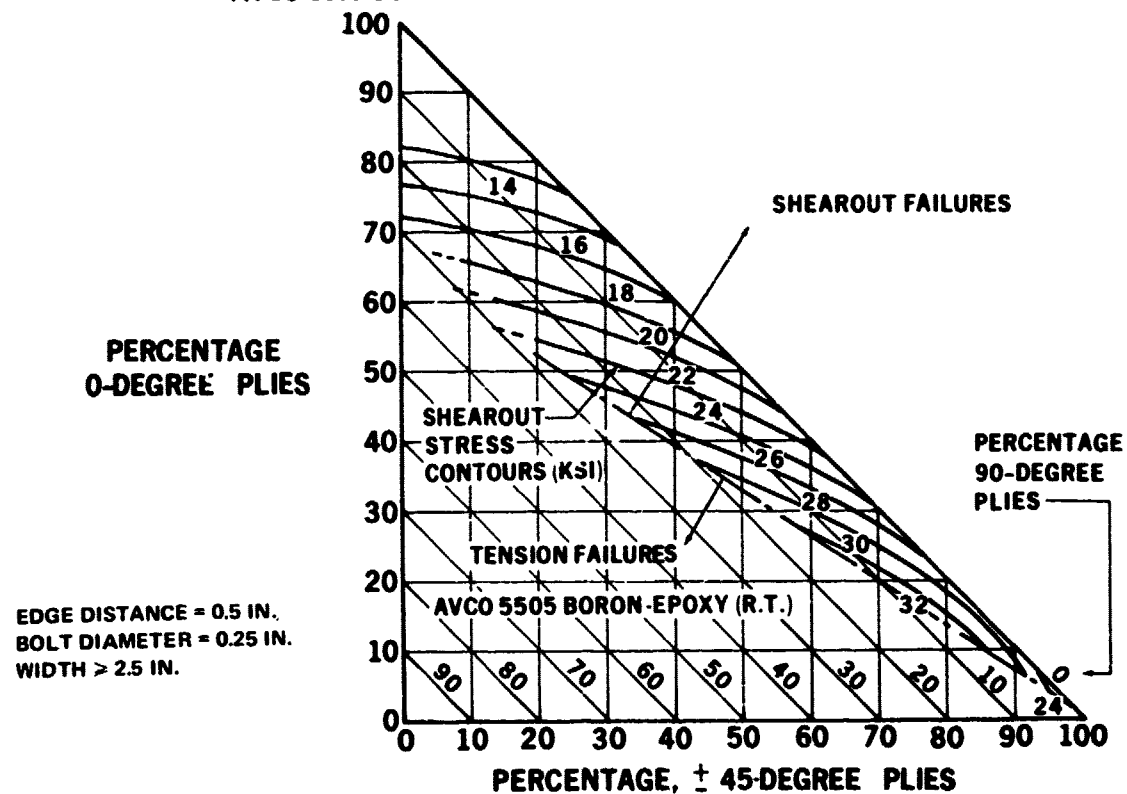


FIGURE 129. SHEAROUT STRESS CONTOURS FOR VARIOUS LAMINATE PATTERNS, AVCO 5505 BORON EPOXY

The bearing stresses were developed with both large w/d and e/d ratios under double shear loading. The specimen design efficiently prevented any influence of tension-through-the-hole failures but two patterns, (0/45/0/-45) and (03/45/0₃/-45), exhibited shearout failures. This confuses the interpretation of the results somewhat but certain conclusions remain clear. Firstly, bearing stresses in the range of 110 and 220 ksi can be developed and, on a specific basis, these are comparable strengths with those of metals. Secondly, as the percentage of 0-degree plies in a laminate increases, the necessary edge distance (or bolt pitch) to develop the full bearing strength potential becomes impractically large. The higher bearing stresses with a high proportion of cross plies makes a strong case in favor of using softening strips to contain the spanwise bolt seams in a highly directional laminate (one with a high proportion of 0-degree plies). The bearing strength of the +45-degree pattern is a respectable 114 ksi with an associated desirable failure mode.

It is evident that the maximum bearing stress of 230 ksi is developed for the (30-percent 0-degree, 70-percent +45-degree) pattern. It is noteworthy that in spite of edge distance ratios $e/d \geq 8$, those patterns with a high percentage of 0-degree plies and a low percentage of 90-degree plies are so weak in shearout as to be inherently incapable of developing a pure bearing failure. The stress contours display a pronounced ridge at the transition in failure modes. Perhaps even greater edge distances would afford some relief from the loss in strength but practical design proportions would prevent taking advantage of it.

The shearout stress contours for AVCO 5505 boron-epoxy shown in Figure 129 indicate the same regularity displayed for the pure bearing failures. The first evident conclusion is that, for patterns with a high proportion of 0-degree plies, either 90-degree or +45-degree plies are nearly equally effective in promoting shearout resistance. The second is that, for patterns with moderate fractions of 0-degree plies, 90-degree plies are much more effective than +45-degree plies in increasing the shearout strength. The third conclusion is that, as the proportion of 0-degree plies is decreased below a certain amount (for each percentage of +45-degree plies) the laminate tensile strength is decreased so much that shearout failures are not developed, even with very wide strips (small d/W ratios).

The mixed graphite-epoxy laminates do not exhibit the regular dependence on the laminate patterns exhibited by the boron-epoxy specimens, either for the bearing or shearout failures (see Figures 130 and 131). Also, the damaged areas were much more extensive for the graphite specimens, with pronounced delaminations (up to 1 inch) even within the confines of the steel doublers on the doublelap specimens. The highest shearout stresses are developed for the (37-1/2 percent 0-degree, 50-percent +45-degree, 12-1/2 percent 90-degree) pattern and the lowest for either predominantly all 0- or +45-degree plies. Both figures exhibit saddles in their contours rather than a single ridge. Part of this unusual behavior should be associated with the low adhesion between the Thornel 75S filaments and the 1004 resin employed.

Some tests were also completed with the 2544 resin system but exhibited problems in cocuring with the Narmco 5206/1004 resin system. In any event, the Thornel 75S fiber failed to adhere to either resin system used in the prepreg.

The data for the mixed graphite-epoxy tests are summarized in Table 52.

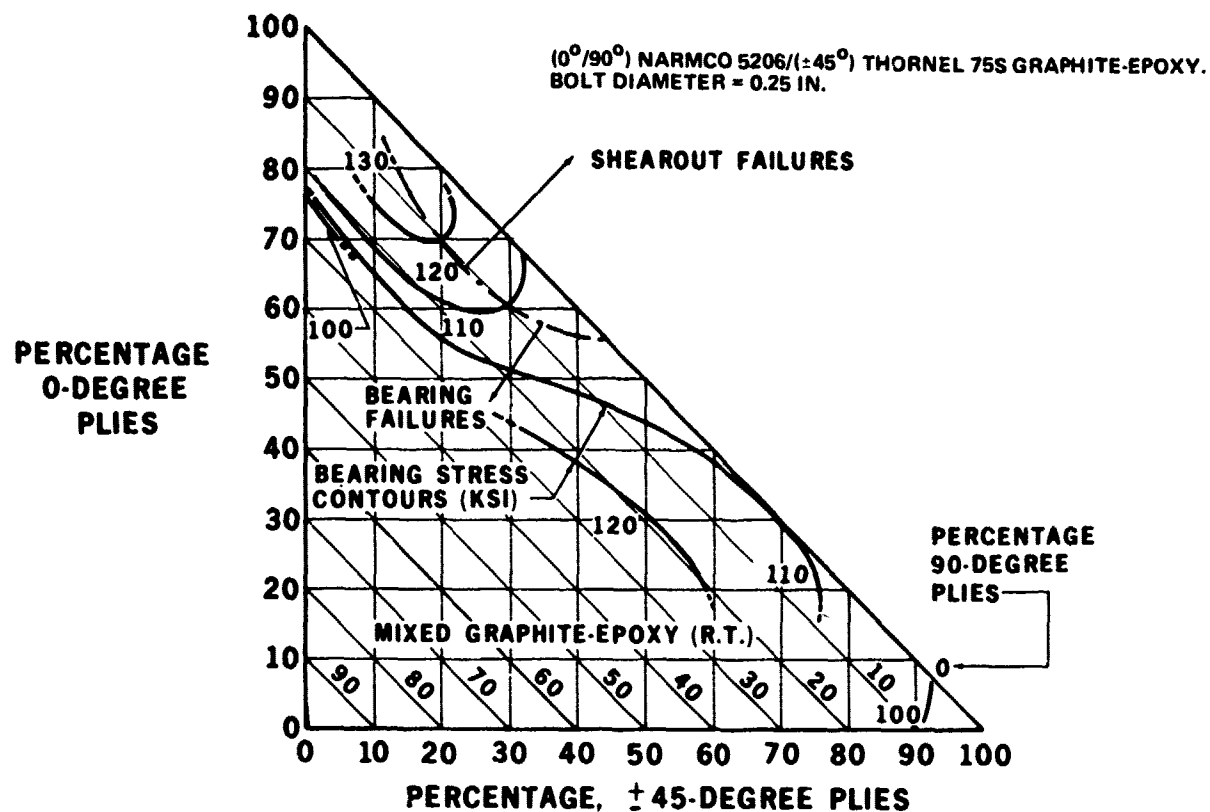


FIGURE 130. BEARING STRESS CONTOURS FOR VARIOUS LAMINATE PATTERNS, MIXED GRAPHITE EPOXY

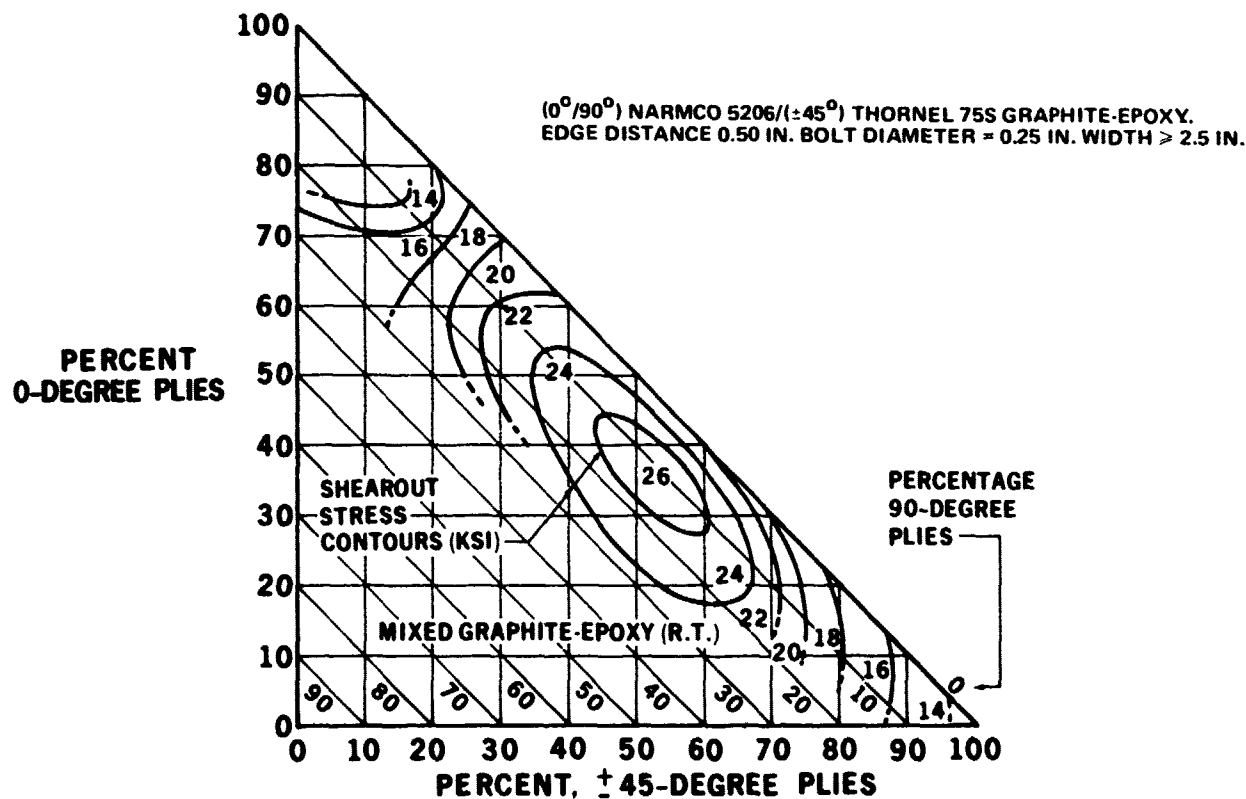


FIGURE 131. SHEAROUT STRESS CONTOURS FOR VARIOUS LAMINATE PATTERNS, MIXED GRAPHITE EPOXY

TABLE 52
DOUBLE-LAP BOLTED JOINT STRENGTH SUMMARY
(0.25-INCH BOLT DIAMETER MIXED GRAPHITE EPOXY)

| CONFIGURATION | LAMINATE THICKNESS (IN.) | LAMINATE WIDTH (IN.) | SHEAROUT TESTS | | | | BEARING TESTS | | | |
|--|--------------------------|----------------------|---------------------|---------------------|---------------------------------------|---------------------------|---------------|---------------------|---------------------|-----------------------|
| | | | EDGE DISTANCE (IN.) | ULTIMATE LOAD (LBS) | FAILURE MODE | STRESSES AT FAILURE (PSI) | | EDGE DISTANCE (IN.) | ULTIMATE LOAD (LBS) | FAILURE MODE |
| | | | | | | BEARING | SHEAROUT | | | |
| -25 (25% 0 DEG, 75% +45 DEG) | | | | | | | | | | |
| NO 1 - 1, 3 | 0.169 | 2.499 | 0.497 | 2,170 | SHEAROUT 0 DEG, +45 DEG, DELAMINATION | 51,360 | 17,263 | 1.813 | 4,370 | BEARING |
| NO 1 - 2, 4 | 0.171 | 2.498 | 0.498 | 2,310 | SHEAROUT 0 DEG, +45 DEG, DELAMINATION | 54,040 | 18,103 | 1.874 | 5,420 | BEARING, DELAMINATION |
| NO 2 - 1, 3 | 0.166 | 2.499 | 0.499 | 2,450 | SHEAROUT 0 DEG, +45 DEG, DELAMINATION | 59,040 | 19,726 | 1.858 | 4,350 | BEARING |
| NO 2 - 2, 4 | 0.170 | 2.503 | 0.496 | 2,375 | SHEAROUT 0 DEG, +45 DEG, DELAMINATION | 55,880 | 18,834 | 1.831 | 4,440 | BEARING |
| -27 (50% 0 DEG, 50% +45 DEG) | | | | | | | | | | |
| NO 1 - 1, 3 | 0.170 | 2.510 | 0.524 | 2,650 | CLEAVAGE | 62,350 | 19,528 | 1.834 | 4,850 | BEARING, DELAMINATION |
| NO 1 - 2, 4 | 0.170 | 2.499 | 0.484 | 2,675 | CLEAVAGE | 62,940 | 21,908 | 1.833 | 4,705 | BEARING |
| NO 2 - 1, 3 | 0.171 | 2.495 | 0.498 | 3,225 | SHEAROUT, DELAMINATION | 75,440 | 25,274 | 1.907 | 4,740 | BEARING |
| NO 2 - 2, 4 | 0.171 | 2.504 | 0.506 | 3,370 | CLEAVAGE | 78,830 | 25,863 | 1.851 | 4,870 | BEARING |
| -29 (75% 0 DEG, 25% +45 DEG) | | | | | | | | | | |
| NO 1 - 1, 3 | 0.164 | 2.002 | 0.491 | 2,275 | SHEAROUT, TENSION | 55,490 | 18,958 | 2.462 | 5,040 | BEARING, DELAMINATION |
| NO 1 - 2, 4 | 0.163 | 2.004 | 0.518 | 2,340 | SHEAROUT | 57,420 | 18,267 | 2.474 | 5,050 | BEARING |
| NO 2 - 1, 3 | 0.165 | 2.004 | 0.499 | 2,190 | SHEAROUT, TENSION | 53,090 | 17,747 | 2.469 | 5,140 | BEARING, DELAMINATION |
| NO 2 - 2, 4 | 0.164 | 2.003 | 0.511 | 2,275 | SHEAROUT, TENSION | 55,490 | 17,970 | 2.475 | 5,080 | BEARING |
| -31 (25% 0 DEG, 12 1/2% 90 DEG, 62 1/2% +45 DEG) | | | | | | | | | | |
| NO 1 - 1, 3 | 0.177 | 2.495 | 0.480 | 2,500 | SHEAROUT, 0 DEG, DELAMINATION | 56,500 | 19,889 | 1.847 | 5,030 | BEARING |
| NO 1 - 2, 4 | 0.177 | 2.495 | 0.513 | 3,930 | SHEAROUT, 0 DEG, DELAMINATION | 88,810 | 28,603 | 1.870 | 5,230 | BEARING |
| NO 2 - 1, 3 | 0.177 | 2.496 | 0.521 | 3,600 | SHEAROUT, 0 DEG, DELAMINATION | 81,360 | 21,678 | 1.914 | 5,050 | BEARING |
| NO 2 - 2, 4 | 0.177 | 2.494 | 0.487 | 3,525 | SHEAROUT, 0 DEG, DELAMINATION | 79,660 | 27,518 | 1.844 | 5,200 | BEARING |
| -33 (50% 0 DEG, 12 1/2% 90 DEG, 37 1/2% +45 DEG) | | | | | | | | | | |
| NO 1 - 1, 3 | 0.177 | 2.509 | 0.497 | 3,300 | SHEAROUT, 0 DEG | 74,580 | 25,057 | 1.832 | 5,190 | BEARING |
| NO 1 - 2, 4 | 0.178 | 2.505 | 0.500 | 3,300 | SHEAROUT, 0 DEG | 74,160 | 24,719 | 1.834 | 5,310 | BEARING |
| NO 2 - 1, 3 | 0.179 | 2.504 | 0.491 | 3,310 | SHEAROUT, 0 DEG | 73,570 | 25,267 | 1.816 | 4,855 | BEARING |
| NO 2 - 2, 4 | 0.180 | 2.503 | 0.501 | 3,300 | SHEAROUT, 0 DEG | 73,330 | 24,372 | 1.853 | 5,315 | BEARING |
| -35 (75% 0 DEG, 12 1/2% 90 DEG, 12 1/2% +45 DEG) | | | | | | | | | | |
| NO 1 - 1, 3 | 0.180 | 2.004 | 0.509 | 1,800 | CLEAVAGE | 41,780 | 13,603 | 2.467 | 6,360 | SHEAROUT*, BEARING |
| NO 1 - 2, 4 | 0.181 | 2.004 | 0.502 | 2,000 | CLEAVAGE, SHEAROUT | 44,200 | 14,652 | 2.486 | 6,160 | SHEAROUT*, BEARING |
| NO 2 - 1, 3 | 0.178 | 2.004 | 0.508 | 1,900 | SHEAROUT | 42,700 | 13,940 | 2.463 | 6,090 | SHEAROUT*, BEARING |
| NO 2 - 2, 4 | 0.179 | 2.004 | 0.495 | 1,800 | SHEAROUT | 40,220 | 13,443 | 2.457 | 5,660 | SHEAROUT*, BEARING |

NOTES: 0 DEG AND 90 DEG PLYS NARMCO 5206, +45 DEG PLYS THORNEL 775 IMPREGNATED WITH NARMCO 1004 RESIN
SHEAROUT STRESSES DERIVED BY FORMULA $\sigma_s = P/L \cdot t$ (P = LOAD, L = PLUG LENGTH, t = PLUG THICKNESS)
STRESSES COMPUTED ON BASIS OF ACTUAL LAMINATE THICKNESS BECAUSE OF DIFFERENT PLY THICKNESSES FOR NARMCO 5206 AND THORNEL 775
*CLEARLY DEFINED 0.25 IN. PLUG SHEARED OUT ALL THE WAY TO THE EDGE

TABLE 52 (CONTINUED)

| CONFIGURATION | LAMINATE THICKNESS (IN.) | LAMINATE WIDTH (IN.) | SHEAROUT TESTS | | | | BEARING TESTS | | | | | | | |
|---|--------------------------|----------------------|---------------------|--------------------|----------------------------------|---------------------------|---------------|--------------|---------------------------|----------|--------------------------------|---------|--|--------|
| | | | EDGE DISTANCE (IN.) | ULTIMATE LOAD (LB) | FAILURE MODE | STRESSES AT FAILURE (PSI) | | FAILURE MODE | STRESSES AT FAILURE (PSI) | | | | | |
| | | | | | | BEARING | SHEAROUT | | BEARING | SHEAROUT | | | | |
| -37 (25% 0 DEG, 25% 90 DEG, 50% +45 DEG) NO 1 - 1, 3 NO 1 - 2, 4 NO 2 - 1, 3 NO 2 - 2, 4 | 0.174 | 2.492 | 0.513 | 3,280 | BEARING | 75,400 | 24,256 | | 1841 | 5,200 | BEARING, TENSION, DELAMINATION | 119,540 | | 13,330 |
| | 0.172 | 2.493 | 0.519 | 3,340 | BEARING, DELAMINATION | 73,810 | 24,649 | | 1867 | 5,600 | BEARING, TENSION, DELAMINATION | 130,233 | | 14,516 |
| | 0.172 | 2.495 | 0.518 | 3,080 | BEARING, DELAMINATION | 71,630 | 22,781 | | 1856 | 5,640 | BEARING, TENSION, DELAMINATION | 131,163 | | 14,606 |
| | 0.172 | 2.495 | 0.509 | 3,320 | BEARING, DELAMINATION | 76,700 | 24,981 | | 1902 | 5,090 | BEARING, TENSION, DELAMINATION | 117,688 | | 13,106 |
| -39 (50% 0 DEG, 25% 90 DEG, 25% +45 DEG) NO 1 - 1, 3 NO 1 - 2, 4 NO 2 - 1, 3 NO 2 - 2, 4 | 0.174 | 2.483 | 0.506 | 2,625 | BEARING | 60,340 | 19,796 | | 1870 | 5,060 | TENSION, BEARING | 116,322 | | |
| | 0.176 | 2.490 | 0.510 | 2,940 | BEARING | 67,200 | 21,197 | | 1856 | 5,260 | BEARING, TENSION | 119,545 | | |
| | 0.173 | 2.489 | 0.522 | 2,580 | BEARING | 59,650 | 18,777 | | 1869 | 4,950 | BEARING, TENSION | 114,451 | | |
| | 0.174 | 2.494 | 0.505 | 2,625 | BEARING, TENSION | 60,340 | 19,856 | | 1563 | 4,980 | BEARING, TENSION | 114,483 | | |
| -41 (75% 0 DEG, 25% 90 DEG) NO 1 - 1, 3 NO 1 - 2, 4 NO 2 - 1, 3 NO 2 - 2, 4 | 0.190 | 2.024 | 0.505 | 2,200 | TENSION, CLEAVAGE | 48,700 | 15,235 | | 2335 | 3,920 | BEARING | 86,000 | | |
| | 0.190 | 2.014 | 0.508 | 2,260 | TENSION, CLEAVAGE | 51,800 | 16,220 | | 1979 | 3,560 | BEARING | 78,100 | | |
| | 0.189 | 1.997 | 0.500 | 2,125 | CLEAVAGE | 46,600 | 14,986 | | 2495 | 3,950 | BEARING | 86,600 | | |
| | 0.191 | 1.994 | 0.496 | 2,185 | TENSION, CLEAVAGE | 47,900 | 15,420 | | 2500 | 3,800 | BEARING | 84,600 | | |
| 43 (100% +45 DEG THORNEL 75S) NO 1 - 1, 3 NO 1 - 2, 4 NO 2 - 1, 3 NO 2 - 2, 4 | 0.179 | 2.485 | 0.492 | 1,820 | TENSION AT +45 DEG, DELAMINATION | 40,670 | 13,851 | | 1894 | 3,740 | BEARING, TENSION AT 45° | 83,575 | | 9,349 |
| | 0.174 | 2.486 | 0.513 | 1,790 | TENSION AT +45 DEG, DELAMINATION | 41,150 | 13,259 | | 1812 | 3,640 | BEARING | 83,678 | | 9,356 |
| | 0.176 | 2.486 | 0.480 | 1,650 | TENSION AT +45 DEG, DELAMINATION | 37,500 | 13,200 | | 1851 | 3,520 | BEARING | 80,000 | | 8,945 |
| | 0.176 | 2.486 | 0.522 | 1,800 | TENSION AT +45 DEG, DELAMINATION | 40,910 | 12,885 | | 1864 | 3,630 | BEARING, TENSION AT 45° | 88,409 | | 9,884 |
| 45 (100% +45 DEG NARMCO 5206) NO 1 - 1, 3 NO 1 - 2, 4 NO 2 - 1, 3 NO 2 - 2, 4 | 0.180 | 2.509 | 0.497 | 3,325 | TENSION AT +45 DEG | 72,900 | 24,832 | | 1667 | 3,445 | BEARING | 75,500 | | |
| | 0.179 | 2.508 | 0.489 | 3,150 | TENSION AT +45 DEG | 69,100 | 24,175 | | 1780 | 3,240 | BEARING | 71,100 | | |
| | 0.180 | 2.496 | 0.498 | 3,130 | TENSION AT +45 DEG | 68,600 | 23,300 | | 1230 | 3,130 | BEARING | 68,600 | | |
| | 0.178 | 2.496 | 0.506 | 3,250 | TENSION AT +45 DEG | 71,300 | 23,968 | | 1205 | 3,290 | BEARING | 72,100 | | |
| 47 (50% +45 DEG THORNEL 75S, 50% +45 DEG NARMCO 5206) NO 1 - 1, 3 NO 1 - 2, 4 NO 2 - 1, 3 NO 2 - 2, 4 | 0.174 | 2.504 | 0.514 | 2,840 | SHEAROUT AT +45 DEG | 65,290 | 20,975 | | 1900 | 4,870 | BEARING, TENSION AT 45° | 111,954 | | 12,417 |
| | 0.176 | 2.505 | 0.490 | 3,040 | SHEAROUT AT +45 DEG | 69,490 | 23,658 | | 1774 | 4,930 | BEARING, TENSION AT 45° | 112,745 | | 12,422 |
| | 0.176 | 2.505 | 0.532 | 3,100 | SHEAROUT AT +45 DEG | 70,450 | 21,633 | | 1882 | 4,820 | BEARING, TENSION AT 45° | 109,545 | | 12,145 |
| | 0.176 | 2.506 | 0.503 | 2,925 | SHEAROUT AT +45 DEG | 66,480 | 21,976 | | 1812 | 4,980 | BEARING | 113,182 | | 12,543 |

NOTES

7.5.3 Open Hole Stress Concentration Factors

The stress concentration factor at a bolted joint in a wing skin derives from two sources. The first is the bearing stress developed at the bolt hole and the second is the interruption in the stress field running past the hole. The latter component is treated as an unloaded hole, for which the elastic isotropic stress concentration factor is 3. For the tension skin on this conceptual wing, the inboard section may be represented by the typical pattern (0/+45/0) with 50-percent spanwise plies. A series of tests was run on unloaded holes in strips of this pattern. The results are reported in Table 53. The interpretation of these results, in conjunction with earlier test on tension failures induced by loaded bolts, leads to the conclusions that the appropriate values of K_{tc} for unloaded holes in a wide panel are

$$K_{tc} = 2.0 \text{ for } [0/\underline{+45}/0]$$

and

$$K_{tc} = 1.3 \text{ for } [0/\underline{+45}/90].$$

TABLE 53
OPEN HOLE STRESS CONCENTRATION FACTORS
NARMCO 5206 GRAPHITE-EPOXY [0/+45/0] LAMINATE PATTERN

| HOLE DIAMETER (IN.) | LAMINATE THICKNESS (IN.) | LAMINATE WIDTH (IN.) | NET CROSS-SECTIONAL AREA (SQ IN.) | FAILURE LOAD (LB) | NET TENSION FAILURE STRESS (PSI) | STRESS CONCENTRATION FACTOR k_{tc} | PREDICTED ELASTIC ISOTROPIC STRESS CONCENTRATION FACTOR k_{te} |
|---------------------|--------------------------|----------------------|-----------------------------------|-------------------|----------------------------------|--------------------------------------|--|
| 0 (CONTROL) | 0.045 (NOM) | 1.0 (NOM) | 0.0479 | | 82,600 | | |
| 0 (CONTROL) | 0.045 (NOM) | 1.0 (NOM) | 0.0470 | | 78,400 | | |
| 0 (CONTROL) | 0.045 (NOM) | 1.0 (NOM) | 0.0478 | | 76,400 | | |
| 0 (CONTROL) | 0.045 (NOM) | 1.0 (NOM) | 0.0484 | | 91,400 | | |
| 0 (CONTROL) | 0.045 (NOM) | 1.0 (NOM) | 0.0478 | | 86,500 | | |
| 0 (CONTROL) | 0.045 (NOM) | 1.0 (NOM) | 0.0471 | | 89,200 | | |
| 0 (CONTROL) | 0.045 (NOM) | 1.0 (NOM) | 0.0482 | | 78,200 | | |
| 0 (CONTROL) | 0.045 (NOM) | 1.0 (NOM) | 0.0464 | | 89,400 | | |
| | | | | | (A'VG) 84,013 | 1.0 (REF) | 1.0 |
| 0.250 | 0.0850 | 1.0045 | 0.0641 | 4290 | 66,927 | 1.25 | |
| 0.250 | 0.0845 | 1.0050 | 0.0638 | 3460 | 54,232 | 1.55 | 2.4 |
| 0.250 | 0.0840 | 1.0040 | 0.0633 | 3350 | 52,923 | 1.59 | |
| 0.444 | 0.0840 | 1.0050 | 0.0471 | 2837 | 60,085 | 1.64 | |
| 0.444 | 0.0850 | 0.9231 | 0.0463 | 2570 | 64,147 | 1.31 | 2.2 |
| 0.444 | 0.0830 | 0.9905 | 0.0454 | 2690 | 59,251 | 1.42 | |
| 0.630 | 0.0845 | 0.9908 | 0.0305 | 1630 | 53,443 | 1.57 | |
| 0.630 | 0.0845 | 0.9901 | 0.0304 | 1770 | 58,224 | 1.44 | 2.0 |
| 0.628 | 0.0835 | 0.9905 | 0.0303 | 1880 | 62,046 | 1.35 | |

NOTES

1. CONTROL SPECIMENS 8 PLIES THICK, FROM EARLIER PROGRAM. Z4829015.
2. HOLE SPECIMENS 16 PLIES THICK, WITH 4-1/2 IN. GAGE LENGTH BETWEEN GRIPS. Z4829017.
3. ALL SPECIMENS MADE FROM SAME MATERIAL, WITH SAME PROCESSING, AT CLOSE TO SAME TIME.

It is apparent that more stress concentration relief is afforded by fewer 0-degree plies.

These values were used for design purposes for this program with interpolation for other patterns. There are potential influences on these values arising from the use of mixed-graphite laminates but the successful satisfaction of other strength requirements would ensure that these changes be relatively small.

An important conclusion is to be drawn from these values which are aggravated by the additional bearing stress contributions. In the design of composite wing skins, one must either accept allowables of only about half those pertaining to purely bonded structures or employ a stress concentration relief technique such as softening strips around the bolt holes.

7.5.4 Compression K_T in Boron Laminates

Test loads, stresses, and stress concentration factors for 18 Z3569982 compression beams are shown in Table 54. Stresses for specimens with a pin in 0.250-inch-diameter holes are computed for both net section area and gross section area because of uncertainty about the mechanism of failure initiation. Specimens 17 and 18 failed at identical loads, yet one had an interference fit fastener while the other was loose. Consequently, the influence of bearing load through the fastener is unclear. It is evident that the stress concentration factors for unloaded holes in a compression panel are quite significant, being comparable with those for tensile loading.

The holes were filled with pins, not torqued bolts, so there was no restraint against the interlaminar tension induced by the compressive load. While lower K_T 's may be obtainable by the use of clampup by protruding head bolts and washers, such relief is not available on exterior skin surfaces with flush fasteners.

The K_T predictions leave something to be desired as the result of making the facings for the -1 beams with too many plies. The capacity of the honeycomb bond in the shear transfer area was exceeded. Despite the efforts to rectify the problem by necking down the test section, no reliable control value was established for the -501 beams; therefore, no meaningful K_T values were determined. The abnormally high control value for the -507 beams is inexplicable. The test results and the laminate pattern have been checked and rechecked. The importance of establishing experimental control stresses is revealed by the -509 beams with very different K_T 's computed, with respect to the -507 control beams and the Design Guide allowables.

7.5.5 Stress Concentration Relief Tests

The need for softening strips to alleviate the stress concentrations at bolt holes in advanced composites has already been demonstrated under both tensile and compressive loadings. Douglas IRAD sandwich beam tests have confirmed the effectiveness of 0-degree glass filaments in minimizing the stress concentrations at unloaded holes. It remained to establish the lower bearing and higher shearout stresses associated with the mixed laminates to be used in the softening strips. The test specimen employed is Z3569985 and the results are documented and interpreted in Table 55 for both spanwise and

TABLE 54
COMPRESSION TESTS ON UNLOADED FILLED HOLES IN BORON-EPOXY

| SPECIMEN Z3569982 | FAILURE LOAD (LB) | GROSS FAILURE STRESS F _{cu} (KSI) | DESIGN GUIDE FAILURE STRESS (KSI) | NET SECTION K _T | | GROSS SECTION K _T | | COMMENT |
|----------------------|-------------------------|---|---|----------------------------|---------------------------|------------------------------|---------------------------|---|
| | | | | W.R.T.* CONTROL | W.R.T. DESIGN GUIDE | W.R.T. CONTROL | W.R.T. DESIGN GUIDE | |
| -1 NO. 1 | 11,895 | — | | | | | | NO TEST. BOND FAILED. TOO MANY 0-DEG PLIES. FAILURE STRESS REDUCED BY NECK DOWN. 8-9°, 8-45°, 2-90° |
| NO. 2 | 5,655 | 148.8 | | | | | | |
| NO. 3 | 6,305 | 164.1 | | | | | | |
| AVG | | 156.5† | 217 | | | | | |
| -501 NO. 4 | 10,530 | 173.7 | | | 1.09 | | 1.25 | ALL FAILURES ACROSS NET SECTION THROUGH HOLE SAME AS -1 EXCEPT 0.25 IN. DIA FILLED HOLE |
| NO. 5 | 10,140 | 165.5 | | | 1.15 | | 1.31 | |
| NO. 6 | 9,300 | 153.5 | | | 1.24 | | 1.41 | |
| AVG | | | | | | | | |
| -503 NO. 7 | 3,675 | 49.5 | | | | | | ALL FAILURES ALONG 45° DIRECTION. 10-45°, 2-90° |
| NO. 8 | 3,725 | 50.1 | | | | | | |
| NO. 9 | 3,650 | 49.1 | | | | | | |
| AVG | | 49.6 | 47 | | | | | |
| 505 NO. 10 | 3,025 | 40.3 | | 1.08 | 1.02 | 1.23 | 1.17 | ALL FAILURES ALONG 45° DIRECTION THROUGH HOLE. SAME AS -503 EXCEPT 0.250 IN. DIA FILLED HOLE. |
| NO. 11 | 2,925 | 38.9 | | 1.12 | 1.06 | 1.28 | 1.21 | |
| NO. 12 | 3,000 | 40.4 | | 1.07 | 1.02 | 1.23 | 1.16 | |
| AVG | | | | | | | | |
| -507 NO. 13 | 10,725 | 203.8 | | | | | | PREMATURE FAILURE OUTSIDE TEST SECTION. FAILED IN TEST SECTION. 4-0°, 8-45°, 4-90°. |
| NO. 14 | 11,650 | 218.7 | | | | | | |
| NO. 15 | 11,375 | 213.5 | | | | | | |
| AVG | | 212.0† | 152 | | | | | |
| -509 NO. 16 | 6,500 | 120.5 | | 1.54 | 1.10 | 1.76 | 1.26 | ALL FAILURES ACROSS NET SECTION IN TEST AREA SAME AS -507 EXCEPT 0.250 IN. DIA FILLED HOLE. |
| NO. 17 | 6,630 | 124.4 | | 1.49 | 1.07 | 1.70 | 1.22 | |
| NO. 18 | 6,630 | 124.4 | | 1.49 | 1.07 | 1.70 | 1.22 | |
| AVG | | | | | | | | |

*WITH RESPECT TO.

†THESE SPECIMENS WERE EXAMINED AFTER FAILURE UNDER THE MICROSCOPE TO DETECT THE 0-DEGREE PLIES AND BY THICKNESS MEASUREMENT TO CONFIRM THAT THE SPECIMENS HAD NOT BEEN MISIDENTIFIED.

TABLE 55

DOUBLE-LAP BOLTED-JOINT STRENGTH SUMMARY
(0.25 IN. BOLT, 0 DEG GLASS SOFTENING STRIP IN 1004 RESIN.
NARMCO 5206 GRAPHITE-EPOXY OR AVCO 5505 BORON-EPOXY)

| CONFIGURATION Z3569985 SPECIMEN I.D. | LAMINATE THICKNESS (IN.) | LAMINATE WIDTH (IN.) | EDGE DISTANCE (IN.) | ULTIMATE LOAD (LB) | FAILURE MODE | STRESSES AT FAILURE | | | |
|--|--------------------------------|----------------------------|---------------------------|--------------------------|-----------------|---------------------|----------|---------|--------|
| | | | | | | BEARING | SHEAROUT | TENSION | |
| SHEAROUT TESTS (125 IN. LB TORQUE) | | | | | | | | | |
| 501 | 5A B | 0.162 | 3.004 | 0.620 | 4130 | TENSION/BEARING | 101,980 | 25,750 | 9,260 |
| | 5A E | 0.163 | 3.004 | 0.620 | 4580 | TENSION/BEARING | 112,390 | 28,380 | 10,200 |
| | 5B B | 0.155 | 3.007 | 0.622 | 1450 | TENSION | 114,840 | 28,880 | 9,960 |
| | 5B E | 0.165 | 3.007 | 0.622 | 3865 | TENSION | 93,700 | 23,570 | 8,500 |
| | AVERAGE | | | | | | 105,730 | 26,640 | 9,480 |
| 503* | 7A B | 0.160 | 3.005 | 0.618 | 3240 | SHEAROUT | 81,000 | 20,540 | 7,350 |
| | 7A E | 0.160 | 3.005 | 0.606 | 3060 | SHEAROUT | 76,500 | 19,880 | 6,940 |
| | 7B B | 0.155 | 3.004 | 0.622 | 2980 | SHEAROUT | 76,900 | 19,340 | 6,980 |
| | 7B E | 0.157 | 3.004 | 0.621 | 3380 | SHEAROUT | 86,110 | 21,700 | 7,820 |
| | AVERAGE | | | | | | 80,130 | 20,370 | 7,270 |
| 505 | 9A B | 0.135 | 2.999 | 0.513 | 3515 | TENSION/BEARING | 104,150 | 33,550 | 9,470 |
| | 9A E | 0.135 | 2.999 | 0.497 | 3550 | TENSION/BEARING | 105,190 | 35,340 | 9,570 |
| | 9B B | 0.135 | 3.007 | 0.514 | 3770 | TENSION/BEARING | 111,700 | 35,890 | 10,130 |
| | 9B E | 0.136 | 3.008 | 0.506 | 3730 | TENSION/BEARING | 109,710 | 35,990 | 9,940 |
| | AVERAGE | | | | | | 107,690 | 35,190 | 9,780 |
| 5051 | 11A B | 0.132 | 3.002 | 0.525 | 3020 | SHEAROUT | 91,520 | 28,600 | 8,310 |
| | 11A E | 0.135 | 3.001 | 0.520 | 2750 | SHEAROUT | 81,480 | 25,790 | 7,400 |
| | 11B B | 0.134 | 2.998 | 0.506 | 2825 | SHEAROUT | 84,330 | 27,670 | 7,670 |
| | 11B E | 0.135 | 3.000 | 0.519 | 2700 | SHEAROUT | 80,000 | 25,380 | 7,270 |
| | AVERAGE | | | | | | 84,330 | 26,860 | 7,660 |
| BEARING TESTS (65 IN. LB TORQUE) | | | | | | | | | |
| 1 | 5A C | 0.162 | 3.004 | 2.120 | 6280 | BEARING | 155,060 | 9,720 | 14,080 |
| | 5A D | 0.163 | 3.004 | 2.102 | 6300 | BEARING | 154,600 | 9,770 | 14,020 |
| | 5B C | 0.155 | 3.007 | 2.113 | 6620 | BEARING | 170,840 | 10,740 | 15,490 |
| | 5B D | 0.165 | 3.007 | 2.119 | 6900 | BEARING | 167,270 | 10,400 | 15,170 |
| | AVERAGE | | | | | | 161,940 | 10,180 | 14,690 |
| 5011 | 7A C | 0.160 | 3.005 | 2.127 | 6340 | BEARING | 158,500 | 9,900 | 14,280 |
| | 7A D | 0.160 | 3.005 | 2.123 | 6360 | BEARING | 159,000 | 9,950 | 14,430 |
| | 7B C | 0.155 | 3.004 | 2.118 | 5610 | BEARING | 144,780 | 9,080 | 13,140 |
| | 7B D | 0.157 | 3.004 | 2.117 | 5960 | BEARING | 151,850 | 9,530 | 13,780 |
| | AVERAGE | | | | | | 153,530 | 9,610 | 13,930 |
| 503* | 9A C | 0.135 | 2.999 | 2.125 | 7010 | TENSION | 207,700 | 12,980 | 18,890 |
| | 9A D | 0.135 | 2.999 | 2.123 | 6940 | TENSION | 205,630 | 12,860 | 18,700 |
| | 9B C | 0.135 | 3.007 | 2.100 | 7130 | TENSION | 211,260 | 13,370 | 19,160 |
| | 9B D | 0.136 | 3.008 | 2.113 | 7050 | TENSION | 207,350 | 13,040 | 18,800 |
| | AVERAGE | | | | | | 207,990 | 13,060 | 18,890 |
| 5051 | 11A C | 0.132 | 3.002 | 2.137 | 6750 | BEARING | 204,550 | 12,710 | 18,580 |
| | 11A D | 0.135 | 3.001 | 2.113 | 6830 | BEARING | 202,370 | 12,720 | 18,390 |
| | 11B C | 0.134 | 2.998 | 2.115 | 6510 | BEARING | 194,330 | 12,210 | 17,680 |
| | 11B D | 0.135 | 3.000 | 2.119 | 6460 | BEARING | 191,410 | 12,000 | 17,400 |
| | AVERAGE | | | | | | 198,170 | 12,410 | 18,040 |

1 (45/90/ 45/90/45/0/ 45/90/45/90/ 45/90)_S } 45° N5206 GRAPHITE EPOXY
 501 (45/0/ 45/0/45/90/ 45/0/45/0/ 45/0)_S } 0°, 90° HTS 5994 GLASS EPOXY

GLASS FIBERS IMPREGNATED WITH NARMCO 1004 RESIN

503 (45/90/ 45/90/45/0/ 45/90/45/90/ 45/90)_S } 45° AVCO 5505 BORON EPOXY
 505 (45/0/ 45/0/45/90/ 45/0/45/0/ 45/0)_S } 0°, 90° HTS 5994 GLASS EPOXY

HOLE SIZES RANGED FROM 0.2483 TO 0.2478 INCH

SHEAROUT STRESSES COMPUTED FROM $\sigma_s = P/(2te)$ (0.50d)

*TESTS REVEALED MULTIPLE PARALLEL TENSION CRACKS OVER MUCH OF WIDTH ASSOCIATED WITH GROSS SHEAR DEFORMATION ON ALL 503 SPECIMENS

†PRONOUNCED COMPRESSION SNAKE S

chordwise loadings. These data indicate that this mixed materials concept has adequate joint load transfer capacity. The bearing strengths are of the same magnitude as for graphite-epoxy and boron-epoxy laminates and the shearout strengths are quite respectable. S-glass HTS finish, with 1004 resin, was used with the Narmco 5206 Type II graphite and Avco 5505 boron. These high strengths appear to be due to the high shear strengths of the +45-degree plies in conjunction with the high-strength, high-elongation, 0-degree glass plies.

7.5.6 Bonded Tension Joint

The first bonded truss-to-cover joint concept (Bond scheme A) was subjected to a tension test, as being most crucial for the joint. See Figure 104 for a detail of the specimen before being bolted to the test machine fixed head. The two legs attached to a load distribution system which permitted equal inclined tension load in each.

The failure load was 1740 pounds or 870 pounds/inch of joint length as compared to a design requirement of 1730 pounds/inch, based on 20-psi wing internal pressure and a 50-percent factor.

Observations during and after testing revealed that initial failure was probable at the bond between the web and the buildup area on the cap. While Non-Destructive Testing by ultrasonic C-scan before testing did not reveal any unbond in this area, the method of specimen manufacture could easily have resulted in inadequate pressure on the EA951 adhesive at this location during final cure. Since there was no failure in the web or the cap, it was decided that the specimen could be repaired and retested with only a small expenditure of effort. The EA951 adhesive bond in the critical area was made first before application of the filler material to ensure adequate pressure. The failure load on the retest was 1380 pounds (690 pounds/inch) and initiated in the graphite plate buildup area. See Figure 132 for failure surface after the initial test.

Because of suspected stress concentration at the heels of the reinforcing angles and the increased cost of fabricating this joint with respect to the scheme B fillet bond concept, fillet bond testing was preferentially pursued.

7.5.7 Bonded Fillet Joint

Tension Tests

While none of the adhesive materials screened by flatwise testing met all of the objectives enumerated under the bonded joint manufacturing feasibility Section (7.1.1), the Hysol EA9306 has such excellent handling characteristics coupled with good bond strengths that it was selected for use in the F3578686-507 test specimen (see Figure 106). This specimen, when tension tested as shown in Figure 133, failed in the graphite plate (close to the adhesive) by interlaminar tension at a test load of 1260 pounds. The desired design ultimate load was 1730 pounds based on 20-psi pressure and a 50-percent bonded joint factor.

The Z3578686-509 configuration shows a revised configuration to reduce joint weight and improve joint geometry. EA951 adhesive plies were interleaved

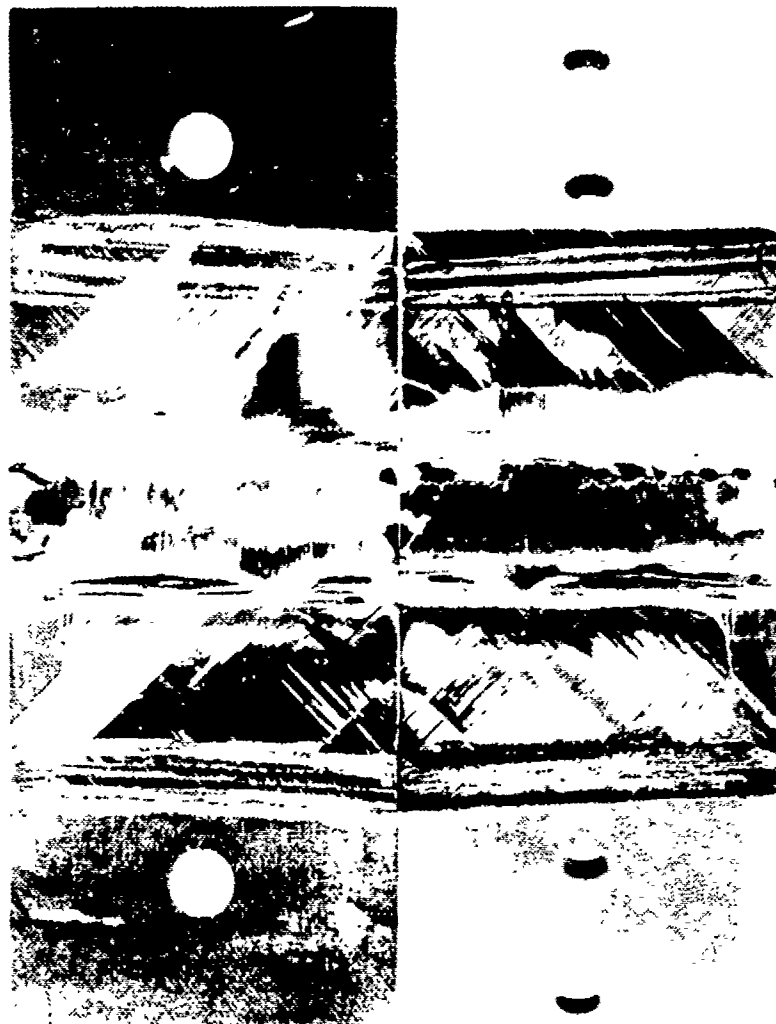


FIGURE 132. Z3578686-1 BONDED TENSION SPECIMEN – INTERNAL FAILURE BEFORE REPAIR

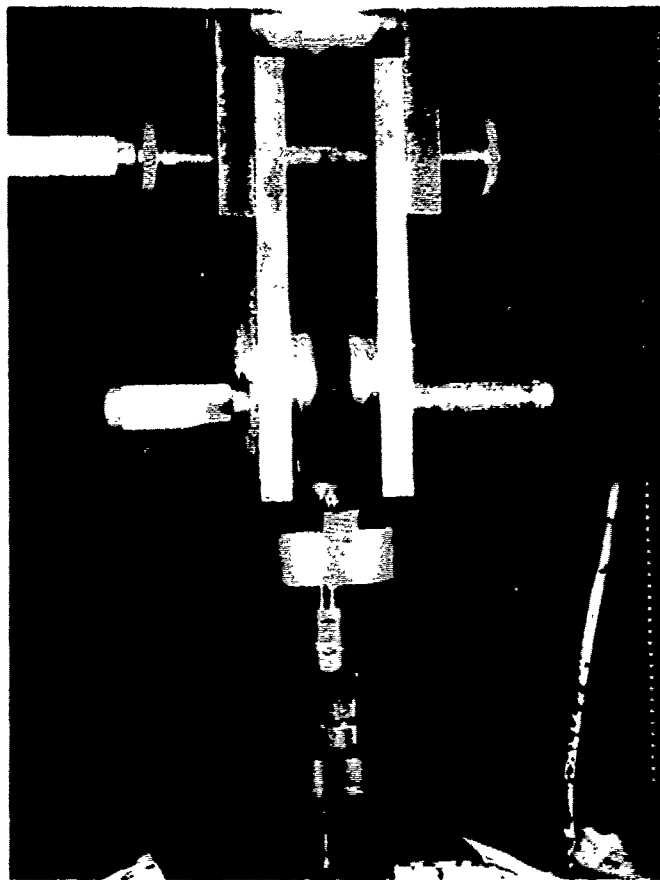


FIGURE 133. Z3578686-509 LOOP TENSION TEST, ROOM TEMPERATURE

in the graphite base plate to improve its strength. The -509 failure load was 2690 pounds, comfortably exceeding the requirement. However, preceding element tests of the adhesive and mixed graphite/adhesive laminate alone had indicated a still higher test load, approaching 4000 or 5000 pounds. At the time, it was believed the -509 failure was premature since failure surface was only 35 percent within the baseplate graphite and passed through a void (stress concentration) in a corner on the filleted adhesive.

Table 56, a summary of all the loop tension tests, shows the -509 value was never exceeded. The four -511 specimens were identical to -509 except that no adhesive was interleaved in the baseplate of -511. Interleaved EA951 produced severe baseplate flexing at elevated temperature. Interleaved FM96, although promising from the standpoint of preliminary interlaminar shear and flexure tests at elevated temperature, proved to have a chemical incompatibility problem when interleaved in a thick laminate. The laminate simply split apart progressively through a number of layers. Since -511 No. 3 more than exceeded its fatigue strength requirement of 10 to 15 percent of 1,731 pounds per inch. -511 No. 4 was static-tested to provide another room temperature data point. The environmental specimen -511 No. 2 was subjected to ten 24-hour cycles of 100°F and 100-percent relative humidity, 160°F at ambient humidity and -67°F, in that sequence. Specimen edges were exposed unlike a real structure. This single test was intended to indicate the extent of any temperature/humidity environmental degradation in adhesive or laminate. The Rangoon cycle test is felt to be a very severe test.

Figure 134 shows three of the failed specimens from this series.

TABLE 56
SUMMARY Z3578686 JOINT TENSION TESTS

| SPECIMEN CONFIGURATION | ENVIRONMENTAL EXPOSURE | TEST TEMP (°F) | FAILURE LOAD (LB) | COMMENT |
|------------------------|--|----------------|-------------------|--|
| -507 | NONE | RT | 1260 | 1730 LB REQUIRED |
| -509 NO. 1 | NONE | RT | 2690 | EA951 INTERLEAVED BASEPLATE FLEXING REBONDED WITH EA951 AFTER INITIAL FAIL AT 300 LB |
| -509 NO. 2 | NONE | 160 | 300 | |
| -509 NO. 2 | NONE | 160 | 780 | |
| -511 NO. 1 | NONE | 160 | 2135 | FATIGUED AT 25 PERCENT DESIGN ULTIMATE. NO FAILURE FROM FATIGUE |
| -511 NO. 2 | 10 "RANGOON" CYCLES | RT | 635 | |
| -511 NO. 3 | 6 x 10 ⁶ FATIGUE CYCLES AT 430 LB MAXIMUM R = 0.05 | RT | 2412 | |
| -511 NO. 4 | NONE | RT | 1920 | |

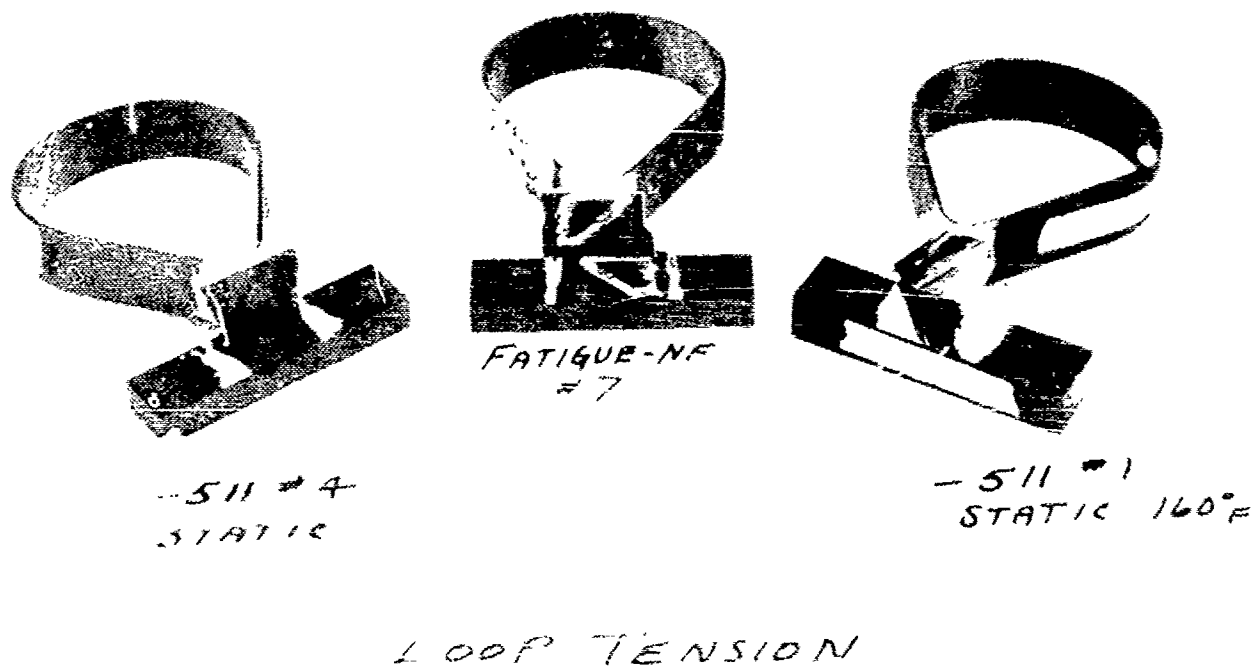


FIGURE 134. Z3578686-511 LOOP TENSION SPECIMENS

Shear Tests

The fillet joint concept shear test series (Drawing Z4569981, Appendix A) includes a progression of tests, the results of which are to be found in Table 57. The -1 configuration tests a uniformly thick bond with steel adherends to assess the adhesive at 0.150-inch thickness and minimum stress concentrations. The rail shear configuration was selected over a beam geometry on the basis of economy. The test results (Table 57) reveal an average bond strength of 5047 psi in spite of significant voids in the bond. The next stage was to employ steel adherends in the fillet joint geometry proposed for the wing. The test results for these -501 specimens were 5300 and 5600 pounds per running inch of joint. These specimens also exhibited some voids, but the favorable geometry minimized them. All these failures were cohesive and not influenced by surface effects. The bonds exhibited extensive cracking in addition to the fracture surface. In every case the fracture surface ran through from one face of the bond to the other. The fracture started adjacent to the loaded adherend at each end of the joint, which is to be expected since the maximum combined stresses occur there. A feature of the designs was that each adherend had the same extensional stiffness as the other so as to make each end of the joint equally critical. Figure 135 shows these failures.

The next stage in the sequence was to include the effects of bonding to graphite epoxy laminates. The -503 specimens were to achieve this end (Figure 135). Although the graphite epoxy has an interlaminar shear strength in excess of that of the EA9306 adhesive, laminate failures induced the breaking of the joint at loads 20 percent less than with the steel adherends. The reason is believed to be the higher transverse tensile and compressive strengths of the adhesive, as compared to those of the laminate. There appears to be a need to protect the ends of the fillet joint by thickening the bondline locally and/or replacing the EA9306 with a compatible ductile adhesive. The -505 specimens were intended to demonstrate the adequate design capacity of 25 percent excess over the ultimate joint load of 5280 pounds per inch (i. e., 6600 pounds per inch). To this end, the more lightly stressed center of the joint was isolated by teflon films to boost the average stress demonstrated to the maximum attained at the end of the joint. In addition, the joint was scaled up to a larger cross section. Because of favorable

TABLE 57
BONDED FILLET JOINT RAIL SHEAR TESTS

| CONFIGURATION SPECIMEN I.D. | FAILURE LOAD (LB) | AVERAGE SHEAR STRENGTH (LB PER INCH) | TEST TEMPERATURE (°F) |
|--------------------------------|-------------------------|--|-----------------------------|
| -1 NO. 3 | 19,500 | 4850 | RT |
| -1 NO. 4 | 20,700 | 5130 | RT |
| -1 NO. 5 | 20,900 | 5160 | RT |
| -501 NO. 1 | 21,300 | 5300 | RT |
| -501 NO. 2 | 22,700 | 5600 | RT |
| -503 NO. 1 | 17,750 | 4330 | RT |
| -503 NO. 2 | 18,000 | 4460 | RT |
| -505 NO. 1 | 7500 | 3750 | RT |
| -505 NO. 2 | 8520 | 4260 | 160 |
| -505 NO. 3 | 7565 | 3780 | 160 |
| -505 NO. 4 | 6100 | 3050 | 200 |

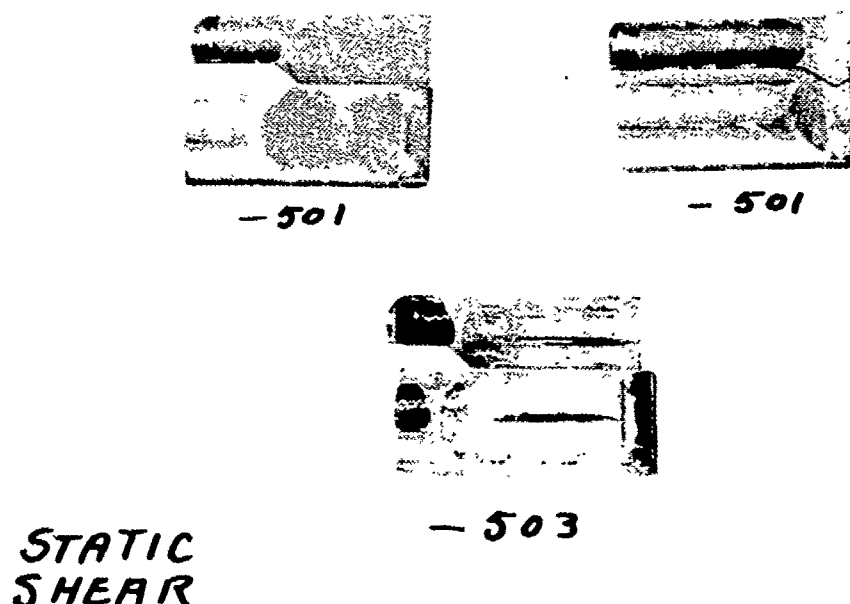


FIGURE 135. Z4569981-501, -503 FILLET JOINT RAIL SHEAR SPECIMENS

bolted-joint test results using 0-degree glass softening strips, the 0-degree plies in the -21 skin were made of glass instead of graphite. Inspection of the failed specimens suggests that the low interlaminar strength of this laminate was responsible for the reduced joint strengths. (The dominant importance of the transverse laminate strength was not appreciated until it was deduced analytically on a concurrent program after these specimens were tested, Figure 136.)

Static and fatigue testing of Z3569983-1 and -501 double-lap shear specimens is summarized in Table 58. The -1 specimen with the mixed 5206/951 adhesive laminate had greater fatigue resistance than the -501 specimen without interleaved adhesive, but the specimens were otherwise identical. The adhesive interleaving improved the joint performance at room temperature, as shown in Figure 137, but the concept has been abandoned because of drop-off in strength at 160°F. The basic problem remains that of the low interlaminar tension strength of the laminate. This precludes the development of the full potential shear strength of the adhesive. The interleaved adhesive renders the inner laminate more ductile, thereby alleviating the problem, as depicted in Figure 138. However, a more marked gain is to be achieved by sacrificing some of the unattained shear strength potential in exchange for relief from the peel stress problem at the end of the outer adherends. This can be accomplished by feathering the ends of the outer adherend over part of the overlap, either alone or in conjunction with a thickened bondline at that location. The measure of effectiveness of the interleaving is revealed by the test on the -1 No. 2 specimen which failed in the outer adherend, as shown in the upper right corner of Figure 138. Failed specimens are pictured in Figure 139.

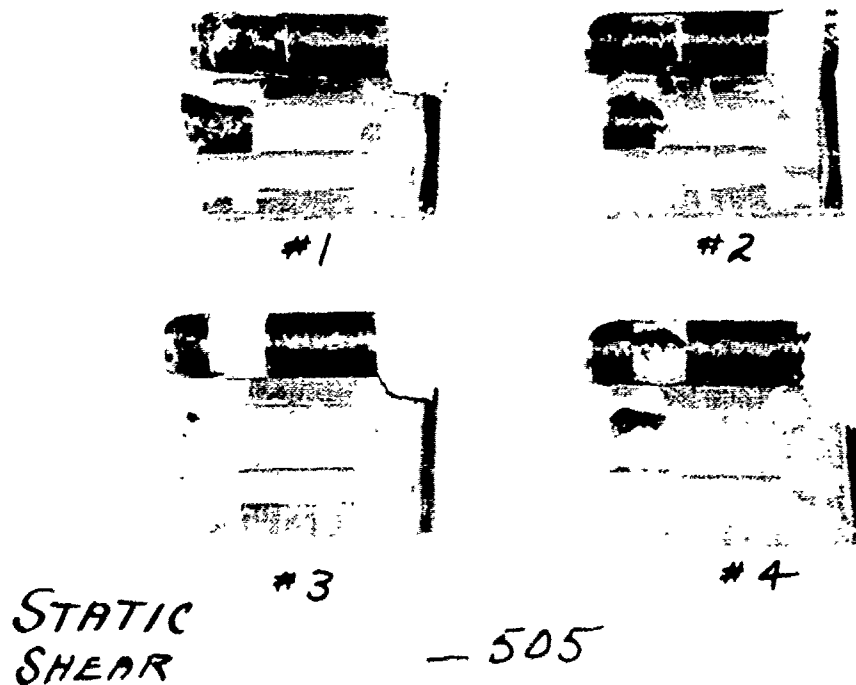


FIGURE 136. Z4569981-505 FILLET JOINT RAIL SHEAR SPECIMENS

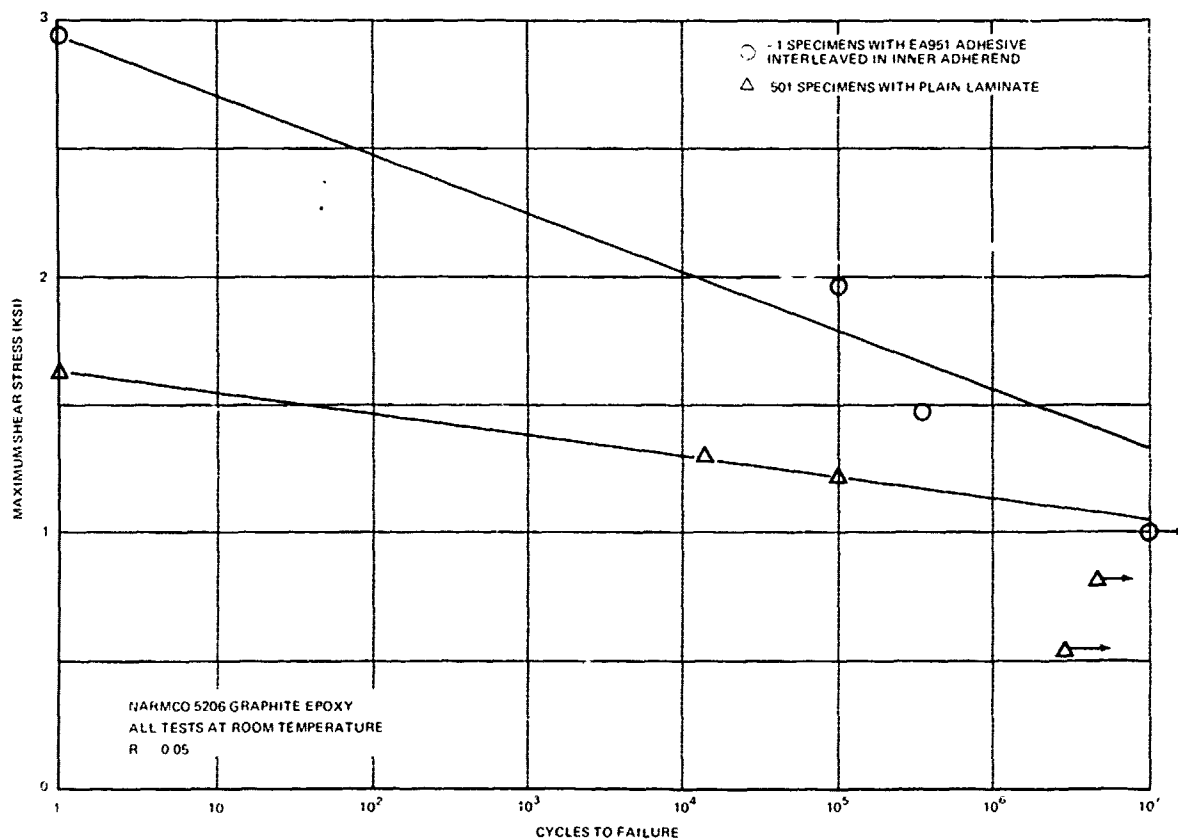


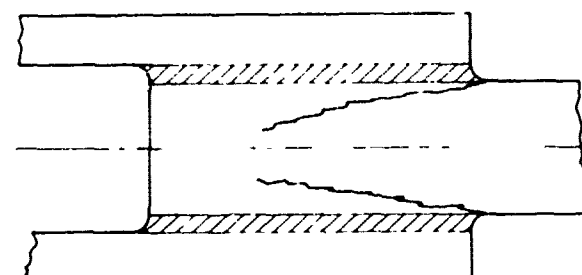
FIGURE 137. DOUBLE-LAP SHEAR TESTS ON Z3569983 SPECIMEN, EA9306 ADHESIVE

TABLE 58
DOUBLE-LAP GRAPHITE-EPOXY EA9306 FATIGUE TESTS (R = 0.05) SPECIMEN Z3569983

| CONFIGURATION* SPECIMEN I.D. | MAXIMUM LOAD (LB) | MAXIMUM SHEAR STRESS (PSI) | CYCLES TO FAILURE | COMMENTS |
|---------------------------------|-------------------------|----------------------------------|--|--|
| -1 NO 1 | 7050 | 2940 | STATIC TEST | FAILED IN INNER ADHEREND |
| -1 NO 2 | 2350 4700 | 980 1960 | 10.36×10^6 1.01×10^5 | NO FAILURE FAILED IN OUTER ADHEREND |
| -1 NO 3 | 3505 | 1470 | 3.55×10^5 | FAILED IN INNER ADHEREND |
| -501 NO 1 | 4100 | 1630 | STATIC TEST | FAILED IN INNER ADHEREND |
| -501 NO 2 | 1353 2050 3000 | 540 815 1215 | 2.84×10^6 4.66×10^6 1.01×10^5 | NO FAILURE NO FAILURE FAILED IN INNER ADHEREND |
| -501 NO 3 | 3000 | 1300 | 1.4×10^4 | FAILED IN INNER ADHEREND |

*-1 INTERLEAVED ADHESIVE IN INNER ADHEREND
 -501 WITHOUT INTERLEAVED ADHESIVE

TESTS AT ROOM TEMPERATURE



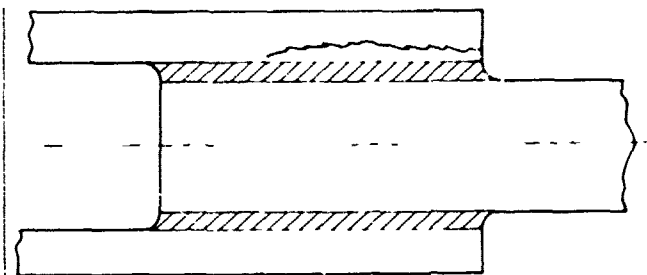
**CHARACTERISTIC FAILURE MODE
FOR THICK COMPOSITE ADHERENDS**



BOND PEEL STRESSES



ASSOCIATED SHEAR STRESSES



**ALTERNATIVE POSSIBLE FAILURE
MODE WHEN INNER LAMINATE IS
SOFTENED BY ADHESIVE**



REDUCED PEEL STRESSES



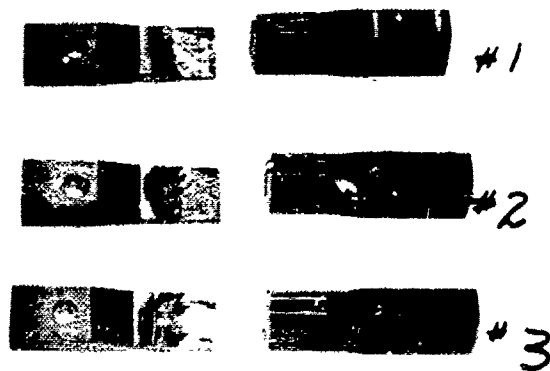
HIGHER AVERAGE SHEAR STRESS



ALTERNATIVE PEEL STRESS RELIEF TECHNIQUES

- (1) CRITICAL PEEL STRESS ALLEVIATED THROUGH REDUCTION IN BENDING STIFFNESS AT END OF OUTER ADHEREND
- (2) EFFICIENCY OF SHEAR TRANSFER AT RIGHT END OF JOINT REDUCED, BUT NOT AS MUCH AS IS GAINED FROM IMPROVED PEEL RESISTANCE
- (3) TECHNIQUES NOT NECESSARY FOR THIN LAMINATES

FIGURE 138. PEEL STRESS FAILURE OF THICK COMPOSITE BONDED JOINTS



DOUBLE LAP SHEAR -501

FIGURE 139. Z3569983-501 DOUBLE LAP SHEAR FATIGUE SPECIMENS

7.5.8 Small Bolted Tension Joint

The Z3578686-501 bolted web-to-cover joint with 1/4-inch countersunk steel bolt in an all-Narmco 5206 cap was pictured in Figure 105. It was tested in tension similarly to the bonded tension joint (7.5.6). The specimen failed within the graphite cover plate at a load of 3100 pounds or 1550 pounds/inch of joint. The design requirement was 1335 pounds/inch, based on 20 psi wing pressure and a 15-percent joint factor. The -503 configuration used the undamaged web and shoulder parts from the -501 but used a boron plate. The -503 failed at 4350 pounds (2175 pounds/inch) again within the plate by bending and interlaminar tension at the countersunk bolt head. The tests were considered sufficient demonstration of the bolted joint adequacy for tension.

7.6 DESIGN VERIFICATION TESTS

The design verification specimen series was conceived to demonstrate the structural integrity of the key structural elements of the truss web design. Although the small joint tests were also called "design verification," they have been reported in the preceding section. The scaling design of the verification specimens has been governed chiefly by the large size of the wings and the difficulty of scaling the joints. This has resulted in roughly one-quarter size parts in which full-scale stresses are developed. The typical truss-to-cover joint was left full size in these specimens since it was felt the 1/4-inch-diameter bolt could not be meaningfully reduced in size.

7.6.1 Wing/Fuselage Joint Tension Tests

The Z3578686-505 graphite strap wraparound tension test (Figure 140) was used to obtain design values for combined transverse bearing and laminate tension stresses in the wing/fuselage joint concept. The small joint represented the larger joint and developed the same bearing and tension stresses at its 4200-pound design load. Two tests were made from the same "tear drop" laminate by cutting it into two pairs of straps.

The first specimen failed in the strap bearing area at 4740 pounds of load. The second failed at 4640 pounds in the same area. See Figure 141 for relation of small joint to large joint tension tests.

Fabrication of the Z5578687-503 large joint tension specimen was discussed in Paragraph 7.2.3. See specimen drawing, Appendix A, and Figure 141. Two sheets of photoelastic coating were bonded to the outer web skin in order to obtain shear distribution emanating from the high strength loading bolt. These can be seen in Figure 142. The specimen was mounted in a fixture (ZD007488) and tested in a Universal Testing Machine (Figure 142). A tension load was applied through an adapter block to the high strength bolt. This central load was reacted at each end of the box beam as a shear parallel to the webs (see Figure 143). Test loading was applied in 5000-pound increments with stress distribution being photographed at each increment.

Figure 148 shows the stress pattern in the photo stress coating (original in color) just prior to failure at 44,000 pounds. Design ultimate load was 34,400 pounds without fitting factor. A fitting factor of 1.25 was applied (assessment of uncertainty in major composite joints). Cracking sounds were noted beginning at approximately 25,000 pounds with the ultimate failure load occurring at 44,000 pounds. Photostress coating on the exterior of the specimen indicated uniform distribution of stress into the shear webs; however, color fringe changes in the immediate joint buildup area indicate presence of stress concentrations. At this point, it is conjectural whether bond failure at one of the internal straps initiated failure with subsequent longitudinal splitting of the web at the cap, or if web splitting initiated at the specimen end due to jig effects, in which case the joint may be stronger than tested.

7.6.2 Truss Action Tests

This test verified several design predictions regarding a chordwise slice of the truss web wing. Both bolted and bonded (Scheme A) joints were tested. These tests measured:

- Maximum transverse load capability of the trussed wing without special provisions for concentrated load introduction
- Joint rotational stiffness
- Compression web stability design.

Paragraph TBD contains photographs of the Z5578684-1 and -501 specimens and closeups of the joints.

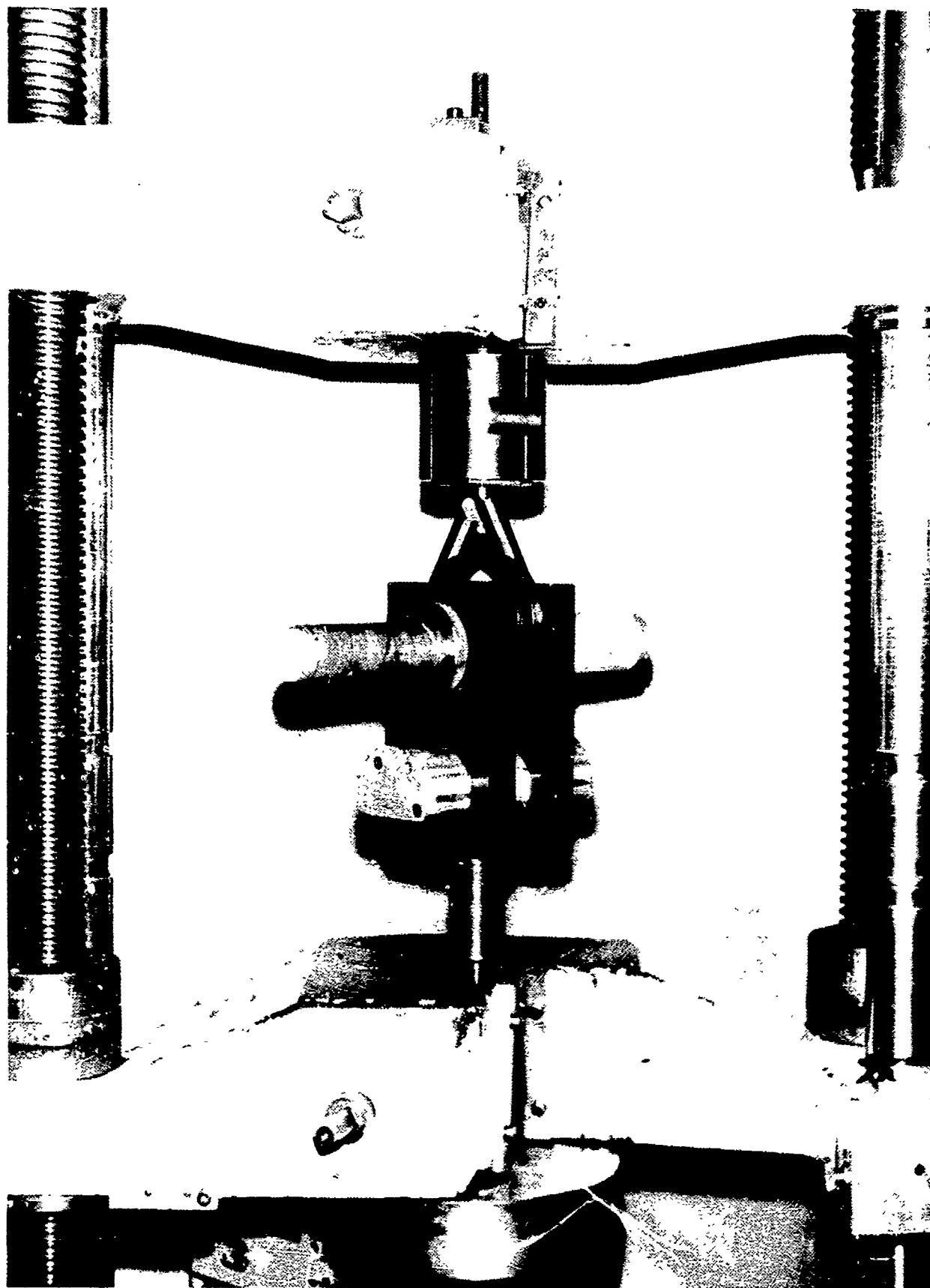


FIGURE 140. Z3578686-505 LAMINATE COMBINED BEARING AND TENSION TEST

DESIGN DEVELOPMENT TEST RESULTS

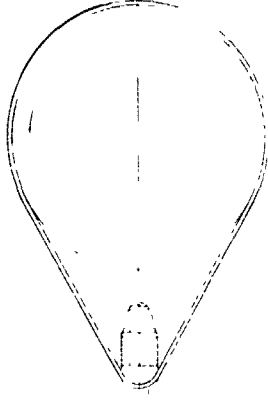
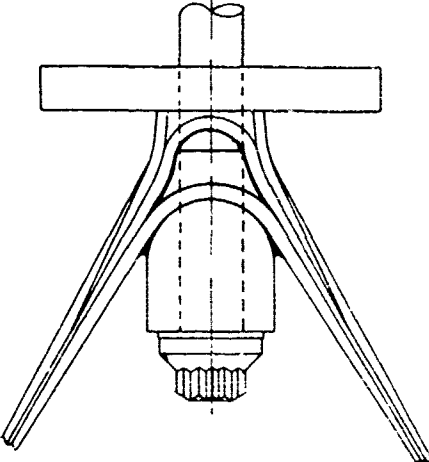
| TEST | SPECIMEN | RESULTS |
|-------------|---|--------------------|
| MAJOR JOINT |  | 4760 LB 4640 LB |
| MAJOR JOINT |  | 44,000 LB |

FIGURE 141. LARGE JOINT TENSION TEST RESULTS

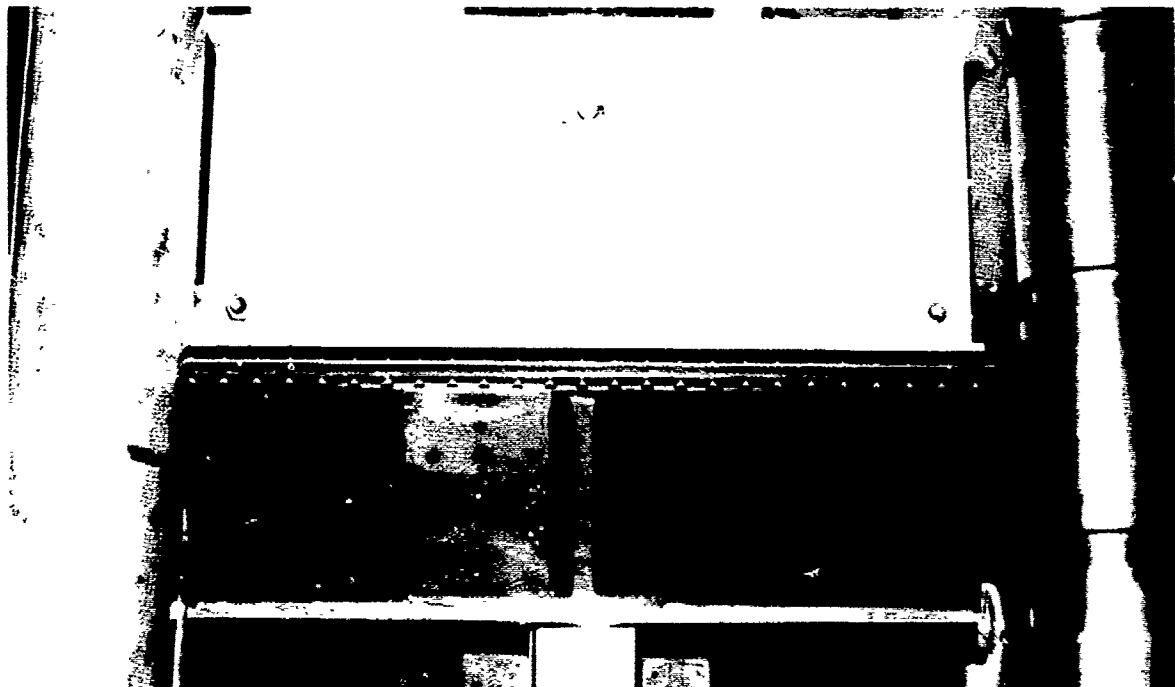


FIGURE 142. Z5578687-503 SPECIMEN IN TEST MACHINE

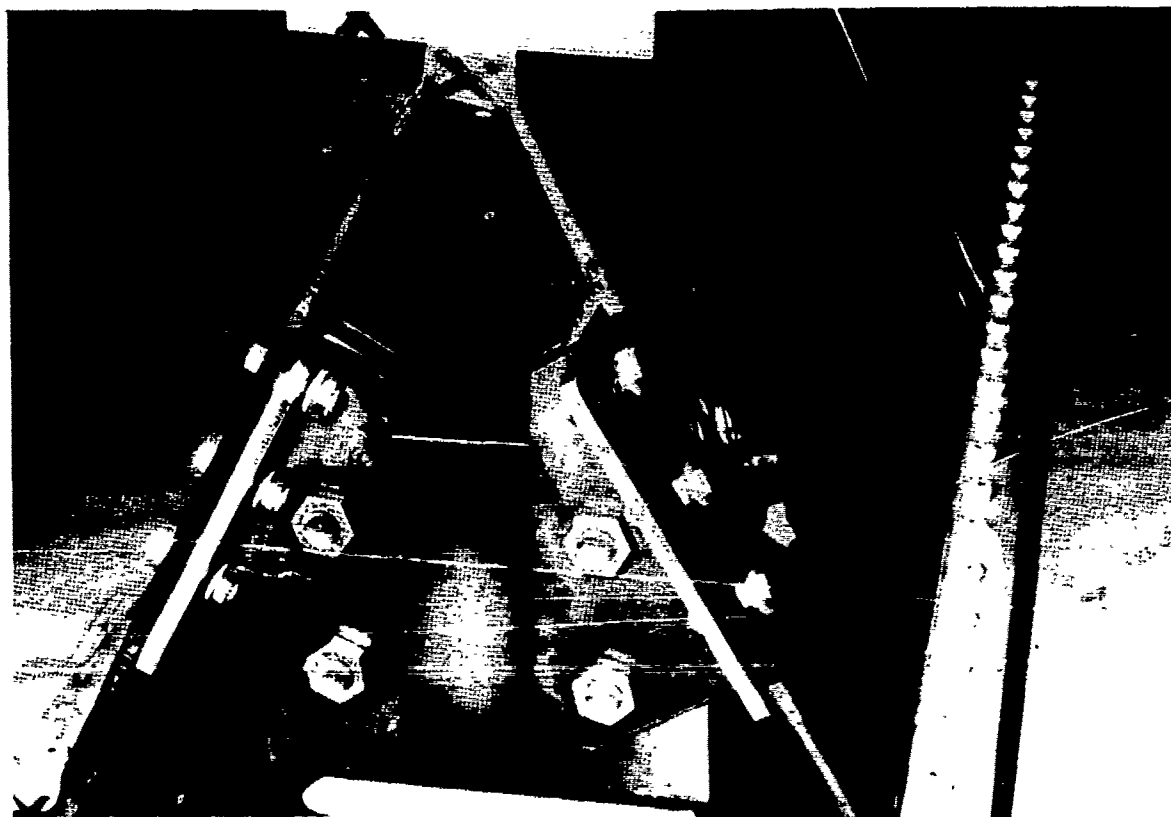


FIGURE 143. 25578687-503 SPECIMEN, SHOWING FAILURES IN END

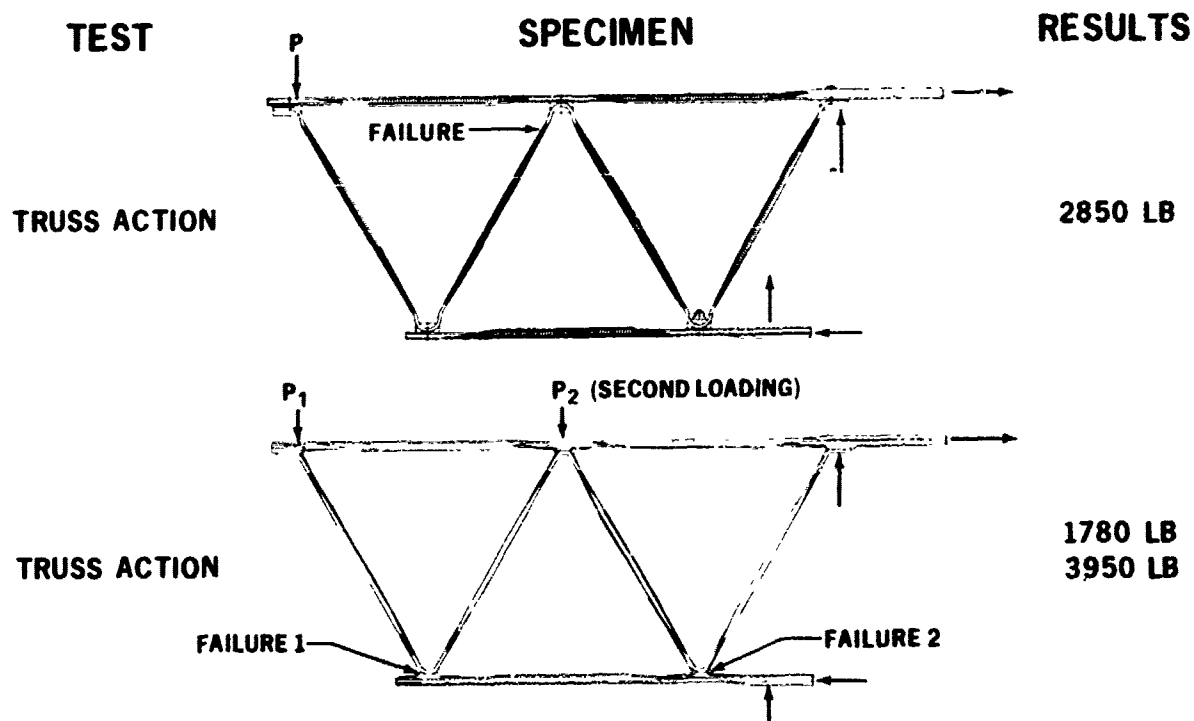


FIGURE 144. TRUSS ACTION SPECIMEN TEST RESULTS

Each specimen was bolted to a test fixture (ZD007331) and the assembly installed in a Universal Testing machine for cantilever beam test to failure as shown in Figure 110.

Figure 144 shows failure results for both specimens. Design load was 2500 pounds in each case.

The bolted joint specimen was instrumented with electrical-resistance strain gages (located as shown on ZA007470, Appendix A), while deflection data were obtained for both specimens. Strain data from upper and lower covers indicated the inner facing of each cover strained differently than the outer facing due primarily to the eccentric neutral axes of the panels. See Figures 145 and 146. This was not significant since at failure load the truss web was tension critical with web failure near the upper cover at the second node (Figure 144).

The bonded joint specimen failed at 1780 pounds by a shearing action within the graphite laminate at the lower web joint to the boron cover. The quality of the laminate in this region was suspect.

The second loading at the next joint produced a much higher failure load, 3950 pounds; however, the proximity of the lower joint to the steel doubler and the jig meant much load was going directly to the jig. The joint failed in an identical manner to the first joint.

Figure 147 shows the load-deflection comparison of the bolted and bonded specimens. Deflection was measured vertically at the point of load application. The bonded specimen proved to be generally stiffer in the load range of possible comparison. It is believed the "yielding" evidenced in the higher load range of the bolted specimen is due to secondary bending of cover panels and compression webs introduced by joint rotations.

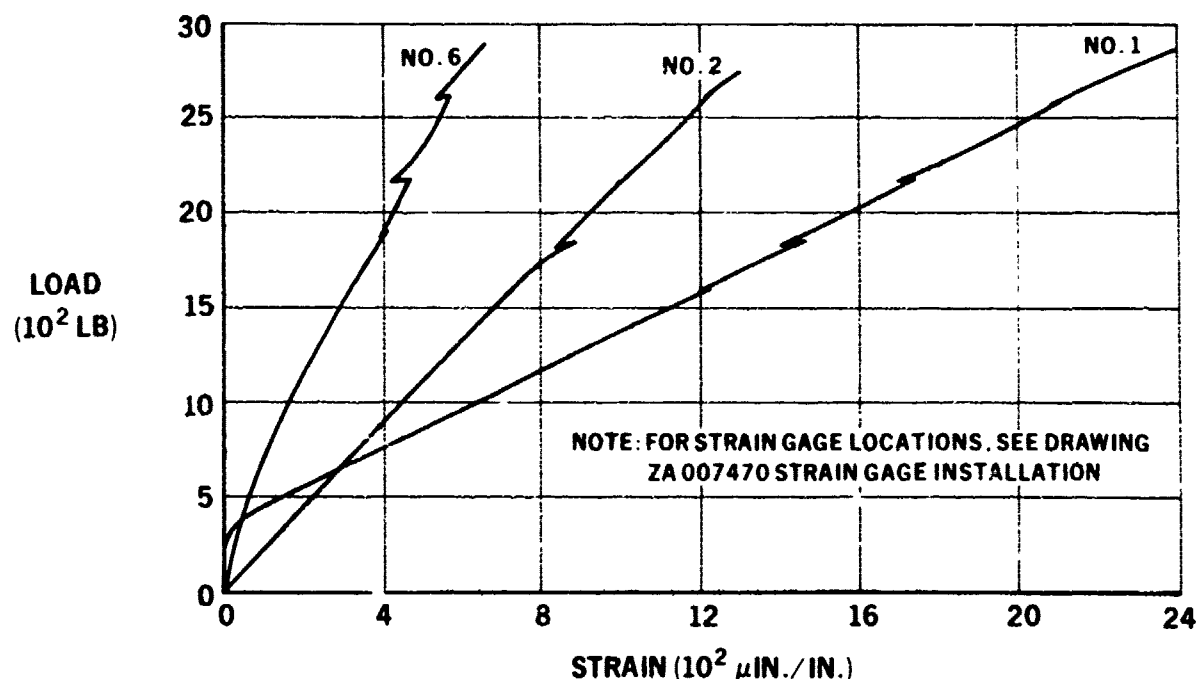


FIGURE 145. LOAD-TENSILE STRAIN RELATIONSHIP FOR Z5578684-1 TRUSS SPECIMEN

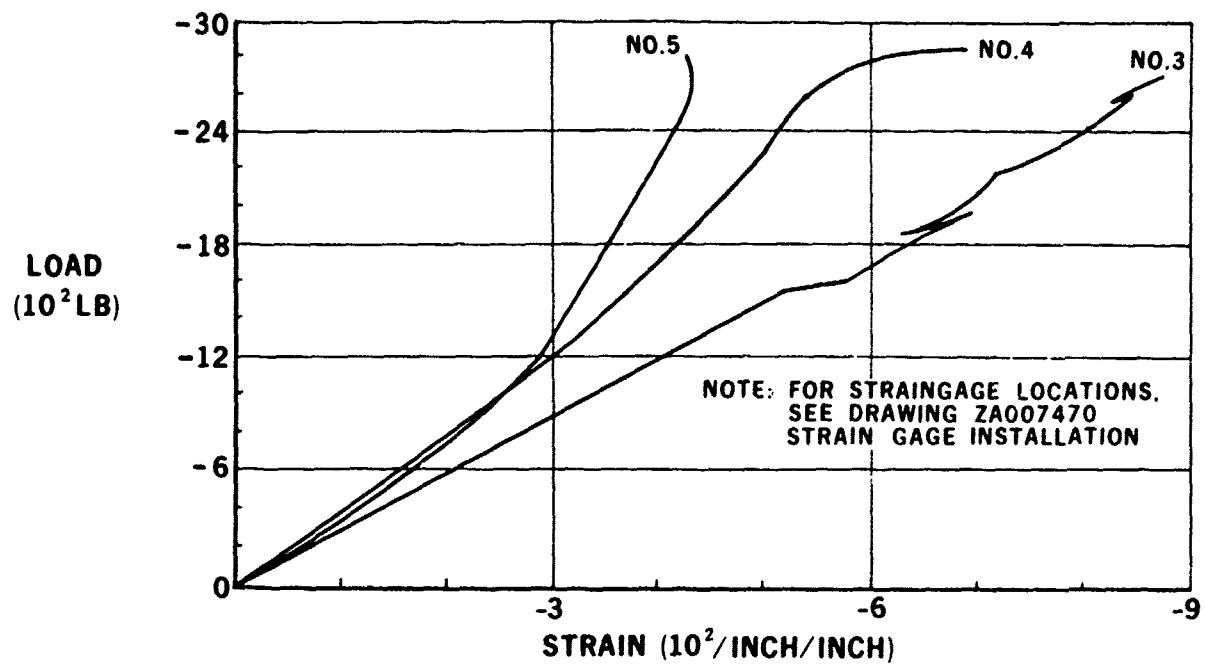


FIGURE 146. LOAD-COMPRESSION STRAIN RELATIONSHIPS FOR Z5578684-1

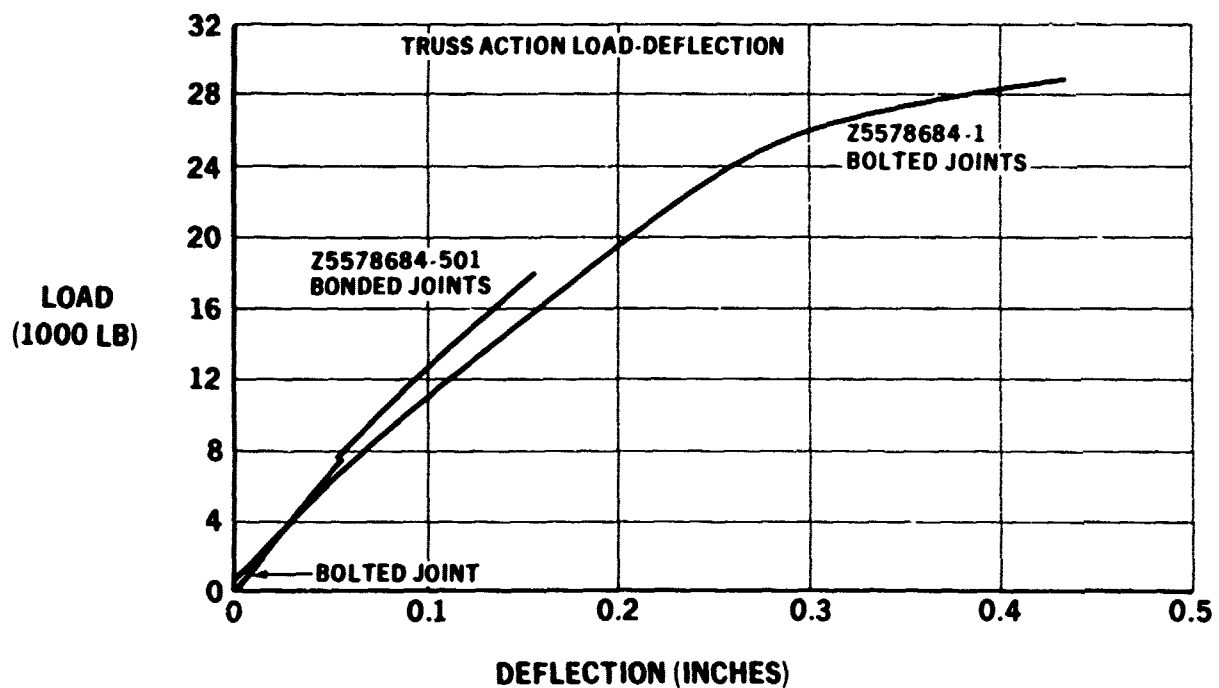


FIGURE 147. COMPARISON OF TRUSS ACTION SPECIMEN DEFLECTIONS



FIGURE 148. PHOTOSTRESS PATTERN IN 5578687-503 NEAR FAILURE

7.6.3 Substructure Tests

Four sandwich struts per Drawing Z3569984 were fabricated and tested, two in compression and two in static tension. The four parts were identical. The first compression specimen was difficult to load uniformly without bending. The compression specimens failed by laminate compression in the test area. The design requirement was 690 pounds (62,700 psi), compression and tension. The specimen was a one-fourth scale representation of a typical center wing section strut.

Static tests were conducted in a Universal Testing Machine, with loads being applied continuously until failure developed. Figure 149 shows tension load being applied through standard test machine clevis fittings and introduced into the specimen through clevis plates bolted to the test article. Compression loads were introduced through angles bolted to the test specimen, as shown in Figure 150.

Strain data were published in Appendix C of Reference 7, while Table 59 summarizes the test data. Note that 121 ksi was achieved in the two-ply compression strut facings and 151 ksi was achieved in the tension strut.

Because of intercell buckling of thin, highly stressed face sheets on this specimen, 1/8-inch cell core is required as well as substantial core shear and compressive moduli to avoid the wrinkling mode of failure. Non-metallic core not being available with these properties, aluminum core was selected.

7.6.4 Box Beam Bending and Torsion Test

Fabrication of the Z5578687-1 box beam was discussed in Paragraph 7.2.3.

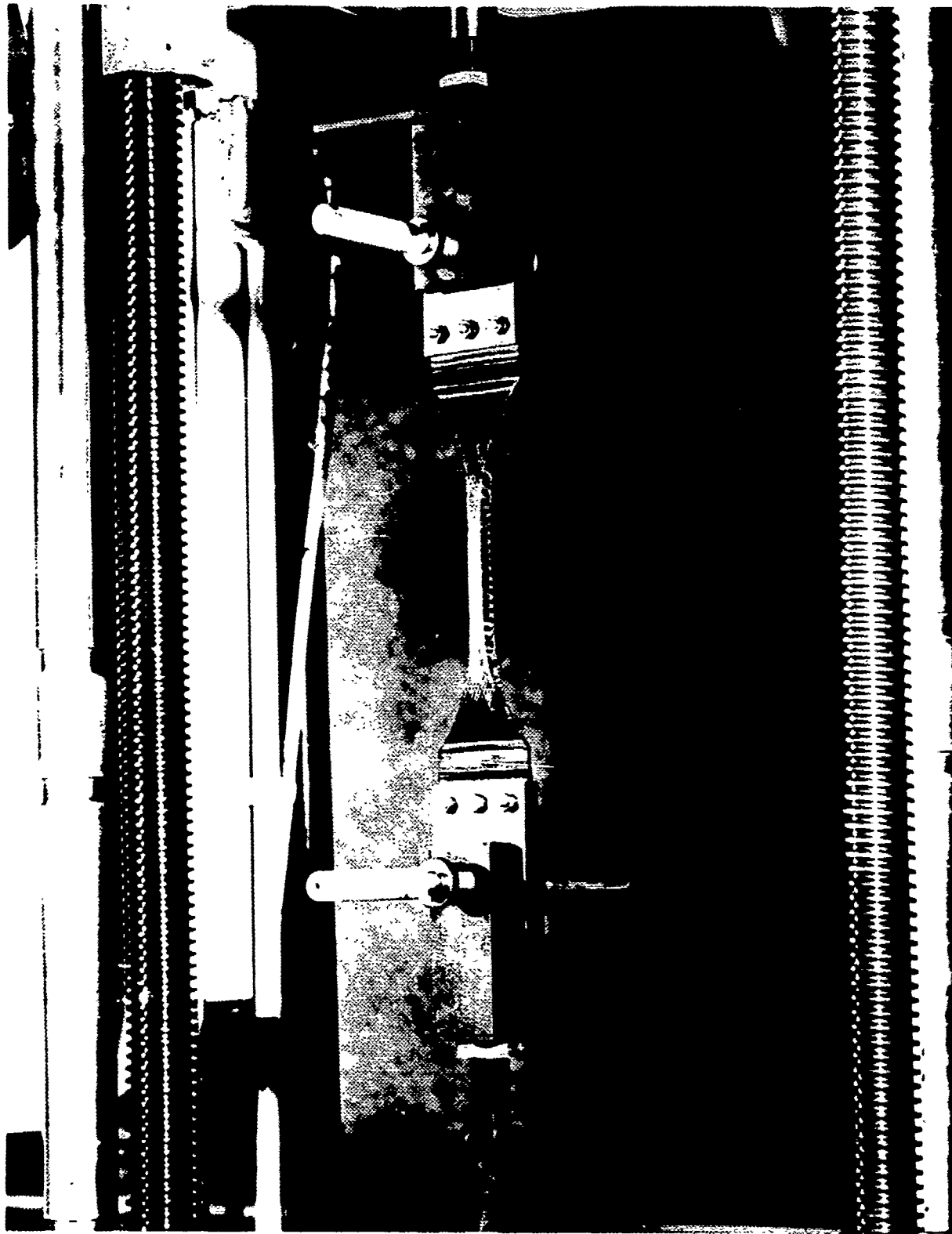


FIGURE 149. CUTOUT TRUSS WEB ELEMENT TENSION TEST SETUP

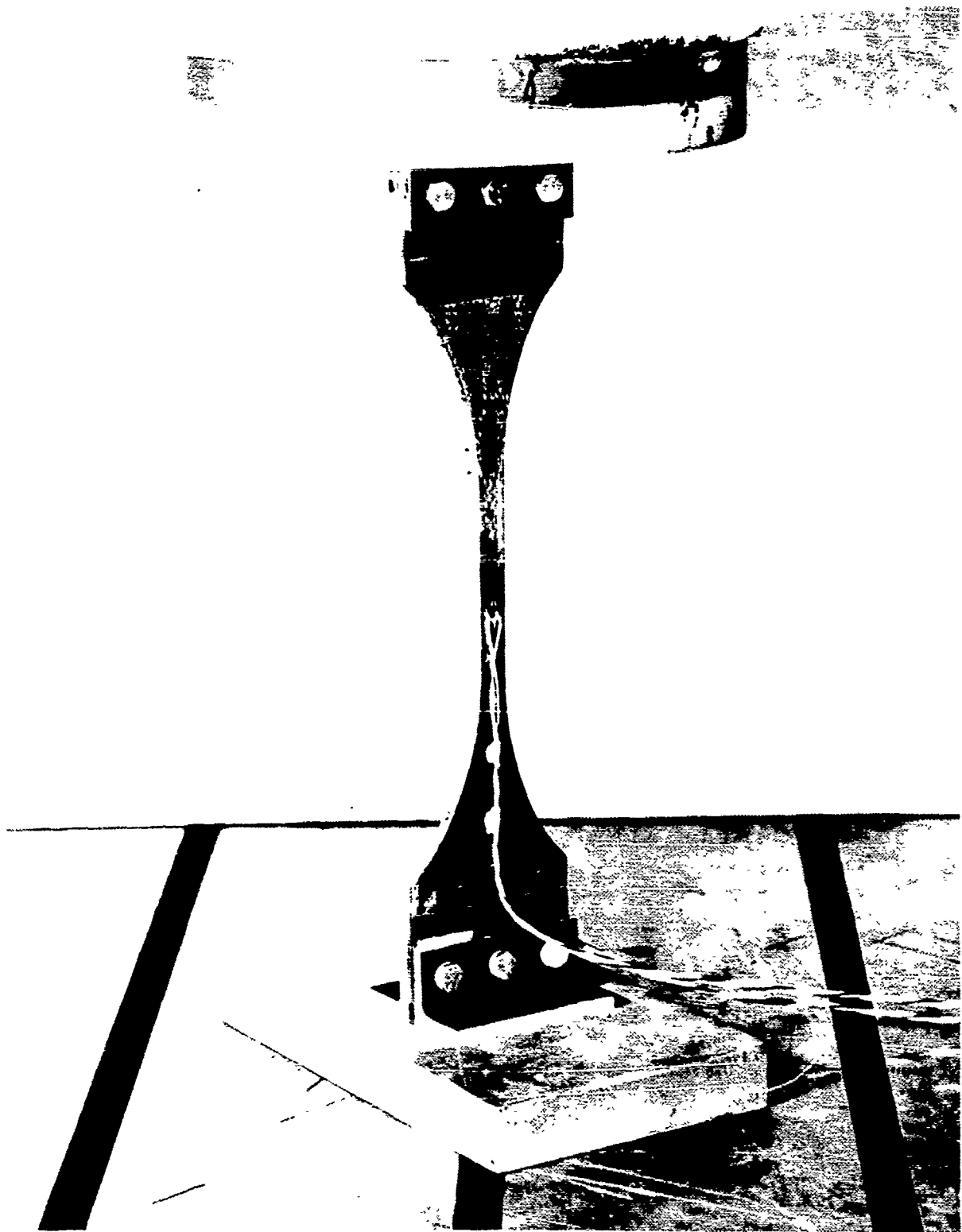


FIGURE 150. CUTOUT TRUSS WEB ELEMENT COMPRESSION TEST SETUP

TABLE 59
SUMMARY OF CUTOUT TRUSS WEB ELEMENT TESTS - Z3569984

| TYPE OF TEST | TOTAL SKIN THICKNESS (IN.) | SKIN WIDTH (IN.) | SKIN AREA (IN. ²) | LOAD (LB) | FACING STRESS (KSI) | MODULUS - E (MSI) | |
|--------------|----------------------------|------------------|-------------------------------|-----------|---------------------|-------------------|------------|
| | | | | | | GAGE NO. 1 | GAGE NO. 2 |
| COMPRESSION | 0.022 | 0.50 | 0.011 | 920 | 83.64 | 21.45 | 17.04 |
| COMPRESSION | 0.022 | 0.50 | 0.011 | 1340 | 121.82 | 22.73 | 20.79 |
| TENSION | 0.022 | 0.50 | 0.011 | 1663 | 151.18 | - | - |
| TENSION | 0.022 | 0.50 | 0.011 | 1657 | 150.64 | - | - |

The box was loaded as shown in Test Setup Drawing ZJ005450 (Appendix A), with a predominantly constant bending moment in conjunction with uniform compression. The lower skin was subjected to a uniform compression of twice the jack load. Relatively small torsional loads were also applied. The box consisted essentially of a boron-epoxy honeycomb compression panel, graphite-epoxy honeycomb shear panels, and a steel cap to represent the tension skin.

The analysis of the box considered the following factors:

1. Buckling of the compression skin under pure compression and in conjunction with shear loading from the applied torque
2. Shear strength and shear buckling of the webs
3. Shear strength and bearing stresses of the various bolts
4. Stress concentrations at the bolt holes in the composites due to both the bearing load and the load running past the bolt hole
5. Different extensional moduli of the various components sharing the applied load.

The test load levels reflected typical patterns and stresses of the wing design. Hence, the ratio of shear stress (torque) to compression stress (bending) was established as $\tau \approx \sigma/5$. The analysis predicted failure of the boron-epoxy panel under combined compression and shear, and the loads to be applied during test were established as shown in Table 60.

TABLE 60
BOX BEAM TEST SUMMARY

| TEST SEQUENCE | TEST CONDITIONS SKIN ASSEMBLY | LOAD SCHEDULE LOADS | | MAXIMUM TEST LOAD | |
|---------------|--------------------------------|---------------------|-----------------|-------------------|-----------------|
| | | BENDING (LB) | TORQUE (IN.-LB) | BENDING (LB) | TORQUE (IN.-LB) |
| 1 | LIMIT COMPRESSION | 30,500 | 0 | 30,500 | 0 |
| 2 | LIMIT SHEAR | 0 | 64,000 | 0 | 64,000 |
| 3 | ULTIMATE COMPRESSION AND SHEAR | PREDICTED FAILURE† | | 40,000* | 32,000* |
| | | 40,000 | 32,000 | | |

* FAILED WITH 40,000 POUNDS BENDING LOAD AND 32,000 INCH-POUNDS TORQUE APPLIED † MAINTAIN $\tau = \sigma/5$ BY KEEPING $P_1 = 0.04 P_2$

7.6.4.1 Design Verification Test Method

The box beam specimen was mounted as a cantilever beam in the ZJ005450 structural test loading fixture, as shown in Figure 151, and statically tested three conditions:

1. Bending only to 100-percent design limit load
2. Torque only to 100-percent design limit load
3. Combined bending and torque to failure at 150-percent design limit load.

Test loads were applied through the ZJ005450-3 loading assembly and introduced into the specimen by the following detail parts (see Figure 152): -7 tee which was attached to the steel skin at the apex of the test article, two -5 clips bolted to the web assembly, and a -55 and -57 angle sandwiched about the skin assembly. The -11 reaction assembly, mounted to the opposite end of the box beam in the same manner as the load assembly, served as an adaptor for attachment of the specimen to the rigid test fixture.

Bending and torque loads were applied by three hydraulic actuators, each incorporating a strain-gaged load cell and an individual servocontrol system. The bending actuator was located 10 inches below the lower skin and parallel to the longitudinal centerline of the specimen, to introduce compression stresses in the skin assembly. The two torque actuators were positioned at the free end of the beam perpendicular to the longitudinal centerline, 20 inches apart, to introduce in-plane shear stresses in the skin and web assemblies. Load applications were in increments of the respective design limit loads and controlled by a manual load control and data acquisition system (see Figure 153) acting through each servo valve, while load cell data were monitored on strip chart pen recorders. Strain and deflection data were gathered from electrical resistance strain gages and displacement transducers. These data were recorded on digital printout paper tape for on-site visual monitoring, punched cards, subsequent computer reduction, and presentation in a tabulated and graphical format. Test loads and conditions were summarized previously in Table 60.

The test structure accepted 100-percent design limit load in the bending only and torque only conditions. Load input was then increased (bending and torque simultaneously) until 150-percent design limit load was attained; however, as load was being brought up beyond this level, an inadvertent setting on the emergency dump system triggered an instantaneous removal of all test loads. Subsequently, loads were again simultaneously applied to 150-percent design limit load. Shortly after achieving this load level, failure developed. The primary and secondary failure modes are displayed in Figures 154 through 156.

7.6.4.2 Failure Analysis of Z5578687-1

The failure occurred at the anticipated load and in the manner predicted. The primary failure was in the boron-epoxy sandwich skin (See Figure 154). This was not associated with complete loss of load capacity across the section because the solid caps at the corners of the webs were not damaged there. Consequently, the bending load was not transferred out of the sand-

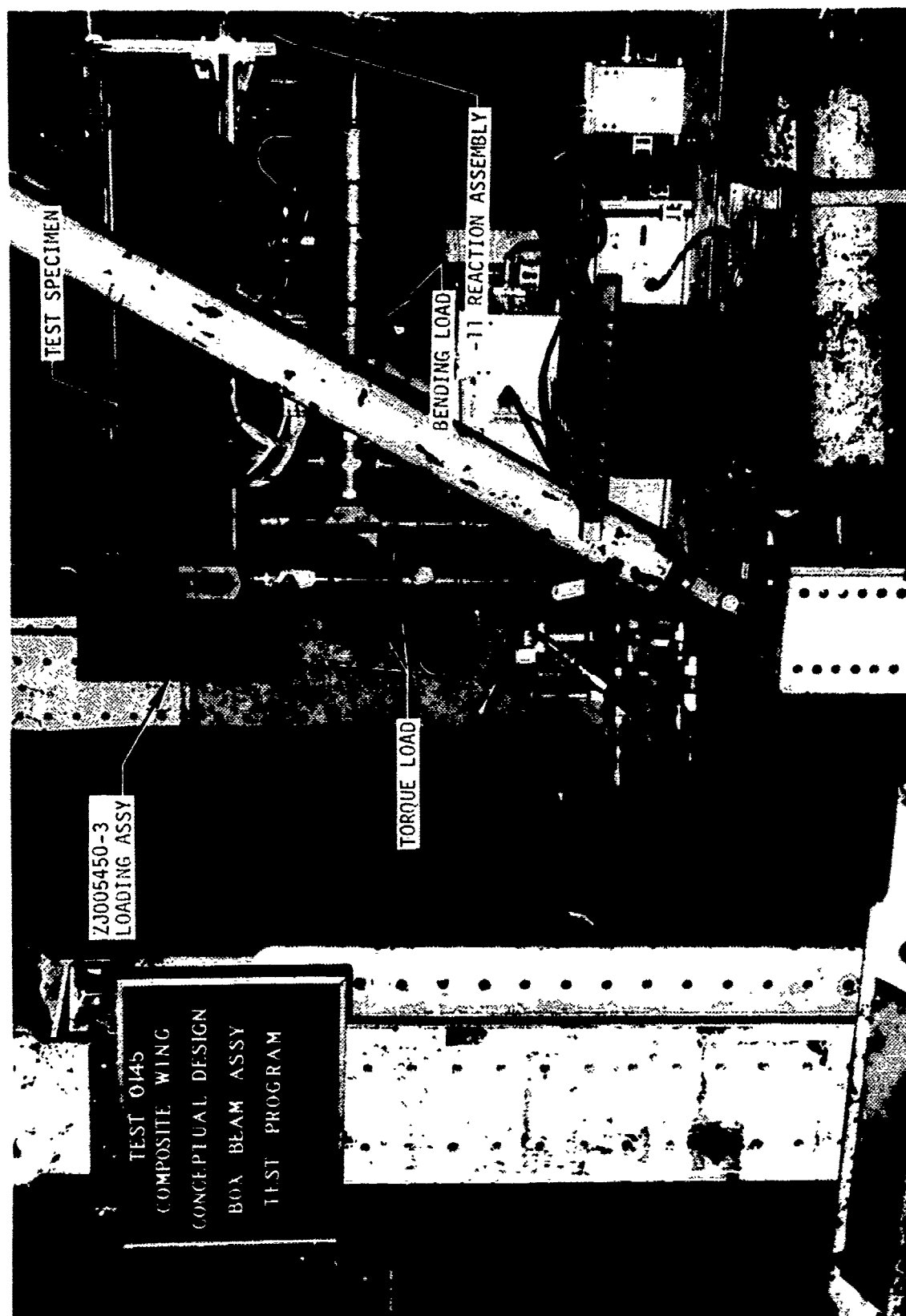


FIGURE 151. BOX BEAM TEST SETUP

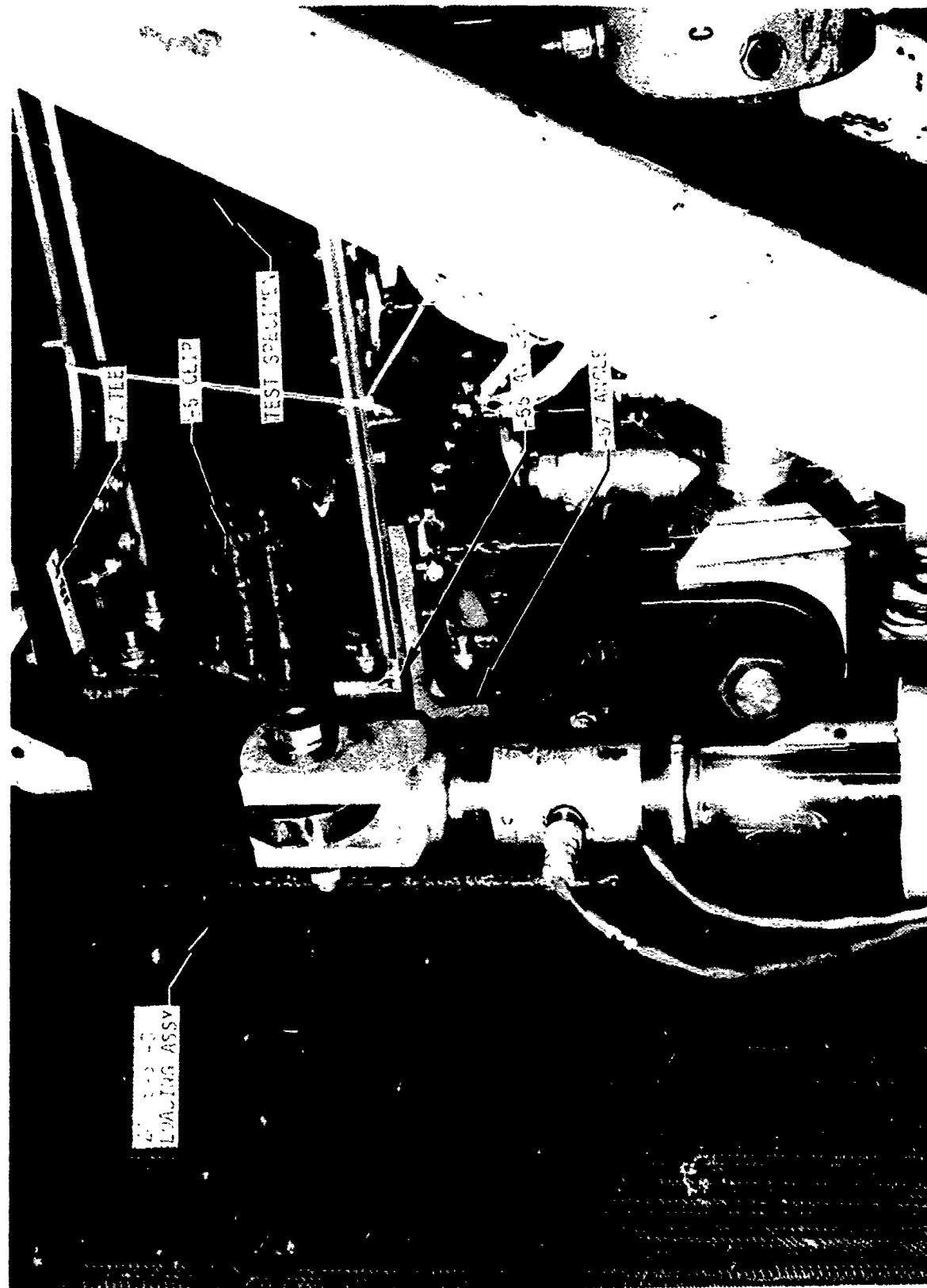


FIGURE 152. BOX BEAM LOAD INTRODUCTION DETAILS

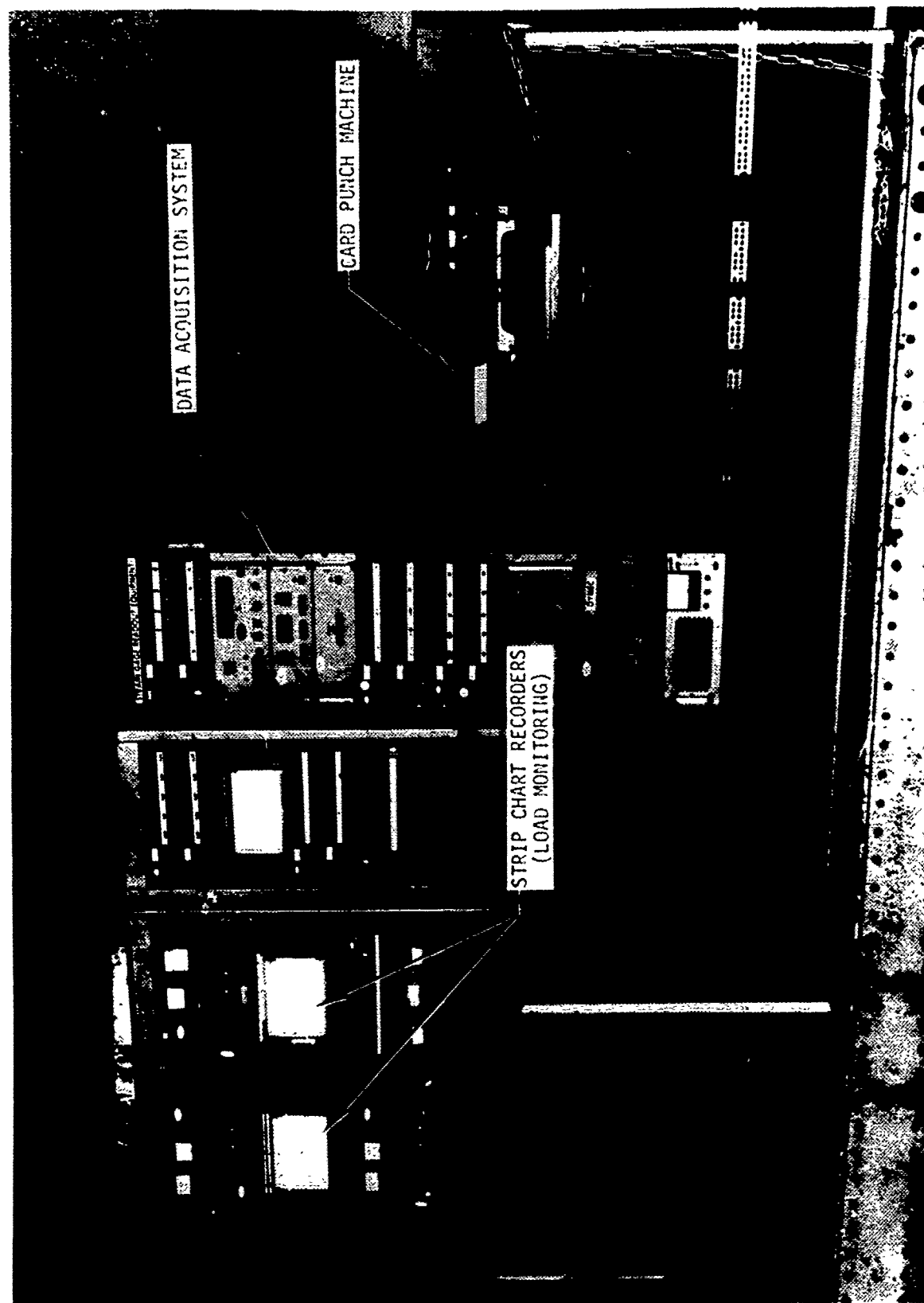


FIGURE 153. LOAD CONTROL AND DATA ACQUISITION SYSTEM



FIGURE 154. PRIMARY FAILURE, SKIN ASSEMBLY - REACTION END

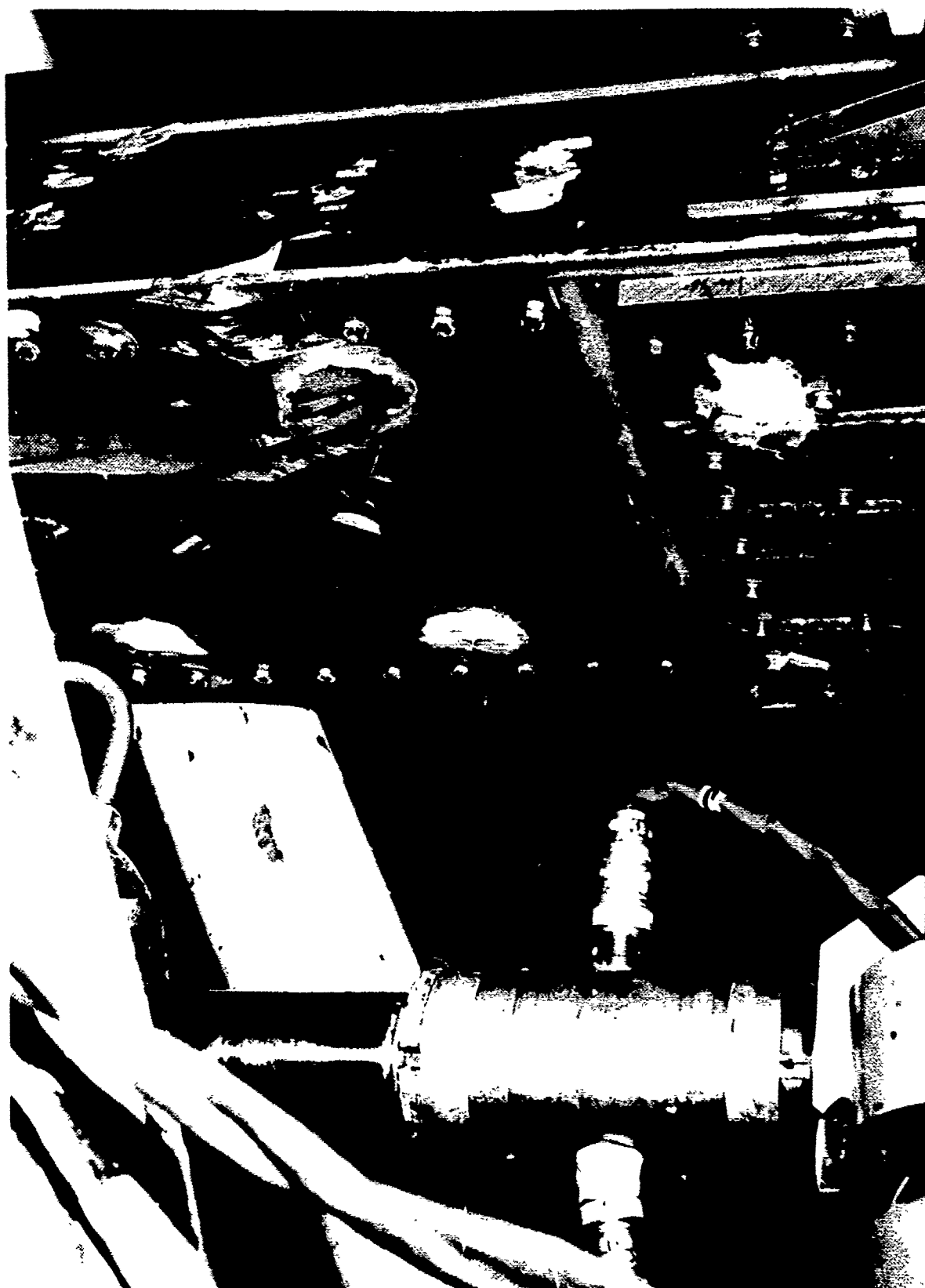


FIGURE 155. SECONDARY FAILURE, SKIN ASSEMBLY – LOADED END

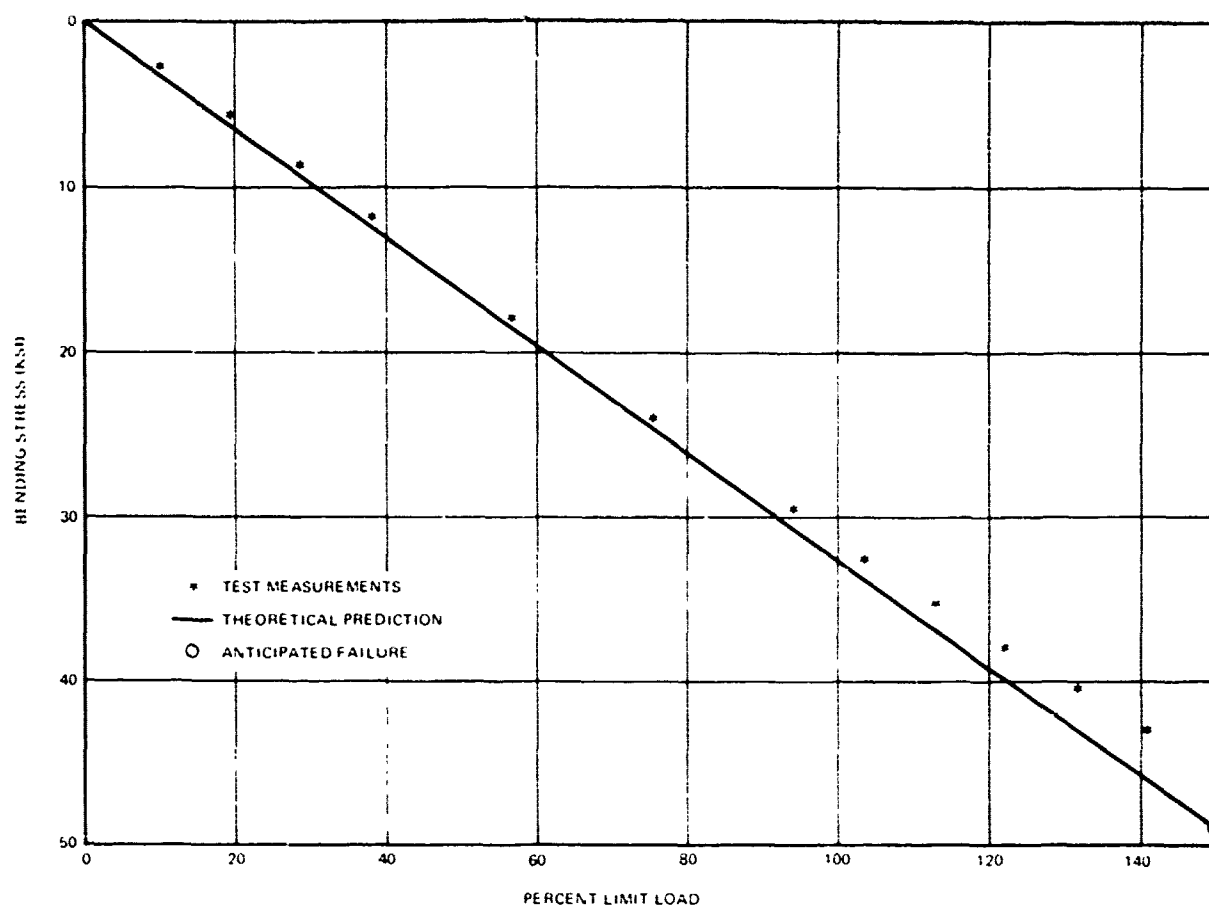


FIGURE 156. SECONDARY FAILURE, WEB ASSEMBLY - LOADED END

wich portion of the lower panel and into the caps formed at the bolted edges of the panels. Having a large proportion of glass fibers at this location, the caps continued to pick up load because their ultimate strain capacity exceeded by far that of the filaments. However, the ultimate load capacity of the caps alone was less than the failure load applied, so the caps failed secondarily at their weakest location, elsewhere along the length (see Figure 155). The secondary failure was associated with the web failure shown in Figure 156. There was audible creaking of the structure, long prior to failure, but both failures occurred so close together as to be indistinguishable to the eye. Were one to hypothesize that failure occurred in the reverse order, one is left with the problem of explaining the lower panel failure after it would have been unloaded by the edge cap failure, as well as the arresting of the edge cap failure without progressing far across the lower panel (see Figure 155).

The test specimen was instrumented with the objective of providing a correlation between analysis and test. While the failure load agreed precisely with the prediction, a comparison of the strain gage readings with the predictions reflecting the local extensional modulus of the laminate revealed that the caps at the corners of the triangular cross section accepted proportionally more load than anticipated. This difference is explained by the comprehensive data acquisition in terms of shear lag in the lower panel. As the cover caps curved downward under the bending load, the lower skin did not deflect down as rapidly. Significant transverse bending stresses were recorded, with most of the transverse bending strains concentrated in the skin sections near the edges of the honeycomb. In order to quantify this discrepancy, it is noted that the Panbuc analysis predicted a compressive buckling stress of 65 ksi for simply supported edges located at the estimated points of inflexion. This value for a uniform panel was reduced to 55 ksi to account for the tapered honeycomb. The limit bending case developed compressive stresses ranging from 32.5 to 35.8 ksi on the outer face and up to 38.5 ksi on the inner face. The transverse stresses changed sign across the honeycomb. The discrepancy in skin stresses due to neglecting consideration of load shifting through transverse deflection of the panel is, consequently, some 1 to 10 percent, as illustrated by the typical load-stress curves in Figure 157. Much the same discrepancy was observed in the failure case under combined load. It seems probable that the reason the predicted load was still attained is that the analysis was based on the old monolayer axial compression allowable of 300 ksi for the boron-epoxy, rather than the current 400 ksi. The caps would therefore carry somewhat more load prior to failure, masking the effect of the distortion of the sandwich panel.

The torque behavior was quite linear to failure also. The shear stress level established was relatively low, being based on the standard rail shear specimen. New IRAD tests performed at Douglas during the program with an improved shear specimen raised the average test result to 60 ksi for shear on +45-degree Narmco 5206 graphite-epoxy. In comparison with the prior test results, it is evident that only about half this result should be used near panel edges, discontinuities, or inserts, but that advantage can be taken of the weight saving due to the much higher allowable in the larger portion of a shear panel.



CHANNELS 8A 8B 8C LOAD TO FAILURE CONDITION

FIGURE 157. COMPARISON BETWEEN THEORY AND TEST FOR TEST TO FAILURE OF Z5578687-1 TRIANGULAR BOX BEAM

7.6.5 Fillet Bonded Box Beam Pressure Test

Fabrication and inspection of the Z5578687-505 box beam is discussed in Paragraph 7.2.3c. It was originally designed to demonstrate a relatively low level of shear adequacy of the fillet bond concept, with a pressure test to failure following the shear test. The objective changed to that of demonstrating the shear strength of a long fillet bond, therefore it was necessary to reinforce the fabricated specimen because of a low margin of safety in the upper bolted connection with respect to the anticipated design ultimate fillet bond shear load (2650 pounds/inch). While this modification was being accomplished, a proof pressure test was conducted to conserve program time and because of analytic assessment that adequate margin of safety existed for the interlaminar tension failure mode, based on previous "loop tension" tests. The inaccuracy of this assessment was proved by the premature failure of the specimen during the pressure test.

The specimen drawing (Z5578687-1, Appendix A) shows 3/16-inch-diameter bolts through the fillet bond line, but these were not installed. It was realized bolts would rotate about the thick bond line during joint shear deformation. Nor would bolts prevent peeling since the toe of the stiff fillet is too far from the bolt centerline.

Figure 158 shows the pressure test setup. Steel plates were sealed against the ends of the specimen and were connected by rods to remove longitudinal forces. Pneumatic pressurization was introduced to design limit pressure, 27 psi, which was scaled to twice actual pressure, ($27 \text{ psi} \approx 2 \times 20 \text{ psi}$) (0.67), since the panel widths were 1/2 scale with respect to the wing station simulated. Failure occurred at 24 psi. The lower cover pulled away from the bond line simultaneously at both bonds, leaving graphite layers in the EA9306 adhesive (Figure 159). A thin, light-colored line of adhesive at the toe of the fillet bond can be seen in the lower portion (Figure 159). The failure originated at the toe of this fillet by combined bending and interlaminar tension within the cover laminate. It is noted that the panel edge was one-half as thick as the wing cover panel would be, thereby increasing panel edge rotation and peeling beyond that present in the full-scale wing, nevertheless the low interlaminar tension strength of the graphite laminate (Narmco 5206) is seen to be a detriment to this bonding concept.

7.6.6 Final Demonstration Component

The aft two cells of the five-cell truss web wing box were selected as a critical segment of the conceptual wing design to be tested. The two-cell specimen was fabricated to approximately 1/4 scale and extended both directions from the sweepbreak a sufficient distance to meaningfully simulate the stressing of the wing.

TEST SPECIMEN

A sketch of the specimen is shown in Figure 160 and is detailed in Engineering Drawing Z5569987. It represents the sweepbreak and fuselage attach points where maximum bending and torque loads occur. The specimen was made approximately 1/4 scale to reduce fabrication costs. Composite materials used in its construction were Avco 5505 boron/epoxy for the upper skin and Narmco 5206 graphite/epoxy for the web structure and lower skin. The upper skin was fastened to the webs with titanium bolts, while the lower skin was joined with Hysol 9306 adhesive.

TEST LOADS

The load condition employed to test the specimen was one which yielded stresses at several specified points matching corresponding peak stresses in the wing box from two critical flight conditions. These conditions were a 3g symmetrical maneuver (max bending), and a fully extended flaps down landing approach at 120 knots (max torque). The test loads were applied to the specimen by four loads (V_1 , R_1 , R_2 , T). The loads R_1 and R_2 were hydraulically applied at the sweepbreak to simulate the wing-fuselage attach points. The load R_1 was applied in tension at the large 3/4-diameter aft attach bolt, while R_2 was applied as a compression load on the front web. The loads V_1 and T were applied at the ends of a very rigid fixture of such magnitude as to match a near-uniform spanwise stress distribution in the covers at the inboard end. The torque was required to compensate for the fore and aft offset of the upper and lower covers. This loading is illustrated in Figure 161.

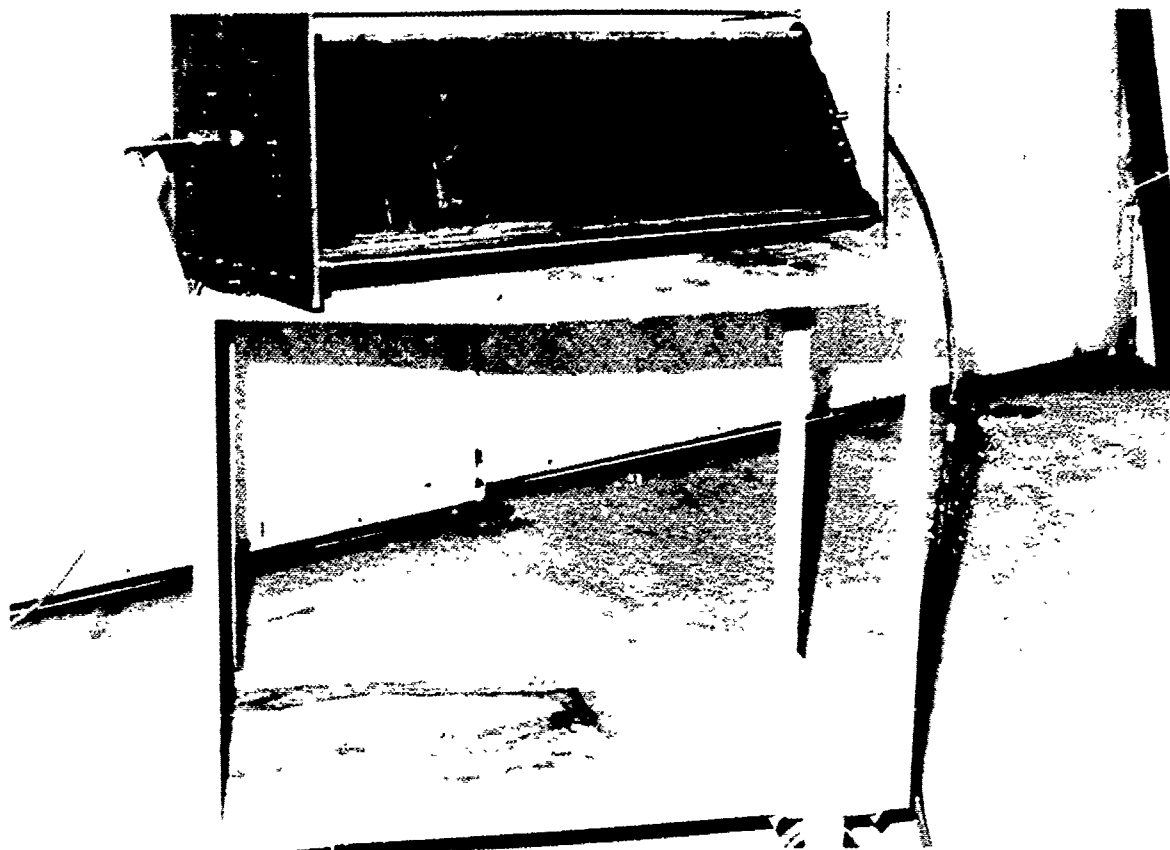


FIGURE 158. FILLET BONDED BOX PRESSURE TEST



FIGURE 159. CLOSEUP OF INTERLAMINAR TENSION FAILURE - Z5578687 WEB

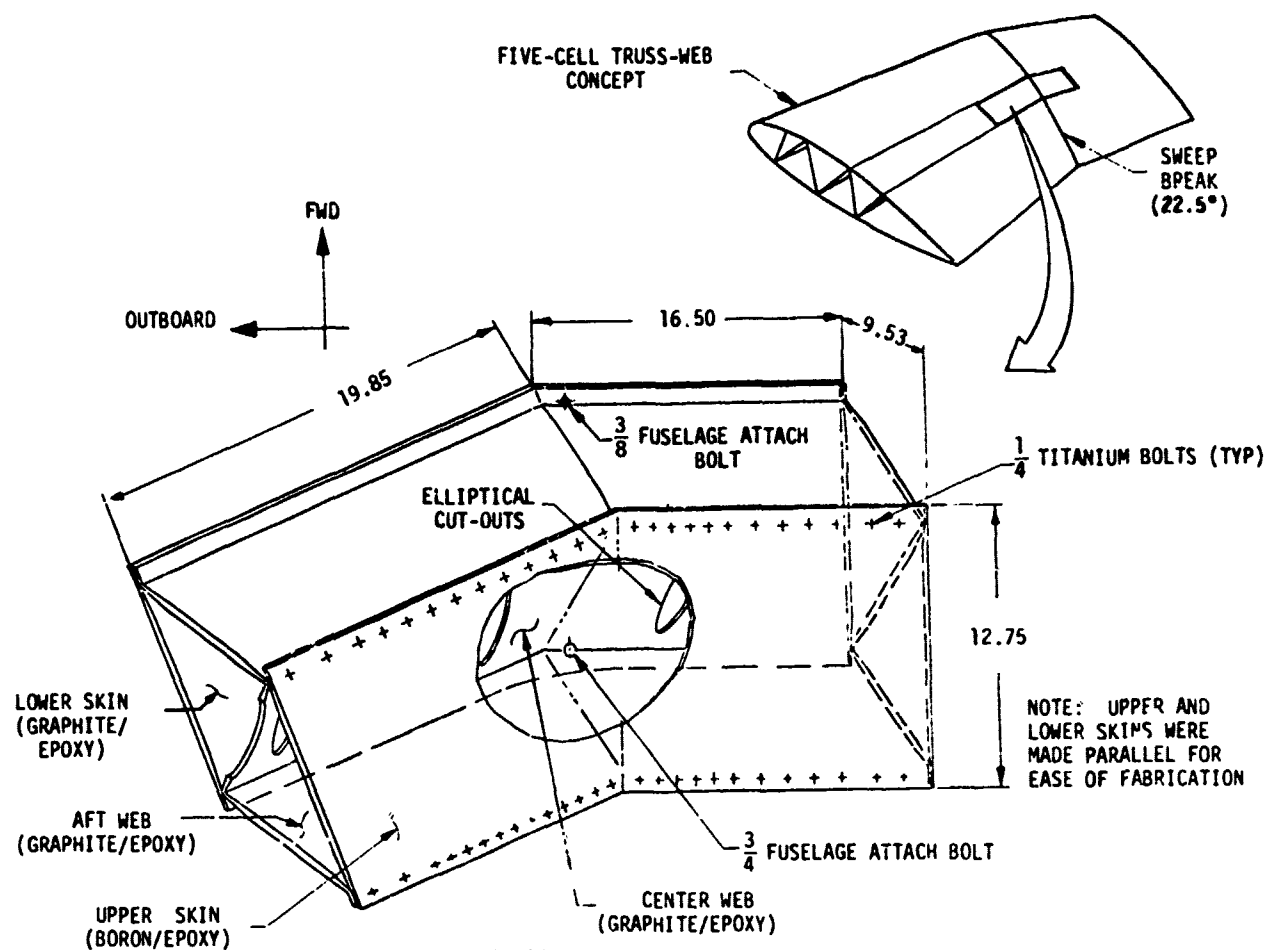


FIGURE 160. CONCEPTUAL WING BENT BOX SPECIMEN

| PT | LOAD (ULT) |
|----------------|--------------|
| V ₁ | 15773 LB |
| R ₁ | 35222 LB |
| R ₂ | 19449 LB |
| T | 295370 IN-LB |

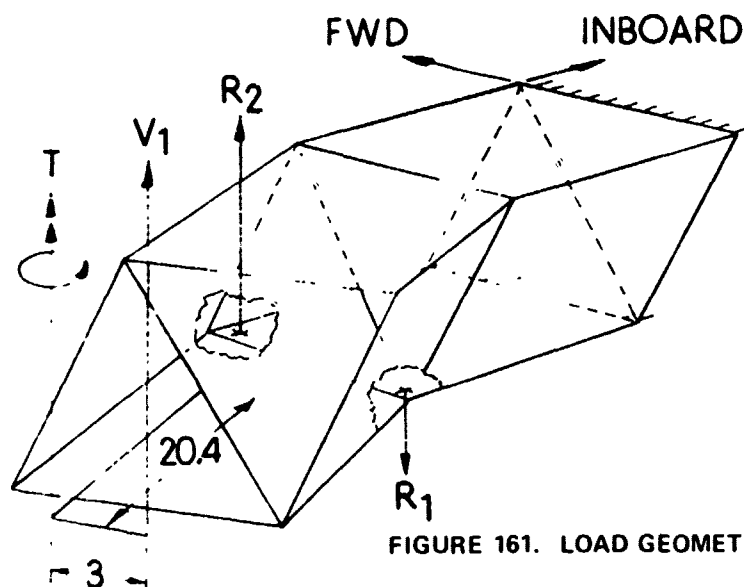
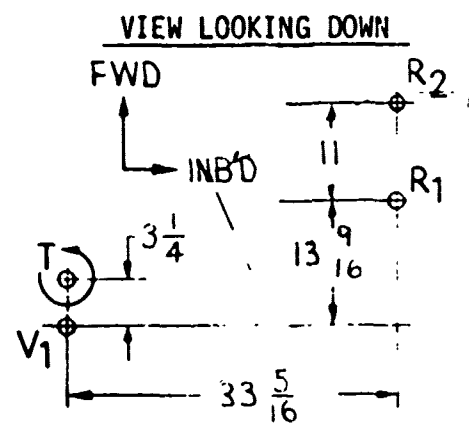


FIGURE 161. LOAD GEOMETRY SKETCH



TEST SETUP

Mechanical

The bent box specimen was supported as a cantilever by its inboard end in the ZJ008353 test fixture as shown in Figure 162. The outboard end of the specimen was fitted with a 20-inch-long steel extension (fixture ZJ008353-3) through which were applied the vertical test load (V_1) and the compensating torque load (T) referred to in the previous section. Two hydraulic actuators were required to apply torque load (T). The reaction loads R_1 and R_2 at the fuselage attach points were applied by a single actuator using the lever arm test fixture ZJ008353-29. All four actuators in the setup were 5-square-inch area on the pressure side and plumbed in parallel to a Sprague hand pump. See illustration of setup in Figure 163.

Electrical

The single pressure system required only one load cell which was installed on the V_1 actuator and connected to a digital readout device. Twenty electrical resistance strain gages were placed on the specimen as illustrated in Figure 164. Data from these gages were recorded by the Dymec Data Acquisition System on digital printout paper tape and subsequently reduced by the Douglas/IBM 370 computer.

TEST PROCEDURE

Preliminary Loading, 12-22-72

A preliminary 40-percent ultimate load was applied in 5-percent increments for the purpose of checking the performance of the loading fixture, strain gages and data acquisition system. Strain information was recorded at each increment. Strain gage R9, located on the inside surface of the lower skin outboard of the sweepbreak, was suspect. It showed lower strain in the chordwise direction than predicted by analyses. A single gage (S2) was installed opposite gage R9 on the outside surface of the lower skin to provide additional data in this area.

Ultimate Loading, 1-8-73

After a 20-percent exercise load was applied and released, strain gage data for zero load and the calibration values were recorded. Then ultimate loading was applied in 20-percent increments (see Table 61) holding approximately 5 seconds at each increment for data acquisition. Minor creaks were heard issuing intermittently from the specimen beginning at 20-percent load until a loud sharp sound signaled failure at 94-percent ultimate load. At that point the load dropped to 62-percent ultimate and stabilized there.

No attempt was made to reapply the load so as to preclude additional specimen damage and the possibility of obscuring the initial failure. The load was removed and the specimen taken down for inspection.

TEST RESULTS

Complete strain gage information as reduced by the Douglas/IBM 370 computer is presented in tabular and graphical format in Reference 8.

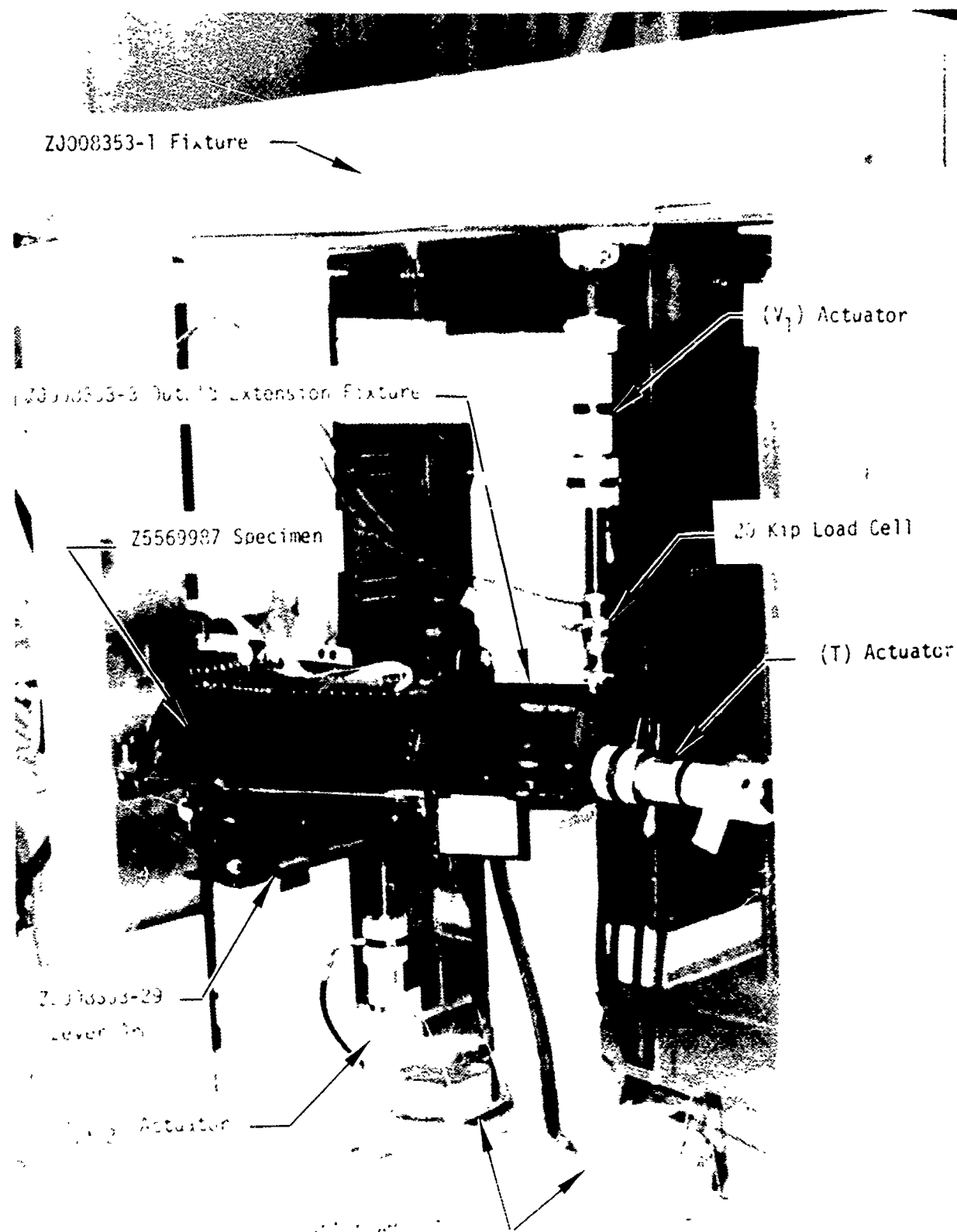


FIGURE 162. TEST SETUP, FINAL COMPONENT

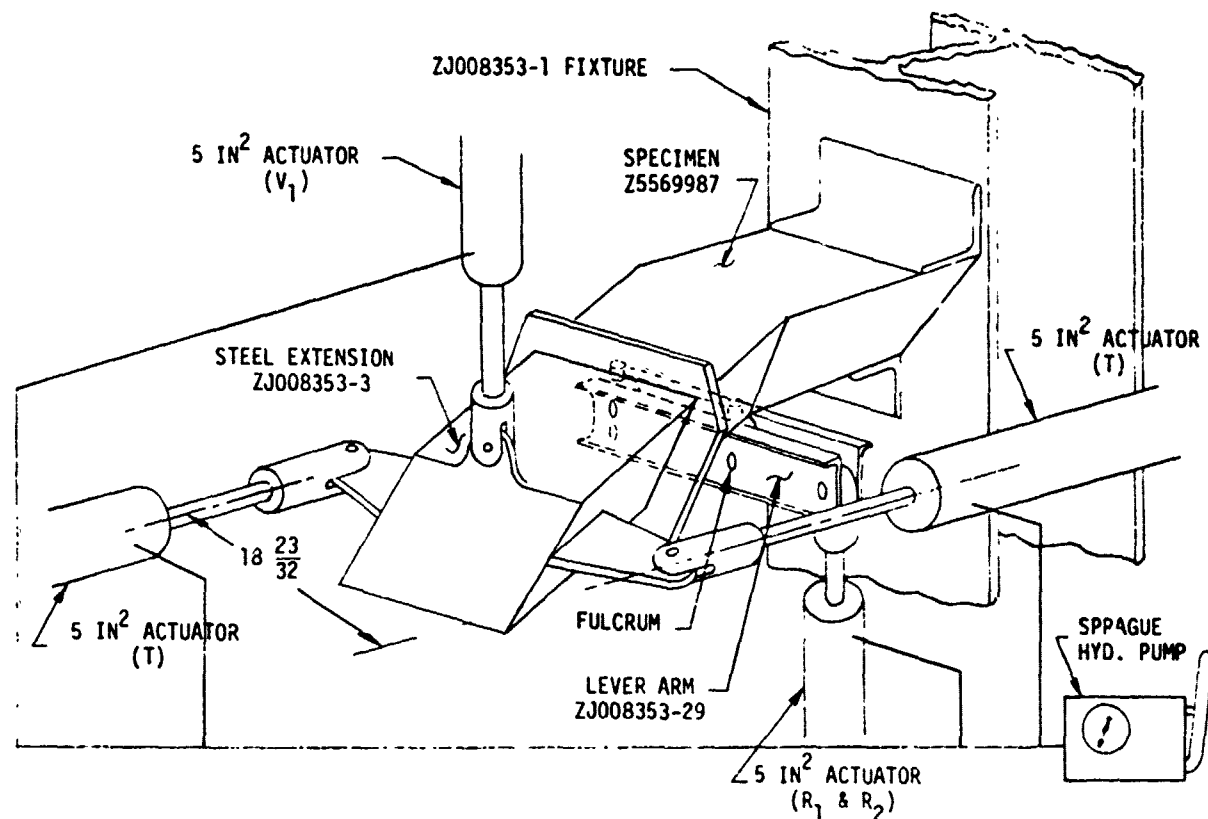


FIGURE 163. ACTUATOR SETUP

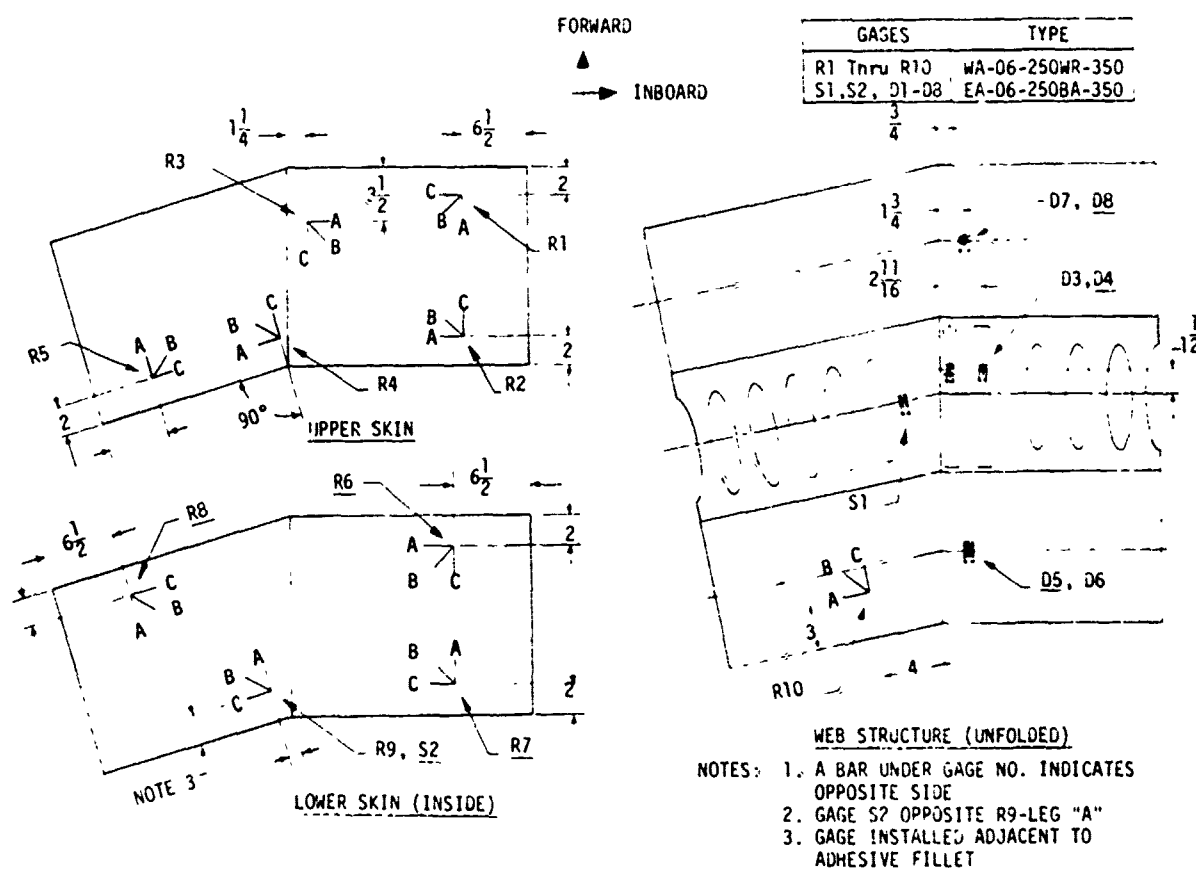
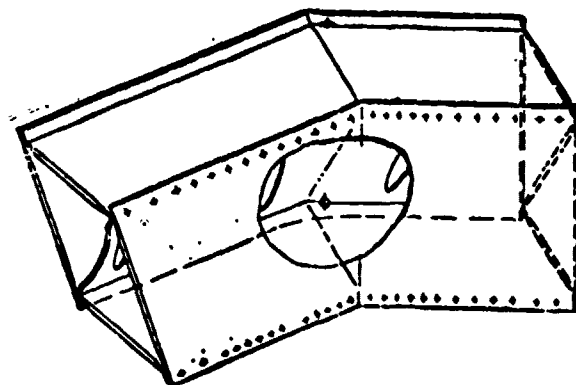
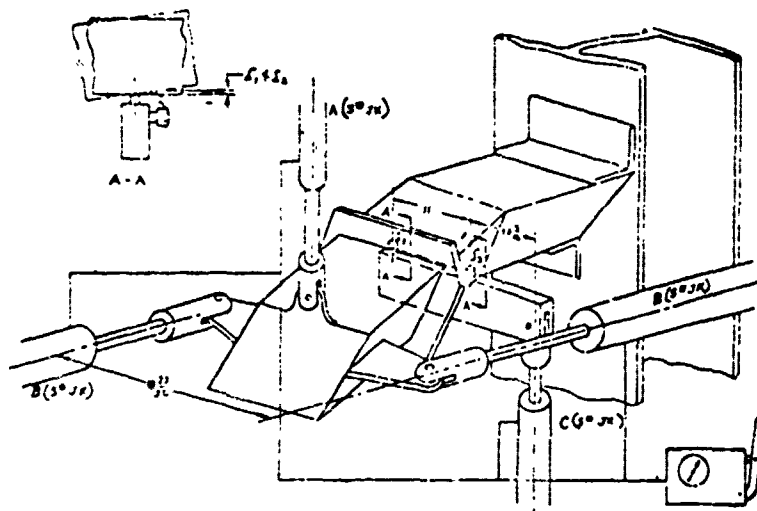


FIGURE 164. STRAIN GAGE INSTALLATION

TABLE 61. ULTIMATE TEST

CONCEPTUAL WING BENT BOX ULTIMATE TEST

| DYMEC SEQUENCE NO. | % ULTIMATE LOAD | LOAD LBS. | LOAD CELL DIGITAL READ OUT MV | JACK PRESS PSI | |
|--------------------------|-----------------------|--------------|--|----------------------|---------|
| 1 | 0 | 0 | 0 | 0 | |
| 2 | CAL | 0 | 6.383 | 0 | |
| 3 | 20 | 3155 | 1.577 | 631 | |
| 4 | 40 | 6309 | 3.154 | 1262 | |
| 5 | 60 | 9464 | 4.732 | 1893 | |
| 6 | 80 | 12618 | 6.309 | 2524 | |
| 7 | 94 | 14819 | 7.409 | 2964 | FAILURE |



Specimen failure occurred at 94-percent ultimate load in the center web as shown in Figures 165, 166, and 167. A path of fractured graphite fibers started at the sweepbreak under the -67 bolt pad and traveled inboard and outboard connecting each of the elliptical cutouts.

The residual load (62-percent ultimate) remaining on the specimen immediately after failure was a function of the elasticity in the hydraulic loading system and the change in the specimen's flexibility due to the loss of center web effectiveness. What load level the specimen could attain in that condition or where the second failure would occur, can only be surmised at this time.

ANALYSIS-TEST CORRELATION

The correlation of stresses between analysis and test is shown in Tables 62 and 63. Two sets of stresses from analysis are listed in these tables. The first set corresponds to a bent box model with stiff straps on the webs, just inboard of the sweepbreak. The straps which introduce the load from the big 3/4-diameter aft attach bolt are denoted as -43 and -45 straps. On the forward web, the added stiffening material used to support the column load from the forward attach bolt is included in the model. The first set of analysis stresses corresponds to an upper bound sweepbreak stiffness solution. The second set of analysis stresses corresponds to a model reflecting a lower bound sweepbreak stiffness. The location of stresses which are tabulated in Table 62 correspond as near as possible to the strain gage locations of the test.

It was expected that the stresses corresponding to strains monitored during the test would fall somewhere between the results of the two analyses since these analyses were based on stiffness bounds of the sweepbreak area. For the most part, the poor correlation is due to several features of the test specimen which were not accurately modeled. These features include:

- Eccentricities of the covers and webs which would cause the strain gage data to be unrepresentative of the average stress
- Flexibility of the adhesive connecting the web and lower cover
- Flexibility of the fiberglass stress relief protection to the upper cover bolt holes
- Defects and inclusions in the adhesive.

In-plane shear stresses are required in the covers to allow turning of the spanwise stresses at the sweepbreak. Consequently, since the shear stiffnesses are reduced at the cover edges, the spanwise stresses are shifted toward the central regions of the covers at the sweepbreak. This is evidenced significantly by the low stresses measured by the rosettes R4 and R9.

A more accurate model of the specimen would have allowed for the inclusion of very narrow rectangular panels running spanwise along the edges of the cover, which could have reflected the larger flexibilities discussed above.



FIGURE 165. SPECIMEN FAILURE

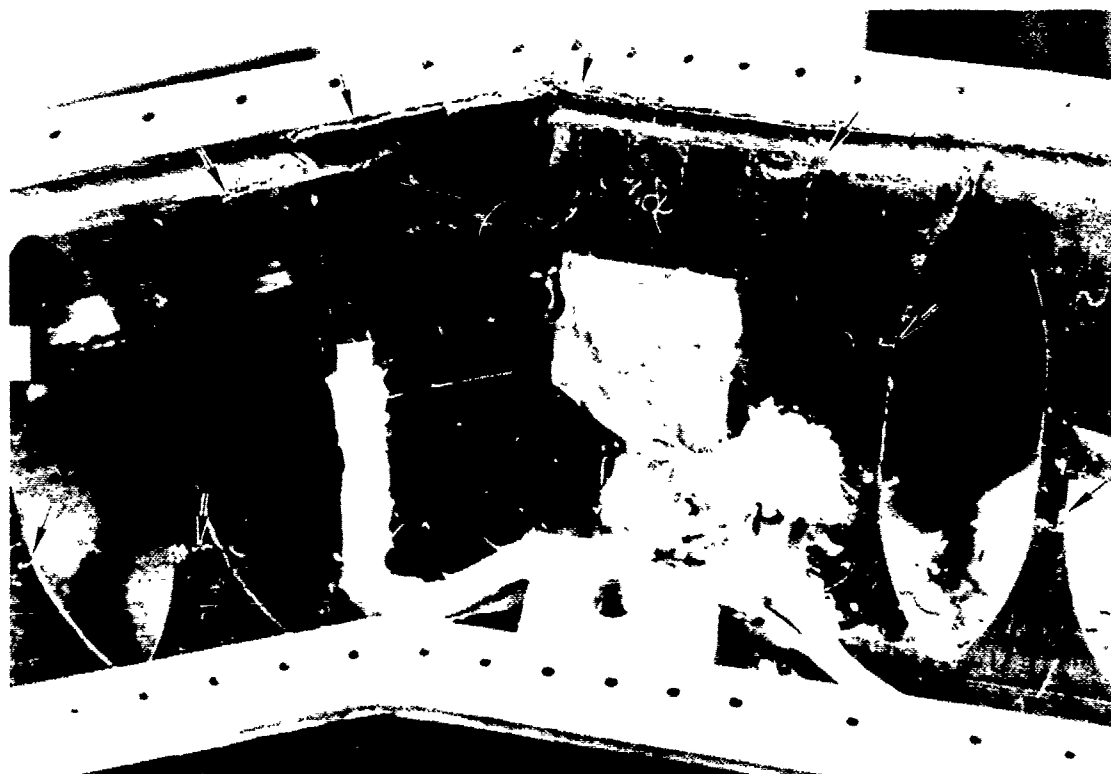


FIGURE 166. SPECIMEN FAILURE - SWEEP BREAK



FIGURE 167. SPECIMEN FAILURE — INBOARD

TABLE 62.
TEST CORRELATION

| GAGE | STIFF ⁽¹⁾ | | | FLEXIBLE ⁽²⁾ | | | TEST ⁽³⁾ | | |
|------|----------------------|------------|--------|-------------------------|------------|--------|---------------------|------------|--------|
| | σ_s | σ_c | τ | σ_s | σ_c | τ | σ_s | σ_c | τ |
| R1 | -59.6 | -2.7 | 0.2 | -59.7 | -5.4 | 0.2 | -39.4 | 0.8 | 2.7 |
| R2 | -55.3 | 0 | 0.7 | -53.4 | 0 | 0.6 | -40.8 | 3.4 | 3.7 |
| R3 | -25.3 | -38.7 | 4.8 | -32.1 | -34.7 | 2.7 | -20.4 | -21.0 | 4.9 |
| R4 | -51.6 | 0 | 8.5 | -76.4 | 0 | 13.2 | -29.2 | -0.6 | 0.2 |
| R5 | -55.7 | -0.4 | 7.0 | -48.6 | -0.2 | 13.3 | -33.7 | 4.1 | 4.8 |
| R6 | 51.6 | 0.6 | 0.1 | 50.7 | -0.9 | 0.2 | 44.5 | 7.5 | 9.5 |
| R7 | 54.9 | -1.4 | 1.1 | 52.4 | -2.7 | 1.2 | 39.1 | 0.1 | 2.1 |
| R8 | 47.2 | 0 | 6.1 | 50.7 | 0 | 6.2 | 35.8 | 0.5 | 3.6 |
| R9 | 58.0 | -2.8 | 7.8 | 53.9 | -4.7 | 7.8 | 18.6 | 1.8 | 3.7 |
| R10 | 0.6 | -2.7 | 21.8 | 1.3 | -3.4 | 22.3 | -0.7 | -3.7 | 25.6 |

(1) STRESSES FROM ANALYSIS WITH STIFF SWEEP-BREAK (KSI)

(2) STRESSES FROM ANALYSIS WITH FLEXIBLE SWEEP-BREAK (KSI)

(3) STRESSES FROM TEST, EXTRAPOLATED TO 100% ULT (KSI)

TABLE 63
TEST CORRELATION

| GAGE | STIFF σ_c | FLEXIBLE σ_c | TEST σ_c |
|------|---------------------|------------------------|--------------------|
| D1 | 26.2 | 22.7 | 29.6 |
| D2 | 26.6 | 22.7 | 31.9 |
| D3 | 26.6 | 22.7 | 33.2 |
| D4 | 26.6 | 22.7 | 29.8 |
| D5 | 6.7 | 1.0 | 13.2 |
| D6 | 6.7 | 1.0 | 16.5 |
| D7 | -30.3 | -35.2 | -29.9 |
| D8 | -30.3 | -35.2 | -23.6 |
| S1 | 42.6 | 90.1 | 59.4 |

FAILURE MODE

The failure mode of the specimen was a bending failure of the center web under the -67 bolt pad, originating, in all probability, at the sweepbreak, and the failure traveled inboard and outboard connecting each of the elliptical cutouts. The failure was caused by bending rather than direct tensile stress because of the 0.405-inch radius at the juncture of the center web and upper cover. The large bending stresses at the location of failure were not considered in the original analysis, the margin of safety at that location being based on the direct stress alone. The following analysis confirms the high bending stresses which initiated failure.

Consider the juncture of the center web and upper cover as shown in Figure 168. The bending effects associated with such a configuration can be realized by treating an initially curved strut in tension as also shown in Figure 168, and solve for M_o .

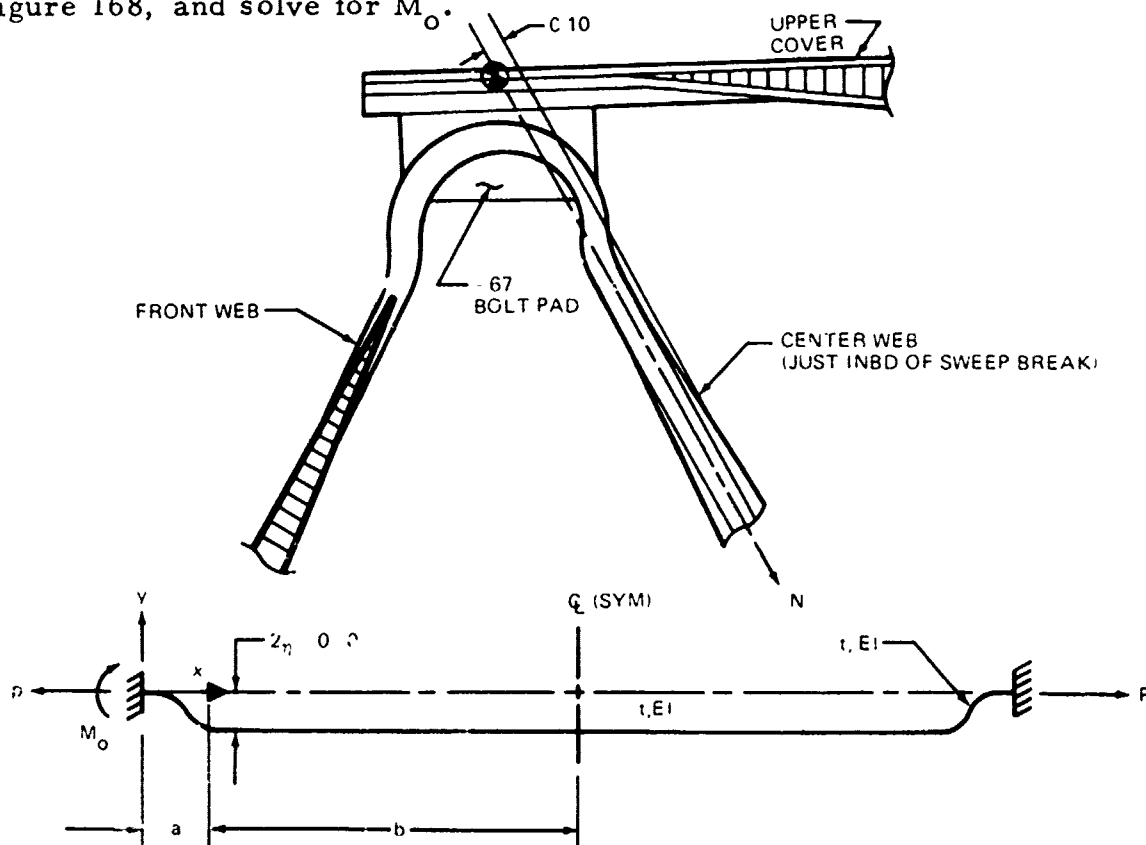


FIGURE 168. IDEAL STRUT WITH INITIAL CURVATURE

Denote $\bar{x} = x - a$ and $\bar{y} = y(\bar{x})$

$$\lambda^2 = \frac{P}{EI} \text{ and } \bar{\lambda}^2 = \frac{P}{\bar{EI}}$$

$$\text{Then } y'' - \lambda^2 y = -\lambda^2 \eta (1 - \cos \frac{\pi x}{a}) + \frac{M_o}{EI} \quad 0 \leq x \leq a$$

$$\bar{y}'' - \bar{\lambda}^2 \bar{y} = -2\bar{\lambda}^2 \eta + \frac{M_o}{\bar{EI}} \quad 0 \leq x \leq b$$

$$y_{(0)} = 0$$

$$y'_{(0)} = 0$$

$$y_{(a)} = \bar{y}_{(0)}$$

$$y'_{(a)} = \bar{y}'_{(0)}$$

$$\bar{y}'_{(b)} = 0 \text{ from symmetry}$$

The solution for the ideal strut is $M_o = \Lambda P \eta$

where

$$\Lambda = \left(1 + \frac{\tanh b\lambda}{\frac{\lambda}{\bar{\lambda}} \sinh a\lambda + \cosh a\lambda \tanh b\bar{\lambda}} \right) \left(1 - \frac{\lambda^2}{\lambda^2 + \frac{\pi^2}{a^2}} \right)$$

For the bent box specimen,

$$a = 0.36$$

$$b = 4.40$$

$$t = 0.132 \quad E_y = 9.0 \times 10^6 \quad \nu_{xy} \nu_{yx} = 0.219$$

$$\bar{t} = 0.176 \quad \bar{E}_y = 16.6 \times 10^6 \quad \bar{\nu}_{xy} \bar{\nu}_{yx} = 0.117$$

For unit width use

$$P = N_y$$

$$EI = \frac{E_y t^3}{12(1 - \nu_{xy} \nu_{yx})}$$

From test, the chordwise load at R3 at failure was

$$N_y = 0.94(21,000)(0.170) = -3356 \text{ lb per inch}$$

and from equilibrium of the joint, the loading in the center web must be the same, but of opposite sign. Hence, from test, a loading of $N_y = 3356$ pounds per inch tension existed in the center web at the upper cover, just inboard of the sweepbreak.

$$\lambda^2 = \frac{12(1 - \nu_{xy}\nu_{yx})N_y}{E_y t^3} = 1.520 \quad \lambda = 1.233$$

$$\bar{\lambda}^2 = \frac{12(1 - \bar{\nu}_{xy}\bar{\nu}_{yx})N_y}{\bar{E}_y \bar{t}^3} = 0.393 \quad \bar{\lambda} = 0.627$$

$$\Lambda = 1.467$$

$$M_o = 1.467(3356)(0.05) = 246 \text{ in.-lb per inch}$$

$$\begin{aligned} \sigma_o &= \frac{6M_o}{t^2} + \frac{N_y}{t} \\ &= \frac{6(246)}{(0.132)^2} + \frac{3356}{0.132} \\ &= 84,700 + 25,400 = 110,100 \text{ psi} \end{aligned}$$

The allowable stress for a pattern of (+45/-45/90) is

$$F_y = 77,000 \text{ psi.}$$

This verifies the failure mode selection.

SECTION VIII

PAYOFF AND RECOMMENDATIONS

8.1 WEIGHT PAYOFF

The truss web conceptual design utilizes high stress levels so stress concentration relief (SCR) becomes of paramount importance in avoiding weight penalties for attachment. SCR has been utilized to remove all stress concentration in spanwise joints because of the predominate spanwise loading. The design itself is "spanwise oriented."

A further weight advantage of truss web was shown in Paragraph 4.1.6 through use of the variably spaced panel facings which come together in solid laminates at spanwise joints, indicating the structural efficiency of those panels with respect to constant depth sandwich panels and the ease of making joints. If constant or variable depth sandwich covers were used for a competing multi-rib concept, heavy, solid laminate sections or frequent potted inserts must be used at rib intersections.

The use of variable depth honeycomb panels also avoids the design and fabrication problems of discrete stiffening which, if parallel, must run out against truss crests, or, if converging, requires continuous change of cross section.

Full wing weights were obtained for truss web fairly early in the program to assess design performance and were updated as knowledge about the design improved.

Full wing weight was calculated as the sum of four terms in a weight formula:

$$W_{\text{wing}} = W_u + W_l + W_{\text{tw}} + W_p$$

where

W_u = weight of upper cover

W_l = weight of lower cover

W_{tw} = weight of truss web substructure

W_p = weight penalties.

Figure 169 illustrates the distribution of weight in the five-cell truss web. Integration and addition of each of the constituent curves provided the total truss web weight, or W_{tw} . It will be noted in Figure 169 that the weight of cover-to-truss-web joints and adhesive for the sandwich construction becomes a large percentage of the total in the outboard wing. The joint weight is relatively invariant with span. For a bonded joint the same relationship holds but joint weight is of lesser magnitude.

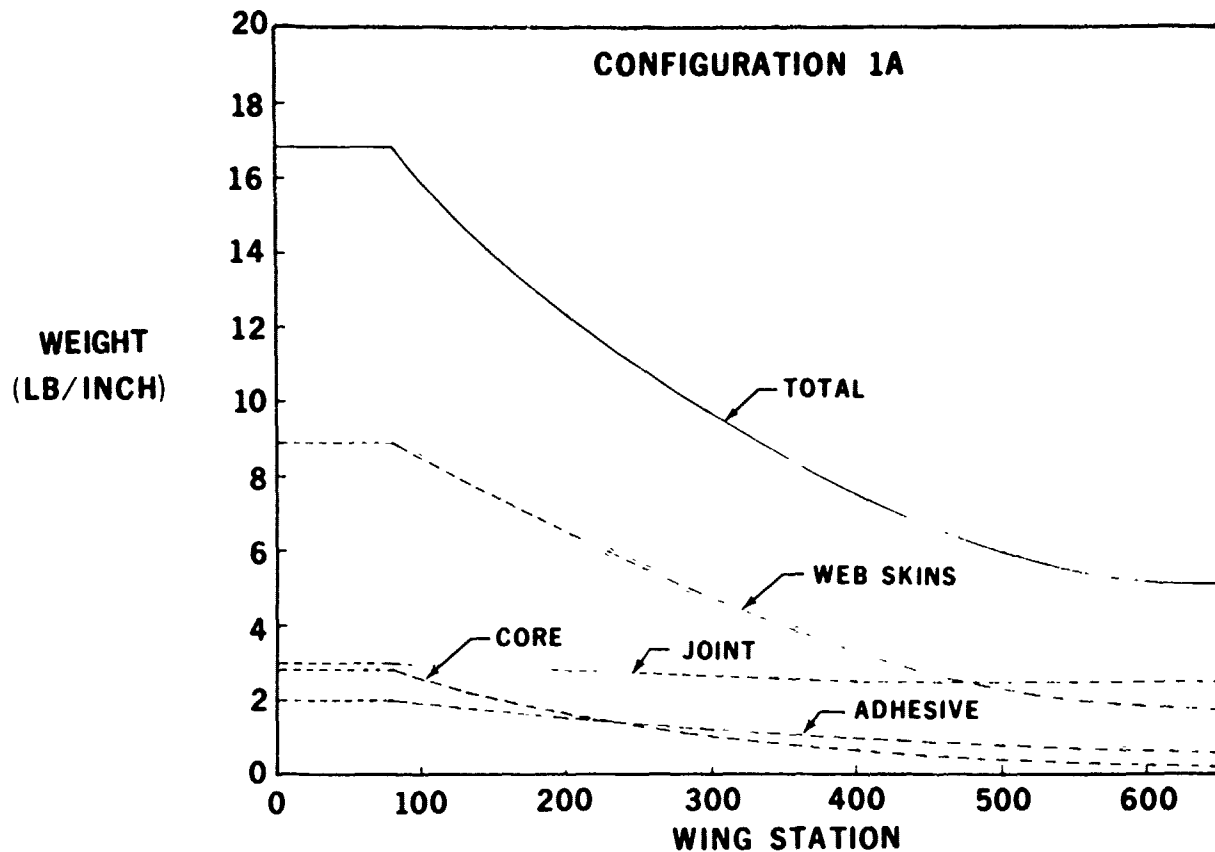


FIGURE 169. TRUSS WEB WEIGHT DISTRIBUTION

The wing cover weight terms likewise consist of constituent parts:

- Facing weights
- Core Weight
- Adhesive
- Bolt Bearing Strips (as applicable).

Facing weight for all-bonded or fully stress concentration relieved covers consists of those laminates of thickness and pattern required for local strength and shear stiffness. For bolted tension covers, a weight penalty factor (WPF) was assigned per the formula:

$$WPF = \frac{\sigma_{\text{working}} \times K_t + 25,000}{\sigma_{\text{allowable}}}$$

WPF was used as a multiplier for the design thickness obtained for the bonded covers. K_t varied with span with maximum values near the root due to higher percentage of 0-degree plies in the laminate patterns. For the upper compression cover, the WPF formula was modified to $0.67 \times$ (working stress) to check the upper cover for tension due to the 2g down bending condition. The upper cover was found to be tension-critical to approximately 25 percent of the half span, thus requiring SCR or application of weight penalty factor for that portion. Initial estimates assumed compression $K_{tc} = 1$ which was later found to be incorrect (Paragraph 7.5). However, later weight estimates used low K_{tc} values because stress relief strips were introduced into the baseline bolted upper cover.

All facing weights were reduced by the web "caps" (or joints) working with the covers as bending material. This was done by removing equivalent 0-degree plies where sufficient plies existed. This could not be done for a multi-rib design. In most of the outboard wing, the truss caps provide excess bending material. Bolt bearing strips were added where sufficient cover thickness did not exist to develop the required countersunk bolt bearing strength ($t_{min} = 0.3$ inch for 1/4-inch-diameter bolt).

Figure 170 shows a typical wing weight distribution by summation of the four constituent weight terms.

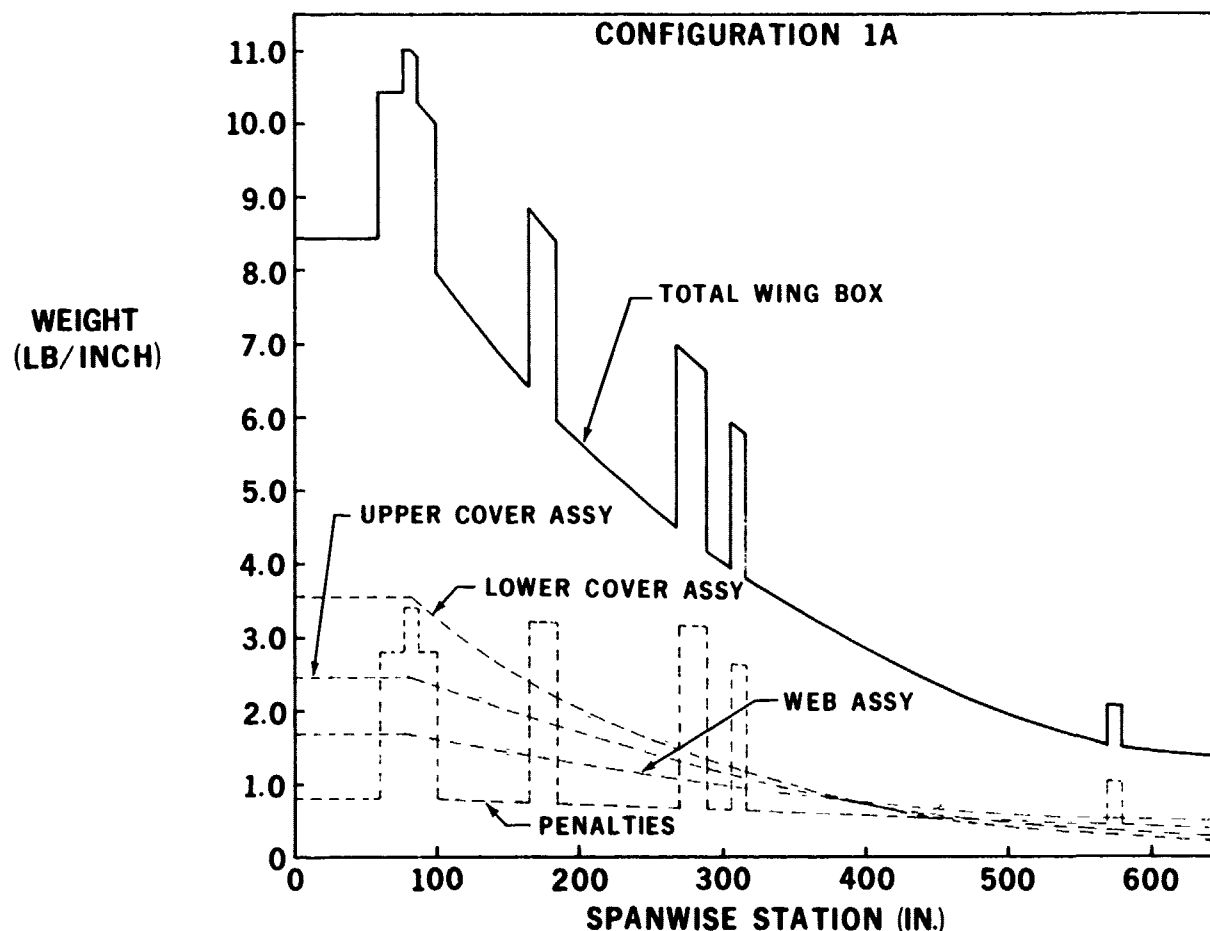


FIGURE 170. EXAMPLE TRUSS WEB WING WEIGHT DISTRIBUTION

Table 64 shows the weight saving on the full-wing basis for the several early study configurations, materials, and cover attachments. In addition, the cocure weight penalty was determined for Configuration 1A and the first cutout web concept was weighed for Configuration 3C2L. Configuration 3C2L contains the "lightened web" and, with the other weight saving design features, provides the maximum 54.6-percent weight saving. Other configurations would also show a corresponding weight saving improvement with a cutout web substructure.

The initial payoff study (Paragraph 4.1.8) showed the weight effect of the various design features and the relative fabrication cost among the study configurations. That will not be repeated here.

Whereas the weight penalties for the metal wing were based on existing past design analysis data, it was necessary to perform separate weight estimates for each weight penalty item of the composite wing to attain realism. Table 65 shows these penalties and the comparative metal wing weights. The greatest contribution of the truss web concept is seen in the low penalties for concentrated load introduction or load redistribution, such as at pylons, wing/fuselage connection, aerodynamic break, and control surface attachments. A center wing pressure bulkhead penalty was not included for the composite wing since the cover panels had already been designed for fuel over-pressure and were adequate for the 7.5-psi cabin pressure plus flight loads. Twenty-two access doors were considered adequate accessibility for the open truss web design whereas the metal configuration showed 32 access doors.

This section will be concluded with final wing weight revisions.

TABLE 64
INITIAL TRUSS WEB WING WEIGHT SAVINGS

| CONFIGURATION | PRECURE (P) COCURE (C) | NO. CELLS | TYPE | PERCENT SAVED | |
|---------------|---------------------------|--------------|----------------------------|-------------------|----------------------|
| | | | | BASE MATERIALS | OPTIMUM MATERIALS |
| 1A | C | 5 | BOLTED | 28.2 | - |
| 1A | P | 5 | BOLTED | 30.85 | 35.6* |
| 1A/2A | P | 5 | BOLTED/BONDED | 38.7 | - |
| 1B2 | P | 6 | BOLTED (SCR) | 40.1 | - |
| 1B | P | 5 | BOLTED (SCR) | 40.2 | 42.2* |
| 2A | P | 5 | BOLTED (SCR)// BONDED A | 41.4 | 43.1* |
| 2B | P | 5 | BOLTED (SCR)// BONDED B | 41.6* | 43.4* |
| 3C | P | 5 | BONDED B | 43.3* | 47.3* |
| 3C2 | P | 6 | BONDED B | 46.1* | 49.8* |
| 3C2L | P | 6 | BONDED B WEB LIGHTENING | 50.9* | 54.6* |

*ESTIMATED BY EXTRAPOLATION (WEIGHT PENALTIES HELD CONSTANT)

The final baseline (Configuration 2B) wing box weights (see Table 65) included the following changes with respect to weights established for Table 64.

- Results of the optimized pressure panel study were incorporated (i.e., "end beam" and maximum core thickness definitions).
- Design of laminates with the Douglas laminate design program rather than with STOP 3 which was judged unconservative.
- Changes in flutter stiffness requirements as a result of Company-funded work. Initial configurations were designed to metal wing stiffness. A 5-percent weight saving due to flutter stiffness reductions was offset by other weight increases.
- Narmco 5206 II/Thornel 75 lower cover replaced by all Narmco 5206 II.
- Cover and front and rear web cores were increased 10 percent over pressure-only design to account for interaction of 20-psi pressure stresses and stresses due to 80-percent design limit loads.
- Recalculated and lightened web-to-cover bolted tension joints.
- Recalculated improved cutout truss web internal structure.
- Penalties not recalculated.
- A 5-percent contingency for positive margin of safety added to composite weights since it had been included in the comparative metal wing weights.

TABLE 65
FINAL WING WEIGHT BREAKDOWN COMPARISON

| CONFIGURATION | METAL (LB) | COMPOSITE BASELINE MATERIALS (LB) | PERCENT SAVED |
|--|---------------|---|------------------|
| UPPER COVER | 2333 0 | 1651 0 | 29.2 |
| LOWER COVER | 2241 0 | 1542 0 | 31.2 |
| SUBSTRUCTURE (INCLUDING SPLICES AND JOINTS) | 1852 0 | 1169 0 | 36.8 |
| BASIC BOX | 6426 0 | 4362 0 | 32.1 |
| WING TO FUSELAGE ATTACH | 234 0 | 95.4 | |
| DOORS, DOUBLERS, ATTACH | 496 0 | 220 0* | |
| WING FUS BULKHEAD | 256 0 | NONE | |
| OUTBOARD WING SPLICE | NONE | 38 0 | |
| POWER PLANT ATTACH. PENALTY | 200 0 | 100 0 | |
| FLAP ATTACH. PENALTY | 305 0 | 160 0 | |
| AILERON ATTACH. PENALTY | 38 0 | 28 0 | |
| SLAT ATTACH. PENALTY | NOT INCLUDED | 35 0 | |
| AERODYNAMIC BREAK PENALTY | 40.0 | NONE | |
| FUEL BULKHEADS | 105 0 | 37.7 | |
| CENTER WING PRESSURE BULKHEAD | 135 0 | NONE | |
| LIGHTNING PROTECTION AND MISC | NONE | 102 0 | |
| 5 PERCENT CONTINGENCY | INCLUDED | 39.9 | |
| PENALTIES | 1809 0 | 856 0 | 52.6 |
| WING BOX | 8235.0 | 5218 0 | 36.6 |

*22 DOORS

8.2 RECOMMENDATIONS

1. A final wing design should be accomplished to explore problems associated with integrating engine pylons, flaps, and composite control surfaces with a basic truss web wing box.
2. Since a chordwise load introduction component was not achieved within the program, it is recommended that this important aspect of the truss web concept be subjected to test.
3. Task VI explored the wing/fuselage interface (Reference 1). However, a further optimization and analysis of this area is desirable, particularly:
 - Method for resisting upper cover anhedral "kick loads" at sweep-break.
 - Advisability of isolating wing bending deflections from fuselage deflections.
4. It is recommended the advantages of this wing concept be explored relative to a thin, highly loaded wing application.
5. Fabrication feasibility and test/analysis correlation work should be accomplished with respect to alternate wing assembly and substructure concepts (such as the micro-corrugated hat section strut concept).
6. Since the fillet bonding concept has broad application potential and promises to be an economical method of joining large composite assemblies and of reducing stress concentration through the elimination of fasteners, additional work should be accomplished in the following areas:
 - Bond material temperature resistance
 - Bond material toughness
 - Bonded laminate interlaminar tension strength
 - Fillet formation manufacturing technique
 - Joint configurations for high loads.
7. Test/analysis correlation work is suggested for the exploration of alternate panel stiffening concepts and also for the promising Arch-Web design concept.

APPENDIX A

REFERENCED ENGINEERING DRAWINGS

This appendix consists of the engineering drawings referenced by drawing number in the text.

244

REVISIONS

| LTR | DESCRIPTION | DATE | APPROVED |
|-----|-------------|------|----------|
| A | SEE E.O. | | |

GENERAL NOTES: UNLESS OTHERWISE NOTED

- IDENTIFY PER DTS 3-02
- BOND -3 TAB TO ALL SPECIMENS WITH NARMCO 252 ADHESIVE OR EQUIVALENT
- PREPARE TABS FROM A CURED LAMINATE OF 0°, 90° STRATOGLOSS OR EQUIVALENT
- FABRICATION AND PROCESSING METHOD PER FACT SHEET Z2578681
- 0° LAYER OF -3 TAB MUST BE ADJACENT TO THE BOND

*** TRUE DIMENSION TO BE RECORDED BEFORE TEST**

| LAYER | Φ | MATL | Φ | MATL |
|-------|--------|------|--------|------|
| 1 | 0 | A | 0 | C |
| 2 | 0 | A | 0 | C |
| 3 | +45 | B | +45 | B |
| 4 | -45 | B | -45 | B |
| 5 | 0 | A | 90 | B |
| 6 | 0 | A | -45 | B |
| 7 | 90 | A | +45 | B |
| 8 | 0 | A | 0 | C |
| 9 | 0 | A | 0 | C |
| 10 | -45 | B | | |
| 11 | +45 | B | | |
| 12 | 0 | A | | |
| 13 | 0 | A | | |
| ± NOM | -0.006 | | -0.050 | |

QUANTITY REQUIRED PER NOTED DASH NO.

| DASH NO. | QUANTITY |
|--------------|----------|
| 4 | 4 |
| 5 | 4 |
| 9 | 4 |
| CANCELLED | 1 |
| NOT REPLACED | 1 |
| 7 | 1 |
| 5 | 1 |
| 1 | 1 |

PARTS LIST

| ITEM NO. | DESCRIPTION | STOCK SIZE | CODE IDENT. NO. | NOMENCLATURE OR DESCRIPTION | PART OR IDENTIFYING NO. |
|----------|-----------------------------------|----------------|-----------------|-----------------------------|-------------------------|
| 1 | STRATOGLASS OR EQUIV. | .050 x .25 x 2 | | SPECIMEN | - 7 |
| 2 | FURNISHED BY DEPT 270 PROCESS LAB | | | SPECIMEN | - 5 |
| 3 | | | | TAB | - 3 |

UNLESS OTHERWISE SPECIFIED, DIMENSIONS ARE IN INCHES. TOLERANCES: ANGLES ±0°-30' 3 PLACE DEC ±0.015 2 PLACE DEC ±0.03 FINISH

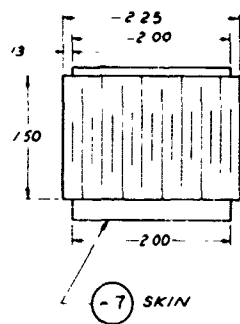
DOUGLAS AIRCRAFT COMPANY
LONG BEACH, CALIFORNIA

SPECIMEN ASSY - CELENESE
LAMINATE COMPRESSION TEST

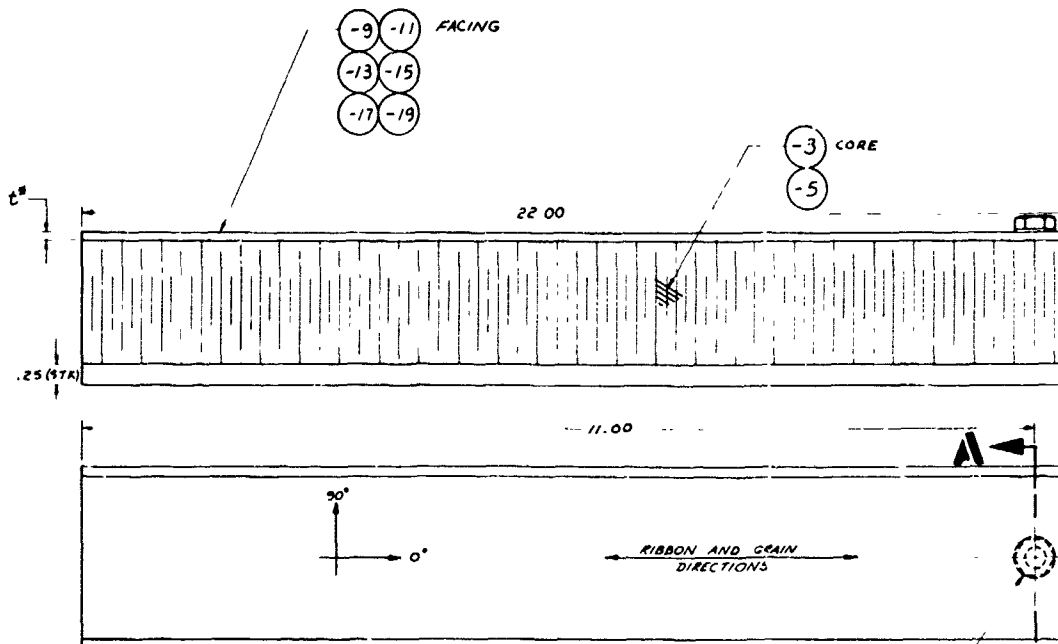
SIZE CODE IDENT NO
B 88277

SCALE 2/1

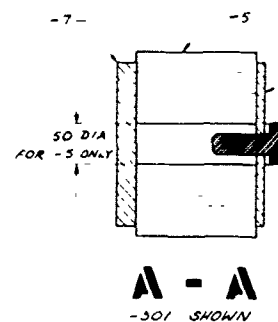
SHEET 1 OF 1



TRUE DIMENSION TO BE
RECORDED BEFORE BONDING



| LAYER | -9, -11 | -13, -15 | -17, -19 |
|--------------|---------|----------|----------|
| 1 | 0° | 45° | 0° |
| 2 | 45° | -45° | 45° |
| 3 | 0° | 45° | 90° |
| 4 | -45° | -45° | -45° |
| 5 | 90° | 90° | 0° |
| 6 | -45° | 45° | 45° |
| 7 | 0° | -45° | 90° |
| 8 | 45° | 45° | -45° |
| 9 | 0° | -45° | -45° |
| 10 | 0° | -45° | 90° |
| 11 | 45° | 45° | 45° |
| 12 | 0° | -45° | 0° |
| 13 | -45° | 45° | -45° |
| 14 | 90° | 90° | 90° |
| 15 | -45° | -45° | 45° |
| 16 | 0° | 45° | 0° |
| 17 | 45° | -45° | |
| 18 | 0° | 45° | |
| (TOLERANCES) | .090 | .090 | .080 |



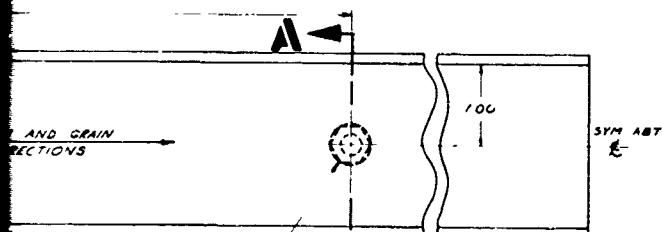
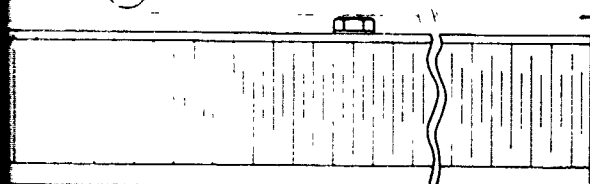
28669982

2

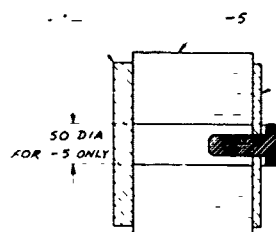
| REVISIONS | | | |
|-----------|-------------|------|----------|
| LTR | DESCRIPTION | DATE | APPROVED |
| | | | |
| | | | |

GENERAL NOTES - UNLESS OTHERWISE SPECIFIED

1. IDENTIFY PER D'S 3 OR
2. BOND ALL FACINGS AND -7 SKIN TO -1 OR -5 CORE WITH EA-951 ADHESIVE PER D'S 1.07
3. HEAT TREAT -7 125-145 KSI PER D'S 5.00
4. FABRICATION AND PROCESSING METHOD PER PROCESS ENGINEERING FACT SHEET PERTAINING TO THIS DRAWING



2495 DIA HOLE IN -11, -15 & -19 ONLY
 2505 NAS 1104-8 BOLT
 NAS 1252-416H WASHER



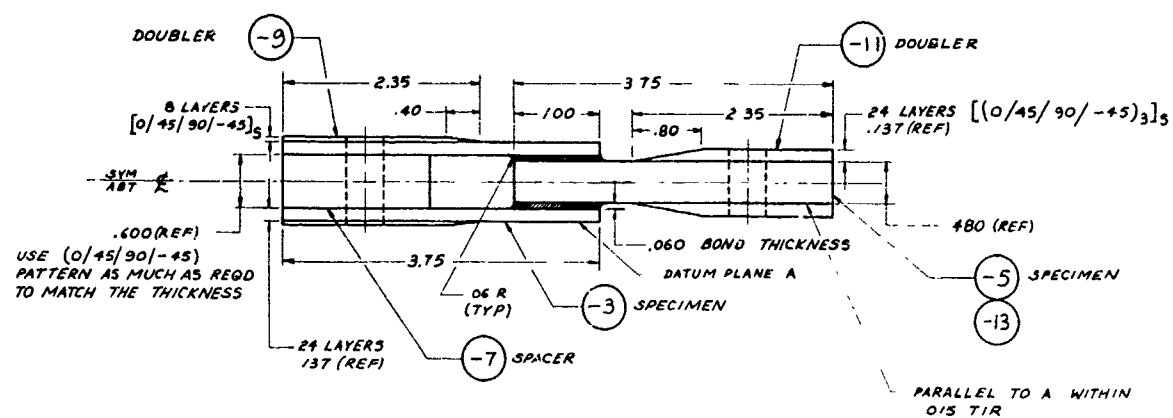
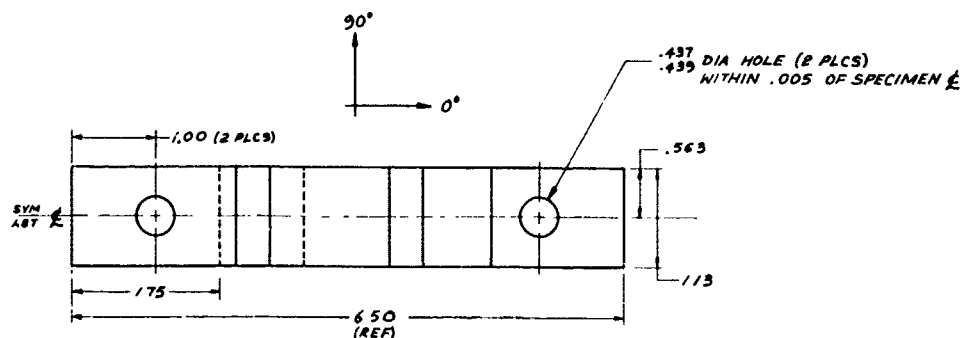
A - A
 -501 SHOWN

| AR | AR | AR | AR | AR | AR | EA-951 | ADHESIVE | | | | DMS 2109 | | |
|------|------|------|------|------|----|------------------------|-----------------------------|------------------------|-----------------------|----------------------|------------------------|---------|------|
| / | / | / | / | / | / | NAS 1252-416H | WASHER | | | | | | |
| / | / | / | / | / | / | NAS 1104-8 | BOLT | | | | | | |
| / | / | / | / | / | / | -19 | FACING | 14 LAYERS x 2 x 22 | AVCO 5505 BORON/EPOXY | DMS 1919 | | | |
| / | / | / | / | / | / | -17 | | 18 LAYERS x 2 x 22 | | | | | |
| / | / | / | / | / | / | -15 | | 18 LAYERS x 2 x 22 | | | | | |
| / | / | / | / | / | / | -13 | | 18 LAYERS x 2 x 22 | | | | | |
| / | / | / | / | / | / | -11 | | 18 LAYERS x 2 x 22 | | | | | |
| / | / | / | / | / | / | -9 | FACING | 18 LAYERS x 2 x 22 | AVCO 5505 BORON/EPOXY | DMS 1919 | | | |
| / | / | / | / | / | / | -7 | SKIN | 25 x 22 STL PLATE 4130 | MIL-S-18729 COND N | | | | |
| / | / | / | / | / | / | -5 | | 3 x 2 | AL HONEYCOMB | PURCHASE FROM HEXCEL | | | |
| / | / | / | / | / | / | -3 | | x 22 | 1/8-5052-006 | | | | |
| -509 | -507 | -505 | -503 | -501 | -1 | PART OR IDENTIFYING NO | NOMENCLATURE OR DESCRIPTION | CODE IDENT NO | STOCK SIZE | MATERIAL DESCRIPTION | MATERIAL SPECIFICATION | FIND NO | ZONE |

PARTS LIST

McDONNELL DOUGLAS CORPORATION PROPRIETARY RIGHTS ARE RESERVED IN THE INFORMATION DISCLOSED HEREIN. ACCEPTANCE BY THE USER OF THIS DOCUMENT AGREES THAT THE USER SHALL BE RESPONSIBLE FOR THE PROTECTION OF THIS INFORMATION FROM DISCLOSURE TO OTHERS FOR MANUFACTURING OR FOR ANY OTHER PURPOSES EXCEPT AS SPECIFICALLY AUTHORIZED IN WRITING BY McDONNELL DOUGLAS CORPORATION.

| | | | | | | | |
|--|--|--|--|--|--|---|--|
| DASH NUMBERS OF THIS DWG ODD DASH NUMBERS SHOWN EVEN DASH NUMBERS OPPOSITE | | UNLESS OTHERWISE SPECIFIED DIMENSIONS ARE IN INCHES TOLERANCES ANGLES ± 0 - 30 3 PLACE DEC ± 0.015 2 PLACE DEC ± 0.03 | | CONTRACT NO F33615-71-C-1340 | | DOUGLAS AIRCRAFT COMPANY LONG BEACH CALIFORNIA | |
| FINISH | | | | STRESS <i>E. SPEARMAN</i> 1-6-72 | | SPECIMEN ASSY - SANDWICH BEAM | |
| ECA 10054 | | CONCEPTUAL WING | | CHECK <i>E. SPEARMAN</i> 1-6-72 | | COMP. STRESS CONCENTRATION TEST | |
| NEXT ASSY | | USED ON | | DESIGN <i>M. ASHMAN</i> 1-4-71 | | | |
| FIRST APPLICATION | | | | PREP BY <i>M. ASHMAN</i> 1-3-71 | | | |
| FOR COMPLETE USAGE DATA SEE ENGINEERING RECORDS | | ORIG SECTION | | RELEASE CODE | | CUSTOMER APPROVAL | |
| JAN 6 1972 | | JAN 6 1972 | | DESIGN ACTIVITY APPROVAL <i>W. J. Nelson</i> 1-5-71 | | SIZE CODE IDENT NO D 88277 | |
| SCALE 1/1 | | | | | | Z3569982 | |
| | | | | | | SHEET 1 OF 1 | |



-3 LAYUP

| LAYER | ANGLE |
|-------|-------|
| 1 | 24 |
| 2 | 23 |
| 3 | 22 |
| 4 | 21 |
| 5 | 20 |
| 6 | 19 |
| 7 | 18 |
| 8 | 17 |
| 9 | 16 |
| 10 | 15 |
| 11 | 14 |
| 12 | 13 |
| 13 | 12 |
| 14 | 11 |
| 15 | 10 |
| 16 | 9 |
| 17 | 8 |
| 18 | 7 |
| 19 | 6 |
| 20 | 5 |
| 21 | 4 |
| 22 | 3 |
| 23 | 2 |
| 24 | 1 |

ε NOMINAL = .137

-5/-13 LAYUP

| LAYER | ANGLE | LAYER | ANGLE |
|-------|-------|-------|-------|
| 1 | 40 | 11 | 30 |
| 2 | 39 | 12 | 29 |
| 3 | 38 | 13 | 28 |
| 4 | 37 | 14 | 27 |
| 5 | 36 | 15 | 26 |
| 6 | 35 | 16 | 25 |
| 7 | 34 | 17 | 24 |
| 8 | 33 | 18 | 23 |
| 9 | 32 | 19 | 22 |
| 10 | 31 | 20 | 21 |

-5. INSERT EA951 A RESIN BETWEEN EACH LAYER NARMCO 5206

-13 INSERT FM96 ADHESIVE BETWEEN EACH LAYER OF NARMCO 5206

2

GENERAL NOTES : UNLESS OTHERWISE SPECIFIED

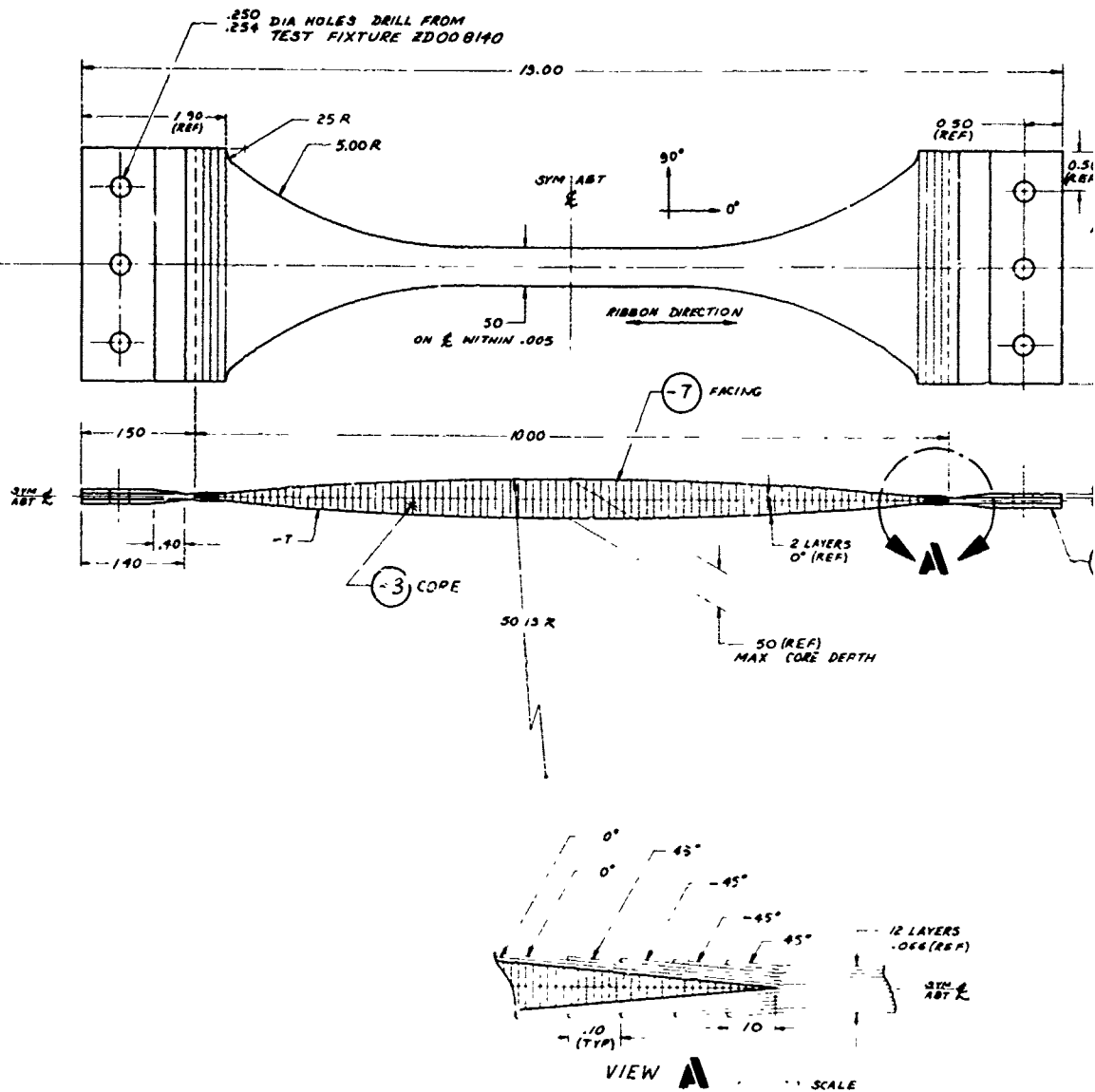
- 1 IDENTIFY PER DRS 3.02
- 2 FABRICATION AND PROCESSING METHOD PER P/E FACT SHEET PERTAINING TO THIS DRAWING
- 3 BOND SPACER AND DOUBLERS WITH EA 951 ADHESIVE

WITHIN

£3569983

1

FORM 100-1124 (7-68)



FIRST RELEASE
OF PRINTS

ORIGINAL
OF DRAWING

48

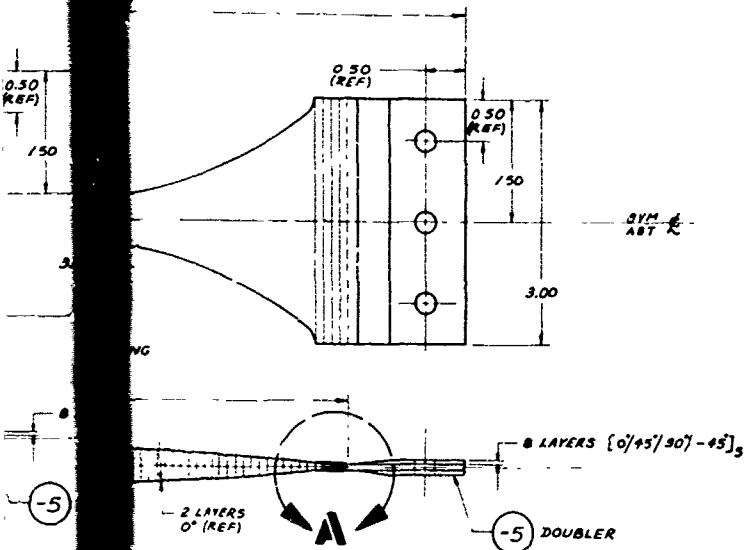
48669984

2

| REVISIONS | | | |
|-----------|-------------|------|----------|
| LTR | DESCRIPTION | DATE | APPROVED |
| | | | |
| | | | |
| | | | |

GENERAL NOTES UNLESS OTHERWISE SPECIFIED

- 1 IDENTIFY PER DPS 302
- 2 FABRICATION AND PROCESSING METHOD PER P/E FACT SHEET PERTAINING TO THIS DRAWING
- 3 ROND DOUBLERS WITH EA 951 ADHESIVE
- 4 CO-CURE AND BOND -7 FACING. USE FM 96 ADHESIVE
- 5 1/8-5052-.001-4.5 AL HONEYCOMB OPTIONAL



0.50 (REF)
MAX CORE DEPTH

45°
12 LAYERS
.066 (REF)
SYM A-BT

TO SCALE

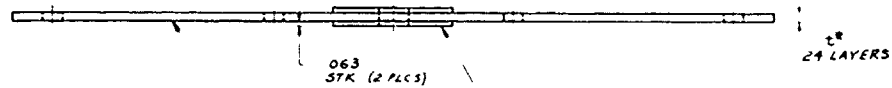
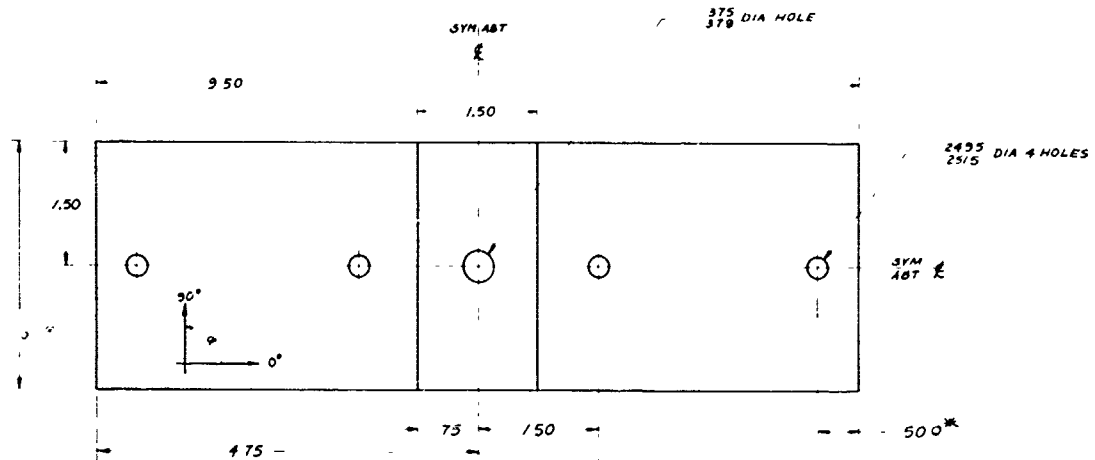
| AR | ADHESIVE | FM 96 SUPPORTED | | | | DMS 1892 |
|------------------------|-----------------------------|-----------------|----------------|--------------------------------|------------------------|----------------------|
| AR | ADHESIVE | EA 951 | | | | DMS 2103 |
| 2 | -7 | FACING | NOTED ON B'D | NARMCO 5206/X | | DMS 1936 |
| 4 | -5 | DOUBLER | 8 LAYERS 2 x 3 | NARMCO 5206/X | | DMS 1936 |
| 1 | -3 | CORE | .5 x 3 x 10 | 1/8-5052-.001-4.5 SEE 56 05 | | PURCHASE FROM HEXCEL |
| PART OR IDENTIFYING NO | NOMENCLATURE OR DESCRIPTION | CODE IDENT NO | STOCK SIZE | MATERIAL DESCRIPTION | MATERIAL SPECIFICATION | FIG NO |

PARTS LIST

ALL INFORMATION CONTAINED HEREIN IS UNCLASSIFIED EXCEPT WHERE SHOWN OTHERWISE BY THE INFORMATION CONTAINED HEREIN. REPRODUCTION OF THIS DOCUMENT IS PROHIBITED EXCEPT WHERE SHOWN OTHERWISE BY THE INFORMATION CONTAINED HEREIN. THIS DOCUMENT IS THE PROPERTY OF THE AIR FORCE AND IS LOANED TO YOU. IT IS TO BE RETURNED TO THE AIR FORCE WHEN NO LONGER REQUIRED. IT IS NOT TO BE DISTRIBUTED OUTSIDE THE AIR FORCE.

| | | | | | | | |
|--|--|--|--|------------------------------------|--|--|--|
| DASH NUMBERS OF THIS DWG ODD DASH NUMBERS SHOWN EVEN DASH NUMBERS OPPOSITE | | UNLESS OTHERWISE SPECIFIED DIMENSIONS ARE IN INCHES. TOLERANCES ANGLES ± 0°-30' 3 PLACE DEC ± 0.015 2 PLACE DEC ± 0.3 | | CONTRACT NO | | DOUGLAS AIRCRAFT COMPANY LONG BEACH, CALIFORNIA | |
| FINISH | | NEXT ASSY USED ON | | STRESS <i>W.D. Nelson</i> 2-10-72 | | SPECIMEN ASSY - CUTOUT TRUSS | |
| FIRST APPLICATION | | DESIGN ACTIVITY APPROVAL <i>W.D. Nelson</i> 2-10-72 | | CHECK <i>E. J. McMillan</i> 2-8-72 | | WEB ELEMENT TEST | |
| FOR COMPLETE USAGE DATA SEE ENGINEERING RECORDS | | ORIG SECTION | | DESIGN <i>W.D. Nelson</i> 2-8-72 | | SIZE CODE IDENT NO | |
| ORIGINAL DATE OF DRAWING SEP 8 1972 | | RELEASE CODE | | PREP BY <i>N. Ashbaugh</i> 2-7-72 | | D 88277 | |
| SHEET 1 OF 1 | | CUSTOMER APPROVAL | | SCALE 1/1 | | Z3569984 | |

1



(-5) SPECIMEN

(-3) DOUBLER

(-7)

* MEASURE AND RECORD BEFORE TEST

(-9)

(-11)

| LAYER | | -5 | -7 | -9 | -11 |
|-------|----|-------|-------|-------|-------|
| 1 | 24 | 45 A | 45 A | 45 B | 45 B |
| 2 | 23 | 90 C | 0 C | 90 C | 0 C |
| 3 | 22 | 45 A | -45 A | -45 B | -45 B |
| 4 | 21 | 90 C | 0 C | 90 C | 0 C |
| 5 | 20 | 45 A | 45 A | 45 B | 45 B |
| 6 | 19 | 0 C | 90 C | 0 C | 90 C |
| 7 | 18 | -45 A | -45 A | -45 B | -45 B |
| 8 | 17 | 90 C | 0 C | 90 C | 0 C |
| 9 | 16 | 45 A | 45 A | 45 B | 45 B |
| 10 | 15 | 90 C | 0 C | 90 C | 0 C |
| 11 | 14 | -45 A | -45 A | -45 B | -45 B |
| 12 | 13 | 90 C | 0 C | 90 C | 0 C |
| THICK | | .156 | .156 | .150 | .150 |

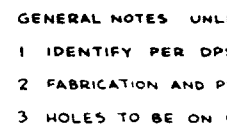
A - NARMCO 5206 GRAPHITE/EPOXY
B - AVCO 5505 BORON/EPOXY
C - HTS-5-99+ FIBERGLASS/EPOXY

** B-STAGE MATERIAL TO BE CURED IN THE ORDER SHOWN IN THE TABLE

FIRST RELEASE
OF PRINTS APR 11 1972

ORIGINAL DATE
OF DRAWING MAR 15

\$898



FOR -47 SPECIMEN GRAPHITE/EPOXY MATERIALS ARE.
NARMCO 5206 FOR LAYERS MARKED #
THORNEL 75S/2544 FOR UNMARKED LAYERS

| | |
|-------|---|
| - 541 | 2 |
| - 539 | 2 |
| - 537 | 2 |
| - 535 | 2 |
| - 533 | 2 |
| - 531 | 2 |
| - 529 | 2 |
| - 527 | 2 |

2

| REVISIONS | | | |
|-----------|-------------|------|----------|
| LTR | DESCRIPTION | DATE | APPROVED |
| | | | |
| | | | |
| | | | |

- 1 IDENTIFY PER DPS 3 02
- 2 FABRICATION AND PROCESSING METHOD PER PROCESS ENGINEERING FACI SHEET
- 3 HOLES TO BE ON CENTER LINE WITHIN .005 TIR

[illegible]

73578689

| |
|---------------------------------|
| QUANTITY REQD PER NOTED DASH NO |
|---------------------------------|

| | |
|--|-----------------|
| DASH NUMBERS OF THIS DWG ODD DASH NUMBERS SHOWN EVEN DASH NUMBERS OPPOSITE | |
| FINISH | |
| ZCA 10046 | CONCEPTUAL WORK |
| NEXT ASSY | USED ON |
| FIRST APPLICATION | |

UNLESS OTHERWISE SPECIFIED
DIMENSIONS ARE IN INCHES

TOLERANCES

ANGLES ± 1° - 30'

3 PLACE DEC ± 0.015

2 PLACE DEC ± 0.1

CONTRACT NO
F33615-71-C-1340

| | | |
|---------|------------------|--------|
| STRESS | L. J. Paul, York | 5-25-7 |
| CHECK | F. J. W. Mann | 5/6/7 |
| DESIGN | R. V. Hawley | 5-24-7 |
| PREP BY | AV HAWLEY | 5-21-7 |

DESIGN, ACTIVITY APPROAL
J. C. G. 1271

DOUGLAS AIRCRAFT COMPANY
LONG BEACH, CALIFORNIA

SPECIMEN ASSY-COMPOSITE
LAMINATE BOLTED JOINT
TEST

| | | | |
|------|-------|---------|----------|
| SIZE | CODE | CENT NO | |
| D | 88277 | | 73578685 |

FOR COMPLETE USAGE DATA
SEE ENGINEERING RECORDS

| | |
|-------------|--|
| ORG SECTION | |
|-------------|--|

RELEASE CODE

CUSTOMER APPROVAL

11708

255000

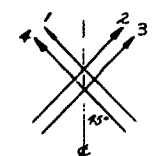
73578685

1

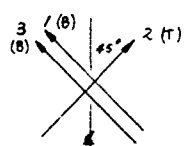
28282827

PLAN SHAPE IS
DOUBLY SYMMETRIC

SKIN PATTERN



-3 & -13 PATTERN

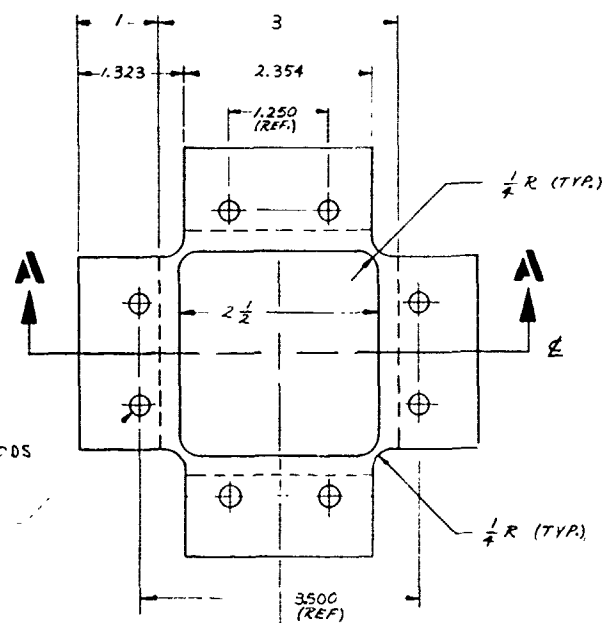


B- BROADGOODS
T- TAPE

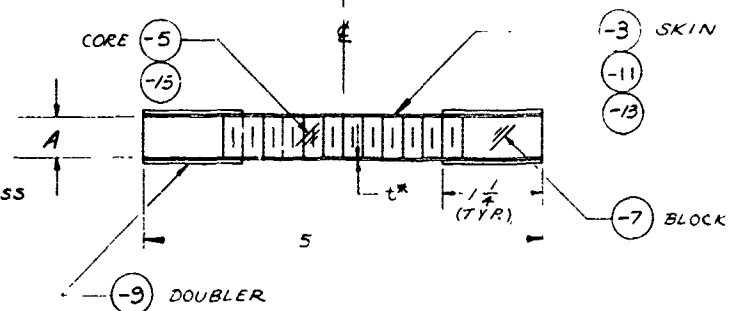
- 11 PATTERN

IT IS PERMISSIBLE TO REPLACE ONE LAYER
OF TAPE WITH TWO LAYERS OF BROADGOODS
WHEN SUITABLE TAPE IS NOT AVAILABLE.
(-3 & -11 ONLY)

DRILL .257 DIA 8 HOLES
.261
DRILL FROM TEST
FRAME 4195751



DIMENSION "A" IS .488 ± .005
FOR -7 AND .500 ± .005
FOR -5 & -15 TO ALLOW FOR
DIFFERENCE IN BOND THICKNESS



SECTION A-A

* DIMENSION MUST BE RECORDED
BEFORE BONDING

S.O.
643997/3

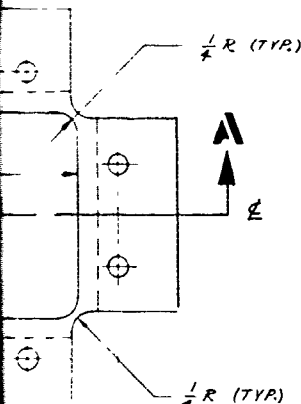
SEE ENGINEERING R

23828782

| REVISIONS | | | |
|-----------|--------------|----------|----------|
| SYM | DESCRIPTION | DATE | APPROVED |
| A | SEE E.O. "A" | 7/15/71 | KJ |
| B | SEE E.O. "B" | 11/24/71 | CRS |

GENERAL NOTES:

1. IDENTIFY PER DPS 3.02
2. NO SCRATCHES OR TOOL MARKS PERMITTED ON SKINS
3. HONEYCOMB RIBBON DIRECTION OPTIONAL WITH RESPECT TO E
4. FABRICATION AND PROCESSING METHODS PER ENGINEERING TECHNICAL REPORT ETR - DAD - 67199
5. INSTRUMENTATION REQUIRED, SEE TAD ZIA 10029 OR ZCA 10044
6. OUTER LAYER OF SKINS MUST BE IN SAME DIRECTION



- (-3) SKIN
- (-11)
- (-13)
- (-7) BLOCK

| | | | | | | | | | |
|---|----|---|----------------------------|--------------------------------|-------------------|--|--|---------------------------|------------|
| 1 | | | - 15 | CORE | | $\frac{1}{2} \times 3 \times 3$ | HRP $\frac{3}{16}$ -4.0 | PURCHASE FROM HEXCELL | |
| 2 | | | - 13 | SKIN | | 4 LAYERS (.003/PLY) 5×5 | ARMAND 5206 | DMS 1936 | |
| | 2 | | - 11 | SKIN | | 3 LAYERS 5×5 | MORGANITE III GRAPHITE LAMINATE | DMS 1936 | |
| 2 | 2 | 2 | - 9 | DOUBLER | | .04 $\times 5 \times 5$ | SHEET LAM GLASS CLOTH EPOXY | DMS 1668 | |
| 4 | 4 | 4 | - 7 | BLOCK | | $\frac{1}{2} \times 1 \times 2\frac{1}{2}$ | SHEET LAM PHENOLIC SEMI-GLOSS | MIL-P-15035 TYPE FBH | |
| | 1 | 1 | - 5 | CORE | | $\frac{1}{2} \times 3 \times 3$ | AL HONEYCOMB $\frac{1}{8}$ -5052-001N | PURCHASE FROM HEXCEL | |
| | | 2 | - 3 | SKIN | | 4 LAYERS (.004/PLY) 5×5 | GRAPHITE LAMINATE | DMS 1936 | |
| 3 | DI | / | PART OR IDENTIFYING NO. | NOMENCLATURE OR DESCRIPTION | CODE IDENT NO. | STOCK SIZE | MATERIAL DESCRIPTION | MATERIAL SPECIFICATION | PHD NO. |

LIST OF MATERIALS

| | | | | | | | | | |
|--|--|----------------------------------|--|---|--|---|--|---|--|
| S.O. 543997/3 | | FINISH | | DIMENSIONS ARE IN INCHES. TOLERANCES FRACTIONS ± 1/32 DECIMALS ± .015 ANGLES ± 1/2° | | WT CHK STR CHK CHECK PR ENGR DES ENGR GR ENGR PREP BY | | DOUGLAS AIRCRAFT COMPANY, INC. LONG BEACH, CALIFORNIA | |
| SEE ENGINEERING RECORDS FOR USAGE DATA | | QUANTITY REQUIRED PER NOTED ASSY | | UNLESS OTHERWISE SPECIFIED | | RELEASE OCT 1 1968 DATE OF DRAWING | | SPECIMEN ASSY - EDGEWISE SHEAR TEST | |
| 88277 | | D | | 23828782 | | CODE IDENT NO. | | SIZE | |
| SCALE | | SHEET 1 OF 1 | | CUSTOMER APPROVAL | | DESIGN ACTIVITY APPROVAL | | PREP BY | |

23828782



GENERAL NOTE UNLESS OTHERWISE NOTED

| | |
|---|---|
| 1 | IDENTIFY PER DPS 3 Q2 |
| 2 | FABRICATION AND PROCESSING METHOD PER P/E |
| 3 | FACT SHEET PERTAINING TO THIS DRAWING |
| 4 | ALL MACHINED SURFACE ROUGHNESS $250 \sqrt{\text{IN}}$ PER MIL-STD-10 |
| 5 | STOCK TO BE PURCHASED HEAT TREATED 125 KSI , TEMPERED |
| 6 | AND COLD FINISHED |
| 7 | HEAT TREAT -9, -11 $\frac{1}{2}$ -17 $125-145 \text{ KSI}$ PER DPS 5 00 |
| 8 | 0° LAYERS OF -19 $\frac{1}{2}$ -21 SKIN MUST BE ADJACENT TO -7 |

PARTS LIST

FIRST RELEASE
OF PRINTS
DEC 21 1978
ORIGINAL DATE
OF DRAWING



74569381

REVISIONS

| LTR | DESCRIPTION | DATE | APPROVED |
|-----|-------------|---------|----------|
| A | SEE E.O. | 7/10/71 | 8827 |

GENERAL NOTES: UNLESS OTHERWISE SPECIFIED

- IDENTIFY PER DPs 9.02
- BOND-LINE THICKNESS, BOND OVERLAP AND SPECIMEN WIDTH TO BE MEASURED AND RECORDED BEFORE TEST.
- ALL MACHINED SURFACE ROUGHNESS 125/PER USAS B46.1
- FABRICATION AND PROCESSING METHOD PER FACT SHEET Z4578680
- MAKE ADHERENDS FROM 13.00 PANELS OF SUFFICIENT WIDTH TO ENABLE NUMBER OF REPLICATES STATED ON E.O. TO BE CUT FROM PANEL. AFTER 45° CUT, MATCHING PAIRS OF ADHERENDS SHALL BE IDENTIFIED A-A OR B-B AS SHOWN.
- ASSEMBLE ON BASE PLATE TO ENSURE ALIGNMENT OF MATCHING PAIRS OF ADHERENDS. SEE VIEW A.
- COMPLETE BONDING PRIOR TO CUTTING INTO 1.00 WIDE SPECIMENS.

QUANTITY REQUIRED PER NOTED DASH NO.

| DASH NO. | QUANTITY |
|----------|----------|
| 500 | 1 |
| 501 | 1 |

UNLESS OTHERWISE SPECIFIED CONTRACT NO. F39415-71-C-1340

STRESS $\frac{1}{2}$ INCHES

CHECK $\frac{1}{2}$ INCHES

DESIGN $\frac{1}{2}$ INCHES

PREP BY $\frac{1}{2}$ INCHES

DESIGN ACTIVITY APPROVAL $\frac{1}{2}$ INCHES

CUSTOMER APPROVAL $\frac{1}{2}$ INCHES

ORIG REGION

RELEASE CODE

FOR COMPLETE USAGE DATA SEE ENGINEERING RECORDS

FIRST RELEASE OF PRINTS 6 971

ORIGINAL DATE OF DRAWING 1/1/71

SHEET 1 OF 1

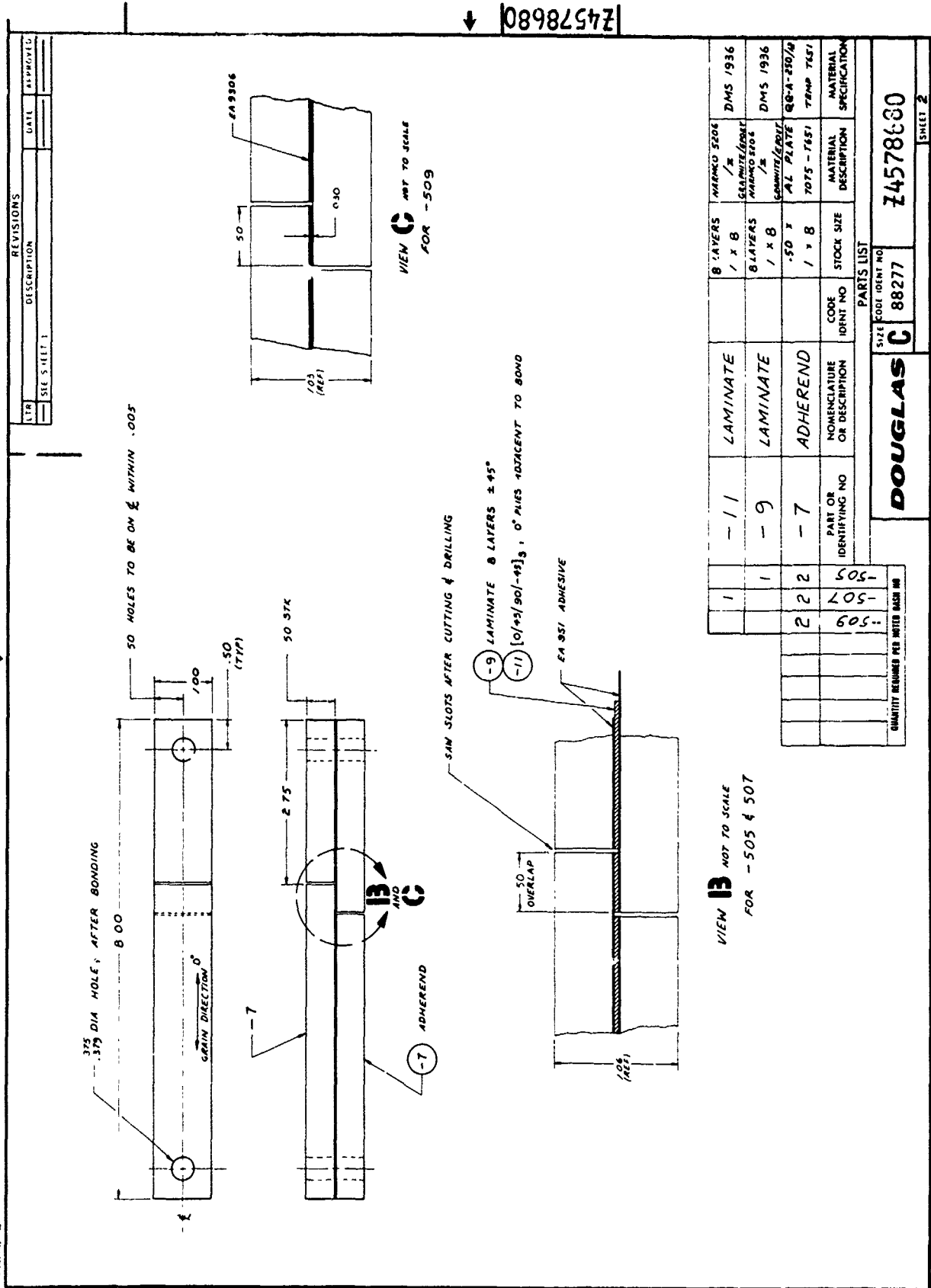
3/16 DIA HOLE 2 PLCS, AFTER BONDING

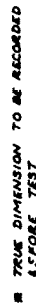
* HOLES TO BE ON CENTER LINE WITHIN .005

THICKNESS DIFFERENCES BETWEEN MATCHING -3A AND -3B ADHERENDS MUST BE CONTROLLED AS SHOWN TO MINIMIZE VARIATION OF ADHESIVE THICKNESS IN TEST REGION

VIEW A
DIAGRAMMATIC ONLY

Z4578680





| REVISIONS | | | |
|-----------|-------------|------|----------|
| LTR | DESCRIPTION | DATE | APPROVED |
| A 566 | EO | | |

PARTS LIST

B-STAGE MATERIAL TO BE CURED FOR -5 AND -7 IN THE ORDER SHOWN IN THE TABLE

| LAYER | 5 | 7 |
|-------|---|---|
| 1 | 0 | 0 |
| 2 | 4 | 0 |
| 3 | 3 | 0 |
| 4 | 0 | 0 |
| 5 | 0 | 0 |
| 6 | 0 | 0 |
| 7 | 4 | 0 |
| 8 | 0 | 0 |
| 9 | 0 | 0 |
| 10 | 4 | 0 |
| 11 | 3 | 0 |
| 12 | 0 | 0 |

| WDM | Wavelength (nm) | Material | Wavelength (nm) |
|-----|-----------------|----------|-----------------|
| A | 5206 | GRAPHITE | 5206 |
| B | 755 | GRAPHITE | 755 |
| C | 5505 | BLU IN | 5505 |

98982623

2

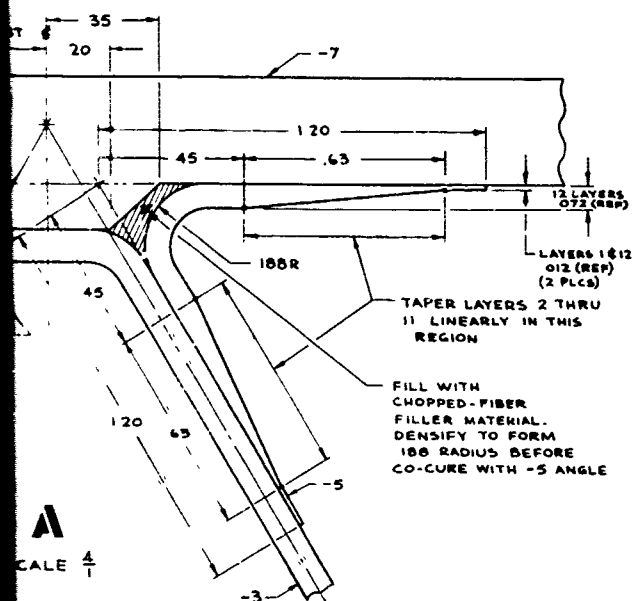
GENERAL NOTES UNLESS OTHERWISE SPECIFIED

- 1 IDENTIFY PER DPS 302
- 2 -5 ANGLES ARE CURED IN POSITION AGAINST THE -5 WEB AND -7 CAP. AT THE SAME TIME, THE -3 WEB, THE -5 ANGLES AND THE -7 CAP ARE BONDED TOGETHER WITH EA 951 ADHESIVE LAYUP -5 ANGLES WITH ALTERNATE $\pm 45^\circ$ LAYERS
- 3 ASSEMBLY SHOP PRACTISE PER DPS 270
4. FABRICATION AND PROCESSING METHOD PER PROCESS ENGINEERING FACT SHEET PERTAINING TO THIS DRAWING
- 5 LAYER SEQUENCE OF -3 & -9 WEBS PER 25578684 ZONE 7 AT NODE
- 6 LAYUP OF -7, -15, -17 & -27 CAPS IS IN SETS OF 0/45/90/-45°, SYMMETRIC ABOUT MID-PLANE OF THE LAMINATE. THE 0° LAYERS ARE ALONG THE 5.00 CAP DIMENSION. THE ADDITIONAL LAYERS OF -7 CAP ARE ADDED AFTER BASIC LAYERS ARE IN POSITION AND ARE SYMMETRIC ABOUT THEIR OWN MID-PLANE
- 7 DELETED

CONTINUED ON SHEET # 2

| REVISIONS | | | |
|-----------|-------------|--------|----------|
| LTR | DESCRIPTION | DATE | APPROVED |
| A | SEE EO | 7/7/71 | 1205 |

CONTINUED ON SHEET 2



| | | | | | | | | | | | | |
|------------|------|------|------|----|---------------------------|--------------------------------|-----------------------|---------------------------------|--|---------------------------|------------|------|
| | | I | | | -17 | CAP | 64 LAYERS X 2 X 4 | BORON/EPOXY AVCO 5505 | DMS 719 | | | |
| | | | | AR | | FILLER | | GRAPHITE/EPOXY CHOPPED FIBER | TO BE PURCHASED BY PROCESS ENGINEERING | | | |
| AR | | | | AR | EA 951 | ADHESIVE | | | | | | |
| | AR | AR | AR | | HYSOL A9- 5120/H2-3690 | ADHESIVE | | | | | | |
| | | I | I | | NAS 1252-416H | WASHER | | | | | | |
| | | I | I | | MS 21042L4 | NUT | | | | | | |
| | | I | I | | NAS 4604UI2 | BOLT | | | | | | |
| | | | I | | -15 | CAP | 56 LAYERS X 2 X 4 | GRAPHITE/EPOXY HARMCO 5206 | DMS 1936 | | | |
| | | | I | I | -13 | BOLT PAD | 24 X 2 X 1 | GRAPHITE/EPOXY HARMCO 5206 | DMS 1936 | | | |
| | | | I | I | -11 | SHOULDER | 2 X 1 X 1 | | | | | |
| | | | I | I | -9 | WEB | 24 LAYERS X 2 X 12 | GRAPHITE/EPOXY HARMCO 5206 | | | | |
| | | | I | | -7 | CAP | 53 LAYERS X 2 X 5 | GRAPHITE/EPOXY HARMCO 5206 | DMS 1936 | | | |
| | | | | 2 | -5 | ANGLE | 12 LAYERS X 2 X 2 | GRAPHITE/EPOXY HARMCO 5206 | DMS 1936 | | | |
| | | | | I | -3 | WEB | 16 LAYERS X 2 X 12 | GRAPHITE/EPOXY HARMCO 5206 | DMS 1936 | | | |
| -507 | -505 | -503 | -501 | -1 | PART OR IDENTIFYING NO | NOMENCLATURE OR DESCRIPTION | CODE IDENT NO | STOCK SIZE | MATERIAL DESCRIPTION | MATERIAL SPECIFICATION | FINL NO | ZONE |
| PARTS LIST | | | | | | | | | | | | |

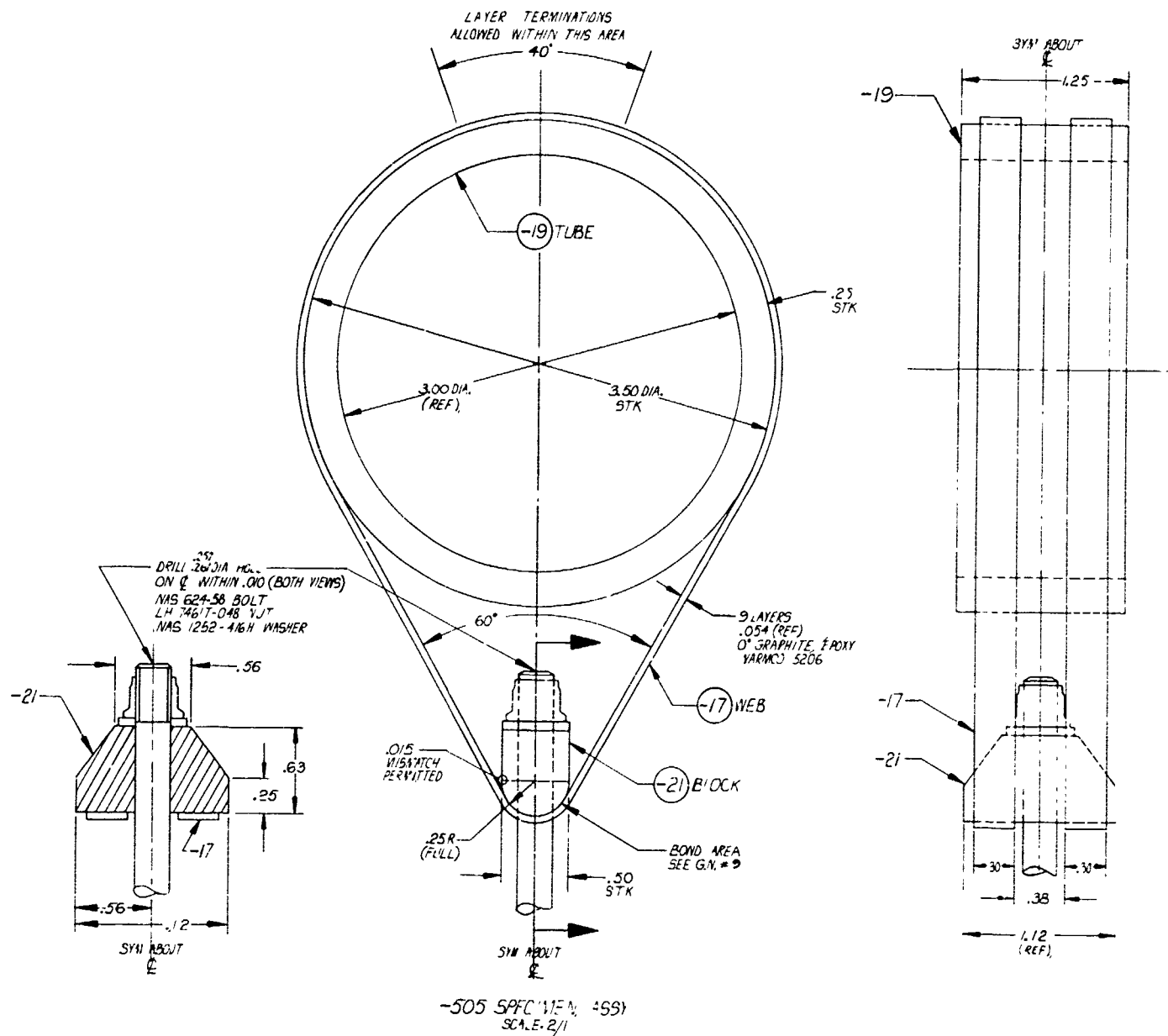
PARTS LIST

QUANTITY REQD PER NOTED DASH NO

| | | | | | | | |
|--|--|--|--|---------------------------------|--|--|--|
| DASH NUMBERS OF THIS DWG ODD DASH NUMBERS SHOWN EVEN DASH NUMBERS OPPOSITE | | UNLESS OTHERWISE SPECIFIED DIMENSIONS ARE IN INCHES. TOLERANCES ANGLES $\pm 0^\circ - 30'$ 3 PLACE DEC ± 0.015 2 PLACE DEC ± 0.03 | | CONTRACT NO F33615-71-C-1340 | | DOUGLAS AIRCRAFT COMPANY LONG BEACH, CALIFORNIA | |
| FINISH | | | | STRESS Rm 6-9-71 | | SPECIMEN ASSY -- TRUSS WEB JOINT TENSION TEST | |
| ECA 10045 CONCEPTUAL WING | | | | CHECK E SPAN 6-9-71 | | | |
| NEXT ASSY USED ON | | | | DESIGN AV 6-4-71 | | | |
| FIRST APPLICATION | | | | PREP BY AV HANLEY 6-4-71 | | | |
| FOR COMPLETE USAGE DATA SEE ENGINEERING RECORDS | | ORIG SECTION | | RELEASE CODE | | DESIGN ACTIVITY APPROVAL | |
| | | | | | | SIZE CODE IDENT NO D 88277 | |
| | | | | | | Z3578686 | |
| | | | | | | SHEET 1 OF 3 | |

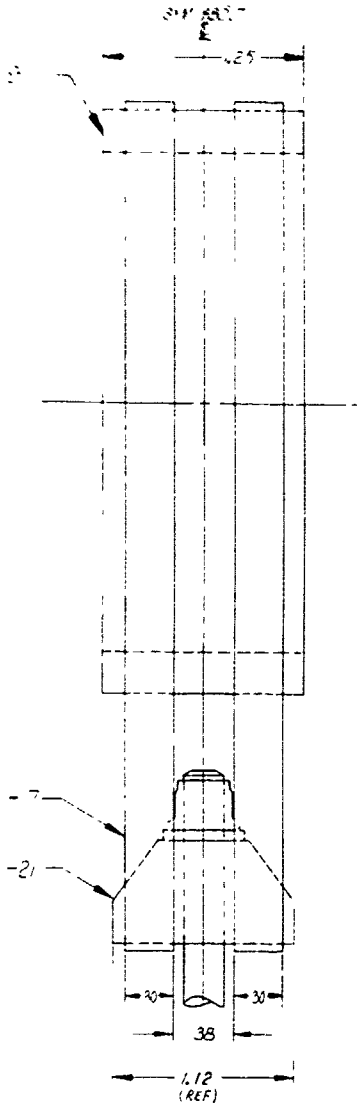
1

3578686



2

| REVISIONS | | | |
|-----------|-------------|------|----------|
| LTR | DESCRIPTION | DATE | APPROVED |
| | SEE SHEET 1 | | |



GENERAL NOTES CONTINUED

9. TO INSURE GOOD FIT, BOND -21 BLOCK TO SMALL END OF -17 WCB WITH
HYSOL A9-5150/H2-3690 ADHESIVE.
ALIGN BOLT ϕ WITH ASSY ϕ DURING BONDING OPERATION.

CONTINUED ON SHEET 3

[illegible]**DOUGLAS**

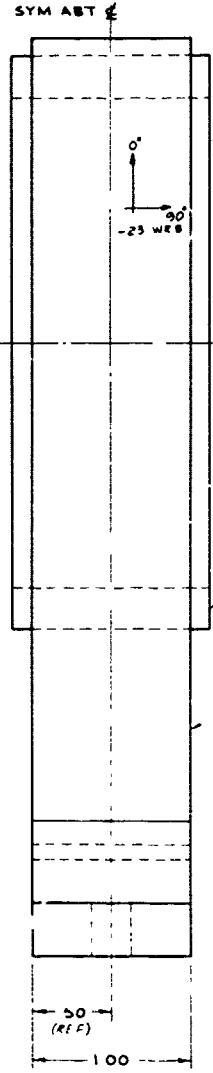
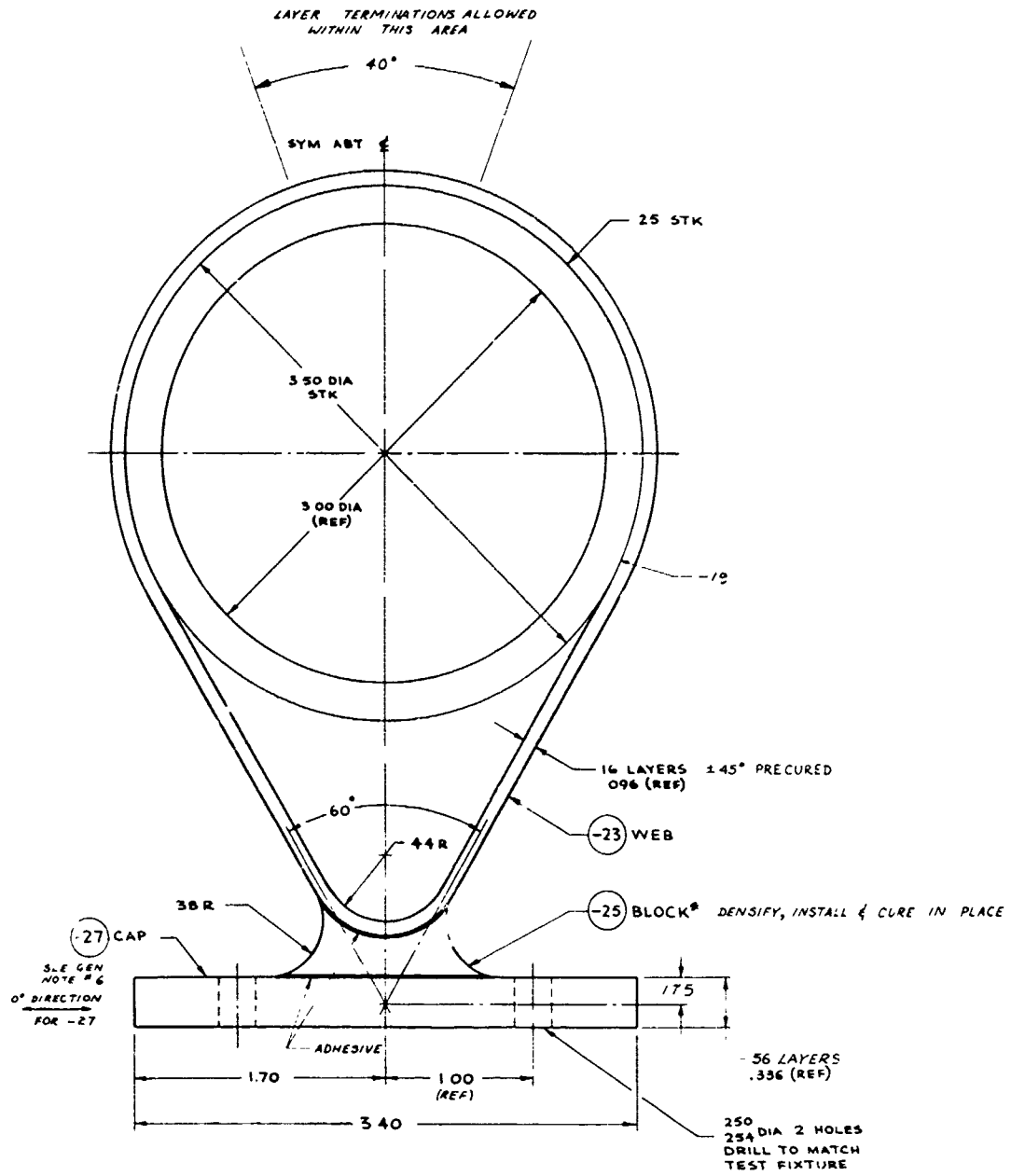
| | |
|------|----------------|
| SIZE | CODE IDENT NO. |
| D | 88277 |

43578686

SHEET 2

1

98981557



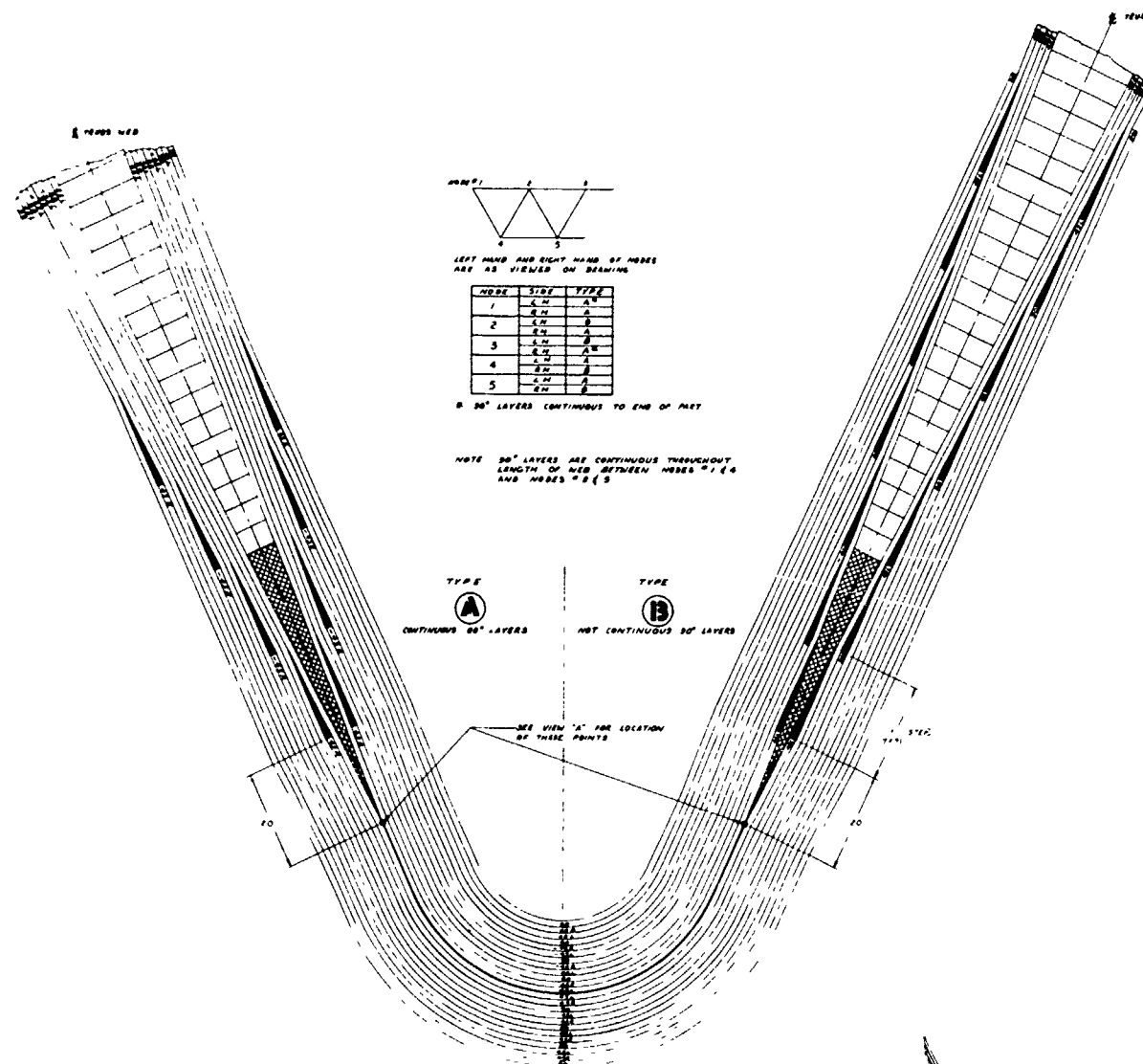
-507 SPECIMEN ASSY
SCALE 2/1

* MATERIAL FOR -25 TO BE DETERMINED BY PROCESS ENGRG WITH DESIGN ENGRG APPROVAL

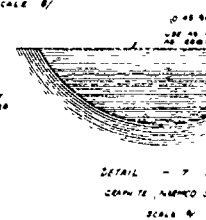
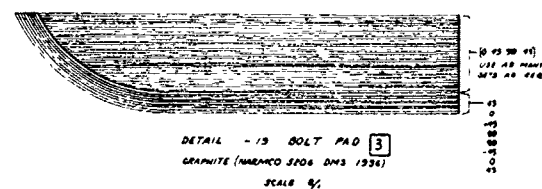
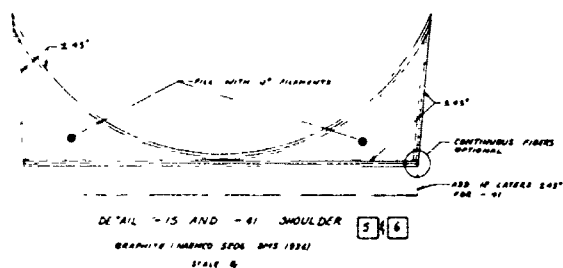
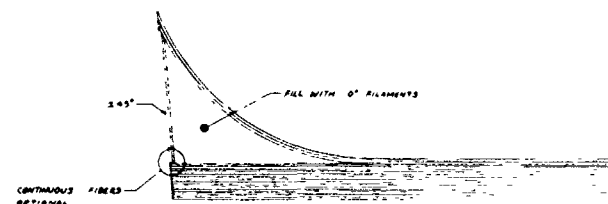
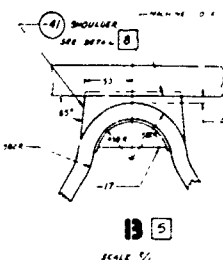
| QUANTITY | DESCRIPTION |
|----------|-------------|
| | |

2

SHEET 3

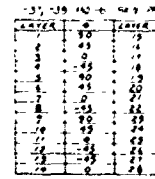


LAYUP SEQUENCE OF -45 AT NODE
(DIAGRAMMATIC ONLY)



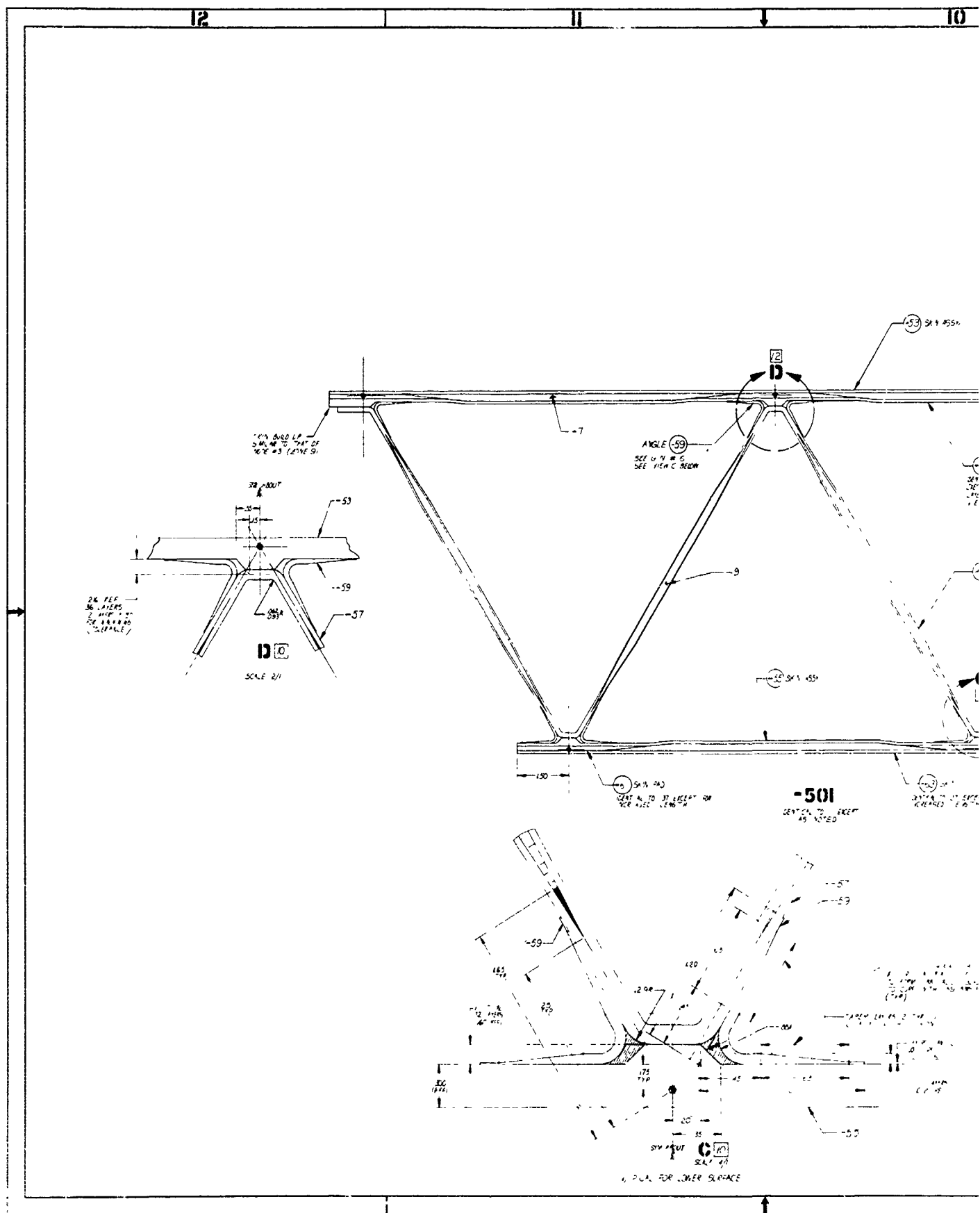
[0 45 50° 45°] = 4 347 (MAY 1970)

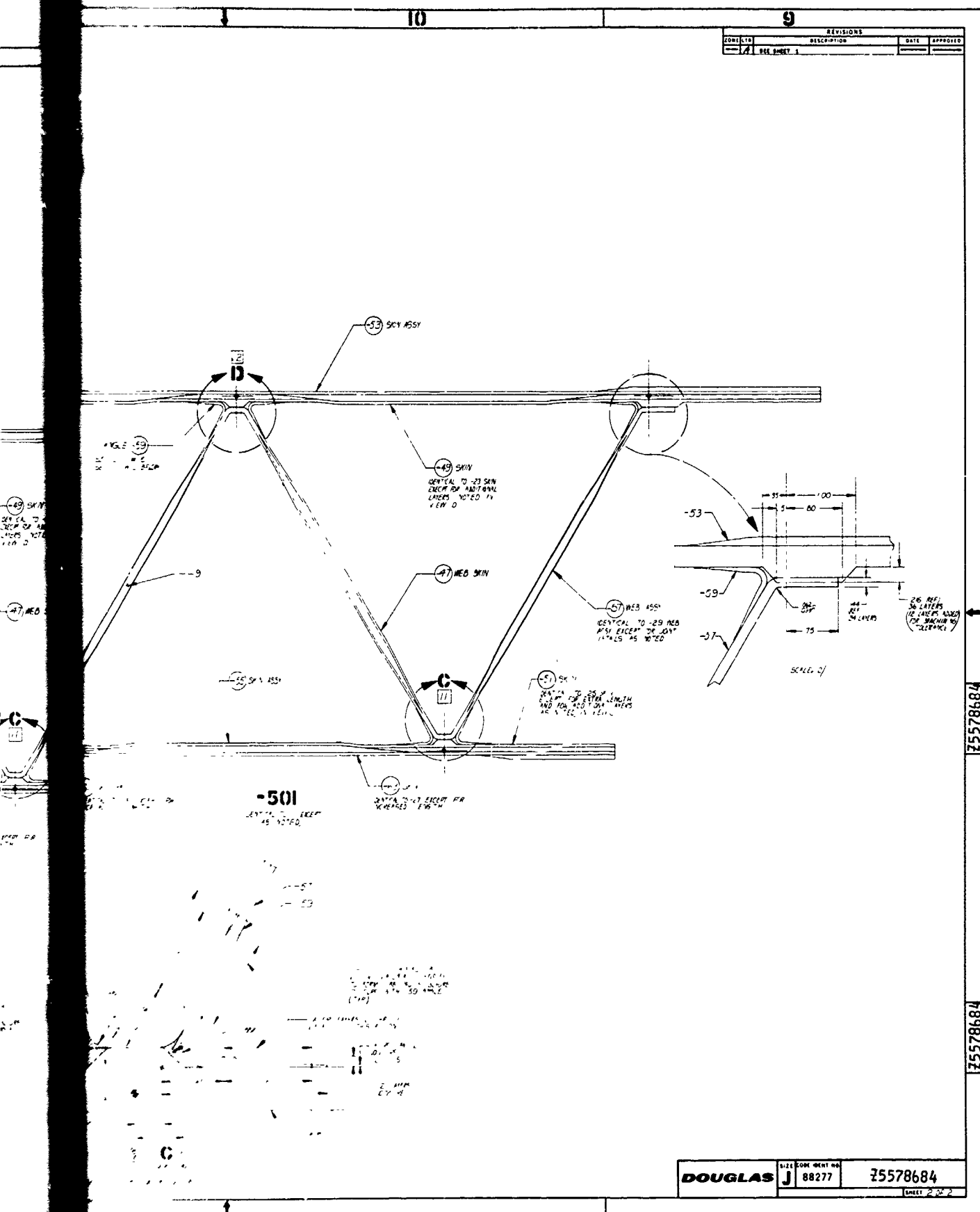
4



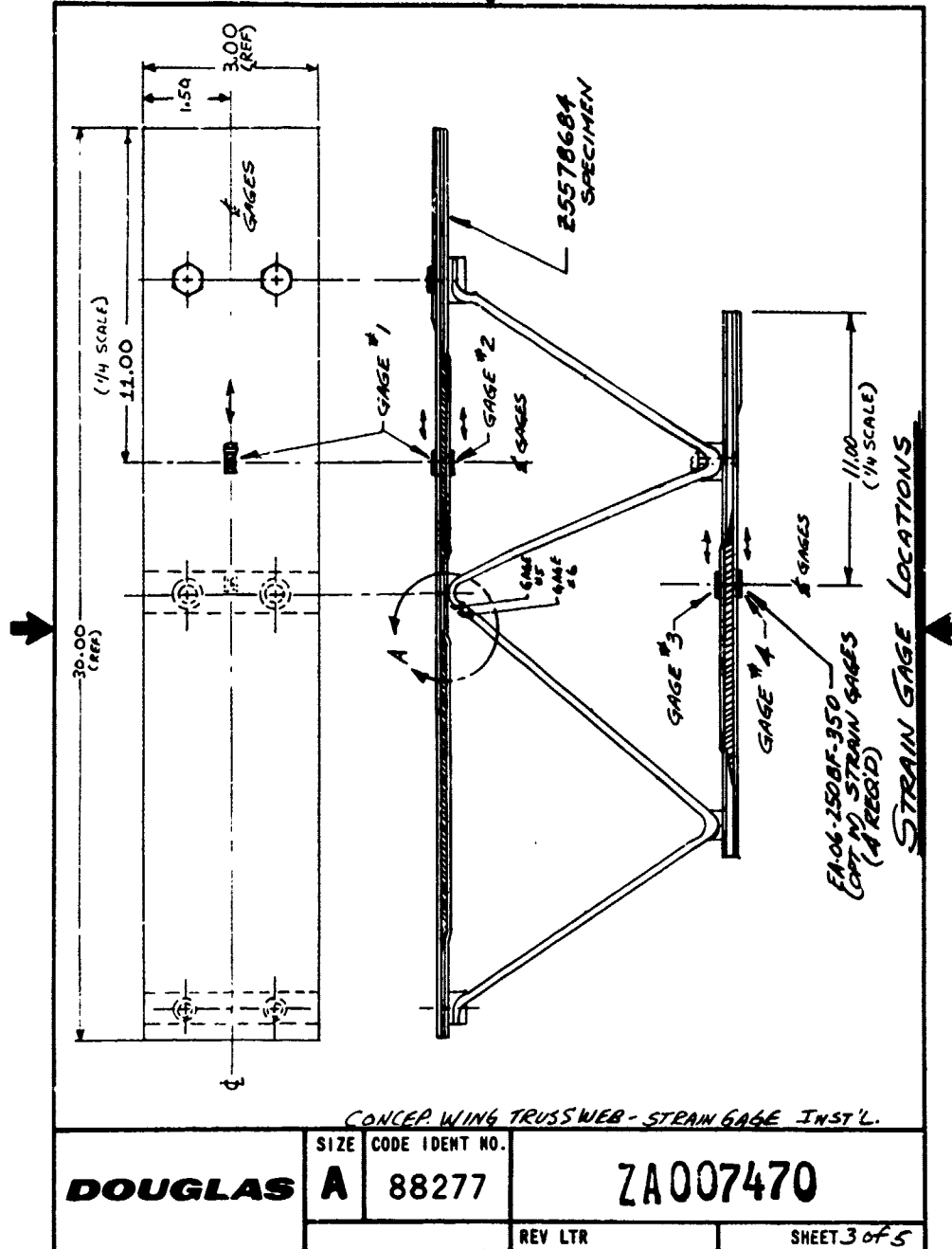
1

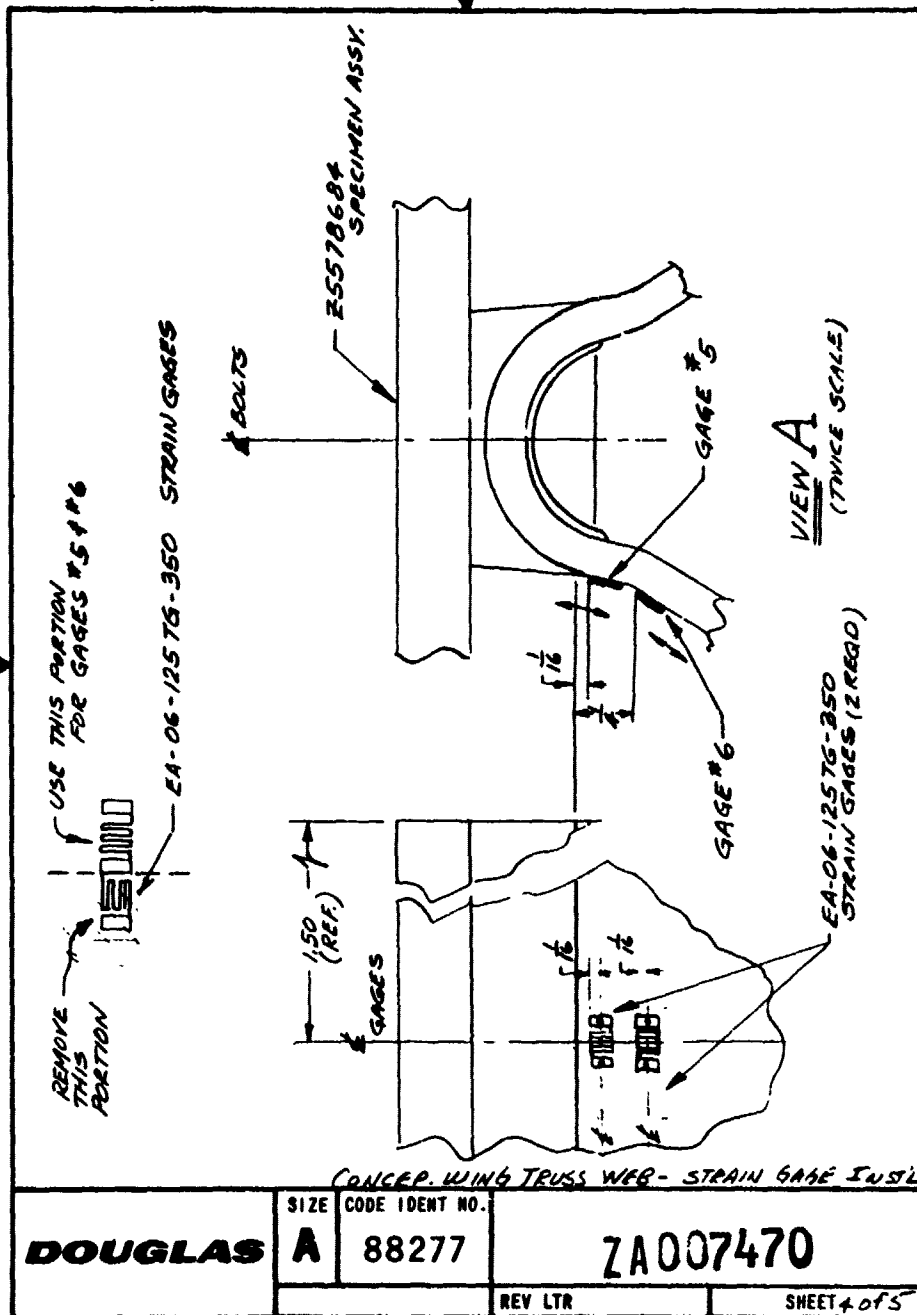
1



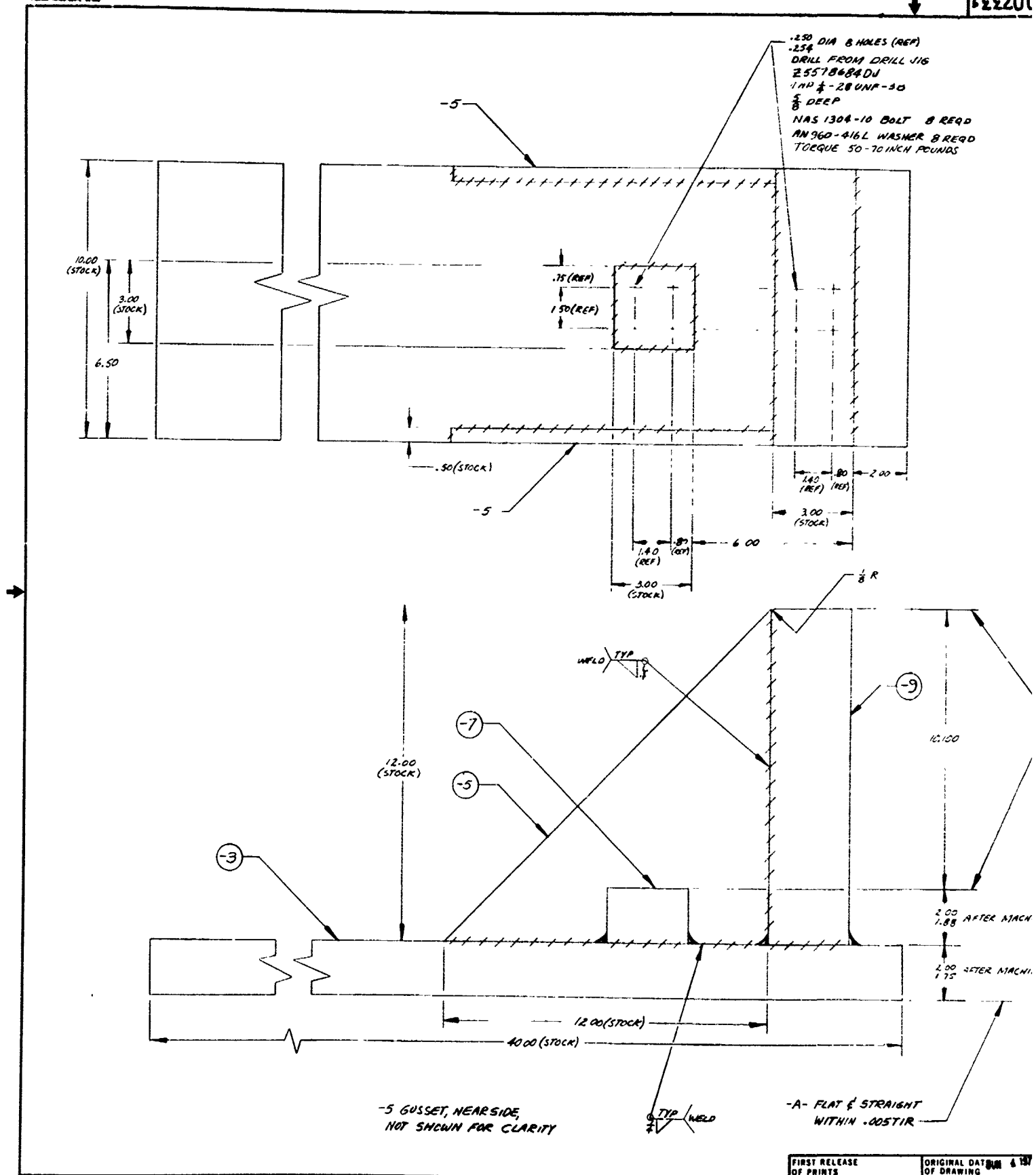


FORM XA60-13A2 (1-68)





007331



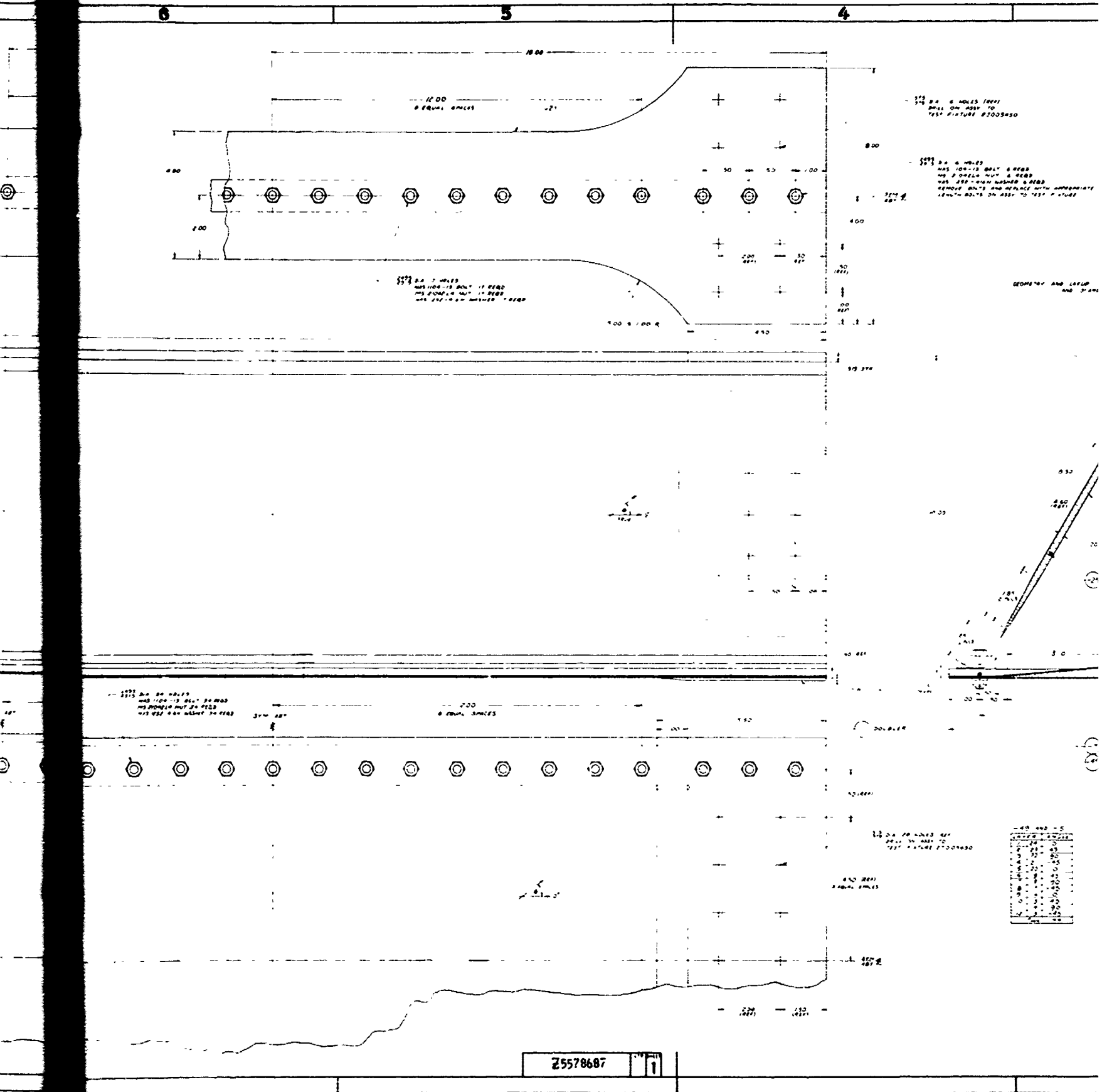
ORIGINAL DATE OF DRAWING JUN 4 197

[illegible]

2

3

4



75578687

1

420

420

370 480 (2) 98 2

1 IDENTIFY PER OPS 3 OF
2 ASSEMBLY AND PRACTICE PER OPS 3 TO
3 IDENTIFICATION AND PROCEEDING METHOD PER 2/3 AND
4 SHEET PERTAINING TO THIS DOCUMENT
5 BOND - 11 - 15 AND - 25 BOUNDED TO BEING WITH
6 100 ADVISORY OR EQUIPMENT CO (CUMULATIVE BONDING
7 OF 20 OPTIMUM
8 MAP 1000 - 21 100 - 100 25 PER OPS 3 00



| | |
|----|----|
| 10 | 43 |
| 13 | 45 |
| 18 | 45 |
| 20 | 49 |
| 22 | 50 |
| 25 | 50 |

[illegible]

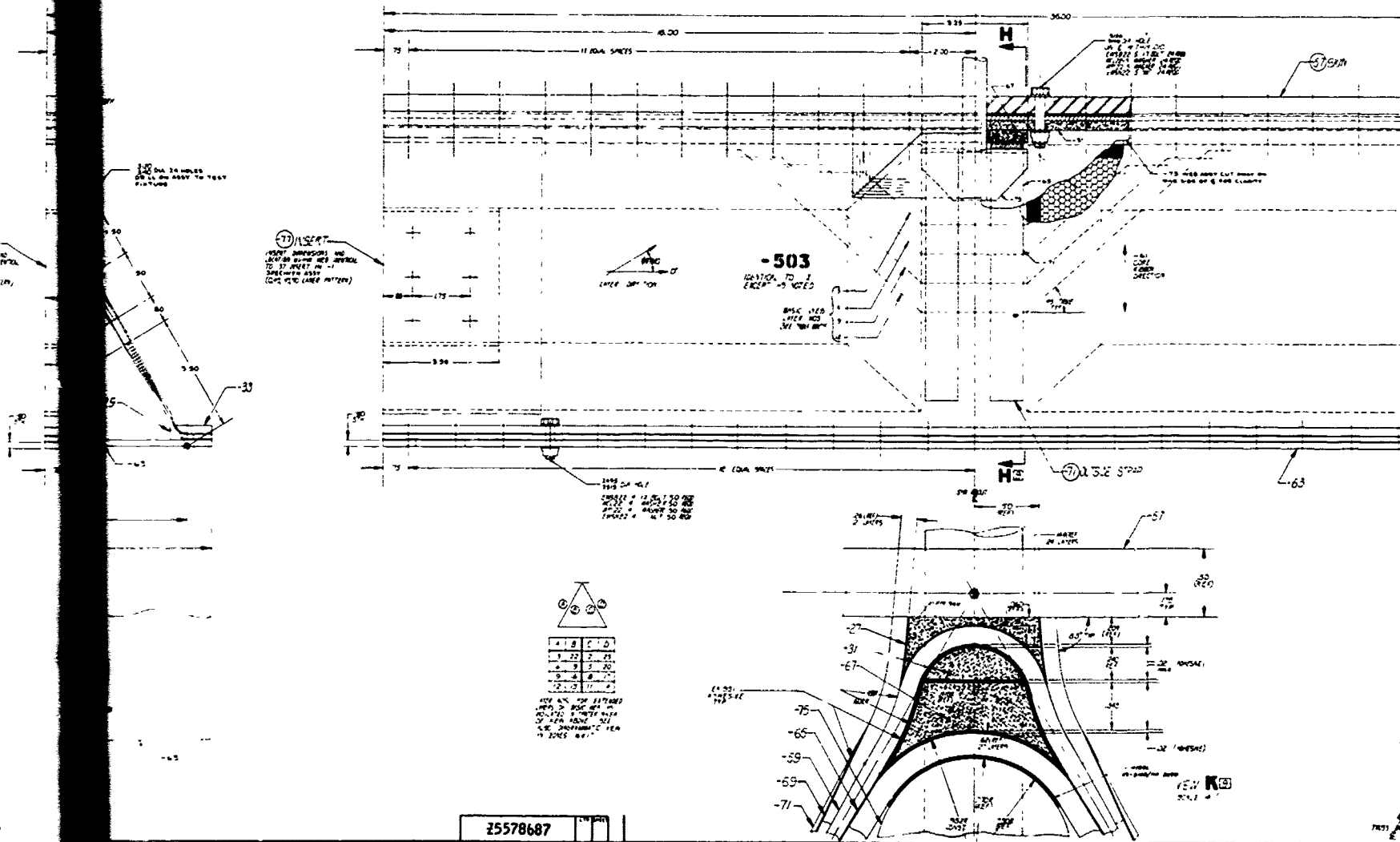
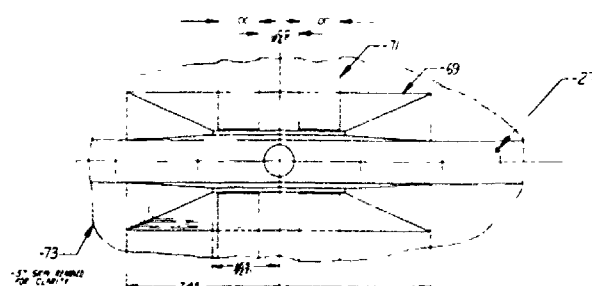
| | | |
|-----------------------------|-------|-----------------------------------|
| 1-017 0(1) 011 01 00-015 | 八 月 廿 | 00-6-00; 0015 01 00-0-06 歲 子 癸 |
|-----------------------------|-------|-----------------------------------|

25578687

[illegible]

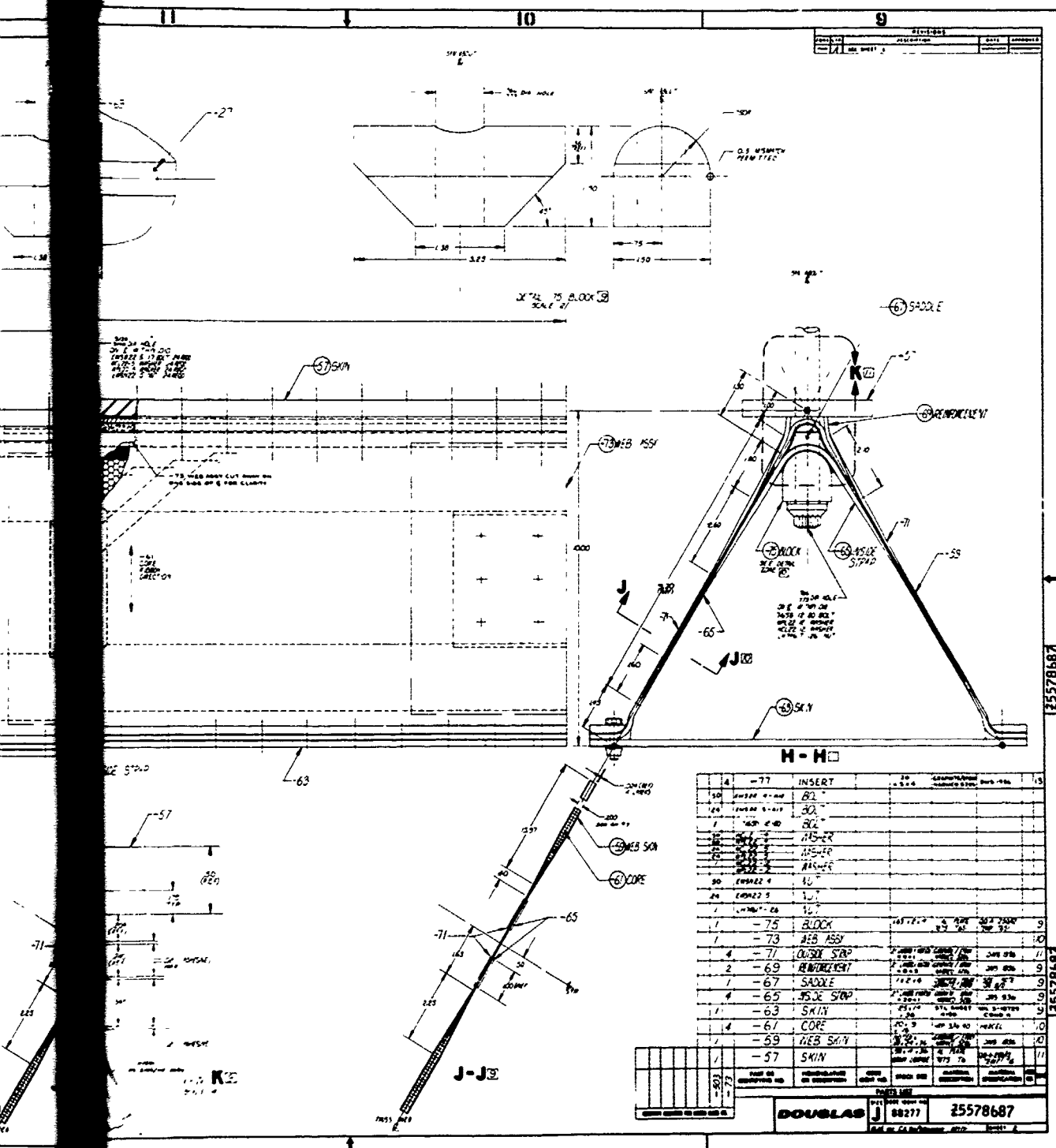
| | | | | | |
|--|--|--|--|--|--|
| 1. INSTRUCTIONS TO THE USER 2. INSTRUCTIONS TO THE USER 3. INSTRUCTIONS TO THE USER | | 4. INSTRUCTIONS TO THE USER 5. INSTRUCTIONS TO THE USER 6. INSTRUCTIONS TO THE USER | | 7. INSTRUCTIONS TO THE USER 8. INSTRUCTIONS TO THE USER 9. INSTRUCTIONS TO THE USER | |
| 10. INSTRUCTIONS TO THE USER 11. INSTRUCTIONS TO THE USER 12. INSTRUCTIONS TO THE USER | | 13. INSTRUCTIONS TO THE USER 14. INSTRUCTIONS TO THE USER 15. INSTRUCTIONS TO THE USER | | 16. INSTRUCTIONS TO THE USER 17. INSTRUCTIONS TO THE USER 18. INSTRUCTIONS TO THE USER | |

[illegible]



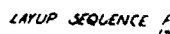
25578687

2



[illegible]

20



2

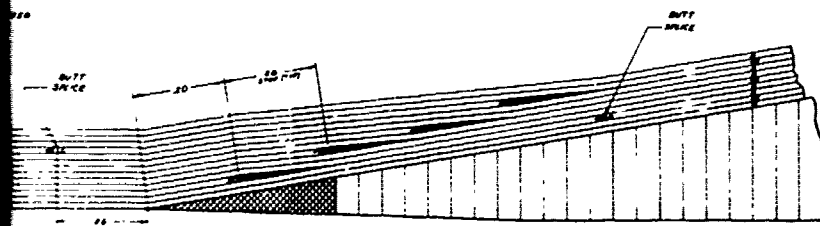
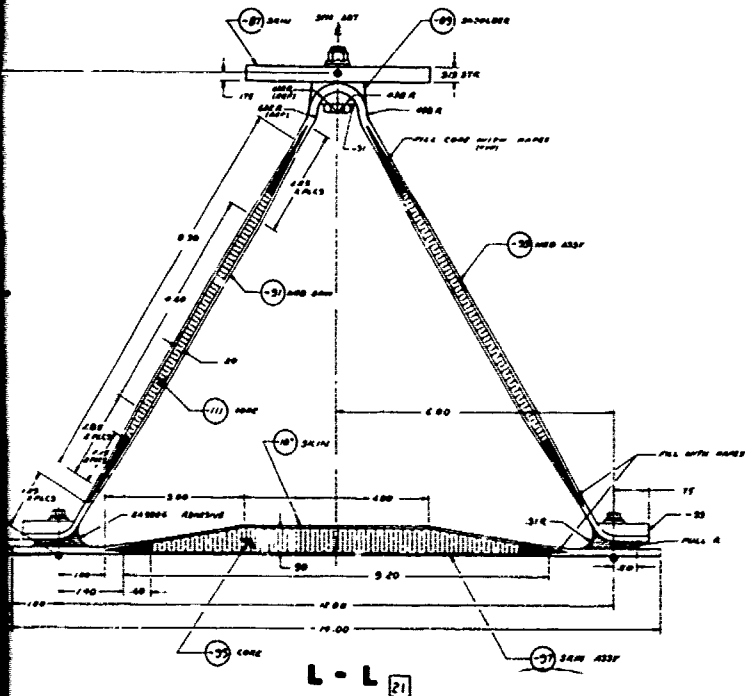
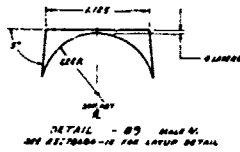
| SECRET | | | |
|-----------|------------|------|-----------|
| FORM 1-70 | DISCLAIMER | DATE | REVISIONS |
| 000 | 000 0000 1 | | |

GENERAL NOTE CONTINUED FROM SHEET 1

8. MEAT TRAY - 11, - 07 @ 103 100 - 100 201 MEA 000 200
0 0000 - 00 WITH 01300 09 - 000/0-0000 AFTER 0001

10. CO-UNION AND BOND - 100 WITH 0100 0000 0000 00
- 100 000000 AND REACHING TO 000 000000

11. 0000 - 00 TO - 00 WITH 00001 0000 - 01 0-00
0 0 00 WITH 00000 00 000/00-0000



LAYOUT SEQUENCE FOR -107 AT LOWER NODE
(DIAGRAMMATIC ONLY)

[illegible]

1

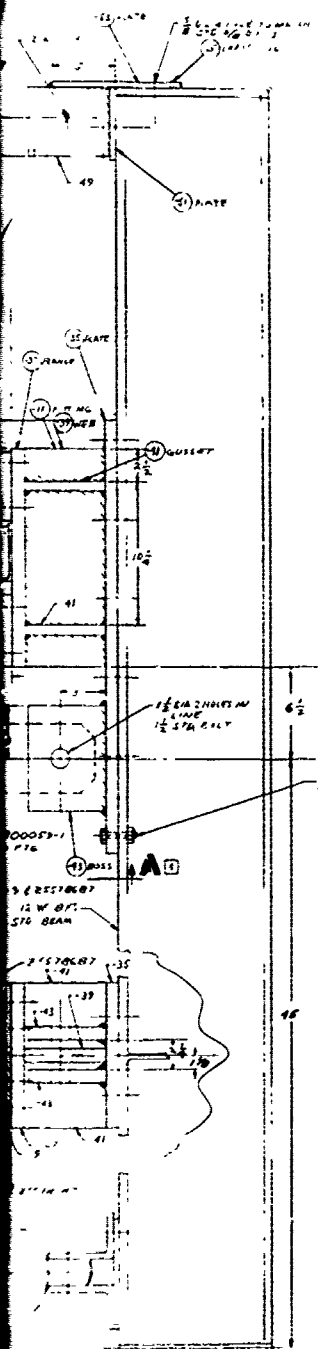
TECHNICAL DRAWING OF A MECHANICAL ASSEMBLY, INCLUDING MAIN VIEW, SECTION A-A, SECTION B-B, AND SECTION C-C.

KEY COMPONENTS AND DIMENSIONS:

- 20A LOAD CELL 2 REFS
- 24000-505 ACTUATOR 2 REFS
- 24000-505 JACK LUG 2 REFS
- 1/2 DIA 2.000 IN 32 PLACES ALL 8 PLACES
- 1/4 DIA 1.000 IN 16 PLACES ALL 8 PLACES
- 1/8 DIA 0.500 IN 16 PLACES ALL 8 PLACES
- 1/16 DIA 0.250 IN 16 PLACES ALL 8 PLACES
- 1/32 DIA 0.125 IN 16 PLACES ALL 8 PLACES
- 1/64 DIA 0.062 IN 16 PLACES ALL 8 PLACES
- 1/128 DIA 0.031 IN 16 PLACES ALL 8 PLACES
- 1/256 DIA 0.015 IN 16 PLACES ALL 8 PLACES
- 1/512 DIA 0.007 IN 16 PLACES ALL 8 PLACES
- 1/1024 DIA 0.003 IN 16 PLACES ALL 8 PLACES
- 1/2048 DIA 0.001 IN 16 PLACES ALL 8 PLACES
- 1/4096 DIA 0.0005 IN 16 PLACES ALL 8 PLACES
- 1/8192 DIA 0.0002 IN 16 PLACES ALL 8 PLACES
- 1/16384 DIA 0.0001 IN 16 PLACES ALL 8 PLACES
- 1/32768 DIA 0.00005 IN 16 PLACES ALL 8 PLACES
- 1/65536 DIA 0.00002 IN 16 PLACES ALL 8 PLACES
- 1/131072 DIA 0.00001 IN 16 PLACES ALL 8 PLACES
- 1/262144 DIA 0.000005 IN 16 PLACES ALL 8 PLACES
- 1/524288 DIA 0.000002 IN 16 PLACES ALL 8 PLACES
- 1/1048576 DIA 0.000001 IN 16 PLACES ALL 8 PLACES
- 1/2097152 DIA 0.0000005 IN 16 PLACES ALL 8 PLACES
- 1/4194304 DIA 0.0000002 IN 16 PLACES ALL 8 PLACES
- 1/8388608 DIA 0.0000001 IN 16 PLACES ALL 8 PLACES
- 1/16777216 DIA 0.00000005 IN 16 PLACES ALL 8 PLACES
- 1/33554432 DIA 0.00000002 IN 16 PLACES ALL 8 PLACES
- 1/67108864 DIA 0.00000001 IN 16 PLACES ALL 8 PLACES
- 1/134217728 DIA 0.000000005 IN 16 PLACES ALL 8 PLACES
- 1/268435456 DIA 0.000000002 IN 16 PLACES ALL 8 PLACES
- 1/536870912 DIA 0.000000001 IN 16 PLACES ALL 8 PLACES
- 1/1073741824 DIA 0.0000000005 IN 16 PLACES ALL 8 PLACES
- 1/2147483648 DIA 0.0000000002 IN 16 PLACES ALL 8 PLACES
- 1/4294967296 DIA 0.0000000001 IN 16 PLACES ALL 8 PLACES
- 1/8589934592 DIA 0.00000000005 IN 16 PLACES ALL 8 PLACES
- 1/17179869184 DIA 0.00000000002 IN 16 PLACES ALL 8 PLACES
- 1/34359738368 DIA 0.00000000001 IN 16 PLACES ALL 8 PLACES
- 1/68719476736 DIA 0.000000000005 IN 16 PLACES ALL 8 PLACES
- 1/137438953472 DIA 0.000000000002 IN 16 PLACES ALL 8 PLACES
- 1/274877907539 DIA 0.000000000001 IN 16 PLACES ALL 8 PLACES
- 1/549755815078 DIA 0.0000000000005 IN 16 PLACES ALL 8 PLACES
- 1/1099511630156 DIA 0.0000000000002 IN 16 PLACES ALL 8 PLACES
- 1/2199023260312 DIA 0.0000000000001 IN 16 PLACES ALL 8 PLACES
- 1/4398046520624 DIA 0.00000000000005 IN 16 PLACES ALL 8 PLACES
- 1/8796093041248 DIA 0.00000000000002 IN 16 PLACES ALL 8 PLACES
- 1/17592186082496 DIA 0.00000000000001 IN 16 PLACES ALL 8 PLACES
- 1/35184372164992 DIA 0.000000000000005 IN 16 PLACES ALL 8 PLACES
- 1/70368744329984 DIA 0.000000000000002 IN 16 PLACES ALL 8 PLACES
- 1/140737488659968 DIA 0.000000000000001 IN 16 PLACES ALL 8 PLACES
- 1/281474977319936 DIA 0.0000000000000005 IN 16 PLACES ALL 8 PLACES
- 1/562949954639872 DIA 0.0000000000000002 IN 16 PLACES ALL 8 PLACES
- 1/1125899909279744 DIA 0.0000000000000001 IN 16 PLACES ALL 8 PLACES
- 1/2251799818559488 DIA 0.00000000000000005 IN 16 PLACES ALL 8 PLACES
- 1/4503599637118976 DIA 0.00000000000000002 IN 16 PLACES ALL 8 PLACES
- 1/9007199274237952 DIA 0.00000000000000001 IN 16 PLACES ALL 8 PLACES
- 1/18014398548475904 DIA 0.000000000000000005 IN 16 PLACES ALL 8 PLACES
- 1/36028797096951808 DIA 0.000000000000000002 IN 16 PLACES ALL 8 PLACES
- 1/72057594193903616 DIA 0.000000000000000001 IN 16 PLACES ALL 8 PLACES
- 1/144115188387807232 DIA 0.0000000000000000005 IN 16 PLACES ALL 8 PLACES
- 1/288230376775614464 DIA 0.0000000000000000002 IN 16 PLACES ALL 8 PLACES
- 1/576460753551228928 DIA 0.0000000000000000001 IN 16 PLACES ALL 8 PLACES
- 1/1152921507102457856 DIA 0.00000000000000000005 IN 16 PLACES ALL 8 PLACES
- 1/2305843014204915712 DIA 0.00000000000000000002 IN 16 PLACES ALL 8 PLACES
- 1/4611686028409831424 DIA 0.00000000000000000001 IN 16 PLACES ALL 8 PLACES
- 1/9223372056819662848 DIA 0.000000000000000000005 IN 16 PLACES ALL 8 PLACES
- 1/18446744113639325696 DIA 0.000000000000000000002 IN 16 PLACES ALL 8 PLACES
- 1/36893488227278651392 DIA 0.000000000000000000001 IN 16 PLACES ALL 8 PLACES
- 1/73786976454557302784 DIA 0.0000000000000000000005 IN 16 PLACES ALL 8 PLACES
- 1/147573952909114605568 DIA 0.0000000000000000000002 IN 16 PLACES ALL 8 PLACES
- 1/295147905818229211136 DIA 0.0000000000000000000001 IN 16 PLACES ALL 8 PLACES
- 1/590295811636458422272 DIA 0.00000000000000000000005 IN 16 PLACES ALL 8 PLACES
- 1/1180591623272916844544 DIA 0.00000000000000000000002 IN 16 PLACES ALL 8 PLACES
- 1/2361183246545833689088 DIA 0.00000000000000000000001 IN 16 PLACES ALL 8 PLACES
- 1/4722366493091667378176 DIA 0.000000000000000000000005 IN 16 PLACES ALL 8 PLACES
- 1/9444732986183334756352 DIA 0.000000000000000000000002 IN 16 PLACES ALL 8 PLACES
- 1/18889465972366669512704 DIA 0.000000000000000000000001 IN 16 PLACES ALL 8 PLACES
- 1/37778931944733339025408 DIA 0.0000000000000000000000005 IN 16 PLACES ALL 8 PLACES
- 1/75557863889466678050816 DIA 0.0000000000000000000000002 IN 16 PLACES ALL 8 PLACES
- 1/151115727778933356101632 DIA 0.0000000000000000000000001 IN 16 PLACES ALL 8 PLACES
- 1/302231455557866712203264 DIA 0.00000000000000000000000005 IN 16 PLACES ALL 8 PLACES
- 1/604462911115

VIEW **B-13**

A-A

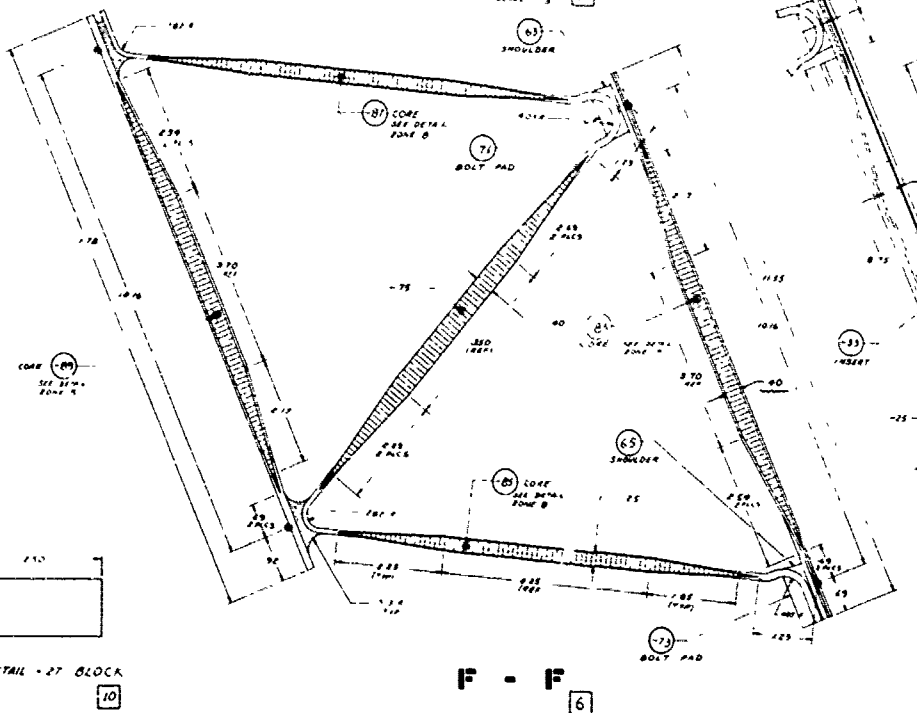
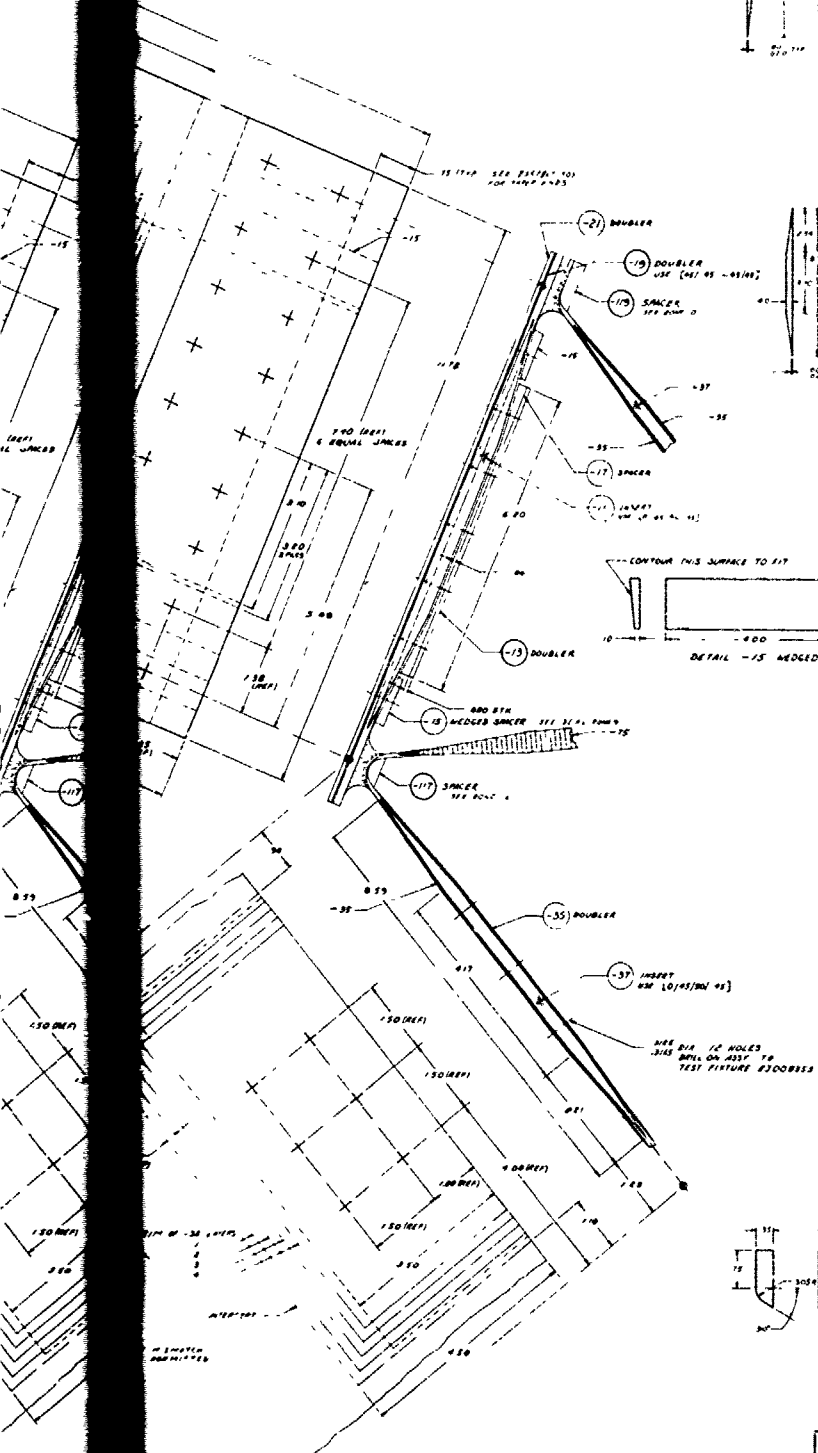
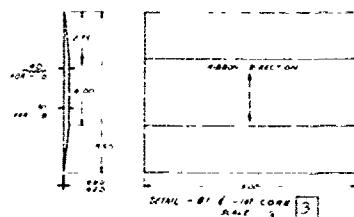
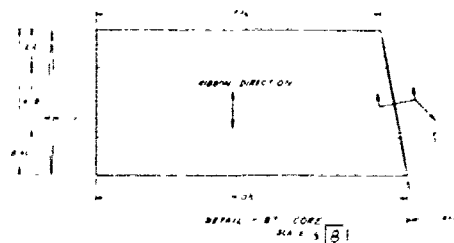
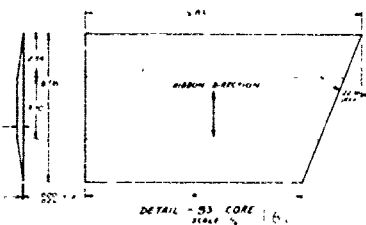
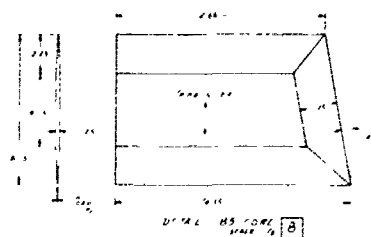
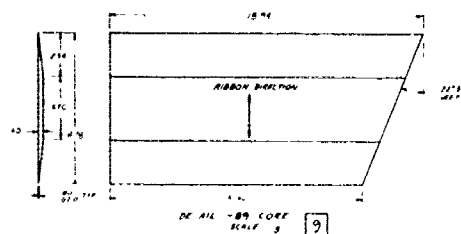


- GEN NOTES:
1. * MATERIAL ORDERED AND DRAWING DETAILS PER DRO 03637
 2. INSTALL - 5", 8", 9" WITH FIXTURE ATTACHES SQUARE & PARALLEL TO TEST SPECIMEN
 3. INFO PER DTS 10254, USE 120,000 PSI COMP. RAD
 4. ALL WELDS ARE 1/2 INCH

[illegible][illegible]

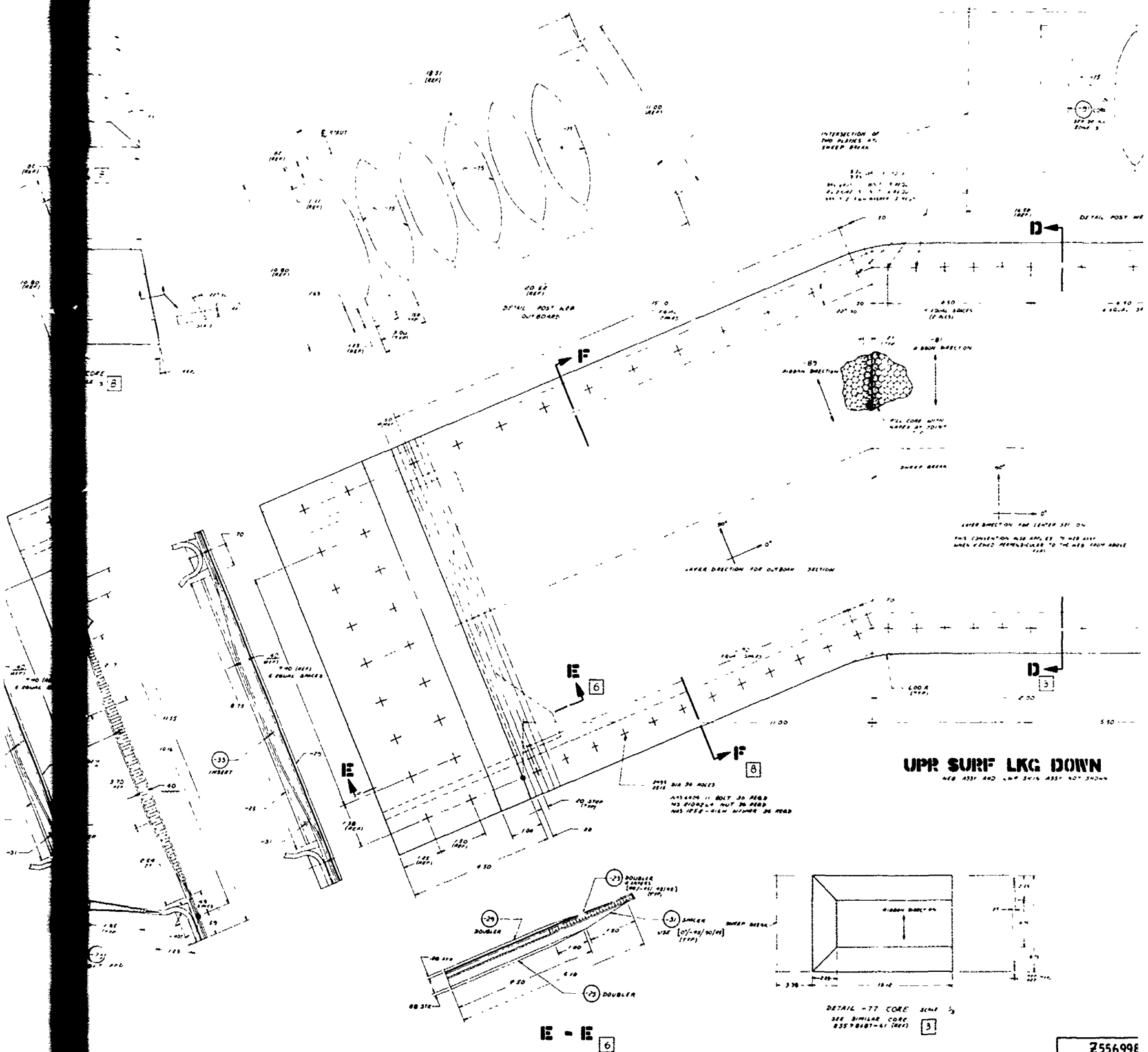
2 J005450



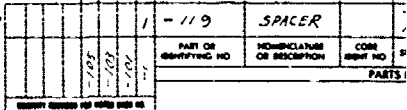


F - F

6



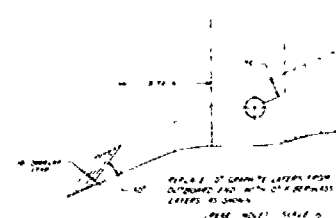
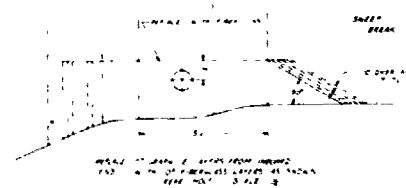
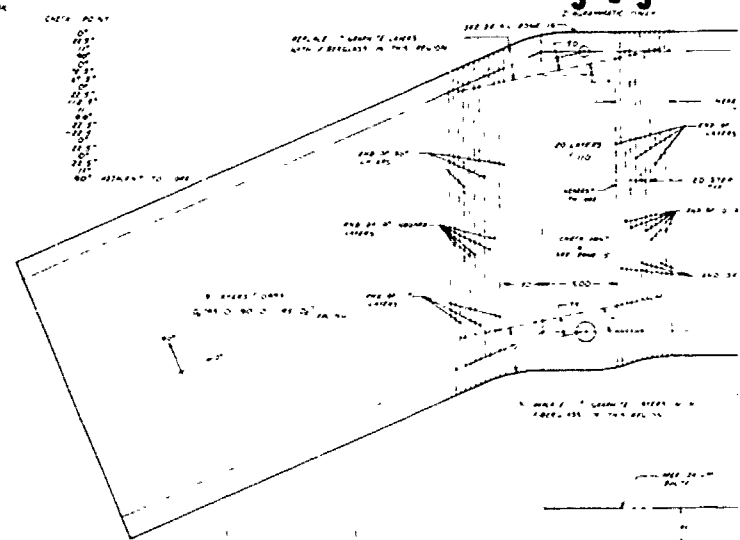
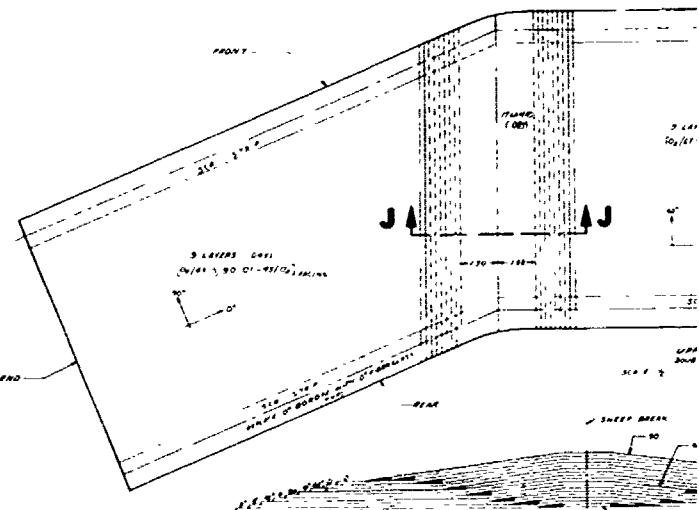
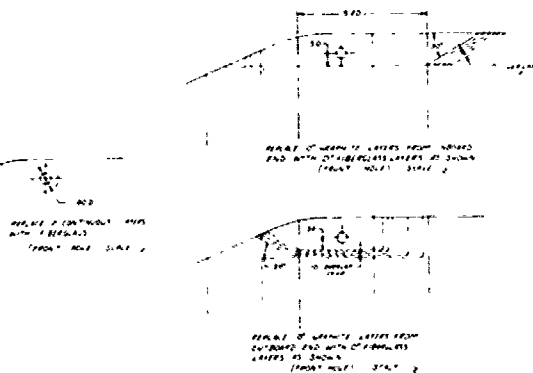
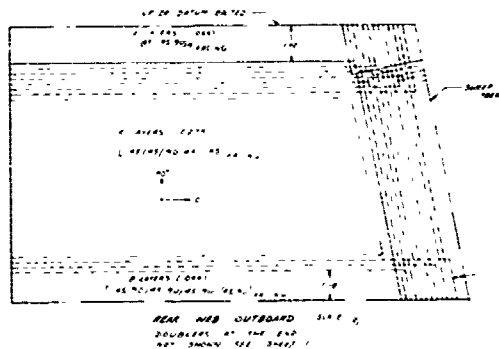
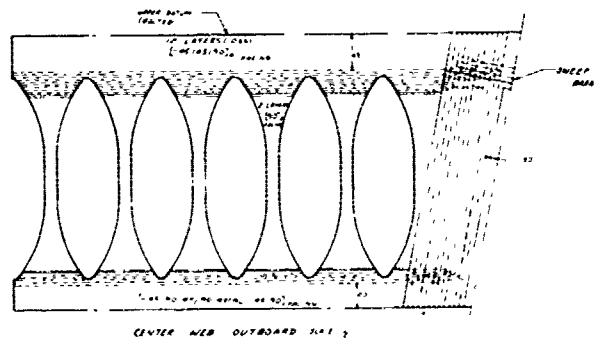
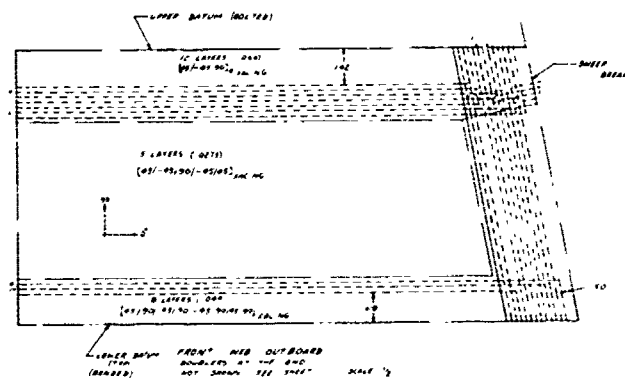
T



16

15

14



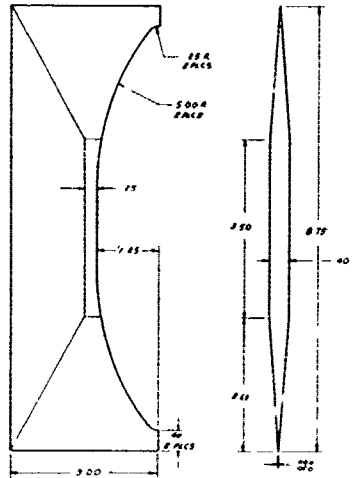
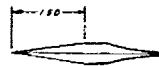
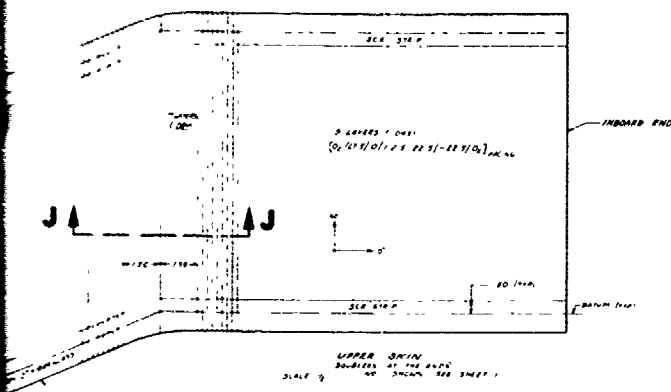
REAR VIEW

2

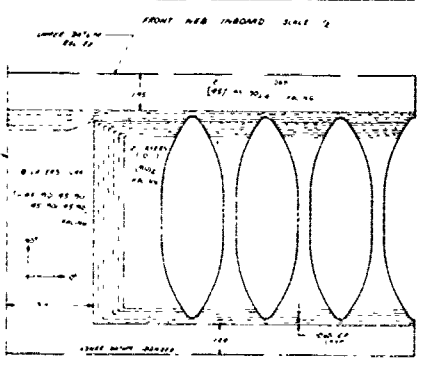
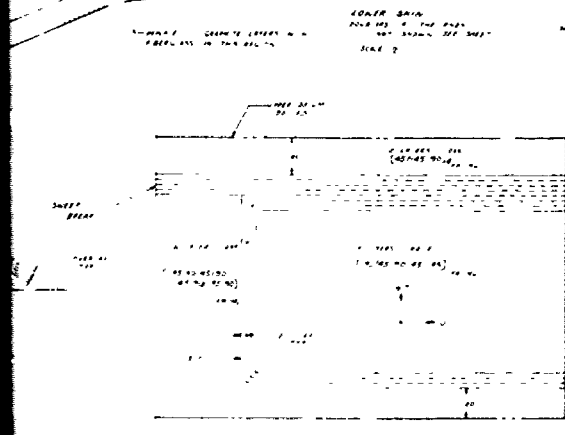
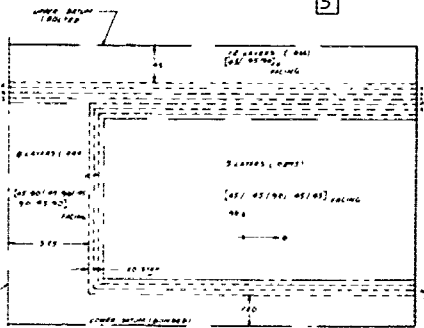
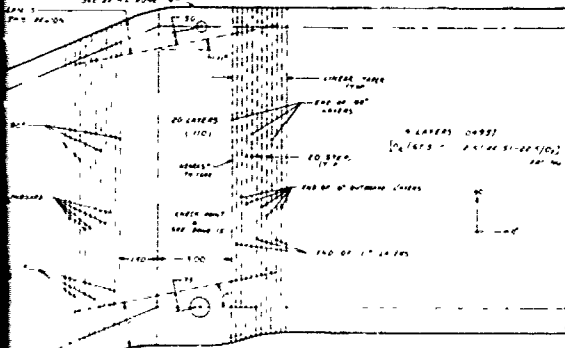
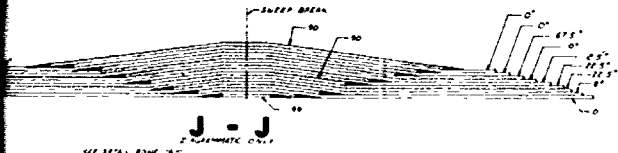
14

13

| DATE | BY | DESCRIPTION | DATE | APPROVED |
|------|----|-------------|------|----------|
| | | REV SHEET 1 | | |



DETAIL - 91 CORE



REAR WEB INBOARD SCALE 1/4

CENTER WEB INBOARD SCALE 1/4

DOUGLAS

DATE

CODE (SHEET NO.)

88277

25569987

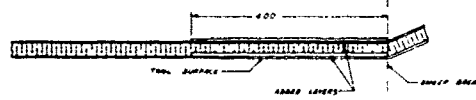
SHEET 2

4

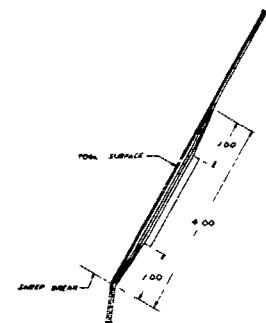
20

19

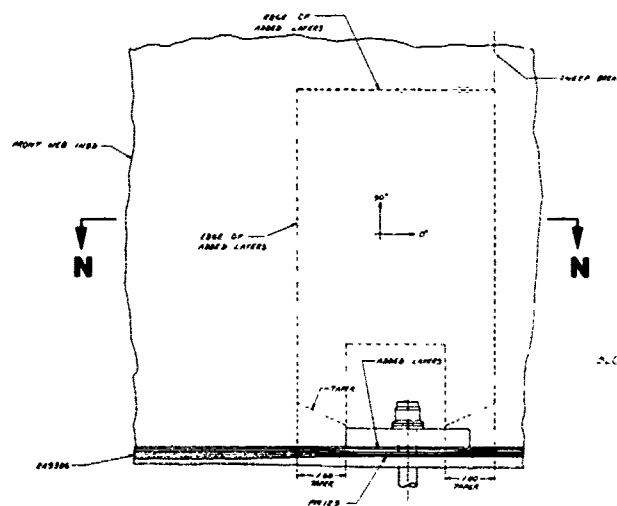
18



N - N

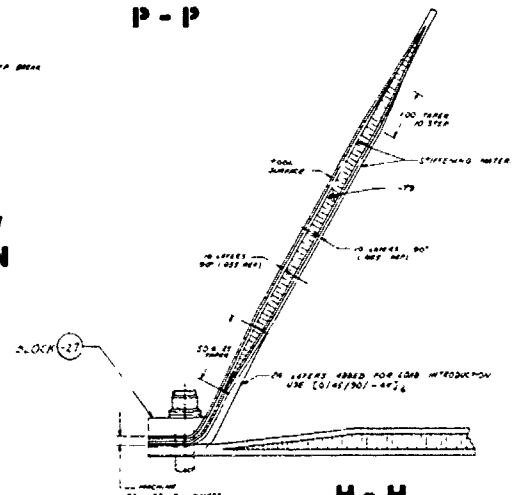


p - p



N

N



H - H

APPENDIX B

RAW MATERIAL QUALITY CONTROL

1. Graphite - Eight batches of Modulite 5206/II graphite/epoxy prepreg were received and tested to DMS 1936B. The test results have been reported for all but Batch 379 (See Table D-1, Reference 3, Table C-1, Reference 10, and Table 9, Reference 9). The data for batch 379 are displayed in Table B-1 of this appendix. The testing of four batches of Thornel 75S was reported in Table D-2 of Reference 3.
2. Boron - Two batches of Rigidite 5505 boron/epoxy prepreg were received and tested to DMS 1919B. The test results for Batch 45 were shown in Table D-3 of Reference 3 and for Batch 47 in Table 8 of Reference 9. Batch 47 was retested before use since some of it was used more than 90 days after the first test. See Table B-2 of this appendix.
3. Mixed Materials - Various tests were conducted to verify the quality of materials and laminations for the mixed graphite studies. The results were reported in Table B-1 of Reference 4.
4. Adhesive - One batch of EA951 and two batches of FM96 were received and tested. See Table D-4 of Reference 3 and Table B-3 of this appendix.

TABLE B-1
PREPREG QUALITY CONTROL RECEIVING INSPECTION REPORT

| | | | | | | | | | | | | | | | | | | | |
|-------------------|--|-----------------|--|----------------------|--|---------|--|---------------|--|----------|--|------|--|--------------|--|----|--|---|--|
| MATERIAL | | MODMORE 11/5206 | | LOT NUMBER | | 379 | | DMS | | 1936-B | | PAGE | | 1 | | OF | | 1 | |
| VENDOR | | NARMCO | | DATE OF MANUFACTURER | | 7-20-72 | | DATE RECEIVED | | 7-26-72 | | | | | | | | | |
| QUANTITY RECEIVED | | 384 | | UNIT SIZE | | 34 Avg. | | S/O | | 16216001 | | P/O | | 201-608384-9 | | | | | |
| NUMBER OF UNITS | | 14 ROLLS | | | | | | | | | | | | | | | | | |

| TEST UNIT IDENTITY | PREPREG PROPERTIES | | | | | LAMINATE PROPERTIES | | | | | THICKNESS PER PLY INCHES | COMMENTS | | |
|------------------------|---------------------|------------------------|------------------|--------|----------|--------------------------|-------------------------------------|---------------------|---------------------|---------------------------------------|--------------------------|-----------|--------------------------------------|------------------------|
| | RESIN CONTENT WT. % | VOLATILE CONTENT WT. % | GEL TIME MINUTES | VISUAL | HANDLING | TENSILE STRENGTH 103 PSI | TENSILE MODULUS 10 ⁶ PSI | RESIN CONTENT WT. % | VOID CONTENT Vol. % | FLEXURAL STRENGTH 10 ³ PSI | | | FLEXURAL MODULUS 10 ⁶ PSI | SHEAR STRENGTH 103 PSI |
| DMS | 39 To 45.0 | 3.0 To Max. | 18 To 26 | — | — | 145.0 Min. | 19.0 Min. | 28 To 34 | 1 Max. | 195.0 Min. | 17.5 Min. | 14.0 Min. | 28 To 34 | 1 Max. |
| REQ'TS | | | | | | | | | | | | | | |
| VENDOR AVERAGE RESULTS | | | | | | | | | | | | | | |
| ROLL 6 -1 | 40.25 | | 22'18" | | | 167.1 | 23.1 | | | 206.4 | 21.0 | 15.4 | 30.48 | .52 |
| -2 | 40.24 | | 21'49" | | | 182.8 | 22.6 | | | 207.0 | 21.0 | 15.1 | 30.46 | .82 |
| -3 | 40.15 | | | | | 184.3 | 20.2 | | | 204.4 | 19.6 | 14.4 | 31.42 | .96 |
| -4 | | | | | | | | | | | | | 32.10 | .91 |
| -5 | | | | | | | | | | | | | | |
| AVE. | 40.2 | .91 | 22'04" | | | 178.1 | 22.0 | | | 205.9 | 20.5 | 15.0 | 31.125 | .80 |
| ROLL 12 -1 | 42.87 | | 22'42" | | | 160.6 | 19.3 | | | 199.1 | 19.6 | 15.1 | 35.13 | 1.15 |
| -2 | 45.00 | | 22'13" | | | 161.8 | 22.5 | | | 215.5 | 22.9 | 14.7 | 33.57 | 1.32 |
| -3 | 44.63 | | | | | 157.2 | 20.4 | | | 191.1 | 20.2 | 15.4 | 33.98 | 1.11 |
| -4 | | | | | | | | | | | | | 33.57 | 1.27 |
| -5 | | | | | | | | | | | | | | |
| AVE. | 44.2 | .86 | 22'28" | | | 159.9 | 20.7 | | | 201.9 | 20.9 | 15.1 | 34.08 | 1.21 |
| ROLL 9 -1 | | | | | | 178.4 | 24.2 | | | | | | | |
| -2 | | | | | | 173.9 | 27.7 | | | | | | | |
| -3 | | | | | | 188.9 | 26.7 | | | | | | | |
| -4 | | | | | | | | | | | | | | |
| -5 | | | | | | | | | | | | | | |
| AVE. | | | | | | 180.4 | 26.2 | | | | | | | |
| SHEET -1 | | | | | | | | | | | | | | |
| -2 | | | | | | | | | | | | | | |
| -3 | | | | | | | | | | | | | | |
| -4 | | | | | | | | | | | | | | |
| -5 | | | | | | | | | | | | | | |
| AVE. | | | | | | | | | | | | | | |
| SHEET -1 | | | | | | | | | | | | | | |
| -2 | | | | | | | | | | | | | | |
| -3 | | | | | | | | | | | | | | |
| -4 | | | | | | | | | | | | | | |
| -5 | | | | | | | | | | | | | | |
| AVE. | | | | | | | | | | | | | | |

| | |
|----------|---|
| REMARKS: | MEETS SPEC. <input checked="" type="checkbox"/> DOES NOT MEET SPEC <input type="checkbox"/> MEETS P.O. <input checked="" type="checkbox"/> DOES NOT MEET P.O. <input type="checkbox"/> O.C. REPRESENTATIVE <u>H. M. Tollner</u> DATE: <u>8-17-72</u> |
|----------|---|

TABLE B-2
BORON CONTROL RECEIVING INSPECTION REPORT

NO. _____

MATERIAL RIGIDITE 5505

DMS 1919B VENDOR AVCO S/O 16216012 P/O 101299339-9 LOT NO. 47

DATE OF MNFG. 9-14-71 DATE RECEIVED 9-21-71 NO. OF ROLLS 2 NO. OF FT. IN ROLL 690

FOLLOWING IS A REPORT ON THE ABOVE MATERIAL, COVERING DETAILED REQUIREMENTS OF APPLICABLE SPECIFICATION.

| TEST | TEST METHOD | SPECIFICATION LIMITS | | TEST OR INSPECTION RESULTS | | DATE TESTED |
|--|-------------|-----------------------------|------|---|-------------|-------------|
| | | MAX. | MIN. | INDV. VALUES | ARITH. MEAN | |
| A) UNCURED MATERIAL | | | | | | |
| 1) RESIN FLOW (% BY WT.) | | | | | | |
| 2) VOLATILES (% BY WT.) | | | | | | |
| 3) RESIN CONTENT (% BY WT.) | | | | | | |
| 4) FILAMENT COUNT AND SPACING | | | | | | |
| 5) ROOM TEMPERATURE WORKING LIFE | | | | | | |
| B) CURED MATERIAL | | | | | | |
| 1) FLEXURAL STRENGTH PSI | DMS 1919 | 225,000 min. | | 321,000, 320,000, 320,000 | 320,000 | 8-10-72 |
| 2) FLEXURAL MODULUS PSI | DMS 1919 | 26.0 x 10 ⁶ min. | | 30.1, 29.7, 30.3 | 30.0 | 8-10-72 |
| 3) ULTIMATE HORIZONTAL SHEAR STRENGTH PSI | DMS 1919 | 8,500 min. | | 11,300, 11,200, 11,300 | 11,000 | 8-10-72 |
| 4) VOID CONTENT (% BY VOL.) | | | | | | |
| 5) RESIN CONTENT (% BY WT.) | | | | | | |
| REMARKS Retest after expiration of shelf-life warranty. | | | | <input checked="" type="checkbox"/> MEETS SPEC. REQ. <input type="checkbox"/> DOES NOT MEET SPEC. REQ. <u>H. M. Toellner</u> COGNIZANT ENGINEER DATE: 8-11-72 | | |

TABLE B-3
RECEIVING QUALITY CONTROL - FM96 ADHESIVE

| PROPERTY | BATCH NO. | TEST RESULT (AVG) | DMS 1892B REQUIREMENT |
|------------------------|-----------|-------------------|-----------------------|
| Tensile Lap Shear, psi | 1639 | 3140 | 2500 |

SECTION IX

PRECEDING PAGE BLANK NOT FILMED

REFERENCES

1. Nelson, W. D., et al., "Composite Medium STOL Transport Structural Integration Study, Task VI of Composite Wing Conceptual Design," Technical Report AFML-TR-72-228, October 1972.
2. First Quarterly Technical Report, "Composite Wing Conceptual Design," McDonnell Douglas Corporation, Report MDC J4129, 14 May 1971.
3. Second Quarterly Technical Report, "Composite Wing Conceptual Design," McDonnell Douglas Corporation Report MDC J4140, 17 August 1971.
4. Fourth Quarterly Technical Report, "Composite Wing Conceptual Design," McDonnell Douglas, Contract F33615-71-C-1340, Report MDC J4170, 17 February 1972.
5. Purdy, D. M., Dietz, C. G; McGrew, J. A., "Optimization of Laminates for Strength and Flutter," Douglas Aircraft Company Paper 6058, presented to Air Force Conference on Fibrous Composites in Flight Vehicle Design, Dayton, Ohio, 26 - 28 September, 1972.
6. Yen, S. W., "Analysis of Thin, Rectangular Sandwich Beam of Variable Thickness Under the Action of Uniform Pressure," Douglas Aircraft Company IRAD Report MDC J5656, May 1972.
7. Fifth Quarterly Technical Report, "Composite Wing Conceptual Design," McDonnell Douglas, Contract F33615-71-C-1340, Report MDC J4181, 17 May 1972.
8. Willoughby, E. G., "Composite Wing Conceptual Design, Final Demonstration Component," Douglas Aircraft Company Test Report DM168, January 1973. Appendix I contains reduction of strain gage data.
9. Sixth Quarterly Technical Report, "Composite Wing Conceptual Design," Contract F33615-71-C-1340, McDonnell Douglas Company Report MD J4187, 17 August 1972.
10. Third Quarterly Technical Report, "Composite Wing Conceptual Design," McDonnell Douglas, Contract F33615-71-C-1340, Report MDC J4110, 17 November 1971.
11. Padawer, G. E. The Strength of Bolted Connections in Graphite/Epoxy Composites Reinforced by Colaminated Boron Film, Composite Materials: Testing and Design (Second Conference), ASTM STP 497, American Society for Testing and Materials, 1972, pp 396-414.
12. Hart-Smith, L. J., "Design and Analysis of Adhesive Bonded Joints," Douglas Aircraft Company Paper 6059, presented to Air Force Conference on Fibrous Composites in Flight Vehicle Design, Dayton, Ohio, 26 - 28 September, 1972.

13. Lehman, G. M., et al., "Development of a Graphite Horizontal Stabilizer," McDonnell Douglas Company Report J0945, December 1970.
14. Leonhardt, J. L. ; Shockey, P. D. ; and Studer, V. J. ; "Advanced Development of Boron Composite Wing Structural Components," Convair Aerospace Division of General Dynamics, Technical Report AFML-TR-70-261, December 1970.

UNCLASSIFIED

Security Classification

DOCUMENT CONTROL DATA - R & D

(Security classification of title, body of abstract and indexing annotation must be entered when the overall report is classified)

| | | | |
|---|--|---|-----------------|
| 1. ORIGINATING ACTIVITY (Corporate author) McDonnell Douglas Corporation Douglas Aircraft Company Long Beach, California 90846 | | 2a. REPORT SECURITY CLASSIFICATION UNCLASSIFIED | |
| | | 2b. GROUP NA | |
| 3. REPORT TITLE COMPOSITE WING CONCEPTUAL DESIGN | | | |
| 4. DESCRIPTIVE NOTES (Type of report and inclusive dates) Final Technical Report of Work Conducted Between 1 February 1971 and 17 January 1973 | | | |
| 5. AUTHOR(S) (First name, middle initial, last name) Nelson, W. D., et. al. | | | |
| 6. REPORT DATE March 1973 | | 7a. TOTAL NO. OF PAGES | 7b. NO. OF REFS |
| 8a. CONTRACT OR GRANT NO. F33615-71-C-1340 | | 9a. ORIGINATOR'S REPORT NUMBER(S) MDC-J 4381 | |
| b. PROJECT NO. 698 CW | | 9b. OTHER REPORT NO(S) (Any other numbers that may be assigned this report) AFML-TR-73-57 | |
| c. | | | |
| d. | | | |
| 10. DISTRIBUTION STATEMENT Distribution limited to U.S. Government agencies; test and evaluation; statement of work must be referred to AFML/LC, Wright-Patterson AFB, Ohio, 45433 | | | |
| 11. SUPPLEMENTARY NOTES | | 12. S. RING MILITARY ACTIVITY Air Force Materials Laboratory Air Force Systems Command Wright-Patterson Air Force Base, Ohio 45433 | |
| 13. ABSTRACT Design, analysis, fabrication and test work are described which were performed to identify and develop the potentials of the advanced composite truss web wing box concept. The aircraft on which the effort is based is the Advanced Medium STOL Transport (AMST). The truss web concept is unique in that it utilizes no ribs or bulkheads to redistribute chordwise loads or to support the covers. A weight savings of 36.6 percent with respect to the metal wing box is achieved for the baseline truss web utilizing a boron-epoxy tapered sandwich lower cover and cutout-lightened substructure. Optimization studies showed an available range of weight savings from 28 to 56 percent, depending on the specific materials used, number of cells in the configuration, method of handling stress relief at bolted joints, bonded joint details, and tailoring of panel stiffening and substructure lightening detail. A multi-rib/multi-web design optimization study is reported. Finite anisotropic element analyses for the wing and final test component are described. Laminate tests utilizing mixed graphite materials are described. Element and subcomponent tests are conducted to verify features of the design, including the fillet bond concept for joining webs to covers. The testing effort culminates in a sweepbreak wing-fuselage intersection component which includes a stress-relieved bolted upper cover and a fillet-bonded lower cover. It achieves 94 percent of ultimate combined bending and torsion load. The major design features under test are validated since failure occurs in a conventional locally overstressed area. | | | |

DD FORM 1 NOV 65 1473

UNCLASSIFIED

Security Classification

UNCLASSIFIED
Security Classification

| 14. KEY WORDS | LINK A | | LINK B | | LINK C | |
|--|--------|----|--------|----|--------|----|
| | ROLE | WT | ROLE | WT | ROLE | WT |
| CONCEPTUAL DESIGN TRUSS WEB WING FINITE ELEMENT ANALYSIS COMPOSITE MATERIALS WEIGHT OPTIMIZATION FILLET BONDING STRESS CONCENTRATION RELIEF ADHESIVE PROPERTIES JOINT DESIGN VERIFICATION TESTING | | | | | | |

UNCLASSIFIED
Security Classification